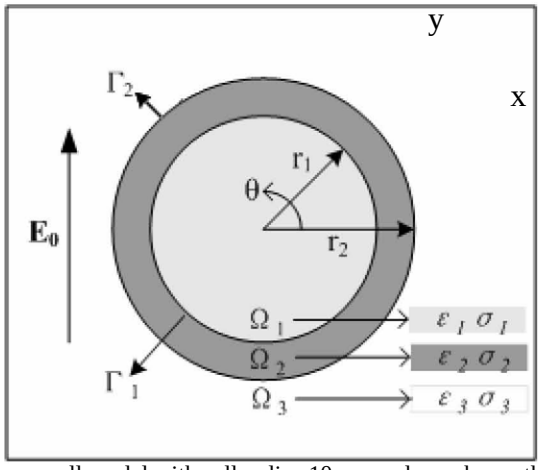


Fig. 1 Double layer cell model with cell radius 10 μm and membrane thickness 10 nm.

2.1 Quasi-static analysis by solving Laplace's equation

The wavelength at the studying frequency band (100MHz ~ 100GHz) is much larger than the cell dimension, so the quasi-static approximation applies in this study. Therefore, Laplace's equation together with the boundary conditions on the interfaces is sufficient to define the problem.

$$\nabla^2\Phi = 0 \qquad \text{In } \Omega_1\ \Omega_2\ \Omega_3 \qquad (1)$$

$$\left(\varepsilon_2\vec{E}_2 - \varepsilon_1\vec{E}_1\right)\cdot\hat{n} = 0 \qquad \text{On } \Gamma_1$$

$$\left(\varepsilon_3\vec{E}_3 - \varepsilon_2\vec{E}_2\right)\cdot\hat{n} = 0 \qquad \text{On } \Gamma_2$$

The analytical solutions of the Laplace's equation in a spherical cell model can be solved as follows.

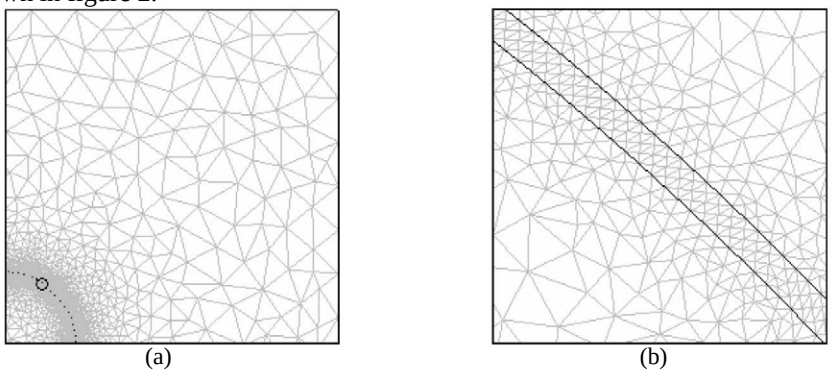
$$E_{1n} = \frac{3\varepsilon_2\varepsilon_3}{\varepsilon_2(\varepsilon_1+2\varepsilon_3)+2\alpha(\varepsilon_1-\varepsilon_2)(\varepsilon_3-\varepsilon_2)}E_0 \qquad \text{In } \Omega_1 \qquad (2a)$$

$$E_{2n} = \frac{\varepsilon_3(\varepsilon_1+2\varepsilon_2)}{\varepsilon_2(\varepsilon_1+2\varepsilon_3)+2\alpha(\varepsilon_1-\varepsilon_2)(\varepsilon_3-\varepsilon_2)}E_0 + \frac{(1+\cos^2\theta)r_1^3}{r^3}\frac{\varepsilon_3(\varepsilon_1-\varepsilon_2)}{\varepsilon_2(\varepsilon_1+2\varepsilon_3)+2\alpha(\varepsilon_1-\varepsilon_2)(\varepsilon_3-\varepsilon_2)}E_0 \qquad \text{In } \Omega_2 \qquad (2b)$$

$$E_{3n} = E_0 + \frac{(1+\cos^2\theta)r_1^3}{r^3}\frac{\varepsilon_2(\varepsilon_1-\varepsilon_3)-\alpha(\varepsilon_1-\varepsilon_2)(\varepsilon_3-\varepsilon_2)}{\varepsilon_2(\varepsilon_1+2\varepsilon_3)+2\alpha(\varepsilon_1-\varepsilon_2)(\varepsilon_3-\varepsilon_2)}E_0 \qquad \text{In } \Omega_3 \qquad (2c)$$

where $\alpha = \frac{1-\left(\frac{r_1}{r_2}\right)^3}{3}$.

In addition to the analytical solution, the Laplace's equation (Equation 1) can also be solved numerically. The numerical solution was performed in the trial version v3.2b of Comsol Multiphysics (FEMLAB) based on FEM (Finite Element Method). Meshing scheme of a quarter of the cell model and the zoom-in view of mesh on the membrane are shown in figure 2.



(a) (b)

Figure 2 Meshing schemes of the cell model: (a) mesh on a quarter of a cell; (b) the zoom-in view of mesh on the membrane

2.2 Full-wave analysis by solving Maxwell's equations

On the other hand, the full wave equation, i.e. Maxwell's equations is a complete description of the problem. The theoretical solution of Maxwell's equations is obtained based on the Mie theory, which solves the Helmholtz's equations in the studying regions. Boundary conditions at the interfaces Γ_1 and Γ_2 are involved with the electric and magnetic fields of the incident wave.

$$\nabla^2\vec{E} + k^2\vec{E} = 0 \qquad \text{In } \Omega_1\ \Omega_2\ \Omega_3 \qquad (3a)$$

$$\nabla^2\vec{H} + k^2\vec{H} = 0 \qquad (3b)$$

$$\left(\vec{E}_2 - \vec{E}_1\right)\times\hat{e}_r = 0; \quad \left(\vec{H}_2 - \vec{H}_1\right)\times\hat{e}_r = 0; \qquad \text{On } \Gamma_1$$

$$\left(\vec{E}_i + \vec{E}_3 - \vec{E}_2\right)\times\hat{e}_r = 0; \quad \left(\vec{H}_i + \vec{H}_3 - \vec{H}_2\right)\times\hat{e}_r = 0; \qquad \text{On } \Gamma_2$$

The calculated electric and magnetic fields are expressed by the vector harmonics $\boldsymbol{M}_{o1n}$, $\boldsymbol{M}_{e1n}$, $\boldsymbol{N}_{o1n}$, $\boldsymbol{N}_{e1n}$ (products of cosine, Legendre and Bessel functions of corresponding parameters in spherical coordinate system) in equation 4. The coefficients a_n, b_n, c_n, d_n, f_n, g_n, v_n and w_n are solved by the wave expressions together with the boundary conditions. The summation of infinite elements in the following equations provides the accurate result, which is not applicable in practical calculation, so the element-summation truncation number N is selected as 12 to balance the accuracy and computation overheads.

$$\vec{E}_1 = E_0\sum_{n=1}^{N} i^n\,\frac{2n+1}{n(n+1)}\left(c_n\vec{M}_{o1n}^{(1)} - id_n\vec{N}_{e1n}^{(1)}\right) \qquad (4a)$$

$$\vec{H}_1 = \frac{-k_1}{\omega\mu_1}E_0\sum_{n=1}^{N} i^n\,\frac{2n+1}{n(n+1)}\left(d_n\vec{M}_{e1n}^{(1)} + ic_n\vec{N}_{o1n}^{(1)}\right) \qquad (4b)$$

$$\vec{E}_2 = E_0\sum_{n=1}^{N} i^n\,\frac{2n+1}{n(n+1)}\left(f_n\vec{M}_{o1n}^{(1)} - ig_n\vec{N}_{e1n}^{(1)} + v_n\vec{M}_{o1n}^{(2)} - iw_n\vec{N}_{e1n}^{(2)}\right) \qquad (4c)$$

$$\vec{H}_2 = \frac{-k_2}{\omega\mu_2}E_0\sum_{n=1}^{N} i^n\,\frac{2n+1}{n(n+1)}\left(g_n\vec{M}_{e1n}^{(1)} + if_n\vec{N}_{o1n}^{(1)} + w_n\vec{M}_{e1n}^{(2)} + iv_n\vec{N}_{o1n}^{(2)}\right) \qquad (4d)$$

$$\vec{E}_3 = E_0\sum_{n=1}^{N} i^n\,\frac{2n+1}{n(n+1)}\left(-b_n\vec{M}_{o1n}^{(3)} + ia_n\vec{N}_{e1n}^{(3)}\right) \qquad (4e)$$

$$\vec{H}_3 = \frac{k}{\omega\mu}E_0\sum_{n=1}^{N} i^n\,\frac{2n+1}{n(n+1)}\left(a_n\vec{M}_{e1n}^{(3)} + ib_n\vec{N}_{o1n}^{(3)}\right) \qquad (4f)$$

The Maxwell's equations are also solved by FEM in the Comsol Multiphysics (FEMLAB) as the full-wave analysis, using the same meshing scheme as the quasi-static method, as shown in figure 2. The scattering boundary conditions are used assuming the boundary is transparent for the scattered wave.

2.3 Results

Figure 3 shows the calculated E-fields by using Mie theory (red dotted line) and the Laplace's solution (red solid line), compared with the numerical calculated results of full-wave (blue dotted line) and quasi-static FEM (blue solid line). It is observed that the two dotted lines (Mie theory and FEM with full-wave) agree with each other quite well, presenting a more accurate evaluation than the other two methods based on the quasi-static approximation (Laplace's solution and FEM with quasi-static). However, the largest discrepancy between them is no more than 5%, which is acceptable in the estimation of the field distribution in cell modelling.

The left part of the separator symbol ('//') on figure 3 shown the electric field distribution near the membrane of the cell. The field inside the cell is slightly higher than the external field strength (1V/m), and the field outside the cell is lower than the external field. The right part (right of '//') showed that the electric field increases while leaving the edge of the cell, and approaches the external field strength gradually.

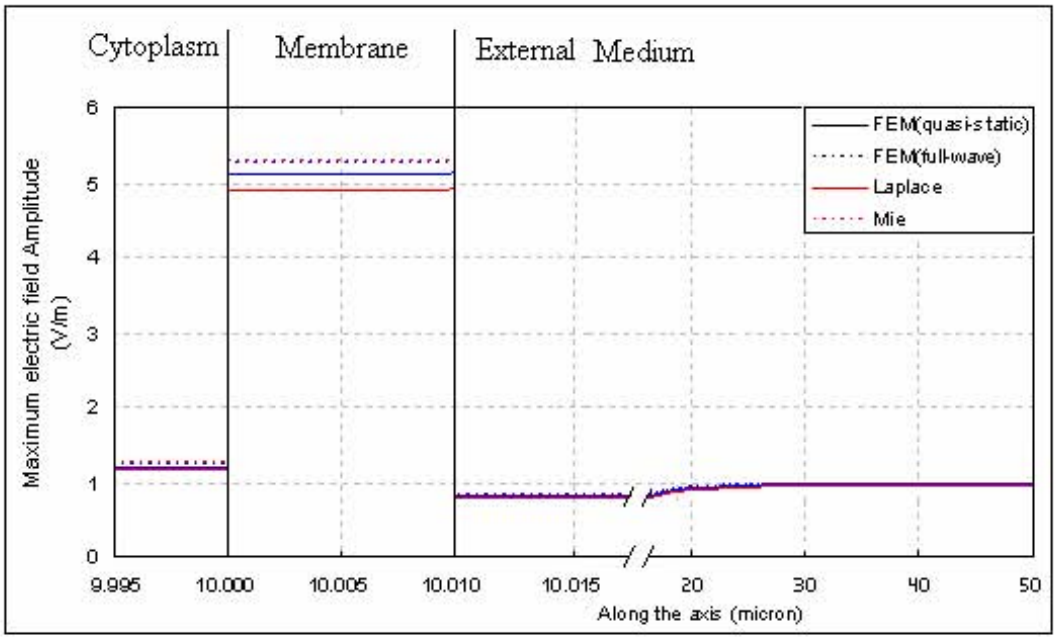


Figure 3 Electric field distributions along the axis parallel to the external field (analytical and numerical)

Solving the 2D cell model with quasi-static approximation took 2 minutes 27 seconds in the simulation software FEMLAB, whereas the full-wave analysis of the same cell model and meshing scheme took 26 hours 48 minutes, both on a 2.80GHz PC with 512M memory. Therefore, the fast microdosimetry based on quasi-static approximation is much more efficient than the traditional full-wave analysis while maintaining acceptable accuracy (<5% error). All the simulations in next two sections use the models based on the quasi-static approximation.

III. Analyses

3.1 Influences of dielectric properties

The cytoplasm was modelled as physiological saline (0.07N) containing a protein volume fraction of 0.262, so the relative permittivity and the conductivity were obtained in literature [3]. As a protein solution, the major dispersion at microwave frequencies is dominated by the water relaxation near 20GHz, and diminished a little due to the proteins' displacement of a corresponding volume of water. The membrane, as a phospholipid bilayer, has a frequency-independent relative permittivity of 11.3 (membrane capacity 1.0μF/cm^2) and conductivity of 0 [4]. The external medium is assumed to have the frequency-dependent dielectric properties of physiological saline (0.15N) [4] with a static and infinite frequency permittivity values of 76 and 5, respectively. There is no apparent difference between the relaxation frequency of the medium and that of the pure water, which is 20GHz at room temperature. The characteristic values of the dielectric properties on the three sub-domains are listed in table 2.

	Cytoplasm (Ω_1)	Membrane (Ω_2)	External (Ω_3)
ε_s	57	11.3	76
ε_{in}	5	0	5
f_c (Hz)	15e9	-	20e9
σ_s (S/m)	0.3	0	1.1

Table 2 Dielectric properties of double layer cell model

The parameters illustrated in table 2 are static relative permittivity, infinite frequency relative permittivity, relaxation frequency and static conductivity, respectively. The frequency dependent permittivities are plotted in figure 4. The electric fields inside and outside the cell are almost uniform, whereas the field concentrated on the membrane varies according to the theta angle in the polar coordinate. The maximum value of the field intensity happens at the zenith angle (90^0), and depends on the frequency, as plotted in figure 5.

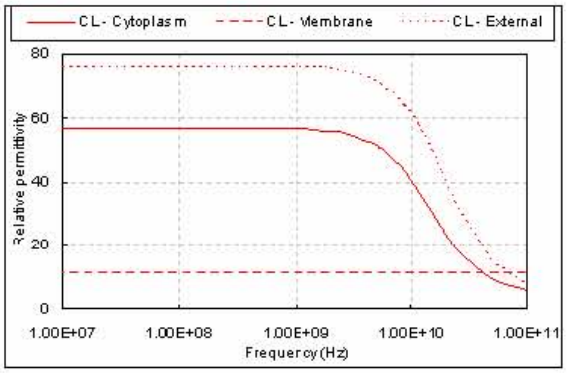


Figure 4 Debye 1st order relaxation properties of cell model (Relative permittivity)

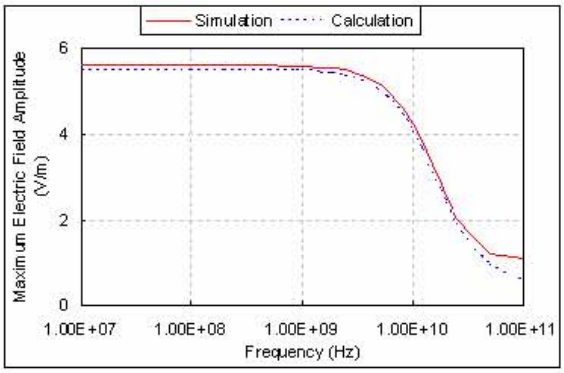


Figure 5 Maximum E fields on the membrane of the spherical cell model

Figure 5 displays the electric field simulated by FEM with quasi-static approximation and calculated by directly solving Laplace's equation. The two curves agree with each other very well. With the logarithm scaled axes, figure 5 illustrates that at the lower frequency band, the E-fields are not significantly dependent on the dielectric model. While at the higher frequency range the maximum electric field is strongly dependent on the frequency, which agrees well with the trends shown in figure 4 of the dielectric properties.

3.2 Elliptical cells

One of the most common cells shapes is ellipsoid, which has one more dimensional variable than the spherical model, axial ratio (the ratio between major and minor axes). When the cell is exposed to the plane wave illumination, the electric field also concentrates on the membrane and the maximum electric field appears at the zenith angle of the cell. The dielectric properties used in the simulations in this section are the same values as listed in table 1. Amplitudes of the maximum electric fields of the cell model with different axial ratios are plotted in figure 6.

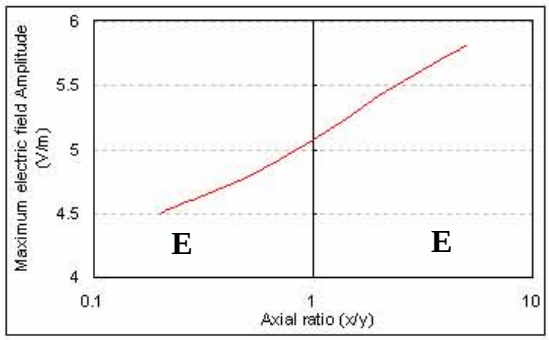


Figure 6 Maximum E fields on the membrane of the ellipsoidal cell (according to different axial ratio)

Figure 6 presents that the maximum electric field is higher when the major axis of the ellipsoidal cell is perpendicular to the external field, and the value decreases while the minor axis increasing. When the major axis is parallel to the external field, the E field value increases with the increasing of the minor axis. Plotting the E field amplitude according to the axial ratio in logarithm scale, this relationship is approximately linear.

The ellipsoid exposed to external electric fields with different polarisations as illustrated in Figure 7 has also been investigated. The maximum value of electric field presents at the frontier of the structure. Figure 8 shows the maximum electric field on the membrane decreasing when the external electric field polarisation changing from 0 degree to 90 degree.

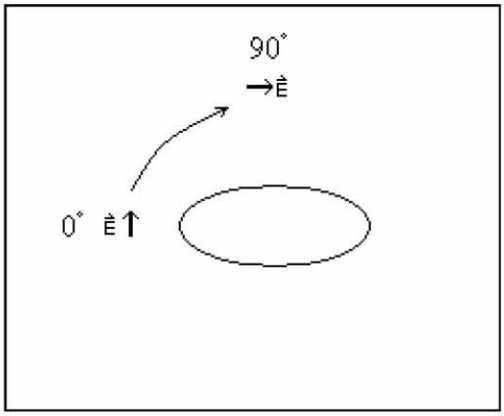


Figure 7 Ellipsoidal cell exposed to electric field with different polarisation

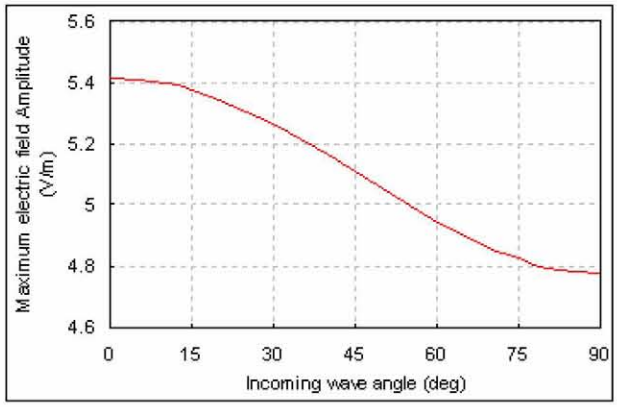


Figure 8 Maximum eelectric fields on the membrane of the ellipsoidal cell (according to different polarisation of external electric field)

3.3 Other shapes of models

The geometric shape of the structure also influences the maximum electric field on the membrane. For a cell model with length 10 microns and width 5 micros, the maximum E fields of the ellipsoids, rods and erythrocytes are compared in Table 3. The "vertical (↑0°)" and "horizontal (→90°)" in Table 3 indicates the directions of external electric field as shown in Figure 4. The location of maximum electric field is labelled by the red circles in Table 3.

	E field (external E_0: horizontal → 90°)	E field (external E_0: vertical ↑0°)
Ellipsoid	4.776	5.415
Rod	4.762	5.492
Erythrocyte	4.779	5.780

Table 3 E fields on the membrane (according to different cell shapes)

IV. Summaries

In this paper, a fast microdosimetry technique based on the quasi-static approximation has been studied. It is demonstrated that the fast microdosimetry technique runs much faster than the one working with full-wave analysis, while maintaining acceptable accuracy. The following analyses of frequency-dependent dielectric properties of the simple cell model have revealed their influences on the electric field concentration on the membrane. In addition, the effects of the various shapes of cell models have been also been investigated. In the future, the fast microdosimetry can be performed on more realistic cell models, in order to study the field distribution and transmembrane potential of the cell.

References

[1] S Munoz San Martin, J L Sebastian, M Sancho and J M Miranda, "*A study of the electric field distribution in erythrocyte and rod shape cells from direct RF exposure*", Phys. Med. Biol. vol.48, 1649-1659, 2003

[2] C Merla, M Liberti, G d'Inzeo, "*Dielectric models of biological cells and quasi-static EM analysis at radio and microwave frequencies: A microdosimetric study*", Proceeding of BEMS Annual meeting, Ireland, 2006

[3] G P Drago, S Ridella, "*Evaluation of electrical fields inside a biological structure*", Br J Cancer (Suppl V), 45: 215-219, 1982.

[4] H P Schwan, K R Foster, "*RF-field interactions with biological systems: Electrical properties and biophysical mechanisms*", Proceedings of IEEE, 68(1): 104 – 113, 1999.

Directional Effects of a Moderate-Intensity Static Magnetic Field on Anomalous Chemical Wave Propagation

Daisuke Akai[a], Hideyuki Okano[b], Hiroyuki Kitahata[c], Kenichi Yoshikawa[c] and Naohide Tomita[a,b]

[a]Department of Mechanical Engineering, Graduate School of Engineering, Kyoto University, Japan
[b]International Innovation Center, Kyoto University, Japan
[c]Department of Physics, Graduate School of Science, Kyoto University, Japan

Abstract
The effect of the spatial magnetic gradient in static magnetic field (SMF) exposure on the velocity of chemical wave in Belousov-Zhabotinsky (BZ) reaction was examined. The BZ medium was exposed to SMF of maximum magnetic flux density 210 mT and maximum spatial gradient 37 mT/mm for a period of up to 20 min at room temperature. The SMF was generated by a parallel pair of attracting rectangular NdFeB magnets positioned opposite to each other. The results suggested three characteristics for the alternation of BZ chemical wave formation: (1) the magnetic gradient could be the dominant factor for the alternation of the chemical wave; (2) the direction of accelerated velocity of chemical wave was vertical to the direction of magnetic gradient; (3) the effect was symmetry to the gradient direction and our experiments demonstrate clearly that The effect of SMF on the chemical wave propagation was affected by the thickness of the BZ medium.

1. Introduction

It has been reported that static magnetic field (SMF) can influence physicochemical reactions [Boga et al., 1990; He et al., 1994] and biochemical reactions [Harkins and Grissom, 1994], and therefore it has been predicted that SMF might affect auto-oscillations in the nonequilibrium system. We used the Belousov-Zhabotinsky (BZ) reaction known as nonequiriblium system and one of the simplest chemical oscillators in order to test this hypothesis. The steady oscillations of BZ reaction can be easily observed for a long period. The present study shows that the spatial magnetic gradient in the SMF exposure affects the velocity of chemical wave propagation. This phenomenon could be attributed primarily to the magnetic force acting the iron ion complexes in the BZ solution.

2. Experiment

The BZ medium of 20 ml contains the following solutions: (1) 7 ml H_2O, (2) 3 ml $NaBrO_3$ (1 M), (3) 2 ml H_2SO_4 (3 M), (4) 2 ml $CH_2(COOH)_2$ (1 M), (5) 2 ml NaBr (3 M), and (6) 4 ml $Fe[(phen)_3]^{2+}$ (20 mM). Every solution from (1) to (5) was added in number order. After these 5 solutions were mixed in a glass vessel, the solution turned yellowish, started to fade and became colorless in some minutes. In the end, solution (6) ferroin was added into the previous solution.

The magnetic device is constructed using a pair of rectangular neodymium magnets (Fig.1). The opposite magnets attracting each other through a 26 mm air gap are fixed parallel to both sides of the stainless frame. The maximum magnetic flux density was measured to be approximately 210 mT at the bottom center of the Petri dish by using a gaussmeter (Model 4048, Hall probe A-4048-002; Bell Technologies, Orlando, FL, USA).

(1) The BZ medium was put into a petri dish with a diameter 140 mm (3030-150; Iwaki Glass Co, Japan), which was put on a magnetic device (Fig.1). BZ reaction was initiated at the center of the Petri dish using a silver wire. The images were taken by a digital video camera (DIGICAM, NV-GS250-S, Panasonic, Japan) from above. The pictures were quantified by using Scion software (Scion Image; Scion, Frederick, MD, USA). All the experiments were carried out at a room temperature. Four independent experiments were averaged per data point. All values are expressed as mean ± SD.

(2) To examine the effect of the thickness of BZ medium on the chemical wave propagation, the thickness of BZ medium was controlled from 0.5 to 0.9 mm at 0.2 mm intervals by slipping some cover glasses with a thickness 0.1 mm in between two square plates. These plates were put on one side of the magnetic device with the edges of the plates parallel to the inner line of the magnet. The BZ medium was poured in between two plates. BZ reaction was initiated from the edge of plates using a silver wire to observe chemical wave propagation from the center of the device. The images were taken by a digital video camera in the same way as

the previous experiment.

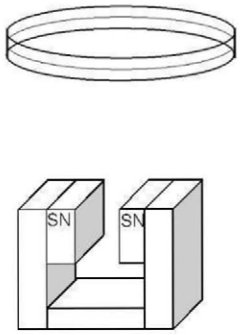


Fig.1. Experimental device
A Petri dish with a diameter 140 mm was put on the magnetic table where, two parallel rectangular magnets (NdFeB, L. 80 × W. 18 × H. 55 mm, TDK Corporation, Japan) attract each other.

3. Results and discussions

The concentric propagation of chemical wave was observed in the BZ medium when sham exposure was performed without magnet (the background geomagnetic field intensity at our laboratory is ~50 μT) (Fig.2A). On the other hand, the different propagation from concentric pattern of chemical wave was observed when the BZ medium was exposed to SMF (Fig.2B). The thickness of BZ medium in the petri dish was 1.3 mm.

These results suggested three characteristics for the alternation of BZ chemical wave formation: (1) the magnetic gradient could be the dominant factor for the alternation of the chemical wave; (2) the direction of accelerated velocity of chemical wave was vertical to the direction of magnetic gradient; (3) the effect was symmetry to the gradient direction.

The velocity of chemical wave of BZ reaction to Y direction was accelerated on the inner line of the magnet where the magnetic gradient to X direction was maximum (Fig.2). This result indicates that the BZ chemical reaction was accelerated to one direction by the magnetic gradient, and that the direction was perpendicular to the gradient. The chemical wave can be visualized by the oxidation-reduction reaction of ferroin. However, BZ reaction is induced by the complicated combination of several chemical reaction steps. Ions produced in the chemical reaction could be affected by the inhomogeneous magnetic field. The alternation of the chemical wave propagation in BZ reaction could be caused by the different orientation of iron ions under SMF exposure from that of sham exposure (no magnet).

In order to quantify the alternation of chemical wave, the angles θ of tangent line of the chemical wave front to the inner line of the magnet defined in Fig.3 were measured under the both conditions of sham exposure (no magnet) and SMF exposure (Fig.4). The deformation rates of chemical wave in SMF exposure were significantly larger and reached their maximum levels earlier than those in sham exposure.

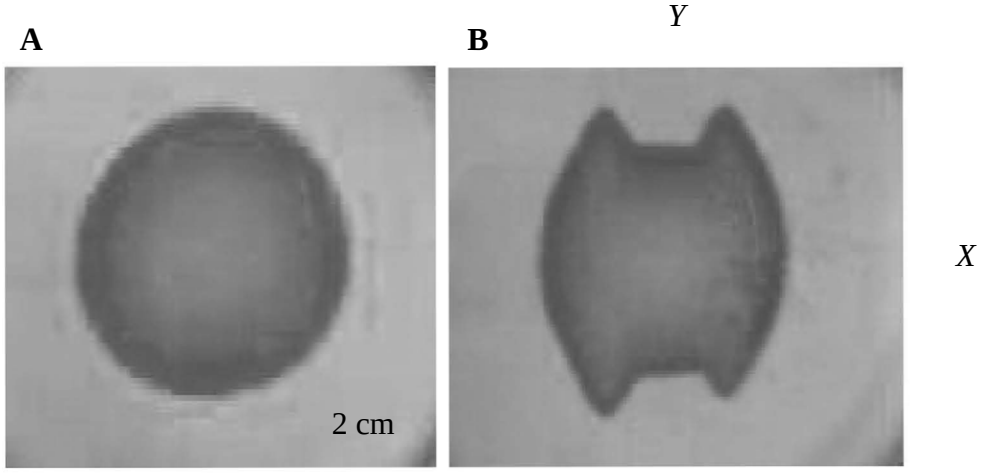


Fig.2. (A) Chemical wave not exposed to magnets (sham exposure) (B) Chemical wave exposed to magnets (SMF exposure; white dashed lines correspond to the position of magnets)

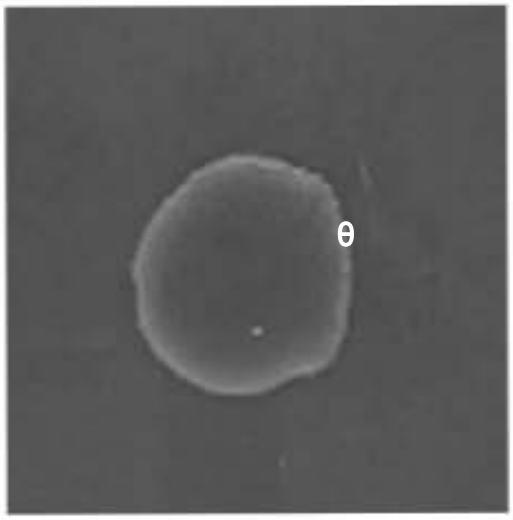


Fig.3. Angle θ of tangent line of the chemical-wave front to an inner line of the magnet (dashed line corresponds to the position of magnet)

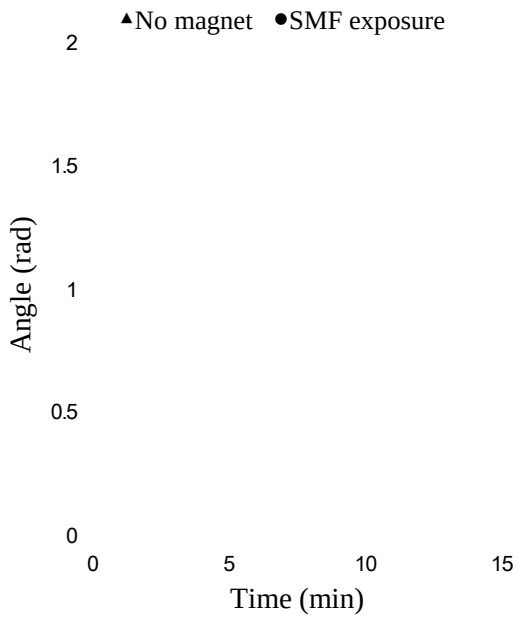


Fig.4. Angles defined in Fig.3 measured per data point in the case of no magnet and SMF exposure

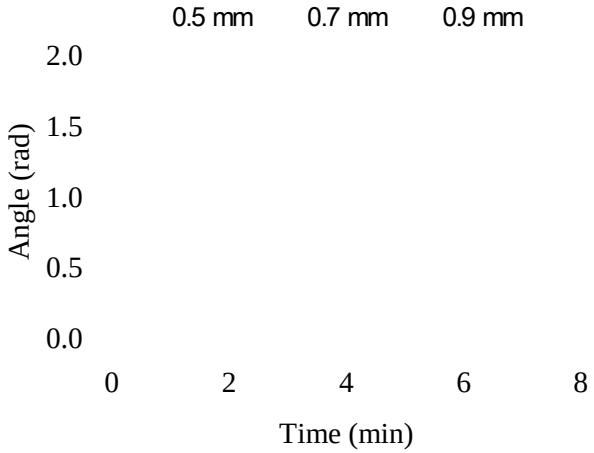


Fig.5. Angles defined in the same way as Fig.3 per data point of BZ reaction of several thickness 0.5, 0.7, 0.9 mm of BZ medium

The effect of SMF on the chemical wave propagation was affected by the thickness of the BZ medium as shown in Fig.5. When the thickness of BZ medium was different, the velocity of reaction front varied. Therefore, the forms of chemical wave propagation were different among three conditions. The thicker the BZ medium was, the larger the deformation rate of chemical wave was. However, there was no significant difference per data point between the thickness 0.7 and 0.9 mm. It is conceivable that the degree of the chemical wave propagation would not change in the case of both more than constant thickness and less than the threshold of thinner thickness. This means that there is a window effect of SMF on the deformation rate of chemical wave depending on the thickness of the BZ medium. The result given in Fig.5 includes the factor of the velocity of the reaction front on the inner line of the magnet. The elements of the distance of reaction front should be taken into account in order to quantify the anomalous propagation in detail.

References

Boga E, Kádár S, Peintler G, Nagypál I. 1990. Effect of magnetic fields on a propagating reaction front. Nature 347:749–751.

Harkins TT, Grissom CB. 1994. Magnetic field effects on B_{12} ethanolamine ammonia lyase: evidence for a radical mechanism. Science 263:958–960.

He X, Kustin K, Nagypál I, Peintler G. 1994. A family of magnetic field dependent chemical waves. Inorg Chem. 33:2077–2078.

COMPARATIVE STUDY OF THE EFFECTS OF EMF-TREATED AND HYDROGEN PEROXIDE-CONTAINING SOLUTIONS ON NEUROMEMBRANE CHEMOSENSITIVITY

SINERIK AYRAPETYAN, ARSEN HUNANYAN

UNESCO CHAIR- LIFE SCIENCES INTERNATIONAL POSTGRADUATE EDUCATIONAL CENTER
31 ACHARYAN ST., YEREVAN, 375040 ARMENIA, LIFE@ARMINCO.COM

Abstract

The hydrogen peroxide (H_2O_2) which is formed in cell bathing aqueous solution upon Electromagnetic Fields (EMF) exposure is very often considered as the most reliable messenger through which the biological effect of EMF is realized. To check this hypothesis the comparative study of the effects of 4Hz EMF-treated and H_2O_2 - containing physiological solutions (PS) on Ach sensitivity of snail neuron as well as on the nerve tissue hydration were studied. The 4 Hz EMF-treated and H_2O_2-containing PS at room temperature (23^0C) had depressing effects on Ach-induced current, while in cold medium (12^0C) these effects disappeared. The EMF-treated ouabain-containing and K-free PS elevated the amplitude of Ach-induced current, while the H_2O_2 – containing PS has inhibitory effect on it. The both, EMF-treated and H_2O_2 -containing PS have dehydration effects on cell hydration in nerve ganglia. It is suggested that the ELF EMF-induced H_2O_2 formation could serve as one of the metabolic pathways through which the depressing effect of ELF EMF on membrane chemosensitivity is realized.

Key words: EMF, H_2O_2,, neuron, acetylcholin -sensitivity, membrane, cell volume.

Introduction

Although, the abundance of experimental data on the biological effect of magnetized water and water solutions on different cells and organisms are available (Klassen, 1982; Ayrapetyan et al., 1994a; Ayrapetyan, 2006), the nature of the messenger transferring the signal of magnetic and electromagnetic fields-induced water structural changes to cell metabolic cascade is not clear yet. As the water molecule dissociation is the most variable water property, it is suggested that the EMF-induced vibration of water dipoles could change water dissociation and its products could serve as possible messengers through which the biological effect of EMF is realized (Ayrapetyan 1994). By privies our work the depressing effect of extremely low frequency (ELF) EMF on specific electrical conductivity (SEC) of water and water solutions (which is marker for its dissociation) was documented (Ayrapetyan et al., 1994). It was also shown that the depressing effect of LF EMF on water SEC as well as its biological effects on various cells are most pronounced at frequency of 4 Hz (Stepanian et al. 1999; Ayrapetyan 2006).

The fact that the vibration of water dipoles in presence of oxygen could generate the H_2O_2, which could initiate the modulation of a number of metabolic pathways in the cell, makes it as one of the most reliable candidates for the messenger able to transfer the ELF EMF-induced water structure changes to cell metabolic cascades (Klassen, 1982). As the acetylcholine (Ach) sensitivity of neuronal membrane is sensitive to the effect of magnetized physiological solutions (MPS) (Ayrapetyan et al., 1994a; Ayrapetyan et al., 2004), it was chosen as an experimental model for testing the above-mentioned hypothesis.

The overall aim of the present review is to present the results of the comparative study of 4 Hz EMF-treated and H_2O_2 –containing PS on snail neuromembrane chemosensitivity, as well as on the nerve tissue hydration which has a crucial role in metabolic regulation of membrane chemosensitivity (Ayrapetyan & Arvanov, 1979).

Method

The experiments were carried out on non-selected giant neurons of the right parietal ganglion of Helix pomatia. The standard Voltage-Clamp method was used to record the Ach-induced current through the neuronal membrane (Ayrapetyan and Arvanov, 1988). The normal physiological solution contains (in mM): NaCl-80,

KCl-4, CaCl2-7, MgCl2-13, Tris-HCl (pH 7.8)-10, glucose-10. In K-free solution 4mM KCI was replaced by 4mM NaCI. Different concentrations of acetylcholine (10^{-4}-10^{-6} M) and H_2O_2 (10^{-4}-10^{-11} M) were prepared from Ach and H_2O_2 stock solution (10^{-2} M) before the experiments. The transient application (less than 30 sec) of Ach was performed by thin (diameter ~1mm) polyethylene tube placed near the investigated neuron. The H_2O_2 was added to the perfusion solution to a final concentration from 10^{-4} to 10^{-11} M and applied to the cells at a rate of 2-3 ml/min. The time of pre-incubation of neurons in tested physiological solution before the Ach application was 3 min.

The tested physiological solution was preliminary exposed to 4Hz EMF with the intensity of 2,5 mT for 30 minutes. The experimental setup consisted of a glass test tube with diameter of 10 mm and volume of 10 ml., EMF generator with low-noise amplifier and a coil. The coil has the cylindrical form with diameter of 154 mm. and height of 106 mm. The coil consists of Helmholtz rings that generate the homogeneous magnetic field. Rings of Helmholtz are formed by two equal ring coils located coaxially and in a parallel way. The distance between ring coils is equal to their radius of 77 mm. The magnetic field created by these rings has high homogeneity. For example, on distance of 0.25R from the center of an axis strength differs from computed by formula only on 0.5 % $H = 71.6 \cdot \omega \cdot \frac{I}{R}$. Herewith, the intensity of generated EMF is equal to 2.5 mT and 4 Hz frequencies. The instrument used for measurement of magnetic field intensity was a Teslometer W1-8 (Armenian Radiophysical Institute). This instrument measures magnetic fields in the range 10^{-3} to 1.6 T (±5%). The magnetic induction converter was a crystal, type X511-1, 1.5 X 0.2 mm^2 and was fixed on non-magnetized material (PX13-1). During the experiment the neurons were perfused with normal and 4Hz EMF treated solutions. The physiological solution treated by 4Hz EMF for 30min. and immediately (interval from the end of the treatment and till the beginning of perfusion was no longer than 1-2 min.) used for perfusion of neuronal ganglia. The control (unexposed) PS taken from the same reservoir of PS (Vol: 1-2 l) also was placed in the same test tube for 30min in an inactive coil system, i.e. the background field was the same for the control (sham exposed) and tested PS. The background of magnetic field in the area of experimental setup in the laboratory, supplied by 60 Hz electricity, was less than 0,001 mT. The holder of the exposure tube and the coil holder were placed in two neighboring tables to excluded the vibration during the exposure.

For determination of tissue hydration, the wet samples of the nerve ganglia were weighted and dried in thermostat at 105^0C, during 24 hours. After determination of dry weight the quantity of water on 1 g. of dry weight was determined by the equation: (A - B) / B , where A- wet weight of the tissue, B- weight of the tissue after drying.

The procedure of measuring a single cell volume has been previously described in Ayrapetyan et al., 1994a. Briefly, single neurons were dissected and isolated from the ganglion under a dissecting microscope (Lomo, B-14, Russian production) on which was mounted a digital video camera (WPI, USA) connected to PC. The system had the sensitivity such that changes of ±0.1 µm could be detected. These neurons had diameters of 50-100 µm.

The mean value, standard deviations, and the statistical probability, determined by Student Test were calculated with the help of computer program Sigma Plot (Version 8.02A).

Results

It is known that three types of neurons can be distinguished according their sensitivity to Ach: (a) insensitive, (b) depolarizing (D), and (c) hyperpolarizing (H) (Shakarov et al., 1969). The present experiments were carried on 22 neurons having D-responses and 20 neurons having H-responses. The membrane potential (MP) of neurons was clamped on the level of resting potential (-40 to -60 mV). After recording the control Ach-induced currents in normal physiological solution (control) the cells were perfused with magnetized PS (MPS) or by different concentrations of hydrogen peroxide- containing PS during 7 minutes and the end of 7-th minutes the application of Ach was performed.

By previous our work was shown that the normal MPS has a reversible depressing effect on Ach-induced membrane current and this effect of MPS was absent in cold (12^oC) medium. The typical record of such responses presented on Figure 1. (Ayrapetyan et al., 2004).

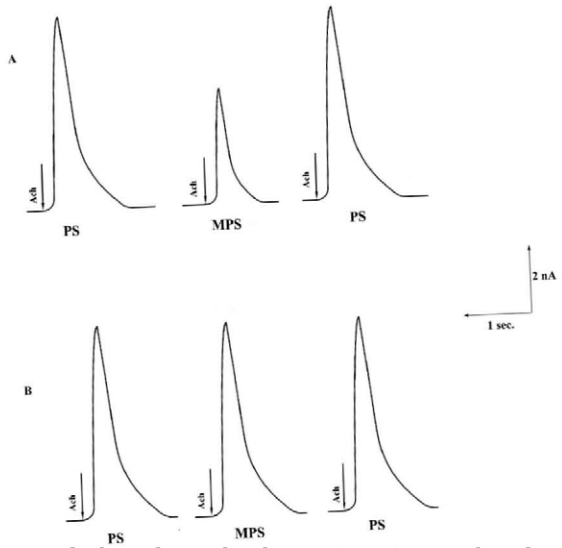


Figure 1. *The effect of magnetized physiological solution (MPS) on Ach-induced current in D type neuron in voltage-clump experiments, where the clumping potential (E_c) was equal to the resting membrane potential (E_r = -50 mV).*
A- at room temperature (23^0C), B- in cold medium (12^0C).
The rows show the transit (30 msec) application of 10^{-4} M Ach containing PS. The time of pre-incubation of neurons in tested physiological solution (PS and MPS), before the application of Ach was 3 min. The intervals between Ach applications was 5 min.

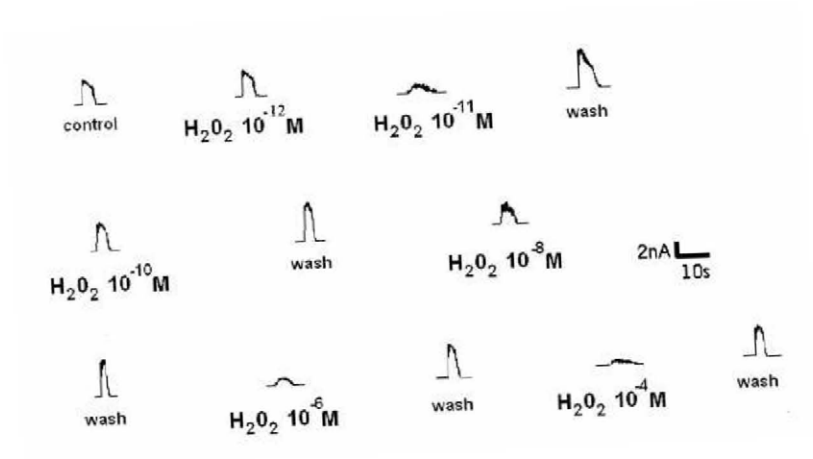


Figure 2. *The typical record of dose-dependent effect of H_2O_2 on Ach-induced current in D-type neuron in voltage-clamp experiments, where the clamping potential (E_c) was equal to the resting membrane potential (E_r = -60mV). Ach concentration was 10^{-4}M. The time of pre-incubation of neurons in H_2O_2 containing physiological solution (PS) was 7 min. All presented data were taken from one neuron. The intervals between Ach application was 5 min.*

As shown in Figure 2, the H_2O_2 at concentrations of 10^{-11}-10^{-4} M also has a depressing effect on Ach (10^{-4} M)-induced ionic currents in D-type neurons. After removing of H_2O_2 from extracellular medium the amplitudes of Ach-induced currents were recovered to their initial level within 5 minutes. The maximum depressing effect of H_2O_2 on Ach-induced current appeared at concentration of 10^{-4} M (75±1.2%), while the threshold of H_2O_2 concentration, unable to change the amplitude of Ach-responses of the membrane during 7 min. pre-incubation, was 10^{-12} M . The character of H_2O_2-induced inhibition of Ach-responses in both, H-and D- types neurons was the same (Figure 3, n=5), which could serve as indicator of potential independence of inhibitory effect of H_2O_2 on Ach responses.

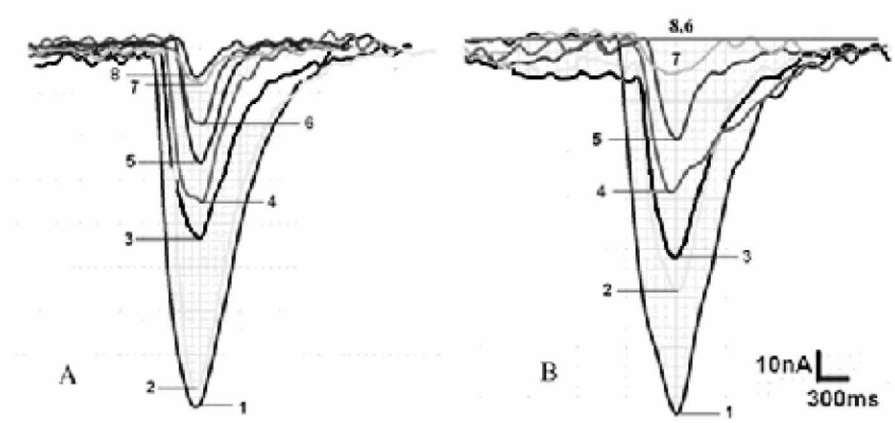


Figure 3. *The dose-dependent effect of H_2O_2 on Ach-induced current in H-type neurons in PS (A) and in K-free solution (B), where the clamping potential (E_c) was equal to the resting membrane potential (E_r = -52mV).*
1- Ach 5 × 10^{-4} M; 2- Ach 10^{-4} M; 3- H_2O_2, Ach 5 × 10^{-4} M; 4- H_2O_2, Ach 10^{-4} M; 5- Ach 10^{-5} M; 6- H_2O_2, Ach 10^{-5} M; 7- Ach 10^{-6} M; 8- H_2O_2, Ach 10^{-6} M.
The data are taken from one neuron. The presented data are typical for all 10 studied neurons. The H_2O_2 concentration was 10^{-6} M. The time of pre-incubation of neurons in H_2O_2 containing PS was 7 min.

This suggestion was confirmed by studying the potential-dependency of inhibitory effect of H_2O_2 on Ach responses, by clamping MP at different levels (Figure 4).

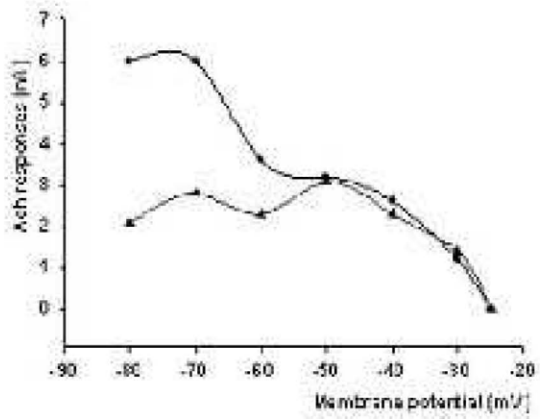


Figure 4. *The Ach-responses (nA) in D-type neuron in voltage-clamp experiments in normal (circles) and 10^{-6} M H_2O_2- containing (triangles) PS, when the membrane potential was clamped on different levels (n=5).*

The study of the potential-dependence of Ach-induced outward currents in normal and H_2O_2 (10^{-6} M) containing solution showed that the Ach-induced currents in presence of H_2O_2 became potential independent in the range of MP= - 50 – - 80 mV (Figure 4, n=5). These data could serve as additional evidence that H_2O_2 – induced depression of Ach-responses could not be explained by modulation of ionic channel activity, determining the Ach-responses. As shown in Figure 5, the depressing effect of H_2O_2 on Ach-responses as in case of MPS (Figure 1B), disappeared in cold medium (5^0C) (Figure 5, n=5), which could be considered as an evidence on the metabolic nature of H_2O_2-induced depression of Ach-responses of the membrane. The low temperature (12^0C) -induced slight elevation of Ach-induced current (Figure 1B) could be interpreted as the increase of the lifetime of agonist-activated ionic channels (Bregetovski et al., 1979).

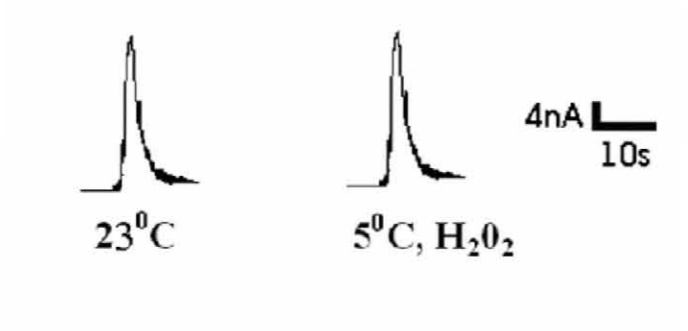


Figure 5. *The absence of depressing effect of H_2O_2 on Ach (10^{-4}M)-induced ionic currents in cold medium (5^0C). H_2O_2 concentration was 10^{-4} M, (n=5).*

The data on temperature sensitivity of the EMF-treated and H_2O_2 –containing PS-induced depressing effects on Ach membrane responses allow us to speculate on their metabolic nature. As shown in our early works the electrogenic Na^+-K^+ pump serves as one of the powerful metabolic mechanism through which the metabolic regulation of membrane chemosensitivity is realized (Ayraperyan and Arvanov, 1988). As shown by the obtained data, these factors have opposite effects on Ach-induced membrane currents in K-free medium, when Na^+-K^+ pump was in inactive state (Thomas 1972): the K-free -induced pump inactivation reversed the effect of EMF-treated PS on Ach-induced membrane current (Figure 6), while the H_2O_2 had more pronounced inhibitory effect in K-free medium than in normal K-containing PS.

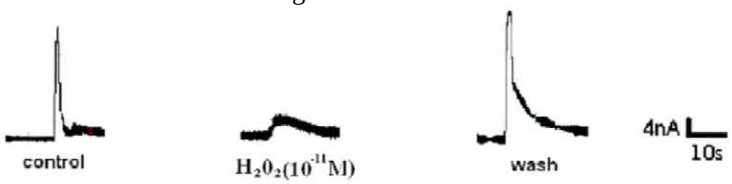


Figure 6. *The depressing effect of 10^{-11} M H_2O_2 in K-free solution on Ach-induced current in D-type neuron in voltage-clamp experiments. Neuron was clamped E_c = -55mV. The data are taken from one neuron. The presented data are typical for all 5 studied neurons.*

As shown in Figure 6, the H_2O_2 at 10^{-11} M in K-free solution has strong (reversible) depressing effect on Ach-induced current amplitude (80±2.5%, n=5) in D-type neurons. No significant differences were observed between H_2O_2 –sensitivity of Ach-responses in D and H-type neurons. These data allow as to conclude that from one side, the both MPS and H_2O_2 -induced modulations of Ach-responses could not be explained by the activation of Na^+-K^+ pump, and from another side, the nature of metabolic pathways through which they modulate the membrane chemosensitivity in K-free medium is different. Therefore, the elucidation of the nature of mechanism of H_2O_2 effect on membrane chemosensitivity would be the subject for the next series of experiments.

It is known that the agonist-induced membrane current changes could be the result of modification of ionic channel properties or the process of interaction between receptors and agonists. As the above-mentioned data on potential independence of the H_2O_2 effect on membrane chemo-sensitivity excluded the role of channel mechanism in this process, the main reliable mechanism through which the H_2O_2-induced depression of Ach-responses is realized is the process of modification of interaction between Ach and its receptors: the changes of the number of functionally active receptors or their affinity to agonist. Therefore, the effect of H_2O_2 on kinetic curve of doze-dependent Ach-induced membrane response was studied.

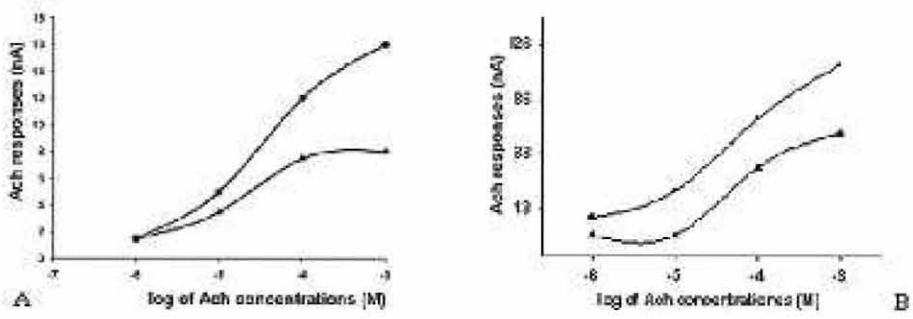


Figure 7. *The effect of 10^{-6} M H_2O_2 on dose-dependent curve of Ach-response in K-containing (A) and K-free (B) mediums in H-type neuron. Circles show the control, the triangles - in the presence of H_2O_2, (n=10).*

As shown in Figure 7A, in H_2O_2-containing solutions the Ach-induced responses reached of their maximum values at 10^{-4} M concentration, while in normal physiological solution the curve wasn't saturated even at 10^{-3} M Ach concentration. Such pronounced depressing effect of H_2O_2 on "maximums" of the doze-dependent curves of Ach could serve as evidence on the decreasing effect of H_2O_2 on the number of functionally active Ach-receptors in the membrane. It is worth to note that, although, in K-free solution the H_2O_2 also has depressing effect on number of receptors involving in generation of Ach-responses, there are significant differences between the kinetics of dose-dependent curves of Ach-responses in K-free and K-containing solutions (Figure 7B), which could be the subject for more detailed investigation.

Thus, it is important to clarify, which metabolic pathways could be responsible for H_2O_2 –induced decrease of number of functionally active receptors interacting with the agonists. It is suggested that the actinolike protein phosphorilation-induced contraction of cytoskeleton could serve as one of such mechanism through which the H_2O_2 could decrease the number of membrane receptors. As the citosceleton (cell) shrinkage is accompanied by the increase of membrane electrical resistance (Carpenter et al., 1992), for testing the above-mentioned suggestion the effect of H_2O_2 on I-V characteristics of membrane was studied (Figure 8).

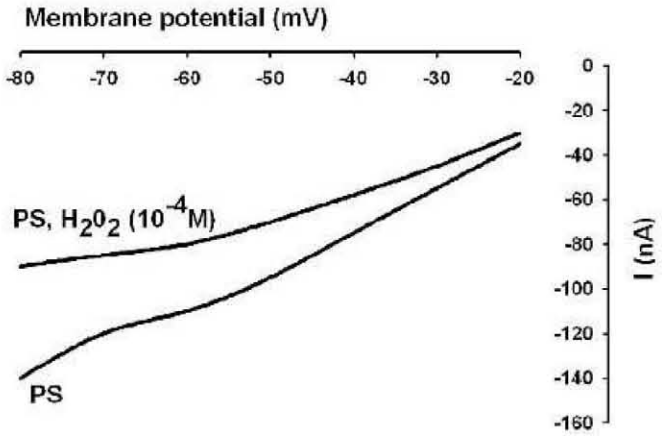


Figure 8. *The effect of H_2O_2 on current-voltage (I-V) characteristic of D-type neurons. The I-V curves in normal and 10^{-4} M H_2O_2-containing solutions were obtained by changing the holding potential from -20 to -80mV. Pre-incubation time in H_2O_2-containing solution was 7min. (n=5).*

As shown in Figure 8 there are significant increase of membrane resistance upon the effect of H_2O_2 and this effect has pronounced elevation tendency by increasing the cell membrane polarization. If the H_2O_2–induced increase of membrane resistance could be explained by the possible decrease of cell volume, the mechanism responsible for potential-dependence of such effect of H_2O_2 is not clear and needs more detailed investigation.

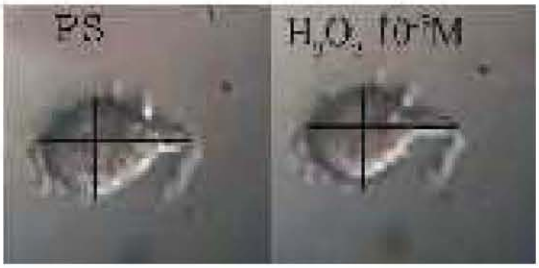


Figure 9. *The effect of 10^{-9} M H_2O_2 on neuronal volume. Scale bar 10μm. (n=5)*

For testing the above mentioned conclusion on H_2O_2 –induced cell volume (shrinkage), which leads to the decrease of membrane active surface (number of receptors in the membrane), in the next series of experiments the effect of H_2O_2 on cell volume was studied by means of light microscopy. Figure 9 shows that H_2O_2 in nM concentrations has shrinking effect on the cell.

Discussion

Although the hypothesis on the role of H_2O_2 as a possible messenger through which the biological effect of magnetized aqueous solutions is realized has long history (Klassen, 1982), its role in biological effect of SMF and ELF EMF is not elaborated yet. This difficulty is due to the absence of reliable theory explaining the cellular and molecular mechanisms of biological effects of ELF EMF from one side, and multisided metabolic effect of the H_2O_2 from the other side. Previous works of our laboratory have shown a crucial role of intracellular messenger-dependent Na^+/Ca^{2+} exchanger in realization of biological effect of magnetized solution (Ayrapetyan et al., 1994b, 2005). As the Na^+/Ca^{2+} exchanger serves as one of powerful mechanisms regulating the intracellular Ca^{2+} homeostasis (Dipolo and Beauge, 2006), which determines the membrane chemo-sensitivity (Bregestovski et al., 1979], the latter could serve as a convenient experimental model for studying the role of H_2O_2 as a potential messenger in realization of biological effect of magnetized solution on cell membrane.

The presented data on similar inhibitory effect of MPS (Figure 1) and H_2O_2 (Figure 2) on Ach-induced current and their temperature dependence, from the first face could be considered as an evidence of their synergic influences on membrane chemosensitivity. In previous our works the following metabolic cascade through which ELF EMF-treated PS can modulate the membrane chemosensitivity was suggested: the MPS-induced activation of cGMP-dependant Na^+/Ca^{2+} exchanger leads to the removal of the intracellular Ca-induced inhibition of Na^+-K^+- ATPase as a result of reactivation of Na^+-K^+ pump, which causes the decrease of a number of receptors in the membrane due to the pump-induced cell shrinkage. While the pump is in inactive state (when the pump-induced cell volume changes are excluded), the ELF EMF-induced elevating effect can be explained by the decrease of intracellular Ca concentration (Ayrapetyan et al., 2004). The fact that in K-free solution the H_2O_2 has more pronounced inhibitory effect on Ach-induced current compared to its effect in normal PS could not be explained from the point of the mentioned metabolic cascades and serves as evidence on different nature of metabolic pathways through which the inhibitory effects of MPS and H_2O_2 are realized.

It is known that the agonist-induced membrane responses could be changed as a result of modification of ionic channel properties and (or) interaction processes between membrane receptors and agonists. The obtained data on potential independence of H_2O_2–induced inhibition of Ach-responses (Figure 4) allow us to exclude the role of ionic channels in this inhibition and it could be explained by the depression of the process of interaction between receptors and agonists. The H_2O_2 –induced depression of the "maximum" in Ach doze-dependent curve serves as evidence on the changes of number of functionally active receptors in the membrane interacting with the agonist molecules (Figure 7). Early our works showed that the Na^+-K^+ pump-induced activation caused the similar inhibition of membrane Ach-sensitivity in result of cell shrinkage (Ayrapetyan and Arvanov, 1979), however the data obtained in present experiments on elevation of H_2O_2–induced depression on Ach- responses in K-free solution (when Na^+-K^+ pump is inactive) (Figures 3B, 7B), excludes the role of Na^+-K^+ pump in this process. The disappearance of such inhibitory effect of H_2O_2 on membrane chemo-sensitivity in cold (5^0C) medium (Figure 5) indicates its metabolic nature. Therefore, it is suggested that the H_2O_2 leads to the decrease of the number of functionally active receptors in the membrane by unknown metabolic mechanisms (not by Na^+-K^+ pump). Previous our works showed the close correlation between membrane active surface (cell volume) and number of functioning chemo-receptors in the membrane (Ayrapetyan and Arvanov, 1979). It is predicted that the H_2O_2–induced depression of membrane Ach-sensitivity could be the result of cell shrinkage. The microscopic study of the H_2O_2 effect on cell volume (Figure 9) proved this suggestion.

Summary

The data obtained in the present work clearly showed that the H_2O_2 in nM concentrations depressed the membrane chemosensitivity by decreasing the number of functioning receptors in the membrane as a result of cell shrinkage (probably by cytoskeleton phosphorylation). We came to the same conclusions in previous our work on studying the effect of magnetized solutions on Ach-induced responses of the membrane (Ayrapetyan et al., 2004). It was shown that the MPS caused the depression of membrane Ach-responses at room temperature (23 ^{0}C), while in cold medium (5 ^{0}C) it had no effect (Ayrapetyan et al., 2004, Figure 1). These effects were explained by MPS-induced cell dehydration which led to the decrease the number of chemo-receptors in the membrane (Danielyan et al., 1999).

Thus, the comparison of the physiological data obtained in the present work on the influences of H_2O_2 with the previous results on the effects of magnetized solution on membrane sensitivity to Ach demonstrates the close synergism between the effects of these two factors on Ach responses in normal PS which are the result of cell dehydration. However, opposite dependence of their effects on Na^+-K^+ pump activity allow us to suggest that H_2O_{2-} -dependent metabolic pathway could serve as one of the metabolic pathways through which the biological effect of ELF EMF is realized.

References

Ayrapetyan SN, Arvanov VL. 1979. On The Mechanism of The Electrogenic Sodium Pump Dependence of Membrane Chemosensitivity. *Comp. Biochem. Physiol.*, **64A**: 601-604.

Ayrapetyan SN, Arvanov VL. 1988. The Metabolic Regulation of Membrane Chemosensitivity. In Salanki (ed): Neurobiology of Invertebrates, Budapest, 36:669-684.

Ayrapetyan SN, Grigorian CV, Avanesian AS. 1994a. On a mechanism of action of magnetic field on the electrical conductivity of water solutions and some properties of Helix neurons. *Bioelectromagnetics*, **15**: 133-142.

Ayrapetyan SN, Avanesian AS, Avetisian TH, Majinian SB. 1994b. Effects of incubation of snail ganglia in physiological solutions exposed to magnetics fields on levels of intracellular cyclic nucleotides. In: *Biological effects of electric and magnetic fields* (Ayrapetyan & Carpenter, eds), Academic press, INC, pp: 185-186.

Ayrapetyan SN, Hunanyan ASh, Hakobyan SN. 2004. 4Hz EMF–treated physiological solution depresses Ach-induced neuromembrane current. *Bioelectromagnetics*. **25**(5): 397-399.

Ayrapetyan GS, Papanyan AV, Hayrapetyan HV, Ayrapetyan SN. 2005. Metabolic pathway of magnetized fluid-induced relaxation effects on heart muscle. *Bioelectromagnetics*. **26**(8): 624-30.

Ayrapetyan SN. 2006. Cell aqua medium as a preliminary target for the effect of electromagnetic fields. In: *Bioelectromagnetics: Current Concepts*, S. Ayrapetyan and M. Markov, eds., NATO Science Series, Springer Press, The Netherlands, pp: 31-64

Bregestovski PD, Bukharaeva EA, Iljin I. 1979. Volotage clamp analysis of acetylcholine receptor desensitization in isolated mollusk neurons. Nature, **279**: 581- 595.

Carpenter DO, Fejtl M, Ayrapetyan SN, Szarowski DH, Turner JN. 1992. Dynamic changes in neuronal volume resulting from osmotic and sodium transport manipulations. Acta Biologica Hungarica, 43: 39-48.

Danielian AA, Ayrapetyan SN. 1999. Changes of Hydration of Rats' Tissues after in Vivo Exposure to 0.2 Tesla Steady Magnetic Field. *Bioelectromagnetics*, **20**(2): 123-128.

Dipolo R, Beauge L. 2006. Sodium/Calcium exchanger: Influence of metabolic regulation on ion carrier interactions. *Physion. Rev*. **86**: 155-203

Klassen 1982; in: *Magnetized Water Systems*. "Chemistry" Press, 296 p (in Russian), English translation: *European Biology and Bioelectromagnetics*, 2006, **1**(2): 201-220

Sakharov DA, Salanki J. 1969. Physiological and pharmacological identification of the neurons in the central nervous system of helix pomatia. *Acta Sci. Hungar*., **35**: 19-30.

Stepanyan R., Ayrapetyan G., Arakelyan A., Ayrapetyan S. 1999. Effect of Mechanical Oscillations on Electrical Conductivity of Water Biophysics, **44**: 197-202.

Thomas RC. 1972. Intracellular sodium activity and the sodium pump in snail neurons. J. Physiol. 220:55-71.

Simulations of ELF Magnetic Shields

Josef Pekar Moshe Netzer Yekutiel Pekar
EMC Engineering & Safety
Haifa, Israel

Abstract
This paper describes a multi-stage algorithm for efficient calculation of magnetic flux contours, for optimizing the design of structural magnetic shielding. The multi-stage algorithm enables albeit medium-power computer system to calculate the effect of shielding materials with a given geometry, in a reasonable timeframe without compromising precision. The outcome results are a large number of electrical utility models and the best cost-effective shielding materials and geometries for ELF magnetic flux reduction per Authority regulations and requirements.
This paper attempts to review methods and principles for calculation of an extremely low frequency (50/60 Hz) electromagnetic field originating from power utilities and power lines, for the purpose of constructing efficient magnetic shielding. The paper points out difficulties in existing methods and proposes a new algorithm for analysis and construction of magnetic shielding.

Introduction

Magnetic field of extremely low frequency (ELF) is produced by utility and industrial electric lines, machines and cables, and various electrical fixtures, devices, and apparatuses all of which are surrounding us and deployed everywhere. Often, the level of the magnetic fields exceed the permissible exposure limits setup by international[1] and national agencies for non-ionizing radiation protection, thus need to be reduce at locations where people dwell. It can be achieved by several cost effective methods, such as: relocation of strong magnetic field emitters; reduction of electrical current; reconstruction of the electrical circuits to reduce the loop areas generating magnetic fields. If any of the above outlined relative simple solutions do not provide the desired results, it might be necessary to install structural magnetic shielding made of various metal types some of which might be very expensive such as μ-metal, co-netic and other metals with great permeability.

Before the actual building of structural magnetic shielding starts, one needs to determinate the magnitude of the magnetic field exposure problem. It can be performed by actual field measurements, or if the electrical utilities are still unavailable or none operational it entails modeling the utilities and solving electro-magnetic equations[3], all of which enables the prediction of magnetic flux contours with and without magnetic shielding buriers.

To determine the best engineering solutions for structural shielding, one needs to employ very complex analysis. The analog approach is impractical because of the uniqueness of each problem and the associated difficult level. Also, the digital approach is still too difficult for the most of today's personal computer systems. Subsequently, the calculation is less accurate and time-consuming. It can take from tens to hundreds of man-hours to prepare models and to solve a single problem.

Strategies and Stages in Planning Magnetic Field Reduction

To first stage in planning the shielding effectiveness required for magnetic field reduction is to obtain the overall worst-case intensity of the ELF magnetic flux in locations where people may reside. This can be doe using two methods – the analytical method (also good for the design stage), and/or field measurements when construction is completed and populated). These two strategies to determine the magnetic field is summarized as follows:

1. **Analytical Prediction:** given the geometry of the structure and the current sources producing the ELF magnetic fields, including the geometry of these magnetic sources, the integrated cumulated field levels in every relevant place (places where there may be people residing) can be predicted.
2. **Measurements:** conducting field level measurements where people work and reside could provide a general picture of the magnetic field including evaluation of maximal loads in maximal power consumption, hence, worst-case magnetic flux contours.
   The decision for the need for magnetic shielding is best taken based on results obtained by strategy 2 – measurements. However, the structural shielding design must use strategy 1 – analytical prediction. It facilitates cost-effective shielding design, placement, barrier dimensions, shielding materials, and installation methods. It enables theoretical examination of the shielding effectiveness elsewhere in the facility. If shielding is insufficient based on phase I of the analytical design effort, it is modified by reselecting of:
   - shielding materials;
   - barrier dimensions;
   - placement

   Phase II of the shielding design commences to obtain the shielding effectiveness of the modified design. Phase II might yield an insufficient engineering solution and go into Phase III, etc., until a best engineering solution is obtained.

Availability of Analytical Methods

The analysis methods available for determining the electromagnetic field levels are many and vary in complexity, accuracy and easiness of pre and post processing. Some of the most known numerical methods are:

- Finite Difference Methods
- Variation Methods
- The Methods of Moments (MoM)
- Finite Element Method[4,5]
- Transmission-line-matrix Method
- Monte Carlo Methods
- Method of Lines

The **Finite Difference Method** requires the performance of the following steps:

1. Divide the region of interest into a grid of nodes (common rectangular, skew, triangular or circular type of grids)
2. Approximate the given differential equation by finite difference. (To relate the dependent variable at a point in the region of interest to its values at the neighboring points)
3. Solve the difference equations subject to the boundary and initial condition.

This method is very intuitive and fairly easy for numeric realization. It is not clear which grid is preferable in every case. A problem arises in cases where the point for which the value is calculated is not exactly on the grid. The ease or programming "balances" in extensive calculation time.
For simple enough problems, when one arrives at a collection of equations (both integral and differential), the problem can be solved by finding functions that give the integrals a minimum value[6]. Problems of this type are called *variational problems.*
This method is limited to theoretical problems, requires a high level of mathematics and seldom used to solve practical problems.

The **MoM** requires the performance of the following steps:

1. Derivation of the appropriate integral equation.
2. Conversion this set of equation into a matrix equation (the process called discretization that is based on using basic functions (kernels) and weighting (or testing) functions.
3. Evaluation of the matrix elements.
4. Solving the matrix equation and obtaining the parameters of interest.

This is a sturdy method that turns problems containing integral equations into matrix equations (of course, accurate calculation requires an extensive calculation power and a large amount of memory). Many of today's solutions are based on this method.

The **Finite Element Method** comes from the area of materials strengthening and has been used for calculating electromagnetic fields since the 1970s.

The **Finite Element Method** requires the performance of the following steps:

1. Discretizing the solution region into a finite number of subregions (called elements). These elements may be one, two or three-dimensional.
2. Deriving governing equations for a typical element.
3. Assembling all elements in the solution region.
4. Solving the system of equations obtained.

Among the method's advantages, it can be used with almost no changes for different areas of problems. The most accepted areas are mechanics and electricity, but lately it has also been used for image processing. It is difficult to match an appropriate element for every problem, and the method required extensive calculation time.

Other methods are more theoretical or methods suitable for solving specific problem types not related to our goals.

It is customary to imagine shielding as an infinite surface or a closed sphere. Only in these cases may accurate analytic methods be obtained. All analysis of other models is semi- empirical. The accuracy of the results decreases as we increase the practical details of the shielding.
The analytical solution for calculating shielding cannot take the form of a method as we must solve a different problem each time (this includes building a new model with range, limit conditions, sources, new geometry etc.).

Solving the problem using a computer somewhat reduces the complexity of the mathematical solution, but adds the problem of a model that is very resource consuming for most existing computers. The problem lies in both memory size and calculation power.

As a result, any calculation (construction of a mathematical or digital model, inputting the problem's data, calculation and examination of probability of the received results) requires hundreds of man hours and dozens of computer hours. It is clear that under these limitations it is impossible to perform a large number of attempts (analysis phases as described above) in order to reach an appropriate solution. The desire to examine a single problem for several shielding solutions, in order to select the best one, often seems as "mission impossible".

Practical Methods Combined with Analysis

The problem we face is: to calculate the electromagnetic field in defined areas generated by known sources with the presence of a given specific shielding burrier design to reduce the EM fields.
There are no analytical systems and algorithms that we know for writing a program that enables inputting of entry data (such as range, sources, shielding location, shielding materials etc.), followed by the required targeted field level in a certain area, let one or more parameters acting as the unknown ones and perform calculations (assuming convergence) that solve the unknown parameters.
Presently, all we can do is as follows: place shielding (using previous practical experience) in places that seems most logical using materials that were suitable in similar cases, calculating the field levels in questioned areas, comparing the results to the values we aim for, and if the results are unsatisfactory, slightly change the shielding size, geometry, location and/or materials.
The form of shielding accepted today is a rectangular plate, inserted between the source and the area in which field level should be reduced. Magnetic shielding includes 3 different effects: reflection, absorption, and fringe radiation (that usually reduces the shielding effectiveness). The theoretical basis for high frequency (radiofrequency) shielding for distant EM field is relatively well developed and has accelerated in recent years. In the case of ELF fields and for an adjacent source – these theories cannot be straightforward adopted. In the case of high impedance, the source if electric field is dominant; in the case of low impedance – the source is a magnetic field is dominant. In this case a separate approach for shielding against the magnetic part and from the electric part of the EM field is the correct approach.
An alternating electromagnetic field, originating from 50 Hz electrical facilities is an "adjacent source" field. The characteristic impedance of the magnetic component is very low while the characteristic impedance of the electric component is high. Therefore, currents in low voltage electric facilities generate dominant magnetic field components; the associated electric field component is negligible. A source of a solely magnetic field does not cause electromagnetic waves. Therefore a 50Hz magnetic field is quasi- static in nature. This field is "static" because it acts as a static field, but is called "quasi" as it is not completely static due its source (alternating field).

Two phenomena exist in magnetic shielding for a quasi- static field – static shielding and dynamic shielding.
Static shielding is independent of the field frequency and works in the same way for both the earth's static magnetic field and for sources of 50 Hz or more. The shielding quality depends on the material's relative permeability (μ) and its geometrical dimensions. The higher the permeability (μ) and the thicker the plate, the more effective is the shielding.
Dynamic shielding depends on the frequency of the primary field and the shielding material's electric conductivity. At 50 Hz the effect is well pronounced. The phenomenon is based on Foucault currents (eddy currents) and Lentz laws. The higher the conductivity and the higher the frequency – the more effective is the shielding.
There are no materials that combine both phenomena well, and so it is customary to use two plates or more for constructing shielding to reduce quasi- static magnetic field. In many cases shielding construction is attempted using no analysis, based only on instinct, experience or luck. In many cases this might not only not decrease field levels, but even raise its intensity in undesirable locations.
The principle of magnetic shielding is based on two phenomena of decrease of the electromagnetic field intensity in different materials: absorption of a magnetic field (absorption loss) and reflection of the field back to the source (reflection loss).

The above discussion is highlighted with a real problem description and shielding planning demonstration.

The field level in an area adjacent to a transformation substation inside a residential building is analyzed.

The area of interest is only the residential area as shown in Figure 1. Analysis show that the level is higher than desirable and shielding must be constructed.
A simplistic calculation with substitution of a plate of finite dimensions with an infinite surface does not give correct results. In this case substitution of the plate creates distortions in the plate ends, and as a result the field level would not only decrease, but may increase. It is clear that in this case the attempt to build magnetic shielding without proper planning might causes more damage than benefit.
Three dimensional shielding against the magnetic field from the transformation substation could be done by covering parts of the walls, ceiling and floor adjacent to the location of the transformers. Walls, ceiling and floor covering is obtained by using special materials that decrease the magnetic flux density caused by the transformer's secondary terminal (low voltage) phase lines and neutral line loops.

Field sources are often having a complex geometry which makes it analysis difficult to solve. It is much more difficult to solve the problem of the shielding effect on the magnetic source flux lines as it is in our example. It is important to note that for our specific problem, the source is 3 currents in the same frequency and different phases, and at every point the field vector is a complex vector value (as are all the matrix analysis).
"Absorption" of a static magnetic field can be done using magnetic materials with a high magnetic permeability. Plates of this material are used for construction of static shielding. The efficiency of the static shielding depends on several factors, as follows:

- Relative magnetic permeability (μ_r) of the plate material.
- Plate width.
- Angle between the direction of the magnetic flux vector and the plane of the plate.

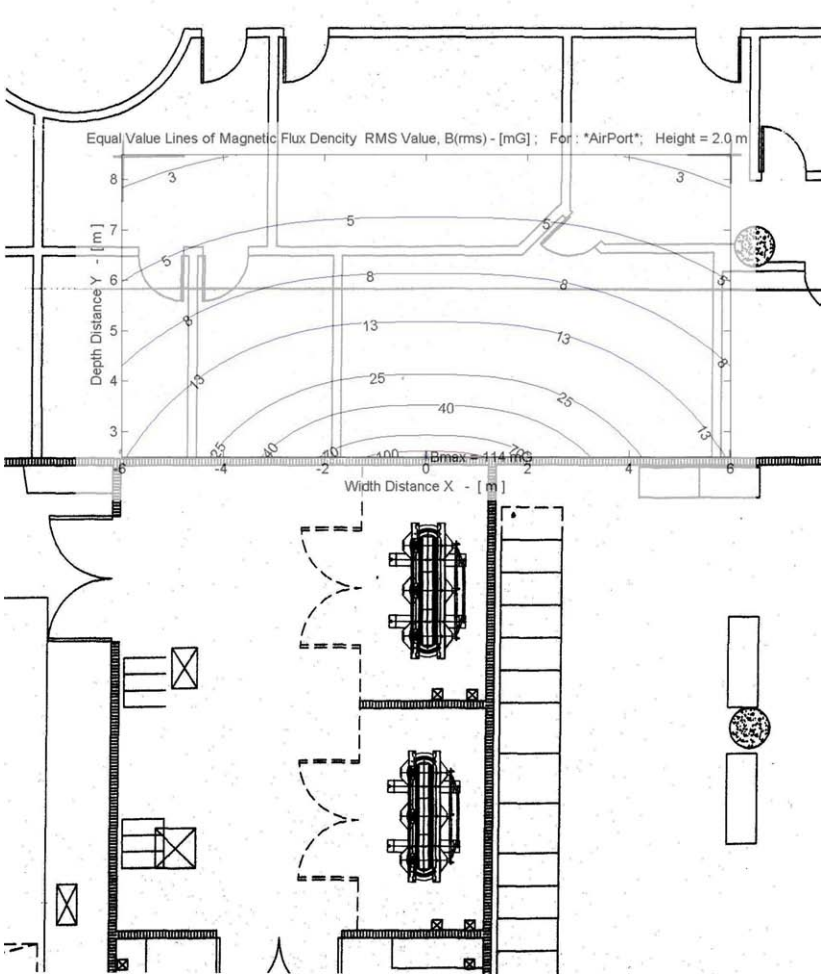


Figure 1: Primary Magnetic Flux Analysis near an Internal Transformation Station

There is no "reflection" phenomenon of a static magnetic field. The reflection phenomenon exists only in an alternating electromagnetic field. The flux of an alternating magnetic field that permeates plates made of a material with electric conductivity creates induced currents known as eddy currents. These currents create a secondary magnetic flux at a direction opposed to the direction of the original magnetic field flux and thus reduce the magnetic field flux. This is known as Lenz's law.

Plates made of metals with high electric conductivity are used for building dynamic shielding. The efficiency of the dynamic shielding depends on several factors, as follows:

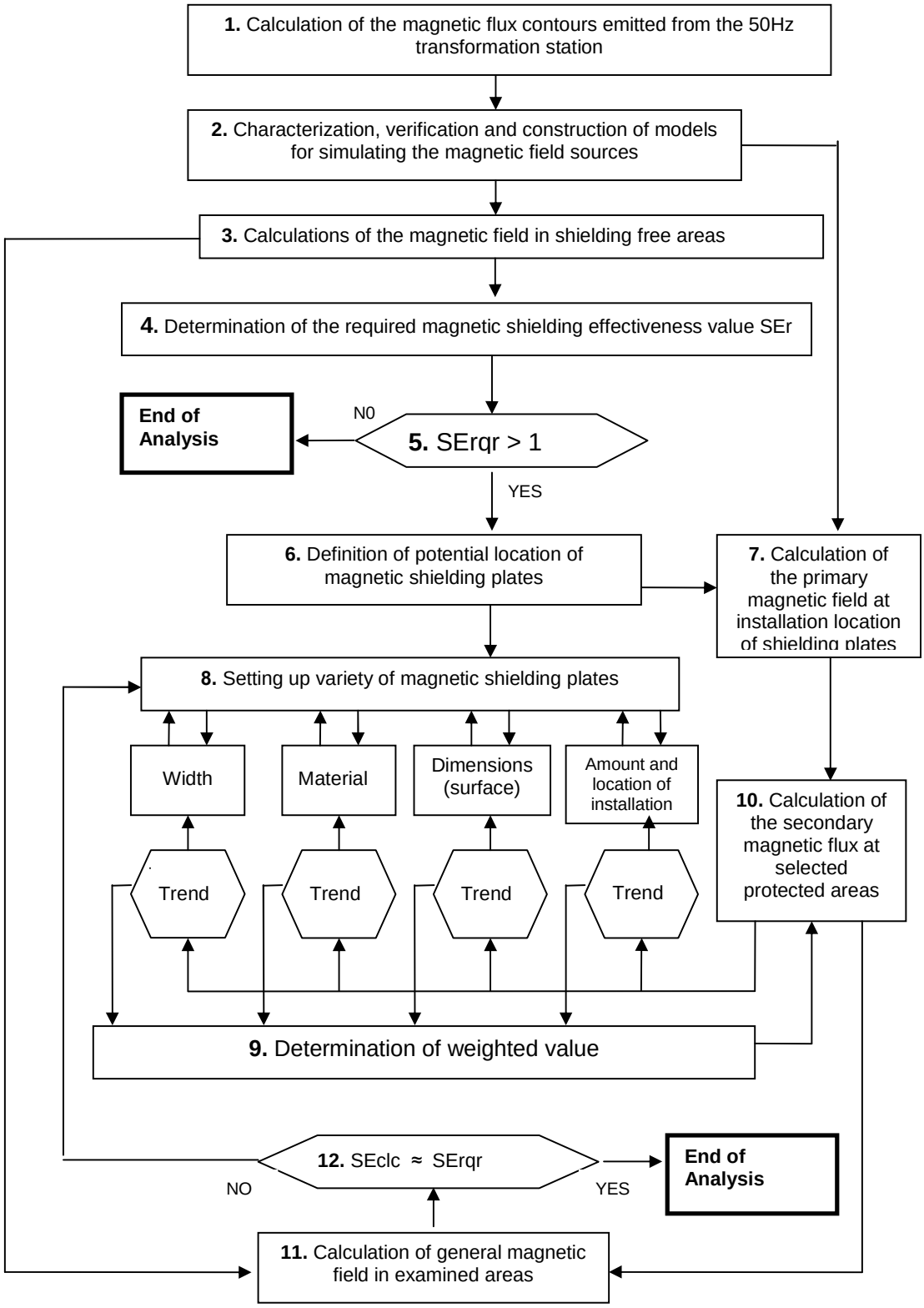
- The plate material's electric conductivity σ.
- Frequency of the alternating magnetic field.
- Plate width (up to a certain width).
- Angle between the direction of the magnetic flux vector and the plate's perpendicular.

The efficiency of static and dynamic shielding, as a rule, is a different and non linear dependence on the parameters outlined above. The main difference, in terms of shielding efficiency, is in the inverse effect on efficiency of the incident angle of the magnetic flux lines on the shielding plate:

- When the direction of the magnetic flux vector is closer to that of the shielding plate's normal direction, the efficiency of dynamic shielding increases while that of static shielding decreases.
- When the direction of the magnetic flux vector is closer to that of the tangent to the shielding plate, the efficiency of dynamic shielding decreases while that of static shielding increases.

As the magnetic flux adjacent to electric facilities is not uniform in size and direction, the highest efficiency in reducing the magnetic flux density in the entire shielded space is accomplished by a combination of static and dynamic shielding.

New Algorithm for Shielding Analysis



The first step is the calculation of the magnetic flux density in the entire space, especially the area we wish to protect and the apace in which we wish to introduce the shielding barrier. Analysis of the **primary field** is done using the laws of Faraday and Ampere. This analysis affords a comprehensive picture of the entire area, and a decision on whether shielding is in fact necessary or can be substituted by simpler less-costly measures, such as relocation of power utilities or personnel.
There are many analysis methods, most popular of which is the finite elements method discussed above. Using this method, the shielding burrier is divided into subcomponents so that lack of uniformity can be neglected and the field is perceived as uniform. This is the second step of the analysis.
In the third step, each point in the shielded area is analyzed as a sum of the effects of each shielding element. This is the **secondary field** reduced from the primary field by the shielding.
Now, as a picture of the effect of the shielding is formed, one can decided on the continuation (or termination) of the process.
Using this method there is no need for difficult neither complex analysis for the entire problem, only for the shielding effect on the secondary field intensity in the examined area. This analysis method greatly reduces analysis complexity, gives accurate results and reduces calculation time by an order of magnitude. The finite elements method enables to perform sufficient iterations in order to obtain the best results among several different shielding barriers from different materials and dimensions and compare the outcome results to select the best solution. The time required for the entire process is equal to the time it would have taken to calculate a single iteration using one of the old methods.

The course of the analysis is presented in the algorithm flow chart.

1. Analysis of 50 Hz magnetic field contours caused by the transformation substation – step 1 of this project is defining the problem and possible solution subset.
2. Construction, verification and determination of models for simulating the magnetic field source. These models can be used to calculate magnetic flux densities in all areas adjacent to the field source.
3. Analysis of the magnetic field in the areas that are examined without any shielding. Analysis is carried out using a computer program based on integrals of complex magnetic moment methods.
4. Determination of the required magnetic shielding effectiveness value SErqr. This action is taken and is presented in table 3 of step 1 of the project (reference 2). The SErqr value is determined by comparing the results of the analysis to the exposure threshold recommended by the Ministry of the Environment or other requirements of the client, using the following formula:

   $$SErqr = Bmax / Brcm$$

   Where:
   - Bmax – the maximal value of the magnetic flux density analyzed in the examined area based on a model of magnetic field source simulation at its typical current, as coordinated with the client.
   - Brcm – the value of magnetic flux density coordinated with and determined by the client based on recommendations set by the Ministry of the Environment for general public magnetic field exposure at 50/60 Hz.
5. Existence of a condition SErqr > 1 (YES) causes the continuation of the project for design and magnetic shielding burrier required, while the (NO) response ends the analysis and the project.
6. Selection of potential locations for installation of magnetic shielding plates. As a rule, it is accepted to cover walls and/or ceilings and/or floors within the area in which the magnetic field source is located. In transformation substation with two transformers, these areas are: the TR01 and TR02 transformer cells and/or the entire transformer room.

The possibility to install shielding around a whole transformer cell is not feasible, as complete and continuous shielding in the cell might hinder the maintenance and natural ventilation of the transformers. Opening ventilation hatches and/or installation of forced ventilation might reduce shielding effectiveness to below requirements.
The feasible shielding practice is to cover all or part of the walls, ceiling and floor of the transformer room.

7. Analysis of the magnetic field in some locations of the shielding plates. As an auxiliary action for calculating shielding effectiveness, the complex vector of the magnetic flux density in the walls, ceiling and floor of the transformer room is analyzed, meaning – primary magnetic field with no shielding, similar to the primary magnetic field in the examined areas (step 3 above).
8. Setting up variety of magnetic shielding plates. This step determines shielding parameters as follows:
   A. Amount and location of shielding plate installation, static and dynamic separately.
   B. Plate size (surface area) for static and dynamic shielding separately.
   C. Static shielding plate's material – magnetic permeability value; dynamic shielding plate's material – electric conductivity value.
   D. Plate width for static and dynamic shielding separately.
9. Determination of weighted value. In this step we prepare the parameter matrix for static and dynamic shielding for the analysis following in step 10.
10. Analysis of the secondary magnetic field created by the shielding plates in the examined area. The analysis is carried out by a computer program based on a Numerical finite element method.

The starting data for analysis are the results of the primary magnetic field analysis described in step 7 above and the data of the shielding plates described in step 8.
At the beginning of the analysis the shielding plate areas are divided into elements in order to reach a state wherein in most separate elements there is a uniform magnetic field incident the single element. The data of the complex vector of the magnetic flux density, $\vec{\mathbf{B}}$ that permeates through the shielding area element, we receive from the primary magnetic field analysis (7).
The elements of the high magnetic permeability shielding material are forced to become magnetic moments under the effect of the primary magnetic field. The magnetic flux density Bmag in the area of these elements increases according to the formula:

$$Bmag = \mu_r \times B_0$$

Where:

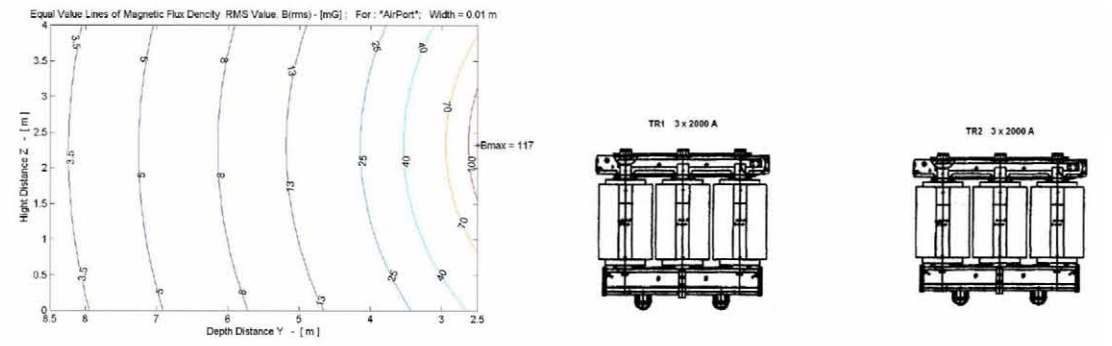
B_0 – primary magnetic flux density

μ_r – relative magnetic permeability through the static shielding material.

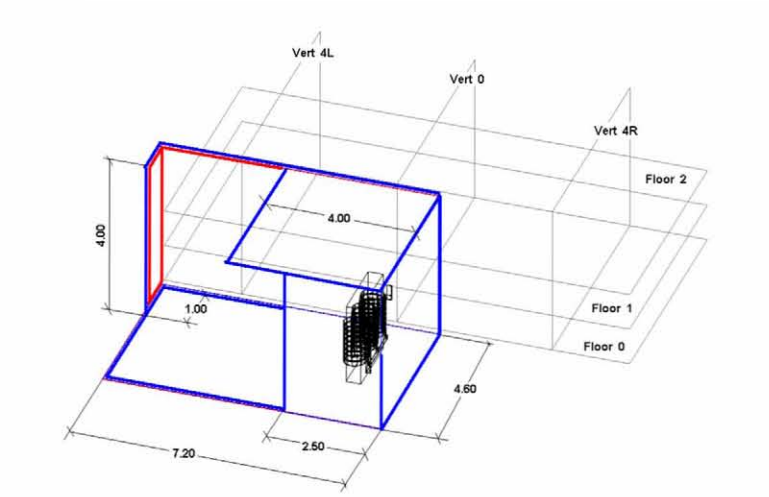
The main direction of the moment vectors from the static shielding plates is tangential to the plane of the plates. Magnetic moments of the static shielding material elements emanate a secondary magnetic field, and thus affect the overall magnetic flux density in the examined areas. Alternating magnetic flux creates eddy currents of elements in the dynamic shielding material with the high electric conductivity. These currents create a secondary magnetic field. The direction of the secondary magnetic field flux is opposed to the direction of the primary magnetic flux, known in physics as Lenz's law. Eddy currents in the dynamic shielding elements are considered to be magnetic moments. The main direction of the moment vectors from the dynamic shielding plates are normal to the plane of the plates. These moments emanate a secondary magnetic field. And thus affect overall magnetic flux density in the examined areas.

11. Analysis of overall magnetic field in the examined areas. The analysis is carried out using a computer program based on a complex vector superposition method.
12. The realization of the SEclc ≈ SErqr (YES) condition ends the analysis, while (NO) causes the continuation of the analysis in a loop including stages 8 – 11. SEclc – the analyzed value of the shielding effectiveness.

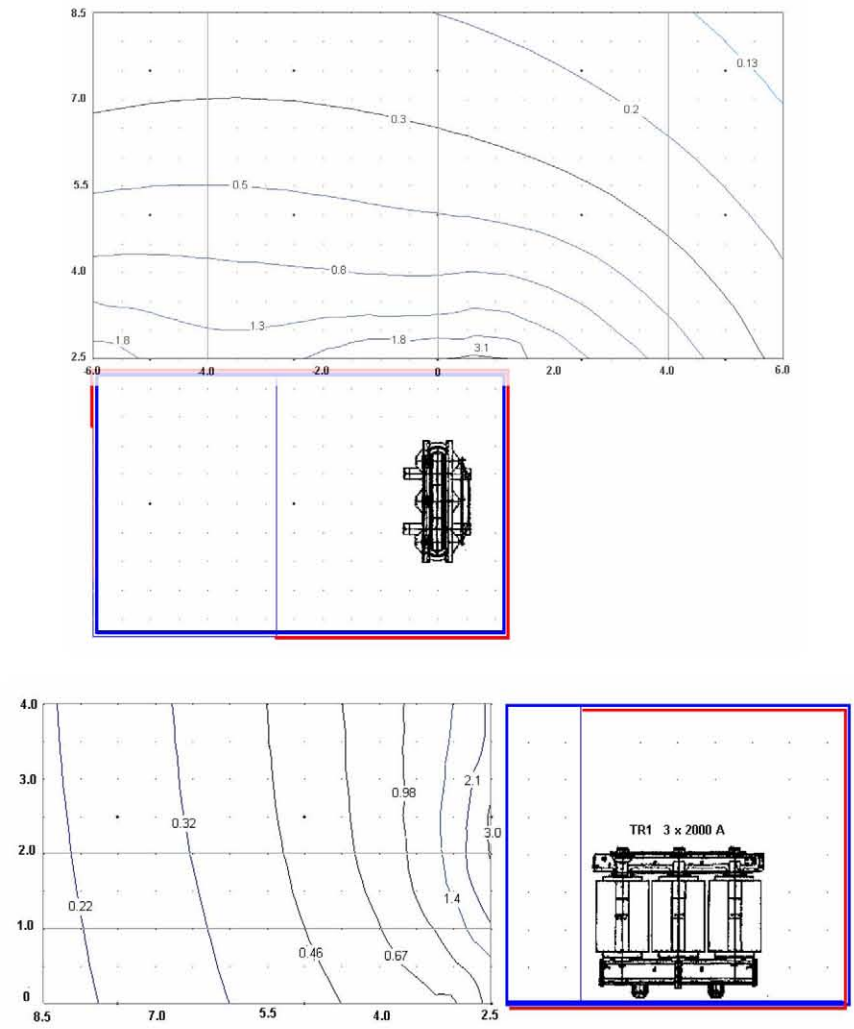
Back to the practical example – an analysis is performed based on this algorithm. The following results were obtained:
Primary flux density analysis (without the shielding plates):



Based on the results tt was decided to shield only the transformer adjacent to the residential area.



Analysis show that the field level decreased to the following levels:



Conclusions

The question of potential adverse effects due to ELF magnetic fields exposure has been discussed and hypnotized in the past years. The potential magnetic field adverse effects on the human body are still under ongoing studies; nevertheless, the adoption of the precautionary principal by many countries and environmental conservation offices owes to minimize personnel exposure[2]. Many countries have already established regulations and limitations for the maximal magnetic field allowed at the workplace and residential areas which is much lower than the WHO ICNIRP[1] guidelines. The best situation exists when a building design (both architecture and infrastructure) considers magnetic flux reduction design. In reality, this does not happen often. At best, magnetic field surveys and shielding design (if needed), is the very last stage before construction is completed. In many cases, construction is completed; inhabited and only thereafter magnetic flux reduction is taken care by the building management. This paper describes a multi-stage algorithm for efficient analysis of magnetic flux contours, for optimizing the design of structural magnetic shielding. The multi-stage algorithm enables albeit medium-power computer system to calculate the effect of shielding materials with a given geometry, in a reasonable timeframe without compromising precision. The outcome results are a large number of electrical utility models and the best cost-effective shielding materials and geometries for ELF magnetic flux reduction per Authority regulations and requirements.

References

[1] "Guidelines on Limits of Exposure to Electromagnetic Fields in the Frequency Range from 1Hz to 300GHz", ICNIRP, 1998
[2] Josef Pekar and M. Netzer, "Graphical Presentation of 50/60 Hz Magnetic Field Contours as an Engineering Tool for Minimizing ELF Fields", Kos Workshop, 2004
[3] Edward M. Purcell, "Electricity and Magnetism", Berkeley Physics Course –Volume 2, McGraw-Hill Book Company, 1970
[4] K.H. Huebner and E.A. Thornton, "*The Finite Element Method for Engineers*", New York: John Wiley and Sons, 1982
[5] P.P. Silvester and R.L. Ferrari, "Finite Elements for Electrical Engineers", Cambridge University Press, 3rd ed., 1996
[6] N. Morita et al., "Integral Equation Methods for Electromagnetics", Boston, MA, Artech House, 1990

A NEW TECHNIQUE FOR REDUCING EXTREMELY LOW FREQUENCY MAGNETIC FIELD EMISSIONS AFFECTING LARGE BUILDING STRUCTURES

[(1)]E. SALINAS, [(2)]J. ATALAYA, [(2)]Y. HAMNERIUS, [(3)]J. SOLANO, [(3)]D. GONZALES, [(3)]C. CONTRERAS, [(3)]C. CHINCHAY, [(3)]M. A. SUMARI, [(1)]S. DIMITRIOU and [(4)]M. REZINKINA

[(1)] CENTRE OF PHYSICAL ELECTRONICS AND MATERIALS, (PEM) FACULTY OF ENGINEERING, SCIENCE AND THE BUILT ENVIRONMENT, LONDON SOUTH BANK UNIVERSITY, 103 BOROUGH ROAD, LONDON SE1 0AA, UK

[(2)] CHALMERS UNIVERSITY OF TECHNOLOGY, GOTHENBURG, SWEDEN

[(3)] UNIVERSIDAD NACIONAL DE INGENIERÍA, LIMA, PERU

[(4)] NATIONAL POLYTECHNIC UNIVERSITY, KIEV, UKRAINE

Abstract

When large structures such as residential compounds or public buildings are under the influence of extremely low frequency (ELF) magnetic fields, such as the one generated by a system of railways fed by 16 ⅔ Hz, standard methods of designing shielding structures by numerical methods usually fail. The latter can be explained by the difficulty posed in the computing process by the large aspect ratios involved due to thin layers of metal (a few millimetres or centimetres) in contrast to the large dimensions of the affected structure (several tens of meters). In some cases one has to utilize special approximations such as surface conductivity, which are not easy to handle when the designed shielding structure is clearly 3-dimensional. Other alternatives such as experimentation *in-situ* are very costly. Here, a new technique is presented of mitigating the field by using 3-dimensional propagation of induced currents optimizing the field reduction factors and minimizing the cost of shielding material. The particular designing method is a hybrid of numerical simulations combined with lab experimentation using scaled models of the large structure. The method is rather cost-effective and flexible as various designs can be easily tested. Results are presented in the form of magnetic field values, at various locations in the buildings, *before* and *after* this mitigation technique is applied.

Introduction

There are two major sources of extremely low frequency magnetic fields (ELF/MF) which are able to affect large scale areas in their extended vicinity (i.e. tens or in some cases even hundreds of metres). One of them is overhead power lines and the other is AC powered railway systems. Mitigation techniques for the first source have been extensively studied for more than two decades and there are a manifold of references in the literature. On the other hand, although some studies related to magnetic fields originated in rail systems have been published [1-6], there is a lack of literature on mitigation techniques of magnetic fields originated from AC railway sources. In this investigation, the magnetic field produced by a system of trains operating at 16 ⅔ Hz (~16.67 Hz) is analyzed and mitigated using a combined technique, i.e. designing a structure able to redirect induced currents improving their effectiveness and performing cost-effective experimental settings at reduced scale. The present study was made before starting the construction of the

buildings. Fig. 1 shows the location of the railway system in the central area of the city of Stockholm. The configuration of the buildings is also shown, which is "L"-shaped formed by two type of buildings, namely: "A+B" and "C" or correspondingly *Frontal and Lateral* the first notation is from the architectural map while the second notation is related to the ways the trains pass with respect to the buildings. Two reasons motivated this study. Firstly, there is a growing concern on suspected harmful effects of ELF/MF on human health. Although several epidemiological studies suggest that long-term exposure to fields in excess of 0.2-1 μT (depending on the study) can explain some bias in the statistics of some deceases. The issue is still not resolved at the moment and there is no clear indication that there will be a conclusive answer in a near future. Some countries are adopting some policies upon limits in residential and public buildings, as low as 1 μT, while others subscribe to ICNIRP recommendations of 100 μT for 50 Hz, limit based on effects of induced currents in the human body [7], [8]. Secondly, this type of field is able to produce interference on electronic equipment driven by electron beams such as TV and computer screens, oscilloscopes and electron microscopes. This interference becomes evident at field values over 0.5-1 μT, depending on the device. For the present study, we have chosen to aim at averaged (per floor) after-mitigation field values not exceeding 0.5 μT while trying to keep peak values at the sub-microtesla level. The feasibility of achieving these values will be explained in the next sections.

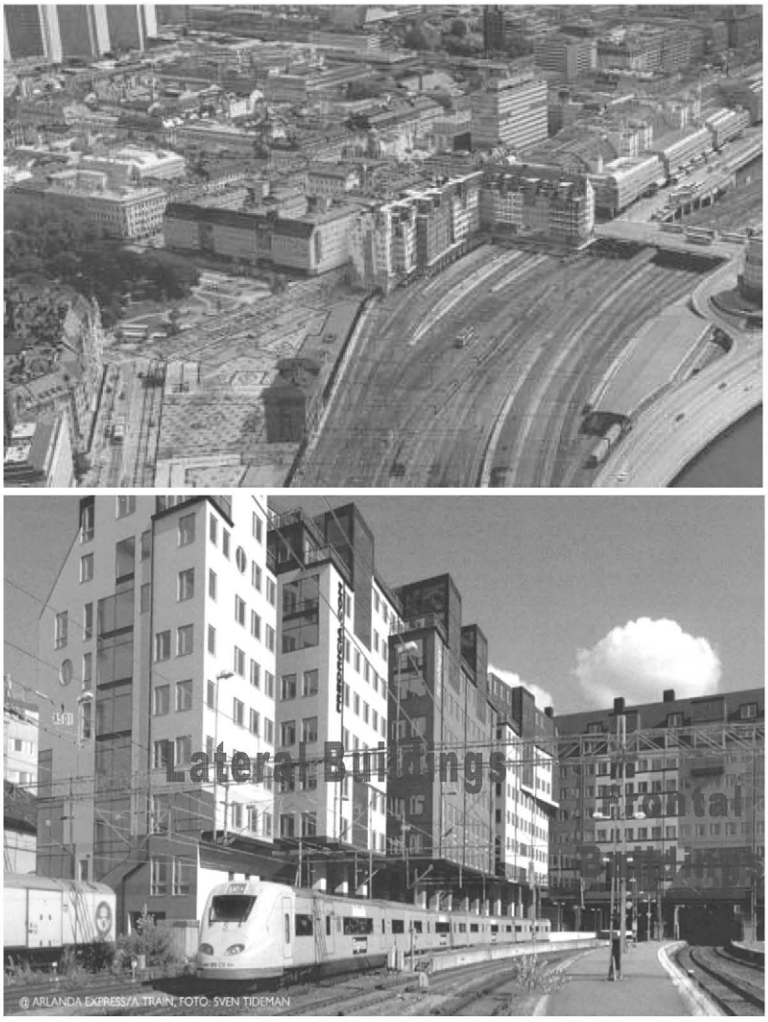


Fig. 1 Location of the buildings in the central part of the city of Stockholm; the pictures are virtual as the study was performed before the buildings were constructed. The lower picture shows the way the trains would pass with respect to the buildings.

The Sources of the Field

Power is supplied to the train system by the overhead wires of 15 kV carrying an average current of 200A (rms). The current's return path follows the rail track (Fig. 2). In fact, the amount of traction current depends on the power consumption of the engine needed to accelerate these trains; which reverts in a complex time-variability. The magnetic field rms values against time are shown in Fig. 3. The measurements shown were taken during 1-hour at a high traffic time. In spite of the short duration of the pulses, these are still rather long compared with the period corresponding to 16.67 Hz. Therefore, this study is concern only with the influence of the periodic signal. The number of trains considered is 10. Two of them, the closest to the lateral buildings, will stop before reaching the frontal buildings. The other eight trains will either not stop or stop for a few minutes and then continue to the next station crossing the frontal buildings.

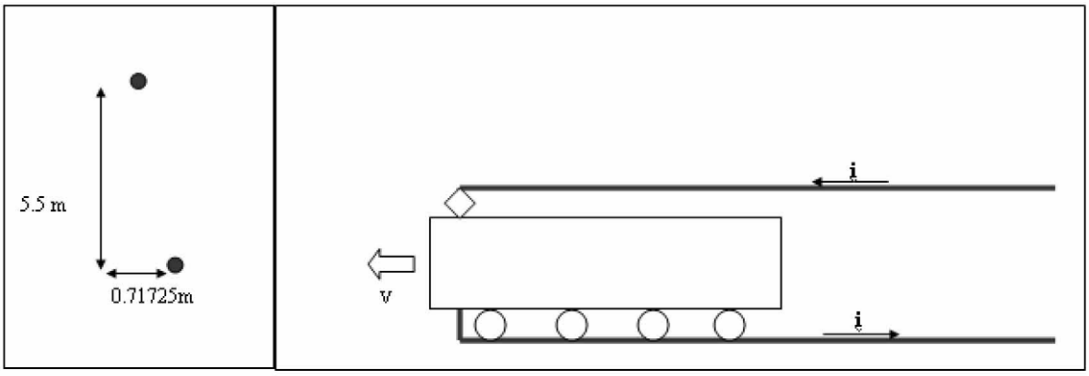


Fig. 2 A simplified diagram of the source of magnetic field. The train is powered by an overhead wire carrying an average current of 200 A. The return path is by one of the rail tracks.

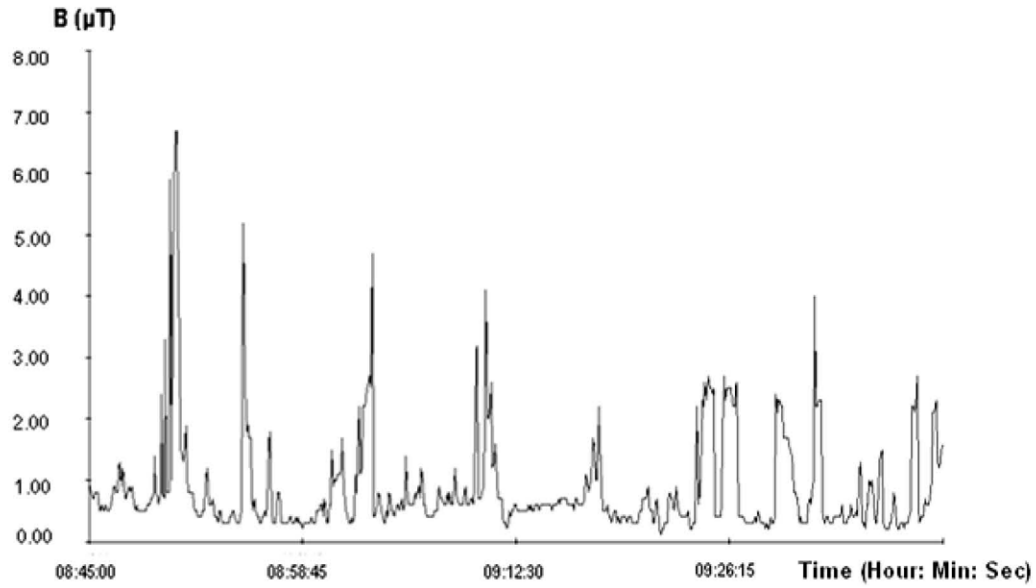


Fig.3 Time variability of the magnetic field. The values were taken at the nearest floor to the rails, near the intersection of the lateral buildings with the frontal buildings. Although the short duration of the pulses; these are still rather long compared with the period of the feeding current

The Shielding Challenges

The dimensions of the building are, for the lateral buildings: (20-30)m x 100m; and for the frontal buildings:18mx65m. The height of both buildings is 34 m. Traditional methods of mitigating magnetic fields suggest placing a metallic plate (shield) between the source of magnetic fields and the affected area. The most commonly used materials for the shield are steel (ferromagnetic), or aluminium (pure conductive). Because of the large dimensions of the building, iron would be excessively heavy, thus aluminium seems to be the obvious choice. However, when an aluminium shield is applied to the **frontal buildings**, some issues arise. The nearest floor (5^{th} floor) to the railway track has an average distance of 1 m to the upper cable of the feeding source; the extreme proximity of the cable poses a challenge to the shielding properties, for most of the eddy currents will be behaving as if they were induced by a homopolar (single cable) source. Fig. 4 shows the similarity of the eddy current pattern on a shield placed on the floor in close proximity to the upper cable of the railway dipole and a single cable in the same location. In the same figure one can also observe that eddy currents try to generate a cancellation field to the source that originated the effect (by Faraday and Lenz laws) with a concentration in the middle of the plate. At the same time they also go towards the edges as they try to reach for a return path. Thus, the result is that an aluminium plate *alone* would not be very effective shield when a train is passing through just under and in close proximity to the shield. The simulations were performed using 3d software Opera and its solver ELEKTRA [9].

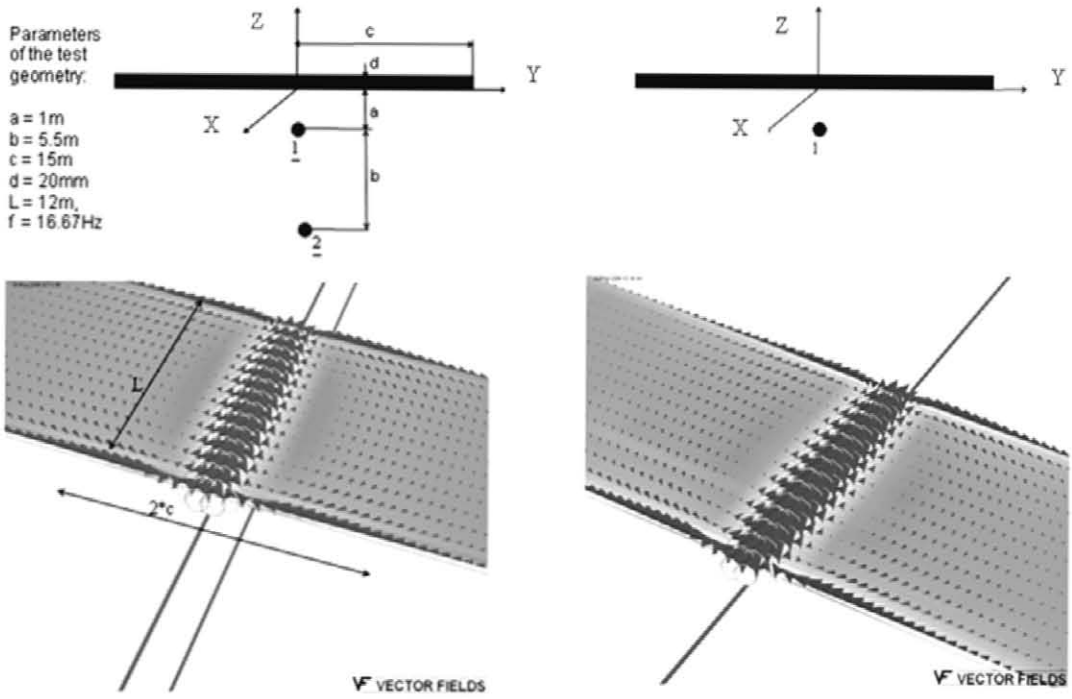


Fig. 4 Comparison between a railway feeding-dipole and a homopolar source; both sources behave similarly in the proximity of an aluminium conducting plate.

A proposed solution to this issue is to redirect the induced currents in a spatial configuration such that the returning paths will become useful to mitigate the field inside the enclosed area. This can be achieved by conductive ribbons joining two plates. The upper plate is used as part of the currents' returning path, thus it can be thinner than the bottom plate (Fig. 5). In some designs the upper plate or even both plates can be replaced by a set of ribbons providing further cost reduction. Yet, as different shielding configurations will yield different results, balance between material cost and mitigation factors has to be considered.

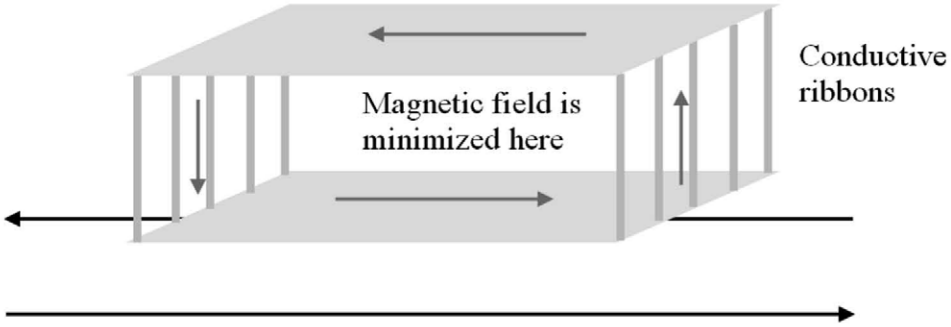


Fig. 5 extended shielding structure that redirects the induced currents creating effective current loops resulting in a minimization the field inside the enclosed region. In some designs, the upper conductive plate (or even both plates) can be replaced by ribbons resulting in further cost reduction.

Considering the **lateral buildings** we note that the sources pass alongside the buildings at different distances, some even under the building, such as the one shown in Fig.1. An aluminium shield alone, even if thick relatively to the skin depth (δ), will neither be optimal nor cost effective. The solution is a combination of optimally positioned system of loops and shields. Because the lateral region is 100m long with a cross-section area 20m(width)x34m(height), such a section can be modelled approximately assuming YZ symmetry (fields do not change in the X direction). Such a simplification can be considered accurate for the central part of the lateral buildings, but it does not model its ends, which are in fact interconnected. From the latter, is noticed that the total eddy current (at the cross section) must be zero. This condition comes from the fact that the eddy currents must find a return path when they meet the physical ends of the longitudinal extension. After performing numerical 2d simulations for the cross section (see Fig. 6), it was found that the results depend on the kind of boundary condition assumed (the total domain boundary is far from the region of interest).

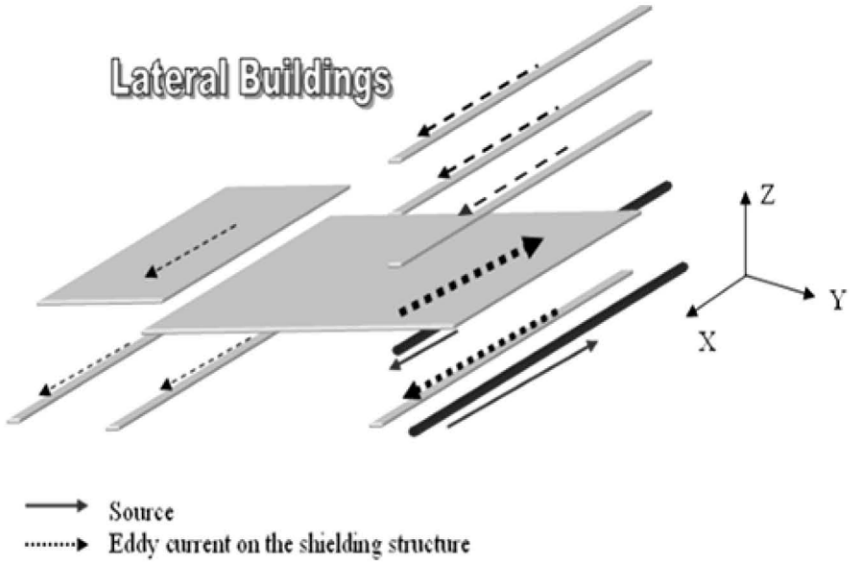


Fig. 6 The lateral shielding structure is shown which can be modelled using YZ symmetry (the field does not depend on the x coordinate). The eddy currents (dotted arrows) on the shielding structure are shown as well as the source (continuous arrows). This simplification can be considered accurate for the central part of the lateral buildings, but it does not model the endings.

It is observed that the boundary condition: $A_x = 0$ at $\partial\,\Omega$ (A_x is the x- component of the magnetic vector potential and Ω is the problem domain) allows a net eddy current flowing at the shielding structure. If the total domain boundary $\partial\,\Omega$ is far from the region of interest, we can assume the magnetic field intensity **H** = **0** at $\partial\,\Omega$ as the boundary condition. This boundary condition makes the net eddy current be zero because its circulation on $\partial\,\Omega$ is zero. Figure 7 shows 2d numerical results using both boundary conditions; the 2d simulations were performed using the code Femlab 3.1 [10]. A line L was added for comparison reference between the two conditions; this will be plotted later when contrasted with experimental validation.

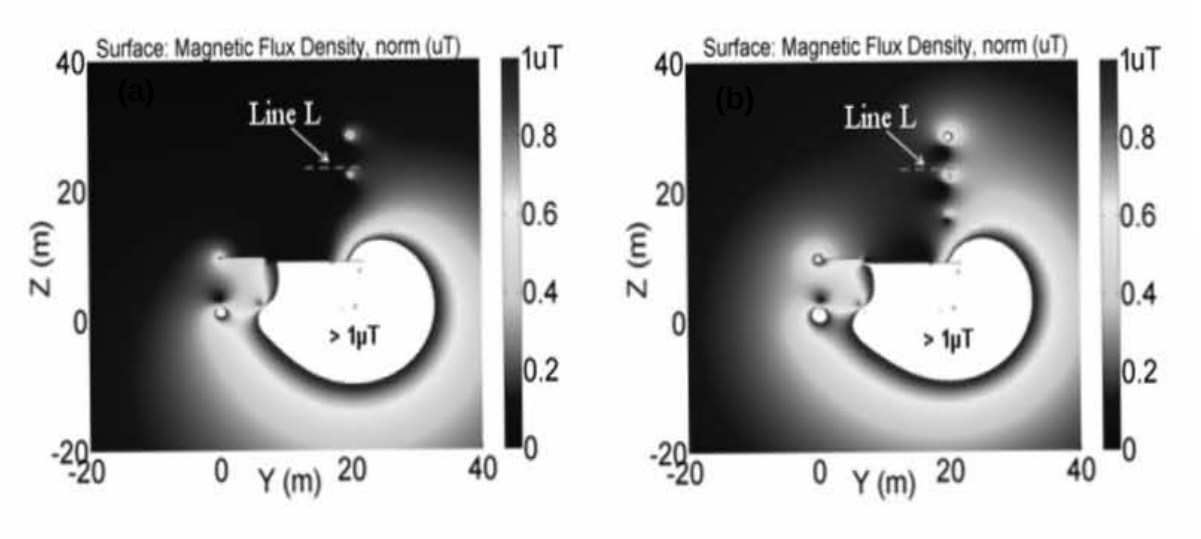


Fig. 7 Numerical results are shown for the two boundary conditions discussed above. In (a) the boundary condition is assumed $A_x = 0$ at $\partial\,\Omega$, while in (b) it was assumed **H** = **0** at $\partial\,\Omega$. The line L is added as comparison reference when contrasted with experimental validation.

Scaling rules

The computation of shielding factors for the frontal structure (which is evidently 3-dimensional) by numerical simulations, is rather complicated as a result of the large aspect ratios involved. Something similar can be said for a fully 3d numerical simulation of the lateral structure, since the 2d- simulations presented can only represent accurately the central region. Here an experimental technique, based on scaling rules, is combined with the suggested 3d structures which are the paths of the induced currents. This technique will make it possible to experiment in a lab with various shielding designs and to predict shielding factors of 3dimensional structures more accurately.

Let the scaling factor between two shielding systems M and M' be k then length, surface and volume scale as $L' = k\,L$; $A' = k^2 A$; $V' = k^3 V$ respectively. A current I is scaled assuming a homogeneous scale-invariant current density J. Then: $J' = J$, $I'/A' = I/A$, and $I'/(k^2 A) = I/A$, therefore: $I' = k^2 I$. Having units of length, the *skin depth* δ scales linearly: $\delta' = k\,\delta$. This expression allows the computation of the scaling rule for the frequency: $(2\mu\pi'\sigma' f')^{-1/2} = k\,(2\sigma\mu\pi f)^{-1/2}$. Assuming scale-invariance and homogeneity of the materials ($\mu = \mu'$, $\sigma = \sigma'$), then the frequency scales as: $f' = (1/k)^2 f$. The application of Ampere law yields the scaling rule for the magnetic field: $B' = k\,B$, i.e. it is linear with respect to scaling. Finally the shielding factors (SF) which are relative comparisons between the magnetic field before and after mitigation become invariant with respect to scaling, i.e. SF' = SF. When applying this method [11], [12] to our study we will adopt a scaling factor k = 1/10. Therefore the frequency for the small system is 1667 Hz. These settings were implemented in a laboratory where the frontal and lateral structures were built and tested independently. Figures 8, 9 and 10 show details of this structure and Fig. 11 shows values obtained, before and after mitigation procedures were applied, for one of the floors (level two stories above the train tracks).

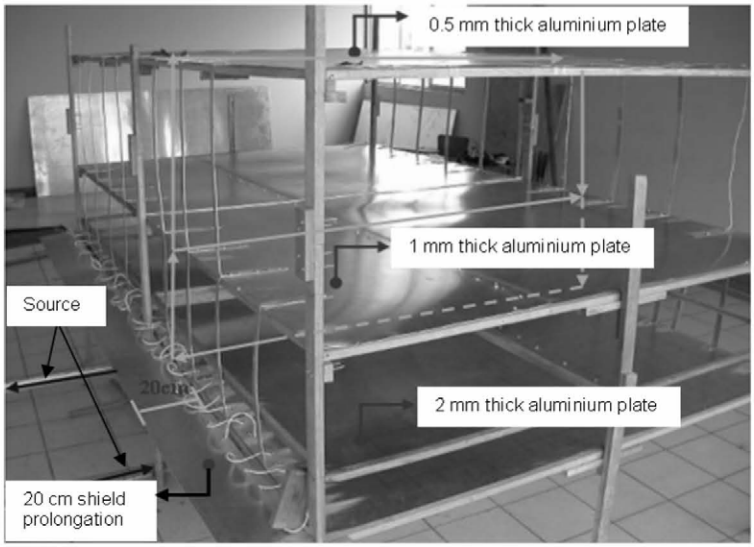


Fig. 8 Scale model ten times reduced (k = 1/10) of the shielding structure for the frontal buildings. The model was built in an electronic laboratory and low power was used to feed the source, which represented the effect of the current loop and the corresponding magnetic field generated by it. Different location of the loop represented different trains.

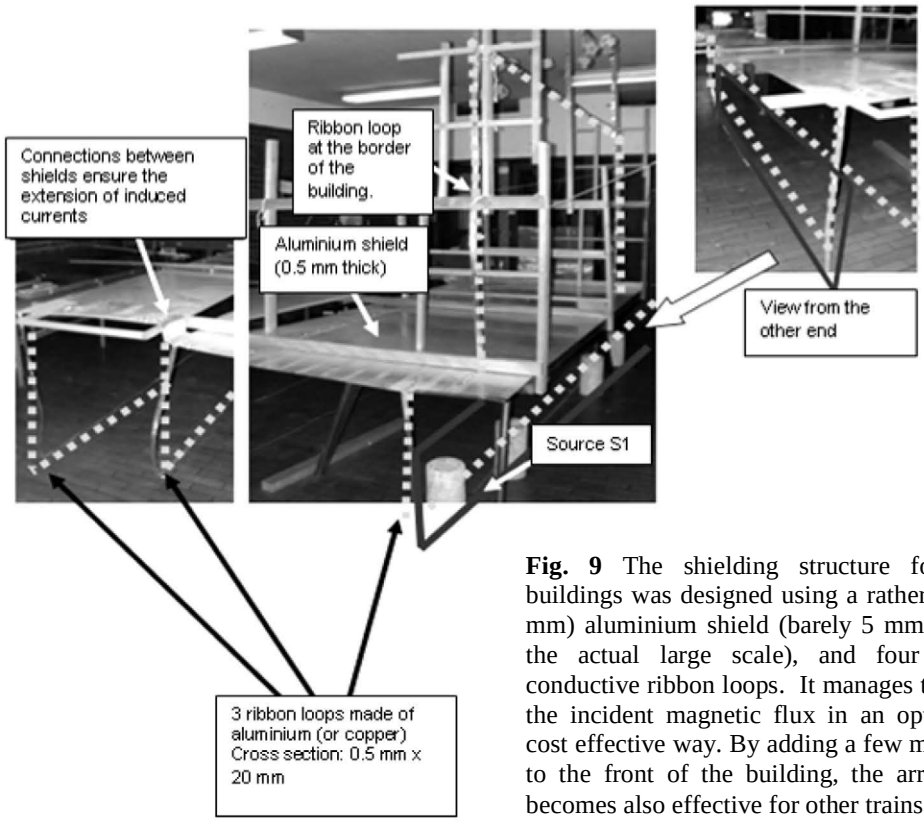


Fig. 9 The shielding structure for lateral buildings was designed using a rather thin (0.5 mm) aluminium shield (barely 5 mm thick for the actual large scale), and four attached conductive ribbon loops. It manages to restrain the incident magnetic flux in an optimal and cost effective way. By adding a few more loops to the front of the building, the arrangement becomes also effective for other trains.

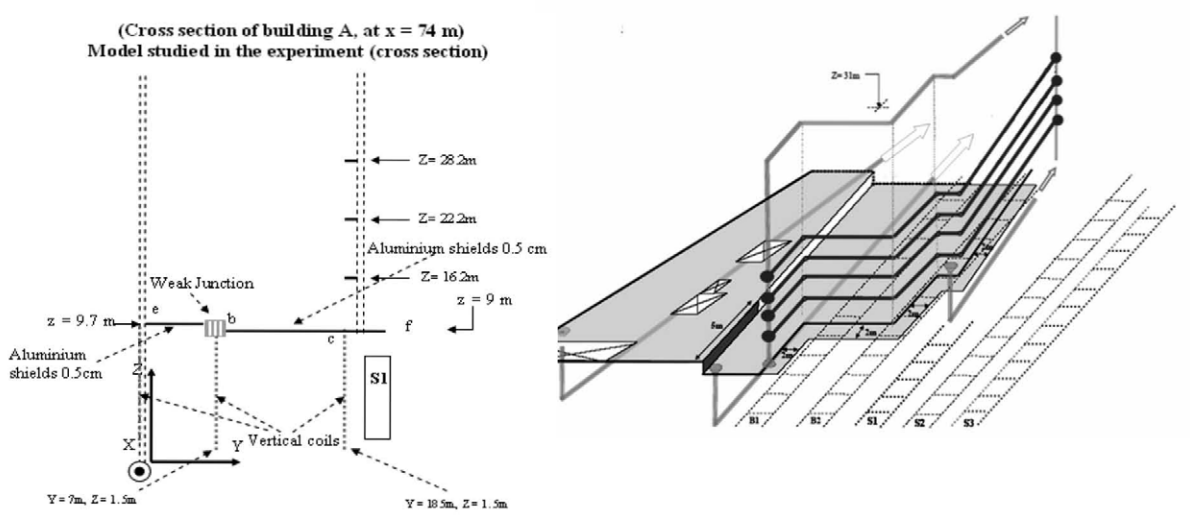


Fig. 10 Cross section (left) and a 3D picture (right) are shown of the final shielding structure for the lateral buildings. The extra loops have been added to consider the influence of any of the 10 trains, namely, B1, B2, S1, S2…or S8.

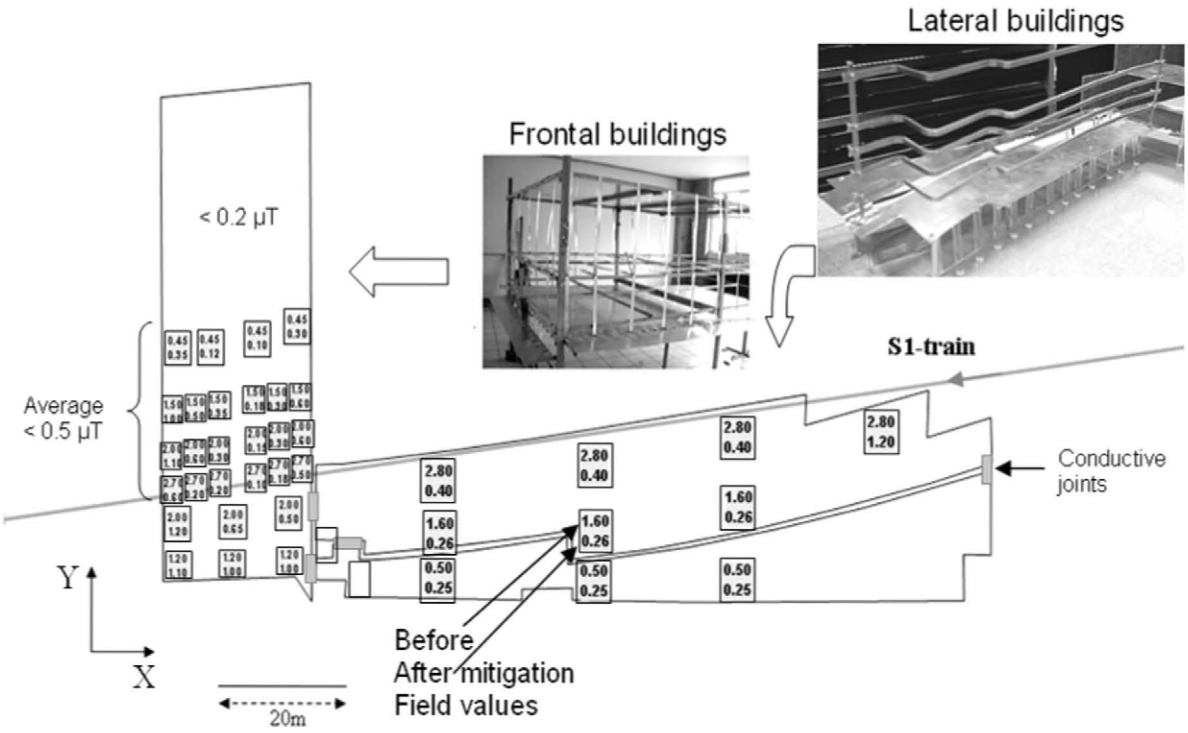


Fig. 11 Before and after mitigation field values are shown for the level located two floors above the train tracks. The resulting average magnetic field levels in each floor were kept below 0.5 μT.

Returning to the shielding issues and numerical modelling, a comparison was made (Fig. 12) between the experimental results and the two results applying two different boundary conditions mentioned in the two-dimensional modelling (see Fig. 7). The line L was taken at z = 22.7 m . The result is that the condition H = 0 fits the obtained data more accurately than $A_x = 0$. This boundary condition is also physically more realistic as it makes the net eddy current be zero; which is demanded in the experiments due to the connecting paths of the shielding loops.

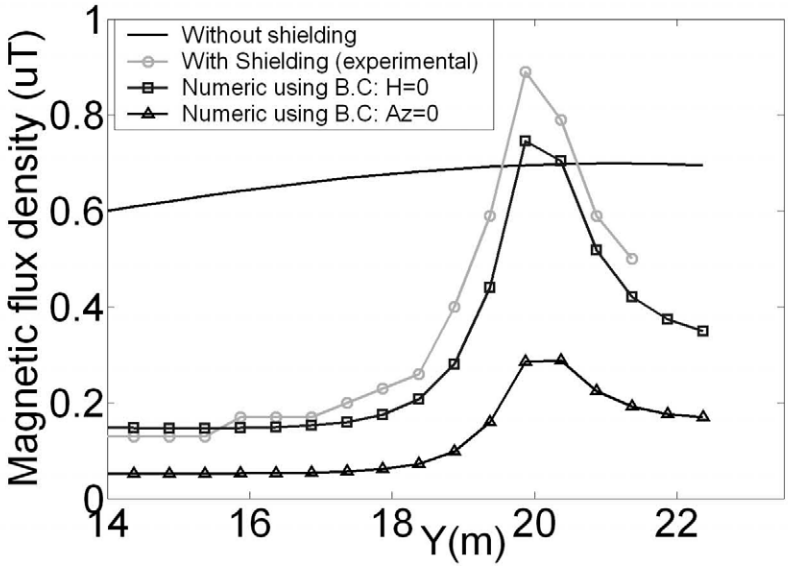


Fig. 12 Comparison between numerical results and experimental data is shown. The values taken over the line L at z = 22.7m (see Fig. 7). Notice that the boundary condition H = 0 agrees more with experimental data. The experimental data is obtained by using the scale model described in this article.

Conclusions

The problem of shielding extremely low frequency magnetic fields of 16.67 Hz that affect large buildings certainly poses several challenges to standard field mitigation schemes and to modern numerical modelling methods too. A new technique was used based on re-directing eddy currents towards ribbon paths that effectively contributed to reduce the magnetic field inside the buildings. Due to the 3-dimensional character of the proposed models the design was elaborated using scaling rules and performing tests in a low-power laboratory. The scaling factor for the experiment was 1/10 and the frequency 1.67 kHz. The division of lateral and frontal buildings proved to be useful in the design of shielding structures. Complex but cost-effective structures based on conductive material consisting on plates and ribbons were built. Good mitigation factors (up to SF=10) were achieved. After shielding averages field values were measured under 0.5 microtesla and peak values were kept (with a few localized exceptions) under 1 microtesla.

Acknowledgements

The authors are grateful to the representatives of the Swedish company *NCC AB* for proposing the problem. We would like to thank the Faculty of Science of the *Universidad Nacional de Ingeniería,* in Lima Peru, for allowing us to use of their lab facilities. Our gratitude also goes to ELFORSK for the grant N° 3950, which enabled us the development of some the methods used in this study.

References

[1] C. Buccella, M. Feliziani, F. Maradei, and G. Manzi, Evaluation of the Magnetic Field Levels Produced by a Railway Line, Proceedings of conf. Environmental Modelling and Simulation – 2004, ref. 432.

[2] P. Chadwick et al: Magnetic fields on British trains. *Ann Occup Hyg* 5:331-335, 1998.

[3] M. Röösli, M. Lörtscher, D. Pfluger, N. Schreier: ELF (16.7 Hz) magnetic field exposure assessment in Swiss railway engineers. Bioelectromagnetics 2005, Dublin, Ireland - Book of abstracts pp. 41-42.

[4] P. Rossi, R. Falsaperla, V. Brugaletta, P. Betti e A. Gaggelli: Occupational exposure to static and ELF magnetic fields on railway engines. VI International Congress of the European BioElectromagnetics Association, EBEA 2003. Budapest Nov. 13-15, 2003, p.31.

[5] Minder, C. E.; Pfluger, D.H., Leukemia, Brain Tumors and Exposure to Extremely Low Frequency of Electromagnetic fields in Swiss Railway Employees, Am J Epidemiol 153(9):825-835.

[6] Information Ventures, Inc. Electromagnetic Fields and Rail Maintenance Workers: Final Report of an Exposure Survey and Feasibility Investigation. Exposure Assessment, http://infoventures.com, 1999.

[7] International Commission on Non-Ionizing Radiation Protection (ICNIRP): Guidance on determining compliance of exposure to pulsed and complex non-sinusoidal waveforms below 100 kHz with ICNIRP guidelines, 2003; 84: pp. 383-387.

[8] ICNIRP. Guidelines for limiting exposure to time-varying electric, magnetic and electromagnetic fields (up to 300 GHz). *Health Phys.*, 74, No. 4, 494–522 (1998).

[9] Opera 3d User manual; solver ELEKTRA, Vector Fields Ltd. 1996.

[10] Comsol AB, Femlab 3.1, *Electromagnetics Module User's Guide*, Sweden, 2004.

[11] E. Salinas, Y. Q. Liu , P. Souza Jr. , J. Atalaya, , P. Cruz , J. Daalder. "Design and Validation of Power-Frequency Magnetic field Conductive Shielding for Underground Cables" *Proceedings of CIRED'2005, 18th International Conference and on Electricity Distribution,* IEE Technical Report, Technical Theme 2, Power Quality and EMC, paper 97 pp 1-4, Turin, 2005.

[12] Ener Salinas, Per Pettersson, Jaap Daalder, Yueqiang Liu, Juan Atalaya, Diego Gonzales, Munish Jassi, Cynthia Contreras, Carlos Leon. Minimization of Power-Frequency Magnetic Fields in Confined Regions Using 3-Dimensional Physical Processes; with Applications to Currently Active Electrical Substations, *ELFORSK Report, project 3950, 2006.*

DAILY PULSED ELECTROMAGNETIC FIELD (PEMF) THERAPY INHIBITS TUMOR ANGIOGENESIS VIA THE HYPOXIA DRIVEN PATHWAY: THERAPEUTIC IMPLICATIONS

IVAN L. CAMERON, NICOLAS J. SHORT, MARKO S. MARKOV

University of Texas Health Science Center at San Antonio, Department of Cellular and Structural Biology, San Antonio, Texas 78229 [I.L.C., N.J.S.], Research International, 135 Arielle Ct, Suite E, Williamsville NY, 14221 [M.M.]

Abstract

Ten minute daily PEMF inhibits hypoxia driven angiogenesis and tumor growth (Williams et *al*. 2001, Cameron et *al*. 2005a) but does not inhibit angiogenesis that normally occurs during embryogenesis and tail fin regeneration in zebrafish (Short et *al*. 2006). As discussed, the reason for this difference may be due to the hypoxic state of the tissues. Daily pulsed electromagnetic field (PEMF) was found to retard angiogenesis and growth of a human breast cancer xenograft, causing the tumor to develop proportionately larger areas of necrosis and hypoxia and smaller areas of proliferatively active cancer cells. It was also demonstrated that the daily PEMF therapy continued to inhibit tumor angiogenesis and tumor regrowth for two weeks following a standard course of ionizing radiation (IR) therapy (Cameron et *al*. 2005a). However, this PEMF therapy renders large areas of the tumor hypoxic and therefore is expected to lessen susceptibility to oxidative damage caused by further IR treatments or by oxidative dependent chemotherapy. The need for a 2-4 day recovery from the anti-angiogenic effects of PEMF prior to the next round of oxidative IR therapy is discussed.

Introduction

There appears to be only two previously published original research reports on use of pulsating electromagnetic field (PEMF) to reduce tumor angiogenesis and tumor growth (Williams et *al.* 2001, Cameron et *al.* 2005a). These two previous reports both indicated that a 15 mT PEMF given for 10 minutes per day safely reduces tumor growth and tumor vascularization. In an accompanying report in these proceedings the effects of the exact same PEMF exposure condition on zebrafish development and tail fin regeneration was reported to be ineffective in retarding fish embryonic development or fin regeneration or to retard the vascularization accompanying these processes (Short et *al.* 2006). What factor or factors might be responsible for the difference in response to the same PEMF exposure conditions between the transplantable tumors in mice and the development and fin regeneration in the fish? Thus, an aim of the current report is to briefly reexamine the results of these two prior reports on growth of a transplantable tumor and on fish development and tail fin regeneration and to explore possible differences in responsiveness to the same PEMF exposure conditions.

It seems likely that clinical oncologists might not be inclined to use PEMF as the sole method of cancer therapy. Thus, it was decided to combine a commonly used form of cancer therapy, specifically a standard course of ionizing radiation (IR) with PEMF therapy in hopes of finding additive or synergistic benefits. The therapeutic implications of the results of the IR and PEMF study are presented and discussed.

Materials and Methods

EMF on Tumor Growth/Angiogenesis—Green fluorescent protein transfected with MDA-MB 231 breast cancer cells were injected into the mammary fat pad of young female athymic mice. Six weeks later, mice were randomly divided into four treatment groups: untreated controls; 10 minute daily PEMF; 200 cGy of IR every other day (total of 800 cGy); IR plus daily PEMF. Detail of the PEMF method and the IR method are given in Cameron et *al.* (2005a). Tumor size and body weight measurements were made

throughout the course of treatment. Some mice in each group were euthanized 24 hours after the end of the IR treatment. PEMF treatment continued for three additional weeks. Tumor sections were stained for: endothelial cells with CD31 and PAS or hypoxia inducible factor 1α (HIF). Tumors were scored for angiogenesis, for metaphase index and for lung metastases.

EMF on Zebrafish Embryonic Development—Newly fertilized zebrafish embryos were given daily PEMF and developmental stages were scored versus untreated control embryos based on developmental designations made my Kimmel et *al*. (1995). Details of the methods are given in accompanying report in these proceedings (Short et *al*. 2006).

Results

Whole body IR and PEMF therapy suppressed tumor growth (Fig. 1), cell proliferation (Fig. 2), lung metastases (Fig. 3) and angiogenesis (Fig. 4).

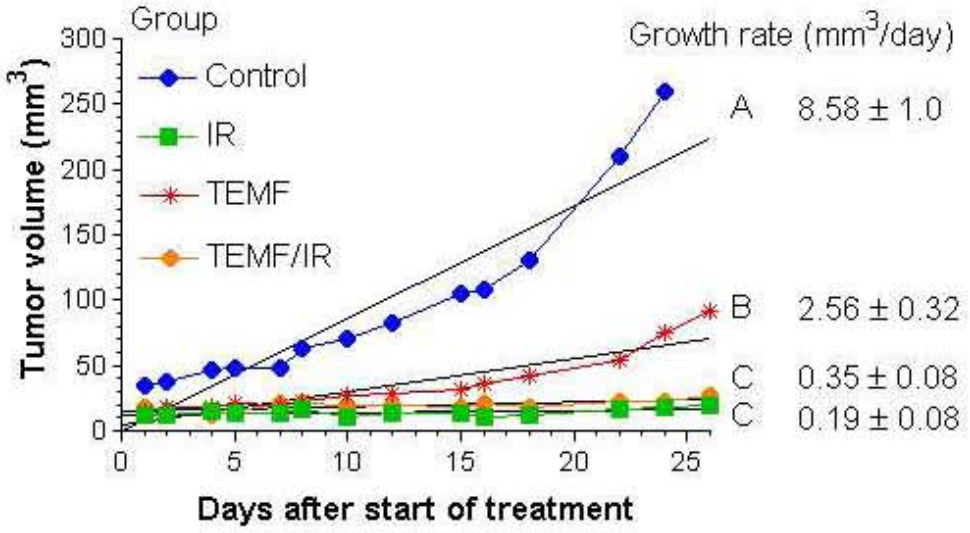


Figure 1. Illustrates the effect on tumor growth of: the 8-day course of gamma irradiation therapy (IR), the daily exposure to the TEMF therapy (TEMF), a combination of gamma irradiation and TEMF therapy (TEMF/IR), and no treatment (Control). The tumors were all 35mm^3 or less at the start of treatment.

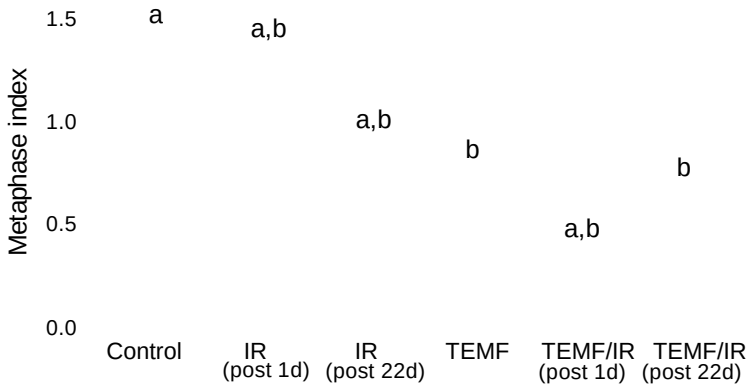


Figure 2. Number of metaphase figures per midaxial histological section of tumor. Column height indicates mean ± SEM. The columns that do not share a common letter are significantly different ($p<0.01$). TEMF significantly suppresses metaphase index in the tumor. Data from the untreated mice (Control) and the TEMF treated mice were pooled from mice of the early and the late sacrifice because there were no significant time of sacrifice differences within these groups. Not shown are data on number of metaphase figures per midaxial histological section of duodenal crypts from mice sacrificed one day after last IR exposure. The data reveal significant decreases in IR treatment. Treatment with IR but not TEMF caused a significant decrease in metaphase index in the intestinal crypts.

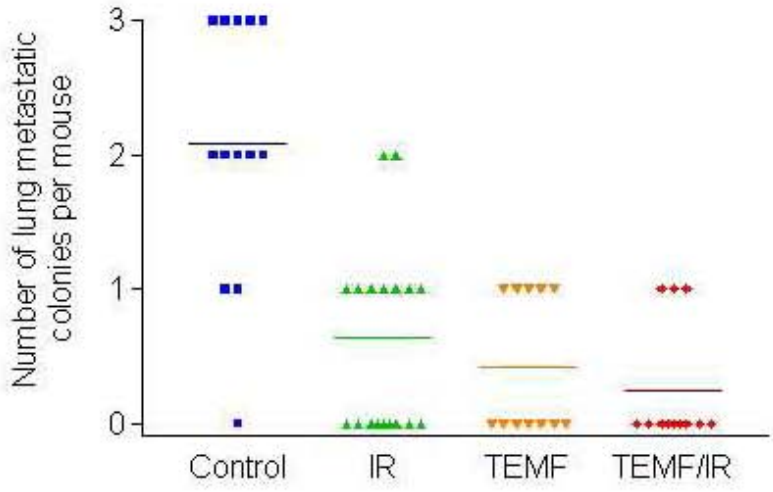


Figure 3. Metastasis of GFP-expressing human breast MDA MB231 cells from the site of inoculation in the inguinal mammary fat pad to lodge in the lungs of mice in each of the four treatment groups. The lungs were removed and smashed between microscopic slides and microcolonies of GFP cells were observed by epilumination using blue light and detected by presence of green fluorescence microcolonies observed using both 3.5× and 10× objective lens. The untreated mice had a significantly higher number of GFP positive microcolonies than the groups of mice that received gamma irradiation therapy or those mice that received EMF therapy. There were no other significant differences between groups in either mean number of microcolonies per lung or in incidence. Horizontal lines indicate mean values for each treatment group.

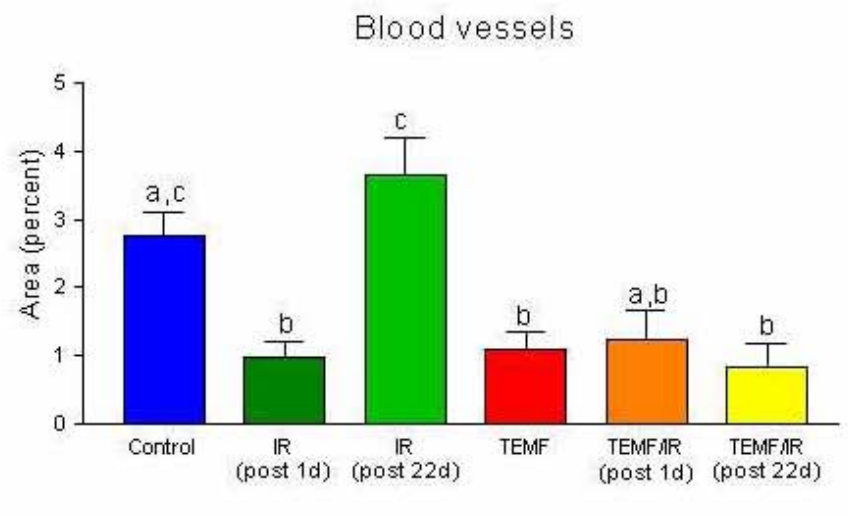


Figure 4. Quantification of changes in tumor vascularization between treatment groups. The percent of area (volume density) of blood vessels was determined using an ocular grid intercept counting method. The mean ± SEM of each treatment group is graphed. Columns that do not share a common letter within a graph are significantly different ($p < 0.01$). The data indicate that gamma irradiation and EMF alone or in combination decreased the total area of blood vessels and increased the total area of pseudopods compared to the control. Data from the untreated mice (Control) and the EMF treated mice (TEMF) were pooled from mice from the early and from the late sacrifice because there was no significant time of sacrifice difference within these groups.

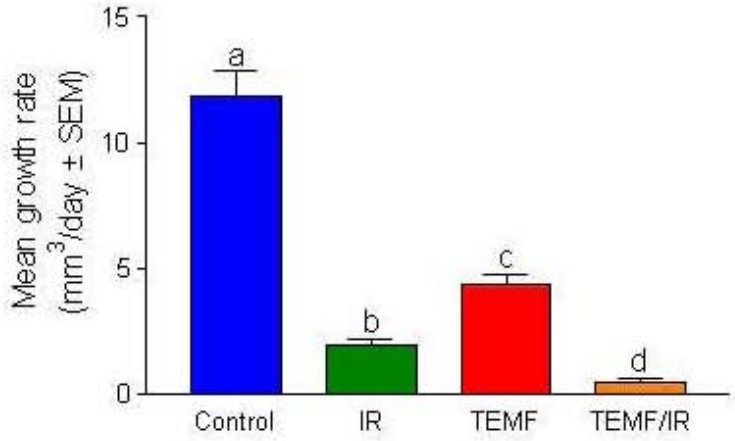


Figure 5. Mean ± SEM tumor growth rate data from day 7 to day 15 post IR therapy in each treatment group. ANOVA was used to determine any statistical differences in growth rates between treatment groups. Different letters demonstrate significant differences. Tumors in the untreated control group grew significantly faster than did tumors in the other three groups. Tumors in the IR/TEMF group had a growth rate significantly lower than that of the other three groups.

Continued daily PEMF therapy following IR treatment prevented angiogenesis and tumor regrowth (Fig. 4-5). PEMF therapy did not result in the body weight decreases nor the decreases in blood elements that IR did (not shown). Embryogenesis was not inhibited by daily PEMF therapy (Fig. 6).

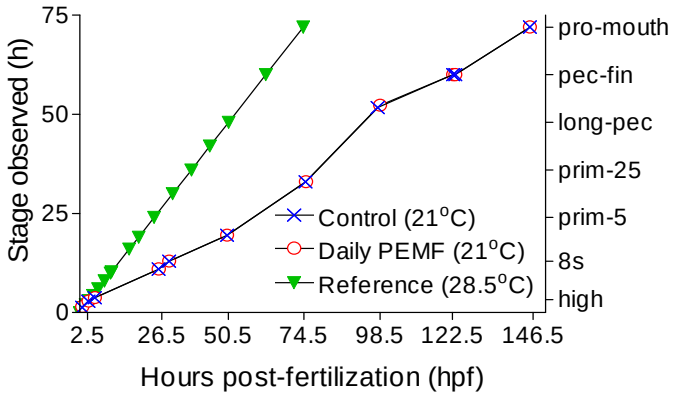


Figure 6. Temperature and 10 minute daily exposure to PEMF on development. The time post-fertilization to reach each stage at 28.5°C (from Kimmel et *al*., 1995) is plotted on the left y-axis. Corresponding morphological stages are listed along the right y-axis. Stage abbreviations used are 8 somite (8s) and protruding mouth (pro-mouth). Times of PEMF exposures are labeled on the x-axis.

Discussion

Angiogenesis in the tumor was hypoxia driven. (see Fig. 7 that summarizes a model of human MDA MB231 breast cancer tumor). Continued daily PEMF therapy following IR treatment prevented tumor angiogenesis and regrowth. However, it did not suppress metaphase index in intestinal crypts. This suggests that PEMF works selectively on hypoxia driven angiogenesis such as that in growing tumors. Angiogenesis during embryogenesis in fish was not inhibited by daily PEMF treatment. Had hypoxia occurred in fish development then developmental retardation or arrest has been demonstrated to occur (Padilla and Roth 2001). Lack of effect of angiogenesis in the fish versus the tumor suggests the difference in response to PEMF is because PEMF interferes with hypoxia driven angiogenesis that occurs in tumors but not in normal fish embryogenesis.

PEMF is an effective adjunct therapy following IR therapy but the continued daily PEMF therapy should be stopped sometime (2-4 days) prior to a second round of IR therapy. The temporary cessation of PEMF prior to the second round of IR is necessary for resumption of angiogenesis, decrease of hypoxic areas and increase in proliferative activity in well oxygenated areas within the tumor, all of which are needed for an effective second round of IR treatment.

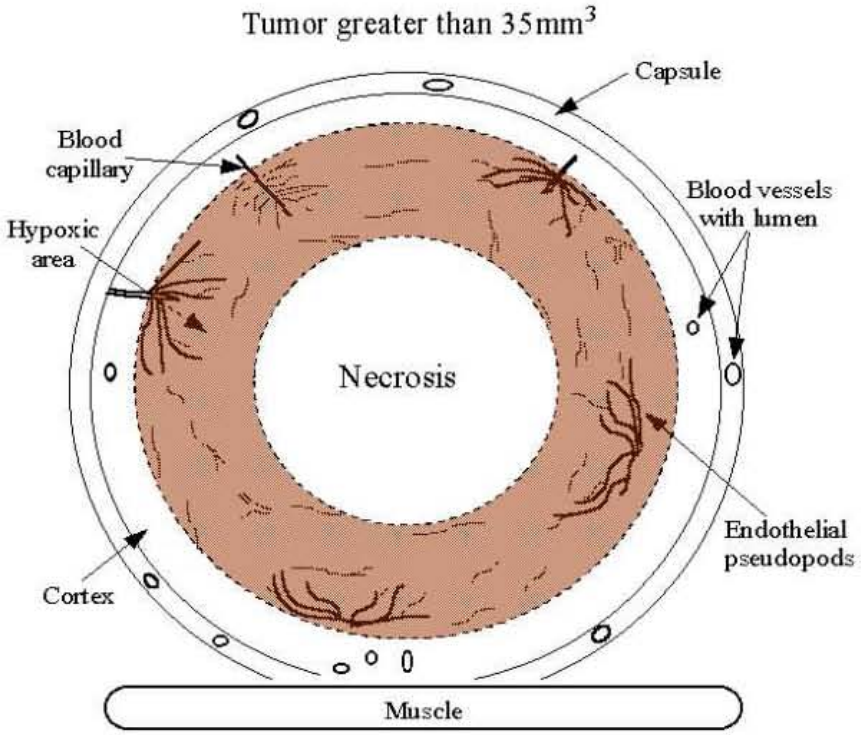


Figure 7. Model of vascularization as observed in the human MDA MB231 breast cancer cell tumor grown as a xenograph in a female nude mouse. The well vascularized tumor capsule overlies the tumor cortex. The cortex extends between 100 and 150 μm beneath the capsule. The HIF-α positive region is located in the subcortical region, at distances greater than 150 μm of the capsule. More endothelial pseudopods are located in this subcortical region than are located in the cortical region of the tumor. Even further away from the vascularized capsule is the region of tumor necrosis which contains no blood vessels or endothelial cell pseudopods. This model is consistent with the conclusion that the hypoxic regions of the tumor produce HIF leading to production of vascular endothelial growth factors and sprouting of endothelial cell pseudopods (Cameron et *al.* 2005b).

Acknowledgements

This work was supported by EMF Therapeutics, Inc. and NIH grant CA 75253. Figures 1-6 are from Cameron et *al.* 2005a, and figure 7 is from Cameron et *al.* 2005b. Cancer Cell International is gratefully acknowledged. The authors wish to thank Matt Cykowski for help with animal handling and photography.

References

Cameron IL, Sun LZ, Short N, Hardman WE, Williams CD. 2005a. Therapeutic electromagnetic field (TEMF) and gamma irradiation on human breast cancer xenograft growth, angiogenesis and metastasis. *Cancer Cell International* 5:23.

Cameron IL, Short N, Sun LZ, Hardman WE. 2005b. Endothelial pseudopods and angiogenesis of breast cancer tumors. *Cancer Cell International* 5:17.

Kimmel CB, Ballard WW, Kimmel SR, Ullmann B, Schilling TF. 1995. Stages of embryonic development of the zebrafish. *Developmental Dynamics* 203:253-310.

Padilla PA, Roth MB. 2001. Oxygen deprivation causes suspended animation in the zebrafish embryo. *PNAS* 98:7331-7335.

Short N, Miera KL, Markov M, Cameron IL. 2006. A pulsed electromagnetic field that inhibits tumor growth fails to delay zebrafish embryonic development and tail fin regeneration. These proceedings.

Williams CD, Markov MS, Hardman WE, Cameron IL. 2001. Therapeutic electromagnetic field effects on aniogenesis and tumor growth. *Anticancer Research* 21:3887-3892.

A PULSED ELECTROMAGNETIC FIELD THAT INHIBITS TUMOR GROWTH FAILS TO DELAY ZEBRAFISH EMBRYONIC DEVELOPMENT AND TAIL FIN REGENERATION

N. SHORT, K. L. MIERA, M. MARKOV[2], P. JAGADEESWARAN, I. L. CAMERON[3]

University of Texas Health Science Center at San Antonio, Department of Cellular and Structural Biology, San Antonio, Texas 78229 [N.S., K.M., P.J., I.L.C.], [2]Research International, 135 Arielle Ct, Suite E, Williamsville NY, 14221 [M.M.]

This work was supported by EMF Therapeutics, Inc. and by National Institutes of Health grants HL63792 and AG20863

[3]To whom requests for reprints should be addressed, at Department of Cellular and Structural Biology, University of Texas Health Science Center, 7703 Floyd Curl Drive, Mail Code 7762, San Antonio, TX 78229-3900. Phone: (210)567-3817; Fax: (210)567-3803; E-mail: cameron@uthscsa.edu.

Abstract

A rectified semi-sinewave signal with an amplitude of 15mT and a frequency of 120 pulses per second (PEMF) given as a 10 minute daily session has proven to be a safe means for retarding tumor growth and angiogenesis in a transplantable tumor in mice. The experiments reported here were designed to test the same PEMF exposure on embryonic development and on caudal fin (tail) regeneration in zebrafish. The results of single and multiple exposures to PEMF at different times during embryonic development and tail fin regeneration demonstrated no significant delay in either embryo development or in tail fin regeneration. Possible difference between the inhibitory effect of PEMF on tumors compared to the lack of effect of the PEMF on embryo development and on tail fin regeneration is discussed.

Background

It has been reported that a 10 minutes per day exposure to a 15mT pulsed electromagnetic field (PEMF) given at 120 pulses per second reduced tumor growth and vascularization and resulted in increased survival time in mice with a breast cancer xenograft [Williams et *al*., 2001, Cameron et *al*., 2005]. The study reported here was designed to investigate the potential effects of the same PEMF on embryonic development and tail fin regeneration of zebrafish (*Danio rerio*).

In the present study it was decided to exactly repeat the PEMF exposure conditions used in the previous breast cancer xenograph experiments. No attempt was made to increase the dose of exposure (time or intensity). Thus, no claims are made to any possible effects outside the dosage range used in the present fish study.

Zebrafish are excellent organisms for the study of embryonic development. A single mating pair can provide 200 newly fertilized eggs that progress through development in synchrony. The zebrafish is a leading model for studies of vertebrate development because one can obtain a large number of transparent, externally and rapidly developing embryos [Kimmel et *al*., 1995]. Thus, even modest experimental perturbations can influence the rate of sequential development in a subset of these fertilized embryos.

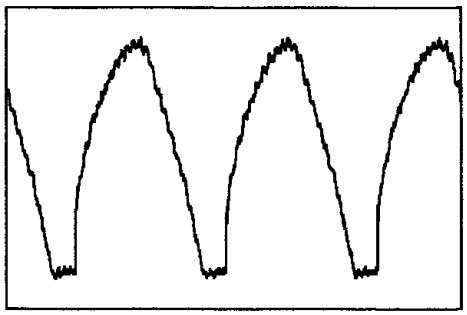
The caudal tail fin is an excellent model organ for studying regeneration. It has a comparatively simple architecture, consisting of several segmented, bony fin rays composed of concave hemirays, which are surrounded by connective tissue, nerves, and blood vessels [Ferretti and Géraudie, 1998]. Hundreds of amputations per hour may be performed. Regeneration is rapid and reliable, with most structures replaced within 1 to 3 weeks. Zebrafish survive their amputation wound, allowing for study of formation of new blood vessels and nerve regeneration [Johnson and Weston, 1995].

Because of the critical events associated with blood vessel formation and circularization between the 21 and 26 somite stages of embryogenesis [Stainier et *al*., 1993] and the need for angiogenesis during tail regeneration as well as the past report that PEMF has anti-angiogenic action in rapidly growing mammalian tumors [Williams et *al*. 2001, Cameron et *al*. 2004], it was decided that exposure of fish embryos and regenerating fish fins to the PEMF at known times of angiogenesis might shed light on the mechanism of action the PEMF on suppression of tumor growth and angiogenesis.

Materials and Methods

A pulsed electromagnetic field (PEMF) system having a proprietary signal designed by EMF Therapeutics, Inc. (Chattanooga, TN, USA) was used (Figure 1). The system generates a pulsating half sinewave magnetic field with a frequency of 120 pulses per second. An ellipsoidal coil with 21" large diameter and 14" small diameter is used to deliver the signal to the target. In the experiment reported here, the magnetic flux density measured in the exposure chamber was 15 mT. This value of magnetic field flux density was chosen based upon our previous dose response experience and data (Williams and Markov 2001 and Williams et al. 2001). A thorough 3-D mapping of the magnetic field was performed for the entire space covered by the coil.





Pulsed (120 pps) rectified semi-sine wave

Figure 1. Photograph of the EMF device and a separately suspended exposure table that was used to avoid vibration of the exposure chamber (left). An illustration of the fully rectified 60Hz signal transferred to 120 pulses per second pulsating magnetic field (right).

The flux density of the magnetic field in the exposure chamber (25 cm long, 10 cm wide and 13 cm high) was consistent within the entire volume of the chamber. The same type chamber was used on sham controls. The temperature inside the exposure chamber before and at the end of the PEMF treatment was the same. The exposure chamber is suspended separately from the EMF device and no vibrations were detected in the chamber during

operation of the EMF device.Zebrafish (4 months old) were purchased from Ekkwill Waterlife Resources (Gibsonton, FL). Zebrafish were cultured according to Westerfield [1989]. Developmental times were determined from the morphological features of the embryos under a dissecting microscope. All experiments were conducted at 21^{o}C. A time point for a particular stage as judged by the morphological staging of each individual embryo in the cohort was assessed and the corresponding time value from Kimmel et *al*., 1995 was then used for statistical analysis. Linear regression analyses of all data obtained revealed a significant linear fit between hours post-fertilization (hpf) from this study and hpf from Kimmel et *al*., 1995 when plotted against one another at various morphological stages. This indicates that the method of scoring development in numerical hours, as done in this study, is justified.

In an attempt to determine an action of the PEMF on embryogenesis, fertilized zebrafish eggs were exposed to the PEMF at designated stages of development. A first group was exposed daily to the PEMF beginning at the 64 cell stage (2.5 hpf) for a total of 7 daily pulses. A second group of fertilized eggs was exposed at either the 8 cell stage (1.6 hpf) or at the 64 cell stage (2.5 hpf), both at times during synchronous cell divisions. The third group was exposed to the PEMF pulse at the sphere/blastula stage (7 hpf), shortly after the initiation of embryonic mRNA transcription [Zamir et al., 1997]. The fourth group was divided into four subgroups: embryos not exposed to the PEMF (controls), embryos exposed to the PEMF at the 4 somite stage (27 hpf), embryos exposed to the PEMF at the 13 somite stage (31 hpf), and embryos exposed to the PEMF at the 25 somite stage (48 hpf). The timing of exposure to the PEMF pulses of these four subgroups was designed to coincide with the time of cardiovascular development in zebrafish (between the 21 and the 26 somite stages) [Stainier et *al*., 1993].

For the caudal fin regeneration study, adult zebrafish were anesthetized in a 10µmol Tricaine solution and the distal one-half of each fish's caudal fin was amputated. Afterwards, the fish were returned to tanks of distilled water and fed brine shrimp every third day. To assess regeneration at 2 days, 7 days and 13 days post-amputation, the fish were anesthetized in 10µmol solution at these times and the amputated fin regeneration areas were determined by assessment of the ratio of the tail fin area regeneration to the tail fin area remaining after amputation. Tail regeneration was observed using images captured using a Nikon CoolPix 995 CCD camera mounted on a Nikon Optiphot microscope using a 4x objective.

To further assess tail fin regeneration, the number of new bone centers per fin ray of the middle five rays from each fish was scored. Finally, the number of fin rays with bifurcated bone segments at the distal end was scored.

Statistical analyses consisted of one- and two-way ANOVA followed by Student Newman Keuls multiple range test. Linear regression analyses were used to assess correlations.

Results

Figure 2 summarizes the results of daily exposure of zebrafish embryos to the 10 minute PEMF. Both the PEMF and the no PEMF controls each had at least 20 embryos. There were no significant differences at any of the times of scoring and the variance from the mean values was so small as not to be visible within the experimental points on the figure. No significant differences were found between the two groups at any time post-fertilization. Linear regression analysis gives a significant linear fit of data.

The slope of the mean rate of embryo development was 0.4983 ± 0.0142 for the control embryos and was 0.4985 ± 0.0147 for the embryos exposed to the daily PEMF. These slope values are not significantly different. The slopes of both the control and the daily PEMF groups, both at 21^{o}C, differed significantly from the reference values at 28.5^{o}C ($p<0.001$).

When embryos were exposed to a single pulse of the PEMF at either the 8 cell stage (1.6 hpf), the 64 cell stage (2.5 hpf), or the sphere/blastula stage (7 hpf) and were followed to the 4 somite stage (26 hpf), no significant differences in development were detected compared to the untreated controls (data not shown).

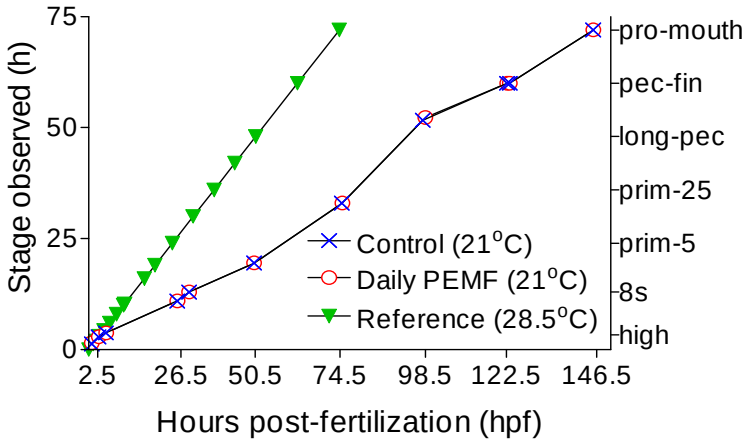


Figure 2 Temperature and 10 minute daily exposure to PEMF on development. The time post-fertilization to reach each stage at 28.5°C (from Kimmel et *al*., 1995) is plotted on the left y-axis. Corresponding morphological stages are listed along the right y-axis. Stage abbreviations used are 8 somite (8s) and protruding mouth (pro-mouth). Times of PEMF exposures are labeled on the x-axis.

In an attempt to bracket PEMF pulse exposure to the time of cardiovascular development in the fish embryo, a single pulse of PEMF was given to subgroups of embryos at: the 4 somite stage (27 hpf), the 13 somite stage (31 hpf), and the 25 somite stage (48 hpf). The results are illustrated in Fig. 3.

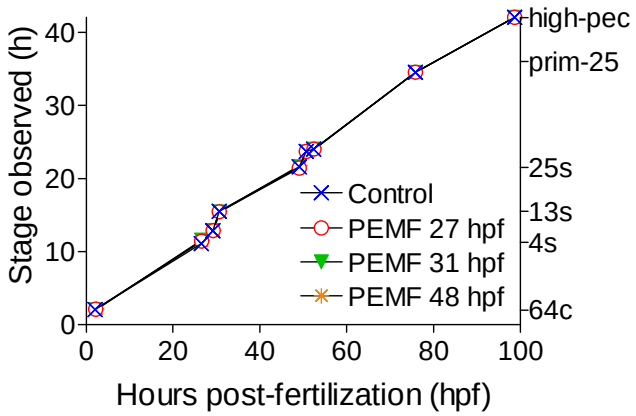


Figure 3 Effect of the PEMF exposure before (4 somite stage, 27 hpf) just prior to (13 somite stage, 31 hpf) and at the end of (25 somite stage, 48 hpf) development of a functional cardiovascular system in the zebrafish embryo (21 to 26 somite stage) [Stainier et *al*., 1993] on rate of embryonic development. The time post-fertilization to reach each stage at 28.5°C (from Kimmel et *al*., 1995) is plotted on the left y-axis. Corresponding morphological stages are listed along the right y-axis. Stage abbreviations used are 64 cell (64c), 4 somite (4s), 13 somite (13s) and 25 somite (25s). Linear regression analyses of the slopes of each of the four groups of embryos from the time of the first PEMF exposure (27 hpf) to the conclusion of the experiment (100 hpf) revealed no significant differences in the rate of development due to PEMF exposure compared to the untreated controls (see text for slope statistics).

There were no significant differences between the four groups at any time after treatment. Variance around the mean values was so small as not to be visible within the points in Fig. 3. Statistical analyses of mean rate of development slopes of each of the four embryo groups yielded the following linear regression slopes: 0.445 ± 0.0075 for the control embryos, 0.4441 ± 0.0073 for the embryos exposed to TEMF 27 hpf, 0.4443 ± 0.0070 for the embryos exposed to the PEMF 31 hpf, and 0.4449 ± 0.0072 for the embryos exposed to the PEMF 48 hpf. These mean slope values are not significantly different.

Table 1 summarizes the results of zebrafish caudal fin regeneration with and without a 10 minutes per day exposure to the PEMF. The ratio of the area regenerated to the area remaining after amputation is presented at 2, 7 and 13 days post-amputation. Statistical analysis reveals a significant increase with time post-amputation but no significant difference between the fish that were exposed to the PEMF and the fish that were not exposed to the PEMF. Likewise, the scoring of newly forming bone centers per fin ray reveals differences with time after amputation but no significant differences between fish with or without the daily PEMF. As fin rays increased in length, they were each observed to have a centrally located artery with veins on each side. Capillaries with circulating blood cells were observed between adjacent rays, indicating return of normal blood vessel morphology by 19 days post-amputation.

Table 1 Analysis of Zebrafish Caudal Fin Regeneration With and Without Daily PEMF Treatments Mean $\pm$ SEM (n=5 fish per group)[a]

Time after amputation in day	Area regenerated / Area remaining after amputation	New bone centers/fin ray[b]
Day 2 - PEMF	.042 $\pm$ .008	0
Day 2 + PEMF	.045 $\pm$ .010	0
Day 7 - PEMF	.739 $\pm$ .140	.600 $\pm$ .167
Day 7 + PEMF	.536 $\pm$ .087	.320 $\pm$ .136
Day 13 - PEMF	1.279 $\pm$ .247	4.320 $\pm$ .361
Day 13 + PEMF	1.258 $\pm$ .168	4.320 $\pm$ .382

[a] Results of two-way ANOVA: Significant increases with time ($p<0.001$) but no significant differences between the group receiving daily PEMF exposure and the group not receiving daily PEMF exposure.

[b] Five middle fin rays were scored in each fish.

Another measurable indicator of fin regeneration is bifurcation of fin rays. As time of regeneration increased, the number of fin rays demonstrating bifurcation increased. The mean percentage of fin rays demonstrating bifurcation did not differ significantly between the control and the PEMF treated experimental groups. For instance, at 13 days post-amputation the PEMF group had (21.0 ± 5.6) % of rays with bifurcation while the control group had (18.8 ± 7.3)% of rays with bifurcation. At 19 days post-amputation, the PEMF group had (70.2 ± 9.4) % of rays with bifurcation while the control group had (68.3 ± 19.0) of rays with bifurcation. Adults whose tails were not amputated and all of the fish in this study with tail amputation demonstrated 100% of the fin rays with bifurcation by 24 days post-amputation.

Discussion

It was shown that a single 10 minute exposure to the PEMF given at either the 8 cell stage (1.6 hpf) or at the 64 cell stage (2.5 hpf) did not delay development indicates that the PEMF is not acting to slow or to interfere with nuclear DNA synthesis, mitosis, or cytokinesis, all of which take place during these synchronous cell division stages. A single 10 minute exposure to the PEMF at the sphere/blastula stage (7 hpf) did not delay development indicates that the PEMF did not interfere with production of zygotic mRNA synthesis known to be needed for continued embryonic development at this stage of development [Zamir et *al*., 1997].

The timing of a pulse of the PEMF at the 4 somite (27 hpf), the 13 somite (31 hpf) or the 25 somite (48 hpf) stages (at times before, just prior to and just after initiation of heart tube formation, respectively)

suggests that the PEMF exposure at these stages of development did not delay normal cardiovascular development known to occur between the 21 and 26 somite stages [Stainier et *al*., 1993]. Clearly, use of the PEMF did not delay embryonic development using any of the experimental conditions tested.

Zebrafish continue to grow throughout life, and fin ray growth occurs by distal addition of bony segments [Iovine and Johnson, 2000]. The caudal fin is a usable model for studying genetics of regeneration [Poss et al., 2002, Akinemko et *al*., 1995] and also as a tool for evaluation of the effects of drugs and natural products [White et *al*., 1994, Santos-Ruiz et *al*., 2001, Zodrow and Tanguay, 2003]. The regeneration process involves: blastema formation, bone formation, nerve regeneration, and formation of new blood vessels (angiogenesis). Because of the usefulness of the regenerating tail fin model for the evaluation of the action of drugs and natural products, it was decided to evaluate the effects of a 10 minutes per day pulse of the PEMF on tail fin regeneration. The question was would a daily 10 minute pulse of PEMF treatment suppress regeneration of the caudal fin of adult zebrafish following partial amputation of the fin? Based on the experimental data in this report, the answer is no.

The failure of daily PEMF to delay development of fish embryogenesis and to delay fin regeneration indicates that daily exposure to the PEMF is without measurable effect. However, the same daily PEMF exposure was effective at slowing growth and angiogenesis of a rapidly growing transplantable tumor in mice [Williams et *al*., 2001, Cameron et *al*., 2005]. What might account for a lack of effect of PEMF on fish development and on wound repair as well as the report that the PEMF inhibits growth and angiogenesis of a transplantable breast cancer in nude mice. One possible explanation may be differences in angiogenesis in the different experimental systems. In the rapidly growing tumor, the cancer cells proliferate so rapidly that development of the needed vascular supply cannot keep pace, thus resulting in hypoxic regions within the tumor. The hypoxic cancer cells respond by production of hypoxia inducible factor, leading to release of vascular endothelial growth factor, which stimulates the subsequent sprouting of new endothelial cell pseudopods into the hypoxic areas of the tumor [Wachsberger et *al*., 2003, Cameron et *al*., 2005]. This eventually leads to formation of new capillaries and blood vessels. Clearly, the angiogenesis process in this tumor system is hypoxia driven. On the other hand, angiogenesis during normal fish development and tail fin regeneration appears not to be hypoxia driven, perhaps because diffusion of oxygen to the embryo and to the regenerating tail fin is adequate enough to avoid hypoxic conditions during normal embryonic development and tail fin regeneration. Thus, angiogenesis in the fish embryo and in fin regeneration may not be hypoxia driven whereas angiogenesis in the rapidly growing tumor is hypoxia driven. This difference between systems may account for the observed differences in response to PEMF. It seems unlikely that zebrafish embryos and adults experienced hypoxia under the experimental conditions based on the fact that induced oxygen deprivation does cause arrest of zebrafish development and heartbeat until returned to normoxia (Padilla and Roth, 2001). A testing of this hypothesis is planned by the authors.

References

1. Akimenko M-A, Johnson SL, Westerfield M, Ekker M. 1995. Differential induction of four *msx* homeobox genes during fin development and regeneration in zebrafish. Development 121:347-357.
2. Cameron IL, Sun LZ, Short N, Hardman WE, Williams CD. 2005. Therapeutic electromagnetic field (TEMF) and gamma irradiation on human breast cancer xenograph growth, angiogenesis and metastasis. Can Cell Int. 5:23.
3. Ferretti P, Géraudie J. 1998. *Cellular and Molecular Basis of Regeneration: From Invertebrates to Humans*. New York: Wiley Press.
4. Iovine MK, Johnson SL. 2000. Genetic analysis of isometric growth control mechanisms in the zebrafish caudal fin. Genetics 155:1321-1329
5. .Johnson SL and Weston JA. 1995. Temperature-sensitive mutations that cause stage specific defects in zebrafish fin regeneration. Genetics 141:1583-1595.
6. Kimmel CB, Ballard WW, Kimmel SR, Ullmann B, Schilling TF. 1995. Stages of embryonic development of the zebrafish. Developmental Dynamics 203:253-310.
7. Padilla PA, Roth MB. 2001. Oxygen deprivation causes suspended animation in the zebrafish embryo. PNAS 98:7331-7335.
8. Poss KD, Nechiporuk A, Hillam AM, Johnson SL, Keating MT. 2002. Mps1 defines a proximal blasternal proliferative compartment essential for zebrafish fin regeneration. Development 129:5141-5149.
9. Santos-Ruiz L, Santamaría JA, Becerra J. 2001. Differential expression of FGF receptors during zebrafish fin regeneration. Int J Dev Biol 45(S1):S131-S132.

10. Stainier DYR, Lee RK, Fishman MC. 1993. Cardiovascular development in the zebrafish. Development 119:31-40.
11. Wachsberger P, Burd R., Dicken AP. 2003. Tumor response to ionizing radiation combined with antiangiogenesis or vascular targeting agents: exploring mechanisms of interaction. Clin Can Res 9: 1957-1971.
12. Westerfield M. 1989. *The Zebrafish Book.* Oregon: University of Oregon Press.
13. White JA, Boffa MB, Jones B, Petkovich M. 1994. A zebrafish retinoic acid receptor expressed in the regeneration caudal fin. Development 120:1861-1872.
14. Williams CD, Markov MS, Hardman WE, Cameron IL. 2001. Therapeutic electromagnetic field effects on angiogenesis and tumor growth. Anticancer Res 21:3887-3892.
15. Williams CD, Markov MS. 2001. Therapeutic electromagnetic field effects on angiogenesis during tumor growth: a pilot study in mice. Electro-and magnetobiology 20:323-329.
16. Zamir E, Kam Z, Yarden A. 1997. Transcription-dependent induction of G1 phase during the zebra fish midblastula transition. Mol Cell Biol 17(2):529-536.
17. Zodrow JM, Tanguay RL. 2003. 2,3,7,8-tetrachlorodibenzo-p-dioxin inhibits zebrafish caudal fin regeneration. Toxicol Sci 76(1):151-161

Acknowledgements

The authors wish to thank Matt Cykowski for help with animal handling and photography.

EMF RISK FOR OPERATORS MOUNTING, ADJUSTING AND MAINTAINING BASE STATIONS

Ts. Shalamanova, I. Iliev, M. Ivanova, M. Israel

National Center of Public Health Protection, Sofia, Bulgaria

ABSTRACT

There are many publications in the last years about the risk of radiofrequency (RF) exposure to the general population from base stations for mobile communication. Unfortunately, very few of them concern the risk to the personnel mounting and maintaining these systems.

Here, we present a pilot study of the exposure to the personnel in selected objects with different types of antennae mounting.

The exposure assessment is made according to the typical work positions corresponding to the operations of the personnel. Calculations of the energetic load are made on the basis of the Bulgarian national legislation.

The data show that the maximal values of power density measured at distances up to 50 cm in front of the antennae reach to 2.5 mW/cm^2. In other locations of the worker: behind, aside and under the antenna, measured values are logically much lower, and corresponding to the exposure limits of ICNIRP Guidelines.

Basing on the results, we recommend future studies in this fields and a special attention to this personnel because of the possible risk of RF overexposure

We propose special protective measures for this particular work group.

INTRODUCTION

There are a lot of recent publications dealing with the emission of mobile communication antennae in settlements affecting the population health. Unfortunately, the results are contradictory and more evidences are needed for the possible effect of electromagnetic fields (EMF) at frequency 900 MHz and 1800 MHz which provokes diseases like cancer, cardiovascular disorders and other health consequences among the population.

Furthermore, little attention was paid to the risk of RF exposure on service staff of base stations and mobile communication antennae up to now. There is evidence that despite the special requirement of the manufacturers that service operations should be performed when antennae are switched off, the personnel frequently works when the antennae emit, i.e. without interrupting the emission, and very close to them. Mild (1) reports similar practice among the service staff of base stations and antennae in Sweden.

AIM AND SCOPE

This study is aimed at assessing the risk of the microwave EMF radiation for the service staff of base stations and mobile communication antennae.

For this purpose typical antennae systems were investigated on routine operations of the personnel which they perform close proximity and around antennae. EMF values were measured and exposure assessment is made for each particular operation. Energetic loading of the organism and whole body SAR were calculated as well. The scenario, technological operations and their average duration were presented by the mobile operator.

The object of investigation is personnel working on base stations antennae emitting EMF with frequencies about 900 MHz, and UMTS systems with 2100 MHz.

On pictures No. 1, 2 and 3 are presented various technological operations in the close proximity of a single antennae for which were made corresponding measurements and evaluations.



Pic. 1
Operation aside and in front of emitting antenna



Pic. 2
Operation behind the antenna



Pic. 3
Operation close to the connectors (lower edge)

On pictures No. 4 and 5 are presented various technological operations in the close proximity of more than one antennae (mounted a pole) for which were made corresponding measurements and evaluations.



Pic. 4
Operation between antennae



Pic. 5
Operation close to lower edges of antennae

This study does not deal with the exposure close to antennae, mounted on telecommunication masts.

The study covers temporary workplaces for adjustment, maintenance and repair of antennae, mounted on base stations. The selected sites cover all possible working conditions, under which the respective service tasks are performed by the staff.

EXPOSURE ASSESSMENT

The evaluation of electromagnetic effects was performed at two stages:

1. Measurement of EMF for various procedures performed by the personnel and evaluation of the compliance with the respective exposure limits

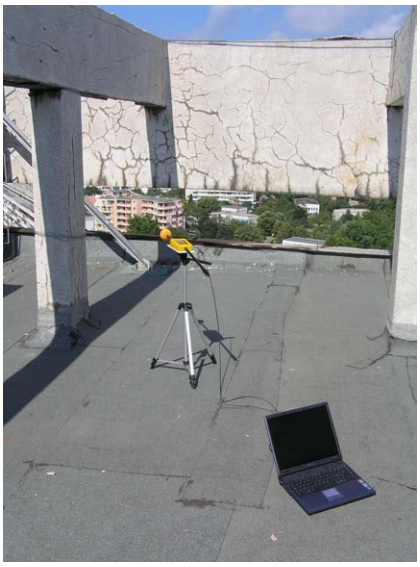
2. Evaluation of the energetic loading (exposure assessment) for various processes, activities and shifts and its compliance with the respective limit values of Bulgarian and European standards.
3. Calculation of Specific Absorption Rate, SAR W/kg.

METHOD AND MATERIALS

Measurement equipment:

Power - meter 'NARDA', model EMR-21C of "NARDA Safety Test Solutions'

The evaluation was performed according to national [2,3], and international standards. [4,5]



Pic. 6
Measurement equipment

Table 1. shows the limit values according to the normative documents listed above.

Table 1

Standard	Power density S, μW/cm^2	Average time t, h	SAR W/kg	Energetic loading W, μW.h/cm^2
ICNIRP				
900 MHz	2250	0.1	0.4	-
1800 MHz	4500	0.1	0.4	-
2100 MHz	5000	0.1	0.4	-
BSS 17137-90				
900 MHz	1000	1	-	200
1800 MHz	1000	1	-	200
2100 MHz	1000	1	-	200

MEASUREMENT METHOD

Measurements were made in wide frequency range by nonselective method.

All measurements were made in few selected typical sites. Measuring device was chosen with probe sensitive to electrical component of EMF.

To avoid human influence on the measurement process handle and optical cable connected to the device. Data were collected using Narda EMR-21C software, installed on laptop. In cases when the height of antenna mounting allows performing measurements from the rooftop level the equipment was mounted on tripod.

Data were collected considering the typical work positions of base station service workers. The average (averaged over 1.5 min) and maximum power densities were measured. The average values for 1.5 min were measured in order to assess the compliance with the international guidelines (ICNIRP), which require determining the (measured) 'reference' values for 6-minute period (0.1 h). This facilitates also the further determination of the energetic loading performed for 1 h. It was calculated with respect to the mean time for performing the above-mentioned work tasks.

In the far field zone, the values of SAR and energetic loading coincide for external exposure to radiation of a 'human equivalent antenna' (receiving antennae equipment corresponding to the resonance and subresonance absorption of incident energy by an average human body size).

Energetic loading of the organism was calculated considering average time duration for performing the described above operations.

On pictures No. 7 to 11 are shown spots where measurements were performed according to the technological operations of the personnel.



Pic. 7



Pic. 8



Pic. 9



Pic. 10



Pic. 11

RESULTS OF MEASUREMENTS AND CALCULATIONS

The results of measurements are shown according to the tasks performed by the service staff of mobile communication antennae and base stations. The measurement points correspond to the location of the subjects at work with respect to the antennae.

In Table 2 are shown the measured values of power density, calculated values of energetic loading of the organism, permissible time duration and whole body SAR values as well.

Table 2

No	Point of measurement according to working position	Measured values		Permissible time duration, t_{max},	Energetic loading of the organism		Operation duration	SAR, W/kg
		S_{avg}, $\mu W/cm^2$	S_{max}, $\mu W/cm^2$		W_{avg}, $\mu W.h/cm^2$	W_{max}, $\mu W.h/cm^2$		
1	2	3	4	6	7	8	9	10
CDMA antennae								
1	**Operation on changing the position of the antenna**	62.00	180.00	1h7min	31.00	90.00	30min	0.012
2	**Single Antennae**							
2.1	**Operation in a close proximity of antennae**							
2.1.1	**Operation behind antennae**	12.00	47.00	4h15min	24.00	94.00	2h	0.002
2.1.2	**Operation in front of antennae**	1240.00	2500.00	Not permissible	2480.00	5000.00	2h	0.242
2.1.3	**Operation close to the lower edge of antennae**	227.00	403.00	30min	454.00	806.00	2h	0.044
2.2	**Operation near emitting antennae (distance up to 2 m)**	390.00	820.00	15min	780.00	1640.00	2h	0.076
2.3	**Operation along the feeder line**	-	6.40	>8h	-	25.60	4h	0.001
3	**Antennae mounted on a pole (wrist type)**							
3.1	**Operation in a close proximity of more than one antenna**							
3.1.1	**Operation in the area among antennae, on a pole**	20.10	27.60	7h15min	120.60	165.60	6h	0.004
3.1.2	**Operation between side edges of antennae**	39.30	73.10	2h44min	235.80	438.60	6h	0.007
3.1.3	**Operation close to the lower edge of antennae**	235.60	620.90	19min	1413.60	3725.40	6h	0.046
3.1.4	**Operation on new near emitting antennae**	331.00	1223.00	Not permissible	1986.00	7338.00	6h	0.064

1	2	3	4	6	7	8	9	10
UMTS antennae								
2	**Single Antennae**							
2.1	**Operation in a close proximity of antennae**							
2.1.1	**Operation behind antennae**	45.00	86.50	Not permissible	888.00	2694.00	2h	0.006
2.1.2	**Operation in front of antennae**	444.00	1347.00	2h19min	90.00	173.00	2h	0.062
2.1.3	**Operation close to the lower edge of antennae**	29.00	60.00	3h20min	58.00	120.00	2h	0..004
2.2	**Operation on new near emitting antennae**	72.80	117.30	1h42min	145.60	234.60	2h	0.010
2.3	**Operation along the feeder line**	-	4.30	>8h	-	17.20	4h	0.001

ANALYSIS OF RESULTS AND CONCLUSIONS

The average and maximum power density S measured at the temporary workplaces for adjustment, maintenance and repair works exceed the limit values of both Bulgarian and European standards. The same is true for all works performed close to antennae at a distance up to 1 m during radiation. Even for short-duration tasks (for up to 2 h) the EMF values exceed the limits. When they are below them, the calculated energetic loading is above the limit.

The energetic loading is within the permissible limits only during works done behind the antennae or along the antenna-feeder lines.

Nevertheless high measured values of power density and calculated values of energetic loading of the organism calculated whole body SAR values correspond to the ICNIRP guidelines basic restriction for occupational exposure. Our legislation is stringent and in some operations forbids stay in such conditions. Although compliance of SAR values to the guidelines we consider that the personnel exposure especially on particular operations is significant.Therefore employers should take the following measures in order to protect the workers' health:

- technological operations in the close proximity of antennae should be performed after switching off emitters;
- use of personal protective equipment (clothes, glasses, etc.) when it is not possible to switch antennae off,
- when protective equipment is not used, combinations of technological operations should be made respecting the following limitation of the exposure:

$$\frac{\Sigma W_i}{W_н} \leq 1,$$

where Wi is the total energetic loading of the organism resulting from the "i" - technological operation;
Wlim is the maximum permissible energetic loading of the body according to the national standards.

Others not less important recommendations for the operators' safety work are the followings:

- permissible time duration specified in Bulgarian regulations should be kept;
- workers should use personal dosimeters, which provide data about the cumulated dose;
- periodical training of the staff about the risks of EMF and protection;

In conclusion, a high risk for EMF exposure is found for workers mounting and maintaining base stations for mobile communication. Hence, measures should be taken to improve the working conditions with respect to EMF by decreasing radiation, carrying administrative and organizational measures, ensuring continuous monitoring and personal protection. The energetic loading should be regularly assessed, while the field should be currently monitored by personal dosimeters. Periodical medical check-ups done by neurologist, cardiologist, therapist and ophthalmologist should be included into the prophylaxis program. Last but not least, the qualification of the staff in standards, biological effect, methods of measurement and protection against microwave fields should be currently maintained. Special attention should be paid to workers with active implants.

Bibliography

1.Mild, K. H., *et.al*, Occupational RF exposure from base stations antennae on roof-tops and buildings, Workshop, Base stations and wireless networks, 15-16 June, 2005, WHO, Geneva.

2. **Ordinance No 7 of 23.09.1999** of the MLSP and the MH on the minimum requirements for healthy and safe working conditions in workplaces and in the use of working equipment (SG No 88/1999.)[2]

3. **Bulgarian State Standard (BSS)17137-90**. Occupational hygiene. Electromagnetic microwave fields. Allowable values and control requirements [3].

4.Guidelines for limiting exposure to time varying electric, magnetic, and electromagnetic fields (up to 300 GHz), ICNIRP, Health Physics, April 1998, Vol.74, No.4.

5.Directive 2004/40/EC of the European parliament and of the council of 29 April 2004 on the minimum health and safety requirements regarding the exposure of workers to the risks arising from physical agents (electromagnetic fields) (18^{th} individual Directive within the meaning of Article 16(1) of Directive 89/391/EEC).

DIRECT AND MEDIATED EFFECTS OF THE EXTREMELY HIGH FREQUENCY COHERENT ELECTROMAGNETIC RADIATION (MILLIMETER WAVES) WITH LOW INTENSITY ON BACTERIA

TADEVOSYAN H.[1], KALANTARYAN V.[2], TRCHOUNIAN A.[1*]

Departments of Biophysics[1] and of High Frequencies Radiophysics and Telecommunication[2] of the Yerevan State University,
1 Alex Manoukian Str., 0025 Yerevan, Armenia
[*]E-mail: Trchounian@ysu.am

Abstract

In addition to bactericidal effect of "noise" electromagnetic irradiation (EMI) of extremely high frequencies [1-2], the coherent EMI of such frequency (the range of frequencies from 45 to 53 GHz) or millimeter waves (the wavelength of 5.6 to 6.7 mm), with low intensity (the flux capacity of 0.06 mW/sm^2), upon direct irradiation (during 30 min or 1 h), affected *Escherichia coli* K12, wild-type, grown under anaerobic conditions with fermentation of sugar (glucose): it caused a decrease in bacterial growth rate, maximal inhibitory effect was achieved at the frequency of 51.8 or 53 GHz. This effect depended on medium pH, the maximal one was at pH 7.5. The noticeable changes in membrane proton conductance, membrane potential, proton fluxes through the membrane of whole cells and total and *N,N'*-dicyclohexylcarbodiimide (DCCD)-inhibited ATPase activity of membrane vesicles were determined. These membranous effects might be accounted in action of EMI. A decrease in sensitivity to reagents (DCCD) by cells was also determined. Moreover, EMI had mediated effects on bacteria. Separate irradiation (the frequency of 51.8 and 53 GHz) of doubly distilled water or some inorganic ions containing Tris-phosphate buffer (pH 7.5), into which grown cells were transferred, during 30 min or 1 h, had changed further growth of these bacteria in different, opposite directions; irradiation of water only caused inhibitory effect. These might point out a role of water in the effects of EMI of extremely high frequency on bacteria. A significant action disappeared upon repeated irradiation at the frequency of 51.8 and 53 GHz during 1 h and with interruption for 2 h. This result indicates some compensatory mechanisms within bacteria.

The *keywords*: coherent electromagnetic radiation of extremely high frequency, bacterial growth, membranous effects, resonant frequencies, water.

INTRODUCTION

The bacterial effects of the electromagnetic irradiation (EMI) of extremely high frequencies, or millimeter waves, with low (low-energetic) intensity and with non-thermal action, are of interest because of two reasons, at least. First of all, bacteria and other cells can interact with each other through EMI (for reviews, see [3-4]). It has been shown, for instance, that bacteria possess the ultrasonic radiation [5-7] or reemission of secondary photons in sub-millimeter frequency range [8]. However radiation of extremely high frequency is not clearly registered in spite of the fact that fine methods have been developed and enough sensitive instruments have been already constructed for last years [9-10]. Secondly, EMI of extremely high frequency is widely used in telecommunication technology and therapeutic practice [2, 11] although low-orbital systems of cosmic communication and different elements of mobile one, and in addition, low-energetic devices used in therapeutic practice radiate EMI of this frequency, small and very small doses of which (low flux capacity of 0.005 mW/sm^2) might affect cells.

The coherent and so named "noise" (with broadband frequencies and accidentally changing phases) EMI of extremely high frequencies with low intensity have been shown to cause different, including bactericidal effects on *Escherichia coli* and the other bacteria [10-14]. Such effects depend on phase and anaerobic or aerobic conditions of

the bacterial growth, composition of growth media, genetic features and peculiarities of the metabolism in bacterial strains. Together with these, coherent and noise EMI of extremely high frequencies can render the different bacterial effects depending on frequency and intensity of EMI, duration of the irradiation and the other parameters [1-2]. Moreover, studies on repeated and mediated action of noise EMI on *E coli* [2] have allowed expecting compensatory mechanisms and role of other factors.

Among cellular mechanisms of bacterial effects of EMI of extremely high frequencies, the membranous changes connected with surface characteristics of plasma membrane, ion and other substances transport across the membrane and energy-conversing processes [1-2, 12-13] are of significance. Action of EMI of extremely high frequency is offered also on structure and properties of water [14-16] leading, for instance, to increase in chemical activity of water or hydration of proteins and other cellular structures. These could also relate to modifications of structure, properties and function of membrane, especially membrane proteins. On the other side, conformational changes in bacterial genome or DNA are also suggested [17]. Bactericidal effect might be determined by transition of bacterial pro-phages from lysogenic to lytic state [18-19].

Finally, effects of such EMI can be a result of the resonant interaction, when in case with *E coli* it is shown that, regardless of intensities of EMI of extremely high frequency, resonance is at the frequencies of 41.5, 51.8 or 70.6 GHz [17-19]; other resonant frequencies are not ruled out. However, effects of EMI on these and other bacteria and cells in generally, especially primary cellular mechanisms of these effects, require the further study.

In the present report with fermenting *E coli*, grown in anaerobic conditions, it is shown that maximal inhibitory effect of coherent EMI of extremely high frequency on bacterial growth rate was observed at the frequencies in 51.8 or 53 GHz. The changes in membrane properties and functions have been determined. The certain effects might be mediated by the other factors and changed by repeated irradiation.

MATERIALS AND METHODS

E coli K12, wild type strain, was used in the study.

The methods for bacterial growth in peptone medium (0.2 % peptone, 0.5 % NaCl and 0.2 % K_2HPO_4) at slightly alkaline (pH 7.4) or the other (specified in text) pH in anaerobic conditions upon fermentation of sugar (glucose, 0.2 %) [1, 20] and determination of bacterial specific growth rate (μ) [1, 21] were described elsewhere. The methods for preparation of whole cells for assays and isolation of membrane vesicles [21-22], for determination of membrane proton conductance (G_m^{H+}) [23], membrane potential ($\Delta\Psi$) [24] and energy-dependent proton efflux (J_H^+) [1, 23-24] from whole cells as well as of ATPase activity of membrane vesicles [21-22], and, in addition, for data processing [25] did not differ from widely described.

The pH of growth medium and assay solutions was measured by using a fine pH-potentiometer with selective (pH) electrode and adjusted by means of HCl and NaOH, although pH of doubly distilled water was 6.5 and did not changed when kept during 2 days at 4 ^{0}C in spite of its less-buffering capacity. The dry weight of bacteria and protein were determined by the method described by Trchounian and Vassilian [21] and Lowry et al. [26], correspondingly. Bacterial titer was calculated by counting colonies grown on solid media with glucose after plating of diluted bacterial suspension.

The irradiation of *E coli*, water or the other solution was produced by means of generator G4-141 (radiating the coherent electromagnetic waves with frequency within the range of 45 to 53 GHz, wavelength of 5.6 to 6.7 mm, correspondingly; the flux capacity was of 0.6 mW/sm^2). The generator was assembled in the Institute of Radiophysics and Electronics of the National Academy of Sciences of Armenia (Ashtarak City). For the others, the conditions of the irradiation of bacteria were similar to those described previously [1]. After direct irradiation of bacterial suspension (grown cells concentrated by centrifugation in water), cells were immediately transferred into the fresh growth (with glucose, 0.2 %) or assay medium.

At determination of the mediated influence of EMI of extremely high frequency on *E coli*, grown cells were transferred into the distilled water or buffer (Tris-phosphate, pH 7.4) containing 0.4 mM $MgSO_4$, 1 mM KCl and 1 mM NaCl, and then, after incubation of 10 min, growth or other assays were carried out immediately. Water or buffer was irradiated during 30 min or 1 h as specified in text. The repeated influence of EMI of extremely high frequency was conducted with interruption of 2 h.

The data processed to be statistical with determination of the standard error and of the Student's validity criteria (p) [26].

RESULTS AND DISCUSSION

Inhibitory effect of coherent EMI of extremely high frequency on bacterial growth

Bactericidal effect of "noise" EMI with frequencies of 53.5 to 68 GHz on *E coli* was installed earlier [1-2]. If such effect is conditioned resonant interaction of EMI of extremely high frequency with bacteria, the range of frequencies of "noise" EMI used does not include the resonant frequencies in 41.5, 51.8 or 70.6 GHz shown for *E coli* [17-19]; the other resonant frequencies may be allowed. Therefore a study of bacterial effects of the coherent EMI with resonance frequency in 51.8 GHz, which is radiated by the generator used (see Materials and methods) was done. Together with this, effects of EMI of extremely high frequency hang from conditions of the growing bacteria [1-2, 11-13] and they can differ in anaerobic conditions, favorable for the majority of pathogenic and conditionally pathogenic bacteria, therefore studies conducted with *E coli*, grown in anaerobic conditions under fermentation of sugar.

Irradiation of *E coli* K12 by coherent EMI with the coherent frequency of 45 to 53 GHz during 30 min (not shown) or 1 h (Fig. 1) brings a gradual decrease in the specific rate of bacterial growth for the frequency of 49 GHz, moreover maximal inhibitory effect was observed at the frequency of 51.8 or 53.0 GHz. Such result complies with those the frequency of 51.8 GHz is resonant for *E coli* [17-19] and, on the other side, the exposition of 1 h is effective to inhibit bacterial growth [11]. The resonances in which proteins and other macromolecules can be entered probably are the basis of membranous and the other mechanisms of the action on bacteria and define bactericidal effect of EMI of extremely high frequency.

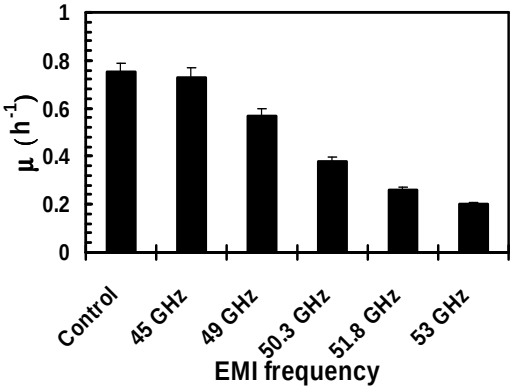


Fig. 1. The changes in the growth rate of *E coli* K12 after direct irradiation with coherent EMI of extremely high frequency. The specific growth rate (μ) was defined as 0,693/time of the reduplication to absorbance (OD) in bacterial suspension (when logarithm of OD linearly increased at time) [10-11]; in checking control, bacteria without irradiation. For the others, see Materials and methods. The average values are from not less than three independent experiments with standard errors.

Note that the inhibitory effect of coherent EMI of extremely high frequency on bacterial growth depends on duration of the irradiation: increase in time of the direct irradiation from 30 min to 1 h at the frequency of 51.8 or 53.0 GHz brings about reinforcement of the effect in 2.2- or 1.6-fold, respectively.

A dependence of the action of EMI of extremely high frequency on *E coli* from pH is of interest: under pH 6.0 and 8.0 in contrast with pH 7.5, inhibitory effect noticeably decreased (Tabl. 1.). Since the specific growth rate practically does not depend on medium pH in noted range (not shown), the change in this rate after irradiation can be indicative of some process as in cells themselves, so and in water medium with determined reaction (pH), in which bacteria grow. Probably, a slightly alkaline medium (pH 7.3-7.5) is chosen not accidentally as the most optimal for growing *E coli* (neutrophilic bacteria) [27].

Table 1. The specific growth rate of *E. coli* K12 irradiated by EMI of extremely high frequency at different pH.

pH*	Growth rate (h^{-1})		
	Control	51.8 GHz	53.0 GHz
6.0	0.86 ± 0.05 (100 %)	0.63 ± 0.03 (73.3 %) ($p<0.05$)**	0.60 ± 0.03 (69.8 %) ($p<0.05$)
7.5	0.82 ± 0.03 (100 %)	0.52 ± 0.02 (34.7 %) ($p<0.01$)	0.34 ± 0.02 (26.7 %) ($p<0.002$)
8.0	0.77 ± 0.03 (100 %)	0.70 ± 0.05 (91.0 %) ($p<0.05$)	0.50 ± 0.02 (64.9 %) ($p<0.05$)

* irradiation time was 1 h, for the other conditions, see Materials and methods and the legends to Fig. 1.

** p is calculated for the difference between the values in checking control and obtained ones; percentage is determined in relation to checking control (100 %).

On mechanisms of bacterial effects of EMI

Determination of some properties and of activity of some key membrane-associated enzymes having a key role in ion and the other substances transport and energy conversation could be of much interest to reveal mechanisms of bacterial effects of EMI. The marked changes in G_m^{H+} (Fig. 2A), $\Delta\Psi$ (Fig. 3) and energy-dependent proton efflux (Fig. 2B) were shown followed irradiation of *E coli* K12 by EMI with the resonant frequency of 51.8 [17-19] or 53 GHz. It is possible to suggest some relationship between these properties of the membrane since the changes in the values of G_m^{H+} and $\Delta\Psi$ were in opposite directions and moreover J_H^+ decreased upon irradiation. Such relationship between G_m^{H+} and $\Delta\Psi$ has been proposed by Akopyan et al. [23] requiring a further study. These changes in the properties of the bacterial membrane might be of significance and could be accounted for decrease in bacterial growth rate.

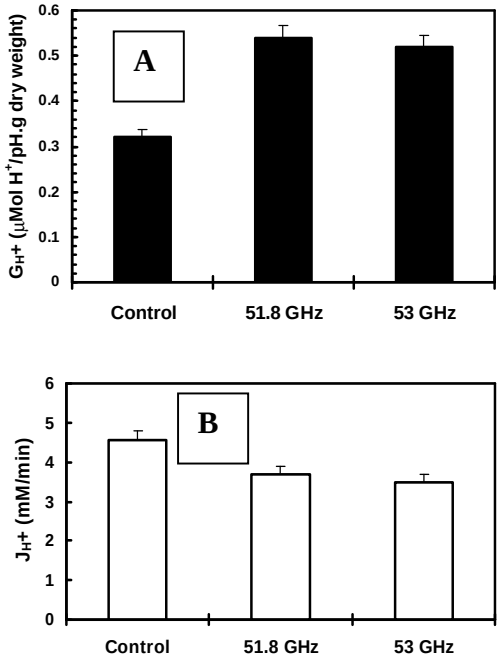


Fig. 2. Changes in membrane proton conductance (G_m^{H+}, A) and energy-dependent proton fluxes (J_H^+, B) of of *E coli* K12 after direct irradiation with coherent EMI of extremely high frequency. The irradiation time was 1 h, the frequency was shown. G_m^{H+} was determined by an acid-pulse technique used before [23]. Energy-dependent ion fluxes were determined by using selective (pH) electrode upon glucose (22 mM) adding; the values represented are for bacterial count of 10^{12} cells [23-24]. For the others, see Materials and methods and the legends to Fig. 1.

Furthermore, total and DCCD-sensitive ATPase activity was inhibited significantly by irradiation with coherent EMI of the frequency of 51.8 or 53 GHz although ATPase activity in the presence of DCCD (0.1 mM) has no changes or, in opposite, is increased a little (Fig. 4). Taken into consideration the fact that DCCD is inhibiting the F_0F_1-ATPase in *E. coli* under fermentation [28], the results obtained indicate that this ATPase may be a target for action of EMI of extremely high frequency.

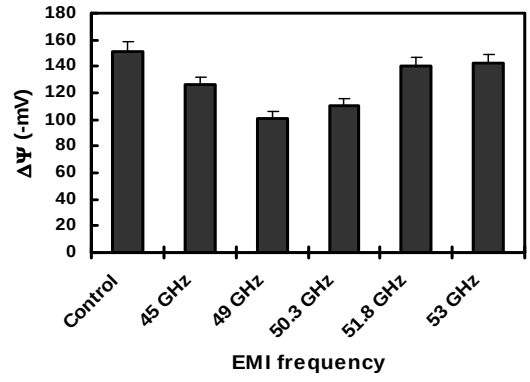
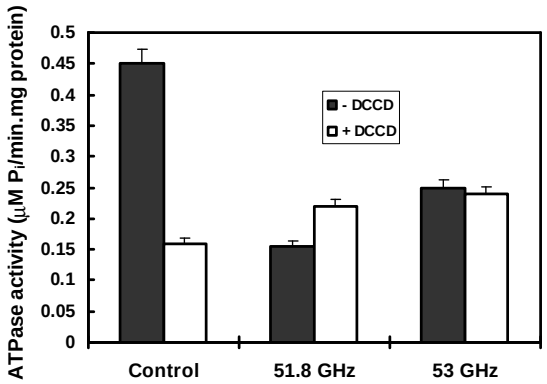


Fig. 3. *E. coli* K12 membrane potential ($\Delta\Psi$) values after irradiation with coherent EMI of extremely high frequency. The irradiation time was 1 h. $\Delta\Psi$ was calculated from distribution of tetraphenyl-phosphonium cation (initial external concentration of 1 μM) between the cytoplasm and the external medium determined with appropriate selective electrode [24]. For the others, see the legends to Fig. 1.

In addition, it should be noted that, in the K^+-less assay medium (concomitant K^+ was of 0.02 mM [21]), total ATPase activity was of lower values close to those in the presence of DCCD (see Fig. 4) having no any marked changes by irradiation with the frequency used (not shown). This is of importance since K^+-sensitive and DCCD-inhibited ATPase activity in *E. coli* has been shown clearly be the F_0F_1-ATPase activity that is associated with K^+ uptake TrkA system [21, 29-30]. Therefore, EMI of extremely high frequency affected K^+-sensitive and DCCD-inhibited ATPase activity suggesting that the F_0F_1-ATPase could be a target for EMI.

Moreover, inhibitory effect of DCCD (in different concentrations of 0.1 to 1 mM) on J_H^+ markedly decreased after irradiation with EMI at the frequency of 51.8 or 53 GHz (Fig. 5) in sprite of different proton fluxes (comp. with Fig. 2B) suggesting that sensitivity of bacteria to inhibitors (DCCD) may be also affected by irradiation with coherent EMI of extremely high frequency. Such an effect was determined with "noise" EMI before [1]. A less sensitivity to DCCD could result from conformational changes in subunits of the F_0F_1-ATPase [31] having a key role in effects of EMI on bacteria. This seems to be in accordance with results reported by Bulgakova et al. [13] that EMI of extremely high frequency with non-thermal intensity could change the sensitivity of *Staphylococcus* to various antibiotics having membranotropic properties. The irradiation (during up to 1 h) is of importance can result in opposite changes inhibiting and stimulating bacterial growth [13]. In all cases, these results might be extrapolated to different reagents and drugs and should be accounted in therapeutic practice. Moreover, this would lead to further study to reveal primary cellular mechanisms for bacterial effects of EMI of extremely high frequency.

Fig. 4. The ATPase activity of membrane vesicles isolated from *E. coli* K12 after irradiation with coherent EMI of extremely high frequency. The irradiation time was 1 h. ATPase activity was calculated by colorimetric determination of liberation of inorganic phosphate (P_i) per time and protein [21-22] upon ATP (3 mM) adding. DCCD was added in final concentration of 0.05 mM in parallel assays. For the others, see Materials and methods and the legends to Fig. 1.



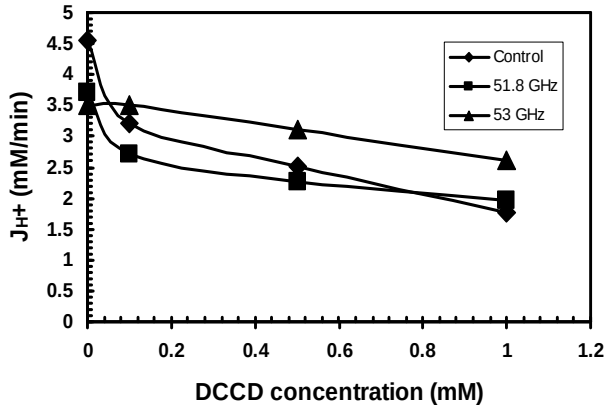


Fig. 5. The changes in inhibitory effect of DCCD on J_H^+ from *E. coli* K12 after direct irradiation with coherent EMI of extremely high frequency. The irradiation time was 1 h, for the others see Materials and methods and the legends to Fig. 1.

Mediated action of EMI on bacteria

The action of EMI of extremely high frequency on bacteria studied under separate irradiation of water or buffers containing different ions (see Materials and methods), in which bacteria are kept under assays [2, 12].

Table 2. Mediated action of EMI of extremely high frequency on the following growth rate of *E. coli* K12.

Conditions*	Growth rate (h^{-1})		
	Control	51.8 GHz	53.0 GHz
Doubly distilled water	0.82 ± 0.03 (100 %)	0.52 ± 0.02 (63.4 %) ($p<0.01$)**	0.34 ± 0.02 (41.5 %) ($p<0.002$)
Assay medium	0.78 ± 0.03 (100 %)	1.22 ± 0.05 (156.4 %) ($p<0.01$)	1.41 ± 0.08 (180.8 %) ($p<0.01$)

* irradiation time was 1 h, for the other conditions, see Materials and methods and the legends to Fig. 1.
** see the legends to Table 1.

When irradiation by the duration of 30 min (not shown) or 1 h (Table 1) and with the frequency of 51.8 or 53.0 GHz was subjected to water, the specific growth rate for *E coli* K12 (after premises in such water during 10 min and then their moving into growth medium with glucose, see Materials and methods) decreased on more than 35 % in comparison with control (Tabl. 2.). But this mediated action was with less effects than direct irradiation of bacteria in the water (comp. with Fig. 1 and Tabl. 1). When irradiation was subjected to the buffer, the growth rate, on the contrary, increased on more than 56 % (Tabl. 2). Evidently, cells may be affected by Tris (hydroximethilaminomethane) or the other buffer components, but data are very poor [2, 32].

Note that water has acidic reaction and transferring cells from slightly acidic medium or slightly alkaline medium could affect growing bacteria. In addition, osmotic shock should be also taken into consideration, since cells are transferring into the medium with greater osmolarity. However, such procedures were shown before do not affect growing *E coli* [33].

Thereby, mediated action of coherent EMI of extremely high frequency on *E coli* might be of different nature. This was observed earlier with "noise" EMI depending on bacterial growth phases and other factors [2]. The results point out a role of water and medium composition in effects of EMI of extremely high frequency on bacteria.

Repeated action of EMI on bacteria

If bacteria have any compensatory mechanisms [2], then these mechanisms possibly become to be important under the repeated irradiation with coherent or "noise" EMI of extremely high frequency. Indeed, the repeated action of coherent EMI with the frequencies in 51.8 or 53.0 GHz on *E coli* K12 (irradiation during 1 h with interruption of 2 h, in checking control repeated irradiation was absent but bacteria were kept with the same time) reduced considerably an inhibitory effect (in 1.7- or 1.9-fold for the frequency of 51.8 or 53.0 GHz, correspondingly; $p<0.01$).

Certainly, compensatory mechanisms in bacteria have not studied, although miscellaneous defensive proteins like those discovered in animal cells [34] might play a role.

Thereby, the results obtained are indicative of negative action of coherent EMI of extremely high frequency on bacteria, when maximal effect is observed at the frequency in 51.8 and 53.0 GHz. The frequency of 51.8 GHz in studied range of EMI (see Materials and methods) is probably a resonant frequency causing maximal effect.

Concluding remarks

The study done defines the bacterial effects of coherent EMI of extremely high frequency with low intensity causing changes in *E. coli* growth and points out some membranous aspects of the mechanisms of such an action. The effects of coherent EMI of the frequency of 51.8 or 53.0 GHz on bacterial growth rate and some properties of the bacterial membrane (see Results and discussion) should be noted to be much stronger than appropriate effects of "noise" EMI of extremely high frequency reported [1-2].

Bacterial effects of "noise" and coherent EMI of extremely high frequency with low intensity shown in the present paper and by different groups [1-6, 10-13, 17-19] are of significance to understand distinguishing role of bacteria in biosphere nowadays leading to changed metabolic pathways and, for instance, to antibiotics resistance (for review, see [35]).

The present results are principal to the further study of mechanisms of biological effects of EMI, on the one hand, and in the same time, for determination of the allowed doses of the long irradiation of the persons and the

other organisms by means of EMI of extremely high frequency to manage appropriate preventive ways. Moreover, it should be necessary to improve using EMI of extremely high frequency in therapeutic purpose, when repeated action can turn out to be inefficient. It is also possible to use EMI for product protection from bacteria. In addition, the results are important for construction of new generators of EMI of extremely high frequency and facilities for telecommunications.

The authors thank L. Arutyunyan and K. Akopyan for help in undertaking some experiments. This study was done within the framework supported by Ministry of Education and Science of the Republic Armenia (Grant # 54).

REFERENCES

1. Trchounian A., Ogandzhanyan E., Sarkisyan E., Gonyan S., Oganesyan A., Oganesyan S. // *Biophysics.* 2001. V 46. P. 69-76.

2. Isakhanyan V., Trchounian A. // *Biophysics.* 2005. V. 50. P. 604-606.

3. Kaprelyants A., Kell D.B // *Trends Microbiol.* 1996. V. 4. P. 237-242.

4. Trushin M.V // *J. Microbiol. Immunol. Infect.* 2003. V. 36. P. 153-160.

5. Matsuhashi M., Pankrushina A.N., Endoh K., Watanabe H., Mano Y., Hyodo M., Fujita T., Kugunita K., Kaneko T., Otani S // *J. Bacteriol.* 1995. V. 177. P. 688-693.

6. Matsuhashi M., Pankrushina A.N., Takeuchi S., Ohshima H., Miyoi H., Endoh K., Murayama K., Watanabe H., Endo S., Tobi M., Mano Y., Hyodo M., Kobayashi H., Kaneko T., Otani S., Yoshimira S., Harata A., Sawada T // *J. Gen. Appl. Microbiol.* 1998. V. 44. P. 49-55.

7. Norris V., Hyland G.J // *Mol. Microbiol.* 1997. V. 24. P. 879-880.

8. Alipov E.D., Scheglov V.S., Sarimov R.M., Belyaev I.Ya. // *Radiats. Biol. Radioecol*. 2003. V. 43. P. 167-171.

9. Alekseev S.I., Ziskin M.C. // *Bioelectromagnetics.* 2000. V. 21. P. 264-271.

10. Chen W.S., Ma P.M., Liu H.L., Yeh C.K., Chen M.S., Chang C.W. // *J. Acoust. Soc. Am.* 2005. V. 117. P. 3740-3749.

11. Akyel Y., Pakhomova O.N., Stuck B.E., Murphy M.R // *Bioelectromagnetics.* 1998. V. 19. P. 393-413.

12. Gub N.M., Luneva I.O., Denisova S.N., Ostrovsky N.V. // *Millimeter waves in medicine and biology*. 10th Russian Symp. with intern. participation. Moscow, 1995. P. 96 (in Russian).

13. Bulgakova V.G., Grishina V.A., Orlova T.I., Petryakina Z.M., Polin A.N., Noks P.P., Kononenko A.A., Rubin A.B. // *Biophysics.* 1996. V. 41. P. 1289-1293.

14. Bechkii O.V., Devytakov N.D., Kislov V.V. // *Crit Rev. Biomed. Eng.* 2000. V. 28. P. 247-268.

15. Fesenko E.E., Geletyuk V.I., Kazachenko V.N., Chemeris N.K // *FEBS Lett.* 1995. V. 366. P. 49-52.

16. Gapeyev A.B., Safronova V.G., Chemeris N.K., Fesenko E.E // *Bioelectrochem. Bioenerg*. 1997. V. 43. P. 217-220.

17. Belyaev I.Ya., Alipov Y.D., Scheglov V.S., Lystsov V.N. // *Z. Naturforsch*. 1992. V. 47. P. 621-627.

18. Lukashevsky K.V., Belyaev I.Ya // *Med. Sci. Res.* 1990. V. 18. P. 955-957.

19. Belyaev I.Ya., Shcheglov V.S., Alipov Y.D., Polunin V.A // *Bioelectromagnetics.* 1996. V. 17. P. 312-321.

20. Trchounian A., Kobayashi H. // *FEBS Lett.* 1999. V. 447. P. 144-148.

21. Trchounian A., Vassilian A. // *J. Bioenerg. Biomembr*. 1994. V. P. 563-571.

22. Bagramyan K., Mnatsakanyan N., Trchounian A. // *Biochem. Biophys. Res. Commun.* 2003. V. 306. P. 361-365.

23. Akopyan K., Zakharyan E., Kirakosian G., Mnatsakanyan N., Bagramyan K., Trchounian A. // *Biophysics.* 2002. V. 47. P. 985-988.

24. Martirosov S.M., Trchounian A., Petrosian L., Vardanyan A. // *Bioelectrochem. Bioenerg*. 1981. V. 8. P. 513-520.

25. Lakin G.F. Biometriya. M.: High School. 1992 (in Russian).

26. Lowry O.H., Rosenbrough N.J., Farr A.C., Randall R.J. // *J. Biol. Chem.* 1951. V. 193. P. 265-275.

27. Kobayashi H // *Recent Res. Devel. Bioenerg*. 2000. V. 1. P. 33-43.

28. Trchounian A., Ohandjanyan E., Bagramyan K., Vardanyan V., Zakharyan E., Vassilian A., Davtian M. // *Biosci. Rep.* 1998. V. 18. P. 143-154.

29. Bagramyan K., Mnatsakanyan N., Poladian A., Vassilian A., Trchounian A // *FEBS Lett.* 2002. V. 516. P. 172-178.

30. Trchounian A. // *Biochem. Biophys. Res. Commun.* 2004. V.315. P. 1051-1057.

31. Nakamoto R.K., Ketchum C.J., Kuo P.H., Al-Shawi M. // *Biochim. Biophys. Acta.* 2000. V. 1458. P. 289-299.

32. Dosch D.C., Helmer G.L., Sutton S.H., Epstein W. // *J. Bacteriol.* 1991. V. 173. P. 687-694.

33. Trchounian A.A., Ogandjanian E.S., Vanian P.A // *Curr. Microbiol.* 1994. V. 27. P. 187-191.

34. Novoselova E.G., Glushkova O.V., Sinotova O.A., Fesenko E.E. // *Dokl. Russ. Acad. Sci.* 2005. V. 401. P. 117-119 (in Russian).

35. *Bacterial Stress Responses.* Storz G., Hengge-Aronis R. (Eds.). ASM Press. Washington DC. 2000. 502 p.

MICROWAVE IONOSPHERIC EMISSION AS A NEW FACTOR OF SOLAR-BIOSPHERE RELATIONS

SERGEI V. AVAKYAN

S.I. VAVILOV STATE OPTICAL INSTITUTE, Tuchkov lane 1, 199034, St. Petersburg, Russia, avak2@mail.ru

Abstract

This paper proposes and provides substantiation for a hypothesis concerning the mechanism by which solar and geomagnetic activity (mainly of solar flares and magnetic storms) affects the biosphere, including man. The hypothesis, including a physical mechanism introduced by the author and new for aeronomy, is that high-lying (Rydberg) states of all gases of the earth's upper atmosphere are excited by ionospheric electrons. Rydberg atoms, molecules and ions of all atmospheric gases emit characteristic radio emission in the spectral range from decimeters to millimeters. This radiation can easily penetrate to low atmosphere and biosphere carrying complete information about power and duration of solar flare and geomagnetic storms to biosphere. The microwave radioemission have the resonances at the spectral range $10^9 \div 10^{12}$ Hz at the biological cells and membranes, DNA and RNA, molecules of hemoglobin, human erythrocytes, and this fact can explain the extremely small threshold for influence of ionospheric radioemission at the monochromatic (characteristic) Rydberg transitions on biological objects, including the viscosity of blood.

The energy estimates of the flux intensity of microwave radiation of the ionosphere from Rydberg states are used to prove for the first time that the values of this flux agree with the experimental data. A method is proposed for distinguishing the contributions of microwave radiation and magnetic perturbation in the geobiocorrelations, taking into account the effect that the magnetic-field variations are not in phase with the flux of corpuscles from the radiation belts in the ionosphere during the period of a geomagnetic storm.

There are several problems in ionospheric and atmospheric physics, biophysics and medicine concerning the investigations of Rydberg excitation role:

- determination of the real spectral distributions for Rydberg ionospheric emission at all transparency windows;
- determination of the perception threshold for the characteristic sharp-resonance microwave Rydberg emission for healthy and sick persons;
- modelling investigations of negative influence of cell telephone. The sporadic increase for the microwave ionospheric Rydberg radioemissions during power solar flares and principal magnetic storms will be taken into account for consideration of the stochastic resonance.

Introduction

One of the fundamental problems of modern natural science is the search for biophysical mechanisms by which solar and geomagnetic activity, and especially solar flares and magnetic storms, affect people and the biosphere as a whole. The accumulated experimental material is mainly evidence, at least in indirect form, of the presence of heliogeobiocorrelations. It is obvious that such correlations are very complex because of their multifactorial nature. At the same time, they indicate that there is some physical mechanism responsible for the transport of the energy given off into the thickness of the lower atmosphere and biosphere when the solar and geomagnetic activity increases. In fact, the main energy flows that vary when there are variations of the solar and geomagnetic activity do not reach the lower atmosphere but are completely absorbed in the earth's upper and middle atmosphere (above 20 km). The chief variations in the electromagnetic radiation flux from the sun actually occur in the region of far- and extreme-UV radiation and soft x rays, which is completely absorbed in the upper atmosphere. It is well known that the radiation flux which ionizes the earth's upper atmosphere in the range from soft x rays to the vacuum UV (with wavelengths from 0.1 to 134 nm) increases most strongly (by a factor of several thousand and sometimes by tens of thousands) in the periods of solar flares. The energy of this flux is 6–7 orders of magnitude higher than that of solar rf radiation in the periods of strong flares.

Corpuscular solar radiation (the solar wind, energetic solar protons and electrons) also do not penetrate into the lower atmosphere. When the geomagnetic activity increases—magnetic storms and substorms, there is a sporadic precipitation of electrons and protons from the earth's radiation belts into the ionosphere, but these flows also completely dissipate at higher altitudes (above 40 km).

The fluxes of charged particles, mainly electrons, as well as protons, that precipitate into the earth's upper atmosphere from the overlying radiation belts also increase by several orders of magnitude during strong

magnetic storms. In periods of solar flares and during magnetic storms, the very first process of complete dissipation of the energy of particle fluxes intruding into the earth's upper atmosphere is the ionization of all the atmospheric gases with the formation of photoelectrons, secondary electrons, and Auger electrons.

The energetics of the variations during the period of geomagnetic perturbations of the geomagnetic field itself with respect to the mean value and even more in absolute magnitudes are insignificant. Therefore, the "*kT* problem" in magnetobiological effects1 is continually being discussed in the literature [1].

In this connection, there is interest in discussing the arguments in favor of the hypothesis of [2, 3] on the importance in heliogeobiospheric correlations of the contribution of the microwave radiation of the earth's ionosphere, detected as sporadic rf radiation when the solar and geomagnetic activity increases [4-6].

Microwave Rydberg radiation of the ionosphere as a factor of the action of solar and geomagnetic perturbations on the biosphere

In 1994, we were the first to propose [7] that the fact that the plasma of the earth's upper atmosphere (and of other planetary atmospheres) unconditionally contains highly excited Rydberg states of atoms, molecules, and their ions should be taken into account in aeronomy and ionospheric physics.. Rydberg states correspond to strong excitation of a valence electron that had been in orbit with high principal quantum number $n>10$. In practice, this is a state of an atomic-molecular particle of any gas of the upper atmosphere close to its ionization potential. The corresponding atomic spectra were experimentally studied for the first time by the Swedish physicist Johannes Robert Rydberg (1854– 1919). These Rydberg states are metastable (long-lived), since most radiative quantum transitions from them have low probability. Transitions from the Rydberg states fill virtually the entire region of the electromagnetic spectrum of the upper atmospheric emissions, beginning from the extreme UV radiation. According to the selection rules for electric dipole transitions, the allowed transitions will be those for which the orbital-momentum quantum number change by an amount $l=\pm1$. Therefore, because of the high values of n and hence of l ($l=n-1$ and below), transitions from high l can occur only between adjacent Rydberg states and consequently lie in the rf region [8].

It should be emphasized that there has been no monitoring of the variations of the absolute magnitude of the fluxes of solar ionizing (soft x rays and EUV) radiation and their spectral composition. There are no experimental data on the spectra or increments of the fluxes in the periods of flares on the sun of various levels and classes. And the only experiment that carries out the tasks involving the total monitoring of solar shortwavelength activity is the Permanent Space Solar Patrol that we proposed. This experiment includes measurements in the entire spectral interval with the spectral resolution needed for solar-terrestrial physics of about 1 nm in the constant regime with continuous scanning of the spectrum every 72 sec, which is close to the duration of subflares and to the pulse phase of powerful flares [9, 10].

In [2, 3, 7, 8] for the physical mechanism of the generation of microwave radiation of the ionosphere, using the process of excitation by electron impact (by ionospheric photoelectrons, auroral and secondary electrons, and also Auger electrons) of the Rydberg states of the components of the upper atmosphere and ionosphere. Specific emissions from Rydberg levels are constantly recorded when the optical radiation of the upper atmosphere is observed [11] as well as in active experiments [12]. These experiments consisted of heating the ionosphere with powerful pulses of radio waves at frequencies of 4.7–6.8 MHz. In response, the ionosphere generated microwave decimeter radiation from the altitude interval from 185 to 240 km, as well as additional emission of the red lines of the oxygen atom. The analysis given in [12] of various ways to generate the detected microwave radiation includes the following: scattering of the earth's thermal radiation at artificial inhomogeneities of the electron concentration, bremsstrahlung of electrons accelerated by high-frequency plasma turbulence to energies of the order of 10–15 eV, and transitions of the electrons between high Rydberg levels of the molecules of the neutral components of the ionospheric plasma excited when they collide with accelerated electrons, showed that the last of the three enumerated mechanisms is the most probable. It was also emphasized in [12] that the region of artificial generation of microwave radiation coincides in altitude (about 200 km) with the position of the maxima of the altitude profiles of the excitation rates of the Rydberg states, calculated in [8] for the ionosphere under natural conditions. Thus, [12] is the first experimental proof of the excitation mechanism of Rydberg levels by energetic ionospheric electrons proposed in [8].

In this investigation the results of calibration for excitation rates of Rydberg states at the altitudes of 95 to 360 km are presented. The main process of this excitation at ionosphere is electron impact, by photoelectrons at the low and middle latitudes and by precipitating from magnitosphereelectron at auroral zones. In the upper atmosphere and ionosphere there are three types of electrons with energies up to several tens and hundreds of electronvolts for which the Rydberg excitation cross sections are maximal:

- photoelectrons, which arise when gases are ionized by the sun's x radiation and extreme UV radiation;
- secondary electrons, formed during ionization by corpuscles (electrons and protons from the radiation belts) precipiteted into the upper atmosphere during geomagnetic storms and substorms;
- Auger electrons, formed both during photoionization and during corpuscular ionization.

The Auger effect in all its manifestations in the ionospheres of the planets also was considered for the first time in our papers [13]. All these ionization electrons in their flux intensity directly track any variations of the solar and geomagnetic activity – from quiet periods to the strongest solar flares and geomagnetic storms and substorms. The Rydberg rf radiation of the ionosphere excited by these electrons accordingly carries full spatiotemporal information concerning all the variations of the ionizing fluxes; i.e., it scans all forms of heliogeophysical activity.

The excitation rate increases with the growth of geomagnetic and solar activities in particular during the solar flares (up to 10 times and more) and during the principal magnetic storms (up to 100 times and more). Unlike the auroral zone, where the excitation rate as a rule shows only one main maximum at the altitude about 100 km, during the solar flare there are usually two maximuma. The first maximum, connected with EUV solar radiation, occurs at the altitude near 200 km and its value increases during a flare by several tens per cents. The second maximum at the altitude above 100 km becomes the main one the large flare. Its increase comes up to ten times and resulted from the X-ray solar radiation. During the quiet Sun the excitation rate of sum of the Rydberg states exceeds the value 10 $cm^{-3}s^{-1}$ for atoms and molecules of oxygen and 100 $cm^{-3}s^{-1}$ for molecules of nitrogen. During solar flare 2B the integral intensity in vertical column is 10^9 photons cm^{-2} s^{-1}. It is important that the increase of excitation rates of the non-Rydberg states in the visual and UV spectral range (for example the LBH system of bands of nitrogen) at the same flare is smaller by factor of three. The centimeter radioemission results from transition with changing the orbital quantum number on 1, for example in atomic oxygen at n = 10 − 20, and the decimeter radioemission occurs at n = 20 − 40, if n is constant. If $\Delta n > 1$ and $n > 10$, there are the millimeter emissions of ionosphere. In the experiments, which registrated sporadic ionospheric radioemission in the range from 3 cm to 2 m with intensity increase of several times during solar flares, particularly when there were sudden ionospheric disturbances (SID), associated with X-ray flux of solar flare [5, 6, 14-17].

It should thus be assumed that a direct information channel from the lowest layers of the atmosphere and the biosphere itself concerning variations of the solar and geomagnetic activity has been determined [2, 3, 8]. For the biosphere and in particular for the human organism, this information, in the form of flux variations of the microwave radiation, can be just the Agent X that was postulated by A.L. Tchijevsky. It should be emphasized that the sun itself emits in the rf region, but this radiation does not directly correlate with the main flare flux—the flux of geoeffective short-wavelength (extreme UV and x-ray) radiation, whose energy is seven orders of magnitude greater than the solar rf flux. The main thing, however, is that the rf radiation of the sun is not monochromatic and consists not of separate lines and bands but has a continuous spectrum.

The latter circumstance can be decisive in demonstrating that the microwave radiation of the ionosphere is biologically effective. In fact, numerous experimental and theoretical papers on studies of the mechanisms by which millimeter and centimeter radiation acts on a living organism emphasize the resonance character of the response of biological cells and erythrocytes to such irradiation. So, there are several works about the theoretical and experimental resonance of living systems: biological cell at the $f = 41.782 \cdot 10^9$ Hz (λ = 7.2 mm) and $f = 83.564\ 10^9$ Hz (λ = 3.6 mm) [20]; DNA-spirale at the $f = 4\ 10^{10}$ Hz (λ = 7.5 mm) [21]; molecule DNA at the $f = 10^9$ Hz (λ = 3 dm) [22], molecule RNA at the $f = 10^9$ Hz (λ = 3 dm) [22], cellular membrane at the $f = 10^{10}$–10^{11} Hz (λ = 3 cm – 3 mm) [22], human erythrocytes at the $f = 10^{10}$ Hz (λ = 3 cm) [23]. It is very important that experimental Δf less than $10^{-3} \div 10^{-4}$ f [21]. Consequently, not only cells of the human organism, but also the blood, have resonance microwave frequencies at which the Rydberg ionosphere excited by flares and magnetic storms radiates. The explanation of how flares and storms act on cardiovascular patients follows from this. Thus, the influence of geomagnetic perturbations on the capillary circulation in patients of ischemic disease of the heart [24] on the day of a magnetic storm and the influence of solar flares and magnetic storms on patients with vascular pathology of the heart and brain [25]. are directly explained by the action of Rydberg rf radiations on the blood, including an increase of the viscosity and deformability of the erythrocytes.

The influence on the blood of a hypothetical signal associated with solar activity and manifested in the period of a flare on the sun and during the subsequent geomagnetic storm (in terms of the statistics of cardiovascular diseases) was discussed in [26]. Of course, these questions were discussed earlier by A. L. Tchijevsky. He proposed in this case that Agent X is (among other things) ‘‘electric vibrations of a definite frequency’’ [27]. and later that the agent of the action of solar activity “is in particular millimeter radiation” [28]. Recently Russian scientists [25] have discovered that the reason that flares on the Sun and following geomagnetic storms have influence the cardiovascular system lies in the change to the physical attributes of the blood. During solar flares changes are experienced in human blood viscosity, red corpuscle proportion in the blood, in the concentration of fibrinogen and the aggregation of blood corpuscles and platelets. These processes take place differently in healthy and meteo-dependent people with cardiovascular problems. In the latter, the blood thickens when magnetic disturbance on the Sun reach the Earth. In the case of healthy people, the organism prepares for the event two days before its advent, immediately after a solar flare. The microwave radioemission have the resonances at the spectral range 10^9 – 10^{12} Hz at the biological cells and membranes, DNA and RNA, human erythrocytes, and this fact can explain the extremely small threshold for influence of

ionospheric radioemission at the monochromatic (characteristic) Rydberg transitions on biological objects. We propose the next scheme of the heliogeobiocorrelations: see Fig. During of high solar activity specially flares at the Sun and also large geomagnetic activity (magnetic storms) there are increased fluxes of EUV and X-rays and precipitating particles from geomagnetosphere, during magnetic storms, which generate the additional ionization of terrestrial ionosphere. This ionization results in production of photoelectrons and secondary electrons and especially Auger electrons. Rydberg excitation of atoms and molecules by these electrons generate microwave monochromatic radiation: (mm, cm, dm), which can produce the resonance reaction of living systems [20-23] during “unfavorable days” for sick people. It is important that microwave radiation in the system that we proposed is capable of acting as the carrier frequency, with modulation by infrasound and internal acoustic-gravity waves of the upper atmosphere, as well as by vibrations of the background electromagnetic field (Alfven and Schuman resonances at the terrestrial ionosphere), including in the region of biorhythms. This amplifies the influence of low-frequency vibrations of the background electromagnetic field, with its high biological efficiency but low energetics of its action [29]. especially because of the surprisingly strong action on biological objects from the side of microwave radiation [1].

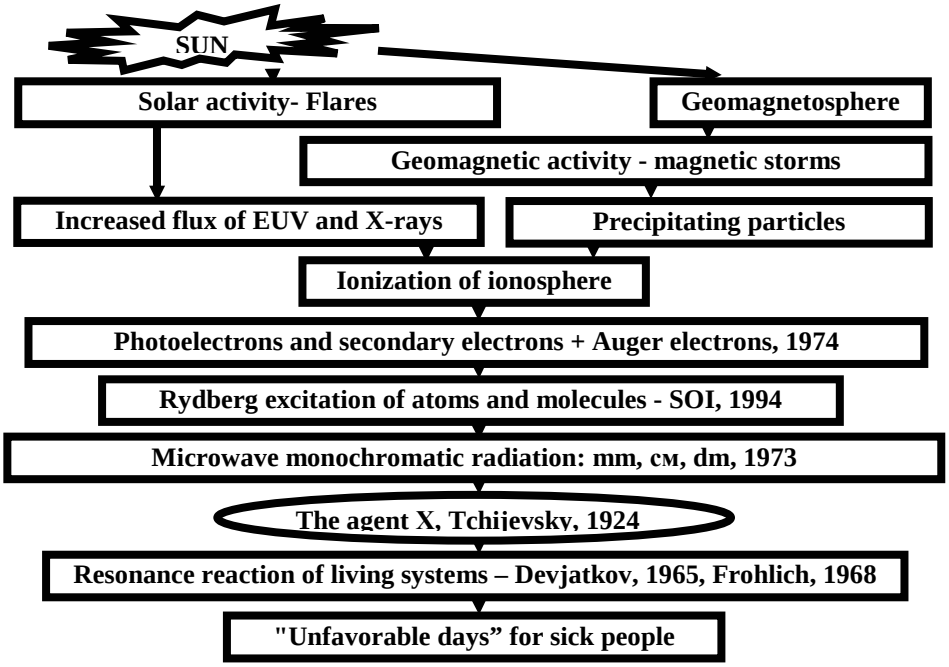


Fig. Biological effects of solar activity and Rydberg states.

There are numerous experimental confirmations that microwave radiation has a biological effect. From the aggregate of such studies, it is possible to expect uniquely low levels of threshold action, all the way to 10^{-15} W/cm2, which is close to the thresholds of perception of vision and hearing [1]. There are a number of considerations in favor of the reliability of such anomalously low threshold levels:

• Fixed action through acupuncture points makes it possible to speak of the possibility of reducing the threshold in actual laboratory experiments.

• Low-frequency modulation of microwave radiation (including in the range of biorhythms) can reduce the action threshold of this radiation.

• When determining spectral resonances, a contribution of the inaccuracy of the resonance is possible when laboratory sources of microwaves are used.

• The contribution of a synergetic effect when several factors are combined (for example, in the period of a geomagnetic storm, microwave radiation of the ionosphere and storm-induced variations of the geomagnetic field become active).

• The appearance of a synergetic effect from the reaction to an external stimulus (for example, a solar flare or magnetic storm) simultaneously of several individuals associating with each other in this case and influencing each other (including via biomagnetism [30]) under the action (in the case under discussion) of sporadic microwave radiation of the ionosphere.

There is an extremely nontrivial effect for the case of a geomagnetic storm, and taking this into account can fundamentally alter the technique and treatment of numerous experiments on magnetobiology. Actually, unlike the standard understanding of the changes of the geomagnetic field during a storm (with a maximum at

the center of the main phase), the precipitation of particles from the radiation belts that accompany these changes experience sharp attenuations (to the recording threshold in the course of 1.5–3 h) at the beginning and end of the main phase. Only at the center of the main phase at middle latitudes in 2–4 h do they actually reach the maximum values – to the level of auroral precipitations [31, 32].

Thus, the mapping of a biophysical experiment on magnetobiology to the values of the generally used indices of geomagnetic activity that semi-quantitatively describe the variation of the earth's magnetic field (*Kp*, *Ap*, or *Dst*), as it is usually done, does not perfectly reflect the intensity of the corpuscular precipitation into the ionosphere in the period of a magnetic storm and hence does not correspond to the intensity level of sporadic microwave radiation of the ionosphere. This may be associated with the appearance of null results when modelling the conditions of a magnetic storm in laboratory experiments on biological objects. The papers [2, 3]. showed that it is the microwave radiation of the ionosphere that must play the main role in the biospheric effect of a magnetic storm. This is confirmed by the increase of the probability of phenomena detected in various statistical studies of the effects of a magnetic storm in medical indices among people [33-35] concurrent with the period of the storm and also for 24–48 h after the storm, when variations in the geomagnetic field no longer exist. At the same time, the experimental fact is well established that the fluxes of corpuscles that pour out in just this time period increase after a storm ([32], p. 290). Incidentally, it is noteworthy in a number of such papers on the statistics of medical cases that the maximum of the effect occurs two days before the storm. [33, 35]. A flare occurs on the sun at just this time [2, 3, 32], and sporadic microwave radiation of the ionosphere also is observed [4-6, 14-17]. A direct correlation has been recorded [36] with solar x-ray flares in the statistics of medical events.

We will discuss more closely at the energy aspect of the problem of how the sporadic microwave (Rydberg) radiation of the ionosphere affects the biosphere and the lower atmosphere. Radiant energy from the sun with a flux density of 1367 W/m^2 reaches the earth's surface, and about 10^{-2} W/m^2 (all of the solar flux of soft x rays and UV radiation with a wavelength of $\lambda<134$ nm, including the L_α line of the hydrogen atom) is absorbed in the ionosphere under quiet heliogeophysical conditions. However, the ratio of the value of absorbed energy per unit mass of atmospheric gas is substantially different: 10^{-3} W/g in the ionosphere, and 7 10^{-5} W/g at the bottom of the troposphere. Thus, per unit mass of atmospheric gas or per one atomic-molecular particle of this gas, an order of magnitude more electromagnetic energy reaches the ionosphere from the sun than reaches the lower layers of the atmosphere. This ratio is still greater in periods of solar flares and geomagnetic storms. The greater part of the energy of the solar EUV radiation and soft x rays with wavelength $\lambda<50$ nm (capable of producing energetic photoelectrons) generates microwave radiation of the ionosphere from the Rydberg levels of all the atmospheric gases, including the minor components. This generation is supplemented by the action of fluxes of charged particles in the auroral zone under virtually any conditions of heliogeophysical activity. The fluxes of short-wavelength solar radiation double (in the spectral region $\lambda<120$ nm) during periods of flares on the sun, and the fluxes of precipitated electrons increase by a factor of 100 or more during geomagnetic storms, not only at high but at middle latitudes. The energy of the electron fluxes precipitated into the upper atmosphere in this case is about a factor of 50 greater than the energy of the ionizing radiation of the quiet sun. It is important that the energy flux of the microwave radiation of the ionosphere completely reaches the earth's surface. We can estimate the energy flux of the sporadic microwave radiation of the ionosphere recorded in [5]. It is important that the radiation signal of the ionosphere exceeded the intensity of the rf flux from the quiet sun by a factor of 2–40 (at a wavelength of $\lambda=50$ cm), where the latter equals (4–6) 10^{-21} W cm^{-2} m^{-1} ([32], p. 13). The width of the surge reached 1 GHz. The flux of ionospheric microwave radiation of the ionosphere at $\lambda=50$ cm in the period of a solar flare is then (according to the data of the measurements of [5]) (3–70) 10^{-16} W cm^{-2}.

This is orders of magnitude greater than the sensitivity threshold of biological objects to microwaves [1] Thus the "Porog" generator [37] for medical purposes, which works efficiently in a wide range of microwaves from superhigh to extremely high frequencies, provides a spectral power density level of 10^{-16} – 10^{-18} W cm^{-2} Hz^{-1}, i.e., an even smaller value. At the same time, a further decrease of the output power of devices with a monochromatic signal (we recall that, according to [2, 3], the microwave radiation of the ionosphere in Rydberg transitions has indeed a monochromatic character) all the way to 10^{-10} – 10^{-12} W, and noise to 10^{-18} – 10^{-20} W cm^{-2} Hz [1], does not reduce the efficiency of the treatment. Moreover, such radical reductions of the output power to the level of counted quanta even increase this efficiency. In [37] pointed out that an explanation of this effect can be found by using a quantum-mechanical approach. When the energy of the entire spectrum of sporadic rf radiation of the ionosphere is taken into account, the threshold value for biological objects (10^{-16} – 10^{-17} W cm^{-2} [1] can be exceeded even by a factor of 10–100. The ratio of the energies dissipated in the ionosphere when there is a medium solar flare and during a geomagnetic storm shows that the flux of microwave radiation can be factor of 10–100 greater in intensity in the period of a magnetic storm. In this case, the radiation in the centimeter and decimeter ranges can now exceed 10^{-11} – 10^{-12} W cm^{-2}.On the other hand, a calculation of the excitation rates of the Rydberg states of the oxygen atom [8] gave a value of about 10^9 particles cm^{-2} sec^{-1} in a column of the ionosphere during the period of a medium class-2B solar flare. Then, for values of the quantum energy in the centimeter range of 2 10^{-23} (for $\lambda=1$ cm) – 2 10^{-24} J (for $\lambda=10$ cm) in this

column in ten allowed transitions, we have a flux density of microwave radiation of $2\ 10^{-13} – 2\ 10^{-14}$ W cm^{-2}. This flux density is the lower limit for transitions with $\Delta n=1$ (only for $\Delta l=1$), i.e., those of the type n', $l'=n'-1 \rightarrow n'-1$, $l'=n'-2$, where $n'=11–20$ for an oxygen atom. This value increases to $10^{-11} – 10^{-12}$ W cm^{-2} during a magnetic storm. Because the densities of oxygen atoms and nitrogen molecules are about equal at an altitude of about 200 km, where, according to [8], there is a maximum of the altitude profiles of the Rydberg excitation rates, and recalling the identical character of the allowed radiative transitions in highly excited (hydrogen-like) atoms and diatomic molecules, it should be expected that the total flux of sporadic rf radiation, taking into account the nitrogen molecules, is approximately doubled [38].

Our energy estimates, without claiming to be complete, show that the experimentally observed sporadic rf radiation of the ionosphere in the period of solar flares and geomagnetic storms is well explained by the energetics of the allowed microwave transitions from the Rydberg excited states of the main gases of the upper atmosphere at altitudes of about 200 km – the oxygen atom and the nitrogen molecule. Thus, the resulting energies of the microwave radiation flux of the ionosphere make it possible to regard this radiation as the main agent in heliogeobiocorrelation effects. According to [2, 39], the microwave radiation itself mainly provides the energy component of the effect, and its modulation by low-frequency oscillations of the electromagnetic and infrasound geomagnetic fields provides the information component. Laboratory experiments in which modulated microwave radiation acts on biological objects show that it is substantially stronger than microwaves with constant intensity. The effect of modulation is most pronounced at lower intensity levels of the microwave flux and also depends on the initial state of the biological system.

Conclusion

Ways of experimentally checking the possible role of the microwave radiation of the earth's ionosphere in heliogeobiocorrelations have been considered, taking into account the variability of its intensity at the different phases of a geomagnetic storm. Energy estimates are presented for the density of such a flux during periods of a moderate solar flare and a magnetic storm, reaching values of 10^{-11} W cm^{-2}. It follows from what has been said that it is necessary to provide constant monitoring of the intensity and spectrum of the microwave radiation of the earth's ionosphere, not only in terms of a methodological improvement of biophysical experiments under conditions of elevated solar and especially geomagnetic activity but also possibly for recording the level of "unfavorability" of the heliogeophysical situation. The medical and biological mechanisms of this problem should be considered, taking into account the phenomenon of stochastic resonance [1], where the background microwave radiation of the ionosphere (before a storm and a flare) plays the role of the noise component. The same phenomenon can be significant in studies of the influence of the microwave frequencies of cellular telephones [38]. Here the role of the noise signal, which sharply increases in the period of solar flares and magnetic storms, will be played by the ionospheric microwave radiation. Since it is very variable, the possible resulting medical effect from cellular telephones and ionospheric sporadic radiations significantly varies in magnitude, and this creates indeterminacy when it is studied. The phenomenon of dissipative resonance can also be relevant to the study of these problems.

There are also other problems in ionospheric and atmospheric physics, biophysics and medicine concerning the investigations of the ionospheric Rydberg excitation role:

- determination of the real spectral distributions for Rydberg ionospheric emission at all transparency windows;
- determination of the perception threshold for the characteristic sharp-resonance microwave Rydberg emission for healthy and sick persons.

These problems can be solved at several Russian institutes by support of the International Science and Technology Center [9, 10, 39].

References

1. Bingi V.N., Magnetobiology. Experiments and Models, IOF RAN, Moscow, 2002.

2. Avakyan S.V., "Microwave Emission of Rydberg States as a New Factor of Solar–Biosphere Relations," in Proceedings of the Fifth International Conference on Problems of Geocosmos, St. Petersburg, 2004, pp. 335–338.

3. Avakyan S.V., "Microwave radiation of the ionosphere as a factor in the way solar flares and geomagnetic storms act on biological systems," Opt. Zh. 72, No. 8, 41 (2005)", [J. Opt. Technol. 72, 608 (2005)].

4. Forsyth P.A., Petrie W., Currie B.W., On the origin of ten centimeter radiation from the polar aurora, Can. J. of Res., 28, ser. A, 3, 324-335, 1950.

5. Troitskii V.S., Starodubtsev A.M., Bondar L.N., et al., "The search for sporadic rf radiation from space at centimeter and decimeter waves," Izv. Vyssh. Uchebn. Zaved., Radiofiz. 16, 323 (1973).

6. Musatenko S.I., “Radio-frequency radiation of near-earth space as a result of the action of solar flares on the earth’s magnetosphere and ionosphere,” Geomag. Aeronom. 20, 884 (1980).

7. Avakyan S.V., ‘‘New factors in the physics of solar-terrestrial relationships—Rydberg states of atoms and molecules,’’ in Abstracts of Reports of the International Conference on the Physics of Solar- Terrestrial Relationships, Almaty, 1994, pp. 3–5.

8. Avakyan S.V., Voronin N.A., and Serova A.E., “The role of Rydberg atoms and molecules in the upper atmosphere,” Geomag. Aeronom. 37, No. 3, 99 (1997).

9. Avakyan S.V., E.P. Andreev, I.M. Afanas’ev, N.B. Leonov, A.V. Savushkin, A.E. Serova, N.A. Voronin; "Creating of the permanent Space Patrol of ionizing solar radiation", In: "Innovative Telescopes and Instrumentation for Solar Astrophysics", USA, Eds. S.L. Keil (NSO, USA), S.V. Avakyan (SOI, Russia), Proc. SPIE, v. 4853, pp. 600-611, 2002.

10. Avakyan S.V. Space Solar Patrol: Absolute measurements of ionizing solar radiation, Advances in Space Research, v. 37, pp. 297-302, 2006.

11. Slanger T.G., Huestis D.L., Cosby P.C., Oxygen atom Rydberg emissions in the equatorial ionosphere from radiative recombination, J. Geophys. Res. 109, A10309, 2004.

12. Grach S.M., Fridman V.M., Lifshits L.M., Podstrigach T.S., Sergeev E.N., and Snegirev S.D., “UHF electromagnetic emission stimulated by HF pumping of the ionosphere,” Ann. Geophys., 20, 1687 (2002).

13. Avakyan S.V., ‘‘Auger processes in the optics of the upper atmosphere,’’ Opt. Zh. 65, No. 11, 4 (1998) [J. Opt. Technol. 65, 870 (1998)].

14. Troitsky V.S., Bondar’ L.N., Starodubtsev A.M., A new type of radio noise. Sporadic radio emission of the near-Earth medium at centimeter and decimeter waves, Dokl. Akad. Nauk SSSR, 212, 3, 607–610, 1973.

15. Bondar’ L.N., Starodubtsev A.M., Troitsky V.S., A search of sporadic radio emission from space, Usp. Fiz. Nauk, 113, 4, 719–723, 1974.

16. Bondar’ L.N., Strezhneva K.M., Troitskiy V.S., Sporadic background radio emission, solar activity and aurorae, Astron. Vestnik, 9, 4, 210–217, 1975.

17. Musatenko S.I. Solar phenomena and the ionospheric UHF radio emission, Solar Data, 8, 92, 1984.

18. Avakyan S.V., ‘‘New processes in aeronomy: the Auger effect - 30 years later, multiple photoionization - 25 years later, Rydberg excitation - 10 years later,’’ in Proceedings of the Fifth International Conference on Problems of Geocosmos, St. Petersburg, 2004, pp. 190–195.

19. Avakyan S.V., ‘‘Biological effects of solar activity and Rydberg states,’’ in the Interdisciplinary Seminar on Biological Effects of Solar Activity: IKI RAN, ITEB RAN, 2004, Pushchino-na-Oke, pp. 45–47.

20. Sevastyanova, L.A., Vilenskaya R.L., A study of the effects of millimeter microwaves on the bone marrow of mice, Sov. Phys. Usp. (Engl. Transl.), 16, 570, 1974.

21. Devyatkov, N.D., Golant M.B., Bezkiy O.B., Millimeter waves and its role in processes of vitalfunctions, M., “Radio i svjaz”, 1991.

22. Frohlich H. The biological effects in microwaves and related questions, in Adv. Electronics and Electron Phys., 53, 85–152, 1980.

23. Pohl H.A., Natural Oscillating fields of cells. In Coherent excitations in biological Systems, eds. H. Frohlich, F. Kremer, Springer, Berlin, p. 198–210, 1983.

24. Gurkinfel Yu.I., Lyubimov V.V., Oraevskii V.N., et al., ‘‘The effect of geomagnetic excitations on capillary circulation,’’ Preprint IZMIRAN, 1994.

25. Ionova V.G., Sazonova E.A., Sergienko N.P., et al., ‘‘The reaction of the human organism to heliogeophysical perturbations,’’ Biofizika 48, No. 2, 380 (2003).

26. Vladimirskii B.M., ‘‘On possible factors of solar activity that affect processes in the biosphere,’’ in The Effect of Solar Activity on the Earth’s Atmosphere and Biosphere (Nauka, Moscow, 1971), pp. 126–141.

27. Tchijevsky A.L., The Cosmic Pulse of Life (Mysl’, Moscow, 1995), pp. 646–647.

28. Tchijevsky A.L., Terrestrial Echo of Solar Storms (Mysl’, Moscow, 1976), p. 327.

29. Temur’yants N.A., Vladimirskii B.M., and Tishkin O.G., Low-Frequency Electromagnetic Signals in the Biological World (Naukova Dumka, Kiev, 1992).

30. Vvedenskii V.L., and Ozhogin V.I., Supersensitive Magnetometry and Biomagnetism, series on Modern Problems of Physics (Nauka, Moscow, 1986).

31. Avakyan S.V., et al., “Electron flows during the magnetic storm of 14–15, December, 1970, from the data of the Kosmos-381 satellite,” Issled. Geomag. Aeron. Fiz. Solntsa 32, 158 (1974).

32. Avakyan S.V., Vdovin A.I., and Pustarnikov V.F., Near-Earth space ionizing and penetrating radiations. Handbook, Gidrometeoizdat, St. Petersburg, 501 pp., 1994.

33. Gurfinkel’ Yu.I., and Lyubimov V.V., “Screened ward in a clinic to protect patients with ischemic heart disease from the action of geomagnetic perturbations,” Med. Phys. 23, No. 3, 34 (2004).

34. Samsonov S.N., Sokolov V.D., Strekalovskaya A.A., and Petrova P.G., “On the relationship of cardiovascular disease exacerbation to heliogeophysical disturbances,” in Proceedings of the Twenty-seventh Annual Seminar, Apatity, 2004, pp. 134–137.

35. Breus T.K., Chibisov S.M., Baevskii R.M., and Shebzukhov K.V., The Chronostructure of the Biorhythms of the Heart and Factors of the External Medium (RUDN, Moscow, 2002).

36. Bobko N.A., Lychak M.M., Il'in V.N., Zelyk Ya.I., Vershigova A.V., Erigina V.T., and Chernyuk S.V., "The effect of heliogeomagnetic perturbations on the appearance of illnesses that require rapid medical treatment," in Transactions of the Russian–European Scientific Conference on Space Weather, Its Influence on Biological Objects and Man, Moscow, 17–18, February, 2005.

37. Sit'ko S.P., Skripnik Yu.A., and Yanenko O.F., "Reaction of the human organism to superlow doses of millimeter radiation," in Abstracts of Reports of the Sixth International Crimean Conference on Space and the Biosphere, Ukraine, 2005, p. 13.

38. Avakyan S.V., Voronin N.A., "Possible mechanisms for the influence of heliogeophysical activity on the biosphere and the weather", Opt. Zh. 73, No. 4, 281-285 (2006) ," [J. Opt. Technol. 73, 78-83 (2006)].

39. Avakyan S.V., "About microwave emissions of the ionosphere and its influence at the biosphere", Proceedings of an International Scientific Workshop "Space weather effects on biological systems and human health" held in Moscow, Russia, February 17-18, 2005, Eds . O.Yu.Atkov, Yu.I.Gurfinkel; Moscow, Reprocenter, 2006, pp. 80-81.

THE HYDROGEN PEROXIDE AS A POSSIBLE MESSENGER FOR MAGNETIZED PHYSIOLOGICAL SOLUTION-INDUCED STIMULATION OF HEART MUSCLE CONTRACTILITY

GAYANE AYRAPETYAN, ANAHIT GRIGORYAN, HOVIK HYRAPETYAN, ERNA DADASYAN

UNESCO CHAIR- LIFE SCIENCES INTERNATIONAL POSTGRADUATE EDUCATIONAL CENTER
31 ACHARYAN ST., YEREVAN, 375040 ARMENIA, LIFE@ARMINCO.COM

Abstract

Previous our works have shown that magnetized physiological solution (MPS) has dual effect on heart muscle contractility: from one hand it leads to muscle relaxation, from the other hand- it stimulates the frequency of heart contractility. If the first effect is explained by the activation of Na^+/Ca^{2+} exchanger, then the mechanism of the second effect is still unclear. It is known that the magnetization of aqua solutions leads to the elevation of the concentration of hydrogen peroxide (H_2O_2) and the later is suggested as one of the possible candidates through which the biological effect of MPS is realized. The purpose of our work was to check this hypothesis for which the comparative study of the effects of MPS and H_2O_2 on isolated and intra-cordially perfused snail heart muscle contractility and intracellular messenger contents were performed.

It was shown that MPS and H_2O_2 have the following synergic effects: it depresses the Na^+-K^+ pump-induced relaxation, intracellular cAMP/cGMP contents and ^{45}Ca-uptake and leads to cell dehydration. It is suggested that the H_2O_2-induced activation of cyclic nucleotide-dependent Na^+/Ca^{2+} exchanger has pivotal role in MPS–induced stimulation of heart contractility; however, the nature of this mechanism could be the subject for future investigations.

Introduction

At present the biological effect of magnetized physiological solution (MPS) on different cells and organisms can be considered as proven fact (Klassen 1982; Ayrapetyan 2006). But the nature of the messenger transferring the signal of EMF-induced water structural changes to the metabolic cascade is not clear yet. By previous our works have shown that MPS has dual effect on heart muscle contractility: from one hand it leads to muscle relaxation, from the other hand- it stimulates the frequency of heart contractility. If the relaxing effect of MPS on heart muscle could be explained by the activation of cGMP-dependant Ca efflux bringing to the deflection of intracellular Ca ions and reactivation of Na^+-K^+ pump (Ayrapetyan et al., 2005), the stimulatory mechanism of the MPS on heart beating is still unclear. As the water molecule dissociation is the most variable water property, it is suggested that the magnetization of water could change the quantity and quality of its dissociation products which are potential messengers through which the biological effect of SMF and EMF on cells could be realized (Ayrapetyan et al. 1994). By previous our study was shown that SMF and ELF EMF has depressing effect on specific electrical conductivity (SEC), It was also shown that the depressing effect of LF EMF on water SEC as well as its biological effects on various cells are most pronounced at frequency of 4 Hz (Stepanian et al. 1999; Ayrapetyan 2006).

Therefore, it is suggesting that the H_2O_2 could serve as one of the most reliable candidate for the messenger transferring EMF-induced water structure changes to cell metabolic cascades (Klassen 1982; Bistolfi 1991). For testing this hypothesis the comparative study of the effects of magnetized and H_2O_2 containing physiological solution (PS) on heart muscle contractility and ^{45}Ca uptake by muscle was performed.

The isolated and intra cordially perfused snail heart muscles, which is able to contract *in vitro* state for more than 24 hours (Azatian et al., 1998), was chosen as an experimental model for the present study.

Methods

Removed snail (Helix pomatia) hearts were cannulated and suspended in bath with physiological solution (PS) for snails that contains (in mM): NaCl (80), KCl (4), CaCl2 (7), Tris-HCl (5), pH 7,5. Continuously intra- and extra-heart perfusion with PS was applied. The intra cordial pressure was controlled by keeping the perfusion solution in reservoirs vessel at a constant level.

The transducer was fixed to the bottom of the heart by a silk suture. To monitor the heart contraction with the electrical signals for subsequent recording with a computer a special setup was constructed, which is schematically presented in Figure 1.

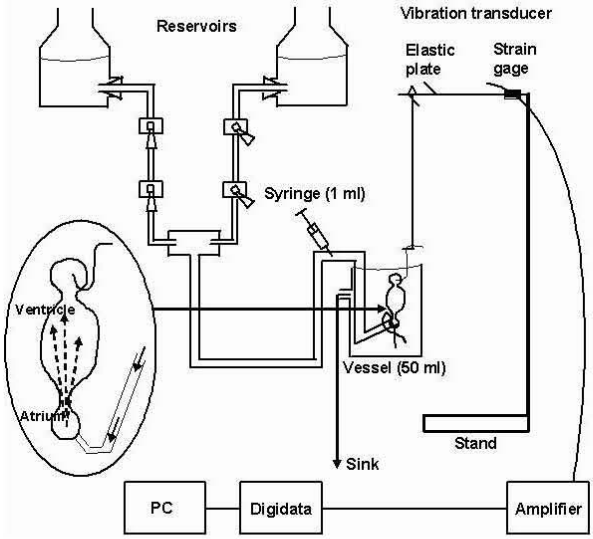


Figure 1. *The setup for the registration of heart muscle contractility. Heart contractions were recorded isotonically and displayed on PC through Digidata 1322A.*

The up and down movements of the baseline of records showed the heart contraction and relaxation, correspondingly. Usually, after heart isolation from the snail, its cannulation and suspension in bath with normal PS, its contraction stops in systole phase (which can be detected visually) or has irregular bursting with short amplitudes of contractions which sometimes could continue 1-2 hours, and then it is gradually relaxed and starts its regular contractions.

The PS treatment by Static Magnetic Field (SMF) was performed by the method described earlier (Ayrapetyan et al. 1994a). PS in a 20 ml glass chamber (50x30x15 mm) was exposed to SMF at intensities of 27 mT generated by a strong magnet for 60 minutes. The magnetic field was homogeneous within the gap in the centre of the magnet (the size of the gap varied from 0 to 15 cm, and at 50 mT the field varied by no more than 5% within a sphere with a diameter of 6 cm. Thus, the size of the vessel was small relative to the size of the homogeneous region). The background of magnetic field in the area of experimental setup in the laboratory, due to the 60 Hz electricity system, was less than 0.001 mT.

The magnetic field intensity was measured with a Teslometer W1-8 (Armenian Radiophysical Institute). This instrument measured magnetic fields in the range 10^{-3} to 1.6 T(±5%). This magnetic induction converter was a crystal type X511-1, 1.5 x 0,2 mm^2 and was fixed on nonmagnetized material (PX13-1).

The sham treatment of PS was performed on the same table and in a same 20 ml glass chamber located at same geometric place, i.e. the sham exposed PS was in the same environmental medium excluding SMF (the static magnet was moved away from the exposure table for ~10m). The both sham and SMF exposed solutions were taken from the same container of stock solution, which was preliminary kept in water bath with stable temperature (21±0,5^o C) during no less than one hour. The temperature of the heart incubated in the chamber was continuously recorded by needle-type thermometer having sensitivity of ±0,1 ^{0}C. The room temperature was 22^{o}C.

In physiological experiments only the reversible effect of MPS-induced changes of heart contractility (frequency, amplitudes and basic line) were considered as a reliable, i.e. when after replacing the MPS by sham exposed solutions, the initial activity of the heart muscle was restored. For each individual heart muscle the number of repetitions of such protocol was varied from 1 to 10 depending on the duration of stabile heart muscle contractility *in vitro*, which for some preparations could prolong until ~24 hours.

The stock solution (10^{-2} M) of H_2O_2 was prepared each day by diluting 3% H_2O_2 by physiological solution and protected it from light to minimize its photo-degradation. H_2O_2 was added to the intra-cordially perfused solution to a final concentration from 10^{-4} to 10^{-12} M. All the experiments were carried out at 18 ± 0.5°C.

^{45}Ca uptake by muscles incubated in normal and magnetized PS was measured by ^{45}Ca isotope having specific activity: 0.185-1.85GBq/mg Ca, 5-50mCi/mg Ca (Amersham Life Science production). Control and experimental groups contained per 10 hearts each(total n=.40) Isolated hearts were incubated in four plastic tubes with control and magnetized normal or K-free solutions containing ^{45}Ca isotopes (0,45 mCi/ml). Then hearts were washed three times per 5min with cold normal or K-free PS (where 4mM KCI was replaced by 4mM NaCl) to remove isotope from the extra cellular spaces. Radioactivity was measured using a liquid scintillation spectrometer (production of Packard TRI-CARB Canberra Cambridge Company) and calculated as pM/mg of wet weight. .

The mean value, standard deviations, and the statistical probability, determined by Student Test were calculated with the help of computer program Sigma Plot (Version 8.02A).

Results

For estimating the role of H_2O_2 in realization of biological effect of MPS on heart contractility the dose-dependent effect of H_2O_2 on heart contractility was studied in normal and K^+-free solution. As seen in Figure 2A the low concentrations (10^{-12}- 10^{-10} M) of H_2O_2 had elevation effect on amplitude of heart contractility, while at higher concentrations (>10^{-7} M) this amplitude was depressed.

In order to estimate the role of electrogenic Na^+-K^+ pump in H_2O_2-induced effect on heart contractility, similar experiments were repeated in K-free solutions, when Na^+-K^+ pump is in inactive state (Figure 2B). It was known that K ions removal from extra cellular medium led to the inactivation of Na^+-K^+ pump, and the restoration of K ions in the medium caused the reactivation of the pump leading to hyper polarization of the cell membrane (Thomas, 1972).

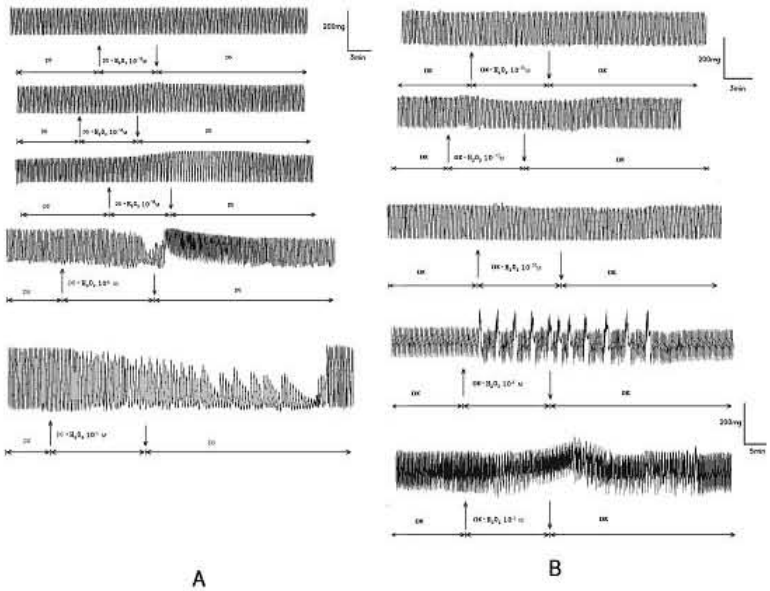


Figure 2. *The dose-dependent effect of H_2O_2 on heart muscle contractility in normal (A) and K-free (B) PS.*

In K-free medium the sensitivity of heart contractions to $H_2O_2$was increased compared to those in normal PS (Figure 2A). If the minimal concentration of H_2O_2 in normal PS able to modulate the heart contractility is 10^{-12} M, in K-free solution it was 10^{-13} M. Previously it was shown that Na^+-K^+ pump activation leads to the inhibition of heart beating (Azatyan et al., 1998). At the same time it was shown that this effect disappeared after perfusion of heart muscle by MPS (Ayrapetyan et al., 2005). In order to find out whether this effect is due to the H_2O_2 formation in MPS, the dose-dependent effect of H_2O_2-containing K-free PS on Na^+-K^+ pump-induced transit inhibition of heart beating was studied (Figure 3A).

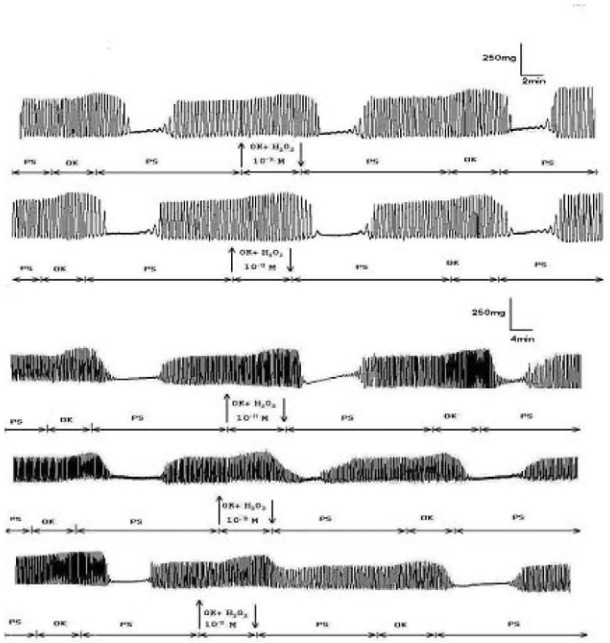


Figure 3. *The dose-dependent effect of hydrogen peroxide in K-free solution on Na-K pump-induced transient inhibition of heart muscle beating.*

It is known that the muscle incubation in K-free solution leads to the increase of intracellular Na ion concentration because of inactivation of Na^+-K^+ pump and its re-incubation in normal K-containing medium, the pump activation was accompanied by depression of heart contractility (Azatyan et al., 1998). As can be seen in Figure 3 the muscle incubation in 10^{-10} M H_2O_2 containing K-free medium in period of pump-induced inhibition of heart beating, the small amplitude of vibration of heart muscle appeared, while in case of 10^{-9} M H_2O_2 this pump-induced transit inhibition of heart beating fully disappeared. Similar effect was obtained when the Na enrichment of muscle was performed in normal K-free and then was re-incubated in H_2O_2-containing normal PS (Figure 4).

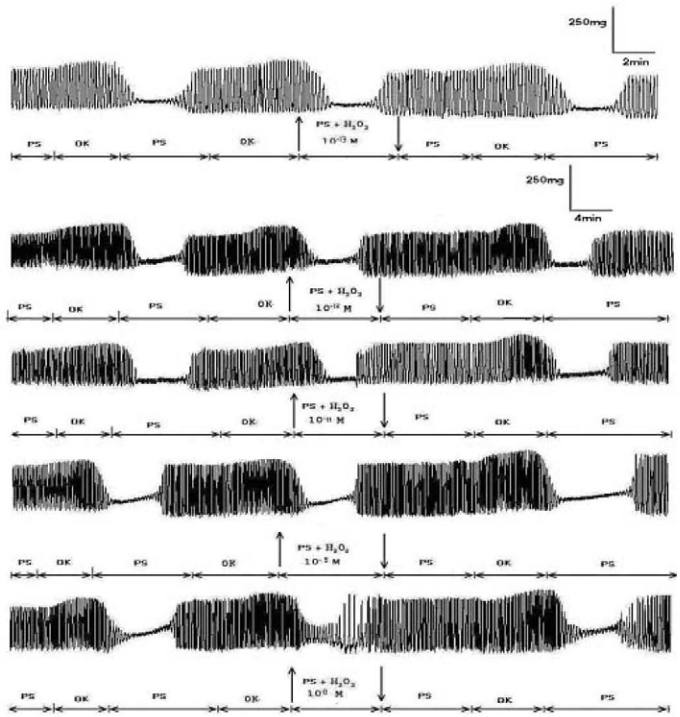


Figure 4*. The dose-dependent effect of hydrogen peroxide in normal PS on Na-K pump-induced transient inhibition of heart muscle beating.*

Thus, the H_2O_2-induced stimulation of heart muscle contractility in period of pump-induced transit inhibition of heart beating is very similar to the effect of MPS (Figure 5).

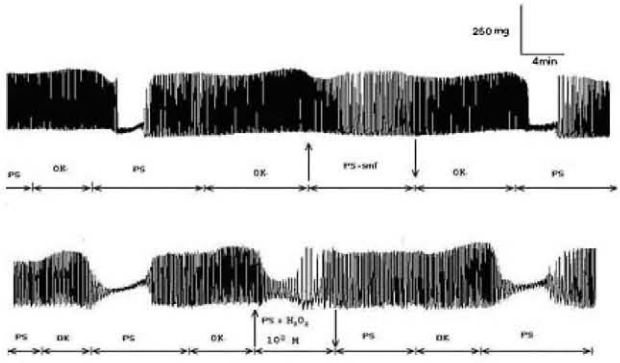


Figure 5. *The effects of magnetized PS (upper) and 10^{-8} M hydrogen peroxide (lower) on Na-K pump-induced transient inhibition of heart muscle beating.*

As intracellular Ca ions concentration has pivotal role in muscle contractility in the next series experiments the comparative study EMF –treated PS and H_2O_2 on ^{45}Ca uptake by muscle was study in Na^+-K^+ pump active (in normal PS) and inactive state (in K-free medium).

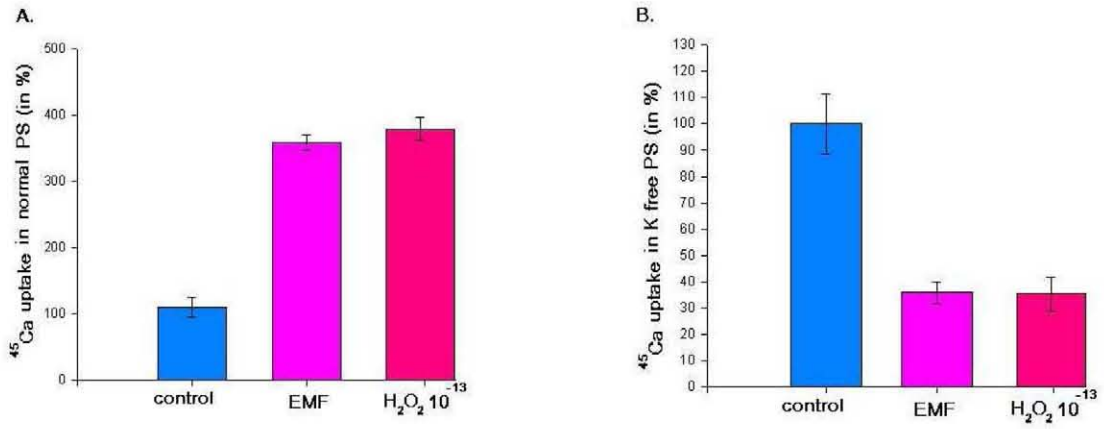


Figure 6. *The effect of MV- and EMF-treated PS (A) and K-free PS (B) in ^{45}Ca uptake by heart muscles (expressed in %, compared to their control value).*

As can be seen in Figure 6 the both EMF-treated and H_2O_2- containing solutions have activation effect on Ca uptake in normal PS, while in K-free solution this effect was reversed, i.d. the both factors have inhibitory effect on ^{45}Ca uptake.

Summary

Previously it was shown that MPS had dual effect on heart muscle contractility: relaxation and stimulation of pacemaker activity (Ayrapetyan et al., 2005). If the relaxation effect of MPS on heart muscle was explained by Ca-deflection of muscle in result of activation of cGMP-dependent Na^+/Ca^{2+} exchanger, the mechanism of MPS-induced stimulation of heart contractility in period of pump-induced inhibition of heart beating still remains unclear. At the same time in literature the experimental data showing the H_2O_2 generation in water medium upon the effect of magnetic fields are available (Klassen 1982). The obtained data on the synergic effects of H_2O_2 and MPS on Na^+-K^+ pump-induced muscle relaxation following the pre-incubation of the heart in K-free medium allow us to conclude that MPS-induced stimulation of heart contractility is due to the H_2O_2 formation in MPS. The data that the activation effects of H_2O_2 and MPS on Na^+-K^+ pump-induced muscle relaxation following the pre-incubation of the heart are present in both cases: in K-free medium or in case of heart re-incubation in K-containing solutions treated by EMF or containing H_2O_2, i.e. when the pump was in active and inactive states, correspondingly, could serve as an evidence on the pump-independent stimulation effects of MPS and H_2O_2 on heart. It is strange that this effect does not depend on Ca metabolisms: in spite that the MPS and H_2O_2 in normal PS have activation and in K-free solution- inactivation effects on Ca uptake, in

both cases MPS and H_2O_2 have stimulation effects on heart muscle contractility.

Thus, the main conclusion from the presented data is that H_2O_2 is one of important messenger through which the biological effect of ELF EMF on heart muscle contractility is realized.

References

Ayrapetyan SN, Grigorian CV, Avanesian AS. 1994a. On a mechanism of action of magnetic field on the electrical conductivity of water solutions and some properties of Helix neurons. *Bioelectromagnetics*, **15**: 133-142.

Ayrapetyan GS, Papanyan AV, Hayrapetyan HV, Ayrapetyan SN. 2005. Metabolic pathway of magnetized fluid-induced relaxation effects on heart muscle. *Bioelectromagnetics*. **26**(8): 624-30.

Ayrapetyan SN. 2006. Cell aqua medium as a preliminary target for the effect of electromagnetic fields. In: *Bioelectromagnetics: Current Concepts*, S. Ayrapetyan and M. Markov, eds., NATO Science Series, Springer Press, The Netherlands, pp: 31-64

Azatian KV, White AR, Walker RJ, Ayrapetyan SN. 1998. Cellular and Molecular Mechanisms of Nitric Oxide-Induced Heart Muscle Relaxation. Gen. Pharmac., **30**: 543-553.

Bistolfi F. 1991. Biostructures and Radiation Order Disorder, Edizioni Minerva Medica, Torino, Italy.

Klassen 1982; in: Magnetized Water Systems. "Chemistry" Press, 296 p (in Russian), English translation: European Biology and *Bioelectromagnetics*, 2006, **1**(2): 201-220

Stepanyan R., Ayrapetyan G., Arakelyan A., Ayrapetyan S. 1999. Effect of Mechanical Oscillations on Electrical Conductivity of Water Biophysics, **44**: 197-202.

EFFECTS OF SURFACE CHARGE AND DC EF FIELDS ON CELLS

RICHARD H.W. FUNK THOMAS K. MONSEES

DEPARTMENT OF ANATOMY, UNIVERSITY OF TECHNOLOGY, DRESDEN, GERMANY

Abstract

In this paper we will concentrate on the effects of surface charge patterns of surfaces which are the substrate for cell adhesion and migration as well as on the effects of static direct current electric (dc EF) fields. Findings in the literature and own results will be discussed.

Results and Discussion

In vitro, the application of static dc EF of physiological power causes directed movement and guiding of bone cells and various other cell types. This phenomenon is called electrotaxis (or galvanotaxis) [Zhao et al., 2002]. In vitro, at field strengths of 0.1–10 V/cm, cells often migrate to the cathode (neural crest cells, fibroblasts, keratinocytes, chondrocytes, rat prostate cancer cells and many epithelial cell types). Only few cell types move to the anode (corneal endothelial cells, bovine lens epithelium, human granulocytes and human vascular endothelial cells). Speed and direction of the movement are voltage dependent: human vascular endothelial cells migrate towards the anode, whereas bovine aortic endothelial cells move to the cathode. During movement, ruffled membranes, lamellipodia and filopodia are formed preferentially in the direction of the anticipated electrotaxis migration [Sulik et al., 1992; Zhao et al., 2002]. Several cell types changed their initial direction of movement by 180° when the current polarity was reversed [Soong et al., 1990; Brown and Loew, 1994; Chao et al., 2000; Wang et al., 2000b]. EF-induced cell migration can be modified by proteins of the ECM. For example, highest cathodal migration was noticed with keratinocytes plated on collagen and plastic, whereas lowest locomotion occurred on laminin. Cell response on fibronectin was in between the two. Similar results were observed for epithelial cell electrotaxis on laminin or fibronectin coatings. Sun et al. [2004] noticed directed movement of fibroblast migration at a field strength as low as 0.1 V/cm in 3-dimensional collagen gels, but not in conventional 2-dimensional cultures. Thus, 3-dimensional conditions seem to reflect the in vivo situation, where dc EF of 0.1 – 0.2 V/cm occur that are important for embryonic development [Nuccitelli, 2003]. Several steps are involved in cell migration: (1) due to their connection to several adaptor proteins, the growing of actin filaments will push the cell membrane in the direction of movement; (2) formation of focal contacts at the leading edge, i.e. specific bindings via membrane bound integrin receptors and ECM proteins, which will also influence several signaling pathways and structural elements of adhesion; (3) focalized proteolysis by recruitment of surface proteases to ECM contacts; (4) cell contraction driven by myosin II binding to actin filaments, and (5) disassembly of focal contacts and detachment of the trailing edge. Many of these events have also been observed in EF-induced cell movement.

If one looks at the level of a single cell in an EF, then elongation of the cell body and alignment of its long axis perpendicular to the field lines are striking phenomena. This behavior was first described for Xenopus myoblasts and thereafter observed in many other cell types including fibroblasts, osteoblasts, chondrocytes, keratinocytes, endothelial and epithelial cells. As dc EF trigger migration and orientation, cells must orchestrate cytoskeletal elements and shape in response to this trigger.

An accumulation of actin stress fibers was observed on the cathodal (leading) edge of several cell types [Sulik et al., 1992; Zhao et al., 2002]. Often, the total amount of filamentous actin transiently increased and became

selectively enriched in the leading lamellipodia. Here, focal contacts were also accumulated. Recent experiments showed that EF-mediated motility in fibroblasts can be halted by inhibition of microfilament dynamics, whereas inhibition of microtubules only reduced migration speed [Finkelstein et al., 2004]. Membrane extensions from the trailing edge of chondrocytes were concomitantly retracted [Chao et al., 2000]. Also osteoblasts and osteoblast-like cells undergo processes of retraction and elongation ultimately resulting in the realignment of the long cellular axis perpendicular to the EF [Curtze et al., 2004]. These authors presented a theory to explain the EF-induced perpendicular orientation of cells: cell attachment is made by the adhesive interaction of ECM proteins with a group of transmembrane adhesion receptors, the integrins. After binding to their specific ligands, integrins cluster within the membrane and recruit several adaptor and signaling proteins to form focal contacts (also called focal adhesions) that anchor the ends of intracellular actin filaments (stress fibers). Vinculin is one of these adaptor proteins and is frequently used as a marker for integrin-based focal contacts. As stated here and elsewhere [Jaffe, 1977; Poo, 1981], dc EF trigger the separation of charged membrane components. In order to achieve perpendicular elongation, a certain self-induced cytoskeletal tension is required along the axis. Assuming that all free integrin receptors drift towards an electrode and accumulate there, the cell is only able to connect to two focal adhesions and increase tension between them if they are on an axis perpendicular to the drift. Cell adhesion is a dynamic process, thus after some time, disassembly of focal contacts on the opposite side of the drift destination leads to another drift. Consequently, the cell is no longer able to maintain protrusions with the same orientation as the EF [Curtze et al., 2004].

Our experiments using corneal endothelial cells support this hypothesis: vinculin proteins, used as a marker for integrin receptors, are normally randomly distributed within the cell with a preference for the cell border. However, after dc EF application, they concentrate on two major spots of focal contacts oriented perpendicular to the EF vector. Mechanical load is also discussed as a possible transducer of EF. EF-induced effects such as dynamic changes in intracellular calcium concentration, cell traction and orientation are similar to the cellular response after mechanical stimulation [Curtze et al., 2004]. Converse flexoelectricity may thereby be a way for cells to sense small dc EF. Charged proteins in the lipid bilayer of the cell membrane repel each other, influencing membrane tension. If the charge on one side of the membrane is changed by dc EF, the membrane tension also changes, resulting in a modified curvature of the membrane. Such flexoelectric effects have already been demonstrated on voltage-clamped cells. Using traction force microscopy, Curtze et al. [2004] noticed a 5–30% increase in average traction force magnitude 10–30 s after dc EF exposure as the first detectable reaction of osteoblasts. The visible retraction phase started after 5–10 min, and then, cells subsequently elongated and oriented perpendicular to the EF lines. Traction forces at the margins tangential to the EF decreased 2–15 min after the start of EF exposure below their initial values. A mean delay of 85 s between EF application and first observable changes in Ca 2+ levels occurred, suggesting that stretch-activated Ca 2+ channels may be responsible for the Ca 2+ influx. Static MF (10 T) also oriented glioblastoma cells in the presence of collagen fibers possibly due to the rearrangement of microtubules [Hirose et al., 2003].

Studies of Erskine and McCaig [1997] and Ohgaki et al. [2001] as well as our own results showed that negatively charged surfaces are a sometimes better interface for cell adhesion and further cell function than positively charged ones. Using controlled surface charge induction on implants, it was shown that the above mentioned charge densities are sufficient to alter cell growth, adhesion and phenotypic. Moreover, specific effects can be observed when cells are plated onto substrates which have been exposed to ELF EMF before plating [McLeod and Rubin, 1994]. Together, these results strongly suggest that the observed effects are associated with an alteration in absorption of charged proteins, and change in the cellular response results from the altered ‘charge environment’.

Seen ‘with the eyes of a cell’, the surface of an implant is covered with water and ions (in vivo serum, in vitro cell culture medium). Then, amino acids and proteins (especially albumin, fibronectin and vitronectin) are absorbed to the surface due to unspecific charge interactions [Vroman, 1988]. At negatively polarized (e.g., glass) and negatively charged surfaces, inorganic cations like calcium and cationic amino acids and proteins may bind to the surface, making it a suitable interface for the negatively charged surface of the cell [Ohgaki et al., 2001]. Additionally, Ca 2+ ions are required for the formation of focal adhesions. Thus, a higher local concentration of Ca 2+ will accelerate specific integrin receptor-mediated binding. In the next step of the attachment sequence, the cell recognizes RGD motifs (a sequence of amino acids which is important for binding processes) of surface-bound proteins, and finally, specific binding occurs at focal adhesions via integrin receptors (early and late). As the ‘missing link’ between the patterns of surface charges and special adhesion proteins described above, Botti et al. [1998] described a class of adhesion proteins that, because of their common electrostatic and structural motif,

were called ‘electrotactins’. These proteins had a functional region common to cholinesterases and exhibitied a special pattern of electrostatical surface potentials.

Responding to extracellular cues like EMF involves a cascade of events, transducing signals from the cell surface to the cytoskeleton. Due to the high dielectric property of the lipid bilayer membrane, externally applied dc EF will be considerably attenuated. For example, a dc EF of 5 V/cm will produce an intracellular field of only 0.5 mV/cm, which is unlikely to produce significant effects [Poo, 1981].

What is the sensor for EF gradients? A suggested mechanism is the electrophoretic mobility of charged molecules in the cell membrane in a dc EF [Jaffe, 1977; Poo, 1981]. In this respect, electroosmosis (see also above) plays a role: the imposition of a dc EF on the negatively charged cell membrane produces a flow of positive counter ions, which will result in a flow of fluid towards the cathodal site of the membrane. By this flow, a negatively charged receptor will be swept to the cathodal side of the membrane if its _ potential is less negative than the potential of the cell surface; otherwise it will accumulate on the anodal site [Poo, 1981; McCaig et al., 2005]. The potential is the electric potential at the interface between a solid surface or membrane and a liquid. Such lateral movements and enrichments of membrane components towards the cathode have been observed in several cell types. Examples are concanavalin A and acetylcholine receptors or positively charged membrane lipids in Xenopus myotomal membrane [Poo, 1981], fibronectin receptor in fibroblasts [Brown and Loew, 1994], lipids and epidermal growth factor (EGF) receptor in keratinocytes [Song et al., 2002], membrane lipids or EGF and hepatocyte growth factor receptors in corneal epithelial cells [Zhao et al., 2002; McBain et al., 2003]. Thus, one can imagine that redistributed membrane molecules can be sensed inside the cell by components of the cytoskeleton and be used as an orientation cue. Some of these mechanisms have been explored in more detail. Finkelstein et al. [2004] recently demonstrated that microtubules are involved in EF-induced cell migration. Signaling molecules such as Rho GTPases and protein kinases interact with microtubules and can effectively hitchhike microtubule-based transport. In this way, they pass signals from the leading edge of the cell via the nucleus to the trailing edge. An EF induces redistribution of hepatocyte growth factor receptors and triggers the mitogen-activated protein kinase pathway downstream that is involved in epithelial cell migration [McBain et al., 2003]. Similarly, EGF receptor kinase activity and redistribution in the cell membrane are necessary for electrotaxis in keratinocytes. In chondrocytes, antagonists of the inositol phospholipid pathway were able to inhibit cathodal migration [Chao et al., 2000]. In contrast to the arising weak internal field, the externally applied dc EF can induce substantial alterations of the membrane potential. The resting potential of a nonexcitable cell is approximately –45 to –75 mV. A usual dc EF of 1–10 V/cm applied to a cell of 10 _ m in radius will hyperpolarize the membrane facing the anode by 1.5– 15 mV and depolarize the cathodal site by the same amount. This is sufficient to induce several physiological effects such as changes in the levels of calcium ions [Poo, 1981; Mycielska and Djamgoz, 2004; Robinson, 1985]. In many cells, dc EF-induced migration depends on changes in intracellular Ca 2+ concentration. Since the cytoplasm on the anode-facing site became more negative, the inward driving force of Ca 2+ was increased at the anode, whereas that on the cathodal site decreased (passive influx). Increasing [Ca 2+] often activates myosin light chain kinase that phosphorylates the regulatory light chain of myosin II. This in turn triggers the actin-activated myosin ATPase, a major regulator in cell contraction. In consequence, the anodal site contracts and the cell will be propelled towards the cathode. If voltage-gated Ca 2+ channels are present, a cathode-faced membrane depolarization should open them, and the Ca 2+ influx following this opening will cause cell migration towards the anode. The calcium waves measured were fast (22.5–50 _ m/s, i.e. faster than electroosmosis) which could possibly explain the very fast cell reactions reported in other EMF studies. However, the net movement (and direction of cell migration) depends on the balance of passive influx and voltage-gated influx of Ca 2+. Calcium ions are also essential for the coupling of other forms of EMF to a biological system.

In conclusion, the cell-guiding effects of static EF have a good explanation with the observations of the electrophoretic mobility of charged cell membrane molecules. However, a cascade of events must be initiated for this effect to be linked to classical biochemical pathways.

Literature

Botti, S.A., C.E. Felder, J.L. Sussman, I. Silman
(1998) Electrotactins: a class of adhesion proteins
with conserved electrostatic and structural
motifs. Protein Eng *11:* 415–420.

Brown MJ, Loew LM: Electric field-directed fibroblast locomotion involves cell surface molecular reorganization and is calcium independent. J Cell Biol 127:117-28, 1994

Chao PHG, Roy R, Mauck RL, Valhmu WB, Hung CT: Chondrocyte translocation response to direct current electric fields.
J Biomech Engineering 122:261-267, 2000

Curtze S, Dembo M, Miron M, Jones B: Dynamic changes in traction forces with DC electric field in osteoblast-like cells. J Cell Sci 117:2721-9, 2004

Erskine L, McCaig CD: Integrated interactions between chondroitin sulphate proteoglycans and weak dc electric fields regulate nerve growth cone guidance in vitro. J Cell Science 110:1957-1965, 1997

Fang K. S., Ionides E., Oster G., Nuccitelli, Isseroff R. R.: Epidermal growth factor receptor relocalization and kinase activity are necessary for directional migration of keratinocytes in DC electric fields. J Cell Sci 112:1967-1978, 1999

Finkelstein E., Chang W., Chao P. H. G., Gruber D., Minden A., Hung C. T., Bulinski J. C.: Roles of microtubules, cell polarity and adhesion in electric-field-mediated motility of 3T3 fibroblasts. J Cell Sci 117:1533-1545, 2004

Hirose H., Nakahara T., Zhang Q. M., Yonei S., Miyakoshi J.: Static magnetic field with a strong magnetic field gradient (41.7 T/m) induces c-Jun expression in HL-60 cells. In Vitro Cell Dev Biol Anim. 39:348-52, 2003

Jaffe L. F.: Electrophoresis along cell membranes. Nature 265: 600-602, 1977

MacBain V. A., Forrester J. V., McCaig C. D.: HGF, MAPK, and a small physiological electric field interact during corneal epithelial cell migration. Invest Ophthalmol Vis Sci 44:540-547, 2003

McCaig, C.D., A.M. Rajnicek, B. Song, M. Zhao
(2005) Controlling cell behavior electrically:
current views and future potential. Physiol Rev
85: 943–978.

McLeod K. J., Rubin C. T.: Regulation of Cell Growth Rates in Vitro by Alteration of Induced Charge Density. The Annual Review of Research on Biological Effects of Electric and Magnetic Fields From the Generation, Delivery and Use of Electricity, Frederick, MD, W/L Associates, Ltd 80:65, 1994

Mu-ming Poo: In situ electrophoresis of membrane components. Ann. Rev. Biophys Bioeng 10:245-76, 1981

Nuccitelli R.: A role for endogenous electric fields in wound healing. Curr Top Dev Biol. 58:1-26, 2003

Ohgaki M., Kizuki T., Katsura M., Yamashita K.: Manipulation of selective cell adhesion and growth by surface charges of electrically polarizes hydroxyapatite. J Biomed mater Res 57:366-373, 2001

Soong H. K., Parkinson W. C., Bafna S., Sulik G. L., Huang S. C. M.: Movements of cultured corneal epithelial cells and stromal fibroblasts in electric fields. Invest Opthalmol Vis Sci 31:2278-2282, 1990

Sulik G. L., Soong H. K., Chang P. C., Parkinson W. C., Elner S. G., Elner V. M.: Effects of steady electric fields on human retinal pigment epithelial cell orientation and migration in culture. Acta Ophthalmol (Copenh) 70:115-122, 1992

Sun, S., J. Wise, M. Cho (2004) Human fi broblast migration in three-dimensional collagen gel in response to noninvasive electrical stimulus. 1. Characterization of induced three-dimensional cell movement. Tissue Eng *10:* 1548–1557.

Vroman, L. (1988) The life of an artifi cial device in contact with blood: initial events and their effect on its fi nal state. Bull N Y Acad Med *64:* 352–357.

Wang E., Zaho M., Forrester J. V., McCaig C. D.: Re-orientation and faster, directed migration of lens epithelial cells in a physiological electric field. Exp Eye Res, 71; 91- 98, 2000b

Zhao M., Pu J., Forrester J. V., McCaig C. D.: Membrane lipids, EGF receptors, and intracellular signals colocalize and are polarized in epithelial cells moving directionally in a physiological electric field. FASEB J (April 10) 10.1096/fj.01-0811fje, 2002.

RETINAL SCANNING OF CRITICAL FUSION FREQUENCY (CFF) OF THE HUMAN EYE

MAGDY S. IBRAHIM

DEPARTMENT OF ENGINEERING MATHEMATICS AND PHYSICS
FACULITY OF ENGINEERING, CAIRO UNIVERSITY, 12211
GIZA, EGYPT

Abstract:

The aim of the present study is to introduce an electronic experimental setting for measuring of critical time (CT) and corresponding critical fusion frequency (CFF) for healthy subjects at different wavelengths and different acuities. The work introduces a simple measuring setting that utilizes an electronic device capable of controlling the frequency of illuminated monochromatic light source.

The investigation considered the size of the stimulus, its luminance, the distance from the eye to the fixed and movable light sources. Particular interest was given to scanning the retina for various CFF responses. The results show that , CFF has a maximum value at fovea and this value decreases nonlinearly as we move to the periphery, explanation of this results is introduced and related to cone and rod distribution at different retinal visual angle as well as the different response of cones to color .

Introduction:

Critical flicker frequency (CFF) is the transition point of an intermittent light source where the flickering light ceases and appears as a continuous light. Accordingly, it is the minimum frequency of a pulsating light source at which the light appears to be fused into continuous, rather than flickering, stimulus. There are a multitude of factors that determine our perception of flicker such as the intensity and size of the test stimulus[1].

Researches in this field are important in diagnosing by the measurements of fusion of the human eye. Braunstein[2] was one of the first to investigate CFF in cases of optic atrophy, optic neuritis and glaucoma. Since then measurements have shown to be sensitive to the presence of retinal or optic nerve diseases when other clinical tests remain unaffected[3, 4].

Several factors such as the light intensity, the target size, and the luminance contrast[5] are affecting on the CFF. Keesey[6] , illustrated that the visual target size affects flicker perception at frequencies higher than 20 Hz , CFF is known to increase with increasing target stimulus size ; under 20 Hz, the sensitivity decrease with increasing target size. Delange[7] demonstrated that for visual stimulus with a fixed temporal frequency; sensitivity to flicker increases as the amplitude of the luminance is increased.

At high frequencies, flicker sensitivity curves for different size of visual stimuli have similar shapes, Kelly[8]. This indicates the visual system responds the temporal characteristics of stimuli in a consistent fashion. At frequency higher than 20 Hz CFF thresholds decreased as target size increases. The age plays an important role, Kim[9], showed that young people in general have higher CFF than older ones. In addition, women enjoy higher CFF than men[10].

CFF is significantly higher than at the fovea when the image is projected at the fovea, also the flicker depends of the background illumination, for dark background, the CFF is lower than that for background at 50 lux[11]. Wolfgang[12], studies the effects of the CFF at the accommodation, convergence and pupil diameter of the human eye. Toshiyuki[13], studied the effects of illumination, distance between the eye and the light source and age on the CFF.

However, very little attention is given to the study of flickering at different point on the retina. Most of the reported literature is concerned with CFF when the image is received at the fovea. In the present work, the CFF at different locations in the visual field for different wavelengths is examined. It employs a device, which enable the researchers to obtain accurate data concerning the effect of the both locations and wavelengths on the CFF value.

Apparatus used:

An electronic device was designed so that light of several wavelengths can produced and jittered from different LEDs. The light pulses are supplied from a square wave function generator. The wave generator produces square pulse, which is differentiated electronically, and then the edge of the pulse was used to initial a rectangular wave using a monostable oscillator. This stage is necessary to control both the pulse duration (T_1) and the time interval between the successive pulses (T_2). At the end, the output of the monostable vibrator is sent to a movable LED 2 light source. The light is filtered so that only the concerned wavelengths are obtained purely.

The pulse is observed using an oscilloscope and fed to PC to record the results. The pulse duration was kept constant while the time interval between pulses varied electronically. The block diagram of electronic circuit can be shown in Figure 1.

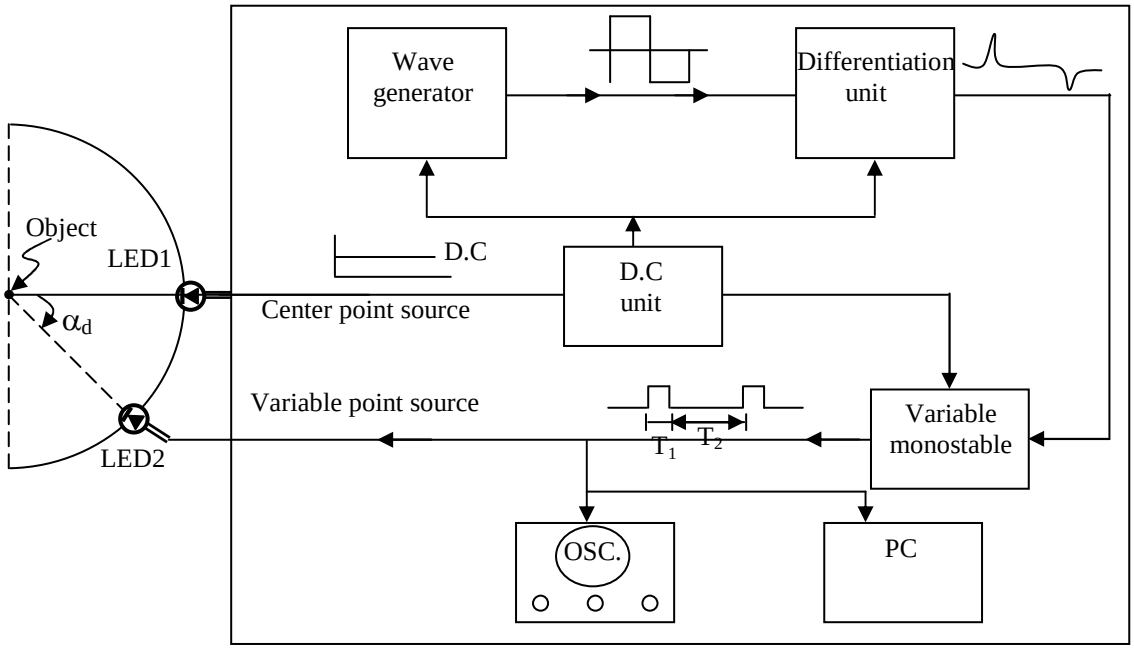
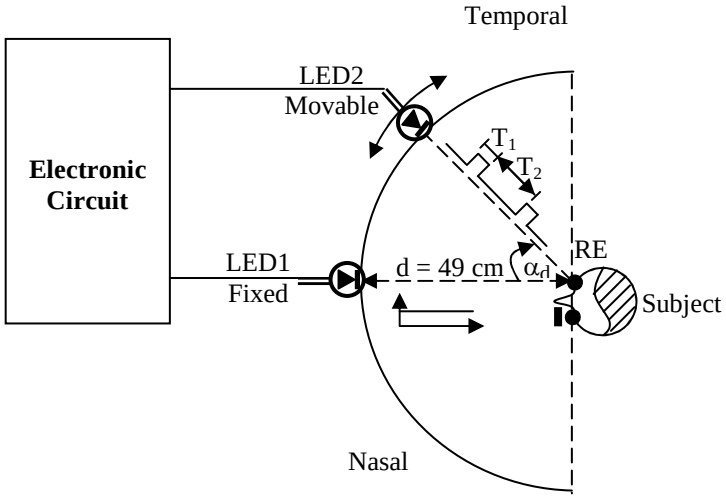
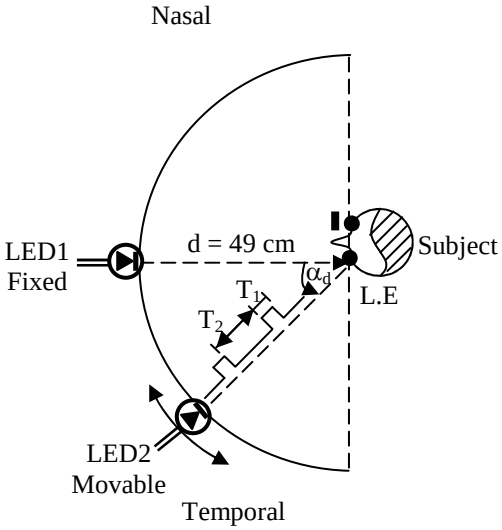


Figure 1

The mechanical device consists of two stand and semi-circular arc of radius 49 cm , the length of the arc is calibrated such that the distance from the center of fixation point to any point on the arc (d) corresponds to an angle α d which is called retinal visual angle at the center of the arc as shown in Figures 2 (a , b) .



Experimental setting for measurement of critical time
Figure 2-a Nasal and Temporal Vision of R.E



R.E
Figure 2-b Nasal and Temporal Vision of L.E

Procedure:

Ten subjects (mean age 30 ± 5 years) were examined for CFF , the visual acuity , sex ,weight , occupation and the state of the health are recorded . The experimental setting is kept under dark conditions. Measurements were taken for each eye separately for each subject. The subject was asked to keep focusing on the center of the arc where a fixed light source LED 1 at the fixed wavelength is located. As the subject is focusing on this source, another source LED 2 of the same wavelength was made to slide slowly on the arc at different positions.

For each position, the light controlled from the second source is made to fluctuate electronically at different frequency, the subject was asked to tell when he sees the light continuously. At that time, the frequency of the light was determined using an oscilloscope. The value of the CFF is obtained an average value for more than six repetitions of the CFF thresholds were obtained.

The procedure was repeated for different wavelengths of λ_1 = 540 nm , λ_2 = 580 nm and λ_3 = 660 nm at different locations on the retinal visual field for each subject. In addition, the effect of the visual acuity was investigated on the CFF thresholds.

Results:

The effects of the different wavelengths on the Critical Time (CT) are measured as shown in Figures 3 and 4. CT has a minimum value at the fovea for all wavelengths; this is because the fovea is the most region of the retina, which contains the maximum concentration of the receptors of, cons (337×10^3 cones). At the temporal side of the eye, CT increases due to the decreasing of the concentration of the cons. CT is higher throughout the periphery than the fovea CT for λ_1 = 540 nm is less than CT for λ_2 = 580 nm and for less than λ_3 = 660 nm .

Fig . 3 - a Critical Time for R.E (Temporal)

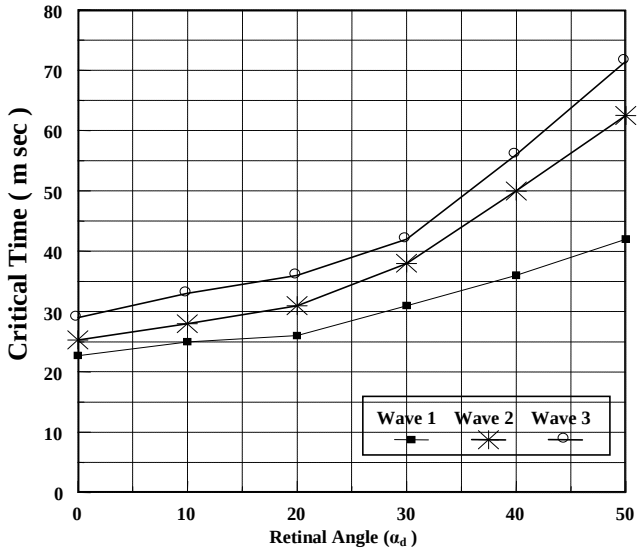


Fig . 3 - b Critical Time for R.E (Nasal)

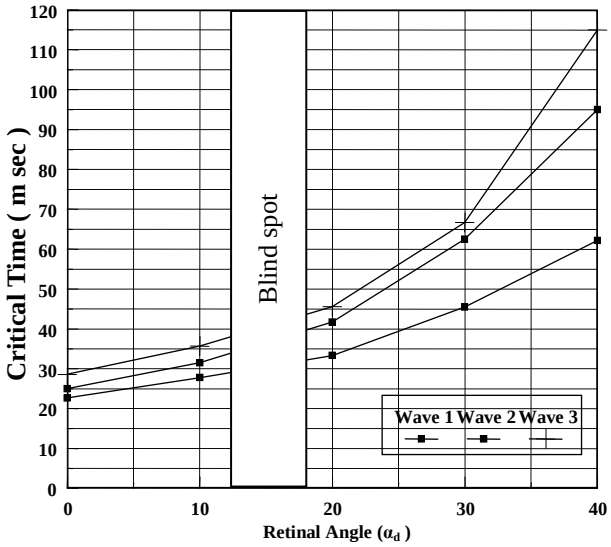


Fig . 4 - a Critical Time for L.E (Temporal)

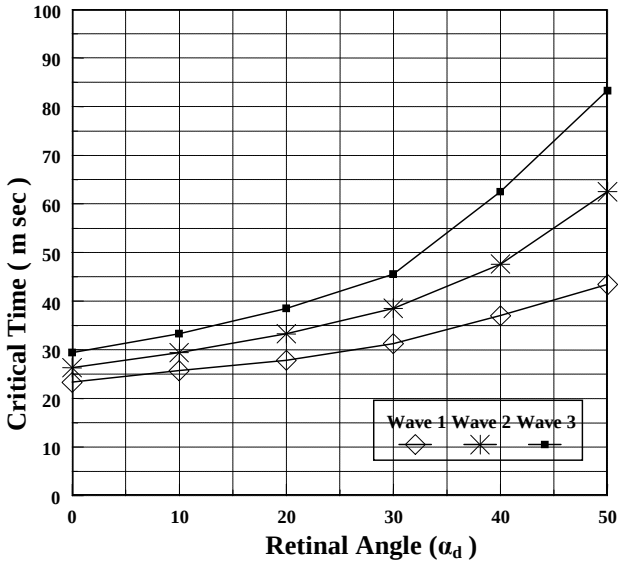
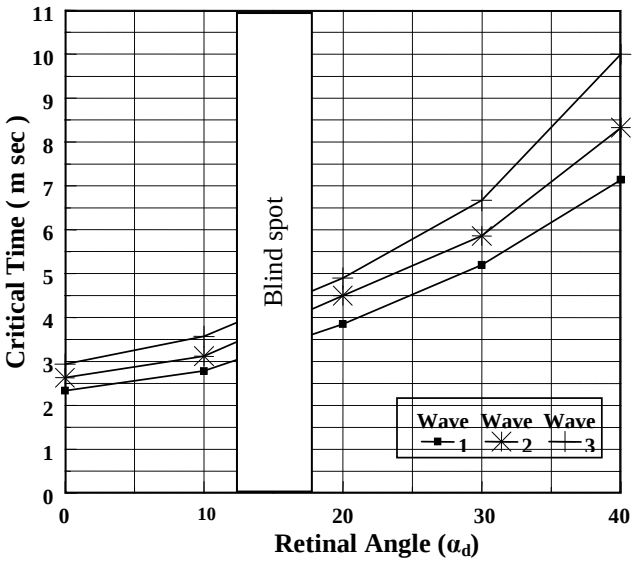


Fig . 4 - b Critical Time for L.E (Nasal)



CFF has a maximum value at fovea (± 2.5º from the visual axis) and this value decreases in the periphery, the reason of this return to the existing of different pathways long (SC) & short (LGN) CFF has a maximum value than in periphery. Also , the different rates , low (blue cone) & high (red and green cones) of neural signal causes that the CFF has a different value at different retinal visual angle, and at different wavelengths of light sources , the values of CFF at different locations of the retina for different wavelengths for right and left eyes respectively are shown in Tables 1,2.

Table 1: CFF values at different locations of visual retinal angle (α_d°) for different wavelengths. (R.E)

Retinal angle (α_d°)	CFF (Hz) Temporal Side		
	Wave 1 λ_1 **= 540 nm**	**Wave 2** λ_2 **= 580 nm**	**Wave 3** λ_3 **= 660 nm**
0º	44	40	35
10º	40	35	30
20º	38	32	28
30º	32	26	24
40º	28	20	18
50º	24	16	14

Table 1-a Temporal side

Retinal angle (α_d°)	CFF (Hz) Nasal Side		
	Wave 1 λ_1 **= 540 nm**	**Wave 2** λ_2 **= 580 nm**	**Wave 3** λ_3 **= 660 nm**
0º	44	40	35
10º	36	32	28
20º	30	24	22
30º	22	16	15
40º	18	10	8

Table 1-b Nasal side

Table 2: CFF values at different locations of visual retinal angle (α_d°) for different wavelengths. (L.E)

Retinal angle (α_d°)	CFF (Hz) Temporal Side		
	Wave 1 λ_1 **= 540 nm**	**Wave 2** λ_2 **= 580 nm**	**Wave 3** λ_3 **= 660 nm**
0º	43	38	34
10º	39	34	30
20º	36	30	26
30º	32	36	22
40º	27	21	16
50º	23	16	12

Table 2-a Temporal side

Retinal angle (α_d°)	CFF (Hz) Nasal Side		
	Wave 1 λ_1 = 540 nm	Wave 2 λ_2 = 580 nm	Wave 3 λ_3 = 660 nm
0º	43	38	34
10º	36	32	28
20º	28	26	24
30º	18	17	15
40º	14	12	8

Table 2-b Nasal side

Figure 5 shows the variation of the Critical Time (CT) with the different visual acuities at different locations of the retina. Critical Time has a minimum value at the fovea and this value is increasing at outside of the fovea. For good visual acuity (20/20), CT is minimum (CFF is maximum) than for low visual acuity (20/120). The values of CFF at different locations of visual angle for different visual acuities are shown in Table 3. In periphery, CFF values did not change almostely for different acuities.

Fig . 5 Critical Time for different visual acuities

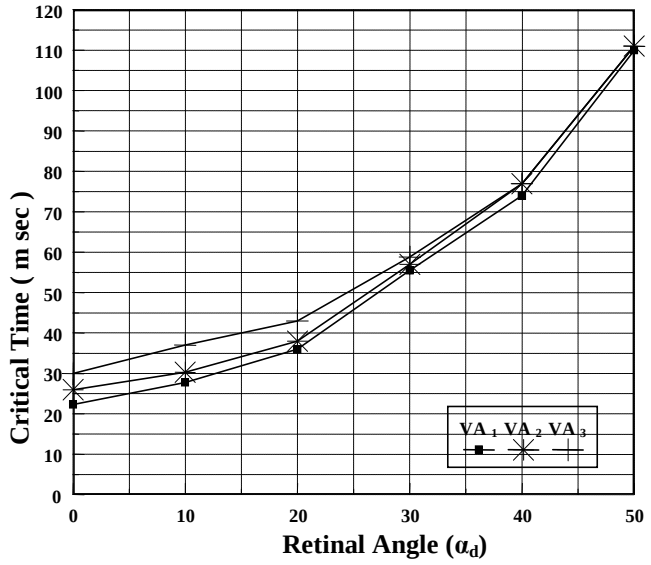


Table 3: CFF values at different locations of visual retinal angle (α_d°) for different acuities. (V.A)

Retinal angle (α_d°)	CFF (Hz)		
	VA_1 20/20	VA_2 20/30	VA_3 20/120
0º	43	42	35
10º	36	33	27
20º	26	25	22
30º	18	17	17
40º	14	13	13
50º	10	9	9

Figures 6 (a , b) Show the visual field of right and left eyes at different wavelengths respectively, the visual field for smallest wavelength is largest area than for largest wavelength .

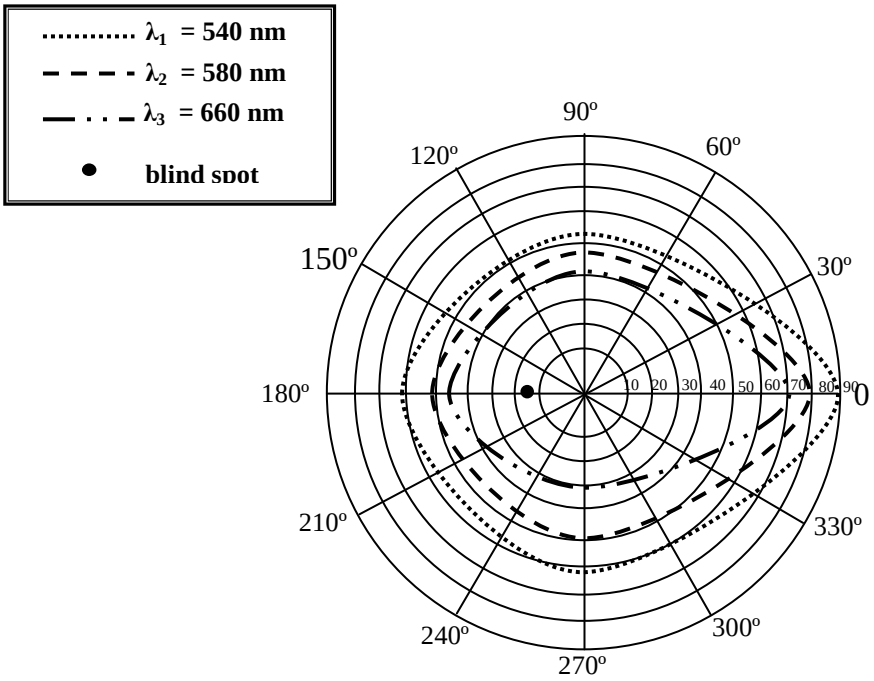


Figure (6 – a) Visual field of R.E

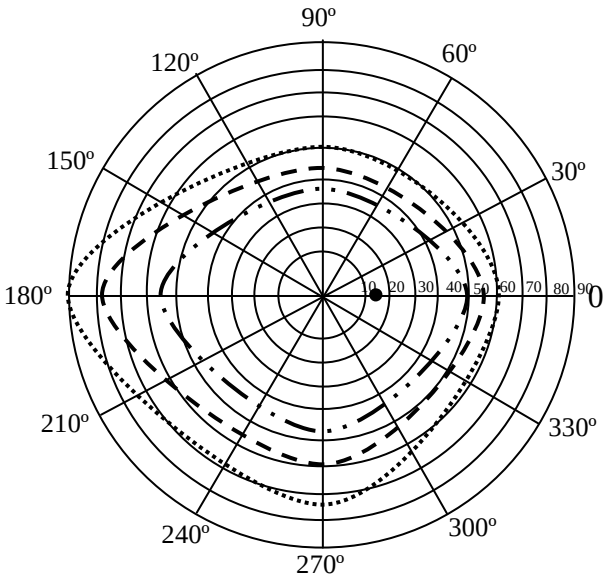


Figure (6 – b) Visual field of L.E

The critical flicker frequency is often used as a measure of the current state of the optical nervous system. As such, it may be affected by several factors; internal as well as external. Internal factors concerned with the subject characteristics, such as stimulus, modulation, luminance (Intensity and area), and wavelength. There are two possible routes for the neural signal from the receptors across the optic nerve to the brain, via the lateral geniculate nuclei (LGN) or via the superior colliculus (SC) as shown in Figure 7. The presence of different pathways {long (SC) & short (LGN)} and different rates {low (Blue cone) & high (Red and Green cones)} of neural signal causes that the CFF has a different value at different retinal visual angle, and its maximum value at fovea.

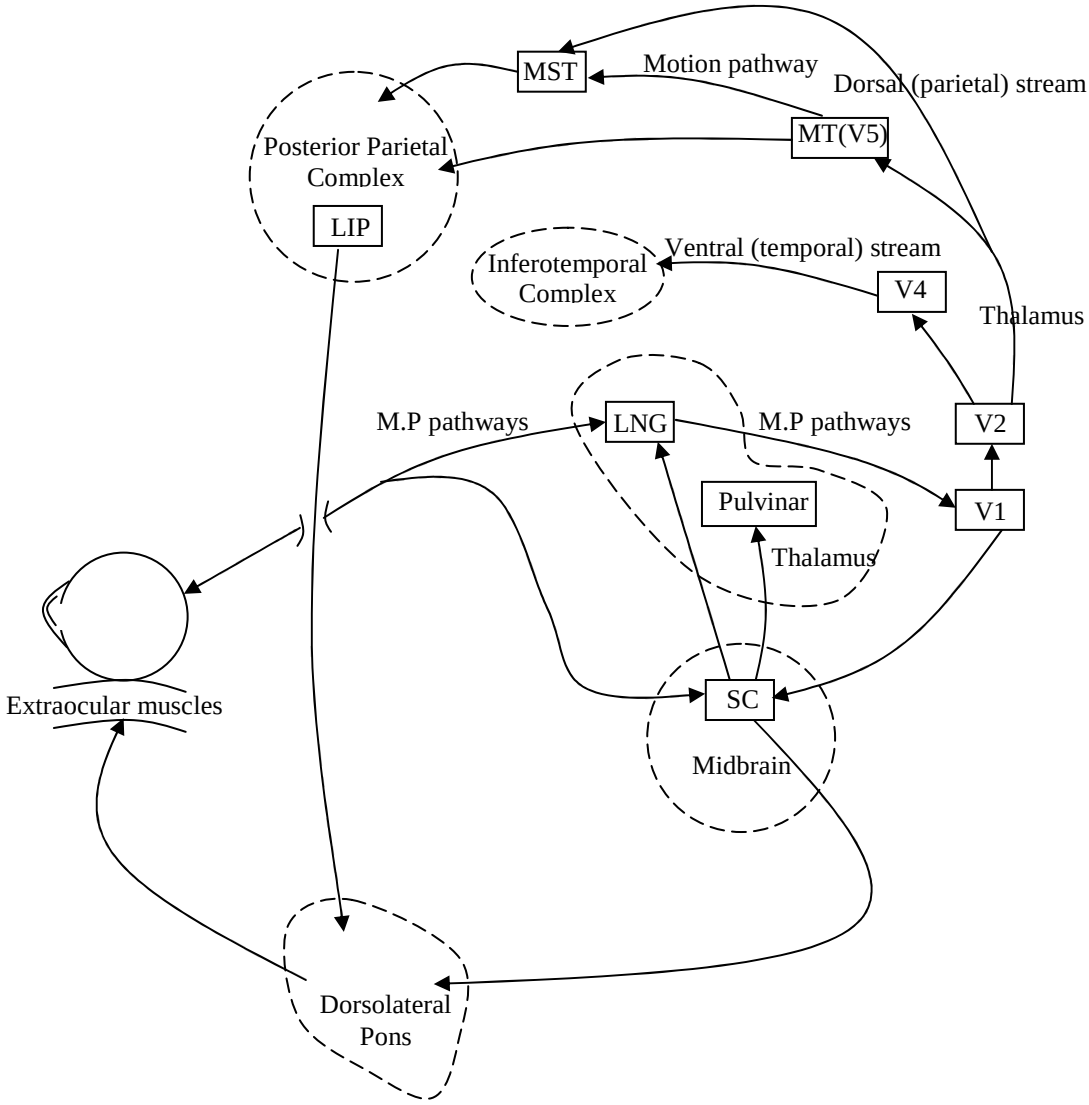


Fig. 7: The brain and the visual pathways

From the pervious results, it is clear that the retina and the occipital cortex synchronize with the flicker, and then CFF is regarded as a function of activity of both the eye and the cerebral cortex. The highest degree of cortical response that is registered when a subject is exposed to flicker is found in the occipital lobe.

Conclusion:

The precedence enables as to examine the variation of CFF with location on the retina as whole. The spatial approach overcomes the pervious literature, which concentrate on the measurement of CFF on the fovea itself. The work also examines the effect of light wavelength on the CFF at different spatial location on the retina and shows that for away from the fovea the CFF decreases.

Also the proposed electronic and mechanical setting have the advantage of simplicity and accuracy for the future work, varying wavelength may be examined and related to know diseases.

References:

1- Martavianya E., William A., Konrad P., " Development of a Critical Flicker/ Fusion Frequency Test for Potential Vision Testing in Media Opacities " Optometry and vision Science, Vol.81, No. 12, December 2004.

2- Braunstein EF : Beitrag Zur lehre des intermittierendem Lichreizes der gesunden and Kranken.Z Psychol. 1903; 33 : 241-88 .

3- Han DP, Thompson Hs , Folk JC. Differentiation between recently resolved optic neuritis and central serous retinopathy . Use of tests of visual function. Arch Ophthalmol 1985 ; 103 : 394 - 6 .

4- Nakamura M, Yamamoto M. Variable pattern of visual recovery of Lebers hereditary optic neuropathy . Br J Ophthalmol 2000 ; 84: 534- 5 .

5- Lachenmayr B J, Gleissner M . Flicker perimetry resists retinal image degradation Invest Ophthalmol Vis Sci 1992; 33 ; 3539- 42 .

6- Keesey U.T. " Flicker and pattern detection " A comparision of thresholds . Journal of the optical society of American , 62 , 446 – 448 , 1972 .

7- Delange H. "Research into the dynamic nature of the human fovea – cortex systems with intermittent and modulated light. Journal of the optical society of American, 48, 777 – 789, 1958.

8- Kelly , D.H. " Flicker , In the Handbook of sensory physiology " vo111/4 ; visual psychophysics D. Jameson and L.M. Hurvich (Eds) New York , spring Verlag , 1972 .

9- Kim , C.B.Y. and mayer , M.J. " Foveal flicker sensitivity in healthy aging eyes Journal of the optical society of American , 11 (7) , 1994 .

10- Amir , T. and Ali , M . R " Critical Flicker Frequency , personality , and sex of Subjects. Perceptual and motor skills , 69 , 1019 – 1026 , 1989 .

11- Jones, M. "Effects of luminance, luminance, viewing angle, and screen test pattern on the perception of flicker in CRT display. Virginia Polytechnic institute and state university, Blacksburg , VA . 1996.

12- Wolfgang J., Matthias B., Edald A., "Accommodation, convergence, pupil diameter and eye blinks at a CRT display flickering near fusion limit" Ergonomics, 1996, Vol. 39 , No. 1 , 152 - 164.

13- Toshiyuki H., Kohki M., Kazuo S., " Basic study of the portable fatigue meter : effects of illumination distance from eyes and age " Ergonomics , 1997, Vol. 40 , No. 9, 887 – 894 .

PLANAR ELLIPTICAL RING BANDPASS FILTER WITH CONTROLLED BANDWIDTH AND OPTIMAL SIZE

MAGDY. S. IBRAHIM

DEPARTMENT OF ENGINEERING MATHEMATICS AND PHYSICS
FACULITY OF ENGINEERING , CAIRO UNIVERSITY, 12211
GIZA, EGYPT

Abstract:

A design of a bandpass filter is presented in this paper and tuned at 2.4 GHz. The resonating element in this design is an elliptical ring with a specific width. The microstrip line is directly connected to the ring. Both the ring and the microstrip line are placed on one side of a dielectric substrate. The slotline is connected to the substrate below the ring. The slotline is electromagnetically coupled to the ring resonator.

A detailed parameter study has been performed for the proposed filter. The results show that both the bandwidth and the surface area of the filter can be controlled via controlling the width and the aspect ratio of the ring.

Introduction:

Bandpass filters play an important role in radio front-end systems. For example a bandpass filter is put immediately after the receiving antenna to reduce the susceptibility of the receiver to unwanted frequencies. Superheterodyne receivers make use of one or more intermediate frequencies with image reject bandpass filters on every intermediate frequency. A passive bandpass filter can be constructed by combining a number of elements [1]. These elements can be either lumped components (such as inductors, capacitors, resistors) or distributed transmission lines [2]. For the bandpass filter based on distributed transmission lines, any type of lines can be used (such as microstrips, coplanar waveguides, slotlines …). Different topologies can be used to achieve the required frequency selection function of the bandpass filter. For example, parallel coupled lines [3] and hairpin resonator [4, 5].

In this paper, a new design of a bandpass filter is presented. The design is based on distributed transmission lines of the microstrip type. The resonator used takes the shape of an elliptical ring of a specific width. Two lines are coupled to this ring. The first line is of microstrip type and directly connected to the ring. The second one is of slot type and coupled electromagnetically, through the substrate, to the ring. Hence, the proposed design is perfectly planar and consists of two metal layers and one dielectric layer.

Section 2 introduces the proposed geometry of the filter. The method used for analysis is mentioned in Section 3. The steps to be followed in order to tune the proposed filter are given in Section 4. A detailed parameter study is performed in Section 5. The important conclusions are stated in Section 6.

Filter Configuration:

Figure 1 shows the proposed design for the bandpass filter. It consists of two planar metallic layers placed on both sides of a dielectric substrate. Without loss of generality, a glass substrate with dielectric constant of 6.2 and thickness of 0.7 mm is selected. This substrate is identical to that used in the multichip module with deposited thin films, MCM-D, technology [6]. The first metal layer is placed on top of the substrate. It includes a microstrip line connected to an elliptical ring resonator. Port 1 is assigned to the microstrip line. The second metal layer is placed on the other side of the substrate. Within this layer, a slotline is etched and connected to port 2. Both metal layers are assumed made up of copper with conductivity of 58×10^6 1/Ωm and thickness of 5 μm.

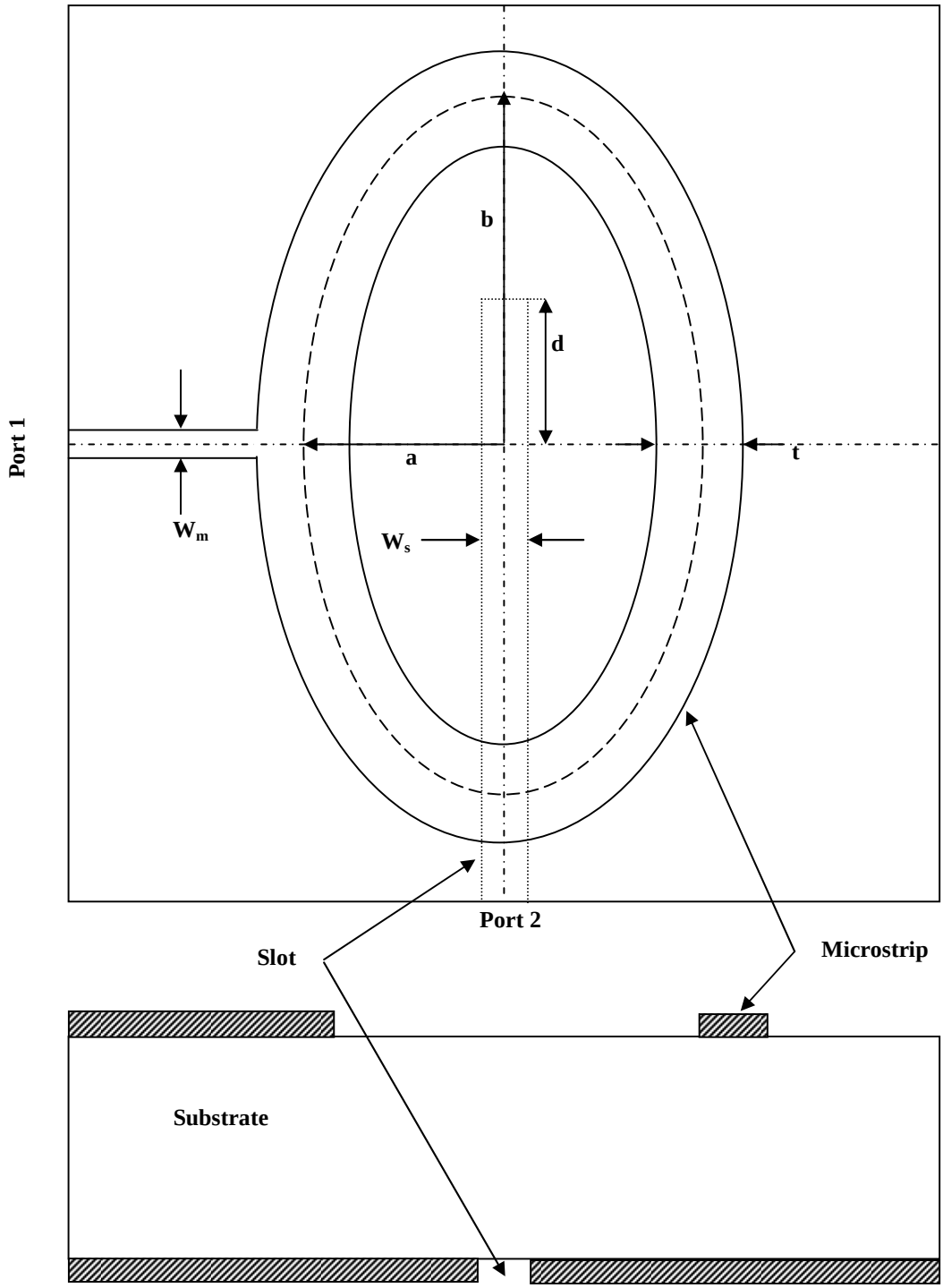


Figure 1 Geometry of the elliptical ring resonator bandpass filter

The proposed filter design has the advantage of allowing the antenna to be of microstrip type, and the rest of the transceiver circuit to be of slot type. This combination is attractive for many practical situations. Being of microstrip type, the integrated antenna, which will be connected to port 1, provides radiation from one side only of the substrate. This feature is desired in several wireless systems. On the other hand, the preferable technology for the rest of the system is either the slotline or the coplanar waveguide (CPW). This is due to the fact that in these technologies both the signal and the ground terminal(s) are brought in the same plane.
This simplifies the integration of shunt lumped elements and active devices and avoids the necessity of drilling via holes through the substrate. It is clear from Fig. 1 that the proposed filter design has 6 feature dimensions. These dimensions are: the minor and major radii of the elliptical ring resonator (*a* and *b*, respectively), the width of the ring *t*, the distance between the edge of the slotline and the center of the ring *d*, the width of the microstrip line W_m, and the width of the slotline W_s. Practically, the last two dimensions are adjusted to achieve specific values for the characteristic impedances of the feeding lines. Knowing the substrate properties and the resonance frequency, 2.4 GHz, the widths which correspond to 100 Ω for both lines are: W_m = 0.21 mm and W_s = 0.8 mm.

The theory of operation of the proposed bandpass filter is that at resonance, the electrical circumference of the elliptical ring equals one guided wavelength λ_g. The width of the microstrip line forming the ring, *t*, defines the corresponding value of the guided wavelength. The satisfaction of this condition, forces the two signal components excited from one port to travel distances of $\lambda_g/4$ and $3\lambda_g/4$ in the two branches of the ring to reach the other port. The resulting 180^0 phase shift is compensated by the 180^0 spatial opposition of the two arms at the other port, which results in an in-phase addition.

Method of Analysis:

The analysis of the proposed bandpass filter is carried out using Agilent-Momentum [7]. Momentum is a 2.5D full-wave solver based on the integral equation formulation solved using the Method of Moments. Since it is a well-known full-wave simulator validated many times in literature, it is possible to rely on its simulation results. For meshing the filter under development, mixed rectangular and triangular segments are used. Twenty five cells per wavelength combined with a narrow edge mesh are adopted.

Filter Design:

As stated in Section 2, the remaining 4 dimensions of the filter to be determined are: *a*, *b*, *t*, and *d*. The first two dimensions can be combined into one parameter called the aspect ratio of the elliptical ring resonator. This new parameter is defined as the ratio between *b* and *a*, i.e. (*b*/*a*). Knowing *b*/*a* and *t*, the last dimension *d* is determined via optimization such that the best impedance matching with the slotline is obtained. This leaves only two independent design parameters, namely *b*/*a* and *t*. Consequently, the design space is a 2D space. The selected range for *b*/*a* starts from 1 up to 5, while the selected range for *t* starts from 0.25 mm up to 0.75 mm. Outside these ranges it has been observed that the response of the filter is unsatisfactory.

The frequency response of the filter at the central point of the design space, *b*/*a* = 3 and *t* = 0.5 mm, is shown in Figure 2. As desired, the resonance frequency of the filter is 2.4 GHz. There are several criteria for defining the percentage bandwidth of a bandpass filter. The selected definition in this paper is $\Delta f / f_0$, where f_0 is the resonance frequency and Δf is the common frequency band which satisfies the following conditions: $|S_{11}| < -10\,\text{dB}$, $|S_{21}| > -1\,\text{dB}$, and $|S_{22}| < -10\,\text{dB}$.
As mentioned in Section 2, once the width of the ring is defined, its circumference become available and equals to the guided wavelength of the microstrip line forming it. However, experimental iterations have shown that the ring circumference is slightly smaller than the corresponding theoretical value. This deviation is mainly due to the excitation of higher order modes around the feeding lines. For the selected width of the ring *t* = 0.5 mm and at *f* = 2.4 GHz, the guided wavelength is 60.62 mm, while the circumference of the ring is found to be 55.83 mm. Since the circumference of the elliptical ring equals $\pi(a + b)$, the specification of the aspect ratio *b*/*a*, results in determining the corresponding values for the minor and major radii, *a* and *b*, respectively.

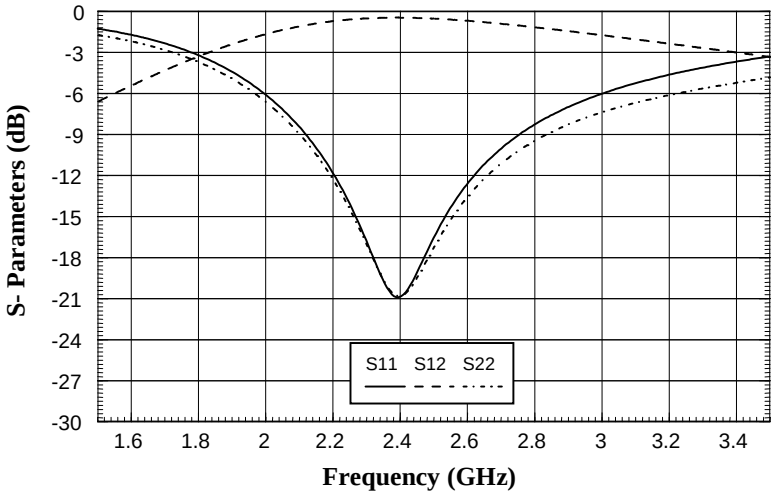


Figure 2 S-parameters versus frequency of the proposed bandpass filter.

Parameter Study:

In this section the effect of varying the independent design parameters on the filter's geometry and response is studied. As mentioned is the previous section, the proposed filter has two independent design parameters, namely the aspect ratio *b*/*a* and the width of the elliptical ring resonator *t*. Of particular interest to many modern wireless systems, is the surface area occupied by the filter. There is a definite trend toward specifying severe restriction on the surface area. For our proposed design the surface area occupied by the filter can be defined as the area of the rectangular which entirely contains the ring. Referring to Figure1, the surface area equals $(2a + t)$ $(2b + t)$. The response of the filter is characterized by its percentage bandwidth, which is defined in Section 4.

Variation of b/a:

In this subsection the aspect ratio of the elliptical ring is continuously varied from 1 to 5. The other independent parameter *t*, takes three discrete values: 0.25 mm, 0.5 mm, and 0.75 mm. Figure 3 shows both the minor radius *a*, and the major radius *b*, versus the aspect ratio. It is clear from the figure that *a* decreases as *b*/*a* increases, while *b* increases. This behavior allows *a* and *b* to provide the required aspect ratio, while keeping their summation approximately constant. The approximately constant summation results in an approximately constant circumference for the ring at the corresponding value of its width. Both *a* and *b* decreases as *t* increases. The reason for that is the guided wavelength, and also the circumference, decreases as *t* increases.

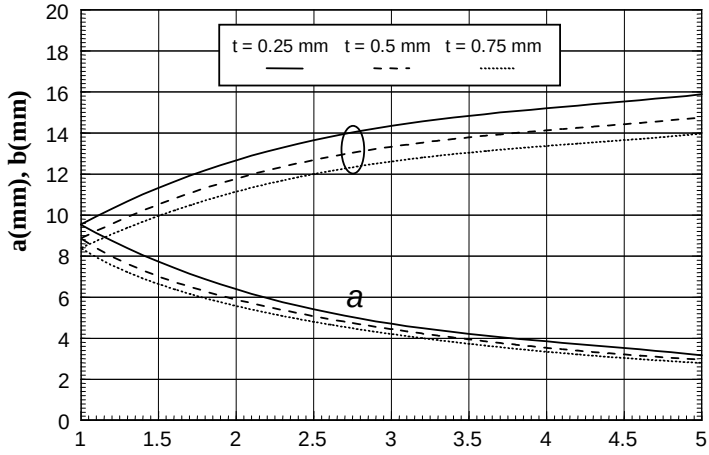


Figure 3 Minor and major radii of the ring versus its aspect ratio

The surface area occupied by the filter is plotted in Figure 4 versus *b*/*a* at three different values of *t*. The figure shows that increasing the aspect ratio *b*/*a*, results in decreasing the surface area. The decrease in the surface area with the increase of the width *t* is expected, because of the decrease of the guided wavelength. Figure 5 shows the optimized values of *d* versus *b*/*a* at the selected values of *t*. The optimization is based on obtaining the best possible match with the slotline of port 2. It is clear from Figure 5 that as *b*/*a* increases the edge of the slotline moves continuously downward. The percentage bandwidth of the filter is plotted versus *b*/*a*, at different values of *t*, in Figure 6. The figure shows that the percentage bandwidth decreases as either *b*/*a* or *t* increases. However, the effect of varying *t* is more pronounced. Based on the surface area and bandwidth specifications, the designer can use Figures 3, 4, 5, and 6 to specify the corresponding values of *a*, *b*, *t*, and *d*.

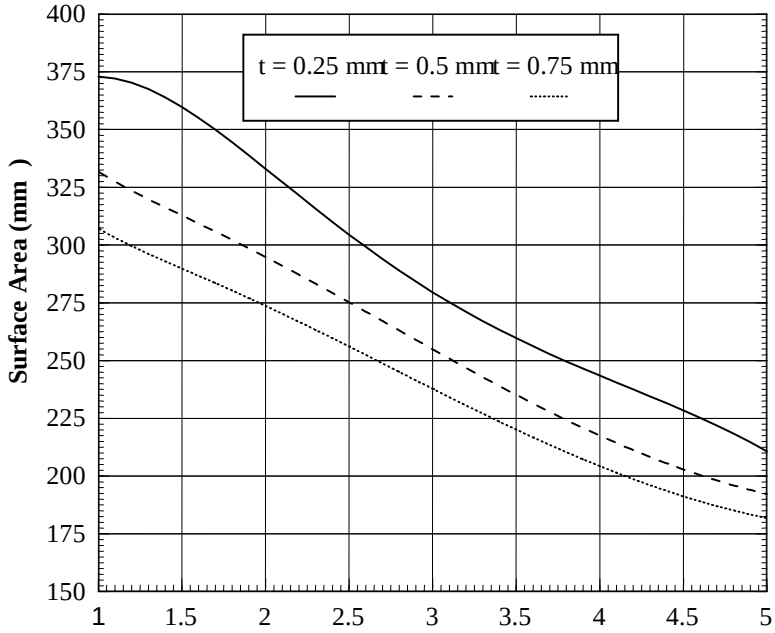


Figure 4 Surface area occupied by filter versus the aspect ratio of its ring

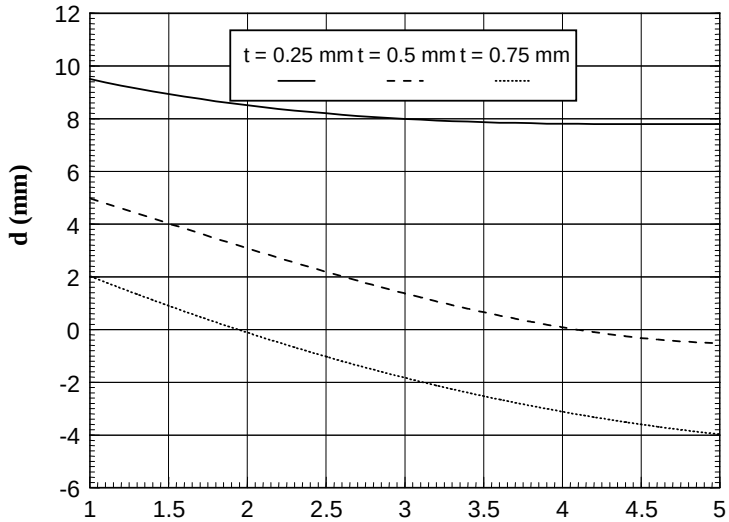


Figure 5 Distance between the edge of the slotline and the center of the ring versus its aspect ratio

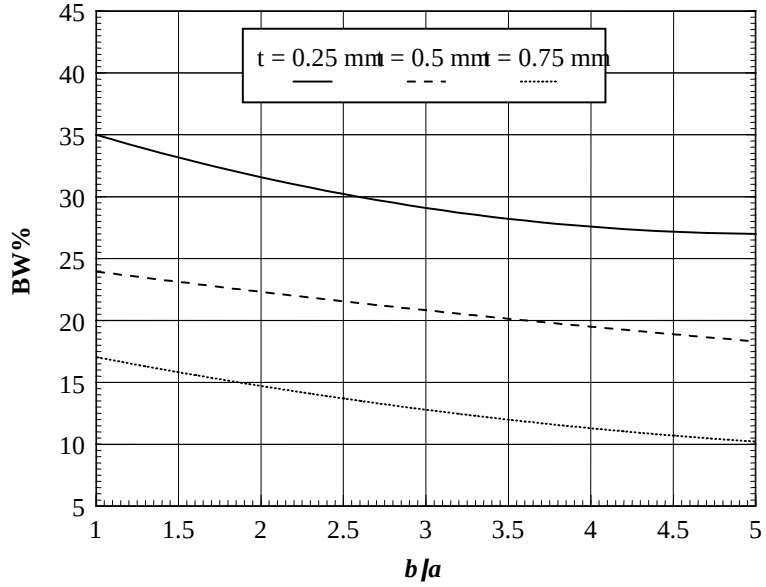


Figure 6 Percentage bandwidth of the proposed filter versus the aspect ratio of its ring

Variation of t

In order to examine the design space in the orthogonal direction, the width *t* of the ring is going to be varied continuously, from 0.25 mm to 0.75 mm, in this subsection. The aspect ratio *b*/*a* will be fixed at three discrete values: 1, 3, and 5. Figure 7 shows both the minor radius *a* and the major radius *b* versus *t*. As *t* increases, both *a* and *b* decreases. This is a result of the reduction of the guided wavelength as well as the circumference of the ring as *t* increases. It is also clear that as *b*/*a* increases *a* decreases, while *b* increases. This behavior allow *a* and *b* to preserve the required aspect ratio while keeping their summation approximately constant at a specific value of *t*.

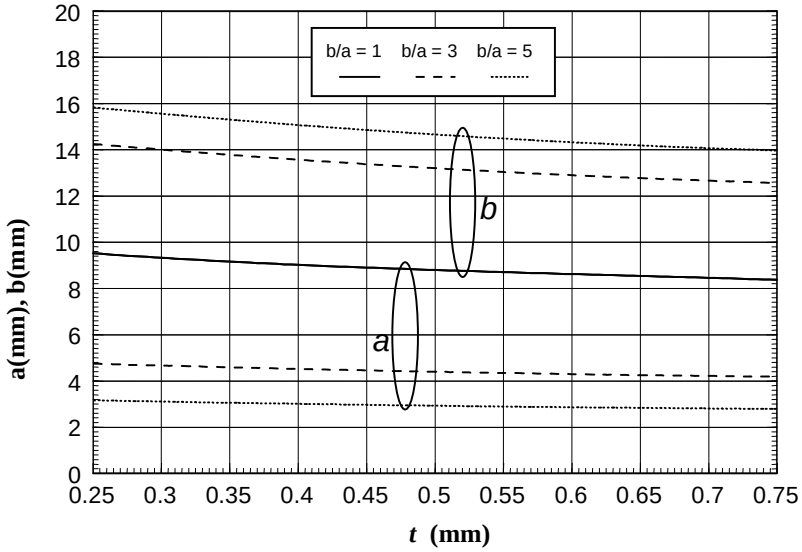


Figure 7 Minor and major radii of the ring versus its width

Knowing *a* and *b*, the surface area occupied by the filter can be calculated. In Figure 8, the surface area is plotted versus *t* at three different values of *b*/*a*. The surface area decreases as either *t* or *b*/*a* increases. The parameter *b*/*a* has more impact on the surface area than that of *t*. After obtaining the radii of the ring, the value of *d* should be optimized in order to achieve the best matching between the slotline and the elliptical ring resonator. The optimum value for *d* is plotted in Figure 9. It is clear from this figure that the distance between the edge of the slot line and the center of the ring decreases as either *t* or *b*/*a* increases.

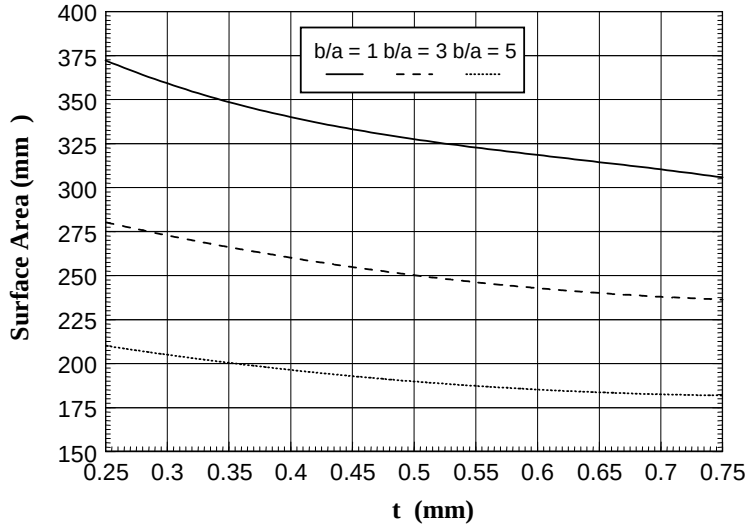


Figure 8 Surface area occupied by the filter versus the width of its ring

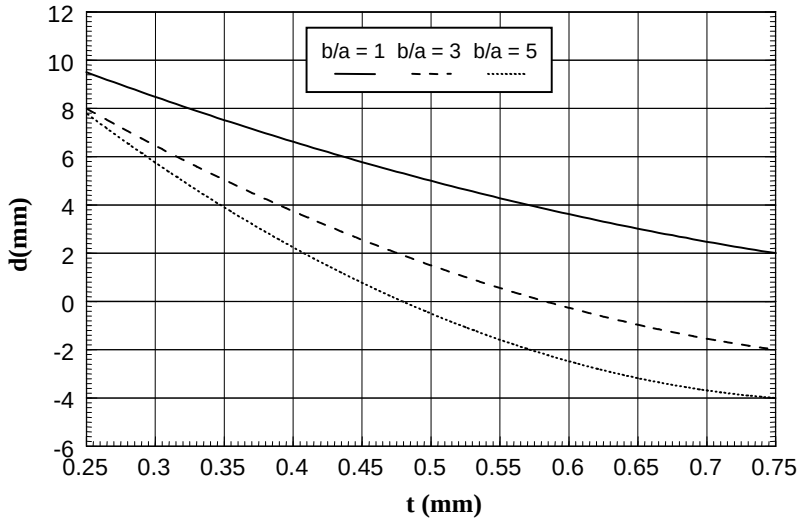


Figure 9 Distance between the edge of the slotline and the center of the ring versus its width

Finally, the percentage bandwidth is presented in Figure 10 versus *t* at the same three values of *b*/*a*. The figure shows that the percentage bandwidth decreases as either *t* or *b*/*a* increases. In consistence with Figure 6, the variation of *t* has stronger effect on the percentage bandwidth than that of *b*/*a*. It is clear from both Figures 6 and 10 that the proposed bandpass filter offers a wide range of bandwidth variation. For the selected ranges of *b*/*a* and *t*, the percentage bandwidth varies from 10% up to 35%.

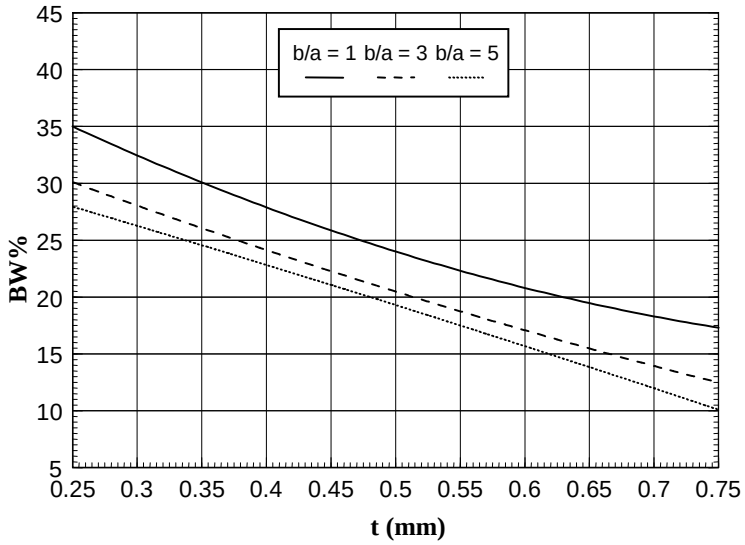


Figure 10 Percentage bandwidth of the proposed filter versus the width of its ring

Conclusion :

This paper presents a new bandpass filter design. The proposed filter is of planar nature which makes it consistent with the modern microwave systems. A rigorous parameter study for the proposed design has been performed via a reliable full-wave commercial software. It has been found that two independent parameters are affecting the performance of the filter. Varying these parameters, it has been demonstrated that the percentage bandwidth of the filter can be controlled within the range from 10% up to 35%. This makes the proposed filter suitable for a wide range of microwave applications. At the selected resonance frequency of 2.4 GHz, it has been also found that changing the independent parameters of the filter results in controlling the surface area of the filter from 373mm^2 down to 182mm^2. This feature indicates that the proposed design is able to satisfy the size reduction requirement of some wireless applications.

References :

1- K. Chang, I. Bahl, and V. Nair, RF and microwave circuit and component design for wireless systems, Wiley, New York, 2002.

2- P. Pieters, K. Vaesen, W. Diels, G. Carchon, S. Brebels, W. De Raedt, E. Beyne, and R.P. Mertens, High-Q integrated spiral inductors for high performance wireless front-end systems, IEEE Radio and Wireless Conference, Denver, Colorado, 11-13, Sept. 2000.

3- E.A. Soliman, M.H. Bakr, and N.K. Nikolova, Accelerated gradient-based optimization of planar circuits, IEEE Trans. Antennas Propagat 53 (2005), 880-883.

4- S.Y. Lee and C.-M. Tsai, New cross-coupled filter design using improved hairpin resonators, IEEE Trans. Microwave Theory Tech 48 (2000), 2482-2490.

5- J.S. Hong and M.J. Lancaster, Cross-coupled microstrip hairpin resonator filters, IEEE Trans. Microwave Theory Tech 46 (1998), 118-122.

6- S. Mestdagh, W. De Raedt, and G.A.E. Vandenbosch, CPW-fed stacked microstrip antennas," IEEE Trans. Antennas Propagat 52 (2004), 74-83.

7- Momentum, version 4.8, Agilent Technologies, 2003.

MULTIPHOTON ABSORPTION IN CHIRAL BRAIN UNDER MICROWAVE RADIATION FROM WLAN'S SYSTEMS

H. TORRES-SILVA* AND M. ZAMORANO

***Instituto de Alta Investigación**
Departamento de Electrónica, Universidad de Tarapacá,
18 de Septiembre 2222, Arica, Chile
E-mail: **htorres@uta.cl**

Abstract
A model formed by chiral bioplasma with a set of macromolecules of DNA, which represents the human head inner structure, makes possible to analyze its behavior, when it is radiated by a microwave electromagnetic field WLAN's. The finite difference time domain, FDTD is used under multiphoton regime deduced from Maxwell equations. The numerical results of the Specific Absorption Rate, SAR, show the SAR behavior in function of the chirality factor. The main conclusions of our work is that the microwave absorption from WLAN's systems is enhanced, compared with classical models, when values of the normalized chiral factor are of order of one. This absorption appears under multiphoton regime in the brain region. To illustrate this effect in our simulations we considerer electromagnetic waves at frequencies of 5.2 and 5.8 GHz.

Keywords: chirality; brain tissue; Maxwell; FDTD; SAR

PACS: 41.20Jb; 02.70.Bf; 52.35; 87.15.Aa

1. Introduction

Even though a lot of work has been done there is still no complete assessed knowledge about the interaction between electromagnetic fields and biological systems . However, there is a general agreement about the relevance of the correct evaluation of the real mechanism. It seems clear that RF fields can have some effects on tissue and it still remains to be determined whether these effects are functionally and pathologically significant.

Different models of human head range from simple models, such as homogeneous sphere to heterogeneous anatomically correct models based on magnetic resonance (MR) imaging. In this paper a FDTD method to determine the absorption of RF waves emitted by WLAN`s is presented. We use a simple model, which takes into account the main interaction between the bioplasma of the brain neurons and the microwave radiation of WLAN's systems. To address the problem and on the basis of our previous approach [1-2], our method have three main steps: 1) modelling of human head through MRI, 2) evaluation of the electromagnetic fields distribution inside the biological target, considering the brain tissue as chiral bioplasmatic media, and 3) SAR simulation for to evaluate both the thermal effect and resonant absorption under multiphoton regime. A explanation of the theoretical base of the technique used and description of the models are given in section 2. Results comparing the computed SAR values in the different models are shown and discussed in the section 3. Finally, conclusions are presented.

2. Fundamentals and models

By looking a special natural chiroplasma like a citoplasma in the human brain the multiphoton mechanism can provide a new approach of the problem of absorption in the human brain. Here the eigenfrequency of collective twist excitation in proteins, DNA and other biological chain molecules can be in the gigahertz range [3-5].

Here, we assume that the electrons within chiral molecules oscillate along a helix and from the averaged electric current [1] we can find the polarization (P) and the magnetization (M) which in a helical geometry may be proportional to $\nabla\times\boldsymbol{E}$ ($\nabla\times\boldsymbol{H}$) respectively. For typical double helices, giving the moment of inertia per unit length, the

torsional factor and the length of a typical chain (I, tor, L), and following [3], For double stranded DNA we estimate I = 300 auA°, torsion constant of 0.8 ev/A°, and L between 200 A° and 2000 A° the frequency falls in the interval between 1 GHz and 10 GHz [4]-[5]. Similar results we can obtain using the Ford's model [7].
In this work we propose that when the multiphoton effect is considered, this microscopic problem is reflected at macroscopic level as thermal absorption combined with resonant absorption. Here, besides the tissue conductivity and dielectric permittivity we considerer the chiral effect caused by the interaction of microwaves and biomolecules of DNA. The chiral wave propagation in bounded helical structures may support mode excitation, mode interactions, mode conversion and amplification of molecular chirality by eigenwaves in a bioplasma [6]

This chiral effect in the brain is considered in this work as a macroscopic mechanism where the typical cell membrane of brain is a fluid bilipid layer with a lot big chiral protein molecules embedded in it. Every protein molecule is polar and will tend to align itself with an electric field and often helical rotate in its socket, so any volume of brain tissue must have a lot of cells bearing protein molecules that happen to resonate at its eigenfrequency which can be similar to the microwave frequency f or when there are n- multiphoton interaction the eigenfrequency can resonate with nf. By contrast with ionizing radiation which damage to genetic structures of cells, microwave may span thousands of cells with a single wavelength. Microwaves set up current in tissue, and any noticeable effect of such current would involve many, many of the relatively weak microwave photons, damage, if any, would be all over the path of the current and would be numerous cells in extend, so damage to general cytoplasm, mitochondria, and so forth would seem likely to be more salient than damage to genetic structure.
Accordingly with the above discussion, we apply the Maxwell´s equations to sets of microtubules and helical molecules embedded in a substrate, characterized by a global chirality factor, T, (equation 1). Chiral media can be characterized by a generalized set of constitutive relations in which the electric and magnetic fields are coupled. In this paper, we consider the Born-Fedorov approach

$$D_{x,y,z} = \varepsilon_0 \varepsilon_r E_{x,y,z} + \varepsilon_0 \varepsilon_r T \left[\frac{\partial E_{z,x,y}}{\partial y, z, x} - \frac{\partial E_{y,z,x}}{\partial z, x, y} \right]; B_{x,y,z} = \mu_0 H_{x,y,z} + \mu_0 T \left[\frac{\partial H_{z,x,y}}{\partial y, z, x} - \frac{\partial H_{y,z,x}}{\partial z, x, y} \right] \quad (1)$$

where ε, μ and T (meter) are the permittivity, permeabilitty and the chiral scalar respectively. Solving Maxwell` equations for a plane electromagnetic wave of frequency ω ($\omega = k_t v = 2\pi f$, k_t is the tissue wavenumber and v is the phase velocity) propagating in a chiral medium, it can be shown that the left- and right hand circularly polarized waves have different wavenumbers, $k = k_t/(1 + k_t T)$, $k = k_t/(1 - k_t T)$ respectively [2]. The chiral parameter T has the dimension of a length, which in an exactly solvable two helical model for a set of oriented handed molecules, is proportional to $\beta N h^2 a \rho$. Here, β is some coefficient determined by the internal elasticity of a molecule, N is the number density of molecules of radius and a pitch h with the charge ρ per unit length of each [1].
Using the MKS system of units, the following system of scalar equations is the set of Maxwell's equations in the rectangular coordinate system (x, y, z):

$$\frac{\partial H_{x,y}}{\partial t} = \mp \frac{1}{\mu} \frac{\partial E_z}{\partial y, x} \pm T \frac{\partial^2 H_z}{\partial y, x \partial t}; \frac{\partial H_z}{\partial t} = \frac{1}{\mu} \left(\frac{\partial E_x}{\partial y} - \frac{\partial E_y}{\partial x} \right) + T \left(\frac{\partial^2 H_y}{\partial x \partial t} - \frac{\partial^2 H_x}{\partial y \partial t} \right) \quad (2)$$

$$\frac{\partial E_{x,y}}{\partial t} = \pm \frac{1}{\varepsilon} \frac{\partial H_z}{\partial y, x} \pm T \frac{\partial^2 E_z}{\partial y, x \partial t} - \sigma E_{x,y}; \frac{\partial E_z}{\partial t} = \frac{1}{\varepsilon} \left(\frac{\partial H_y}{\partial x} - \frac{\partial H_x}{\partial y} \right) + T \left(\frac{\partial^2 E_y}{\partial x \partial t} - \frac{\partial^2 E_x}{\partial y \partial t} \right) - \sigma E_z \quad (3)$$

where σ (mho/m) is the tissue electrical conductivity. The main difficulty for an analytic treatment of this system is in the partial derivatives of space and time in which the chiral parameter T is present. For this reason, equations (2)-(3) can't be reduced to a typical differential equation with known solution. In our formulation, the second order approximation of Mur is used for the near-field irradiation problems in an achiral-chiral interface case. After calculation of the induced chiral electric field by the FDTD method, the local specific absorption rate SAR, is

calculated as

$$SAR_{i,j}(T) = \frac{\sigma_{i,j}\, E_T^2\big|_{i,j}}{2\rho_{i,j}}; with\, E_T\big|_{i,j}(T) = \sqrt{\frac{1}{n}\sum_{1}^{n}\left(E_y^2\big|_{i,j}^{n} + E_x^2\big|_{i,j}^{n} + E_z^2\big|_{i,j}^{n} \right)} \qquad (4)$$

3. SAR simulation and analysis of results

For the numerical calculation we normalize the chiral factor as kT where k is the wave number in the tissue layer, in some case it may be $k_t = nk_0$, ($k_0 = \omega / c$ is the vacuum wave number), with n = 1, 2, 3…n. It is necessary to take into account the multiphoton absorption when the resonance absorption at macromolecular level become important. For the brain we considerer $k = k_b /(1 - k_b T)$ because, the clusters of DNA molecules have eigenwaves like right hand circularly polarized waves and for the rest of tissues we considerer $kT = k_t T = 0$. The values for kT are choose by considering $T \approx \beta N h^2 a \rho \approx 1 - 10 \mu m$, $k = k_b /(1 - k_b T) >> k_b \approx k_0 \sqrt{\varepsilon_b}$, $k_0 T$ is of the order of $10^{-4} - 10^{-3}$ so when the multiphoton effect appears, $k_b T \approx n k_0 T$, $1 - n k_0 T \le 1$ and then kT is of order of one and this effect increases when kT increases Here we suppose that the macromolecules vibrations of the helical structures inside typical brain cells are likely to lead to reasonably absorption enhanced by the proteinic water in which these molecules are immersed (induced chirality).

Stages of the bioplasmatic model for SAR determination are shown in reference [1]. Using the linear FDTD algorithm with chirality, obtained from equations (4) simulations for the mobile phones microwave spectrum are made. The model of human head was constructed with 540,000 cubic cells of 2.5 mm side each. The total number of layers, counted from the bottom of head, used in this model was 54. Here we choose the layers 34, 35 and 36, because there are great concentrations of brain tissue. The figure 1 shows these layers in digitalized version (matrix of 100x100), likewise is exhibited the antenna position. Both, the dielectric constant and the conductivity of the brain were obtained from literature [9-10]. In order to study and isolate the chiral effect, calculations are made for plane wave assumption, powers of 0.1 W were used, at frequencies of 5.2 and 5.8 GHz respectively. Four types of tissues (skin, bone, blood and brain) are considered. Simulations were made in a systematic way, in order to determine the effect that the variation of the chiral coefficient have over the absorption of coefficient SAR and results, for layer 35th, are shown in figures 2-3. Owing to the different electromagnetic properties of the tissues the power absorption is not a monotonically decreasing function of depth. For kT = 0, absorption is highest in the skin, low in the skull, but higher again in the brain. These curves were obtained performing similar simulations and then obtaining a statistical average of the SAR. As the wave penetrates the head, it traverses the different parts of which the head model is made and the value of the SAR is attenuated quickly due to the change in medium and the increase of the distance from the emitting source (antenna). SAR maximum (hot point) is in outer part (skin). After passing through the bone level, the SAR is much attenuated (between cells 5 and 10) and around cell 10, the SAR increases at brain level. Here, starting on cell 10 approximately is important to analyze the performance of our bioplasmatic model.

The profile of the SAR for 35th layer, at 5.2 GHz, as function of distance for different values of chiral factor kT, is showed in figure 2, where the variation is observed for $0 < kT \le 3.0$ values of chiral factor. A SAR of 0,48 W/kg, is observed in the brain region, for a null chiral factor (kT = 0). For kT = 1 the SAR found was 0,65 W/kg, an increase of 35% with respect to the achiral case (kT = 0) and a SAR of 0.75 W/kg was found for kT = 3.0, with an increase 56%. This increase corresponds to the power absorbed by the brain region.

Figures 3 shows the distribution of the SAR for 35th layer, as function of distance, for different values of the chiral factor when the work frequency is 5.8 GHz. The maximum SAR found, in the blood-brain region, was 0.6 W/kg for to kT = 0 and 0.8 W/kg for kT = 1, i.e. an increase of 33% with respect to the achiral case. For a high value of chiral factor, kT = 3.0, the maximum SAR found was 0.93 W/kg with an increase of 55%. Also, this increase corresponds to the power absorbed by the brain region. Following the same procedure, similar results for the layers 34 and 36 are obtained. Here with kT=3 we have an enhanced multiphoton effect which is reflected in strong absorption, SAR=0.93 (5.8GHz).

Apparently the SAR appears to increase as the square root of the power, because in the numerical calculation as initial condition we start with an initial varying electric field $E_i = (V/\Delta)\sin \omega t$ where the voltage is proportional to the square root of the power with constant impedance [5]. Important results are the values of SAR obtained for 5.2 and 5.8 GHz, where a remarkable characteristic is found: at higher frequency the absorption is bigger in the brain

tissue where a lower absorption by skin effect was expected.

The classical skin effect does not occur in our simulation, because the effective induced current penetrate inside the head where the multiphoton resonance is active.

This "inverse skin effect" phenomenon is verified in the brain layers, as shown in figures 2 and 3, where it is possible to observe that in all cases, for any chiral factor and input power values, the maximum SAR at 5.8 GHz is larger than at 5.2 GHz.

4. Conclusions

A bioplasmatic chiral model of the human head has been presented that allows determination and evaluation of the absorption induced by the radiation of cellular phone. After having obtained the digitalized layers of correspondent MR images, the electromagnetic fields radiated were determined firstly by means of the FDTD technique and then the specific absorption coefficient (SAR). It is shown that the use of a more realistic model of the human head, derived from the magnetic resonance of images allows for improved determination of the chiral near fields induced in the head.

Using the proposed bioplasmatic chiral model, the simulation of SAR distribution in layers with high quantity of brain tissue (layers 34, 35 and 36) was made. These results shows that the power absorbed by the head increases with the chiral factor. Other important result found is that the absorption at 5.8 GHz, in the brain tissue, is larger that at 5.2 GHz, therefore there is an effect like an "inverse skin effect" phenomenon. In this calculation it is not possible that chain molecule can alter their conformation and a breaking of the chain can result having in mind the restricting forces which are higher than the EM forces.

Here we are studied a more elaborated model of the head (with chiral effect), but with a simple model for the antenna. For real antennas the proximity of tissue clearly alter the radiation pattern, the antenna gain and the input impedance a more general numerical simulation techniques and an accurate model have to be developed. However for left-hand circular, right-hand circular and helical antennas, now available for isotropic and omni-directional radiation, our analysis on SAR have correct conclusions regarding the chiral effect. Certainly for systems to greater frequencies (wireless LANs) the chiral effect will be more pronounced. This makes it worth to check the first results by means of still more advanced models.

Acknowledgments

The authors thank the University of Tarapacá Projects: 8721-06 and 8722-06.

References

[1] Torres-Silva H and Zamorano M. 2003. SAR simulation for chiral waves in head model. *Revista Facultad de Ingeniería* UTA, Vol. 11, pp. 3-11.

[2] Torres-Silva H and Zamorano M. 2003. Chiral Effect on Optical Soliton, *The Journal Mathematics and Computers in Simulation*, Vol. 62, pp. 149-161.

[3] Bhor H. 1997. Molecular wring resonances in chain molecules, *Bioelectromagnetics*, Vol. 18, pp. 187-189.

[4] Davis C C and Swicird M L, 1982. Microwaves absorption of DNA between 8 and 12 GHz, *Biopolymers* Vol. 21, pp. 2453.

[5] Edwards G S et al, 1984. Resonant of selected DNA molecules, *Physical review letters* 53, pp. 1248-1287.

[6] Nina P. et al, 1996. Dynamic control and amplification of molecular chirality by circular polarized light, *Science*, Vol. 273, pp. 1686-1688

[7] Ford L H. 2003. An estimate of the vibrational frequencies of spherical virus particles, *arXiv:physics/0303089*, Vol. 1.

[8] Belyaev Y I et al, 2000. Nonthermal Effects of Extremely High-Frequency Microwaves on Chromatin Conformation in Cells *in vitro* - Dependence on Physical, Physiological, and Genetic Factors, *IEEE Transactions on Microwave Theory and techniques*, Vol. 48, pp. 2172-2179.

[9] Bernardi P. Cavagnaro and Pisa S. 1997. Assessment of the potential risk exposed to millimeter-wave wireless LANs *Wireless networks* Vol. 3, pp. 511-517.

[10] Taflove A and Hagness SC, Ed. 2000. C*omputational Electrodynamics: The Finite-Difference Time Domain Method*, Artech House, pp. 35-171.

figures caption

Fig. 1a,b,c The structure of layer 34th, 35th and 36th.

Fig. 2 SAR variation as function of the transverse distance, for $0 < kT \leq 3.0$ at 5.2 GHz. Layer 35th.

Fig. 3 SAR variation, as function of the transverse distance, for $0 < kT \leq 3.0$ at 5.8 GHz. Layer 35th.

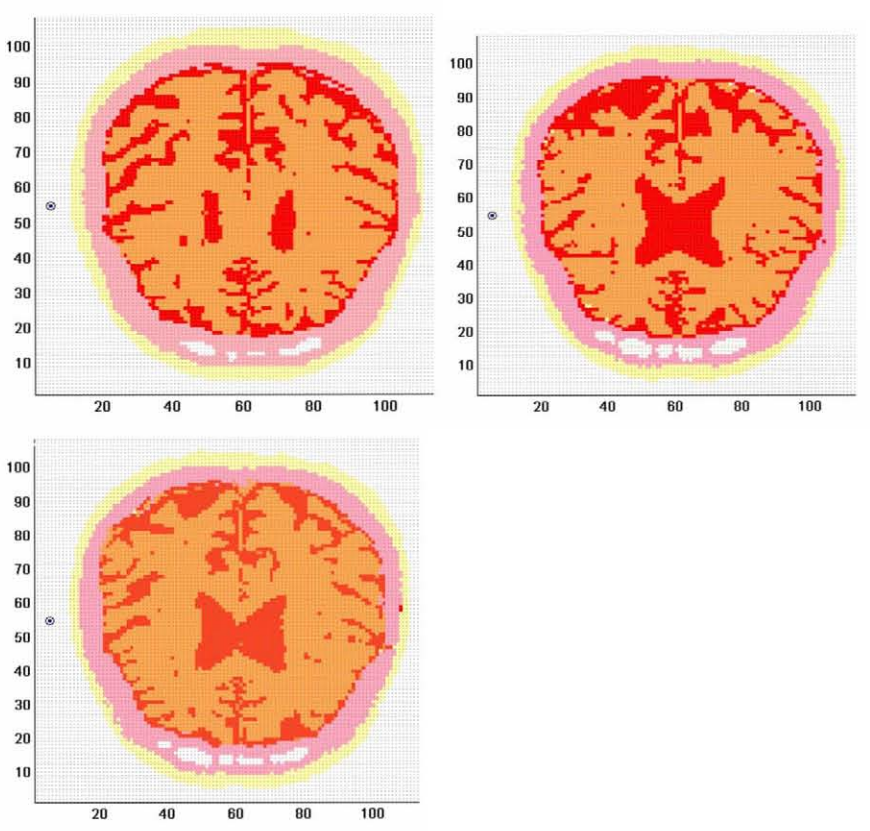


Fig 1

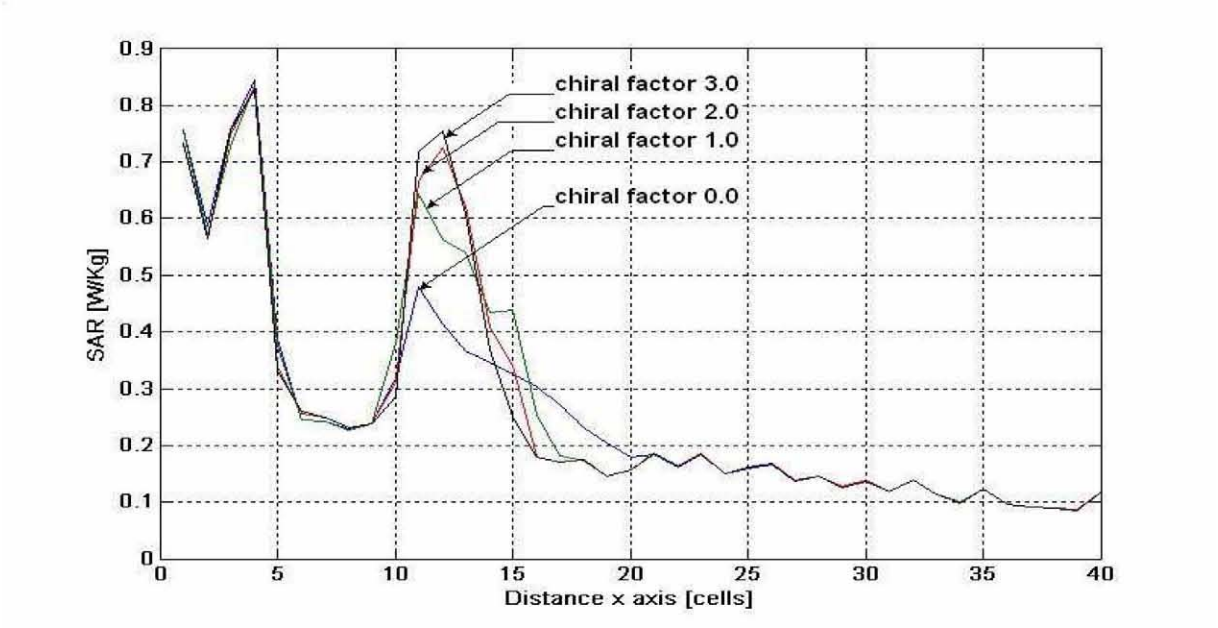


figure2

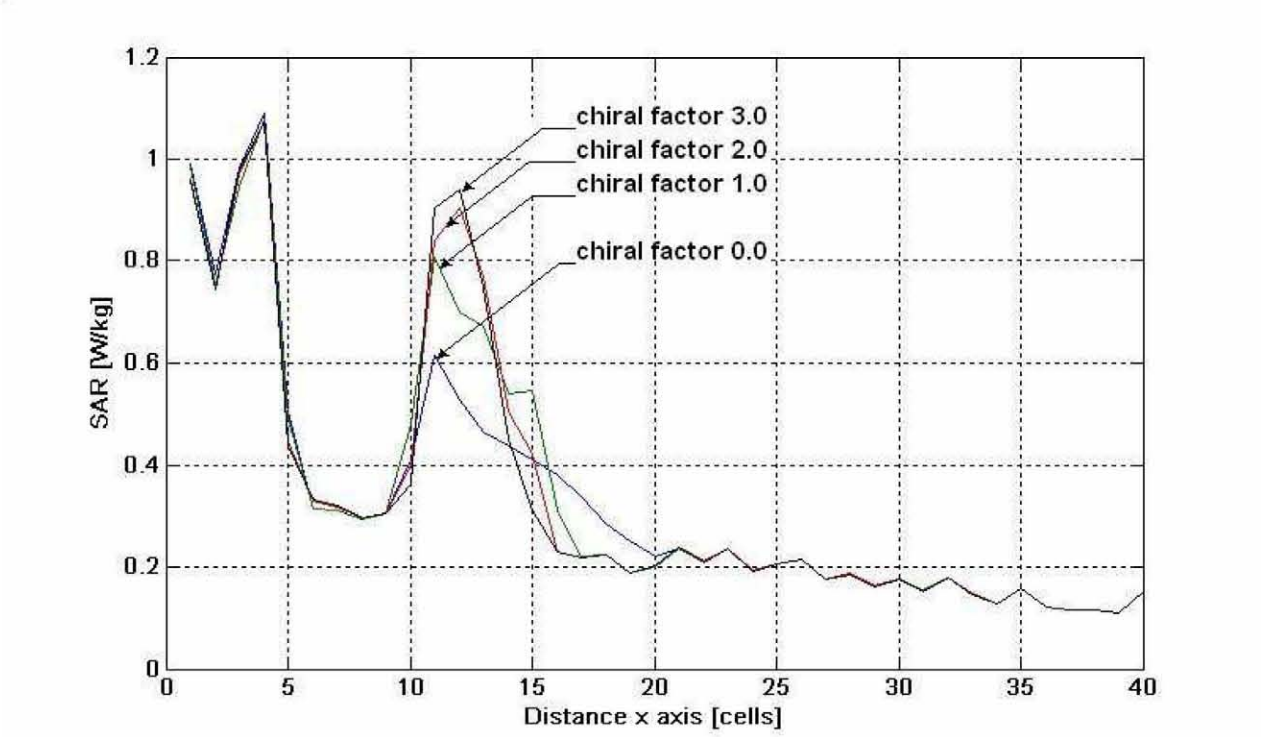


figure 3

INCREASE OF CELL DEATH IN SUSPENTION-CULTURED TOBACCO CELLS FOLLOWING EXPOSURE TO STATIC MAGNETIC FIELD

PARVIZ ABDOLMALEKI, FAEZEH GHANATI

FACULTY OF SCIENCE, TARBIAT MODARES UNIVERSITY, P.O. BOX 14115/175, TEHRAN, IRAN.

Despite to studies demonstrating the effect of static magnetic field (SMS) on animal and/or human cell death fewer studies have been conducted on plant cells. In the present study suspension cultures of tobacco cell in the exponential phase of the growth were exposed continuously for 5 days each 5 hours to SMF of 10 and 30 mT. The viability, lipid proxidation as well as morphological features of the cells were then studied and compared to those of the control cells. The level of peroxidation of membrane lipids in the treated cells was significantly increased compared to those of non-exposed (control) cells while the viability of the treated cells was decreased. In addition, certain characteristics of programmed cell death (PCD) or necrosis e.g., vacuolization and fragmentation of nucleus were remarkably visible in the treated cells, compared to the control cells which had intact nuclei with clear nucleoli. The control cells also excluded ethidium bromide from their walls, whereas most of the treated cells allowed ethidium bromide to penetrate into the cells, emphasizing induction of cell death by magnetic field. Our result suggests that SMF can increase the rate of death in tobacco cells.

Introduction

Electromagnetic fields (EMF) are widely distributed in the environment and their effects are increasing with the burgeoning development of electrical machines [1, 2]. This make the concern about the possible risk of functional disorders in biological systems being growing. Results of the numerous experimental, epidemiological and theoretical studies are rather controversial, and in all areas so far, no unanimous conclusions have been reached [1-3]. Several studies on bacterial and animal cells have shown that EMF exert influence on a large variety of cellular functions, nevertheless the exact mechanism of the interaction with living cells are still unclear [4, 5].

Considering the cell as an electrical system provide a framework to investigate the exact mechanisms of the effect of the electric, magnetic and electromagnetic fields in the physiological behavior of the cell. Taking into consideration the previous reports on the presence of window effect this question raised whether or not a cell absorbed the energy in EMF like a receiver which work in a special band of frequency. If it is positive these fields can therefore act like primary messengers such as hormones. Then it is justified to say that the cells respond to physical stimulus (like EMF) in the same way that they respond to the hormones. Also, it would be helpful to understand whether the exposure of cells to the magnetic fields has any effect on the apoptosis. In the other words the magnetic field works as pro-apoptosis factor or as anti-apoptosis factor. If the MF had a pro-apoptosis role it will be useful in cancer treatment because one possible mechanism through which cells are prompted to develop cancer is the disruption of the equilibrium between the processes of proliferation and apoptosis [6,7. However, apoptosis is a part of normal cell physiology which includes both proliferation and differentiation. It is a major component of both normal cell development and disease. The morphological demonstration of apoptosis is characterized by rapid condensation of the cytoplasm and nuclear chromatin, resulting in DNA fragmentation and membrane blebbing followed by fragmentation of the cells into apoptotic bodies, made up of condensed cytoplasm, nuclear material and/or whole organelles surrounded by intact plasma membranes. [7-9].

There are reports about the short-term EMF exposure that elicited an immune response [10]. A potential link between EMF and its effects on living organisms is the fact that EMF causes an oxidative stress i.e., increase in the activity, concentration, and life time of free radicals [11-13]. Oxidative stress is a function of oxidative metabolites, free radicals and reactive oxygen species (ROS) which are highly reactive by-products of normal metabolism and immune defense [11-13]. It brings changes in enzyme activity, gene expression, and release of

calcium from intracellular storage sites. Oxidative stress also affects membrane structure, cell growth, and cell death, thereby contribute to cancers and leukemia [11-14].

Less studies of this kind have been conducted on plant cells and few available literatures, have particularly directed their attention to the effects of magnetic fields on the germination of seeds, pollen germination and plant growth and development [15, 16].

The goal of the present study was to determine a potential relationship between viability, lipid proxidation as well as morphological features of the suspension-cultured tobacco cells which exposed to static magnetic fields. It may help us to improve the general knowledge about mechanism(s) of the responses of the living systems to EMF.

Suspension cultures established from calli of tobacco cells (Nicotiana tabacum L. cv. Burley 21) that had been maintained in our laboratory for 52 subcultures. Both calli and subsequent suspensions were grown in a modified Murashige and Skoog medium without glycine and containing 3% sucrose. The medium was containing: (NH4)NO3 20.61 mM; KH2PO4, 1.25 mM; CaCl2, 2.99 mM; MgSO4, 1.50 mM; MnSO4, 0.1 mM; Fe-EDTA, 0.1 mM; H3BO3, 0.1 mM; CoCl2, 0.11 μM ; CuSO4, 0.1 μM;; Na2MoO4 μM, 1.03; ZnSO4, 29.91 μM , KI, 5 μM . pH was adjusted to 5.8. All chemicals were purchased from Sigma, Japan. Suspension-cultured cells were grown at 25 °C in darkness on an orbital shaker at 120 rpm and were sub-cultured every 7 day, when they were still in their logarithmic growth phase [17]. Frequent subcultures provided us homogenous and undifferentiated batches of tobacco cells that no longer have kept their original properties and their physiological response to EMF could resemble physiological response of plant cells regardless of their species.

Exposure to EMF was performed by a locally designed EMF generator The electrical power was provided using a 220 V AC power supply equipped with variable transformer as well as a single-phase full-wave rectifier. The maximum power and passing current were 1 KW and 50 A DC, respectively. This system was designed to generate EMF in range of 0.5 μT – 30 mT with stable conditions. It consisted of two coils (each 3000 turns of 3 mm copper wire) equipped with a U-shaped laminated iron core (to prevent eddy current losses). Using two vertical connectors, the arms of the U-shaped iron core were terminated to four circular iron plates covered with thin layer of Nickel (each 23 mm thickness, 260 cm in diameter). A water circulation system around the coils was employed to avoid the increase of the temperature. The temperature between the circular iron plates (exposure sites of samples) ,measured by a thermometer, was almost the same as other parts of the room (e.g., the site of the control cells) ±1°C. Nevertheless, the control cells were kept far enough from the apparatus, to avoid any potential exposure to the magnetic field from aforesaid generator. Since no other appliance was working, the control samples were only exposed to the extremely low MF of the earth, as the treatment group was too.

An electronic board was used to stabilize the system so that we always got a uniform MF. Calibration of the system as well as tests for the accuracy and uniformity of the magnetic fields were performed by a teslameter (PHYWE, Germany) with a probe type of Hall Sound. The accuracy of the system was ±0.1% for static field and the range of measurements was 3 μT – 30 mT.

It is generally accepted that household and office levels of magnetic fields vary between 0.01 to 0.1 mT and levels near a power transmission line are between 10-30mT and much higher levels are expected in occupational exposures [18]. A magnetic field of 30mT is also a limit requiring controlled access - being a level at which magnetic materials may move under the influence of a field. Therefore, the present study was undertaken to test the effects of 10 and 30 mT on plant cells. The cells in their exponential growth phase were continuously exposed to EMF by magnitudes of 10 or 30mT, for 5 days (from day 3 to 7). After the period of treatment the cells were harvested and frozen in liquid N2 and kept at – 80 °C until used for biochemical analysis.

Viability of both treated and control samples of the suspension-cultured tobacco cells was obtained by staining the cells with 0.1% aqueous solution of Evans Blue for 3 min and washed with deionized water. Then it was observed using a light microscope (Olympus, BH2, Japan) with different magnifications. The cells with complete blue color was considered dead and the ones in which the membrane inhibited insertion of the blue dye was considered live. Consequently by counting the live and dead cells the viability of both treated as well as the control cells was obtained.

Level of damage of membranes was determined by measuring malonyldealdehyde (MDA) as the end product of peroxidation of membrane lipids [19]. In brief, samples were homogenized in an aqueous solution of trichloroacetic acid (TCA) (10% w/v) and aliquots of the filtrates were heated in 0.25% thiobarbituric acid (TBA). The amount of MDA was determined from the absorbance at 532 nm followed by correction for the nonspecific absorbance at 600 nm. The amount of MDA-TBA complex was calculated from the extinction coefficient 155mM-1cm-1and expressed against mg of protein.

Cell wall preparations were obtained by homogenization of frozen samples in water with a mortar and pestle followed by centrifugation at 1000g and sequential washing of the pellet with EtOH, CHCl3-MeOH (2: 1) and acetone and then drying in air. Lignin content of wall preparations was measured via a modified acetyl bromide

procedure. The lignin content was determined by measuring of absorbance at 280 nm using specific absorption coefficient value 20.0 g-1 liter cm -1.

Cells were stained with acridine orange (10µg/mL distilled water) or ethidium bromide (10µg/mL distilled water) to extract the morphological features of both treated and control cells. Observations were made with an Olympus BH2 fluorescence microscope equipped with filter combinations WU (330-385-nm excitation and 420-nm barrier filters) and WBV (400- to 440-nm excitation and 475-nm barrier filters).

All of the experiments were carried out with at least three independent repetitions, each three samples, and all data were expressed as the mean values ± standard deviation (SD). Statistical analysis was performed using Student's t- Test and the differences between treatments were expressed as significant at level of $P<0.05$.

The tobacco cells in suspension culture were seen in different shapes such as round, cylindrical as well as ellipse (Figure 1). As mentioned in material and method we exposed the prepared cells in exponential phase which started from day 3 - 8 (Figure 2). The dimension of these cells is presented in table 1. Our results showed that the average size of the treated cells with both 10 and 30 mT SMF was significantly decreased compared to the control cells. Although, the growth rate of the treated cells decreased compared to the control cells by measuring the weight of cells, but it was not significant (Table 1). Exposure to SMF significantly increased the level of the peroxidation of membrane lipids of suspension-cultured tobacco cells, compared to those of non-exposed (control) cells. The MDA level did not show a noticeable difference in both 10 and 30 mT.

Figure 3 shows the MDA level in treated cells compared with the control cells. The obtained average for MDA level on treatment group (10 mT) was 1.16 ± 0.03 (MDA/g Fw) while the obtained average for MDA level on control group was 0.89±0.02 (MDA/g Fw). Similarly, the obtained average for MDA level on treatment group (30 mT) was 1.13±0.04 (MDA/g Fw) while the obtained average for MDA level on control group was 0.84±0.12 (MDA/g Fw). However, there was not significant difference between the levels of lipid peroxidation of 10 and 30 mT of SMF-exposed cells.

Figure 4 shows the lignin content of wall in treated cells compared with the control cells. The results showed that the exposure of the magnetic field caused a significant increase in the lignin content of wall in treated cells (n=24) compared with the controls (n=24). However the lignin content did not show a noticeable difference in both 10 and 30 mT. The obtained average for lignin content on treated groups (10 and 30 mT) were 7.09 ± 0.45 and 6.96 ± 0.08, respectively. While the obtained average for lignin content on control groups were 6.17±0.26 and 5.7 ±0.06, respectively.

The viability of the treated cells as well as control cells using Evans Blue and ethidium bromide were presented in figure 5 and 6. These results showed that the viability of the treated cell (30 mT) was approximately 68% while the viability of treated cells (10 mT) was 72%. The viability of the control cells was 84%.

Certain characteristics of programmed cell death (PCD) or necrosis e.g., nuclear vacuolization and fragmentation were observed in tobacco cells exposed to the static magnetic fields (Figure 7A, Figure 7B), compared to the control cells who had intact nuclei with clearly visible nucleoli (Fig.7D). The latter also excluded ethidium bromide in their walls (Figure 6), whereas most of the magnetic field-exposed cells allowed ethidium bromide to penetrate into the cells, emphasizing induction of cell death by magnetic field (Figure 7)

Table 1: demonstrating the obtained average diementions and weight of treated cells compared with control cells.

SMF(mT)	Diameter(μ_m)		Weight(g/flask)
	Width	Length	
0	48.2±13[a]	40.5±12.5[a]	13.3±.22[a]
10	37.8±10.8[b]	33.6±8.3[b]	12.1±1.01[a]
0	41.8±17.9[a]	49.2±10.8[a]	11.6±1.07[a]
30	29.3±5.9[b]	37.2±10.2[b]	10.9±1.06[a]

Different letters refer to significant differences at the level of $p\leq0.05$ according to student t-test.



Figure 1: A tobacco cell under the light microscope showing cell wall (CW), nucleus (Nu), and Cytoplasmic strands (CS), X660.

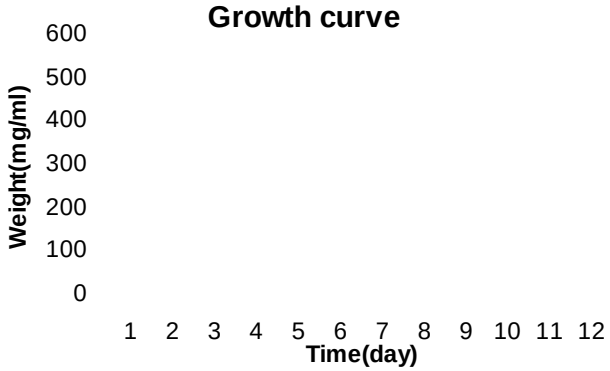


Figure 2: Growth curve of suspension-cultured tobacco cells.

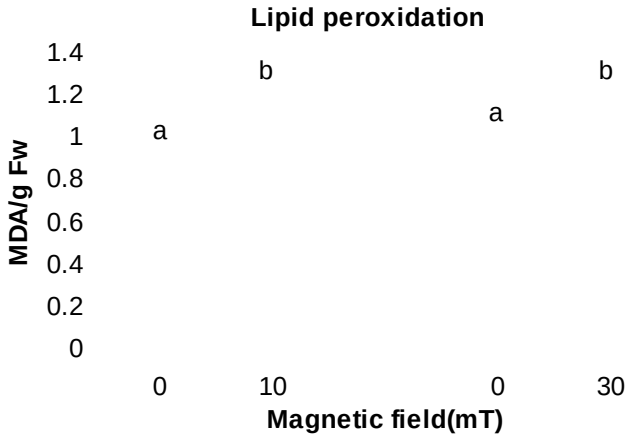


Figure 3. Effect of SMF on the rate of lipid peroxidation of suspension-cultured tobacco cells. Data are means ± SD, n=3. Signs with different letters in each group indicate significant differences at $P < 0.05$ according to Student's t-Test.

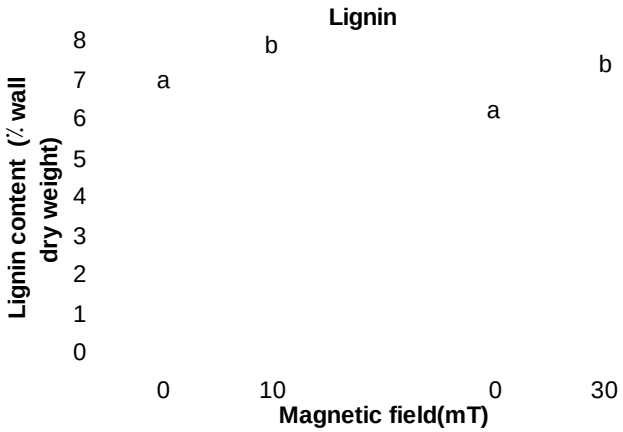
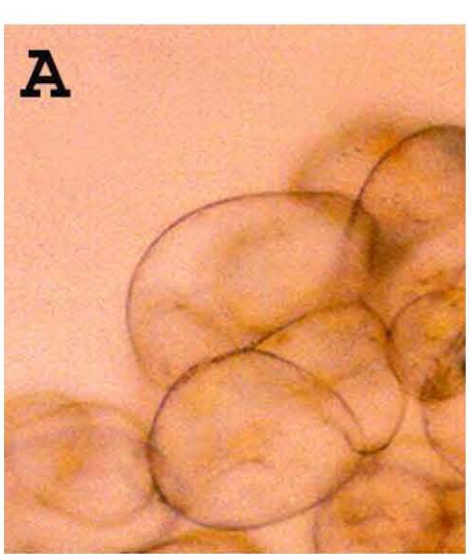
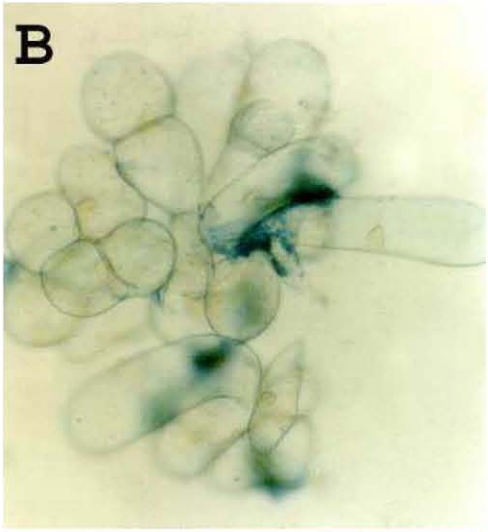
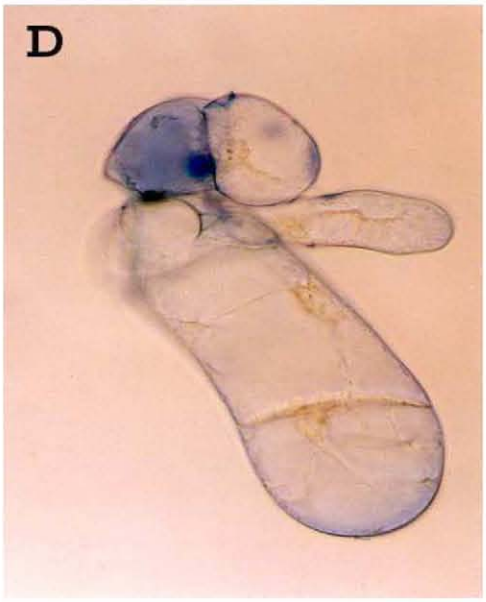


Figure 4.Effects of 10mTand 30mT SMF 5h for 5day on lignin content in tobacco cell. Each column indicates the mean ± SD, n=3.







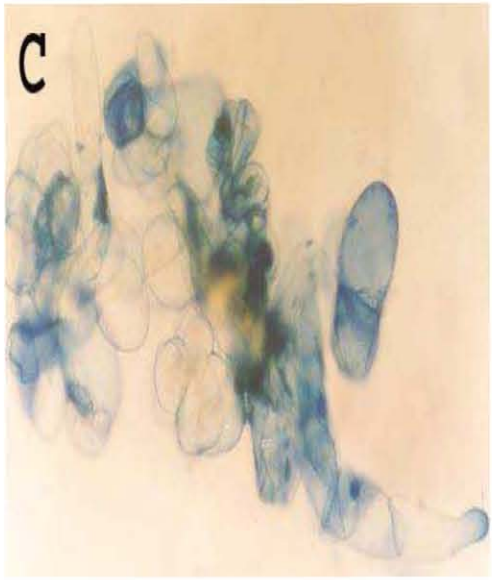


Figure 5: Showing the viability of treated cells (C and D) compared with the control cells (A and B), A-C, X330; D, X660.

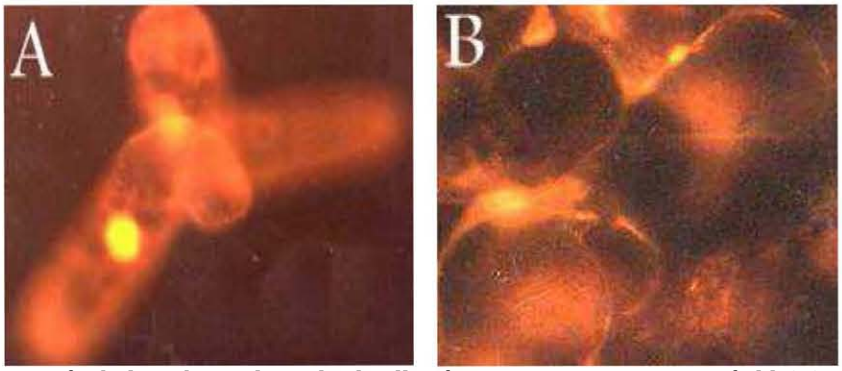


Figure 6. Penetration of ethidium bromide in dead cells after exposure to magnetic field (A), compared to the control cells where excluded dye in their walls (B). Magnifications of both X 660.

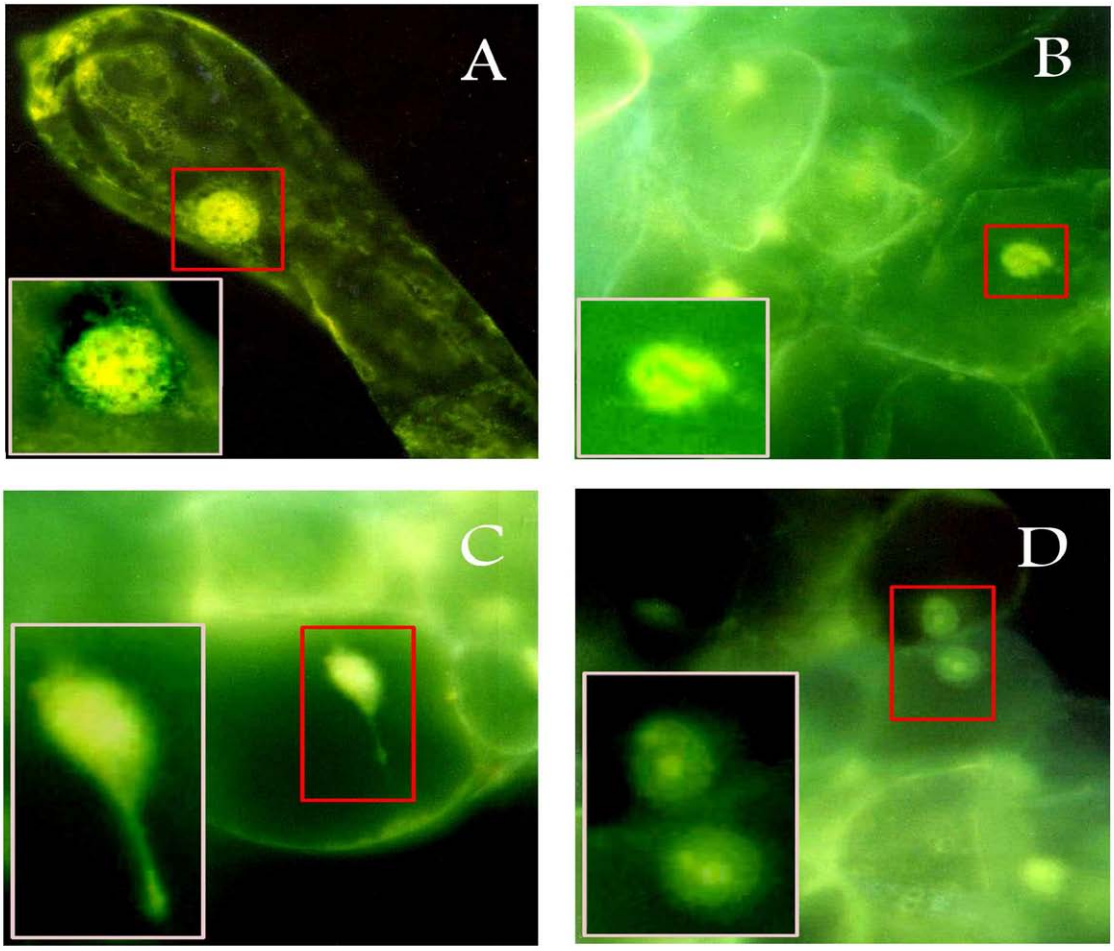


Figure 7. Morphological features of suspension-cultured tobacco cells exposed to static magnetic fields. Cleavage of nucleus of tobacco cells exposed to 10 (A) and 30 mT static magnetic fields (B, C), compared to the control cells with intact nuclei and clearly visible nucleoli (D). Cells were stained with acridine orange and observed under epifluorescence microscope. Magnifications of A, X1320 and of B, C, and D, X660.

Summary

Electromagnetic fields for many years were considered as an absolutely neutral form of radiation, but epidemiological data and results of experimental in vivo studies have attracted more attention to the biological effects of EMF. Primary action of SMF in biological systems is the induction of electrical charges and currents [18]. One of the major molecular effects of magnetic fields is their influence on nuclear spins of paramagnetic molecules. This mechanism plays an important role when in the course of a chemical reaction the chemical bound is disrupted and two molecules with unpaired electrons are formed (a pair of radicals). Depending on their spin orientations, radical recombination or diffusion and formation of free radicals (e.g., Oxygen radicals) may take place [20]. The radical pairs may be affected for a long and continuous time interval by the static magnetic field [21]. This may extend the life time of the free radical and its potential damage could be exaggerated. Although formed in normal cell metabolism, free radicals are potentially damaging and can initiate chain reactions to form new free radicals. A main protective role against free radicals is attributed to SOD in catalyzing and dismutation of superoxide anions to O_2 and H_2O_2 [22]. We showed somewhere else that the exposure to SMF increased the activity of SOD in tobacco cells compared to those corresponding control groups. It implies the first step of the increased production of free radicals by SMF in tobacco cells. An increase in SOD activity might enhance cytotoxicity by active oxygen species likely owing to the accelerated H_2 O_2 generation and subsequent $OH^{\bullet}$ overproduction by the metal catalyzed Haber-Weiss reaction [23]. Scavenging and detoxification of H_2O_2 that is produced by SOD, can be achieved by either non-enzymatic antioxidants or scavenging enzymes, e.g., CAT. Likewise, the activity of CAT was also reduced by SMF.

Accumulation of H_2O_2 and other reactive species of oxygen in SMF-exposed tobacco cells may subsequently result in peroxidation of membrane lipids as well as damage of DNA [24]. Ishisaka and his colleagues (2000) showed H_2O_2 -induced rapid fragmentation of DNA and a slow decrease in the viability of human cancer cell line HL-60[25]. In the same cell line, Robison and his colleagues presented data demonstrating that a decrease in the DNA repair may occur following oxidative burst induced by EMF [26]. Although morphological features of programmed cell death and necrosis of plant cells, to some extent, differ from those in animal cells, however some of these features, e.g., cleavage of DNA to internucleosomal fragments and increase of lipid peroxidation (membrane lysis) were observed more in SMF-exposed cells, compared to the control cells.

MDA measurement also indicates that 10, 30mT SMF exposure induces lipid peroxidative stress. This implies that SMF is somehow involved with free radical reaction in tobacco cells. It means that increase in lipid peroxidation can be another proof for the accumulation of H2O2 in treated tobacco cells compared to the controls. These results indicate that exposing to the SMF can induse oxidative stress due to activity of the free radicals and it will therefore caser more lipid peroxidation. Increase in the lipid peroxidation of the membrane in both 10 and 30 mT SMF also showed that the failure of the antioxidant defence system of treated cells against the free radicals. The results presented in table 1 indicated that the treated cells become smaller in size and less prolifrative compared to the control cells. This could be explained by this suggestion that the SMF shortened the cell cycle and it also inhibitated the extention of the cell membrane. Exposing to the SMF was the main reason for Increase in SOD activity may represent a compensatory reaction against oxidative stress. Increase in lignin content of treated cells (7.09 ± 0.45 and 6.96 ± 0.08 for 10 and 30mT) compared to the control (6.17 ± 0.26 and 5.7 ± 0.06) demonstrating the wall loosening through increasing the wall stiffening. This can possibly decrease the cellular growth.

Taken all together, the results presented here reveal that SMF can cause an inconsistency in the function of antioxidant enzymes in suspension-cultured tobacco cells thereby, lead to oxidative burst and cell death.

References

[1] Patterson RM, Exposure assessment for electric and magnetic field ,J.Expo. Am.Environ.Epidemial 2 (1992)159-176.

[2] Breysse P, Lees PS, McDiamid MA, curbow B., ELF magnetic field exposure in an office environment, Am.J.Ind.Med.25 (1994)177-185.

[3] Ilulbert Al, Metcalfc J, Ilesketh R, Biological response to electromagnetic fields, FASEB.J.12 (1998)395-420.

[4] Lai H, Singh NP, Melatonin and N-tert-butyl-alpha-phenylnitrone block 60-Hz magnetic field –induced DNA single and double strand breaks in rat brain cells, J.Pineal Res.22 (1997)152-162.

[5] Potschka H, Thun-Battersby S, Lioscher W, Effect of low –intensity 50-Hz magnetic fields on kinding acquisition and fully kindled seizures in rats, Brain Res 809(1998)269-276.

[6] Dini L, Abbro L. Bioeffects of moderate-intensity static magnetic fields on cell cultures. Micron 36 (2005) 195–217.

[7] Liu MC, Marshall JL, Pestell RG, 2004. Novel strategies in cancer therapeutics: targeting enzymes involved in cell cycle regulation and cellular proliferation. Current Cancer Drug Targets 4, 403–424.

[8] Alenzi FQ, 2004. Links between apoptosis, proliferation and the cell cycle. British Journal of Biomedical Science 61, 99–102.
[9] Dini L., Coppola, S., Ruzittu, M., Ghibelli, L., 1996. Multiple pathways for apoptotic nuclear fragmentation. Experimental Cell Research 223, 340–347.
[10] Repacholi MH, Greenebaum B. 1999. Interaction of static and extremely low frequency electric and magnetic fields with living systems: Health effects and research needs. Bioelectromagnetics 20: 133-160.
[11] Scaiano JC, Cozens FL, Mclean J. 1994. Model for the rationalization of magnetic field In vivo. Application of the radical-pair mechanism to biological systems. Photochemistry and Photobiology 59: 585-589.
[12] Sobczak A, Kula B, Dancii A. 2002. Effects of electromagnetic field on free-radical processes in steelworkers. Part II: Magnetic field influence on vitamin A, E and selenium concentrations in plasma .J Occup Health 44: 230-233.
[13] Dat JF, Van Montagu M, Inze D, Van Breusegem F. 2001. Catalase-deficient tobacco plants: tools for in planta studies on the role of hydrogen peroxide. Redox Report 6: 37-42.
[14] Green LM, Miller AB, Agnew DA, Greenberg ML, Li J, Villeneuve JP, Tibshirani R. 1999. Childhood leukemia and personal monitoring of residential exposures to electric and magnetic fields in Ontario. Canada. Cancer Causes Control 10: 233-243.
[15] Yano A, Hidaka E, Fujiwara K, Iimoto M. 2001. Induction of primary root curvature in radish seedlings in a static magnetic field. Bioelectromagnetics 22:194-199.
[16] Rakosy-Tican L, Aurori CM, Morariu VV. 2005. Influence of near null magnetic field on in vitro growth of potato and wild solanum species. Bioelectromagnetics 26: 548-557.
[17] Ghanati F, Morit A, Yokota H. 2001. Selection and partial characterization of a boron-tolerant tobacco cell line, Soil Science and Plant Nutrition 47: 405-410.
[18] Roy C, Repacholi M. 2005. Electromagnetic field and Health, A WHO perspective, World Health Organization, Geneva, Switzerland, Available from: http://www.world-aluminium.org/news/ montreal/roy.htm.
[19] De Vos CHR, Schat H, De Waal MAD, Vooijs R, Ernst WHO. 1991. Increased resistance to copper-induced damage of the root plasma membrane in copper tolerant Silene cucubalus. Physiol Plant 82: 523-528
[20] Kula A. Sobczak, Kuska R. 2002. Effects of electromagnetic field on free-radical processes in steelworkers. Part I: Magnetic field influence on the antioxidant activity in red blood cells and plasma. J Occup Health 44: 226-229.
[21] Zmyslony M, Palus J, Jajte J, Dziubaltowska E, Rajkowska E. 2000. DNA damage in rat lymphocytes treated in vitro with iron cations and exposed to 7mT magnetic fields (static or 50HZ). Mutation Res 453: 89-96.
[22] Sreenivasulu N, Grimm B, Wobus U, Weschke W. 2000. Differential response of antioxidant compounds to salinity stress in salt-tolerant and salt-sensitive seedlings of foxtail millet (Setaria italica), Physiol. Plant. 109: 435-442.
[23] Piacentini MP, Fraternale D, Piatti E, Ricci D, Vetrano F. 2001. Senescence delay and change of antioxidant enzyme levels in Cucumis sativus L.etiolated seedling by ELF magnetic fields. Plant Science 161: 45-53.
[24] Jajte J, Grzegorczyk J, Zmyslony M, Rajkowska E, Kowalska MS, Kowalski ML. 2001. Influence of a 7mT static magnetic field and irons on apoptosis and necrosis in rat blood lymphocytes. J Occup Health 43: 379-381.
[25] Ishisaka R, Kanno T, Inai Y, Nakahara H, Akiyama J, Yoshioka T, Utsumi K. 2000, Effects of a magnetic fields on the various functions of subcellular organelles and cells. Pathophysiology 7: 149-152.
[26] Robison JG, Pendleton AR, Monson KO, Murray BK, O'Neill KL. 2002. Decreased DNA repair rates and protection from heat induced apoptosis mediated by electromagnetic field exposure. Bioelectromagnetics 23: 106-112.

IMPLICIT FDTD METHODS AND THE SAMPLING THEOREM

ĽUBOMÍR ŠUMICHRAST

INSTITUTE OF ELECTROMAGNETIC THEORY, SLOVAK UNIVERSITY OF TECHNOLOGY, ILKOVIČOVA 3, SK-81219 BRATISLAVA, SLOVAKIA

Abstract

The numerical properties of two factorized implicit formulations of the method of Finite-Differences-in-Time-Domain (FDTD) for the simulation of electromagnetic wave propagation are investigated and compared with explicit Yee-FDTD and full Crank-Nicolson FDTD formulation. It is shown that the ADI-FDTD factorization approaches asymptotically the Nyquist limit and can be used with arbitrarily large time steps. Also from the point of view of numerical dispersion gives acceptably small deviations from the full Crank-Nicolson FDTD formulation. On the other hand the CNSS-FDTD factorization does not fulfill Nyquist limit for arbitrarily large time steps.

Introduction

Numerical simulations are routinely used for modeling electromagnetic wave propagation problems in the area of high frequency electromagnetics and photonics. The finite-difference time-domain (FDTD) method of explicit type designed by Yee [1] was for long years the preferred numerical technique for such simulations due to its flexibility, since it allows the inclusion of arbitrarily heterogeneous objects in the region to be simulated. In the course of numerical computations artificial artifacts are introduced, such as numerical amplification of the wave power-flow-density (stability issues) as well as the numerical dispersion. For the explicit-type methods the well-known Courant-Friedrichs-Levy (CFL) condition concerning the stability of the calculations must be met, limiting thus the step-length of the in-time-forward-marching algorithm. The extent of literature in this area is huge, including several book publications, e.g. [2].

Recently the implicit types of FDTD methods has been constructed - the "Alternating Directions Implicit" (ADI) FDTD method [3], [4] and the "Crank-Nicholson Split-Step" (CNSS) FDTD method [5], [6]. Both are implicit procedures requiring inversion of tridiagonal matrices in two half steps. Both are theoretically unconditionally stable, i.e. they enable one to avoid the severe CFL condition and use the unlimited length of the time step in the course of calculation. However, another kind of bounds on the length of the time step, due to aliasing effects with growing time step, is imposed on both these methods.

Explicit and implicit FDTD formulations

The Maxwell equations

$$\operatorname{curl} \boldsymbol{H} = \varepsilon \frac{\partial \boldsymbol{E}}{\partial t}, \qquad \operatorname{curl} \boldsymbol{E} = -\mu \frac{\partial \boldsymbol{H}}{\partial t} \tag{1}$$

are for the simplicity taken in the simple form for lossless isotropic homogeneous linear medium without external sources, i.e. the permeability μ and the permittivity ε are constants. Here $\boldsymbol{E}(\boldsymbol{r},t)$ and $\boldsymbol{H}(\boldsymbol{r},t)$ are the electromagnetic field intensities for arbitrary time dependence.

In the Yee-FDTD method are Maxwell equations (1) discretised taking so called staggered grids [1] on all three spatial axes and in time with equidistant intervals $\{\Delta_x, \Delta_y, \Delta_z, \Delta_t\}$ (denoted by the serial indexes $\{i, j, m, n,\}$, i.e.

$$E_x\left([i+\tfrac{1}{2}]\Delta_x, j\Delta_y, m\Delta_z, [n+\tfrac{1}{2}]\Delta_t\right) = E_x\big|_{i+\frac{1}{2},j,m}^{n+\frac{1}{2}} \qquad H_x\left(i\Delta_x, [j+\tfrac{1}{2}]\Delta_y, [m+\tfrac{1}{2}]\Delta_z, n\Delta_t\right) = H_x\big|_{i,j+\frac{1}{2},m+\frac{1}{2}}^{n}$$
$$E_y\left(i\Delta_x, [j+\tfrac{1}{2}]\Delta_y, m\Delta_z, [n+\tfrac{1}{2}]\Delta_t\right) = E_y\big|_{i,j+\frac{1}{2},m}^{n+\frac{1}{2}}, \qquad H_y\left([i+\tfrac{1}{2}]\Delta_x, j\Delta_y, [m+\tfrac{1}{2}]\Delta_z, n\Delta_t\right) = H_y\big|_{i+\frac{1}{2},j,m+\frac{1}{2}}^{n} \tag{2}$$
$$E_z\left(i\Delta_x, j\Delta_y, [m+\tfrac{1}{2}]\Delta_z, [n+\tfrac{1}{2}]\Delta_t\right) = E_z\big|_{i,j,m+\frac{1}{2}}^{n+\frac{1}{2}} \qquad H_z\left([i+\tfrac{1}{2}]\Delta_x, [j+\tfrac{1}{2}]\Delta_y, m\Delta_z, n\Delta_t\right) = H_z\big|_{i+\frac{1}{2},j+\frac{1}{2},m}^{n}$$

Discretised Maxwell equations (only the E_x and H_x are considered bellow) take the form

$$\varepsilon\frac{E_x\big|_{i+\frac{1}{2},j,m}^{n+\frac{1}{2}} - E_x\big|_{i+\frac{1}{2},j,m}^{n-\frac{1}{2}}}{\Delta_t} = \frac{H_z\big|_{i+\frac{1}{2},j+\frac{1}{2},m}^{n} - H_z\big|_{i+\frac{1}{2},j-\frac{1}{2},m}^{n}}{\Delta_y} - \frac{H_y\big|_{i+\frac{1}{2},j,m+\frac{1}{2}}^{n} - H_y\big|_{i+\frac{1}{2},j,m-\frac{1}{2}}^{n}}{\Delta_z}, \tag{3}$$

$$\mu\frac{H_x\big|_{i,j+\frac{1}{2},m+\frac{1}{2}}^{n+1} - H_x\big|_{i,j+\frac{1}{2},m+\frac{1}{2}}^{n}}{\Delta_t} = \frac{E_y\big|_{i,j+\frac{1}{2},m+1}^{n+\frac{1}{2}} - E_y\big|_{i,j+\frac{1}{2},m}^{n+\frac{1}{2}}}{\Delta_z} - \frac{E_z\big|_{i,j+1,m+\frac{1}{2}}^{n+\frac{1}{2}} - E_z\big|_{i,j,m+\frac{1}{2}}^{n+\frac{1}{2}}}{\Delta_y}. \tag{4}$$

Yee-FDTD method as represented by the equations (3) and (4) is the explicit method: the values $E_x\big|_{i+\frac{1}{2},j,m}^{n+\frac{1}{2}}$ in (3) in the "new" time layer $n+\frac{1}{2}$ are directly calculated from the "old" known values in layers $n-\frac{1}{2}$ and n. Similar holds for $H_x\big|_{i,j+\frac{1}{2},m+\frac{1}{2}}^{n+1}$ in (4). The main drawback of the Yee-FDTD explicit method is its conditional stability. In order to have conserved the wave-power-flow-density in the computational window, the CFL-condition

$$c\Delta_t\sqrt{\Delta_x^{-2}+\Delta_y^{-2}+\Delta_z^{-2}} < 1 \tag{5}$$

where $c = (\mu\varepsilon)^{-1/2}$ is the phase velocity in the lossless medium, has to be met, limiting thus severely the permissible length of the time steps Δ_t.

In the matrix notation (1) reads

$$\varepsilon\frac{\partial}{\partial t}\boldsymbol{E} = \boldsymbol{\Delta}\cdot\boldsymbol{H} \qquad -\mu\frac{\partial}{\partial t}\boldsymbol{H} = \boldsymbol{\Delta}\cdot\boldsymbol{E} \tag{6}$$

where $\boldsymbol{E} = \left[E_x, E_y, E_z\right]^T$ and $\boldsymbol{H} = \left[H_x, H_y, H_z\right]^T$ are column vectors of field components and $\boldsymbol{\Delta}$ is given as

$$\boldsymbol{\Delta} = \boldsymbol{\Delta}_1 - \boldsymbol{\Delta}_2 = \begin{bmatrix} 0 & -\partial/\partial z & \partial/\partial y \\ \partial/\partial z & 0 & -\partial/\partial x \\ -\partial/\partial y & \partial/\partial x & 0 \end{bmatrix}, \quad \boldsymbol{\Delta}_1 = \begin{bmatrix} 0 & 0 & \partial/\partial y \\ \partial/\partial z & 0 & 0 \\ 0 & \partial/\partial x & 0 \end{bmatrix}, \quad \boldsymbol{\Delta}_2 = \begin{bmatrix} 0 & \partial/\partial z & 0 \\ 0 & 0 & \partial/\partial x \\ \partial/\partial y & 0 & 0 \end{bmatrix}. \tag{7}$$

Combining $\boldsymbol{E}$ and $\boldsymbol{H}$ into one vector $\boldsymbol{F}$

$$\boldsymbol{F} = \begin{bmatrix} \boldsymbol{E}/\sqrt{Z} \\ \boldsymbol{H}\sqrt{Z} \end{bmatrix}, \tag{8}$$

where $Z = \sqrt{\mu/\varepsilon}$ is the wave impedance of the lossless medium, one arrives to the equation

$$c^{-1}\frac{\partial}{\partial t}\boldsymbol{F} = \boldsymbol{D}\cdot\boldsymbol{F}, \tag{9}$$

where

$$\boldsymbol{D} = \begin{bmatrix} \boldsymbol{0} & \boldsymbol{\Delta}_1 - \boldsymbol{\Delta}_2 \\ \boldsymbol{\Delta}_2 - \boldsymbol{\Delta}_1 & \boldsymbol{0} \end{bmatrix}, \quad \boldsymbol{D} = \boldsymbol{D}_1 + \boldsymbol{D}_2 = \boldsymbol{D}_{12} - \boldsymbol{D}_{21}, \tag{10}$$

$$\boldsymbol{D}_1 = \begin{bmatrix} 0 & \boldsymbol{\Delta}_1 \\ -\boldsymbol{\Delta}_1 & 0 \end{bmatrix}, \quad \boldsymbol{D}_2 = \begin{bmatrix} 0 & -\boldsymbol{\Delta}_2 \\ \boldsymbol{\Delta}_2 & 0 \end{bmatrix}, \quad \boldsymbol{D}_{12} = \begin{bmatrix} 0 & \boldsymbol{\Delta}_1 \\ \boldsymbol{\Delta}_2 & 0 \end{bmatrix}, \quad \boldsymbol{D}_{21} = \begin{bmatrix} 0 & \boldsymbol{\Delta}_2 \\ \boldsymbol{\Delta}_1 & 0 \end{bmatrix}. \tag{11}$$

Crank-Nicolson formulation of discretisation of differential equation is known to be unconditionally stable. For (9) with respect to the time derivative it yields

$$\frac{\boldsymbol{F}^{n+1} - \boldsymbol{F}^{n}}{c\Delta_t} = \boldsymbol{D}\cdot\frac{\boldsymbol{F}^{n+1} + \boldsymbol{F}^{n}}{2}, \tag{12}$$

Equation (12) can be put in the following form

$$\left\{\boldsymbol{I}-\frac{2}{c\Delta_t}\left(\boldsymbol{D}_1+\boldsymbol{D}_2\right)\right\}\cdot\boldsymbol{F}^{n+1}=\left\{\boldsymbol{I}+\frac{2}{c\Delta_t}\left(\boldsymbol{D}_1+\boldsymbol{D}_2\right)\right\}\cdot\boldsymbol{F}^{n}, \tag{13}$$

which can after some calculation be re-cast into the following form (see e.g. [7])

$$\left\{\boldsymbol{I}-\frac{2}{c\Delta_t}\boldsymbol{D}_1\right\}\cdot\left\{\boldsymbol{I}-\frac{2}{c\Delta_t}\boldsymbol{D}_2\right\}\cdot\boldsymbol{F}^{n+1}-\frac{4}{c^2\Delta_t^2}\boldsymbol{D}_1\cdot\boldsymbol{D}_2\cdot\boldsymbol{F}^{n+1}=$$

$$=\left\{\boldsymbol{I}+\frac{2}{c\Delta_t}\boldsymbol{D}_2\right\}\cdot\left\{\boldsymbol{I}+\frac{2}{c\Delta_t}\boldsymbol{D}_1\right\}\cdot\boldsymbol{F}^{n}-\frac{4}{c^2\Delta_t^2}\boldsymbol{D}_2\cdot\boldsymbol{D}_1\cdot\boldsymbol{F}^{n}. \tag{14}$$

Solving the full system of implicit equations (13), (14) is far beyond the capabilities of common computational machinery. Therefore after having neglected last terms on the RHS and LHS of (14), one can split the approximate equation

$$\left\{\boldsymbol{I}-\frac{2}{c\Delta_t}\boldsymbol{D}_1\right\}\cdot\left\{\boldsymbol{I}-\frac{2}{c\Delta_t}\boldsymbol{D}_2\right\}\cdot\boldsymbol{F}^{n+1}=\left\{\boldsymbol{I}+\frac{2}{c\Delta_t}\boldsymbol{D}_2\right\}\cdot\left\{\boldsymbol{I}+\frac{2}{c\Delta_t}\boldsymbol{D}_1\right\}\cdot\boldsymbol{F}^{n} \tag{15}$$

into two subsequent steps

$$\left\{\boldsymbol{I}-\frac{2}{c\Delta_t}\boldsymbol{D}_2\right\}\cdot\boldsymbol{F}^{n+1/2}=\left\{\boldsymbol{I}+\frac{2}{c\Delta_t}\boldsymbol{D}_1\right\}\cdot\boldsymbol{F}^{n},\qquad\left\{\boldsymbol{I}-\frac{2}{c\Delta_t}\boldsymbol{D}_1\right\}\cdot\boldsymbol{F}^{n+1}=\left\{\boldsymbol{I}+\frac{2}{c\Delta_t}\boldsymbol{D}_2\right\}\cdot\boldsymbol{F}^{n+1/2}. \tag{16}$$

where $\boldsymbol{F}^{n+1/2}$ denotes the intermediate value after the first sub step. This procedure is called Alternating-Directions-Implicit (ADI)-FDTD method. If there are N spatial discretisation points along each axis x, y, and z, then the algorithm for (16) can be organized in such a way that it requires six inversions of the tri-diagonal $(N\times N)$ matrices. The original problem (13) requires inversion of the $\left(6N^3\times 6N^3\right)$ sparse matrix. This is already for moderate number of sampling points N an unrealizable task.

Alternatively can (12) be expressed in the following way

$$\left\{\boldsymbol{I}-\frac{2}{c\Delta_t}\left(\boldsymbol{D}_{12}-\boldsymbol{D}_{21}\right)\right\}\cdot\boldsymbol{F}^{n+1}=\left\{\boldsymbol{I}+\frac{2}{c\Delta_t}\left(\boldsymbol{D}_{12}-\boldsymbol{D}_{21}\right)\right\}\cdot\boldsymbol{F}^{n} \tag{17}$$

and then similarly recast into the form

$$\left\{\boldsymbol{I}-\frac{2}{c\Delta_t}\boldsymbol{D}_{12}\right\}\cdot\left\{\boldsymbol{I}+\frac{2}{c\Delta_t}\boldsymbol{D}_{21}\right\}\cdot\boldsymbol{F}^{n+1}+\frac{4}{c^2\Delta_t^2}\boldsymbol{D}_{12}\cdot\boldsymbol{D}_{21}\cdot\boldsymbol{F}^{n+1}=$$

$$=\left\{\boldsymbol{I}+\frac{2}{c\Delta_t}\boldsymbol{D}_{12}\right\}\cdot\left\{\boldsymbol{I}-\frac{2}{c\Delta_t}\boldsymbol{D}_{21}\right\}\cdot\boldsymbol{F}^{n}+\frac{4}{c^2\Delta_t^2}\boldsymbol{D}_{12}\cdot\boldsymbol{D}_{21}\cdot\boldsymbol{F}^{n}. \tag{18}$$

After having neglected last terms on RHS and LHS of (18) one again arrives to analogous equation as (15)

$$\left\{\boldsymbol{I}-\frac{2}{c\Delta_t}\boldsymbol{D}_{12}\right\}\cdot\left\{\boldsymbol{I}+\frac{2}{c\Delta_t}\boldsymbol{D}_{21}\right\}\cdot\boldsymbol{F}^{n+1}=\left\{\boldsymbol{I}+\frac{2}{c\Delta_t}\boldsymbol{D}_{12}\right\}\cdot\left\{\boldsymbol{I}-\frac{2}{c\Delta_t}\boldsymbol{D}_{21}\right\}\cdot\boldsymbol{F}^{n}. \tag{19}$$

which can again be splitted into two subsequent sub steps

$$\left\{\boldsymbol{I}+\frac{2}{c\Delta_t}\boldsymbol{D}_{21}\right\}\cdot\boldsymbol{F}^{n+1/2}=\left\{\boldsymbol{I}-\frac{2}{c\Delta_t}\boldsymbol{D}_{21}\right\}\cdot\boldsymbol{F}^{n},\qquad\left\{\boldsymbol{I}-\frac{2}{c\Delta_t}\boldsymbol{D}_{12}\right\}\cdot\boldsymbol{F}^{n+1}=\left\{\boldsymbol{I}+\frac{2}{c\Delta_t}\boldsymbol{D}_{12}\right\}\cdot\boldsymbol{F}^{n+1/2}. \tag{20}$$

This procedure is called Crank-Nicolson-Split-Step (CNSS)-FDTD method. In both methods are the terms of the second order on the RHS and the LHS of (14) and (18) neglected. Therefore both are in Δ_t second order approximate in comparison with the full Crank-Nicolson formulation (13) or (17).

Numerical dispersion

For the sake of simplicity let us consider the two-dimensional case only. Waves of any temporal and/or spatial shape can be Fourier expanded into the angular spectrum of either TM or TE monochromatic plane waves. Propagation of a spatio-temporal spectral TM component having the vectorial components

$\{E_y, H_x, H_z\}$ in the direction given by the k_x, k_z components of the wave vector $\boldsymbol{k}$, $|\boldsymbol{k}| = k = \sqrt{k_x^2 + k_z^2}$, is described in two dimensions *x* and *z* by

$$E_y = E_0 \exp(j\omega t)\exp(-jk_x x)\exp(-jk_z z), \tag{21}$$

where the angular frequency ω is given as $\omega = kc = c\sqrt{k_x^2 + k_z^2}$, and *c* is the "physical" phase velocity in the given medium.

The FDTD discretisation is performed on the so-called staggered grids [1]. The discretised TM plane wave using (21) is then given by

$$E_y\big|_{i,m}^{n} \approx \xi^n \exp(-jk_x\Delta_x i)\exp(-jk_z\Delta_z m), \tag{22}$$

and similarly for $H_x\big|_{i,m+\frac{1}{2}}^{n}$ and $H_z\big|_{i+\frac{1}{2},m}^{n}$, where $\xi = \exp(j\omega\Delta_t)$ should hold. However, during the numerical simulation of the wave propagation instead of differential equations the difference equations are being solved. Therefore, instead of the above correct terms for ω and *c*, one obtains different values ω_A and v_p from the formula $\xi = \exp(j\omega_A\Delta_t) = \exp(jkv_p\Delta_t)$, where $v_p = \text{phase}(\xi)/k\Delta_t$ is the numerical phase velocity different from the "physical" phase velocity *c* due to the numerical dispersion. The numerical dispersion, i.e. the differences between *c* and v_p are artifacts stemming from the nature of the numerical procedure itself. To avoid aliasing effects for all discretisations the sampling theorem must be fulfilled, i.e.

$$k_x\Delta_x \le \pi, \quad k_z\Delta_z \le \pi, \quad \omega_A\Delta_t = \text{phase}(\xi) \le \pi. \tag{23}$$

For the full Crank Nicolson formulation of the FDTD method using discretised Maxwell equations one obtains the result

$$\xi = \left\{1 - A_x^2 - A_z^2 + j2\sqrt{A_x^2 + A_z^2}\right\} \Big/ \left(1 + A_x^2 + A_z^2\right) \tag{24}$$

where

$$A_x = (c\Delta_t/\Delta_x)\sin(k_x\Delta_x/2), \quad A_z = (c\Delta_t/\Delta_z)\sin(k_z\Delta_z/2). \tag{25}$$

For the ADI-FDTD for each of two simulation-half-steps $\Delta_t/2$ the result

$$\sqrt{\xi_{1,2}} = \left\{1 + j\sqrt{\left(1 + A_{x,z}^2\right)\left(1 + A_{z,x}^2\right) - 1}\right\} \Big/ \left(1 + A_{x,z}^2\right), \tag{26}$$

. For the CNSS-FDTD method one similarly obtains the formula

$$\sqrt{\xi_{1,2}} = \left(2 - A_{x,z}^2 + j2\sqrt{2}A_{x,z}\right) \Big/ \left(2 + A_{x,z}^2\right). \tag{27}$$

The power-flow-density for the full step Δ_t is in all cases unconditionally conserved since either in (24) $|\xi| = 1$, or in (26) and (27) $|\xi| = \left|\sqrt{\xi_1}\right|\left|\sqrt{\xi_2}\right| = 1$, holds. The dispersion characteristics are fully determined by the phase of ξ in the case of full Crank-Nicolson formulation (24)

$$\text{phase}(\xi) = \arctan\frac{2\sqrt{A_x^2 + A_z^2}}{1 - A_x^2 - A_z^2} \tag{28}$$

or by the phase of $\xi = \sqrt{\xi_1}\sqrt{\xi_2}$ using (26) and (27)

$$\text{phase}\left(\sqrt{\xi_1\xi_2}\right) = 2\arctan\sqrt{\left(1 + A_x^2\right)\left(1 + A_z^2\right) - 1}, \quad \text{phase}\left(\sqrt{\xi_1\xi_2}\right) = \arctan\frac{2\sqrt{2}A_x}{2 - A_x^2} + \arctan\frac{2\sqrt{2}A_z}{2 - A_z^2}. \tag{29}$$

For the sake of comparison we show the result for the classical explicit Yee-FDTD. Here one obtains

$$\xi = 1 - 2\left(A_x^2 + A_z^2\right) \pm j\sqrt{1 - \left\{1 - 2\left(A_x^2 + A_z^2\right)\right\}^2} \tag{30}$$

In order to have the stability condition fulfilled the term under the square root must be positive, therefore $\left(A_x^2 + A_z^2\right) < 1$, or

$$c\Delta_t\left\{\frac{\sin^2(k_x\Delta_x/2)}{\Delta_x^2} + \frac{\sin^2(k_z\Delta_z/2)}{\Delta_z^2}\right\} < 1 \tag{31}$$

Since the spatial harmonics due to the sampling theorem (Nyquist limit) can have maximum wave numbers equal to $k_x = 2/\Delta_x$, $k_z = 2/\Delta_z$, i.e. the sine functions in (31) are equal to one and the ultimate CFL-limit

$$c\Delta_t \sqrt{\Delta_x^{-2} + \Delta_z^{-2}} < 1 \tag{32}$$

is obtained. Depending on the actual length of Δ_t the formula (32) defines so-called Courant number that cannot be in case of explicit Yee-FDTD larger than one. For the unconditionally stable methods such as CN-FDTD, ADI-FDTD, or CNSS- FDTD can however reach any values larger than one.

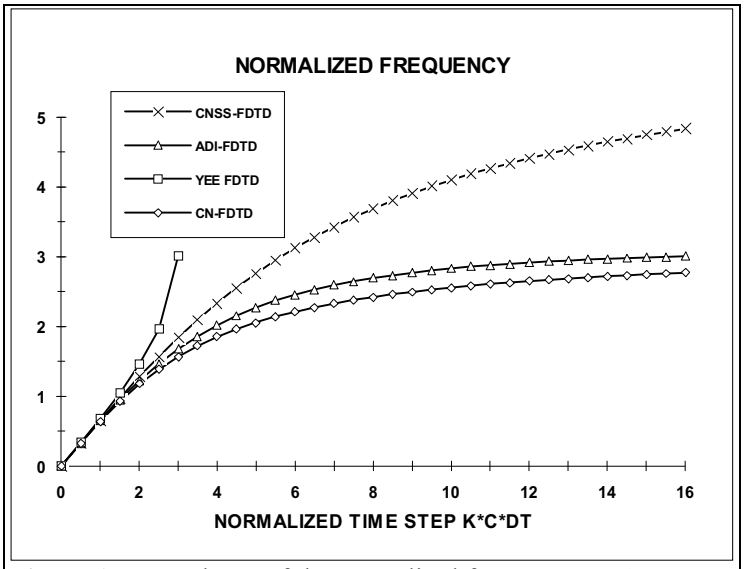


Figure 1. Dependance of the normalised frequency $\omega_A \Delta_t \le \pi$ on the normalised time step $kc\Delta_t$ for $k_x\Delta_x = 3$, $k_z\Delta_z = 3$.

Conclusions

Wave propagation characteristics using the ADI-FDTD and CNSS-FDTD methods are illustrated in Fig.1. For the explicit Yee-FDTD the values can be calculated until the Courant limit is reached. Here the normalized frequency arrives at the Nyquist limit $\omega_A \Delta_t = \pi$. For CN-FDTD and ADI-FDTD it seems that the Nyquist limit $\omega_A \Delta_t = \pi$ is approached asymptotically with increasing Δ_t . Thus, it is inferred that the sampling theorem criteria are fulfilled for any step length for the CN-FDTD and the ADI-FDTD method. As seen from the comparison of curves for CN-FDTD and ADI-FDTD neglecting the second order terms in ADI-FDTD factorization (16) does not cause any substantial error as compared with the "exact" Crank-Nicolson formulation. As it can be easily seen the condition (23), i.e. $\omega_A \Delta_t \le \pi$, is fulfilled for CNSS-FDTD only until the normalized time step value reaches $kc\Delta_t \approx 6$ .This is a substantial not yet published difference between ADI-FDTD and CNSS-FDTD. Moreover, the possibility of the arbitrarily large Δ_t steps in the ADI-FDTD method does not necessarily mean any advantage, since with growing Δ_t the phase velocity $v_p = \text{phase}(\xi)/k\Delta_t$ decreases, i.e. the simulated spatial propagation path pertaining to increased time step remains effectively the same.

Acknowledgment: This work has been supported by the Slovak government grant agency under the VEGA Grant No. 1/1056/04.

References:

[1] K. S. Yee, "Numerical solution of initial boundary value problems involving Maxwell's equations in isotropic media", *IEEE Trans. Antennas & Propagation*, **AP-14**(1966), pp. 302–307.

[2] A. Taflove, S. C. Hagness, Computational Electrodynamics: The Finite-Difference Time-Domain Method, 2nd ed. Boston, MA: Artech, 2000.

[3] F. Zheng, Z. Chen, J. Zhang, "A finite-difference time-domain method without the Courant stability conditions", *IEEE Microwave & Guided Wave Lett.*, **9**(1999), pp. 441–443.

[4] F. Zheng, Z. Chen, J. Zhang, "Toward the Development of a Three-Dimensional Unconditionally Stable Finite-Difference Time-Domain Method", *IEEE Trans. Microwave Theory & Techn.*, **MTT-48**(2000), No. 9, pp. 1550-1558.

[5] J. Lee, B. Fornberg, "A split step approach for the 3-D Maxwell's equations", *J. Comp. Appl. Math.*, **158**(2003), pp. 185-505.

[6] J. Lee, B. Fornberg, "Some unconditionally stable time stepping methods for the 3D Maxwell's equations", *J. Comp. & Appl. Math*., **166**(2004), pp. 497-523.
[7] S. G. Garcia, R. G. Rubio, A. R. Bretones, R. G. Martin, "On the Dispersion Relation of ADI -FDTD, *IEEE Microwave & Wireless Comp. Lett.*, **16**(2006), pp. 354–356.

SIMULATION OF A BIOPLASMATIC CHIRAL MODEL FOR HUMAN HEAD RADIATED BY MICROWAVES BETWEEN 1 TO 100 GHZ

M. ZAMORANO[(1)] AND H. TORRES-SILVA[(2)]

[(1)] Escuela de Electricidad y Electrónica - [(2)] Instituto de Alta Investigación
Universidad de Tarapacá, 18 de Septiembre 2222, Arica, Chile
E-mail: mhzlucero@uta.cl : htorres@uta.cl

Abstract
A bioplasmatic chiral model of the human head, constructed with 540,000 cubic cells in 54 layers derived of MR images, that allows us to simulate and to evaluate the absorption induced by the radiation microwaves wireless systems between 1 to 100 GHz is presented. The procedure to determine the absorption of microwaves waves emitted by wireless systems consisting of the following three main steps: 1) evaluation of the electromagnetic fields distribution inside the biological target, 2) modeling of human head, and 3) SAR simulation by including chirality effects. The simulations were developed by means of the FDTD technique and the specific absorption coefficient (SAR) was determined for a layer with great concentrations of brain tissue (layer 35). The results show the evolution of SAR coefficient, as function of input power and chiral factor.

Keywords: chirality; brain tissue; Maxwell; FDTD; SAR
PACS: 41.20Jb; 02.70.Bf; 52.35; 87.15.Aa

1. Introduction

In recent years, there has been a continuing explosion in the growth of microwave and radio frequency communications, particularly a dramatic acceleration in the use of cellular phones and wireless local area networks (WLANs).This has resulted in public concern about the health hazards of microwave electromagnetic fields emitted by these systems. This growth has raised the research on the effects of microwave interaction with biological tissues. Cellular phones use low-speed data transmission (e.g., voice data) over wide geographical areas, while WLANs and wireless Internet are adopted in services requiring high-speed data transmission over small confined areas (e.g., inside a building). It is important to assess the risk, if any, of the wireless revolution and determine if need exists for the establishment of new regulations for evaluation of the mechanisms of interaction between electromagnetic fields and biological systems. [1]

To transmit data, wireless LAN systems use a directive antenna placed at a mobile personal terminal (computer, telephone, camera, etc.) and a wide beam antenna placed at a fixed site (the base station) usually located on the room ceiling. In this arrangement, the user can find him self in close proximity to the radiating mobile antenna, where the EMF assumes its highest values. As a consequence, it is important to consider the possible health hazard due to such systems. Specifically, the heads of many users are exposed to a sequence of microwave fields modulated in substantially different ways [2]. When the cellular phone is close to the head, background levels are sharply distorted, with 40 to 50 percent of radiated phone energy absorbed in the hand and the head of an user [3]. Its emission at the head surface is typically 10,000 times stronger than fields reaching the head of a user standing within 30 m of the base of a typical mobile phone relay transponder mounted on a tower 30m above ground.

In a technical perspective, the carrier wave remains constant in amplitude throughout the transmission epoch, all data information being transmitted in the frequency domain, where systems generally transmit at 900, 1800 MHz and 2.4 GHz. When the antenna is close to the head, background levels are sharply distorted, with 40 to 50 percent of radiated phone energy absorbed in the hand and the head of a user [4].

In this paper, we propose to use a simple chiro-electrodynamical model, which takes into account the main interaction between the bioplasma of the brain neurons and the microwave radiation of mobile phone or wireless systems. To address the problem and on the basis of our previous experience [2][6], our method consists of the following three main steps: (1) modelling of human head through MRI, (2) evaluation of the EM distribution inside the biological target, considering the brain tissue as chiral bioplasmatic media, and (3) SAR simulation to evaluate the thermal effect. A brief explanation of the theoretical base of the technique used and description of the models are given in section 2. Results comparing the computed SAR values in the different models are shown and discussed in section 3. Finally, conclusions are presented.

2. Electrodynamic point of view.

To characterize the microwave absorption by the brain tissue, radiated by cellular phones, it is assumed that the brain tissue media is chiral. This chiral effect is due to a microscopic mechanism where the typical cell membrane of brain is a fluid bilipid layer with a lot big chiral protein molecules embedded in it. Every protein molecule is polar and will tend to align itself with an electric field and often helical rotate in its socket, so any volume of brain tissue must have a lot of cells bearing protein molecules that happen to resonate at its rotation frequency.

Studies on DNA have shown that large electron flows are possible with the stacked base pairs of the double helix and a collective interaction of large ionic ensembles where the electromagnetic field is assumed in aqueous solutions of amino acids. Also when the twisted DNA molecule is a right-handed helix is transcribed into RNA, the DNA molecule can be unwound. And it is possible that signaling inside neurons can have two twists. Here, we propose the hypothesis that all these features can be explained in a unified manner, namely the chiral-electrodynamics model, where the bioplasma is divided into two very thin layers separated by a permeable membrane, having cylindrical microtubules or helical structures. The dimmers α and β can exist in two different geometric configurations which correspond to the electric polarization states of dimmers, whose helicoidal structure can be right (R) or left (L). Then, since the protein medium is chiral, an electromagnetic wave in this medium necessarily will rotate its polarization plane in accordance with the dominant biological structure. Preliminary calculus show that the medium frequencies are between 10 and 20 GHz (microwave radiation). The eigenfrequencies, for typical proteins become between 10 GHz -12 GHz and for cluster DNA molecules the interval is between 1 GHz to 12 GHz. These frequencies are typical for microwave radiation. Accordingly with the above discussion, we consider the brain tissue as a chiral bioplasma immersed in a low magnetic field, characterized by a global chirality factor, T, so the Born-Fedorov constitutive equations are

$$\boldsymbol{D} = \varepsilon\left(\boldsymbol{E} + T\nabla\times\boldsymbol{E}\right),...\boldsymbol{B} = \mu\left(\boldsymbol{H} + T\nabla\times\boldsymbol{H}\right) \tag{1}$$

where ε, μ and T are the permittivity, the permeability and the chiral scalar, respectively. Solving Maxwell`s equations for a plane electromagnetic wave of frequency ω ($\omega = k_t v = 2\pi f$, k_t is the tissue wave number and v is the phase velocity) propagating in a chiral medium, it can be shown that the left- and right-hand circularly polarized waves have different wave numbers, $k = k_t/(1+k_t T)$ and $k = k_t/(1-k_t T)$, respectively. The chiral parameter T has the dimension of a length. Here, the rotor of polarization plane can be predicted from Maxwell´s equations, considering that the $\boldsymbol{P}$ or $\boldsymbol{M}$ vector has a proportional additional term to rotor $\boldsymbol{E}$ or rotor $\boldsymbol{H}$, respectively. If it is assumed that the medium is isotropic, non-permeable and non-dispersive, the Cartesian field components are [7]

$$D_{x,y,z} = \varepsilon_0\varepsilon_r E_{x,y,z} + \varepsilon_0\varepsilon_r T\left[\frac{\partial E_{z,x,y}}{\partial y,z,x} - \frac{\partial E_{y,z,x}}{\partial z,x,y}\right],..B_{x,y,z} = \mu_0 H_{x,y,z} + \mu_0 T\left[\frac{\partial H_{z,x,y}}{\partial y,z,x} - \frac{\partial H_{y,z,x}}{\partial z,x,y}\right] \tag{2}$$

Using the MKS system of units, the following system of scalar equations is the set of Maxwell's equations in the rectangular coordinate system (x, y, z)

$$\frac{\partial H_{x,y}}{\partial t} = \mp\frac{1}{\mu}\frac{\partial E_z}{\partial y,x} \pm T\frac{\partial^2 H_z}{\partial y,x\partial t},..\frac{\partial H_z}{\partial t} = \frac{1}{\mu}\left(\frac{\partial E_x}{\partial y} - \frac{\partial E_y}{\partial x}\right) + T\left(\frac{\partial^2 H_y}{\partial x\partial t} - \frac{\partial^2 H_x}{\partial y\partial t}\right) \tag{3}$$

$$\frac{\partial E_{x,y}}{\partial t} = \pm\frac{1}{\varepsilon}\frac{\partial H_z}{\partial y,x} \pm T\frac{\partial^2 E_z}{\partial y,x\partial t} - \sigma E_{x,y},..\frac{\partial E_z}{\partial t} = \frac{1}{\varepsilon}\left(\frac{\partial H_y}{\partial x} - \frac{\partial H_x}{\partial y}\right) + T\left(\frac{\partial^2 E_y}{\partial x\partial t} - \frac{\partial^2 E_x}{\partial y\partial t}\right) - \sigma E_z \tag{4}$$

where σ (S m^{-1}) is the tissue electrical conductivity. After calculation of the induced chiral electric field by the FDTD method, the local specific absorption rate SAR is obtained as

$$SAR_{i,j}(T) = \frac{\sigma_{i,j}\left.E_T^2\right|_{i,j}}{2\rho_{i,j}} \tag{5}$$

where

$$\left.E_T\right|_{i,j}(T) = \sqrt{\frac{1}{n}\sum_1^n\left(\left.E_y^2\right|_{i,j}^n + \left.E_x^2\right|_{i,j}^n + \left.E_z^2\right|_{i,j}^n\right)} \tag{6}$$

In these equations, the electric (magnetic) fields depend not only on $\boldsymbol{E}$ (resp. $\boldsymbol{H}$) but also on the transverse components.

3. SAR simulation and analysis of results

For the numerical calculation, the chiral factor is normalized as *kT*, where *k* is the wave number in the tissue layer, in some cases it may be $k_t = nk_0$ ($k_0 = \omega / c$ is the vacuum wave number), with *n* = 1, 2, 3…, taking into account the multiphoton absorption when the resonance absorption at macromolecular level becomes important. For the brain, we considered $k = k_b /(1 - k_b T)$ because the clusters of DNA molecules have eigenwaves representing right-hand circularly polarized waves and for the rest of the tissues we considered $kT = k_t T = 0$. Calculation stages of the bioplasmatic model for SAR determination are shown in figure 1. Using the linear FDTD algorithm with chirality, obtained from equations (3)-(6), simulations for microwave spectrum are made. The model of human head was constructed with 540000 cubic cells of 2.5 mm side each. The total number of layers, counted from the bottom of head, used in this model was 54. Here we choose layer 35, because it has a large concentrations of brain tissue. Figure 2 shows these layers in digitalized version (matrix of 100 × 100), likewise is exhibited the antenna position. Both, the dielectric constant and the conductivity of the brain were obtained from literature. In order to study and isolate the chiral effect, calculations are made for plane wave assumption, powers of 1.25, 12.5 and 125 mW were used, at frequencies of 0.9, 1.8. 2.4, 5.2, 5.8, 30, 60 and 100 GHz, respectively, having the cellular phone antenna an impedance of 180 Ω. Four types of tissues (skin, bone, blood and brain) are considered. Simulations were made in a systematic way, in order to determine the effect that the variation of the chiral coefficient had over the absorption of coefficient SAR, and results, for layer 35, are shown in figures 3-9. Owing to the different electromagnetic properties of the tissues, the power absorption is not a monotonically decreasing function of depth. For $kT = 0$, absorption is highest in the skin, low in the skull, but higher again in the brain. These curves were obtained performing similar simulations and then obtaining a statistical average of the SAR. In all curves, as the wave penetrates the head, it traverses the different parts of which the head model is made and the value of the SAR is attenuated quickly due to the change in medium and the increase of the distance from the emitting source (antenna). It is important to say that the SAR maximum (hot point) is in the outer part (skin). After passing through the bone level, the SAR is much attenuated (between cells 5 and 10) and around cell 10 the SAR increases at brain level. Here, starting from cell 10 approximately it is important to analyze the performance of our bioplasmatic model.

The profile of the SAR for 35th layer, at 0.9 GHz as function of distance for different values of chiral factor *kT*, is shown in figure 3, where the variation is observed for values of chiral factor $0 < kT \leq 3$. A SAR of 0.032 W kg^{-1}, is observed in the brain region, for a null chiral factor ($kT = 0$). For $kT = 1$, the SAR found was 0.036 W kg^{-1}, an increase of 12.5% with respect to the achiral case ($kT = 0$), and a SAR of 0.043 W kg^{-1} was found for $kT = 3$, with an increase 34%. This increase corresponds to the power absorbed by the head. Figure 4 shows the distribution of the SAR for 35th layer, as a function of distance, for different values of the chiral factor when the work frequency is 1.8 GHz. The maximum SAR found, in the blood-brain region, was 0.08 W kg^{-1} for to $kT = 0$ and 0.116 W kg^{-1} for $kT = 1$, i.e. an increase of 45% with respect to the achiral case. For a high value of chiral factor, $kT = 3$, the maximum SAR found was 0.12 W kg^{-1} with an increase of 50%. Again, this increase corresponds to the power absorbed by the head. Figure 5 shows the distribution of the SAR for 35th layer, as a function of distance, for different values of the chiral factor when the work frequency is 2.4 GHz. The maximum SAR found, in the blood-brain region, was 0.09 W kg^{-1} for to kT = 0 and 0.13 W kg^{-1} for $kT = 1$, i.e. an increase of 44% with respect to the achiral case. For a high value of chiral factor, $kT = 3$, the maximum SAR found was 0.16 W kg^{-1} with an increase of 77%.

Figures 6-8 show the distribution of the SAR, for 35th layer as a function of distance, for different values of the chiral factor, when the work frequency is 30, 60 and 100 GHz. The SAR found in the blood-brain region increase when the power get higher also for chiral factor 0, 1, and 2, the SAR is barely increase, for each power simulated. Figure 9 show the distribution of the SAR maximums in the blood-brain region, as a function of frequency, for different powers and chiral factors as summary of all the simulations made it. The consequence of being at such frequency is the fact that the human tissue (especially brain tissue) absorptivity of microwave radiation increase with frequency in this spectrum region. Theses must be verified by using more advanced models. The results of figure 9 are similar to those of Curry [8].

4. Conclusions

A bioplasmatic chiral model of the human head has been presented that allows determination and evaluation of the absorption induced by the radiation of cellular phone and wireless systems. Electromagnetic fields radiated were determined firstly by means of the FDTD technique and then the specific absorption coefficient (SAR). It is shown that the use of a cell model, combined with a real model of the human head, derived from the magnetic resonance of images allows exact determination of the near fields induced in the head when the brain chirality is considered. The simulations are made for the 35th layer. The results also show the evolution of the specific

absorption rate, (SAR coefficient), as function of input power and chiral factor. The more importants conclusion of our work are: 1) with the chiral electrodynamics model the head absorption of microwave fields, produced by cellular phones and wireless systems, is bigger that the results obtained for classical models, and 2) the absorption of microwave radiation increase with frequency.

Acknowledgments
The authors thank the University of Tarapacá Project Nº 8721-06 and 8722-06. Also, we greatly appreciate the help received from M. Sc. Enrique Fuentes H.

References

[1] Lang S., "Recents advances in Bioelectromagnetics Research on Mobile Telephony and Health" *Progress in Electromagnetics Research Symposium*, Cambridge, USA, March, 29-29, 2006.
[2] Torres-Silva H. et al. "Los campos electromagnéticos en la telefonía celular, su interacción con el sustrato neuronal". *Revista Facultad de Ingeniería* UTA, Vol. 9, pp. 3-19, 2001.
[3] Torres-Silva H. and Zamorano M. "Chiral Effect on Optical Soliton". *The Journal Mathematics and Computers in Simulation*, Vol. 62, pp. 149-161, 2003.
[4] Torres-Silva H. and Zamorano M. "SAR Simulation for Chiral Waves in Head Model". *Revista Facultad de Ingeniería* UTA, Vol. 11, pp. 3-11, 2003.
[5] Zamorano M. and Torres-Silva H. "Ecuación de Schrödinger para una Fibra Óptica Quiral". *Revista Mexicana de Física*, 46(1), pp. 62-66, 2000.
[6] Zamorano M. and Torres-Silva H. "Efecto de la Quiralidad sobre Solitones Polarizados en un Medio Anisotrópico". *Revista Mexicana de Física*, Vol. 49(1), pp. 20-27, 2003.
[7] Taflove A and Hagness SC, Ed. C*omputational Electrodynamics: The Finite-Difference Time Domain Method*, Artech House, pp. 35-171., 2000.
[8] Curry B. Ph.D. Consulting Physicist; http://www.emrnetwork.org/schools/curry_broward.pdf

FIGURES CAPTION

Fig. 1 Stages of the bioplasmatic model for SAR determination.
Fig. 2 The structure of layer 35.
Fig. 3 SAR variation, as function of the transverse distance, for $0 < kT \leq 3$ at 900 MHz. Layer 35.
Fig. 4 SAR variation, as function of the transverse distance, for $0 < kT \leq 3$ at 1800 MHz. Layer 35.
Fig. 5 SAR variation, as function of the transverse distance, for $0 < kT \leq 3$ at 2400 MHz. Layer 35.
Fig. 6 SAR variation, as function of the transverse distance, for $0 < kT \leq 2$ at 30 GHz. Layer 35.
Fig. 7 SAR variation, as function of the transverse distance, for $0 < kT \leq 2$ at 60 GHz. Layer 35.
Fig. 8 SAR variation, as function of the transverse distance, for $0 < kT \leq 2$ at 100 GHz. Layer 35
Fig. 9 SARmax variation in the blood-brain region, as function of frequency for $0 < kT \leq 2$ and different power. Layer 35.

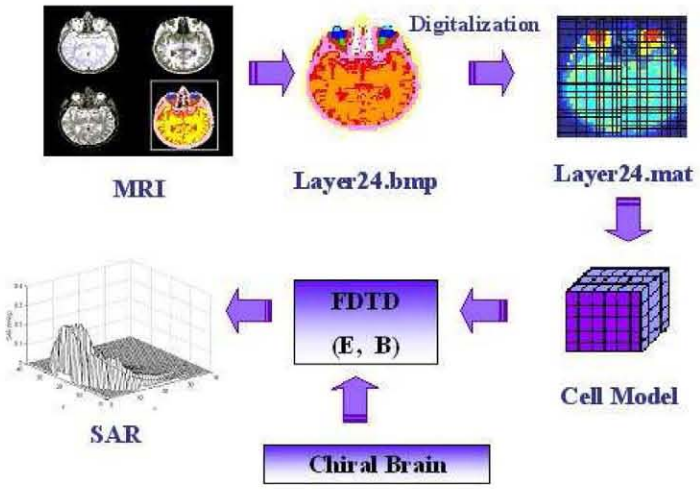


Figure 1

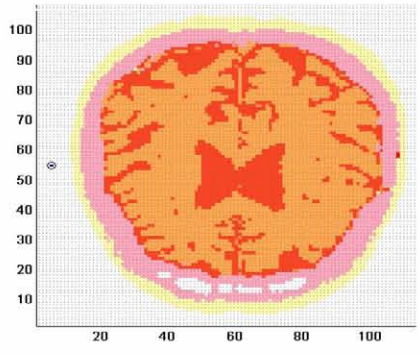


Figure 2

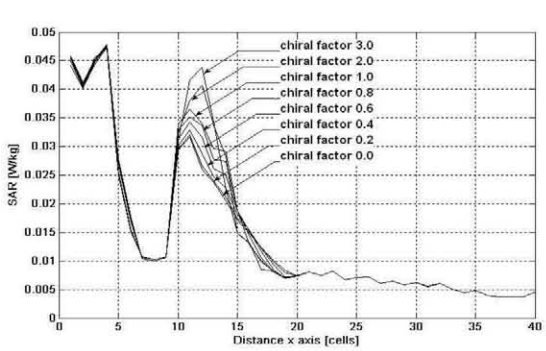


Figure 3

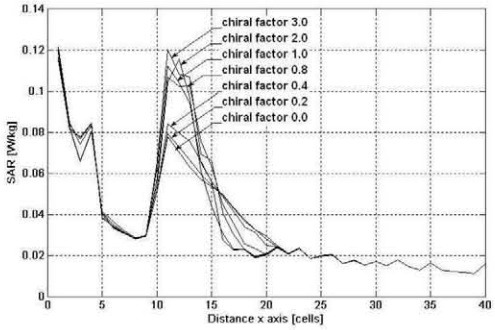


Figure 4

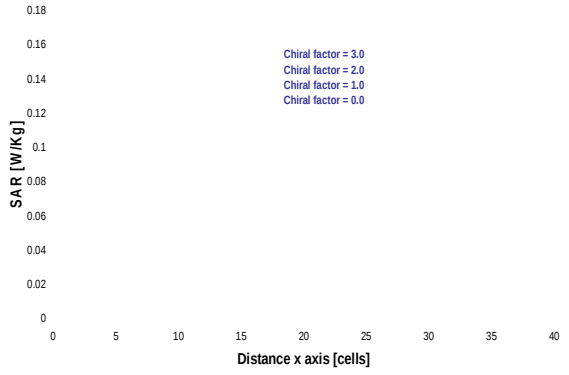


Figure 5

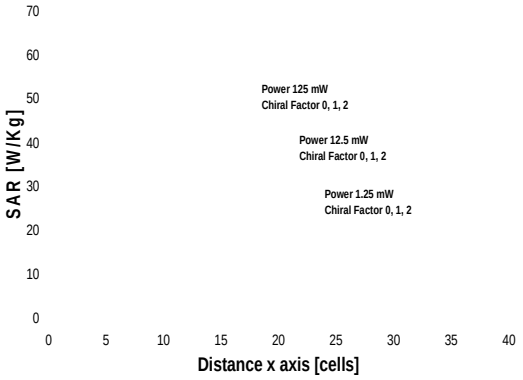


Figure 6

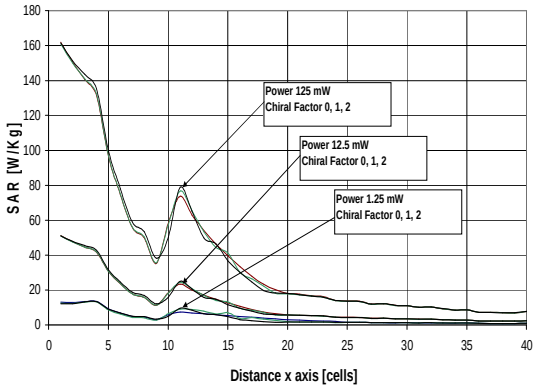


Figure 7

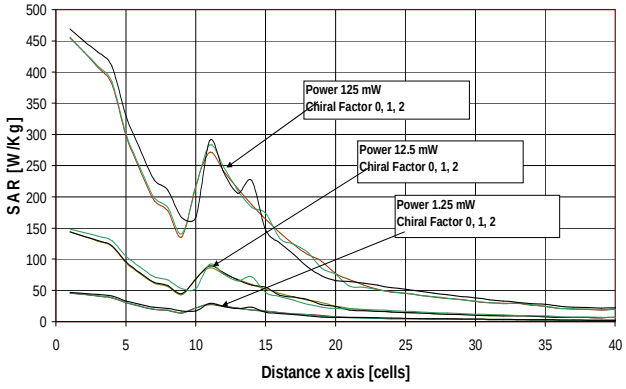


Figure 8

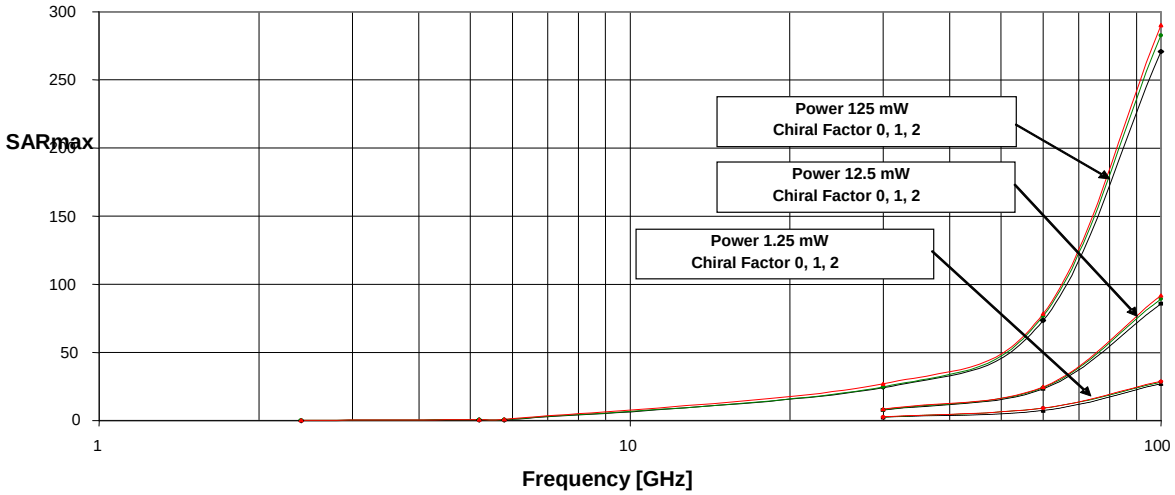


Figure 9

ELECTROMAGNETIC FIELD LEVELS IN THE WORKING ENVIRONMENT IN RADIO AND TV STATIONS. PROGRAM FOR HEALTH PROMOTION

Ivanova, M., V. Zaryabova, Ts. Shalamanova, M. Israel

National Center of Public Health Protection, Sofia, Bulgaria

Abstract

Electromagnetic field sources used for communication always are subject of serious interest. There are many publications concerning exposure and risk assessment of the working in such environment. Results of epidemiological study performed in Bulgaria in 90s (Varna, Proceedings 2001) show exceeding of the maximal permissible values especially in radio stations for the personnel in 24 h working shift.

In the last years the situation is strongly influenced by the development of the technology which leads to changes in equipment in radio and TV stations, using lower power, facilitate the working regime.

Paper presents data of exposure assessment of different professional groups in selected radio and TV stations. Assessment is being performed on basis of EMF parameters values and energetic load calculations according to the national legislation. Data are compared with the results of previous investigation to evaluate the new situation in this branch. Exposure levels are much lower than those in the last study, and lower compared to the exposure limits, as well.

INTRODUCTION

The policy of the World Health Organization (WHO) after its establishment incorporates occupational health issues. Numerous important WHO documents, such as the Constitution, Alma Ata Declaration, "Health for All" Strategy, working programs and certain resolutions of the World Health Assembly underline the necessity to protect and strengthen health and safety at work through prevention and control of workplace hazardous factors and promotion of workers' health and work ability.

The transition during the past two decades experienced by European socioeconomic communities contributed to accelerated changes in labor conditions and market. Many European countries show a tendency to re-orienting the occupational health and safety policy towards improved workers' work ability and significant reduction of increasing social costs for work-related health disorders, injuries and disability.

The new global strategy of the EU Commission and International Labor Organization (ILO) is fully focused on improving the activities on health and safety at work (HSW) at enterprise and national level. The developed systems for HSW control are a successful approach to fulfillment of the responsibilities and gaining maximal benefits through their incorporation in company and national policy, moreover, these systems are implemented in many countries, including a number of Bulgarian companies. They are built on the belief that good work management and reduction of workplace risk are based on self-control, self-assessment and adequate measures for improved safety. Such management is much more effective and with better results than just observing the regulations, moreover, ILO methodological guidelines for systems for control of health and safety at work are not mandatory. They are recommendations to the employer on achievement of better prevention level; reduction of risk for work accidents and occupational diseases and following costs and company losses; reduction of occupational risk and hence – improvement of the company image; improved work quality leading to elevated company competence; last, but not least – functional social dialogue.

The employer has to present his HSW policy as a written program, after consultations with the employees and their representatives.

A very interesting professional group exposed to high levels EMF is those of operators working in radio and TV stations. Electromagnetic field sources used for communication always are subject of serious interest. A wide-spread set of communication systems exists in each country and its types and number is ever increasing.

An epidemiological study carried out in Bulgaria in 90 [5] showed exposure to the personnel of such stations above the permissible levels accepted in the country, especially in the cases of 24-hour working shifts. The results showed that the long-term service of emitting systems results in serious health problems for operating staff, charged with broadcasting.

The present study is a continuation of the previous epidemiological study [5] and one of its goals is to assess how the development of the technology which leads to changes in equipment in radio and TV stations, using lower power, facilitation of the working regime affects the exposure of the operators. The investigation

covers a part of previously studied stations, which gives an opportunity for direct comparison of the results for the personnel's' exposure.

MATERIAL AND METHODS

Objects of study

This study was performed on radio broadcasting system of short waves (SW), television (TV), and on satellite systems. The study covers the following stations:

- ***Radio broadcasting*** station on short waves (SW) - from 6 to 25 MHz;
- ***TV station 1 with sources emitting EMF with frequencies from*** 66 MHz (UHF) to microwaves up to 6 GHz;
- ***TV station 2 with sources emitting EMF with frequencies*** 101 MHz (UHF) to microwaves up to 6 GHz;
- ***TV station 3 with sources emitting EMF with frequencies*** UHF и microwaves;
- ***Satellite station*** – frequencies from 5 GHz to 7 GHz.

We found 5 types of work shifts - A, B, C, D и G as follows:

- A – 5 days a week, 8 h per day – ordinary shift. The rest of the time the personnel is outside the station;
- B – one twenty-four hour period (24 h) in the working environment being followed three subsequent twenty-four hour periods of rest at home;
- C – four subsequent twenty-four hour periods in working environment being followed by three subsequent twenty-four hour periods of rest at home; During its stay in the station the personnel is 10 hours on shift (active working) and 14 h on disposal;
- D –7 days in the working environment followed by 14 days outside (rest at home). During its stay in the station the personnel 5 days is 12 hours on shift (active working) and 12 h on disposal and the other two days are resting in the station;
- G – two subsequent twenty-four hour periods in working environment being followed by two subsequent twenty-four hour periods of rest at home.

The following jobs were characterized: radio engineer, engineer (both with master degrees), mechanic, technician, fitter, sound-technician, radio technician, power engineer, electric fitter, electrician, electric technician, mast operator. Every station depending on its type, equipment, geographical position, etc. has different professionals. Here, we present the results for the next groups: operator on duty, chief of station, power engineer.

Additionally results for a group "other staff" being not directly engaged in the transmitters' service is presented. It includes: cleaners (other assistant jobs) and canteen managers.

Measurement equipment

The measurements of the EMF exposures were made using the following equipment:

N F M - 1 (made in Germany):

- measuring values: E = 2 to 40 kV/m for f = 50 Hz
  E = 2 to 1500 V/m for f = 0.06-350 MHz
  H = 0.1 to 10 A/m for f = 0.06-10 MHz
- uncertainty: $\sigma = \pm 20$ %;
- probes - dipole and frame.

RAHAM 495, model 40, "General Microwave Corporation"(USA).

- Frequency range: 200 kHz - 40 GHz;
- Measurement ranges – 0.02, 0.2, 2 and 20 mW/cm^2;
- Uncertainty ± 20 %;
- Minimal measured value – 0.5 μW/cm^2
- Probe – isotropic.

The devices measure the EMF values in a wide frequency range so specific methods for exposure assessment are used.

Measurement procedure

The measurements were made for typical permanent and temporary work places:

In closed premises: transmission's halls, in front of the transmitters, central desks and central control desks, central control rooms, in front of the final cascades of multipliers, near the antenna control boards, etc. All measurements were made on three levels above the ground (floor) - on the levels of head, chest and genitals of the operator, and the hygienic assessment was formed according to the maximum measured value.

On the antennae's field area we measured the field strength both under the feeder lines (feeders) at the same three levels, and along the roots of the antennas, at different depending on the area. In case of TV towers measurements were made on some of the platforms with antennae as well.

In living rooms only the maximum values of EMF measured have been taken for hygienic assessment.

All measurements were made while the transmitters worked at maximum power of radiation.

On the time of measurements the serving operators stayed on minimal distance of 5 to 10 meters behind the measurer.

The hygienic assessment of the measured values of EMF in the living rooms was made according to Ordinance No:9 for exposure to the general population (Table 3) as the personnel staying in this rooms should not be considered as performing its work tasks. The measured values of EMF in living rooms were added to the common assessment for the energetic loading of the organisms of the workers for 24 hours.

Table 3. Maximum permissible levels (MPL) according to the Bulgarian standards

STANDARD	**FREQUENCY RANGE**	$\mathbf{E_{max}}$, V/m	$\mathbf{H_{max}}$, A/m	$\mathbf{S_{max}}$, μW/cm²	$\mathbf{W_E}=E^2.T$, $(V/m)^2.h$	$\mathbf{W_H}=H^2.T$, $(A/m)^2.h$	$\mathbf{W_S}=S.T$, μW.h/cm
BNS 14525-90	60kHz - 3MHz	500	50	-	20000	200	-
	3MHz - 30MHz	200	50	-	3200	200	-
	30MHz-300MHz	60	-	-	800	-	-
BNS 17137-90	300MHz -300GHz	-	-	1000	-	-	200
Ordinance No.9 - 1991	3MHz - 30MHz	10	-	-	-	-	-
	30MHz-300 MHz	3	-	-	-	-	-
	300MHz – 30GHz	-	-	10	-	-	-

Parameters for exposure assessment

For exposure assessment the following parameters were used:

- *energetic loading of organism*:

$$W_E = \sum_i E_i^2.t_i \text{ , V}^2\text{.h/m}^2; \qquad W_S = \sum_i S_{,i}.t_i \text{ , μW.h/cm}^2;$$

Energetic loading of the organism was calculated for the average and maximal measured values on “i” measurement point (place of stay or premise) respectively for electric field strength (V/m) and power density (μW/cm^2), depending on the frequency of emitted EMF;

- *Time weighted average (TWA) values* of electric field strength and power density, TWA:

$$TWA = \frac{\sum_i E_i.t_i}{T} \text{ , V/m} \qquad TWA = \frac{\sum_i S_i.t_i}{T} \text{ , μW/cm}^2$$

where E_i and S_i are the measured values on the “i” workplace; t_i is the time duration of exposure on the same place, i = 1,...n; $T = \sum_{i=1}^{n} t_i$.

For the described stations TWA of electric field strength and power density are calculated for the average and maximal measured value of EMF on the corresponding places of stay of the personnel. Calculations for two averaging periods were made:

- for one working day – 8h, 10 h, 12 h and 24 h corresponding to the work shift duration and work cycle. Here, the real working time, time on disposal, time of rest in the station, time of rest outside the station were taken into account.
- For 120 h (5 twenty-four hour periods – one working week), taking into account the shift type (A, B, C, D и G).

Energetic loading of the organism is considered for zero for the stay outside the station.

Calculated TWA values for SW range (V/m) are presented in units μW/cm^2 “equivalent power density” for plane wave.

The real time of exposure was determined in the following ways:

- "script or scenario" method - an expert method, based on repeated measurements and for long findings of the working process. It was applied for the three groups of personnel (those, working for 24 h in a shift, others working for 8 h - normal shift, and for the "other" workers) at all studied sites, namely radio stations, TV stations and radio relay stations.

- calculating the maximum permissible time duration. The requirements of the Bulgarian National Standards (BNS) were used when determining the limits of the energetic loading of the organism. Maximum permissible time duration of every working place was calculated according to the average values of EMF by using the formulae:

$$T_{\max} = \frac{W_E}{E^2}, \qquad T_{\max} = \frac{W_S}{S}$$

where W_E , W_H and W_S are values of the energetic loading of organism for corresponding frequency range according to national legislation (Table 3).

RESULTS AND DISCUSSION

Measured EMF values in relative units compared to the limits for corresponding frequency range are presented in Table No.4.

Table No.4.

Station	Average values	Maximal values
Radio station		
transmission's halls	0.02	0.09
antennae field	0,15	0.95
TV station 1		
transmission's halls	0.003	0.05
antennae field	0.20	0.06
TV station 2		
transmission's halls	0.0075	0.0196
antennae field	0.38	0.085
TV station 3		
transmission's halls	0.0045	0.00305
antennae field	0.002	0.00175
Satelite station		
transmission's halls	0.004	0.0163
antennae field	-	

Calculated TWA values are presented in Table No.5.

Table No.5

Professional groups	Radio station		TV station 1		TV station 2		TV station 3		Satelite station	
	$TWA_{avg.}$ $\mu W/cm^2$	TWA_{max} $\mu W/cm^2$	$TWA_{avg.}$ $\mu W/cm^2$	TWA_{max} $\mu W/cm^2$	$TWA_{avg.}$ $\mu W/cm^2$	TWA_{max} $\mu W/cm^2$	$TWA_{avg.}$ $\mu W/cm^2$	TWA_{max} $\mu W/cm^2$	$TWA_{avg.}$ $\mu W/cm^2$	TWA_{max} $\mu W/cm^2$

For one working shift										
Operator on duty	3.10 (B)	137.0 (B)	1.89 (B)	5.24 (B)	1.49 (D)	3.63 (D)	1.19 (G)	1.28 (G)	1.60 (B)	3.57 (B)
Chief of station	3.96	66.90	2.56 (C)	15.41 (C)	0.96 (C)	2.38 (C)	1.57 (A)	2.22 (A)	1.88 (B)	3.67 (B)
Power engineer	0.74 (B)	6.19 (B)	1.69 (B)	4.89 (B)	-	-	-	-	1.43 (B)	3.22 (B)
Worker/ cleaner	2.40 (A)	26.56 (A)	2.12 (A)	17.22 (A)	1.03 (D)	2.18 (D)	0.96 (A)	1.2 (A)	1.83 (A)	3.65 (A)
Canteen manager	0.34 (A)	0.99 (A)	0.80 (A)	1.44 (A)	0.64 (C)	1.40 (C)	0.82 (A)	0.91 (A)	0.79 (A)	1.28 (A)
For 1 working week – 120 h										
Operator on duty	0.30 (B)	1.40 (B)	0.76 (B)	2.09 (B)	0.42 (D)	1.01 (D)	0.52 (G)	0.57 (G)	0.69 (B)	1.51 (B)
Chief of station	0.44 (B)	7.42 (B)	1.03 (C)	6.16 (C)	0.77 (C)	1.81 (C)	0.52 (A)	0.74 (A)	0.75 (B)	1.53 (B)
Power engineer	0.15 (B)	1.53 (B)	0.56 (B)	1.40 (B)	-	-	-	-	0.66 (B)	1.44 (B)
Worker cleaner	0.27 (A)	2.94 (A)	0.71 (A)	5.74 (A)	0.31 (D)	0.66 (D)	0.34 (A)	0.43 (A)	0.61 (A)	1.22 (A)
Canteen manager	0.04 (A)	0.11 (A)	0.27 (A)	0.48 (A)	0.12 (C)	0.26 (C)	0.27 (A)	0.30 (A)	0.26 (A)	0.43 (A)

Calculated values of the energetic loading of organism are presented in Table No. 6

Table No.6

Professional groups	Radio station		TV station 1		TV station 2		TV station 3		Satelite station	
	$W_{avg.}$ $(V/m)^2.h$	W_{max} $(V/m)^2.h$	$W_{avg.}$ $\mu W.h/cm^2$	W_{max} $\mu W.h/cm^2$	$W_{avg.}$ $\mu W.h/cm^2$	W_{max} $\mu W.h/cm^2$	$W_{avg.}$ $\mu W.h/cm^2$	W_{max} $\mu W.h/cm^2$	$W_{avg.}$ $\mu W.h/cm^2$	W_{max} $\mu W.h/cm^2$
For one working shift										
Operator on duty	342.79 (B)	1644.00 (B)	45.30 (B)	125.75 (B)	35.86 (D)	87.20 (D)	14.27 (G)	15.38 (G)	19.25 (B)	42.88 (B)
Chief of station	332.73 (A)	10336.0 (A)	61.98 (C)	369.75 (C)	23.12 (C)	57.38 (C)	12.53 (A)	17.75 (A)	22.61 (B)	44.00 (B)
Power engineer	121.79 (B)	1610.0 (B)	19.69 (B)	58.75 (B)	-	-	-	-	17.21 (B)	38.75 (B)
Worker/ cleaner	83.68 (A)	1312.00 (A)	16.96 (A)	137.75 (A)	24.73 (D)	52.20 (D)	8.18 (A)	10.25 (A)	14.65 (A)	29.25 (A)
Canteen manager	13.03 (A)	32.0 (A)	6.43 (A)	11.50 (A)	15.43 (C)	33.70 (C)	6.56 (A)	7.25 (A)	6.32 (A)	10.25 (A)
For 1 working week – 120 h										
Operator on duty	738.26 (B)	3392.0 (B)	90.60 (B)	251.50 (B)	49.83 (D)	120.95 (D)	61.94 (G)	68.63 (G)	83.40 (B)	181.76 (B)
Chief of station	1663.65 (B)	51680 (B)	180.80 (C)	1287.00 (C)	92.48 (C)	229.52 (C)	62.63 (A)	88.75 (A)	89.92 (B)	184.00 (B)
Power engineer	243.58	3220.0	67.50 (B)	167.50 (B)	-	-	-	-	79.12 (B)	173.50 (B)
Worker cleaner	418.40 (A)	6560.00 (A)	84.80 (A)	688.75 (A)	36.58 (D)	79.28 (D)	40.90 (A)	51.25 (A)	73.25 (A)	146.25 (A)
Canteen manager	65.15 (A)	160.0 (A)	32.15 (A)	57.50 (A)	14.69 (C)	32.09 (C)	32.80 (A)	36.25 (A)	31.60 (A)	51.25 (A)

*The types of shifts are mentioned in brackets

The investigation showed the highest exposure for the personnel in radio station.

The highest values of EMF for every station are measured near the final cascades of the amplifiers, when setting up or repairs are carried out, in the antenna's field (around the irradiating antenna), near the feeders or antenna control board. For these places maximal permissible time of stay was calculated. By professional groups the highest energetic loading of the organism values were found for the professional groups which tasks require prolonged work in antennae field and comutator premises, namely operator on duty and chief of station.

The average values of the energetic loading of the organism in relative units compared to the limit values are between 0.003 и 0.31 depending on the professional group and the working shift type. The calculation for the maximal values (worst case) gives ratio of 3.23 for the SW radio station. In the previous study 3,58 times

exceeding of the energetic loading limit value was established for the 24 h shifts for SW transmitters and up to 0,7 of the limit value for the 24 h shift in the TV stations.

The previous study had shown exceeding of the energetic loading values for 28.1% and 43 % of the working places in the SW stations for 8 h and 24 h shift respectively, exceeding of EMF values was found in 14,3 % of working places in TV stations.

In the present study the exceeding of the maximal permissible values was found only for single cases in antennae field.

There were not measured EMF values above the limits for the general public in the living rooms in stations. Previously, in 67,4% of the studied living rooms EMF values exceeded the limits for the general public.

On the basis of conducted study and estimated exposure to the personnel we propose a risk communication and management program following requirements of WHO and the Precautionary Principle.

Activities concerning risk communication

An acting, addressed towards workers in EMF conditions program demands adhering to WHO requirements for informing the workers, training and limiting the risk to minimal levels. The effectiveness of the program is specified as from the permanent analysis of the taken measures as from the traceability of the actions and from the back link with the management and the group developed the program furthermore.

In this case we recommend outlining the following main actions:

1. Towards EMF levels:
   - adhering to the maximal permissible levels in the current hygienic standards.
   - observing the permissible time duration of stay in sites, where the electric field strength and/or power density exceed the maximal permissible level for corresponding frequency;
2. Control (dosemeters, measurements etc.,)
   - regular check of EMF values, considering different powers or changes in the equipment.
   - each station should be equipped with at least one control measuring instrument (dosemeter), especially for performing tasks in antenna field;
3. Prophylaxis (technical, medical)
   - Periodical control of the technical equipment;
   - periodical check up of the health status of the staff including specialized surveillance: cardiovascular, nervous system, analysers, blood cells, germinative functions.
4. Collective and personal means for protection:
   - use and control of the protection measures and equipment
5. Compensations (nutrition, vitamines, etc.)

In cases when other prophylaxis is impossible or insufficient compensations could be applied. This approach is very extreme, and is applied only when all other possibilities are spent.

6. Training

There is necessity for topical courses on the main activities. The staff is well qualified concerning labour safety. The idea is to widen the training in the field of their specialities, work conditions, and the influence of the factors in the working environment.

7. Living conditions; resting rooms

It is clear that this is very important issue, and takes a special place in the risk communication and management. It ensures special attitude in workers.

8. Precautions (labels and fences, briefings, informational sheets and newsletters)

It is necessary precautionary labels, signs and fences (with bright and reflection colours), briefings, informational sheets and newsletters to be developed, and placed on appropriate places to show areas for stay and crossing, to warn for a possible accidents. Boards indicating the limited stay in the antenna field to be placed.

The materials prepared by the management concerning information about the communication program both for activities and results of the control, prophylaxis measures, preventive actions for health protection of the workers, news about the company organization, cases of accidents, etc., should be distributed on appropriate areas (working places, restrooms, dining rooms) aiming to inform the whole personnel.

Special attention should be paid to pregnant women and persons wearing active implants.

Mechanisms for back link

This part is fundamental for realizing the program. This could be performed by the management through an Occupational Health Service, Labour Committee, and Human Resources Department.

CONCLUSIONS

The comparison of results of the two considered studies shows decreasing of EMF exposure to the specific group of operators working in radio and TV stations. This result could be associated with the development of the technology which leads to changes in equipment in radio and TV stations, using lower power, using better shielding in the control rooms, facilitating the working regime.

REFERENCES

1. BNS 14525-90 Labour protection. Electromagnetic fields - Radiofrequency range. Permissible Exposure Levels and Requirements for Safety
2. BNS 17137-90. Labour protection. Electromagnetic fields - Microwaves. Permissible Exposure Levels and Requirements for Safety.
3. Dobrev B., D. Dimitrov, M. Israel, G. Dimitrov. Hygienic assessment of RF EMF as a factor of the working environment in radio and TV stations. Annals, No. 6, 1978.(in Bulgarian)
4. Electromagnetic Fields in the Frequency Range from 100 kHz to 300 GHz, Health Physics,54,115-123.
5. Israel M., P. Tomov: Epidemiological study of the effects of radiofrequency radiation on operators in radio, TV and relay stations, Proceeding of the Eastern European Regional Meeting and Workshop “Measurements and Criteria for Standard Harmonization in the field of EMF Exposure” and WHO EMF Standards Harmonization Meeting, Varna, Bulgaria, 28 April – 3 May, 2001, pp.145-153
6. Ordinance No.9, for maximal permissible levels of electromagnetic fields in populated areas and determining hygienic safety zones around objects emitting EMR, Ministry of Health, Ministry of Environment, State gazette 35, 1991
7. Report No.2.1/01 NCHMEN, 2004. Assessment of the effect of low-level radiofrequency electromagnetic radiation on the secretion of melatonin, the level of stress hormones and cardiovascular system, NCHMEN, Sofia (in Bulgarian)
8.Tzenova B., M. Israel, M. Topalova – Well-being and Biochemical Correlates of Non-24-Hour Sleep Schedule in Communication, Shiftwork International Newsletter, 1995, vol.12, N:1, p.103
9.WHO Environmental Health Criteria 137,1991,Geneva,Regional Office for Europe.

Biological Effects and Potential Hazards of Microwaves used in Cellular Phone System on Infertility

***Farzaneh Ahmadi*[1]**
***S. Hamed Rohani*[2]**

1. MSc. Communication Engineering; University of Tehran.
2. General Physician; Azad University of Tehran; Member of Young Researchers Club

ABSTRACT
Although recent researches approved that EM waves cause harm to CNS and bone marrow systems [1-6], they are not studied to have health effects on other systems of human body, Nevertheless possible health effects of EM waves on genitalia system is also a question as this system has also dividing cells (like CNS and bone marrow) in males and females. In this case possible effects of E-M waves on infertility is a matter of concern.

This research is done to investigate infertile couples about possession and usage methods of mobile handsets and also to discuss the role of the proximity of housing/occupation to BTSs of GSM (900, 1800) mobile phone network as a means of possible cellular phone exposure and so having possible influence on infertility.
The research has been done by questionnaires and as cross-sectional. Collected data then was analyzed using SPSS software.

The results of the study show that these variables have correlation with infertility:

1. duration which these patients use cellular phone for speech
2. place of holding cellular phone regarding body
3. model of cellular phone
4. Proximity of the handset regarding body

1. INTORDUCTION
Although recent researches have approved that E-M waves may cause harm to CNS and bone marrow systems [1-4], they are not studied to have health effects on other systems of human body. As CNS and bone marrow systems are made of dividing cells in all individuals and are proved to be affected by E-M waves of power lines and Radio frequency which have resulted Brain Cancers and different kinds of Leukemia, this idea is formed that E-M waves may have possible effects on genitalia system also as this system has dividing cells in males and females.

Indeed, a large segment of the world's population is now exposed to RF and microwave radiation. We need a better understanding of the biological effects of RF electromagnetic field so that we can safeguard against possible harms to the general population and increase its beneficial medical uses.

We have chosen the Microwaves used in cellular phone system as a course of study for possible effects on urogenital system. There are many usages of Microwaves in urban lives like satellites, point to point links, and cellular phones. The last one has a higher energy regarding its frequency and also higher amplitude regarding its usage and also is more globally used. Other forms of RF waves do not have remarkable values regarding microwaves used in cellular phone systems. With the widespread use of mobile phones, the question of cellular phone health hazards should be answered. That’s why this research is focused mainly on the study of possible effects of cell phone microwaves on infertility.

2. BIOLOGICAL EFFECTS CAUSED BY MICROWAVES

Our knowledge regarding the biological effects of RF radiation have increased for many decades. It has become a focus of attention because of the accelerated use of RF radiation for wireless communication over the past few years. It is fairly well established that at sufficiently high power levels, RF and microwave energy can produce deleterious biological effects. Wireless communication systems use low power modulated forms of RF and microwave radiation that were not investigated extensively in the past.

Nevertheless, available data do not suggest any immediate cause for concern of an impending threat to the health of the population from acute or short term exposure to low level RF radiation. Investigations to answer some of the questions have already begun. Many of them are designed to study the effects of long term exposure. When considering repeated, low level radiation, the possibility of cumulative effects has been raised. While there is presently few confirmed evidence for cumulative effect, there is little information to the contrary.

Large scale epidemiological investigations should also be undertaken among the mobile telecommunication and cellular telephone users who may be exposed to varying levels of RF radiation over time. Better understanding is needed of the mechanisms of interaction between RF and microwave radiation and biological systems, and the significance of any observed effects. Enormous progress has been made in the difficult area of dosimetry. However, measurement of energy distribution in and around a subject for exposure assessment remains a challenge, more so for large numbers of people. This type of quantitative information is also required for extrapolation from animal experimentation to human response.

3. CHARACTERISTICS OF CELLULAR COMMUNICATION SYSTEMS

The research is focused on the health effects of cellular telephones. Cellular telephones operate at frequencies close to 850 and 1900 MHz in GSM[1] systems (these frequencies may vary for different countries.) The cellular phone system mainly consists of Base Transceiver Stations (BTS) and handsets for signal transmission. So studying the radiations of this system should be focused on these two parts.

Handsets transmit at low power levels. 0.6 watts for hand-held units in the first generation mobile telephones which were based on analog technology. Digital communication systems have made digital mobile technology competitive at power consumption as low as 10 mW. But, while in use, are located very close to the user's head. They are also to be used as placed on the belt or heart other locations near body for long hours when are on but not used for speech. They may also be in places near the body while sleeping. This has naturally led to concerns about potential health effects of handset radiations.

Returning to the BTS, the total MW power that could be transmitted from each BTS antenna at a cell site depends on the number of radio channels (transmitters) that have been authorized and the power of each transmitter. Typically, for a cellular base station, a maximum of 21 channels per sector (depending on the system) could be used. Thus, for a typical cell site utilizing sector antennas, each of the three transmitting antennas could be connected to up to 21 transmitters for a total of 63 transmitters per site. When omni directional antennas are used, up to 96 transmitters could be implemented at a cell site, but this would be unusual. While a typical base station could have as many as 63 transmitters, not all of the transmitters would be expected to operate simultaneously thus reducing overall emission levels.

Although an ***effective radiated power*** (ERP) of up to 500 watts per channel (depending on the tower height) is permitted, the majority of cellular base stations in urban and suburban areas operate at an ERP of 100 watts per channel or less. An ERP of 100 watts corresponds to an ***actual*** radiated power of about 5-10 watts, depending on the type of antenna used (ERP is not equivalent to the power that is radiated but, rather, is a quantity that takes into consideration transmitter power and antenna directivity). As the capacity of a system is expanded by dividing cells, i.e., adding additional base stations, lower ERPs are normally used. In urban areas, an ERP of 10 watts per channel (corresponding to a radiated power of 0.5 - 1 watt) or less is commonly used.

The signal from a cellular base station antenna is essentially directed toward the horizon in a relatively narrow pattern in the vertical plane. The radiation pattern for an omni-directional antenna might be compared to a thin doughnut or pancake centered around the antenna while the pattern for a sector antenna is fan-shaped, like a wedge cut from a pie. As with all forms of electromagnetic energy, the power density from a cellular or PCS transmitter decreases rapidly (according to an inverse square law) as one moves away from the antenna. Consequently, normal ground-level exposure is much less than exposures that might be encountered if one were very close to the antenna and in its main transmitted beam.

Measurements made near typical cellular installations, especially those with tower-mounted antennas, have shown that ground-level power densities are well below limits recommended by RF/microwave safety standards [7-9]. For example, for a base-station transmitting frequency of 869 MHz the RF exposure guidelines recommend a Maximum Permissible Exposure level for the public ("general population/uncontrolled" exposure) of about 580 microwatts per square centimeter (μW/cm2).

[1] Global Service Mobile system

This limit is many times greater than MW levels found near the base of typical cellular towers or in the vicinity of lower-powered cellular base station transmitters, such as might be mounted on rooftops or sides of buildings. Measurement data obtained from various sources have consistently indicated that "worst-case" ground-level power densities near typical cellular towers are on the order of 1 µW/cm2 or less (usually significantly less). Calculations corresponding to a "worst-case" situation (all transmitters operating simultaneously and continuously at the maximum licensed power) show that in order to be exposed to levels near limits for cellular frequencies, an individual would essentially have to remain in the main transmitting beam (at the height of the antenna) and within a few feet from the antenna.

This makes it extremely unlikely that a member of the general public could be exposed to MW levels in excess of these guidelines due to cellular base station transmitters. When cellular antennas are mounted at rooftop locations it is possible that ambient MW levels greater than 1 µW/cm2 could be present on the rooftop itself. However, exposures approaching or exceeding the safety guidelines are only likely to be encountered very close to or directly in front of the antennas. For sector-type antennas MW levels to the side and in back of these antennas are insignificant.

Even if MW levels were higher than desirable on a rooftop, appropriate restrictions could be placed on access. Factoring in the time-averaging aspects of safety standards could also be used to reduce potential exposure of workers who might have to access a rooftop for maintenance tasks or other reasons. The fact that rooftop cellular and PCS antennas usually operate at lower power levels than antennas on free-standing towers makes excessive exposure conditions on rooftops unlikely. In addition, the significant signal attenuation of a building's roof minimizes any chance for persons living or working within the building itself to be exposed to RF levels that could approach or exceed applicable safety limits. With this deduction, we have focused mainly on the radiation of the handsets while considering health effects on infertility.

4. MATERIAL AND METHOD

Isfahan is regarded to be Iran's second big city which has a vast cellular phone system. The population of infertile couples in Isfahan is rather high. Isfahan Fertility and Infertility Center (IFIC) is a place for the study of infertility and thus possible effects of microwaves used in cell phones on infertility.

This project is done as a cross-sectional research using questioners. As it was stated before, in lack of quantitative data about the exposure effects of microwave frequency band used in cellular phone system, the questioner based method will be useful to analyze situation. The questioner was designed to gather information about the usage and brand of mobile handsets and also the proximity of housing/occupation to BTSs of cellular phone network. The questioner was to get information of infertile couples that have visited the IFIC in a specific period of time. Our inclusion criteria was (1) visiting the IFIC in the interval of Sep. 2004 – Feb. 2005 (2) Owning a cellular phone.

As to omit the mixture results of Ionizing radiations and power frequencies, our exclusion criteria was (1) proximity of houses to nuclear equipments, (2) occupation in them and (3) occupation and living by power line frequencies sources, (4) power plants, (5) radio stations, and (6) Broadcast, satellite stations, so these cases were omitted of the study set. Data was gathered by interviewing and ask questions to fill the questionnaire. In this period, 209 cases who had the two inclusion criteria and did not have the exclusion criteria included in the study. Table 1 shows some inquiries made by the questioner.

The collected data was then analyzed by SPSS 11.5 and these to summarize data these types of charts used:

- ✔ Pie chart to summarize data of a nominal variable
- ✔ Histogram chart to summarize data of a scale variable

Table 1 shows the most significant inquiries made by the questioner.

Table 1. The inquiries made by the questioner

Personal Information
Name , Home address, Work address, Occupation
Date of infertility notice
Distance between Home and nearest BTS
Distance between work place and nearest BTS
Brand and model of hand set
Hours using handsets a day
Hours having the phone turned on near the body (less than one meter)
Place holding the phone when turned on (by body side)
Place holding the phone when turned on (while speaking)
How long is the phone turned on while sleeping?
How long do you speak with your phone a day
Do you use hands free? Wireless or wired?

5. Results and Findings

The measurement of duration which each case has used cell phone shows that the mean of this time is 4.05 years.

Table 2. Duration which each case has used cell

Duration which each case has used cell	N	Min	Max	Mean	Std. Dev.
Cell Phone Duration	**209**	**1**	**11**	**4.05**	**2.122**
Valid N (listwise)	**209**				

We measured the mean amount of time in which the cell phone is on and in a distance less than one meter regarding the body in each day. 77.9% of them have their cellular within this distance more than 10 hours (including near bed when sleeping).

Table 3. The mean amount of time more is than 10 hours

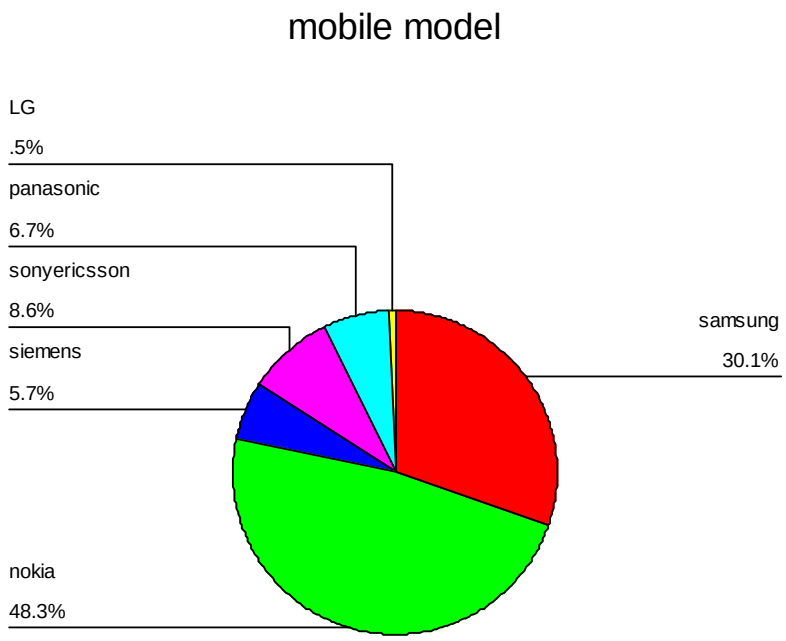
The mean amount of time more is than 10 hours		Frequency	Percent
Valid answer	**yes**	**163**	**77.9**
	no	**45**	22.1
Total		209	100.0

The study of cellular phones' model performed and the results below were achieved:

Table 4. Cellular phones' model

Cellular phones' model		Freq.	Valid Percent
Valid	**Samsung**	**63**	**30.1**
	Nokia	**101**	**48.3**
	Siemens	**12**	**5.7**
	Sonyericsson	**18**	**8.6**
	Panasonic	**14**	**6.7**
	LG	**1**	**0.5**
Total		209	100.0

The next Pie chart summarizes data above:

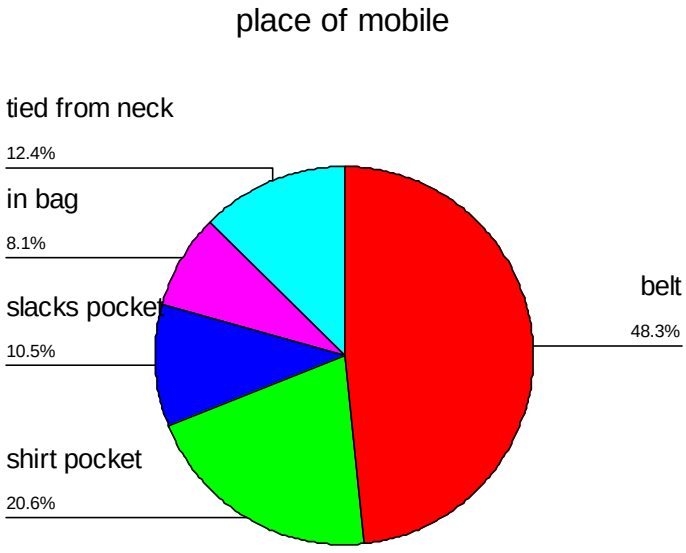


We also studied where each patient holds the cellular phone when it is on but not in use, so the results below achieved:

Table 5. Where does each patient hold the cellular phone?

Where does each patient hold the cellular phone		Frequency	Percent
Valid Answer	**Belt**	101	48.3
	Shirt pocket	43	20.6
	Slacks pocket	22	10.5
	In bag	17	8.1
	Tied from neck	26	12.4
Total		**209**	**100.0**

This Pie chart shows the latter data:



The measurement of the time which each patient calls with cellular phone each day was asked and showed that the mean of this time is 62.61 minutes/day for them. This table shows the data collected:

Table 6. The time each patient calls with cellular phone a day

speech time	**209**	**100**	**10**	**110**	**62.61**	**7.093**
Valid N (listwise)	**209**					

This graph represents the number of cases which calls with cellular phone in each specific duration:

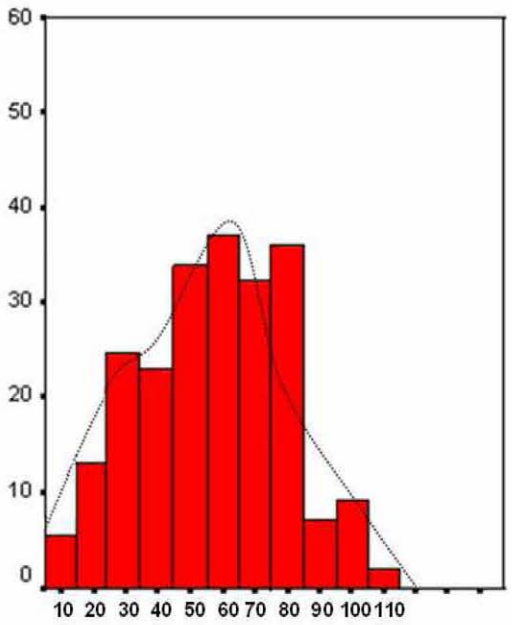


Figure 1. The number of people (vertical) regarding their speech time a day (horizontal)

The study of relation between the duration which these patients uses cellular phone and the duration of infertility shows a relation with correlation coefficient of P= 0.345 (ρ =0.037). This study performed by Bivariate Correlation and usage of Spearman coefficient[1].

[1] In statistics, ***Spearman's rank correlation coefficient,*** ρ (rho), is a non-parametric measure of correlation, it does not require the assumption that the relationship between the variables is linear,

In principle, ρ is simply a special case of the Pearson product-moment coefficient in which the data are converted to ranks before calculating the coefficient. In practice, however, a simpler procedure is normally used to calculate ρ. The raw scores are converted to ranks, and the differences *D* between the ranks of each observation on the two variables are calculated. ρ is then given by:

$$\rho = 1 - \frac{6 \sum D^2}{N(N^2 - 1)}$$

where:

D = the difference between the ranks of corresponding values of *X* and *Y*, and
N = the number of pairs of values.

The study of duration of infertility and distance between job/living place and the distance to the closest electric communication antenna shows a relation with correlation coefficient of P=0.0261 (ρ =0.0046). which shows weak correlation between the two variable. This study performed by Bivariate Correlation and usage of Spearman coefficient.

6. CONCLUSION

In this research, we investigated the possible effect of cellular phone system radiations on infertility. The result of our studies shows possible influences of cell phone handsets on the cases that have been sampled. The study shows that these variables have correlation with infertility:

5. duration which these patients use cellular phone for speech
   So that the increase of usage of mobile phone from 10 to 60 minutes a day yields to an increase of infertile couples
6. place of holding cellular phone regarding body
   48.3% of the cased hold their headsets on their belts
7. model of cellular phone
   48.3% of the cased used Nokia brand
8. Proximity of the handset regarding body
   77.9 of the cases had their handsets on and near the body more than 10 hours in 24 hours.

The study of relation between the duration which these patients uses cellular phone and the duration of infertility shows a relation with correlation coefficient of P = 0.345 (ρ =0.037) which shows a slight linear correlation.

The study of duration of infertility and distance between job/living place and the distance to the closest electric communication antenna shows a relation with correlation coefficient of P = 0.0261 (ρ =0.0046) which shows little correspondence between the two variables so the parameter: Distance between living/job place and the closest electric communication antenna, did not show any meaningful relationship with the infertility date, as was presumed by the discussion presented in section 2.

7. ACKNOWLEDGEMENT

The Authors wish to thank Dr. M. Ahmadi, member of IFIC, for his kindest cooperation in the research. They are also grateful of Mr. E and F. Ahmadi for spreading and gathering up the questioners.

8. REFERENCES

1. Savitz DA et al. Magnetic field exposure in relation to leukemia and brain cancer mortality and electric utility workers. *American Journal of Epidemiology*. 1995; 141: 1-12.
2. Theriault G et al. Cancer risk associated with occupational exposure to magnetic fields among utility workers in Ontario and Quebec, Canada and France. *American Journal of Epidemiology*. 1994; 139: 550-572.
3. National Institute of Environmental Health Sciences. Health effects from exposure to power-line frequency electric and magnetic fields. *NIEH Final Report of Congress.* 1998.
4.
a) Coleman Metal. Leukaemia and residence near electricity transmission equipment: A case-control study. *British Journal of Cancer*. 1989; 60:793-98.
b) London SJ et al. Exposure to residential electric and magnetic fields and risk of childhood leukemia. *American Journal of Epidemiology*. 1991; 134:923-37.
c) Feychting M. et al. Magnetic fields and cancer in children residing near Swedish high-voltage power lines. *American Journal of Epidemiology*. 1993; 138:467-81.

5. Sahl JD et al. Cohort and nested case-control studies of hematopoietic cancers and brain cancer among electric utility workers. *Epidemiology*. 1993; 4: 104-114.
6. National Institute of Environmental Health Sciences. Assessment of health effects from exposure to power-line frequency electric and magnetic fields. *NIEH Working Group Report.* 1998.
7. U.S. Federal Communications Commission (FCC), Guidelines for Evaluating the Environmental Effects of Radiofrequency Radiation, *Report and Order*, ET Docket 93-62, FCC 96-326, adopted August 1, 1996, 61 Federal Register 41006 (1996).

8. U.S. Federal Communications Commission (FCC), Guidelines for Evaluating the Environmental Effects of Radiofrequency Radiation, *Second Memorandum Opinion and Order and Notice of Proposed Rule Making*, ET Docket 93-62 (WT Docket 97-192), FCC 97- 303, adopted August 25, 1997, 62 Federal Register 47,960, 49,557 and 61,447 (1997).
9. Klauenberg, B.J., Grandolfo, M. and D.N. Erwin (eds.), *Radiofrequency Radiation Standards, Biological Effects, Dosimetry, Epidemiology and Public Health Policy*. NATO ASI Series A: Life Sciences, Plenum Press (1994).

10. List of web sited where one can gather more information

American National Standards Institute: www.ansi.org
Bioelectromagnetics Society: www.bioelectromagnetics.org
European Bioelectromagnetics Association: www.ebea.org
Electromagnetic Energy Association: www.elecenergy.com
US Federal Communications Commission: www.fcc.gov/oet/rfsafety
ICNIRP (Europe): www.icnirp.de
IEEE Committee on Man & Radiation: www.seas.upenn.edu/~kfoster/comar.htm
International Microwave Power Institute: www.impi.org
Microwave News: www.microwavenews.com
US National Council on Radiation Protection & Measurements: www.ncrp.com
US OSHA: www.osha-slc.gov/SLTC
Wireless Industry (CTIA): www.wow-com.com
Wireless Industry (PCIA): www.pcia.com
World Health Organization EMF Project: www.who.ch/peh-emf

IN VIVO EFFECTS OF ELF MAGNETIC FIELDS ON ANTIOXIDANT DEFENSE SYSTEM IN KIDNEY

AYSE G. CANSEVEN[*], SULE COSKUN[**], NESRIN SEYHAN[*]

[*] ***DEPARTMENT OF BIOPHYSICS, GAZI UNIVERSITY, FACULTY OF MEDICINE, 06510 BESEVLER ANKARA, TURKEY***
[**] ***DEPARTMENT OF BIOLOGY, GAZI UNIVERSITY, FACULTY OF ART AND SCIENCE, 06500 TEKNIKOKULLAR ANKARA, TURKEY***
canseven@gazi.edu.tr

Abstract

Electromagnetic Fields (EMF) can affect biological systems by increasing the amount of free oxygen radicals. Antioxidants are able to reduce the effects of free radicals formed in body. Glutathione (GSH) is one of the important antioxidants in body defense system for free radical. In this study, we examined the effects of 50 Hz magnetic fields on GSH level in kidney. A total of 56 male guinea pigs were used. Forty-nine guinea pigs were exposed to 50 Hz, 1 mT, 2 mT and 3 mT fields with the exposure periods of 4 and 8 hours/day for 5 days. Seven subjects were handled in an identical manner with the exposed animals in the same laboratory. They were used as control without being exposed to any magnetic fields. The GSH levels were determined spectrophotometrically by modified Aykaç et al. method. Increased GSH levels were found in kidneys of guinea pigs exposed to 1 mT magnetic field for the exposure periods of 4 hours. For the magnetic fields of 2 mT and 3 mT applied with the period of 8 hours, increased levels of GSH were also found. It seems that ELF magnetic fields promote the levels of GSH which has a protective role against the oxidative damage.

Deleted: it was

Deleted: w

Introduction

Exposure of human bodies to extremely low frequency electromagnetic fields (ELF EMF) have been increased by growing use of electrical devices, which emit EMF. It has been showed that EMF influence enzymatic activity in biological systems (Noda, 2000). Several studies on effects of EMF have shown that EMF can induce cell proliferation, variations of calcium concentrations, alteration of DNA integrity, changes in transcription of immediate early genes and protein synthesis (Boland, 2002; Ishisaka, 2000; Gold, 1994; Kenneth, 1987; Guler, 1996a; Guler, 1996b; Guler, 1999; Seyhan, 2006; Canseven, 1996; Canseven, 1999, Canseven, 2005a; Canseven 2005b; Liboff, 1987; Liburdy, 1993) and perturbations of central nervous system (Ilhan, 2004; Jelenkovic, 2006; Jin, 1998; Lai, 1996; Lai, 2004). It is known that ELF magnetic fields (MFs) may cause an increase in free radicals activity in living organisms (Boland, 2002; Kula, 2002; Kula, 2000; Roy, 1995; Khadir, 1999; Simko, 2001; Seyhan, 2006; Guler, 2006). Free radicals are very reactive and unstable molecules that can initiate chain reactions to form new free radicals. Antioxidants are able to reduce the effects of free radicals formed in body. Cells are also equipped with the enzymatic antioxidant mechanisms that play an important role in the elimination of free radicals (Gorenek, 2006; Guler 2006; Ozgur, 2006; Seyhan, 2006) Glutathione (GSH), the most abundant non-enzymatic antioxidant present in the cell, plays an important role in the defense against oxidative-stress-induced cell injury.

Deleted: has

Deleted: been

Deleted: molecular species

It has been showed that exposures of magnetic fields with various frequency and intensity can change the antioxidant activity of human and animal bodies (Harakawa, 2005; Kashalda, 1995; Fiorani, 1997; Ozguner, 2005; Canseven et al., 2005c).

This study was designed to find the effects of exposure to 1 mT, 2 mT and 3 mT of 50 Hz magnetic fields on GSH levels in kidneys of guinea pigs in various exposure periods.

Materials and Methods

Animals

The experimental protocol was reviewed and approved by the Laboratory Animal Care Committee of Gazi University (Report no: 36-7838). A total of 56 male, 250-300 g weighted guinea pigs were used in this experiment. All animals were kept under laboratory conditions and fed standard pellet food.

Magnetic Field Exposure

The system used to generate the magnetic fields was Helmholtz coils' system which was specially designed by Bioelectromagnetic Laboratory at Biophysics Department of Medical Faculty of Gazi University (Canseven, 2005d). This system consisted of two parallel horizontal flat circular coils of 42.75 cm diameter, with a common axis, and separated by 21.375 cm. Each coil has 154 turns and was constructed by insulated copper wire. Sinusoidal current of frequency 50 Hz was generated by the specially designed variable transformer, 2.7 kVA in power. The intensity of MF was modulated by the transformer. The magnetic field generated by the coils is classified as vertical field since the field lines perpendicular to the bottom plane of the animal's cage.

Forty nine guinea pigs were housed in the centre of the Helmholtz coils, 2 per plexiglas cage and were exposed to 50 Hz, 1 mT, 2 mT and 3 mT fields with the exposure period of 4 hours/day or 8 hours/day over 5 days. Seven subjects were handled in an identical manner without being exposed to any magnetic field and studied as controls.

The temperature of laboratory was held constant at 23° C with day and night cycle of 12 hours and ambient geomagnetic field of 30 μT. To eliminate possible variations due to circadian rhythm, the exposure periods of magnetic fields were chosen as 8:00 - 12:00 a.m for 4 hours of exposure periods and 8:00 a.m - 4:00 p.m for 8 hours of exposure periods.

Following 12 h of starvation, guinea pigs were injected intramuscularly with ketamine (30 mg/kg) and xylazine (2 mg/kg) and 250 IU/kg heparin. Kidneys were sampled immediately. They shocked by liquid nitrogen and stored in deep freezer at -80°C until performing analysis.

Determination of GSH levels

The GSH levels were determined by modified Aykaç et al. (Aykac, 1985) method. Tissues were homogenized in nine volumes of cold 10% TCA solution and the homogenate was centrifuged for 15 min. at 3000xg at 4°C. The supernatants were transferred to glass test tubes.0.5 ml of supernatant was added to the 2 ml of 0.3 M $Na_2HPO_4.2H_2O$ solution.a 0.2 ml solution of dithiobisnitrobenzoate (0.4 mg/ml 1% sodium citrate)was added and absorbance at 412 nm was measured immediately after mixing.The GSH levels were calculated using an extiction coefficient of 13.600 $mol^{-1}cm^{-1}$.

All experiments were run in a blind manner.

Statistics

Statistical analyses were carried out using SPSS software (SPSS 11.5 for windows, SPSS Inc., Chicago, USA).

The p value was considered significant at $p<0.05$.

Mann Whitney-U and Kruskal-Wallis tests were used in statistical analysis. Comparisons between exposed groups and controls were made by using Mann Whitney-U test while magnetic fields of 1mT, 2 mT and 3 mT were compared with Kruskal-Wallis test with respect to exposure periods of 4 hours and 8 hours.

Results

In this study, GSH levels were measured in kidney of guinea pigs, which were exposed to magnetic fields of 1 mT, 2 mT and 3 mT fields with the exposure periods of 4 and 8 hours/day for 5 days. For both of the exposure periods, GSH levels were found increased with respect to controls in kidney of guinea pigs exposed to the 50 Hz magnetic fields of 1 mT, 2 mT and 3 mT, except 1 mT, 8 hours. The increases in GSH levels were found statistically significant for 1 mT , 4 hours ($p=0.000$), 2 mT, 8 hours ($p=0.000$) and 3 mT, 8 hours ($p=0.021$) in kidneys by Mann-Whitney U test.

Field intensities were compared with respect to exposure periods by Kruskal-Wallis test. Significant differences were determined between field intensities of 1 mT, 2 mT and 3 mT in kidney tissues for both of the exposure periods ($p=0.001$ and $p=0.000$ for 4 hours and 8 hours respectively).

Discussion

Glutathione is a major non protein thiol in living organisms.It plays a crucial role in coordinating the body's antioxidant defense process. Several studies have reported the effects of 50 Hz magnetic fields on antioxidant defense system activity or GSH levels (Kashkalda, 1995; Harakawa, 2005; Fiorani, 1997; Canseven, 2005d). Fiorani et al. reported that the fields are able to potentiate the cellular damage induced in vitro by oxiding agents (Fiorani, 1997).

Table 1 . GSH (micromole/g tissue) levels in kidney tissues of 1 mT, 2 mT and 3 mT exposed and control guinea pigs. Exposure periods were 4 hours/day and 8 hours/day for 5 days.

GROUPS	n	GSH Level (micromol/g tissue) mean ± sem
Control	7	3.09±0.48
1 mT; 4 hours	8	6.44±0.42
1 mT; 8 hours	10	2.43±0.17
2 mT, 4 hours	6	3.40±0.32
2 mT, 8 hours	8	5.93±0.33
3 mT; 4 hours	9	4.63±0.41
3 mT; 8 hours	8	5.16±0.50

To evaluate the effects of magnetic fields on antioxidant defense system, GSH levels were measured on guinea pigs exposed to magnetic fields of 1 mT, 2 mT and 3 mT fields with the exposure periods of 4 hours/day and 8 hours/day for 5 days, in this study. Our data clearly showed that GSH levels increase with respect to controls under the lowest magnetic field intensity with the relatively short exposure period, i.e. 4 hours.
Although statistically significant increased GSH levels were found for the magnetic fields of 1 mT for 4 hours, 2mT and 3 mT for 8 hours in tissues, no matter what the exposure period was, kidney GSH level started to increase at and after 2 mT exposures.
Antioxidants are able to reduce the effects of free radicals formed in body. Our results indicate that chronic exposure to various ELF magnetic fields increase GSH levels, which are free radical scavengers in kidney.

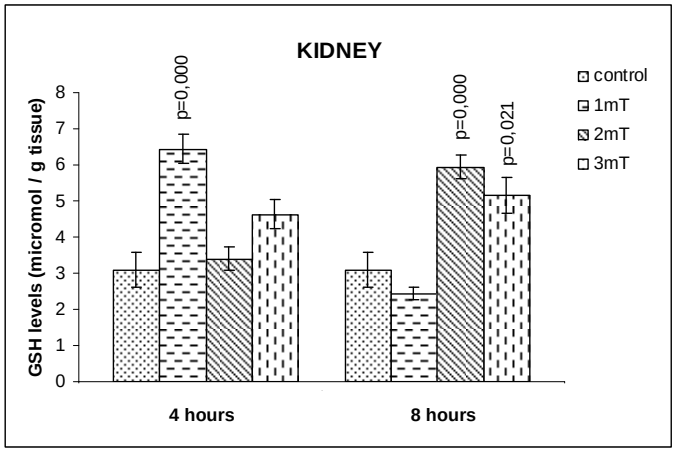


Figure 1. GSH levels in kidneys under effects of 50 Hz magnetic fields of 1 mT, 2 mT and 3 mT with the exposure periods of 4 hours and 8 hours.

References

Aykac G, Uysal M, Yalcin AS, Kocak-Toker N, Sivas A, Oz H. (1985). The effect of chronic ethanol ingestion on hepatic lipid peroxide, glutathione, glutathione peroxidase and glutathione transferase in rats. *Toxicology* 36: 71-76.

Canseven A.G., Seyhan N., Aydin, A., Cevik, C., Isimer, A. (2005a). Effects of Ambient ELF Magnetic Fields: Variations in Electrolytes Levels of Brain and Blood Plasma, Gazi Medical Journal, 16: 121 – 127.

Canseven, A.G., Atalay Seyhan, N. (1996). Is It Possible to Trigger the Collagen Synthesis by Electric Current in Skin Wounds?, *Indian J Biochem Biophys* 33, 223-227.

Canseven, A.G., Coskun S., Seyhan, N. (2005c): Magnetic fields have an effect on antioxidant defense system in heart tissue IFMBE Proceedings, Vol. 11. Prague: IFMBE, 2005. ISSN 1727-1983.Editors: Jiri Hozman, Peter Kneppo (Proceedings of the 3rd European Medical & Biological Engineering Conference - EMBEC´05. Prague, Czech Republic, 20-25.11.2005). pp: 2226-2228

Canseven, A.G., Coskun S., Seyhan, N. (2005e): Magnetic fields have an effect on antioxidant defense system in heart tissue IFMBE Proceedings, Vol. 11. Prague: IFMBE, 2005. ISSN 1727-1983.Editors: Jiri Hozman, Peter Kneppo (Proceedings of the 3rd European Medical & Biological Engineering Conference - EMBEC´05. Prague, Czech Republic, 20-25.11.2005). pp: 2226-2228

Canseven, A.G., Seyhan, N. (2005b). Effects of Ambient ELF Magnetic Fields: Variations In Collagen Synthesis of Guinea Pigs' Skin and Scaling From Animals To Human. *Gazi Medical Journal* 16 : 160 – 165 *(Turkish)*.

Canseven, A.G., Seyhan, N. (2005d). Design, installation and standardization of homogenous magnetic field systems for experimental animals IFMBE Proceedings, Vol. 11. Prague: IFMBE, 2005. ISSN 1727-1983. Editors: Jiri Hozman, Peter Kneppo (Proceedings of the 3rd European Medical&Biological Engineering Conference - EMBEC´05.Prague, Czech Republic, 20- 25.11.2005). pp: 2333-2338

Canseven, A.G., Seyhan, N., et al. (1999). Extremely Low Frequency Electromagnetic Field Effect on Brain Tissue and Blood Plasma Electrolytes, *Med & Biol Eng & Comput*., 37 (Suppl. 2): 1336-1337.

Fiorani, M., Biagiarelli, B., Vetrano, F., Guidi, G., Dacha, M., Stocchi, V. (1997). In vitro effects of 50 Hz Magnetic fields on oxidatively damaged rabbit red blood cells. *Bioelectromagnetics.* 18: 125-131.

Gold, S., Goodman, R., Henderson, A.S. (1994). Exposure of Simian Virus-40-Transformed Human Cells to Magnetic Fields Results in Increased Levels of T-Antigen mRNA and Protein. *Bioelectromagnetics.* 15 **:** 329-336.

Gorenek L., Acar A., Aydin A., Eyigun C. P., Cetinkaya A., Eken A., Sayal A. (2006). Oxidative stress and antioxidant defense in patients with chronic hepatitis C patients before and after pegylated interferon alfa-2b plus ribavirin Therapy. J Transl Med. Jun 20;4 (1) : 25.

Guler, G., Atalay Seyhan, N. (1996a). Changes in Hydroxyproline Levels in Electric Field Tissue Interaction. *Indian Journal Of Biochemistry and Biophysics* 33: 531-533.

Guler, G., Atalay Seyhan, N., Özoğul, C., Erdoğan, D. (1996b). Biochemical and Structural Approach to Collagen Synthesis Under Electric Fields. *Gen. Physiol. Biophys* 15: 429-440.

Guler, G., Atalay Seyhan, N. (1999). Extremely Low Frequency (ELF) Electric Field with Different Application Times Inhibits Protein Synthesis. *Med & Biol Eng & Comput* 37, (Suppl. 2) : 1338-1339.

Guler, G., Seyhan, N., Arıcıoglu, A. (2006). Effects of Static and 50 Hz Alternating Electric Fields on Superoxide Dismutase Activity and TBARS Levels in Guinea Pigs. *Gen. Physiol. Biophys* 25: 177-193.

Harakawa, S., Inoue, N., Hori, T., Tochio, K., Kariya, T., Takahashi, K., Doge, F., Suzuki, H., Nagasawa, H. (2005). Effects of 50 Hz electric field on plasma lipid peroxide level and antioxidant activity in rats. *Bioelectromagnetics.* 26: 589-594.

Ilhan, A., Gurel, A., Armutcu, F., Kamisli, S., Iraz, M., Akyol, O., Ozen, S. (2004). Ginkgo biloba prevents mobile phone-induced oxidative stress in rat brain. *Clin Chim Acta.* 340: 153-162.

Jelenkovic, A., Janac, B., Pesic, V., Jovanovic, D.M., Vasiljevic, I., Prolic, Z. (2006). Effects of extremely low-frequency magnetic field in the brain of rats. *Brain Research Bulletin.* 68: 355-360.

Jin, Y., Wang, H., Cheng, Y., Gu, H. (1998). Effects of static magnetic fields on free radical metabolism of human body. *Wei Sheng Yan Jiu*. 27: 97-99.

Kashkalda, D.A., Pashenko, E.A, Ziubanova, L.F. (1995). Effects of an impulse magnetic field on lipid peroxidation and the antioxidant system of the testes in animal experiments. *Med Tr Prom Ekol*. 10: 14-17.

Kenneth, J.M., Lee, R.C., Ehrlich, H.P. (1987). Frequency Dependence of Electric Field Modulation of Fibroblasts Protein Synthesis. *Science* 236 : 1465-1469.

Khadir, R., Morgan, J.L., Murray, J.J. (1999). Effects of 60 Hz magnetic field exposure on polymorphonuclear leukocyte activation, *Biochim Biophys Acta*, **1472** : 359-367.

Kula, B., Sobczak, A., Kuska, R. (2000). Effects of static and ELF magnetic fields on free- radical processes in rat liver and kidney, *Electro and Magnetobiology*, **19** : 99-105.

Kula, B., Sobczak, A., Kuska, R. (2002). Effects of electromagnetic field on free radical processes in steelworkers. Part I. Magnetic field influence on the antioxidant activity in red blood cells and plasma, *J. Occup Health*, **44** : 226-229.

Lai, H., Singh, N.P. (2004). Magnetic field-induced DNA strand breaks in brain cells of the rat, *Environmental Health perspectives*, **112** : 687-694 .

Liboff, A.R., Smith, S.D., Mc Leod, B.R. (1987). Experimental Evidence for Ion Cyclotron Resonance Mediation of Membrane Transport. In Blank, M., Findl, E., eds. *Mechanistic Approaches to Interactions of Electric and Electromagnetic Fields with Living Systems*. New York: Plenum Press; pp. 109-132.

Liburdy, R.P., Yost, M.G. (1993). Time Varying and Static Magnetic Fields Act in Combination to Alter Calcium Signal Transduction in the Lymphocyte. In Blank, M., ed. *Electricity and Magnetism in Biology and Medicine*. USA: San Francisco Press, Inc.; pp. 331-334.

Ozguner, F., Oktem, F., Ayata, A., Koyu, A., Yilmaz, H.R. (2005). A novel antioxidant agent caffeic acid phenethyl ester prevents long-term mobile phone exposure-induced renal impairment in rat. Prognostic value of malondialdehyde, N-acetyl-beta-D-glucosaminidase and nitric oxide determination. *Mol Cell Biochem*. 277: 73-80.

Ozgur, E., Guler, G., Seyhan, N. Effects Of Electromagnetıc Fıeld From Power Lines on the Oxidant and Antioxidant Levels in Guine pigs. *International Conference and COST 281 Workshop on Emerging EMF Technologies, Potential Sensitive Groups and Health*, April 20-21, 2006, Graz, Austria

Roy, S., Noda, Y., Eckert, V., Traber, M.G., Mori, A., Liburdy, R., Packer, L. (1995). The phorbol 12-myristate 13-acetate (PMA)-induced oxidative burst in rat peritoneal neutrophils is increased by a 0.1 mT (60 Hz) magnetic field, *FEBS Letters*, **376** : 164-166.

Seyhan N., Canseven A. G., Güler G. (2006). Animal Studies on the Effects of ELF and Static EMF. In Ayrapetyan S.N., Markov M.S., eds. *Bioelectromagnetics Current Concepts, The Mechanisms of the Biological Effect of Extremely High Power Pulses* . NATO Security through Science Series B: Physics and Biophysics, Vol. 5, pp: 195-212.

Simko, M., Droste, M., Kriehuber, R., Weiss D.G. (2001). Stimulation of phagocytosis and free radical production in murine macrophages by 50 Hz electromagnetic fields., *Eur J Cell Biol*, **80** : 562-566.

EFFECT OF INTERMITTENT AND CONTINUOUS EXPOSURE TO 50 Hz, 1.5 mT ON LIPID PEROXIDATION IN LIVER

AYSE G. CANSEVEN*, ARIN TOMRUK*, SULE COSKUN**, NESRIN SEYHAN*

**** DEPARTMENT OF BIOPHYSICS, GAZI UNIVERSITY, FACULTY OF MEDICINE, 06510 BESEVLER ANKARA, TURKEY***

*****DEPARTMENT OF BIOLOGY, GAZI UNIVERSITY, FACULTY OF ART AND SCIENCE, 06500 TEKNIKOKULLAR ANKARA, TURKEY***

canseven@gazi.edu.tr

Abstract

We investigated the effects of continuous and intermittent exposure to extremely low frequency (ELF) electromagnetic fields (EMF) on thiobarbituric acid reactive substances (TBARS) in liver. A total of 18 male, ten-twelve-weeks-old guinea pigs were used. Homogeneous magnetic fields were generated from a specially designed Helmholtz coil system. The subjects were divided into one control and two exposure groups which were exposed continuously (4 hours/day) or intermittently (2 hours on/ 2 hours off / 2 hours on) to 50 Hz magnetic field of 1.5 mT for 4 days. TBARS levels were determined by spectrophotometric method. Mann Whitney-U test was applied for statistical analysis. Increased TBARS levels were found in liver tissues for both of the continuous and intermittent exposures of 1.5 mT. These increases were found to be statistically significant ($p<0.05$). In conclusion, both types of the exposure to ELF electromagnetic fields (continuous or intermittent) could play a role in lipid peroxidation process.

Introduction

Although the development of technology provides people various facility, each of advanced technological devices are electromagnetic fields (EMF) sources. People are exposed to EMF seriously by wide usage of these devices. Most scientists have thought that EMF have adverse effects on people health. Several studies have been conducted on the effects of EMF as epidemiological and laboratory studies. It has been suggested that there is a link between ELF magnetic field exposure and the increased incidence of certain types of tumor, particularly in leukemia and brain cancer (Kheifets, 1995, 1997, 2004; Lin, 1985; Preston-Martin, 1989; Bastuji-Garin, 1990; Feychting, 1993; Wertheimer, 1979,1995; Hakansson, 2002; Savitz, 1988). Eextremely low frequency (ELF) electric and magnetic field exposure have recently been classified as a possible carcinogen class 3 and 2B respectively (NIEHS, 1998; IARC 2002). Electromagnetic field effects on protein synthesis (Canseven, 2005a; Guler, 1995) gene expression, signal transduction (Liburdy, 1992,1993), DNA damage (Lai, 2004; Jajte, 2001,2002), immune system functions (Canseven, 2006), apoptosis induction (Blumenthal, 1997), enzyme regulation (Canseven, 2003a,2003b,2004,2005b; Brocklehust, 1996; Khadir, 1999), free radical activity (Guler, 2004; Kula, 2000) have been investigated and reported in vivo and/or in vitro experiments. Studies conducted on free radical activities show that EMF Magnetic fields increase the activation of free radicals in tissues (Boland, 2002). The amounts and the activities of free radicals are important for tissue metabolism. Because free radicals are very reactive and unstable molecular species, they can initiate chain reactions to form new free radicals. Increased free radical activity in cellular levels can cause increase in lipid peroxidation which is known as a major factor in formation of the oxidative stress.

To answer the question “Can intermittent or continuous exposures to extremely low frequency magnetic field increase lipid peroxidation in liver?”, we examined the effect of continous or intermittently exposure of 1.5 mT magnetic field in this study. Guinea pigs were exposed to continuous and intermittent magnetic fields with the period of 4 hours/day for 4 days and lipid peroxidation was determined by measuring levels of TBARS in liver.

Materials and Methods

EMF System and Exposure

The experimental protocol was reviewed and approved by the Laboratory Animal Care Committee of Gazi University (Report no : 39-5858). A total of 18 male guinea pigs weighting between 250 and 300g were used in this study. All animals were kept under laboratory conditions and fed standard pellet food.

50 Hz magnetic field was produced by 42.75 cm diameter Helmholtz coil with winding embedded in an open wooden circular frame (Canseven, 2005c). Each coil was constructed by insulated copper wire with 154 turns. Sinusoidal current of frequency 50 Hz was supplied by a specially designed variable transformer (2.7 kilo Volt Amper-kVA) in power to feed the coils. A Hall-Effect Gaussmeter measured the magnetic field at the center of exposure system. Frequency and wave form of the magnetic field was monitored over an ossiloscope.The plexiglas animal cage was put at the center.

Animals were divided into three groups, controls and two magnetic field exposure groups. Exposure groups were exposed to continuously (4 hours/day) or intermittently (2 hours on/ 2 hours off/ 2 hours on) to 50 Hz MF of 1.5 mT with the exposure periods of for 4 days. Controls were handled in an identical manner without being exposed to any magnetic field.

Following 12 h of starvation, guinea pigs were injected intramuscularly with ketamine (30 mg/kg) and xylazine (2 mg/kg) combined with 250 IU/kg heparin. The liver was sampled immediately. They shocked by liquid nitrogen and stored in deep freezer at -80°C until performing analysis.

Determination of Lipid Peroxidation

Lipid peroxidation was quantified by measuring the formation of thiobarbituric acid reactive substances (TBARS). TBARS level of liver tissues was determined according to the Cassini et al.'s spectrophotometric method (Cassini, 1986). Tissues were homogenized in nine volumes of cold 10 % TCA solution and the homogenate was centrifuged for 15 min. At 3000xg at 4°C. The supernatants were transferred to glass test tubes containing 0.375 % (w/v) thiobarbituric acid and 0.02 % (w/v) butylated hydroxytoluene to prevent further peroxidation of lipids during subsequent steps. The samples were then heated for 15 min at 100°C in a boiling water bath, cooled and centrifuged to remove precipitant. The absorbance of each sample was determined at 532 nm. All experiments were run in a blind manner.

Statistics

Statistical analyses were carried out using SPSS software (SPSS 11.5 for windows, SPSS Inc., Chicago, USA). The p value was considered significant at $p<0.05$. Both comparisons between exposed groups and controls, and comparisons between intermittent and continuous exposed groups were made by using Mann Whitney-U test.

Results

In this study, TBARS level was investigated in liver tissues of guinea pigs which were continuously or intermittently exposed to 50 Hz magnetic field of 1.5 mT with the daily exposure of 4 hours for 4 days. Compared with the control TBARS levels were found significantly increased both continuous (p=0,009) and intermittent (p=0.016) exposures in liver tissues (Table1-Fig 1). Continuous and intermittent exposures were compared and found that there was no any statistical difference between them (p=0.093).

Table 1. Levels of TBARS (nmol/gr) in livers under 50 Hz magnetic field of 1.5 mT

GROUPS	n	TBARS (nmol/g tissue) mean ± sem
Control	6	79,32±3,65
Continuous Exposure	6	90,81±1,16
Intermittent Exposure	6	94,98±2,79

Discussion

Levels of TBARS were measured in livers to determine the lipid peroxidation which is one of the major factor in formation of oxidative stress.
We found significantly increased liver TBARS levels of guinea pigs which were exposed to 1.5 mT continuous (4 hours/day) and intermittent (2 hours on/ 2 hours off/ 2 hours on) exposures for 4 days compared with the control groups. This was in agrement with our previous studies in MDA (Coskun, 2006). We found statistically significant increases in liver MDA levels under the magnetic fields of 1mT (p=0.023) and 2 mT (p=0,027) with 4 hours of daily continuous exposure for 5 days These data reveal that increase of MDA levels as an indicator of lipid peroxidation may give rise to formation of oxidative stress in tissues.

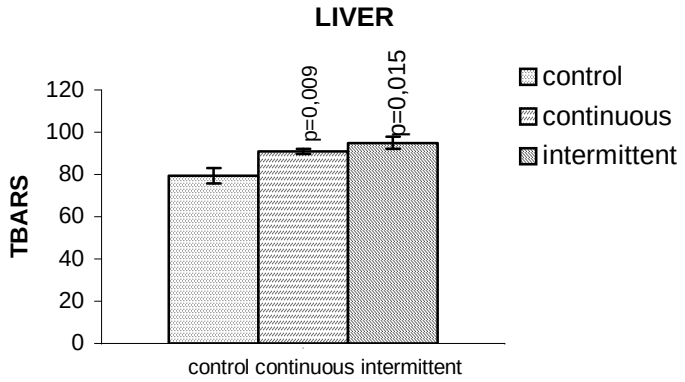


Figure 1. TBARS (nmol/g tissue) levels in liver of 1.5 mT exposed and control guinea pigs. Exposure was continous or intermittent for 4 days.

References

BASTUJI-GARİN S., RICHARDSON S., ZITTOUN R. (1990). Acute leukaemia in workers exposed to electromagnetic fields., *Eur. J. Cancer*., 26 : 1119-1120.

BOLAND A., DELAPIERRE D., MOSSAY D., DRESSE A., SEUTIN V. (2002). Effect of Intermittent and Contiuous Exposure to Electromagnetic Fields on Cultered Hippocampal Cells, Bioelectromagnetics, 23 : 97-105.

BROCKLEHURST B., MCLAUCHLAN KA. (1996). Free radical mechanism for the effects of environmental electromagnetic fields on biological systems., *Int. J. Radiat. Biol*., 69 : 3-24.

CANSEVEN, A.G., SEYHAN, N. (2005c). Design, installation and standardization of homogenous magnetic field systems for experimental animals IFMBE Proceedings, Vol. 11. Prague: IFMBE, 2005. ISSN 1727-1983. Editors: Jiri Hozman, Peter Kneppo (Proceedings of the 3rd European Medical&Biological Engineering Conference - EMBEC´05.Prague, Czech Republic, 20- 25.11.2005). pp: 2333-2338

CANSEVEN, A.G., OZEL U., BILGIHAN, A., SEYHAN, N. (2005b). Effects of environmental ELF magnetic fields on myeloperoxidase (MPO) activity. IFMBE Proceedings, Vol. 11. Prague: IFMBE, 2005. ISSN 1727-1983. Editors: Jiri Hozman, Peter Kneppo (Proceedings of the 3rd European Medical&Biological Engineering Conference - EMBEC´05. Prague, Czech Republic,20-25.11.2005). 2232-2236

CANSEVEN A. G., OZEL U., BILGIHAN A., SEYHAN N. (2004). Does ELF Magnetic Field Effect The Myeloperoxidase (MPO) Activity in the Lung., 11th International Congress of the International Radiation Protection Association, 23-28 May 2004, Madrid, Spain, ID 591

CANSEVEN, A.G., SEYHAN, N. (2005a). Effects of Ambient ELF Magnetic Fields: Variations In Collagen Synthesis of Guinea Pigs' Skin and Scaling From Animals To Human. *Gazi Medical Journal* 16 : 160 – 165 *(Turkish).*

CANSEVEN A. G., OZEL U., BILGIHAN A., SEYHAN N. (2003a). Myeloperoxidase (MPO) Activities in Brain, Lung and Renal Tissues After Exposure to Magnetic Fields of 50 Hz., 13th Balkan Biochemical Biophysical Days & Meeting on Metabolic Disorders, 12-15 October 2003, Kusadasi, TURKEY, P94

CANSEVEN A. G., OZEL U., BILGIHAN A., SEYHAN N. (2003a). The Effect of ELF Magnetic Field Exposure on Kidney Myeloperoxidase (MPO) Activity., 13th Balkan Biochemical Biophysical Days & Meeting on Metabolic Disorders, 12-15 October 2003, Kusadasi, TURKEY, 2003, P96

CANSEVEN, A.G., SEYHAN, N., MIRSHAHIDI, S., IMIR, T. (2006). Suppression of Natural Killer Cell Activity on *Candida Stellatoidea* by a 50 Hz Magnetic Field. *Electromagnetic Biology and Medicine,* 25 (2) : 79-85.

CASSINI A., F M, POMPELAM A, MAELLARO A, COMBORTI M. (1986). Lipid peroxidation and cellular damage in extrahepatic tissues of bromobenzene intoxicated mice., *Am J Pathol*; **123** : 520-31.

COSKUN, S., SEYHAN, N., CANSEVEN, A.G. (2006). Alterations induced in the lipid peroxidation levels of heart and liver tissues with ELF Magnetic Fields. International Conference and COST 281 Workshop on Emerging EMF Technologies, Potential Sensitive Groups and Health Graz, April 20/21.

FEYCHTING M., AHLBOM A. (1993). Magnetic fields and cancer in children residing near Swedish high-voltage power lines., *Am. J. Epidemiol*., 138 : 467-481.

GULER G., ATALAY SEYHAN N. (1995).The Interaction of Electric Field with Biological Systems I: Liver Hydroxyproline, *Gazi Medical Journal*, 6, 125-129.

GULER G., SEYHAN N., ARICIOGLU A. (2004). Effects of Electric Fields on Radical and Antioxidant Enzymes Levels in Spleen and Testis of Guinea Pigs, *Gazi Medical Journal* , 2, pp: 99-104.

HAKANSSON N., FLODERUS B., GUSTAVSSONB P., JOHANSEN C., OLSEN JH. (2002). Cancer incidence and magnetic field exposure in industries using resistance welding in welding in Sweden., *Occup. Environ. Med*., 59, pp: 481-486.

JAJTE J., ZMYSLONY M., PALUS J., DZIUBALTOWSKA, E., RAJKOWSKA, E. (2001). Protective effect of melatonin against in vitro iron ions and 7 mT 50 Hz magnetic field-induced DNA damage in rat lymphocytes., *Mutation Research*, 483, pp: 57-64.

JAJTE, J., GRZEGORCZYK J., ZMYSLONY, M., RAJKOWSKA (2002). Effect of 7 mT static magnetic field and iron ions on rat lymphocytes: apoptosis, necrosis and free radical processes., *Bioelectrochemistry*, 57, pp: 107-111.

KHADIR R., MORGAN JL., MURRAY JJ. (1999). Effects of 60 Hz magnetic field exposure on polymorphonuclear leukocyte activation., *Biochim Biophys Acta*, 1472, pp: 359-367.

KHEIFETS L. (2004). Childhood Leukemia and EMF, WHO EMF Project, Sensitivity of Children to EMF Exposure Workshop Proceedings, Istanbul.

KHEIFETS LI., AFIFI AA., BUFFLER PA., ZHANG ZW., MATKIN CC. (1997). Occupational electric and magnetic field exposure and leukemia. A meta-analysis., *J. Occup. Environ. Med*., 39, pp: 1074-1191.

KHEIFETS LI., AFIFI AA., BUFFLER PA., ZHANG ZW., MATKİN CC. (1995). Occupational electric and magnetic field exposure and brain cancer: a meta-analysis., *J. Occup. Environ. Med*., 37, pp: 1327-1341.

KULA B., SOBCZAK A., KUSKA R. (2000). Effects of static and ELF magnetic fields on free- radical processes in rat liver and kidney., *Electro and Magnetobiology*, 19 , pp: 99-105.

LAI H., SINGH NP. (2004). Magnetic field-induced DNA strand breaks in brain cells of the rat., *Environmental Health perspectives*, 112, 687-694.

LIBURDY, R.P. (1992). Biological interactions of cellular systems with time- varying magnetic fields. *Ann. N.Y. Acad. Sci*, 6, pp: 125-129.

LIBURDY, R.P., COLLAHAN DE., HASLAND J., DUNHAM E., SLOMA T. R., YASWEN P. (1993). Experimental evidence for 60 Hz magnetic fields operating through the signal transduction cascade. Effects on Calcium influx and C-MYC mRNA induction FEBS LETT. 334 pp:301-308.

LIN RS., DISCHINGER PC., CONDE J., FARRELL KP. (1985). Occupational exposure to electromagnetic fields and the occurrence of brain tumors. An analysis of possible associations., *J. Occup. Med*., 27, pp: 413-419.

PRESTON-MARTIN S., MACK W., HENDERSON BE. (1989). Risk factors for gliomas and meningiomas in males in Los Angeles County., *Cancer Res.*, 49, pp: 6137-6143.

SAVITZ DA., WACHTEL H., BARNES FA., JOHN EM., TVRDIK JG. (1988). Case-control study of childhood cancer and exposure to 60-Hz magnetic fields., *Am. J. Epidemiol*.,128, pp: 21-38.

WERTHEIMER N, SAVITZ DA, LEEPER E. (1995). Childhood cancer in relation to indicators of magnetic fields from ground current sources., *Bioelectromagnetics.*, 16, pp.:86-96.

WERTHEIMER N., LEEPER E. (1979). Electrical wiring configurations and childhood cancer., *Am. J. Epidemiol*., 109, pp:273-84.

INTERMITTENT EXPOSURE TO 50 HZ, 1.5 mT AND INCREASE IN NITRIC OXIDE (NO) LEVELS IN KIDNEY

AYSE G. CANSEVEN*, MEHMET Z. TUYSUZ*, SULE COSKUN** NESRIN SEYHAN*

DEPARTMENT OF BIOPHYSICS, GAZI UNIVERSITY, FACULTY OF MEDICINE,06510 BESEVLER ANKARA, TURKEY

**** DEPARTMENT OF BIOLOGY, GAZI UNIVERSITY, FACULTY OF ART AND SCIENCE, 06500 TEKNIKOKULLAR ANKARA, TURKEY***

canseven@gazi.edu.tr

Abstract

Reactive oxygen species (ROS) are constantly generated in small amounts during metabolic processes. Recent studies have demonstrated that electromagnetic fields (EMF) can cause increase in ROS formation and resulting oxidative stress. The aim of this study was to investigate the effects of continuous and intermittent exposure to a magnetic field (MF) on NOx levels in the kidneys in guinea pigs. A total of 18 male guinea pigs weighing 250-300 g were used. The subjects were divided into one control and two exposure groups which were continuously or intermittently exposed to 50 Hz MF of 1.5 mT with 4 hours daily exposure for 4 days. Determinations of NOx were performed by spectrophotometric methods. The Mann Whitney-U test was used in statistical analysis. Statistically significant increases in NOx level was found for the intermittent exposure to MF. These findings indicate that increased NOx levels may reflect formation of reactive nitrogen species following intermittent exposure to 50 Hz MF

Introduction

Recently, the concerns of people about the possible effects of the electromagnetic fields (EMF) on their health have been heightened with the increasing distribution and utilization of electrical machines, electronic equipments, broadcasting and telecommunication systems (Takebe, 1999). For this reason, most scientists have focused on the effects of EMF exposure on people's health and they have conducted several epidemiological and laboratory studies to define the risks of electromagnetic field exposures. Based on the results of these studies, there is growing evidence that electromagnetic fields, the power line frequency (50-60 Hz) and magnetic field (MF), may increase the risk of certain cancers, likely by a tumor-promoting / co – promoting effect. Long-term and as well as short-term electromagnetic field exposure can cause DNA damage and the risk of tumor development. Taking into consideration of the possible adverse effects of extremely low frequency (ELF) electric and magnetic field exposure, they have been recently classified as a possible carcinogens class 3 and 2B respectively, in NIEHS 1998 and IARC 2002 guidelines (Tuncel, 2003; Koifman, 1994; Parola, 1994).Especially, the cellular effects of ELF electric and magnetic field exposure have been investigated intensively. Studies have shown that EMF can induce cell proliferation, variations of calcium concentrations (Canseven, 1996; Canseven, 1999; Canseven, 2005a), alteration of DNA integrity, changes in transcription of immediate early genes and in protein synthesis (Boland, 2002; Ishisaka, 2000; Gold,1994; Canseven, 2005b) and perturbations of the central nervous system inducing behavioral disturbances in animals (Lai, 1996). In addition, EMF are also able to affect biological systems by increasing the level of free radicals produced by various oxidative stress (Boland, 2002). Oxidative stress is, a physiological condition characterized by an elevated level of oxygen free radical species that cause cellular damage and change vital functions and, is critically important for human health. Oxidative stress occurs due to increased production of reactive oxygen species (ROS) such as, super radical, hydrogen peroxide, and hydroxyl radical at the time of reperfusion, which in turn overwhelm the endogenous antioxidant defense (Narang, 2004). The increase in reactive oxygen species formation can cause the initiation of cumulative damage in the proteins, lipids and nucleic acids' structures. Actually, reactive oxygen species formations are related to the metabolic rate of an organism. In summary, there is a balance between reactive oxygen species formation and antioxidative defense which is important to maintain homeostasis within cells and tissues (Simko, 2004).

In the formation of Reactive Oxygen Species, one of the most important reactants is nitric oxide (NO). Nitric oxide (NO) can undergo numerous reactions as an endogenous mediator of numerous physiological processes. It has an important role in both oxidative stress and nitrosative stress. That is, NO can interact with ROS in many ways resulting in oxidative stress and it can also undergo many reactions that result in the formation of reactive nitrogen species (RNOS) which cause nitrosative stress. NO acts as biological messenger in many physiological processes and plays a role in pathogenesis of many disorders (Jelenkovic et al., 2006). It was suggested that nitric oxide synthase (NOS) activity or NO level could have a prognostic value, which may show the degree of EMF induced tissue damage (Noda et al., 2000; Ilhan et al., 2004; Ozguner et al., 2005).
In this study, the effect of continuous and intermittent exposure of 50 Hz, 1.5 mT magnetic field with the exposure period of 4 hours/day for 4 days on NOx levels was investigated.

Materials and Methods

Animals and Magnetic Field Exposure
The experimental protocol was reviewed and approved by the Laboratory Animal Care Committee of Gazi University (Report no : 39-5858). A total of 18 male, 250-300g weighted guinea pigs were used in this study. All animals were kept under laboratory conditions and fed standard pellet food.
Homogenous MF was generated by Helmholtz coils' system. The exposure system developed in our laboratory has been described in detail elsewhere (Canseven, 2005c).
Animals were divided into three groups, controls and two magnetic field exposure groups. Exposure groups were exposed to continuously (4 hours/day) or intermittently (2 hours on/ 2 hours off/ 2 hours on) to 50 Hz MF of 1.5 mT with the exposure periods of for 4 days. Controls were handled in an identical manner without being exposed to any magnetic field.
Following 12 h of starvation, guinea pigs were intramuscularly injected with combinations of ketamine (30 mg/kg), xylazine (2 mg/kg) and 250 IU/kg heparin. The kidney were sampled, shocked by liquid nitrogen and stored at -80°C until performing analysis. All experiments were run in a blinded manner.

Determination of NO Levels
NOx levels - stable end products of nitric oxide- in kidney tissues were measured by the Griess reaction (Green, 1982).
Tissue samples were homogenized in five volumes of phosphate buffer (pH= 7.5) and centrifuged at 2000x g for 5 min. to supernatants (0.5 ml) 0.25 ml of 0.3 M NaOH were added. After incubation for 5 min at room temperature, 0.25 ml of 10% (w/v) $ZnSO_4$ was added for deproteinization. This mixture was then centrifuged at 14000x g for 5 min and supernatants were used for the Griess assay.
Nitrate levels in tissue homogenates were determined spectrophotometrically, based on the reduction of nitrate to nitrite by VaCI3 (Miranda, 2001). Nitrite levels were measured by the Griess reaction. Sodium nitrite and nitrate solutions (1, 10, 50, 100 μM) were used as standards.

Statistics
Statistical analyses were carried out using SPSS software (SPSS 11.5 for windows, SPSS Inc., Chicago, USA). The p value was considered significant at $p<0.05$. The Mann Whitney-U test was used in statistical analysis.
Both comparisons between exposed groups and controls, and comparisons between intermittent and continuous exposed groups were made by using Mann Whitney-U test.

Results

In this study, guinea pigs were continuously or intermittently exposed to magnetic field of 1.5 mT with 4 hours daily exposure for 4 days and levels of NOx in kidney were determined. An increased level of NOx was found in intermittent exposed animals (385.58± 18.79) with respect to controls (302.42± 6.18). This increase was statistically significant (p=0.009).
Continuous and intermittent exposures were also compared. Significant difference (p=0.016) was determined between continuous and intermittent exposed groups. Although both of the exposures increased the levels of NOx, intermittent exposure was more effective than continuous exposure in this study (Table 1- Figure 1)..

Table 1. NOx levels (µmol/g) in kidney of guinea pigs under 50 Hz magnetic fields of 1.5 mT

KIDNEY	Total (µmol/gr) mean±sem
Control	30.,42 ± 6.18
Continuous Exposure	314.30 ± 10.71
Intermittent Exposure	385.58 ± 18.79

Discussion

NO (Nitric oxide), one of the primary indicators of ROS (reactive oxygen species) production, may contribute to the pathophysiology of EMF - induced renal impairment. It can also undergo many reactions that result in the formation of reactive nitrogen species (RNOS), which cause nitrosative stress. Nitrogen derived species (RNOS), most notably the $ONOO^-$ (peroxynitrite) and peroxynitrous acid (ONOOH) are likely involved in renal damage during oxidative stress in all tissues (Wink, 2000; Ozguner, 2005).

In this study, we found significantly increased NOx levels in kidneys under intermittent exposure to 50 Hz magnetic field of 1.5 mT.

Our results indicate that, intermittent magnetic field exposure may cause the change in renal functions with the high levels of reactive oxygen species production.

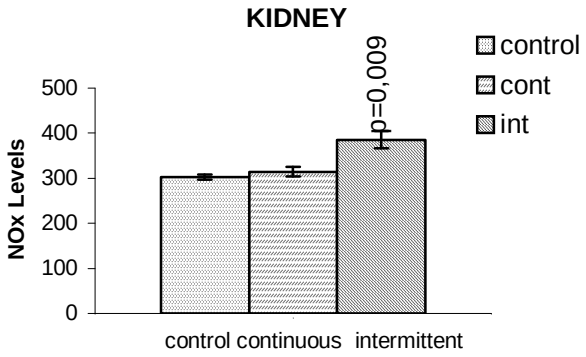


Figure 1. NOx levels (µmol/gr) in kidneys under 50 Hz magnetic fields of 1.5 mT.

References

Boland A., Delapierre D., Mossay D., Dresse A., Seutin V. (2002). Effect of Intermittent and Contiuous Exposure to Electromagnetic Fields on Cultered Hippocampal Cells., *Bioelectromagnetics*, 23:97-105.

Canseven A.G., Seyhan N., Aydin, A., Cevik, C., Isimer, A. (2005a). Effects of Ambient ELF Magnetic Fields: Variations in Electrolytes Levels of Brain and Blood Plasma, Gazi Medical Journal, 16: 121 – 127.

Canseven, A.G., Seyhan, N., Aydin, A., Isimer, A (1999). Extremely Low Frequency Electromagnetic Field Effect on Brain Tissue and Blood Plasma Electrolytes, *Med & Biol Eng & Comput.*, 37 (Suppl. 2): 1336-1337.

Canseven, A.G., Seyhan, N. (2005b). Effects of Ambient ELF Magnetic Fields: Variations In Collagen Synthesis of Guinea Pigs' Skin and Scaling From Animals To Human. *Gazi Medical Journal* 16 : 160 – 165 *(Turkish).*

Canseven, A.G., Seyhan, N. (2005c). Design, installation and standardization of homogenous magnetic field systems for experimental animals IFMBE Proceedings, Vol. 11. Prague: IFMBE, 2005. ISSN 1727-1983. Editors: Jiri Hozman, Peter Kneppo (Proceedings of the 3rd European Medical&Biological Engineering Conference - EMBEC´05.Prague, Czech Republic, 20- 25.11.2005). pp: 2333-2338

Canseven A. G., Seyhan N. (1996). Is it Possible to Trigger Collagen Synthesis by Electric Current in Skin Wounds?., *Indian Journal of Biochemistry & Biophysics*, 33, pp:223-227.

Gold S., Goodman R., Shirley-Henderson A., (1994). Exposure of Simian virus-40-Transformed Human Cells to Magnetic Fields Results in Increased Levels of T-Antigen mRNA and Protein., *Bioelectromagnetics*, 15:329-336.

Green LC, Wagner DA, Glogowski J, Skipper PL, Wishnok JS, Tannenbaum SR. (1982). Analyses of nitrate, nitrite and [^{15}N] nitrate in biological fluids. *Anal Biochem*, **126**: 131-8.

Guler G., Canseven A.G., Seyhan N., (1994). DC Electric Field Effect on Tissues Hydroxyproline Level., *Physics in Medicine & Biology*, 39a, pp:767.

Guler G., Seyhan N. (1996). Changes in Hydroxyproline Levels in Electric Field Tissue interaction. , *Indian Journal of Biochemistry & Biophysics*, 33, pp: 531-533.

Guler G., Seyhan N., (1996). The Effect of Vertical and Horizontal Electric Fields on Collagen Synthesis., *Progress in Biophysics& Molecular Biology* , 65:1, pp: 215.

Ilhan, A., Gurel, A., Armutcu, F., Kamisli, S., Iraz, M., Akyol, O., Ozen, S. (2004). Ginkgo biloba prevents mobile phone-induced oxidative stress in rat brain., *Clin Chim Acta.* 340: 153-162.

Ishisaka R., Kanno T., Inai Y., Nakahara H., Akiyama J., Yoshioka T., Utsumi K., (2000). Effects of a magnetic fields on the various functions of subcellular organelles and cells., *Pathophysiology*, 7:149-152.

Jelenkovic, A., Janac, B., Pesic, V., Jovanovic, D.M., Vasiljevic, I., Prolic, Z. (2006). Effects of extremely low-frequency magnetic field in the brain of rats.. *Brain Research Bulletin*. 68: 355-360.

Koifman S., Theriault G. (1994). Electric and Magnetic Fields and Cancer:the Use of Field Exposure Measurements in Epidemiological Studies.,Eds:Carpenter D.O., Ayrapetyan S.,"Biological Effects of Electric and Magnetic fields:Beneficial and Harmful Effects", Academic Press Inc.,California, pp.201-231,

Lai H. (1996). Spatial learning deficit in the rat after exposure to a 60 Hz magnetic field, Bioelectromagnetics, 17: 494-496.

Miranda KM, Espey MG, Wink DA. (2001). A rapid simple spectrophotometric method for simultaneous detection of nitrate and nitrite. Nitric Oxide, 5: 67-71.

Narang D., Sood S., Thomas M. K., Dinda A. K., Maulik S. K., (2004). Effect of dietary palm olein oil on oxidative stress associated with ischemic-reperfusion injury in isolated rat heart., *BMC Pharmacology* , 4:29.

Noda, Y., Mori, A., Liburdy, R.P., Packer L. (2000). Pulsed magnetic fields enhance nitric oxide synthase activity in rat cerebellum. *Pathophysiology.* 7: 127-130.

Ozguner F., Oktem F., Ayata A., Koyu A., Yilmaz H. R. (2005). A novel antioxidant agent caffeic acid phenethyl ester prevents long-term mobile phone exposure-induced renal impairment in rat: Prognostic value of malondialdehyde, N-acetyl-β-D-glucosaminidase and nitric oxide determination, *Molecular and Cellular Biochemistry*; 277: 73-80.

Parola A. H., Markel A. (1994). Electric and Magnetic Fields and Carcinogenesis, Eds:Carpenter D.O., Ayrapetyan S.,"Biological Effects of Electric and Magnetic fields:Beneficial and Harmful Effects", Academic Press Inc.,California, pp:177-197.

Simko M., Mattson M.O., (2004). Extremely Low Frequency Electromagnetic Fields as Effectors of Cellular Response In Vıtro: Possible Immune Cell Activation. *Journal of Cellular Biochemistry*, 93: 83-92.

Takebe H., Shiga T., Kato M., Masada E. (1999). Biological and Health Effects from Exposure to Power- line Frequency Electromagnetic Fields: Confirmation of Absence of Any Effects at Environmental Field Strengths. Ohmsa Ltd., Japan, pp:76-113,.

Tuncel H. "Effects of Electromagnetic Fields on the Immune System", Eds:Stavroulakis P. "Biological Effects of Electromagnetic Fields", Springer-Verlag Berlin Heidelberg New York 2003 pp: 503-544.

Wink D.A., Miranda K.M., Espey M.G., Mitchell J.B., Grisham M.B., Fukuto J., Feelish M. (2000). The chemical Biology of Nitric Oxide, Balancing Nitric Oxide with Oxidative and Nitrosative Stress.,Eds:Mayer B., Handbook of Experimental Pharmacology, Springer , pp:7-29.

EFFECTS OF CONTINUOUS EXPOSURE TO 50 Hz MAGNETIC FIELDS ON NITRIC OXIDE LEVELS IN LUNG

AYSE G. CANSEVEN[*], SULE COSKUN[**], NESRIN SEYHAN[*]

[*] DEPARTMENT OF BIOPHYSICS, GAZI UNIVERSITY, FACULTY OF MEDICINE, 06510 BESEVLER ANKARA, TURKEY
[**] DEPARTMENT OF BIOLOGY, GAZI UNIVERSITY, FACULTY OF ART AND SCIENCE, 06500 TEKNIKOKULLAR ANKARA, TURKEY
canseven@gazi.edu.tr

Abstract

Interest in researches on the health effects of extremely low frequency electromagnetic fields (ELF EMF) is rapidly growing. ELF EMF has been classified as 2B, possibly carcinogenic to humans, by the International Agency for Research on Cancer. It is believed that ELF EMF prolongs the life of free radicals and can act as a promoter or co-promoter of cancer**.** It is also known that magnetic fields cause an increase in free radicals activity in living organisms. Free radicals are very reactive and unstable molecular species that can initiate chain reactions to form new free radicals. In the present study, we investigated the effect of various magnetic fields on lung tissue damage resulting from oxidative stress by measuring nitric oxide (NOx) levels. Twenty-three guinea pigs were exposed to 50 Hz, 1 mT and 3 mT fields with the exposure periods of 4 hours/day and 8 hours/day for 5 days. Control subjects (n=9) were handled in an identical manner with the exposed animals in the same laboratory. NOx levels - stable end products of nitric oxide - in lung tissues were determined spectrophotometrically using he Griess reaction. For both of the application periods, increases in NOx level were found by the effect of 3 mT MF whereas increased NOx level was determined only for groups of 1 mT, 4 hours. Nitric oxide (NO) has play an important role related to ELF magnetic fields' exposure in lung tissue.

Introduction

In recent years, scientists have focused on the effects of electromagnetic fields (EMF) on living organisms in cellular levels. These major interests have been born of the overexposure of people to extremely low frequency (ELF) electromagnetic fields (EMF) with the increase of wide use of technological devices in their daily life. In many epidemiological and laboratory studies, it has been suggested that there is a link between ELF magnetic field exposure and the increased incidence of certain types of tumor, particularly in leukemia and brain cancer (Lin, 1985; Preston-Martin, 1989; Bastuji-Garin, 1990; Feychting, 1993; Wertheimer, 1979, 1995; Savitz, 1988;). A variety of EMF effects on biological and biochemical responses such as protein synthesis (Kenneth, 1987; Gold, 1994; Canseven, 2005b), gene expression, signal transduction and DNA damage (Liburdy, 1992, 1993; Jajte, 2001; Lai, 2004), immune system functions (Canseven, 2006; Seyhan, 2006; Walleczek, 1992; De Seze, 1993; Blumenthal, 1997; House, 2000, 1996; Tremblay, 1996), apoptosis induction (Blumenthal, 1997; Jajte, 2002), enzyme regulation (Canseven, 2003a, Canseven, 2003b; Canseven, 2004; Canseven, 2005a, Brocklehurst, 1996), free radical activity (Kula, 2000; Kula, 2002; Roy, 1995; Khadir, 1999; Simko, 2001; Sboczak, 2002; Yokus, 2005; Watanabe, 1997; Fiorani, 1997; Mohtat, 1998; Kashkalda, 1995; Jin, 1998) have been described in the reports of many in vivo and/or in vitro experiments. Magnetic fields penetrate the cells and can alter cell membrane potential and the concentration of ions (Canseven, 1999; Canseven, 2005c; Garcia-Sancho, 1994). These alterations may affect free radical processes within the cell. EMF could be also able to affect biological systems by increasing the amount of free radical produced by various oxidative stress (Boland, 2002). ELF EMF has been thought to prolong the life of free radicals and can act as a promoter or co-promoter of cancer (Yokus, 2005). Free radicals, which are known as reactive oxygen species (ROS) are continuously formed in small amounts in biological systems. Depending on the oxygen consumption, the production of ROS increases; however there is a balance between ROS formation and antioxidant defense within cells and tissues. In the case of increase in the formation of ROS, it has been seen the initiation cumulative damage to proteins, lipids and nucleic acids and various physiological conditions, like oxidative stress has been observed. There are many factors, which cause the formation of oxidative stress; among them ROS production is one of the most important.
Nitric oxide (NO) can undergo numerous reactions as an endogenous mediator of numerous physiological

processes. NO plays an important role in both oxidative stress and nitrosative stress.
Taking into consideration the activation of free radicals in biological systems, the behavior of free radicals was investigated. NOx levels were measured in lung tissues of guinea pigs exposed to 50 Hz, 1 mT and 3 mT fields with the exposure periods of 4 hours/day and 8 hours/day for 5 days to determine the effects of electromagnetic fields on ROS production.

Materials and Methods

Animals

The experimental protocol was reviewed and approved by the Laboratory Animal Care Committee of Gazi University (Report no: 36-7838). A total of 32 male guinea pigs weighing between 250 and 300g were used in this study. All animals were kept under laboratory conditions and fed standard pellet food.

Magnetic Field Exposure

50 Hz magnetic field was produced by 42.75 cm diameter Helmholtz coil with winding embedded in an open wooden circular frame (Canseven, 2005d). Each coil was constructed by insulated copper wire and made of 154 turns. To feed the coils, sinusoidal current of frequency 50 Hz was supplied by a specially designed variable transformer, 2.7 kVA (kilo Volt Amper) in power. Magnetic field at the center of exposure system was measured by a Hall-Effect Gaussmeter. Frequency and wave form of the magnetic field were monitored over an ossiloscope. The animal cage without magnetic material was put at the center.
Twenty-three guinea pigs were exposed to 50 Hz, 1 mT and 3 mT fields with the exposure periods of 4 hours/day and 8 hours/day for 5 days. Control subjects (n=9) were handled in an identical manner with the exposed animals in the same laboratory.
Following 12 h of starvation, guinea pigs were injected intramuscularly with ketamine (30 mg/kg) and xylazine (2 mg/kg) combined with 250 IU/kg heparin. Lungs were sampled immediately. They shocked by liquid nitrogen and stored in deep freezer at -80°C until performing analysis. All experiments were run in a blind manner.

Determination of NO Levels

NOx levels - stable end products of nitric oxide- in lung tissues were determined by the Griess reaction (Green et al., 1982).
Tissue samples were homogenized in five volumes of phosphate buffer (pH= 7.5) and centrifuged at 2000 x *g* for 5 min. to supernatants (0.5 ml) 0.25 ml of 0.3 M NaOH were added. After incubation for 5 min at room temperature, 0.25 ml of 10% (w/v) $ZnSO_4$ was added for deproteinization. This mixture was then centrifuged at 14000 x *g* for 5 min and supernatants were used for the Griess assay.
Nitrate levels in tissue homogenates were determined spectrophotometrically, based on the reduction of nitrate to nitrite by $VaCI_3$ (Miranda et al., 2001). Nitrite levels were measured by the Griess reaction. Sodium nitrite and nitrate solutions (1, 10, 50, 100 μM) were used as standards.

Statistics

Statistical analyses were carried out using SPSS software (SPSS 11.5 for windows, SPSS Inc., Chicago, USA). The p value was considered significant at $p<0.05$.

Mann Whitney-U and Kruskal-Wallis tests were used in statistical analysis. Comparisons between exposed groups and controls were made by using Mann Whitney-U test while magnetic fields of 1mT and 3 mT were compared with Kruskal-Wallis test with respect to exposure periods of 4 hours and 8 hours.

Results

In this study, the NOx level was investigated in lung tissues of guinea pigs which were exposed to magnetic fields of 1mT and 3 mT with the exposure periods of 4 hours/day and 8 hours/day for 5 days. For both of the application periods, NOx levels were found increased with respect to controls in lung tissues of guinea pigs exposed to both of the magnetic fields (Table 1- Figure 1).
The increases in NOx levels were found statistically significant for 1 mT, 4 hours ($p=0.003$), 3 mT, 4 hours ($p=0.001$) and 3 mT, 8 hours ($p=0.000$) in lung tissues by Mann-Whitney U test.
Field intensities were compared with respect to exposure periods by Kruskal-Wallis test. Significant differences were determined between field intensities of 1 mT and 3 mT in lung tissues for only exposure period of 8 hours ($p=0.004$).

Table 1. Lung NOx levels of guinea pigs under the effects of 50 Hz magnetic fields of 1 mT and 3 mT with the exposure periods of 4 hours/day and 8 hours/day for 5 days.

GROUPS	n	NO_x Level (µmol/g tissue) (mean ± sem)
Control	9	103.61 ± 3.80
1 mT; 4 hours	4	141.65 ± 3.61
1 mT; 8 hours	4	110.78 ± 1.40
3 mT; 4 hours	7	133.31 ± 4.90
3 mT; 8 hours	8	131.99 ± 3.08

Discussion

For both of the exposure periods, significant increases in NOx levels were found by the effect of 3 mT magnetic field whereas increased NOx levels were found only for groups of 1 mT, 4 hours.
TBARS levels in the same tissue for the same exposure conditions were also investigated in our laboratory (Canseven 2005e). The increased NOx levels in lung for 1 mT, 4 hours and 3 mT, 4 hours was found consistent with the increases of TBARS in these tissues.
Further studies are required to better elucidate the mechanisms of the effect of ELF MFs on lipid peroxidation or oxidative stress in tissues.

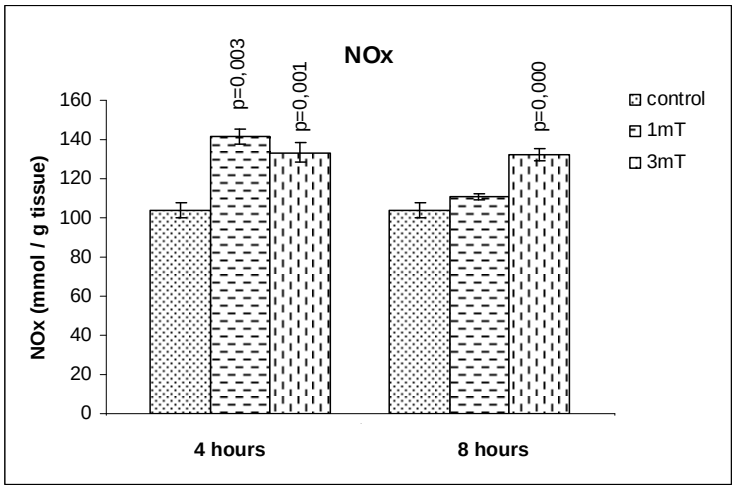


Figure 1. Lung NOx levels of 1 mT and 3 mT exposed and control guinea pigs.

References

BASTUJI-GARIN S., RICHARDSON S., ZITTOUN R. (1990). Acute leukaemia in workers exposed to electromagnetic fields, *Eur. J. Cancer*., 26 : 1119-1120.

BLUMENTHAL NC., RICCI J., BREGER L., ZYCHLINSKY A., SOLOMON H., CHEN GG., KUZNETSOV D., DORFMAN R. (1997). Effects of Low Intensity AC and/or DC Electromagnetic Fields on Cell Attechment and Induction of Apoptosis, *Bioelectromagnetics*, 18 : 264-272.

BOLAND A., DELAPIERRE D., MOSSAY D., DRESSE A., SEUTIN V. (2002). Effect of Intermittent and Contiuous Exposure to Electromagnetic Fields on Cultered Hippocampal Cells, Bioelectromagnetics, 23:97-105.

BROCKLEHURST B., MCLAUCHLAN KA. (1996). Free radical mechanism for the effects of environmental electromagnetic fields on biological systems., *Int. J. Radiat. Biol*., 69:. 3-24 .

CANSEVEN A.G., SEYHAN N., AYDIN, A., CEVIK, C., ISIMER, A. (2005c). Effects of Ambient ELF Magnetic Fields: Variations in Electrolytes Levels of Brain and Blood Plasma, *Gazi Medical Journal*, 16: 121 – 127.

CANSEVEN AG., OZEL U., BILGIHAN A., and SEYHAN N (2004). Does ELF Magnetic Field Effect The Myeloperoxidase (MPO) Activity in the Lung', 11th International Congress of the International Radiation Protection Association, 23-28 May 2004, Madrid, Spain, ID 591

CANSEVEN AG., SEYHAN N., AYDIN A., ISIMER A. (1999). Extremely Low Frequency Electromagnetic Field Effect on Brain Tissue and Blood Plasma Electrolytes., *Med & Biol Eng & Comput*, 37 : 1336-1337.

CANSEVEN, A.G., COSKUN, S., SEYHAN, N. (2005e). ELF magnetic fields' effecst on lipid peroxidation in lung and kidney. IFMBE Proceedings, Vol. 11. Prague: IFMBE, 2005. ISSN 1727-1983.Editors: Jiri Hozman, Peter Kneppo (Proceedings of the 3rd European Medical & Biological Engineering Conference - EMBEC´05. Prague, Czech Republic, 20-25.11.2005). pp: 4748-4752

CANSEVEN, A.G., OZEL U., BILGIHAN, A., SEYHAN, N. (2005a). Effects of environmental ELF magnetic fields on myeloperoxidase (MPO) activity. IFMBE Proceedings, Vol. 11. Prague: IFMBE, 2005. ISSN 1727-1983. Editors: Jiri Hozman, Peter Kneppo (Proceedings of the 3rd European Medical&Biological Engineering Conference - EMBEC´05. Prague, Czech Republic,20-25.11.2005). pp: 2232-2236

CANSEVEN, A.G., OZEL, U., BILGIHAN, A., SEYHAN, N. (2003a). Myeloperoxidase (MPO) Activities in Brain, Lung and Renal Tissues After Exposure to Magnetic Fields of 50 Hz. *13th Balkan Biochemical Biophysical Days & Meeting on Metabolic Disorders*, October 12-15, 2003, Kusadası, TURKEY, P94 (Abstract)

CANSEVEN, A.G., OZEL, U., BILGIHAN, A., SEYHAN, N. (2003b). The Effect of ELF Magnetic Field Exposure on Kidney Myeloperoxidase (MPO) Activity, *13th Balkan Biochemical Biophysical Days & Meeting on Metabolic Disorders*, October 12-15, 2003, Kusadası, TURKEY, P96 (Abstract)

CANSEVEN, A.G., SEYHAN, N. (2005b). Effects of Ambient ELF Magnetic Fields: Variations In Collagen Synthesis of Guinea Pigs' Skin and Scaling From Animals To Human. *Gazi Medical Journal* 16 : 160 – 165 *(Turkish)*.

CANSEVEN, A.G., SEYHAN, N. (2005d). Design, installation and standardization of homogenous magnetic field systems for experimental animals IFMBE Proceedings, Vol. 11. Prague: IFMBE, 2005. ISSN 1727-1983. Editors: Jiri Hozman, Peter Kneppo (Proceedings of the 3rd European Medical&Biological Engineering Conference - EMBEC´05.Prague, Czech Republic, 20- 25.11.2005). pp: 2333-2338.

CANSEVEN, A.G., SEYHAN, N., MIRSHAHIDI, S., IMIR, T. (2006). Suppression of Natural Killer Cell Activity on *Candida Stellatoidea* by a 50 Hz Magnetic Field. *Electromagnetic Biology and Medicine*, 25 (2) : 79-85.

DE SEZE R., BOUTHET C., TUFFET S., DESCHAUX P., CARISTAN A., MOREAU JM., VEYRET B. (1993). Effects of Time-Varying Uniform Magnetic Fields on Natural Killer Cell Activity and Antibody Response in Mice., *Bioelectromagnetics*, 14: 405-412.

FEYCHTING M., AHLBOM A. (1993). Magnetic fields and cancer in children residing near Swedish high-voltage power lines., *Am. J. Epidemiol*., 138 : 467-481.

FIORANI M., BIAGIARELLI B., VETRANO F., GUIDI G., DACHA M., STOCCHI V. (1997). In vitro effects of 50 Hz magnetic fields on oxidatively damaged rabbit red blood cells, *Bioelectromagnetics*.,18:. 125-131

GARCIA-SANCHO J., MONTERO M., ALVAREZ J., FONTERIZ RI., SANCHEZ A (1994). Effects of Extremely Low Frequency Electromagnetic Fields on Ion Transport in Several Mammalian Cells., *Bioelectromagnetics*, 15 : 579-588.

GOLD, S., GOODMAN R., HENDERSON, A.S. (1994). Exposure of Simian Virus-40-Transformed Human Cells to Magnetic Fields Results in Increased Levels of T-Antigen mRNA and Protein', *Bioelectromagnetics*, 15: 329-336.

GREEN LC, WAGNER DA, GLOGOWSKI J, SKIPPER PL, WISHNOK JS, TANNENBAUM SR. (1982). Analyses of nitrate, nitrite and [^{15}N] nitrate in biological fluids. *Anal Biochem* 126: 131-8.

HOUSE, R. V., MCCORMİCK, D. L. (2000). Modulation of natural killer cell function after exposure to 60Hz magnetic fields: confirmation of the effect in mature B6C3F1 mice. *Radiation Res.* 153:722–724.

HOUSE, R. V., RATAJCZAK, H. V., GAUGER, J. R., JOHNSON, T. R., THOMAS, P. T., MCCORMİCK, D. (1996). Immune function and host defense in rodents exposed to 60Hz magnetic fields. *Fund. Appl. Toxicol.* 34:228–239.

JAJTE J., ZMYSLONY M., PALUS J., DZIUBALTOWSKA, E., RAJKOWSKA, E (2001). Protective effect of melatonin against in vitro iron ions and 7 mT 50 Hz magnetic field-induced DNA damage in rat lymphocytes, *Mutation Research*, 483 : 57-64.

JAJTE, J., GRZEGORCZYK J., ZMYSLONY, M., RAJKOWSKA (2002). E.Effect of 7 mT static magnetic field and iron ions on rat lymphocytes: apoptosis, necrosis and free radical processes, *Bioelectrochemistry*,

57, pp. 107-111
JIN Y., WANG H., CHENG Y., GU H (1998). Effects of static magnetic fields on free radical metabolism of human body., *Wei Sheng Yan Jiu*., 27: 97-99.
KASHKALDA DA., PASHENKO EA., ZİUBANOVA LF. (1995). Effects of an impulse magnetic field on lipid peroxidation and the antioxidant system of the testes in animal experiments, *Med Tr Prom Ekol*., 10: 14-17.
KENNETH JM., LEE RC., EHRLICH, HP. (1987). Frequency Dependence of Electric Field Modulation of Fibroblasts Protein Synthesis, *Science*, 236, pp. 1465-1469.
KHADIR R., MORGAN JL., and MURRAY JJ. (1999). Effects of 60 Hz magnetic field exposure on polymorphonuclear leukocyte activation, *Biochim Biophys Acta*, 1472: 359-367.
KULA B., SOBCZAK A., and KUSKA R. (2002). Effects of electromagnetic field on free radical processes in steelworkers.Part I. Magnetic field influence on the antioxidant activity in red blood cells and plasma, *J. Occup Health*, 44: 226-229.
KULA B., SOBCZAK A., KUSKA R. (2000). Effects of static and ELF magnetic fields on free- radical processes in rat liver and kidney., *Electro and Magnetobiology*, 19 : 99-105.
LAI H., SINGH NP (2004). Magnetic field-induced DNA strand breaks in brain cells of the rat, *Environmental Health perspectives*, 112 : 687-694.
LIBURDY RP., CALLAHAN DE., HARLAND J., DUNHAM E., SLOMA TR., YASWEN P. (1993). Experimental evidence for 60 Hz magnetic fields operating through the signal transduction cascade. Effects on calcium influx and c-MYC mRNA induction., *FEBS LETT*., 334: 301-308.
LIBURDY, R.P. (1992). Biological interactions of cellular systems with time-varying magnetic fields,, *Ann .N.Y. Acad. Sci*., 649: 74-94.
LIN RS., DISCHINGER PC., CONDE J., FARRELL KP. (1985). Occupational exposure to electromagnetic fields and the occurrence of brain tumors. An analysis of possible associations., *J. Occup. Med*., 27: 413-419.
MIRANDA KM, ESPEY MG, WINK DA. (2001). A rapid simple spectrophotometric method for simultaneous detection of nitrate and nitrite. *Nitric Oxide* 5: 67-71.
MOHTAT N., COZENS FL., HANCOCK-CHEN T., SCAİANO JC., MCLEAN J., KİM J. (1998). Magnetic field effects on the behavior of radicals in protein and DNA environments., *Photochem Photobiol*, 67 : 111-118.
PRESTON-MARTIN S., MACK W., HENDERSON BE. (1989). Risk factors for gliomas and meningiomas in males in Los Angeles County., *Cancer Res*., 49 : 6137-6143.
ROY S., NODA Y., ECKERT V., TRABER MG., MORI A., LIBURDY R., PACKER L. (1995). The phorbol 12-myristate 13-acetate (PMA)-induced oxidative burst in rat peritoneal neutrophils is increased by a 0.1 mT (60 Hz) magnetic field, *FEBS Letters*, 376 : 164-166.
SAVİTZ DA., WACHTEL H., BARNES FA., JOHN EM., TVRDİK JG. (1988). Case-control study of childhood cancer and exposure to 60-Hz magnetic fields., *Am. J. Epidemiol*.,128 : 21-38.
SBOCZAK A., KULA B., AND DANCH A (2002). Effects of electromagnetic field on free radical processes in steelworkers. Part II: Magnetic influence on vitamin A, E and Selenium concentrarions in plasma., *J. Occup health*., 44 : 230-233.
SEYHAN N., CANSEVEN A. G., GULER G. (2006). Animal Studies on the Effects of ELF and Static EMF. In Ayrapetyan S.N., Markov M.S., eds. *Bioelectromagnetics Current Concepts, The Mechanisms of the Biological Effect of Extremely High Power Pulses* . NATO Security through Science Series B: Physics and Biophysics, Vol. 5, pp: 195-212.
SIMKO M., DROSTE S., KRIEHUBER R., WEISS DG. (2001). Stimulation of phagocytosis and free radical production in murine macrophages by 50 Hz electromagnetic fields.', *Eur J Cell Biol*, 80 : 562-566.
TREMBLAY, L., HOUDE, M., MERCİER, G., GAGNON, J., MANDEVİLLE, R. (1996). Differential modulation of natural and adaptive immunity in Fisher rats exposed for 6 weeks to 60Hz linear sinusoidal continuous-wave magnetic fields. *Bioelectromagnetics* 17: 373–383.
WALLECZEK J. (1992). Electromagnetic field effects on cell of the immune system: the role of calcium signaling. *FASEB J.*, 6 : 3177-3185.
WATANABE Y., NAKAGAWA M., MİYAKOSHİ Y (1997). Enhancement of lipid peroxidation in the liver of mice exposed to magnetic fields, *Ind. Health*., 35 : 285-290.
WERTHEIMER N, SAVITZ DA, LEEPER E. (1995). Childhood cancer in relation to indicators of magnetic fields from ground current sources., *Bioelectromagnetics*., 16 : 86-96.
WERTHEIMER N., LEEPER E. (1979). Electrical wiring configurations and childhood cancer., Am. *J. Epidemiol*., 109 : 273-84.
YOKUS B., CAKIR DU., AKDAG MZ., SERT C., METE N (2005). Oxidative DNA damage in rats exposed to extremely low frequency electro magnetic fields, *Free. Radic. Res*., 39: 317-323.

A DOUBLE LAYER ARTERIAL WALL MODEL UNDER PULSATING BLOOD PRESSURE

MONA A. EL-NAGGAR

DEPT. OF ENGINEERING PHYSICS, FACULTY OF ENGINEERING, CAIRO UNIVERSITY, GIZA, EGYPT

Abstract

The behavior of a double layer arterial section of unit length is studied under the effect of radial pressure. The proposed model considers that the radial pressure follows an exponential rise exponential decay biphasic periodic function mathematically represented by a Fourier series. The dependence of the arterial strain response on viscoelastic properties of each layer is studied. The dissipated and stored power per unit length of the vessel, are computed. The stress-strain response is modeled for each layer. Storage and loss moduli are deduced as well**.**

Introduction

The study of the viscoelastic properties and response of the blood vessels have been one of the most important and biomechanical field of research for quite a while. This study represents an essential step towards controlling the efficiency of the blood pulse propagation process. The blood pulse propagates along the axis of the blood vessels, namely arteries, with a radial component pulsating on the inner wall. This propagation is similar to the propagation of waves in media. The arterial pulse is considered as a pressure wave travelling down the multilayer wall associated with a strain wave. The arterial strain response is the main issue here as it can be considered as an energy storage element that pushes the blood spurts forward down the artery. The rigidity or distensibility of the arteries causes the pressure to be very high during systole and it would fall to low values during diastole. The blood flow as a result of this would be intermittent. Furthermore, the reduced distensibility of the arterial wall has a direct effect on the efficiency of the heart markedly increasing its oxygen consumption making its attack more likely. It is thus extremely important to simulate the pressure wave propagation and its pulsating radial component. The problem is complicated not only because of the non-linearity in blood vessels elasticity, but because of the varying nature of the pulse wave as well. The anisotropic, multilayer and nonlinear viscoelastic properties of the arterial walls lead to certain mathematical complications when the radial dimensions are considered under the effect of pulsating pressure.

Previous work was concerned with mechanical and mathematical simulation to produce stress-strain relation for different soft tissues. Yu Q. et al. [1] evaluated the force-deformation relations for different layers of blood vessels by studying the non axis symmetric deformation of the vessel wall. This was done by imposing bending on the vessel. Young's modulus is given for the intima media and the adventitial layers of the thoracic artery. The circumferential stretch and axial stretch of abdominal arteries are given for different pressure values by Schulz-Bauer et al. [2] for both normal and hypertensive patients. They proposed a method to determine nonlinear constitutive models for human arteries from clinical data using a strain energy function. Mechanical properties are obtained by reliable experimental setups especially for different arterial layers, collagen and body tissues [3]. The degree of nonlinearity and blood vessel elasticity was studied by J. Zhou and Y. C. Fung [4] introducing a pseudo strain energy function and fitting experimental data to produce its parameters. Furthermore the relationship between wall shear stress and intimal thickening for the abdominal aorta was determined by Micheal Bonert et al. [5], who measured experimentally the wall shear stress using the laser photochromic dye tracer technique.

Imaging the mechanical properties of thrombosis, plaques and arterial wall can aid in the characterizing and understanding of the pathogenesis of the cardiovascular disease. Intravascular ultrasound is a widely used method of imaging the coronary arteries. Strain and elasticity images are generated to determine mechanical properties of arterial tissues [6], [7], [8]. Toshiaki Shishido *et al.* developed a new technique by applying minute vibrations at various frequencies to evaluate regional myocardial elastance and Young,s moduli at different

regions [9]. Blood flow and pressure in the larger systemic arteries are modelled by structuring a tree attached to the terminal branches in which the root impedance is estimated using an approach based on a linearization of the viscous axisymmetric Navier-Stokes equations[10].

In the present work, periodic pressure pulses are assumed to act in a radial direction on the inner wall of an arterial section. The periodic pulses are represented mathematically by a Fourier series. These pulses are considered to fluctuate between maximum values of a fraction of the mean arterial pressure. They approximately follow the known shape of the arterial pulse. Though the *in vivo* reported arterial pulses show faster rise than decay [11], we assume here that they are symmetric pulses. Biaxial symmetry of the artery is assumed as well. The radial pressure pulses are assumed to follow the heart beats with the same frequency. Some of the reported values concerning mechanical responses of arteries [1], [2], [3], [12] are adopted.

An R-L-C double section series circuit is proposed to simulate the double layer arterial wall. The flow of electric charge in the circuit is analogous to the strain fluctuations, the input voltage to the radial pressure pulses and the current is the pulse velocity. Parameters required to implement the mathematical model at hand are changed in appropriate ranges to show arterial stiffness, pulse damping, variation of the elasticity constant and heat loss.

The Model

A simplified model, introduced earlier [13], simulates the viscoelastic behaviour of a single layer blood vessel in response of the blood pulses acting in a radial direction on its inner wall. The proposed double layer arterial section is modelled as shown in Fig. 1.

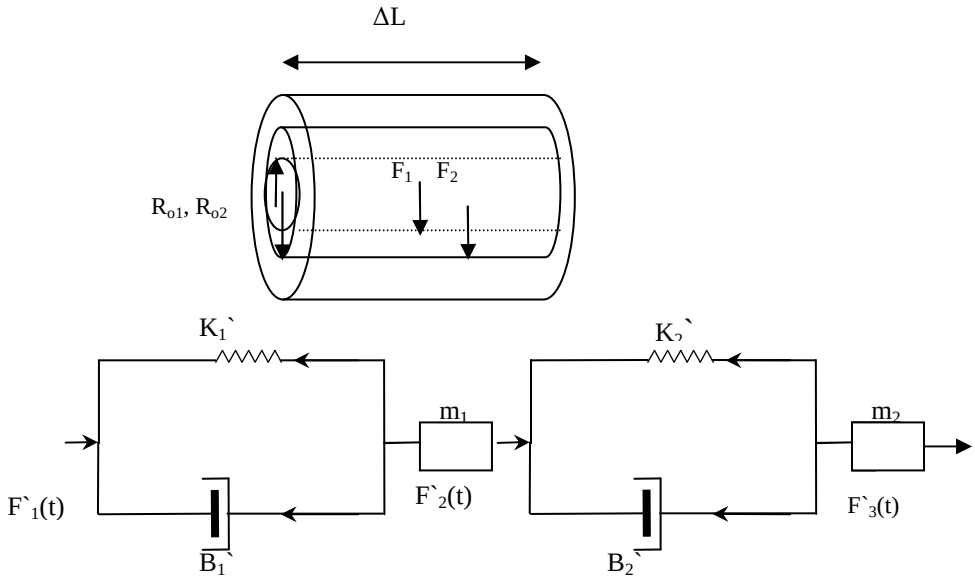


Fig.1. Double layer mechanical model

A section of unit length of the artery is assumed to be a double layer viscoelastic cylindrical tube. The inner layer is assumed to be the intima media layer with elasticity modulus, E_1, while the outer one is the adventitial layer with E_2 . The inner radii of the two layers are R_{01} and R_{02} .The elastic behaviour of the artery segment is represented by that of a spring with spring constants, K_1`and $K_2$` while its viscous component is represented by a dash pot of friction coefficients B_1` and $B_2$` for the first and second layers respectively.

The second degree differential equation that governs the strain functions, $\varepsilon_1(t)$ and $\varepsilon_2(t)$ of the interface of the two layers and the inertial forces on them is as follows:

$$\frac{d^2\varepsilon_1(t)}{dt^2} = F_1(t) - B_1\frac{d\varepsilon_1(t)}{dt} - K_1\varepsilon_1(t)$$
$$\frac{d^2\varepsilon_2(t)}{dt^2} = F_2(t) - B_2\frac{d\varepsilon_2(t)}{dt} - K_2\varepsilon_2(t) \qquad (1)$$

where $B_1=B_1`/\rho_{\ell 1}$ , $K_1=K_1`/\rho_{\ell 1}$, $B_2=B_2`/\rho_{\ell 2}$ , $K_2=K_2`/\rho_{\ell 2}$, are normalized viscosity and elasticity coefficients to the linear mass densities, $\rho_{\ell 1}$, $\rho_{\ell 2}$ for inner and outer layers respectively. $F_1(t)$ is defined as the normalized radial component of the force due to blood pressure pulses, $P_1(t)$, pulsating on the inner layer such that:

$$F_1(t) = 2\pi P_1(t) / \rho_{\ell 1} \qquad F_2(t) = 2\pi P_2(t) / \rho_{\ell 2} \tag{2}$$

Mathematical Analysis

Firstly, $P_1(t)$ is assumed to take the waveform of a biphasic exponential rise exponential decay periodic function, given below:

$$P_1(t) = \begin{cases} P_o(1-2e^{-t\pi/T}) & 0 \le t \ge T \\ P_o(2e^{-\pi(t-T)/T} - 1) & T \le t \ge 2T \end{cases} \tag{3}$$

The proposed model assumes the same time interval, T, for the rise and decay pulse components and hence equal decay constants. It is assumed that the pulses fluctuate between equal values $\pm P_o$.

A Fourier series is deduced to represent $P_1(t)$. The coefficients of the Fourier series, produced by integration on the two time intervals given in eq.(3), give a final form of:

$$P_r(t) = \frac{2}{\pi} P_0 \sum_{n=1}^{\infty} \frac{(e^{-\pi}(\cos n\pi - 1) - (\cos n\pi + 1))\cos \frac{n\pi t}{T}}{+\frac{1}{n}(e^{-\pi}(\cos n\pi - 2) - (\cos n\pi + 1))\sin \frac{n\pi t}{T} - \frac{1}{n} e^{-\pi} \cos n\pi} \tag{4}$$

Fig. 2 shows the pressure periodic waveform. The maximum value P_0, is assumed to be a 10% of the mean arterial pressure in adults.

s

Fig. 2. The figure shows a simulation of the rise and fall of the radial pressure in Pa

An equivalent electrical model, introduced as a double R-L-C series circuit, is analogous to the mechanical model above. We give full analogy between the mechanical system and the equivalent electrical circuit in details in appendix 1. We should note that the stress on each layer is the difference in pressures on the lining interfaces. Thus the stress on the inner layer, T_1, is difference in pressure, P_1-P_2, and the stress, T_2, on the outer layer is P_2-P_3, where P_1 is the pressure on the inner wall, P_2 on the interface between the two layers and P_3 is that on the outer wall.

Consequently, the strain is calculated as:

$$\epsilon_1(t) = q_1 - q_2$$
$$\epsilon_2(t) = q_2 - q_3 \tag{5}$$

where q_1, q_2 and q_3 are related to the respective currents in the equivalent electric circuit as follows:

$$q_1(t) = \int_0^t i1(t)\,dt, \quad q_2(t) = \int_0^t i2(t)\,dt, \quad q3(t) = \int_0^t i3(t)\,dt \tag{6}$$

Since P_1, P_2 and P_3 are analogous with V_1, V_2 and V_3, thus we can deduce the involved quantities in the *s*-domain as follows:

$$I_1(s) = Y_{eq}(s) V_1(s) \tag{7}$$

where Y_{eq} represents the total admittance of the two circuit section.

$$V_2(s) = V_1(s) - I_1(s)(R_1 + \frac{1}{sc_1})$$
$$V_3(s) = V_2(s) - I_3(s)(R_2 + \frac{1}{sc_2}) \quad (8)$$

Results

The stress and the strain waveform for each layer can be produced by eqs.(5-8). Strain pulses follow those of the applied radial pressure having the same frequency with a time delay. They fluctuate between equal values of $\pm \epsilon_0$.

Taking the strain response to be the difference between strains of boundary interfaces, results are given for different parameter sets in Table 1. The periodic time for one pressure pulse is 1s.

The first parameter set, is a simulation of normal performance with elasticity constants close to those of intima media and advetitia layers of real arteries.



Fig.3. The stress waveform acting on the inner layer real and imaginary components in kPa vs. time in s



Fig.4. The strain waveform acting on the inner layer real and imaginary components vs. time in s



Fig.5. The stress waveform acting on the second layer, real and imaginary components in kPa vs. time in s



Fig.6. The strain waveform acting on the second layer, real and imaginary components vs. time in s

Figures 3 and 4 show the stress-strain response for the inner layer, intima media; whereas, Figs. 5 and 6 show the stress-strain response for the adventitia, outer layer. They show elastic response of about 3%, which is much higher than the inner layer. This is taken into account by parameters adjustment

Table 1. Normalized Parameter sets used as input for computer runs.

set	K_1 10^6 s^{-2}	K_2 10^6 s^{-2}	ϵ_{01r} 10^{-3}%	ϵ_{01i} 10^{-3}%	ϵ_{02r} %	ϵ_{02i} %	P_{diss} *w*/m	P_{str} *w*/m
1	8	0.05	3	0.03	3	2	83.850	101.640
2	4	0.8	0.5	0.008	0.4	0.4	13.775	19.7611
3	0.4	.02	0.1	8	6	6	1502.75	2486.04

For all sets P_0 and T are kept constant at 1.6 kPa and 0.5s respectively. $\rho_{\ell 1}$, $\rho_{\ell 2}$ are kept at 25*g/m* and 12*g/m* and B_1, B_2 have the values $0.4s^{-1}$ and $0.417s^{-1}$ respectively.

Fig. 7 shows the computed power versus time. The real component, P_{diss}, corresponds to the energy loss per second while the imaginary component represents the stored energy per second, P_{str}. The average values of the power dissipated and that stored, measured in *w/m*, computed over one pressure pulse for each set are given in Table 1.

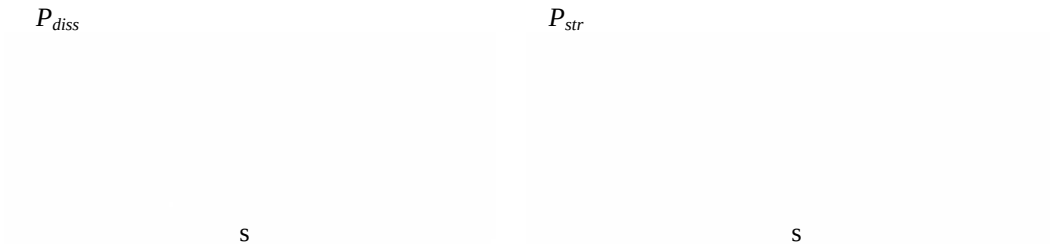


Fig.7. The power dissipated and that stored in *w*/m vs. time in s

The storage and loss moduli are computed using the above parameter sets. The average values calculated are shown in Table 2.

Table 2. Storage and loss moduli for a double layer section.

set	E_{loss1} 10^3 *kPa*	E_{str1} 10^3 *kPa*	E_{loss2} *kPa*	E_{str2} *kPa*
1	432.031	460.852	23.822	46.442
2	3744.905	4024.505	125.022	237.566
3	10.3577	11.0498	0.9822	1.8067

DISCUSSION:

Despite the enormous difficulties studying pulsating flow in an elastic tube of anisotropic material, the elastic analogy offers an adequate tool for approaching this case. The proposed model assumes linear stress-strain relationship and biaxial isotropy of the blood vessel. It offers a new perception towards the understanding of the mechanism of arterial pulsating nature. The elasticity modulus is computed using the stress and the strain complex functions for each layer.

The equivalent resistance, R_{eq}, is the component that is responsible for the dissipated energy per pulse per meter, e_{diss}. Whereas the equivalent reactance, X_{eq}, is the component that is responsible for the stored energy per pulse per meter, e_{st}. These can be deduced as follows:

$$e_{diss}(\mathrm{t}) = \frac{1}{T}\int_0^T i_1^2(t) R_{eq}\, dt, \quad e_{st}(\mathrm{t}) = \frac{1}{T}\int_0^T i_1^2(t) X_{eq}\, dt \qquad (9)$$

The results offer an understanding of how energy is stored and dissipated through a cyclic change of the radial pressure. Also the complex nature of the elasticity modulus is illustrated, in the absence of reliable experimental values for many biological constants of blood vessels. This work has to deal with hypothetical set of values that are believed to approach some previously reported values.

Accordingly the stress-strain pattern, the elasticity moduli, as well as the stored and dissipated power are dependant on the chosen set of values. The model proposed is valid to some extent according to reported experimental data. Furthermore, it shows that under all circumstances the strain developed, in both layers, lags the radial pressure and follows the pulsating wave shape. The elasticity, dissipated and stored power per unit length of both layers do as well.

References

[1] Yu Q,Zhou J, and Fung Y C, "Neutral axis location in bending and Young's modulus of different layers of arterial wall", Am J Physiol, H52-60, p 265, Jul 1993.

[2] Schulze-Bauer and Holzapfel, J.Biomechanics, 2003, Internet communications.

[3] Y. C. Fung, "Mechanical properties of living tissues", Springer, New York, second edition, 1993.

[4] J. Zhou. and Y. C. Fung, "The degree of nonlinearity and anisotropy of blood vessel elasticity", Proc. Natl. Acad. Sci. USA Vol. 94, pp. 14255-14260, Dec. 1997.

[5] Micheal Bonert, Richard L. Keask, Jagdish Butany, C. Ross Ethier, Jerry G. Myers, K. Wayne Johnston, and Matadial Ojha, "The relationship between wall shear stress distributions and intimal thickening in the human abdominal", Biomedical Engineering On Line, 2:18, doi:10.1186/1475-925x-2-18, 2003.

[6] Charles Choi, Biomedical Engineering Dept., Biomedical Ultrasonic lab., Univ. of Michigan, internet communication.

[7] Mingxi Wan, Yangamei Li, Junbo Li Yaoyao Cui, and Xiaodong Zhou, "Strain imaging and Elasticity Reconstruction of Arteries Based on Intravascular Ultrasound Video Images" IEEE Transactions on Biomedical Engineering, Vol. 48, No. 1, 2001.

[8]S. Cirovic, C. Walsh, W. D. Fraser, "A model of pulse transmission in the intracranial arteries", Intrnet communications.

[9] T.Shishido, M. Sugimachi, O. Kawaguchi, H.Miyano, T. Kawada, W. Matsuura, Y. Ikeda, T. Sato, J. Alexander Jr., and Kenji Sunagawa, "A new method to measure regional myocardial time-varying elastance using minute vibration", Am J Physiol Heart Circ Physiol, Vol. 274, issue 4, H1404-H1415, April 1998.

[10] Mette S. Olufsen, "Structured tree outflow condition for blood flow in larger systemic arteries. " Am J Physiol Heart Circ Physiol, Vol. 276, issue 1, H257-H268, January 1999.

[11] Harold J. Metcalf, " Topics in Classical Biophysics", Prentice-Hall, inc., New Jersey, May 1979.

[12] Ed VanBavel, Pier Siersma, and Jos A.E.Spaan, "Elasticity of Passive Blood Vessels: A New Concept", Am J Physiol Heart Circ Physiol, Vol.10, July 2003.

[13] M. A. El-Naggar, and M. A. El-Messiery, "The viscoelastic response of blood vessels under the effect of pulsating pressure", Proceedings of the biological effects of the EMFs, 3rd international workshop, Kos, Greece, Vol.11, Oct. 2004.

APPENDIX 1

The second order differential equation that governs the electrical charge Q with circuit components and input voltage V_0 is:

$$\frac{d^2Q(t)}{dt^2} = V_0(t)/L - \frac{R}{L}\frac{dQ(t)}{dt} - \frac{1}{LC}Q(t) \qquad (10)$$

By analogy between the two systems, mechanical and electrical, we note that:

$V_0(t) \leftrightarrow 2\pi P_1(t)$, $R/L \leftrightarrow B$, $1/LC \leftrightarrow K$, $L \leftrightarrow \rho_\ell$

THE ELECTROMAGNETIC WAVES OF 950 MHz, GSM MOBILE PHONE SYSTEM AND ACQUISITION PHASE OF SPATIAL MEMORY

MAJID JADIDI

PHYSIOLOGY RESEARCH CENTER, SEMNAN UNIVERSITY OF MEDICAL SCIENCES, SEMNAN, IRAN
Jadidim@Hotmail.com

S.M.P. FIROOZABADI

DEPARTMENT OF MEDICAL PHYSICS, TARBIAT MODARES UNIVERSITY, TEHRAN, IRAN
Pourmir@Modares.ac.ir

ALI RASHIDY-POUR

PHYSIOLOGY RESEARCH CENTER, SEMNAN UNIVERSITY OF MEDICAL SCIENCES, SEMNAN, IRAN
Rashidy-pour@Sem-ums.ac.ir

BAHRAM BOLOURI

DEPARTMENT OF MEDICAL PHYSICS, IRAN UNIVERSITY OF MEDICAL SCIENCES, TEHRAN, IRAN
BBolouri@Iums.ac.ir

YAGHOUB FATHOLLAHI

DEPARTMENT OF PHYSIOLOGY, TARBIAT MODARES UNIVERSITY, TEHRAN, IRAN
Fatolahi@modares.ac.ir

Abstract

With increasing in mobile communications, exposure to electromagnetic fields due to base station antenna has increased. This study was planned for evaluating the effects of whole-body exposure to 950 MHz GSM electromagnetic field on acquisition phase of spatial memory.

35 naive male Wistar Rats (3 month old, 220 $^{+}$15 g) randomly divided in three groups (control, sham-exposed and exposed) and were trained in a circular Morris water maze (3 days at 2 blocks, with 3 hours interval between blocks) to locate a submerged platform. The exposure program was planned for 10 session (45 min. and Power density = 0.835 mW/cm^2). According to water maze training, exposure was done just before each training session.

Performances of animals were tested 24 hours after the last training, by a 60 second probe test. Evaluation indexes were escape latency at target and opposite quadrants, swim speed and length.

Analysis of the probe data test showed no significant difference between control, sham and 950 MHz exposed groups.

Results of this study provide no evidence indicating that acquisition phase of spatial memory can be affected by the whole-body exposure to 950 MHz electromagnetic field.

Keywords: Electromagnetic field, Base station, Spatial memory, Morris water maze

Introduction

The RF radiations engage the spectrum of electromagnetic waves between 3 KHz - 300 GHz. This field can induce thermal or non-thermal effects on biological medium. Stimulation of excitable tissues will occur readily below 1 MHz, while thermal effects occur at higher frequencies [5].

In the last decade, many researches studied the effects of exposure to electromagnetic fields (EMF) on different nervous system functions such as memory in human and animals. Some of these studies have revealed deficits on memory due to EMF exposure [4; 8-21], whereas other studies did not [2, 3, 6, 7, 26, 31]. Nowadays, with increase in mobile communications, exposure to EMF due to mobile handset and base station antenna has increased. There are concerns about the effects of mobile phone electromagnetic waves on human body functions. These concerns emerge from results of epidemiological studies contributed to effects of mobile phone on human body. For example some of reports indicated that, mobile phone waves not only in regular power density but also in power density less than limited allowed (1 mW/cm^2), can produce headaches, warmth on ear, memory loss and fatigue.

These reports suggest that there is a significant association between calling time/number of calls per day and prevalence of these signs [10, 11, 12, 25, 29]. Although these results are important but in most of these studies the mobile phone handset frequency has been used and the effects of base station antenna waves have been less noticeable.

The GSM mobile phone system that is used in most of the countries has a frequency of either 900 or 1800 MHz (pulsed at 217 Hz, Band width of 200 KHz). The spectrum of 900 MHz has two band areas: 890-915 MHz that is specific for handset and 935-960 MHz that is specific for base station antenna.

To date, a few studies have evaluated the effects of EMF on memory functions in rodents. Studies performed by Wang and Lai [32] and Lai and Carino [18] reported deficits in two spatial learning tasks (Morris water maze and radial maze) after 45-min exposure to 2450 MHz EMF. On the other hand, studies reported by Cassel and colleagues failed to show any impairment of memory performance of rats in a radial maze after 45 min of whole-body exposure to a 2450- MHz EMF [2]. Findings of the last study were confirmed by recent studies showing no effect in spatial memory after daily 45 min of 900-MHz GSM exposure [6, 7]. The above findings indicate that the effects of GSM exposure on memory functions are still controversial. Moreover, to this date, we know no reports regarding the effects of exposure to 950 MHz waves, as a frequency in middle of base station band (935-960 MHz) on the memory function. There fore, the aim of this study was to examine the effects of exposure to 950 MHz waves, emitted by base station antenna, on acquisition phase of spatial memory in a Morris water maze.

Materials and methods

Subjects

35 naive male Wista rats (3 month old, 225 $^{+}$25 g) were divided randomly in to three groups: control (n=12), sham-exposed (n=11) and EMF exposed (n=12). Rats were maintained on a 12-h light-dark cycle and with an ambient temperature of 21^{o}C.They were housed in a maximum of six rats per breeding cage and allowed access to food and water ad libitum. All experiments were performed between 9:00 a.m and 13:00 p.m during the light cycle.

Morris Water Maze training

The behavioral training and testing was conducted in a water maze. The water maze was a blue circular pool (140 cm in diameter and 50 cm high) filled to a 25 cm depth with 22±2 ^{0}C water [27]. A circular glass platform (diameter: 11cm) was placed at the center of one quadrant (North-East quadrant) of the maze and submerged 3 cm below the surface of the water. The maze was located in a room containing several visual extra-maze cues.

Each animal was released into the water from the wall of the maze at arbitrarily defined east, south, west, and north points. The sequence of points of release into the water followed a random order. The animal was allowed to find the platform and land on it. If it could not find the platform within 1 minute, it was guided manually to the platform.

After finding the platform, it was allowed to stay there for 45 second before another trial. Performance in the maze was carried out and saved in a computer by an infrared receiver mounted on the roof.

The Morris water maze training program was planned for 3 days at 2 blocks, with 3 hours interval between blocks and 5 trials in each block. Performance of each rat was tested 24 hours after the final training day in a probe trial (60s) during which the platform was removed. Evaluation indexes were time spent in target quadrant, swim speed and total swim length during the probe test.

Electromagnetic field exposure

For whole body exposure to EMF, a 950 MHz GSM simulator (pulsed at 217 Hz and band width of 200 KHz, made by Khaje–Nasir Toosi University, Tehran, Iran) was used. It was connected to a 15 cm rod antenna fixed at the center of a circular plastic chamber (diameter = 30 cm). The animal could freely move inside the chamber. To prevent unknown exposure to reactive area of EMF, some of the near field restricted by a plastic mesh (radius = 5 cm). The power density inside the chamber was measured with RF meter (Narda 8716, USA) in different distances with 5 cm height from the base of antenna. With these records, the average value for power density was 0.835 mW/cm^2. The exposure program was consisted of ten 45 minute irradiation (as Lai et al., 1994). One day before running maze training, each animal exposed or sham-exposed to 4 sessions of 45 minute EMF with intervals of 1 hour. Subsequently, in 3 days, prior to each training session, animals were exposed to EMF or sham-exposed for 45 minute. The exposure room was adjacent to the experimental room.

Statistical analysis

The training data was analyzed with a one way analysis of variance (ANOVA) with trials as a repeated measure. Probe trial retention measures were analyzed with a two–way ANOVA. Tukey's *posthoc* test was performed to determine the source of detected significances. Values of $P<0.05$ were considered as significant

Results

All rats learned to locate the platform during training as indicated by decreasing escape latencies as training progressed (Fig.1). A two way ANOVA (group × block) with block as repeated measures showed significant effects of block ($P<0.001$), and no significant effects of groups [$F(3, 33) = 1.596$, $p=0.217$].

Fig.2, illustrates the retention performance as assessed by time spent in the four quadrants. A two way ANOVA (group × quadrant) showed significant effects of quadrants ($P<0.001$), and no significant effects of groups [$F(3, 33) = 1.02$, $p=0.368$].

Fig.3, illustrates the swim path data during the probe test. One- way ANOVA indicated no significant differences among the groups [$F(2, 31) = 2.334$, $p=0.114$].

Fig. 4 illustrates mean swim speed of rats during probe test. A one way ANOVA showed no significant differences between groups ($p>0.05$).

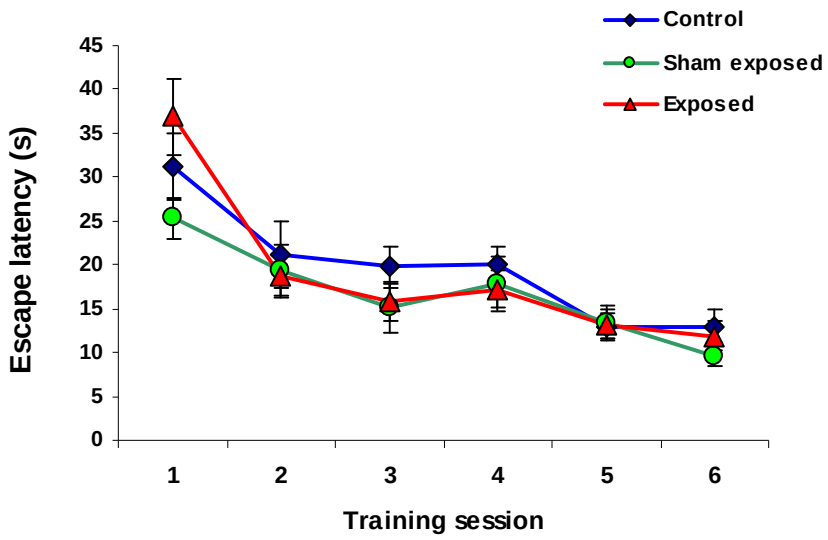


Fig. 1: Average escape time (Mean ± SEM); time to reach the platform after release into the water, during the trials.

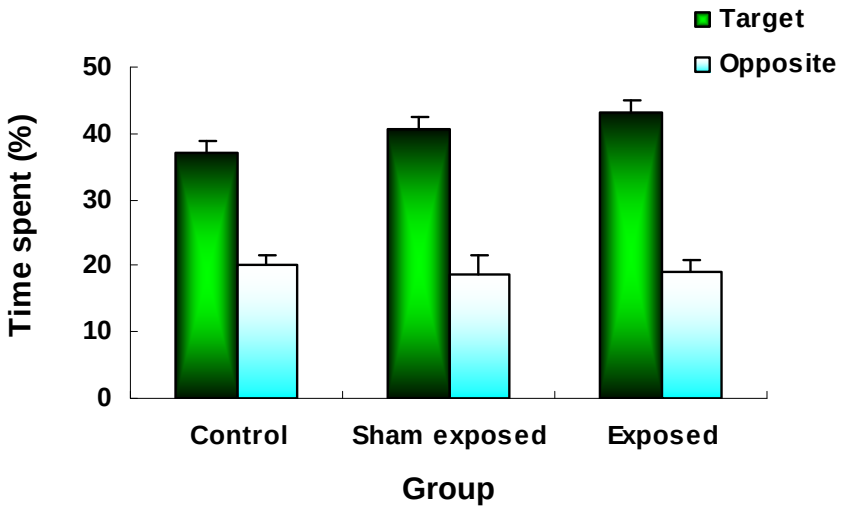


Fig 2: Average time spent (Mean + SEM) in three groups for target and opposite areas during probe trials.

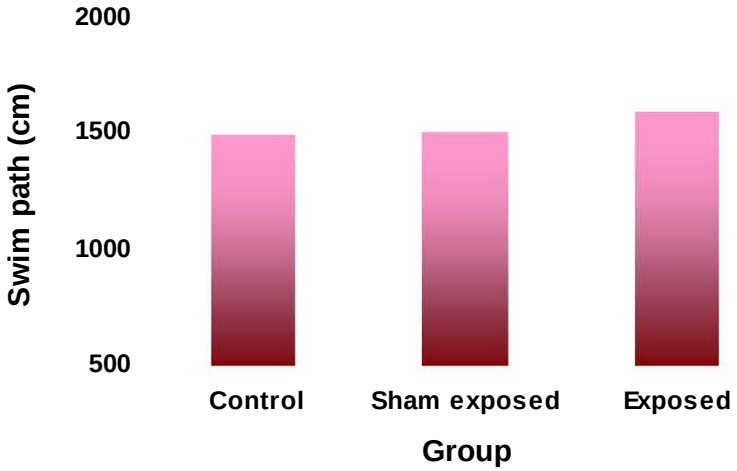


Fig. 3: Average swim path (Mean + SEM) in four groups during probe trials of acquisition phase.

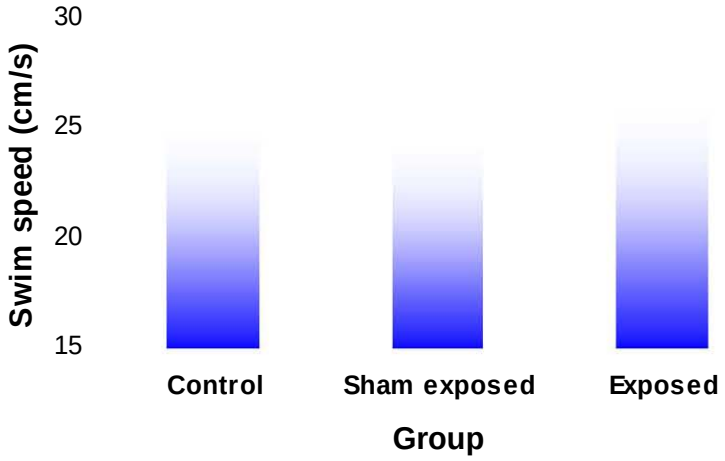


Fig. 4: Average swim speed (Mean + SEM) of the rats during probe trials in acquisition phase.

Discussion

The RF radiations engage the spectrum of electromagnetic waves between 3 KHz - 300 GHz. This field can induce thermal or non-thermal effects on biological medium. Stimulation of excitable tissues will occur readily below 1 MHz, while thermal effects occur at higher frequencies [5]. The mobile phones and their base station electromagnetic fields have low specific absorption rate that induce very low rise in brain temperature. Thus, the possible biological effects of mobile phone systems on brain would be expected to be the non-thermal effects [13]. Thus, the aim of this study was to examine the effect of exposure to 950 MHz waves, emitted by base station antenna, on spatial memory.

The findings of the present experiments indicate that acute whole body exposure to 950 MHz waves of GSM mobile phone system (pulsed at 217 Hz) dose not affect acquisition of spatial navigation in rat.

Our finding is in agreement with recent studies showing no effects of electromagnetic field on performance of rat or mice in an 8-arm radial-maze task [2, 17, 31]. Moreover, studies of Dubreuil et al., [6, 7] showed that head only exposure to GSM 900-MHz electromagnetic fields, did not alter rat's memory in spatial (radial maze) and non-spatial tasks. On the other hand the results of studies performed by Wang and Lai [32] and Lai and his colleagues [19] indicated that 45 min exposure to a 2450–MHZ electromagnetic fields induced deficits in spatial memory functions in Morris water maze and radial maze tasks.

Lai et al., [18] have shown that low level microwave irradiation could alter the cholinergic transmission in the hippocampus and cortex. Since cholinergic system plays an important role in memory processing, Lai et al., claimed that exposure to 2450–MHZ electromagnetic fields alter activity of this system in a way that produces impairment in spatial memory functions [17, 19].

The results of the present study are in contrast with the study of Wang and Lai indicting an impairment of spatial memory in a water maze induced by an acute exposure to electromagnetic fields. This discrepancy may be due to some subtle differences in the training paradigm (two blocks of five trials with a 3 min interval versus two blocks of 6 trials with a 3 h interval), time of probe test (24 h versus 1 h after the last training) or the characteristics of the used electromagnetic fields (950 MHz pulsed with 217 pulses/s, average power density 0.835 mW/cm^2 versus 2450-MHz pulsed with 500 pulses/s, average power density 2 mW/cm^2), and duration of exposure (45 min versus 1 h immediately before each training session). Moreover, previous studies have shown that hyperthermia can induce memory impairment [23], thus it is more likely that impairment reported by Wang and Lai can be due to consequences of a hyperthermia related to the whole body exposure [7].

The epidemiological studies were performed on human cases showed different results like animal experiments. Hocking et al., Oftedal et al. and Sandstrom et al., suggest that there is a direct relationship between the signs and calling time/number of calls per day [10, 11, 12, 25, 29]. In agreement with these results, studies on who lived in areas near the base station antenna showed irritability, depression, memory loss, concentration difficulties, vertigo, headache, sleep disturbances, feelings of discomfort and fatigue [2, 24, 28, 30]. The reported signs depend on duration of exposure, and the distance from antenna, and the antenna characteristics [2].

The results of the present study indicate that exposure to 950 MHz waves emitted by base station antenna had no effect on acquisition of rat's spatial memory in a water maze. Although this study was used as a model for understanding the effect of GSM electromagnetic field on acquisition phase of memory, further studies with a variety of intensities and durations of GSM electromagnetic fields are needed to test their effect on memory processing.

Acknowledgements

This study was supported by Iran Telecommunication Research Center, Tarbiat Modares University and Semnan University of Medical Sciences.

References

1] Bornkessel C, Stocker-Meier E. 2003. Results of a measurement programme concerning mobile phone base station emissions in North Rhine-Westphalia. Mobile Phone Base Station and Health. Dublin, May 15th and 16th, 2003.

2] Cassel JC, Cosquer B, Galiani R, Kuster N. 2004. Whole body exposure to 2.45 GHz electromagnetic fields does not alter radial-maze performance in rats. Behav Brain Res 155(1):37-43.

3] Cosquer B, Galini R, Kuster N, Cassel JC. 2005. Whole-body exposure to 2.45 GHz electromagnetic fields does not alter anxiety responses in rats: a plus-maze study including test validation. Behav Brain Res 156 (1):65-74.

4] Croft RJ, Chandler JS, Burgess AP, Barry RJ, Williams JD, Clarke AR. 2002. Acute mobile phone operation affects neural function in human. Clin Neurophysiol 113:1623-1632.

5] D'Andrea JA, Adair ER, Lorge JO. 2003. Behavioral and cognitive effects of microwave exposure. Bioelectromagnetics Supplement 6:S39-S62.

6] Dubreuil D, Jay T, Edeline JM. 2002. Does head-only exposure to GSM-900 electromagnetic fields effect the performance of rats in spatial learning tasks? Behav Brain Res 129:203-210.

7] Dubreuil D, Jay T, Edeline JM. 2003. Head only exposure to GSM 900 MHz electromagnetic fields does not alter rats memory in spatial and non-spatial tasks. Behav Brain Res 145:51-61.

8] Haarala C, Bjornberg L, Ek M, Laine M, Revonsuo A, Koivisto M, Hamalainen H. 2003. Effect of 902 MHz electromagnetic field emitted by mobile phone on human cognitive function: A replication study. Bioelectromagnetics 24(4):283-288.

9] Hermann DM, Hossmann KA. 1997. Neurological effects of microwave exposure related to mobile communication. J Neurol Sci 152:1-14.

10] Hocking B. 1998. Preliminary report: Symptoms associated with mobile phone use. Occup Med 48(6):357-360.
11] Hocking B, Westerman R. 2001. Neurological abnormalities associated with CDMA exposure. Occup Med 51(6):410-413.
12] Hocking B, Westerman R. 2003. Neurological effects of radiofrequency radiation. Occup Med 53:123-127.
13] Ilhan A, Gurel A, Armutcu F, Kamisli S, Iraz M, Akyol O, Ozen S. 2004. Ginkgo biloba prevents mobile phone-induced oxidative stress in rat brain. Clinica Chimica Acta 340:153-162.
14] Jadidi M, Firoozabadi SMP, Sajadi AA, Taherian AA. 2005. Acute exposure to 50 Hz, 8 mT Magnetic field can impair rat spatial memory. 3rd European Medical & Biological Engineering Conference. Prague, November 20th -25th, 2005.
15] Koivisto M, Krause CM, Revonsuo A, Laine M, Hamalainnen H. 2000a. The effects of electromagnetic field emitted by GSM phones on working memory. Neuroreport 11:1641-1643.
16] Koivisto M, Revonsvo A, Krause C, Haarola C, Sillanmaki L, Laine M, Hamalainen H. 2000b. Effects of 902 MHz electromagnetic field emitted by cellular telephones on response times in humans. Neuroreport 11:413-415.
17] Lai H. 2004. Interaction of microwaves and a temporally incoherent magnetic field on spatial learning in the rat. Physiology & Behavior 82:785-789.
18] Lai H, Carino M. 1999. 60 Hz magnetic fields and central cholinergic activity: effects of exposure intensity and duration. Bioelectromagnetics 20:284-289.
19] Lai H, Horita A, Guy AW. 1994. Microwave irradiation affects radial-arm maze performance in the Rat. Bioelectromagnetics 15:95-104.
20] Lass J, Tuulik V, Ferenets R, Riisalo R, Hinrikus H. 2002. Effects of 7 Hz-modulated 450 MHz electromagnetic radiation on human performance in visual memory tasks. Int J Radiat Biol 78(10):937-944.
21] Mann K, Roschke J. 1996. Effects of pulsed high-frequency electromagnetic fields on human sleep. Neuropsychology 33: 41-47.
22] McEwen BS, Sapolsky RM. 1995. Stress and cognitive function. Current Opinion in Neurobiology 5:205–216.
23] Mickley GA, Cobb BL, Mason PA, Farrell S. 1994. Disruption of a pulsative working memory task and selective expression of brain c-fos following microwave-induced hyperthermia. Physiol Behav 55:1029-1038.
24] Navarro EA, Segura J, Gomez-Perretta C, Portoles M, Maestu C, Bardasano JL. 2003. About the effects of microwave exposure from cellular phone base stations: A first approach. Mobile Phone Base Station and Health. Dublin, May 15th and 16th, 2003.
25] Oftedal G, Wilen J, Sandstrom M, Mild KH. 2000. Symptoms experienced in connection with mobile phone use. Occup Med 50(4):237-245.
26] Preece AW, Davies-smith A, Wesnes K, Butler S, Lim E, Varey A. 1999. Effect of 915 MHz simulated mobile phone signal on cognitive function in man. Int J Biol. 75(4):447-456.
27] Rashidy-Pour A, Motamedi F, Motaghed-Laijani, Z. 1996. Effects of reversible inactivation of the medial septal area on reference and working memory versions of the Morris water maze. Brain Res 709:131-40.
28] Roosli M, Moser M, Meier M, Braun-Fahlander C. 2003. Health symptoms associated with electromagnetic radiation – A questionnaire survey. Mobile Phone Base Station and Health. Dublin, May 15th and 16th, 2003.
29] Sandstrom M, Wilen J, Oftedal G, Hansson Mild K. 2001. Mobile phone use and subject symptoms.Comparision of symptoms experienced by users of analogue and digital mobile phones. Occup Med 51(1):25-35.
30] Santini R, Santini P, Danze JM, Le Ruz P, Seigne M. 2002. Study of the health of people living in the vicinity of mobile phone base stations: I. Influences of distance and sex. Pathol Biol 50:369-73.
31] Sienkiewicz ZJ, Blackwell RP, Haylock RG, Saunders RD, Cobb BL. 2000. Low-level exposure to pulsed 900 MHz microwave radiation does not cause deficits in the performance of a spatial learning task in mice. Bioelectromagnetics 21:151-158.
32] Wang B, Lai H. 2000. Acute exposure to pulsed 2450 MHz microwaves affects water-maze performance of rats. Bioelectromagnetics 21:52-56.

LOW-POWER DENSITY OF 950 MHz FIELD OF GSM MOBILE PHONE SYSTEM DOES NOT AFFECTS LONG-TERM POTENTIATION IN THE DENTATE GYRUS

MAJID JADIDI

DEPARTMENT OF MEDICAL PHYSICS, TARBIAT MODARES UNIVERSITY, TEHRAN, IRAN
Jadidi@modares.ac.ir

S. M.P. FIROOZABADI

DEPARTMENT OF MEDICAL PHYSICS, TARBIAT MODARES UNIVERSITY, TEHRAN, IRAN
Pourmir@Modares.ac.ir

ALI RASHIDY-POUR

PHYSIOLOGY RESEARCH CENTER, SEMNAN UNIVERSITY OF MEDICAL SCIENCES, SEMNAN, IRAN
Rashidy-pour@Sem-ums.ac.ir

BAHRAM BOLOURI

DEPARTMENT OF MEDICAL PHYSICS, IRAN UNIVERSITY OF MEDICAL SCIENCES, TEHRAN, IRAN
BBolouri@Iums.ac.ir

YAGHOUB FATHOLLAHI

DEPARTMENT OF PHYSIOLOGY, TARBIAT MODARES UNIVERSITY, TEHRAN, IRAN
Fatolahi@modares.ac.ir

Abstract

Over the last decade, exposure to electromagnetic field due to base station antenna has increased. This in vivo study was planned for evaluating the effects of whole-body exposure to 950 MHz field of GSM mobile phone system on dentate gyrus long-term potentiation.

24 naive male Wistar rats (3 month old, 225 $\pm$ 25 g) randomly divided in three groups (sham–exposed, GSM and continuous field exposed).

The exposure program was planned for 10 sessions at 3 days. Animals were exposed to electromagnetic field for 45-min in a circular plastic chamber (mean power density = 0.835 mW/cm^2). Immediately after end exposure, anesthesia was induced for LTP induction. Field potentials were recorded and analyzed using the population spike amplitude and EPSP slope for 60-min.

There were no significant differences in population spike amplitude, EPSP slope and EPSP slope maintenance among the three groups.

This experiment provides no evidence indicating that long-term potentiation can be affected by the whole-body exposure to low-power density of 950 MHz field of GSM mobile phone system.

Keywords: Electromagnetic field, Base station, Long-term Potentiation

Introduction

Nowadays, with increase in mobile communications, exposure to EMF due to mobile handset and base station antenna has increased. The GSM mobile phone system that is used in most of the countries has a frequency of either 900 or 1800 MHz (pulsed at 217 Hz, Band width of 200 KHz). The spectrum of 900 MHz has two band areas: 890-915 MHz that is specific for handset and 935-960 MHz that is specific for base station antenna.

In the last decade, many researches studied the effects of exposure to mobile phone electromagnetic fields (EMF) on different nervous system functions such as memory in human and animals. Some of these studies have revealed deficits on memory due to EMF exposure [5, 8-20, 23, 28], whereas other studies did not [3, 4, 6, 7, 31].

A number of studies have suggested that low frequency EMF may interact with learning and memory processes [18, 24]. Nevertheless, other studies have suggested that much higher frequency fields may also affect spatial memory [16, 18, 33]. Wang and Lai [18, 33] reported deficits in two spatial learning tasks (Morris water maze and radial maze) after 45-min exposure to continuous or pulsed, 2450 MHz EMF.

Since the spatial memory was accepted to have a substantial hippocampal involvement, these studies suggest that EMF may affect hippocampal function. This is supported by a report that exposure to 700 MHz continuous field can change electrical activity in the hippocampus of rat [32].

Long-term potentiation (LTP) is a long-lasting increase in synaptic efficacy resulting from the high-frequency stimulation of afferent fibers [1]. LTP in the hippocampus is thought to be a typical model of synaptic plasticity related to learning and memory [21].

To get insights into the cellular effects that 950 MHz exposure (as a frequency in middle of base station band) could induce on hippocampus, we decided to conduct a general study and investigated the consequences of exposure to continuous and pulsed (GSM) waves of 950 MHz EMF. Thus, the aim of this study was to examine the effects of exposure to 950 MHz fields on dentate gyrus (DG) long-term potentiation.

Materials and methods

Electromagnetic field exposure

For whole body exposure to EMF, a 950 MHz GSM simulator (made by Khaje–Nasir Toosi University, Tehran, Iran) was used to produce 950 MHz fields, in continuous (without any modulation) or GSM (217 Hz modulated and band width of 200 KHz) waveform. It was connected to a 15 cm rod antenna fixed at the center of a circular plastic chamber (diameter = 30 cm). The animal could freely move inside the chamber. To prevent unknown exposure to reactive area of EMF, some of the near field restricted by a plastic mesh (radius = 5 cm). The power density inside the chamber was measured with RF meter (Narda 8716, USA) in different distances with 5 cm height from the base of antenna. With these records, the average value for power density was 0.835 mW/cm^2. The exposure room was adjacent to the experimental room.

The exposure program was consisted of ten × 45-min irradiation, delivered at 3 days. In the first and second days, each animal's exposed or sham-exposed to 4 sessions of 45-min irradiation, with 1 hour interval. Subsequently, in the third day, animals had two irradiation sessions. Immediately after the end exposure, anesthesia was delivered for LTP induction.

Animals

.

24 naive male Wistar rats (3 month old, 225 $^{+}$ 25 g) randomly divided in three groups: sham–exposed (n=8), GSM (n=8) and continuous field exposed (n=8). Rats were maintained on a 12-h light-dark cycle and with an ambient temperature of 21^{o}C. They were housed in a maximum of 8 rats per breeding cage and allowed access to food and water ad libitum. All experiments were performed between 9:00 a.m and 13:00 p.m during the light cycle.

Surgical method

Animals were food and water deprived for 1 hour prior to surgery. For electrophysiological recording, the rats were anesthetized with Urethane (1.5 g/Kg, i.p., with supplemental injections as required) and stereotaxically implanted with a bipolar Teflon-coated silver electrode (125 µm diameter) in the perforant pathway (coordinates: AP -6.8 mm, L -4.1 mm, DV -3 mm, from skull surface) and a recording electrode (glass micropipette, 1- 3 MΩ, filled with physiological saline) in the dentate gyrus granule cell layer (coordinates: AP -2.8 mm, L -1.8 mm, DV-3 mm, from skull surface).

Electrophysiological recordings

The stimulating and recording electrodes were adjusted to produce maximum field potentials by applying a single pulse stimulus (0.1 Hz, 200µs pulse width) and recording field potentials in the DG granule cell layer.

Test stimulus intensity, sufficient to produce population spike (PS) with approximately 50% of maximum amplitude, was selected. After the 15-min base line recording, for LTP induction, two high frequency stimulus (250 Hz, 1s, 30s interval) were delivered to the perforant pathway with test stimulus intensity. The field potentials were recorded at 10, 20, 30, 40, 50 and 60-min after the tetanic stimulations, with 0.1 Hz pulse stimulus. The evoked responses were amplified, filtered (band-pass: 5 Hz – 3 KHz), sampled at a rate of 20 KHz and stored.

Evaluation indexes were PS amplitude, excitatory postsynaptic potentiation (EPSP) slop and EPSP maintenance. The LTP signal parameters were extracted as shown in Fig. 1. For EPSP maintenance, the percent of changes in each recording time calculated as: (Last record value – first record value / first record value) × 100. Data were statistically analyzed by repeated measures of ANOVA.

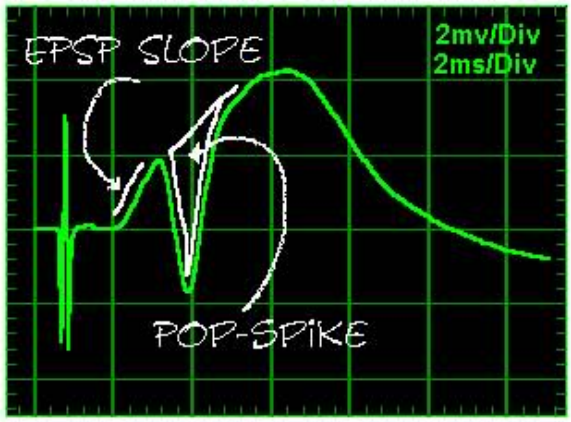


Fig.1: EPSP slope and PS amplitude that extracted from LTP signal.

Results

The results of EPSP slope of three groups, during the base line and 60-min recording are shown in fig.2. One-way ANOVA showed no significant differences among the groups.

Fig.3, illustrates the EPSP slope maintenance during the recording time. One-way ANOVA indicated no significant differences among the groups.

Results of the population spike amplitude are presented in fig.4. There were no significant differences between amplitudes of three groups during the base line recording and after LTP induction.

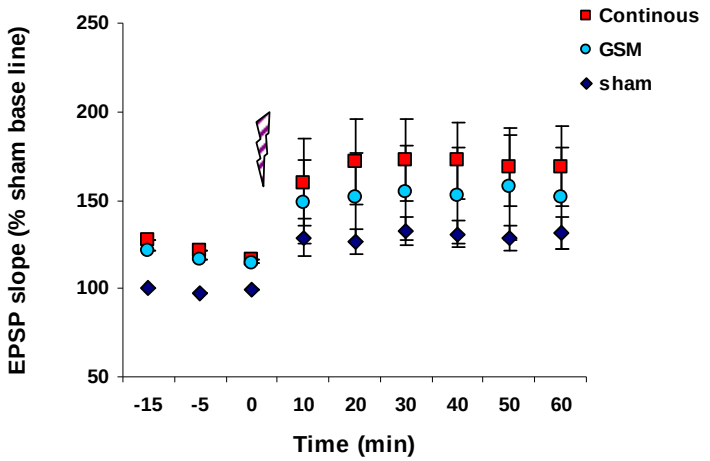


Fig.2: EPSP slope of three experimental groups (Mean ± SEM). Analysis of the data showed no significant differences between sham, continuous and GSM exposed groups.

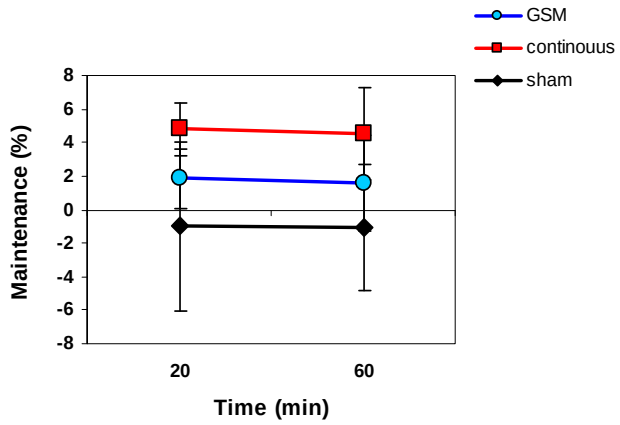


Fig.3: EPSP slope maintenance among the groups (Mean ± SEM). There was no significant difference between maintenance phase of the stimulated and sham exposed groups.

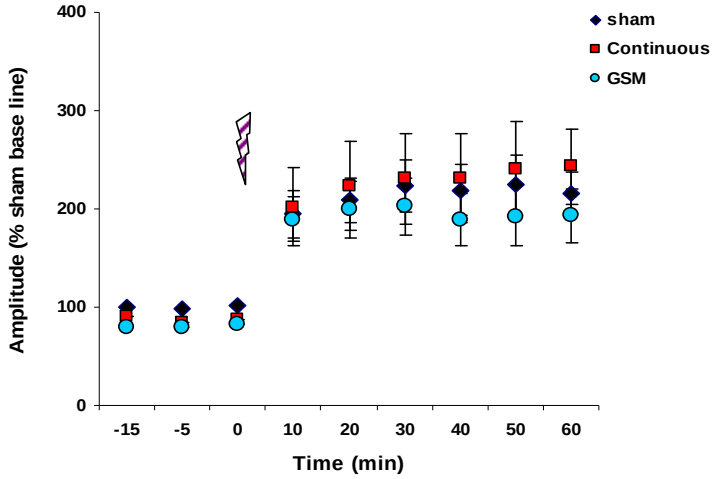


Fig.4: Population spike amplitude (Mean ± SEM). There were no significant differences between LTP induction and PS amplitude in the sham, continuous and GSM exposed groups.

Discussion

The mobile phones and their base station electromagnetic fields have low specific absorption rate that induce very low rise in brain temperature. Thus, the possible biological effects of mobile phone systems on brain would be expected to be the non-thermal effects [13]. This experiment results showed that exposure to continuous or GSM waves of 950 MHz EMF did not affect the LTP parameters. This is in agreement with recent studies showing that 900MHz EMF, in head-only exposure conditions, can not alter performances of rats in spatial memory and non-spatial memory tasks [7, 8]. Another study shows that 900MHz GSM EMF, dose not alter mice performance in an 8-arm radial-maze experiment [31].

On the other hand, Tattersall [32] indicated that exposure to 700 MHz continuous EMF for 5-15 minute reduced spontaneous epileptiform activity of rat hippocampus. Moreover, the results of Ogiue-Ikeda [26, 27] experiments signified the effect of low frequency magnetic field on EPSP slope of LTP.

Lai and Carino [18] found that low level microwave irradiations can alter the cholinergic functions in the rat hippocampus and cortex .This decrease in cholinergic activity in the brain can impair rat spatial memory [18].

Wang et al. and Lai [18, 33] showed that 45-min exposure to 2.45 GHz microwaves can alter spatial memory. But, Cassel et al. [3] could not access the same results, although their testing protocol was as similar as possible to that of the Lai et al. study.

The memory impairment reported by Lai et al and Wang and Lai [18, 33] can be related to a hyperthermia, because hyperthermia can produce amnesic effects [8].

Results of epidemiologic studies that performed on the effects of EMF, on who lived in areas near the base station antennas, showed that people's complaints (sleep disorders, headaches, concentration difficulties and fatigue) are due to EMF [25, 29] . These signs appeared after exposure and decreased slowly. Santini et al [30] suggest that the signs differ with increase of distance from antenna. In addition to distance, it seems that the antenna characteristics are important factors.

Bornkessel and Stocker-Meier [2] studies on 24 antennas showed that although electrical fields' intensities of these antennas are in standard limit, these results are time dependent and can differ with different antenna traffic along day. Although some of these studies suggest that exposure level is less than allowed level by ICNIRP in areas near the base station antenna, but the probability of long term exposure dangers of these waves for whom live in these areas are not rejected. In agreement with this point, Lai et al [17] showed, intensity and duration of exposure have interactions in effectiveness of the field on memory so that high-intensity/short-duration exposure and lower-intensity/longer-duration exposure have similar effects on frontal cortex and hippocampus cholinergic activity and memory. In addition, it is showed that chronic exposure to EMF can increase plasma corticosterone level [23]. This elevated level of corticosterone can induce time–dependent neuronal damage in hippocampus and impair cognitive function [22].

In the present research, the effect of exposure to 950 MHz waves emitted by base station antenna on electrical activity of hippocampus was investigated via the long-term potentiation. Although, this set of experiment provides no evidence indicating that LTP signal can be affected by the continuous or GSM waveform of 950 MHz EMF, further studies are needed to test other durations and intensities on brain activity. In addition, with

rapid increase of number of mobile phone users in the world and base station antenna in urban area, it seems that the knowledge about the effects of EMF on human body especially human brain is a necessity.

Acknowledgements

This study was supported by Iran Telecommunication Research Center, Tarbiat Modares University and Semnan University of Medical Sciences.

References

1] Bliss TVP, Lomo T. 1973. Long-lasting potentiation of synaptic transmission in the dentate area of the anaesthetized rabbit following stimulation of the perforant path. J Physiol. 232:357-374.
2] Bornkessel C, Stocker-Meier E. 2003. Results of a measurement programme concerning mobile phone base station emissions in North Rhine-Westphalia. Mobile Phone Base Station and Health. Dublin, May 15th and 16th, 2003.
3] Cassel JC, Cosquer B, Galiani R, Kuster N. 2004. Whole body exposure to 2.45 GHz electromagnetic fields does not alter radial-maze performance in rats. Behav Brain Res 155(1):37-43.
4] Cosquer B, Galini R, Kuster N, Cassel JC. 2005. Whole-body exposure to 2.45 GHz electromagnetic fields does not alter anxiety responses in rats: a plus-maze study including test validation. Behav Brain Res 156 (1):65-74.
5] Croft RJ, Chandler JS, Burgess AP, Barry RJ, Williams JD, Clarke AR. 2002. Acute mobile phone operation affects neural function in human. Clin Neurophysiol 113:1623-1632.
6] Dubreuil D, Jay T, Edeline JM. 2002. Does head-only exposure to GSM-900 electromagnetic fields effect the performance of rats in spatial learning tasks? Behav Brain Res 129:203-210.
7] Dubreuil D, Jay T, Edeline JM. 2003. Head only exposure to GSM 900 MHz electromagnetic fields does not alter rats memory in spatial and non-spatial tasks. Behav Brain Res 145:51-61.
8] Haarala C, Bjornberg L, Ek M, Laine M, Revonsuo A, Koivisto M, Hamalainen H. 2003. Effect of 902 MHz electromagnetic field emitted by mobile phone on human cognitive function: A replication study. Bioelectromagnetics 24(4):283-288.
9] Hermann DM, Hossmann KA. 1997. Neurological effects of microwave exposure related to mobile communication. J Neurol Sci 152:1-14.
10] Hocking B. 1998. Preliminary report: Symptoms associated with mobile phone use. Occup Med 48(6):357-360.
11] Hocking B, Westerman R. 2001. Neurological abnormalities associated with CDMA exposure. Occup Med 51(6):410-413.
12] Hocking B, Westerman R. 2003. Neurological effects of radiofrequency radiation. Occup Med 53:123-127.
13] Ilhan A, Gurel A, Armutcu F, Kamisli S, Iraz M, Akyol O, Ozen S. 2004. Ginkgo biloba prevents mobile phone-induced oxidative stress in rat brain. Clinica Chimica Acta 340:153-162.
14] Koivisto M, Krause CM, Revonsuo A, Laine M, Hamalainnen H. 2000a. The effects of electromagnetic field emitted by GSM phones on working memory. Neuroreport 11:1641-1643.
15] Koivisto M, Revonsvo A, Krause C, Haarola C, Sillanmaki L, Laine M, Hamalainen H. 2000b. Effects of 902 MHz electromagnetic field emitted by cellular telephones on response times in humans. Neuroreport 11:413-415.
16] Lai H. 2004. Interaction of microwaves and a temporally incoherent magnetic field on spatial learning in the rat. Physiology & Behavior 82:785-789.
17] Lai H, Carino M. 1999. 60 Hz magnetic fields and central cholinergic activity: effects of exposure intensity and duration. Bioelectromagnetics 20:284-289.
18] Lai H, Horita A, Guy AW. 1994. Microwave irradiation affects radial-arm maze performance in the Rat. Bioelectromagnetics 15:95-104.
19] Lass J, Tuulik V, Ferenets R, Riisalo R, Hinrikus H. 2002. Effects of 7 Hz-modulated 450 MHz electromagnetic radiation on human performance in visual memory tasks. Int J Radiat Biol 78(10):937-944.
20] Mann K, Roschke J. 1996. Effects of pulsed high-frequency electromagnetic fields on human sleep. Neuropsychology 33: 41-47.
21] Maren S, Baudry M. 1995. Properties and mechanisms of long-term synaptic plasticity in the mammalian brain: relationships to learning and memory. Neurobiol Learn Mem. 63:1-18.
22] McEwen BS, Sapolsky RM. 1995. Stress and cognitive function. Current Opinion in Neurobiology 5:205–216.
23] Mickley GA, Cobb BL, Mason PA, Farrell S. 1994. Disruption of a pulsative working memory task and selective expression of brain c-fos following microwave-induced hyperthermia. Physiol Behav 55:1029-1038.
24] Mostafa RM, Mostafa YM, Ennaceur A. 2002. Effects of exposure to extremely low-frequency magnetic field of 2 G intensity on memory and corticosterone level in rats. Physiology & Behavior 76:589- 595.

.

25] Navarro EA, Segura J, Gomez-Perretta C, Portoles M, Maestu C, Bardasano JL. 2003. About the effects of microwave exposure from cellular phone base stations: A first approach. Mobile Phone Base Station and Health. Dublin, May 15th and 16th, 2003.
26] Ogiue-Ikeda M, Kawato S, Ueno S. 2003. The effect of transcranial magnetic stimulation on long-term potentiation in rat hippocampus. IEEE Transactons on Magnetics 39(5):3390-3392.
27] Ogiue-Ikeda M, Kawato S, Ueno S. 2003. The effect of repetitive transcranial magnetic stimulation on long-term potentiation in rat hippocampus depends on stimulus intensity. Brain Res 993:222-226.
28] Preece AW, Davies-smith A, Wesnes K, Butler S, Lim E, Varey A. 1999. Effect of 915 MHz simulated mobile phone signal on cognitive function in man. Int J Biol. 75(4):447-456.
29] Roosli M., Moser M., Meier M., Braun-Fahlander C. Health symptoms associated with electromagnetic radiation – A questionnaire survey. Mobile Phone Base Station and Health. Dublin, May 15th and 16th, 2003.
30] Santini R, Santini P, Danze JM, Le Ruz P, Seigne M. 2002. Study of the health of people living in the vicinity of mobile phone base stations: I. Influences of distance and sex. Pathol Biol 50:369-373.
31] Sienkiewicz ZJ, Blackwell RP, Haylock RG, Saunders RD, Cobb BL. 2000. Low-level exposure to pulsed 900 MHz microwave radiation does not cause deficits in the performance of a spatial learning task in mice. Bioelectromagnetics 21:151-158.
32] Tattersall JEH, Scott IR, Wood SJ. 2001. Effects of low intensity radiofrequency electromagnetic fields on electrical activity in rat hypocampial slices. Brain Research 904:43-53.
33] Wang B, Lai H. 2000. Acute exposure to pulsed 2450 MHz microwaves affects water-maze performance of rats. Bioelectromagnetics 21:52-56.

INVESTIGATION ON THE CHANGES IN THE COMPOSITION OF AROMATIC COMPOUNDS OF RED CABBAGE IN RESPONSE TO STATIC MAGNETIC FIELD

MARYAM KHOSHSOKHAN MOZAFFAR[1], FAEZEH GHANATI[2], PARVIZ ABDOLMALEKI[2]

[1]DEPARTMENT OF BIOLOGY, FACULTY OF SCIENCE , AZAD UNIVERSITY OF QOM, QOM, IRAN
[2]DEPARTMENT OF BIOLOGY, FACULTY OF SCIENCE, TARBIAT MODARRES UNIVERSITY(TMU) , POB 14115-175, TEHRAN, IRAN.

Abstract
Treatment of Red cabbage (*Brassica oleracea* L. CV. Saccata) in vegetative growth phase with a 30 mT static magnetic field (SMF) resulted in altered content of lignin, anthocyanin and wall-bound phenolic compounds, compared with those of non-treated plants.
Exposure of red cabbage to the aforesaid static magnetic field during vegetative phase also induced the growth of the plants. The growth was accompanied by a delayed maturation and a lowered content of lignin in shoot and root system.

Introduction
During the past decade considerable evidence has been accumulated with regard to the biological effects of magnetic fields. Although several studies on bacterial and animal cells have shown that the magnetic fields influence a large variety of cellular functions, the mechanisms of its interaction with the living cells are still unclear and less studies have been conducted on plant cells. So far, many temporal and spatial electric phenomena occur during plant development (Moon 1999). Nevertheless, the magnetic field effects on the appearing of some cancers in human, embryogenesis in animals have been studied, seed germination and ion current and pollen-tube emergence in plants under MF also have been studied. The MF-induced inhibitory or stimulatory effects on the growth of plant tissues have seen to be species- specific, dependent on seasonal biological rhythms, field frequency and daily period of exposure (Moon 1999). In the present investigation the effect of static magnetic field on the growth and the metabolism of certain phenolic compounds of *Brassica oleracea* L. CV. saccata was subjected to study. It is well-known that phenolic compounds have various ecological and physiological roles and their contribution to defense system and UV protection have been studied. Phenolic compounds also inducible by different environmental stress and chemical stimuli (otto et al. 1999).
Brassica oleracea L. CV. saccata seeds were sterilized superficially with NaOCl and soaked in sterile Petri dishes on filter paper moisturized in distilled water. Seedlings were germinated and grown for 5 days at a constant temperature(25± 2°C) in a dark. after germination, the similar and entire seedlings were transferred to flower- pots and kept with a controlled condition at a constant temperature and light (25± 2°C and 6800 Luxe).
The plants were watered every day with ordinary water and every 15 days they were watered with Hoagland . after one month in the vegetative phase, the intact plants were selected and divided to treated and controlled groups. The treated groups were exposed to a 30 mT static magnetic field during 5 days and 5 hours in every day. The control group were maintained under a same environmental conditions as unexposed control. the samples were harvested in the end of treatment term.
Exposure to MF was performed by a locally designed MF generator. The electrical power was provided using a 220 V AC power supply equipped with variable transformer as well as a single-phase full wave rectifier. The maximum power and passing current were 1 KW and 50 A DC, respectively.
This system was designed to generate MF in range of 0.5 µT-30 mT. it consisted of two coils (each with 3000 turns of mm copper wire) on a U-shaped laminated iron core (to prevent eddy current losses). Using two vertical connectors, the arms of the U-shaped iron core were terminated in four circular iron plates covered with thin

layer of nickel (each 23 mm thickness, 260 cm in diameter). A water circulation system around the coils was employed to avoid the increase of the temperature. Without this system, the temperature of the coils increased, after the apparatus was working for 10 min, from 25 to 40 °C. Applying the water circulation system helped us to use apparatus for long exposures (5 h) as well as to keep the maintenance of the apparatus. The control cells were kept far enough from the MF producing apparatus, to avoid any potential exposure to the MF. Moreover, other electric appliances and laboratory facilities were not working; the control samples were therefore exposed only to the extremely low MF of the earth (60± 5 μT), as the treatment groups were too.

PPO was extracted from shoot and root systems, separately, in freshly prepared 200mM k-phosphate buffer (PH 6.8) followed by centrifugation at 12000x g . all these procedures were carried out at 2-4°C. Aliquots of supernatant were added to 200 mM k-phosphate buffer (PH 6.8) and freshly prepared 4-methylcatechol at a final concentration of 0.02 M. Enzyme activity was expressed as a change in absorbance at 410 nm per min per mg protein content of the homogenate. Protein concentration was determined by the method of Bradford (1976), using BSA as standard (Ghanati et al. 2002).

PO was extracted and the activity was determined in two fractions: the soluble PO fraction which is involved in the stress response(Pondolfini et al 1992) and the wall- bound PO fraction which is related to the lignification and suberization of cells(Fukuda and Komamine 1982 and Pando;fini et al 1992). The shoot and root systems , separately, were homogenized in 200 mM k-phosphate buffer (PH6.8) and centrifuged at 12000x g for 15 min at 2°C. the supernatant was used to assay soluble Po. The activity of wall- bound PO was determined in the ionically and covalently bound fractions, in turn. Pellets of the centrifugation were pooled, incubated with 0.2 M CaCl2 for 2h at room temperature, and centrifuged at was used to measure the activity of ionically wall- bound Po. The pellet was used directly for the assay of the covalently bound enzyme (Fukuda and Komamine 1982). The final reaction mixture (3 ml) was contained 200 mM k- phosphate buffer (PH 6.8) , 28 mM guaiacol and 5 mM H2O2. the enzyme activity of soluble and ionically fractions were expressed as the change in absorbance at 470 nm per min per mg protein content. The covalently enzyme activity was determined as the change in absorbance at 470 nm per min per cell wall dry weight (Ghanati et al. 2002).

The shoot and root systems, separately, were homogenized in ice- cold k-borate buffer (0.01 M, PH 8.8) containing 2 mM 2-mercaptoethanol and centrifuged at 16000x g for 10 min at 2°C. The supernatant was used as a crude enzyme solution. The reaction mixture (total 2ml) was composed of 0.5 ml of crude enzyme and 1 ml of extraction buffer (without 2-mercaptoethanol). The reaction started with addition of 0.5ml of 4mM phenylalanine and after 1 h incubation at 37°C, was stopped with 100 μl of 0.5 M HCl. The mixture was extracted three times with EtOAc. The EtOAc extract was air- dried, re- dissolved in 50% MeOH and analyzed by HPLC on an ODS-18 Ts column (15 cm x 6.0) at a flow rate of 0.5 ml min^{-1} with a linear gradient of 40-80% MeOH containing 0.1% HoAC and detected at 273 nm. The enzyme activity was expressed as the amounts of CA for 1h per mg of protein in the reaction mixture (Ghanati et al. 2002).

The shoot and root systems, separately, were homogenized in water after centrifugation at 1000x g, the pellet was sequentially washed with 10 volumes (v/w) of 0.5 mM CaCl2, EtOH, CHCl3- MeOH (2:1 v/v) and acetone followed by air- drying. Air-dried materials were desired as wall preparation. Phenolics were liberated from the wall preparations of samples with ammonium oxalate (20 mM, 70°C) and then with 0.1 M NaOH, under N2 for 24h. After acidification of both fractions to approximately PH 3.0 with HCl, phenolics were extracted three times with EtOAC, air- dried and re- dissolved in 50% MeOH before determination by HPLC as described for the determination of the PAL activity. Phenolics was detected at 280 nm (Ghanati et al. 2002; Liyama and Wallis 1990).

Isolation of cell walls was carried out as described for the determination of wall- bound phenolics. Lignin content was measured via a modified acetyl bromide procedure (Iiyama and Wallis 1990). In brief, 6 mg of fine-powdered wall preparation was treated with a mixture (total 2.5 ml) of 25% (w/w) AcBr in HOAC and 0.1 ml of 70% HClO4 at 70°C for 30 min with shaking at 10 min intervals. After cooling with ice, the digestion mixture was transferred to a 25 ml volumetric flask containing 5 ml of 2 M NaOH and 6 ml HOAC and made up to 25 ml. The lignin content was determined by measuring the absorbance at 273 nm using a specific absorption coefficient of 20.0g^{-1} L cm^{-1} (Ghanati et al. 2002; Liyama and Wallis 1990).

The anthocyanin of the shoot system tissues were extracted with cold methanol: water: acetic acid (11: 5: 1). The extraction was spun at 12000x g for 10 min. Anthocyanin concentration was determined by measuring optical absorption at 530 nm (Masakazu et al. 2003).

measurement of total sugar content in shoots and roots was based on phenol- sulfuric method, using glucose as standard (Duboise et al. 1956).

All experiments were repeated at least three times in triplicate. The data shown in the tables and figures are means ± SD. The significance of differences between treatments was evaluated by student's T- test.

PPO activity in shoot and root system were determined in both control and treatment groups. The activity PPO of root system of treated plants was higher than those of the control groups. The activity of PPO of shoot system of the treated plants was lower than that the control ones (Fig. 1).The activity of Po was measured in three fractions including soluble, ionically- and covalently-bound fractions (Table 1). The activity of three fractions

of PO increased in shoot system of treated plants under static magnetic field compared with those of the control groups. The results from measurement of PO activity in root system showed declining in treated plants in the three fractions relation to control ones. PAL enzyme was extracted from root and shoot system of red cabbage. PAL activity in the shoot and root system of treated plants was lower than those of the control ones (Fig. 2). The content of the phenols esterified to the wall polysaccharides of the shoot and root system under the control conditions and treatment with magnetic field, is shown in table 2.The content of these phenolics of root and shoot system under MF was significantly higher than those of the control ones. The lignin content of MF-treated shoot and root system decreased compared to control ones (Table 2).The results shown that the anthocyanin in shoot system has been increased in treated plants with 30 mT static magnetic field in comparison to the control groups (Fig. 3).
The total sugar were measured based on glucose standard curve in shoot and root system of samples. Compared to the samples under the control conditions, treatment samples significantly decreased total sugar (Fig. 4).

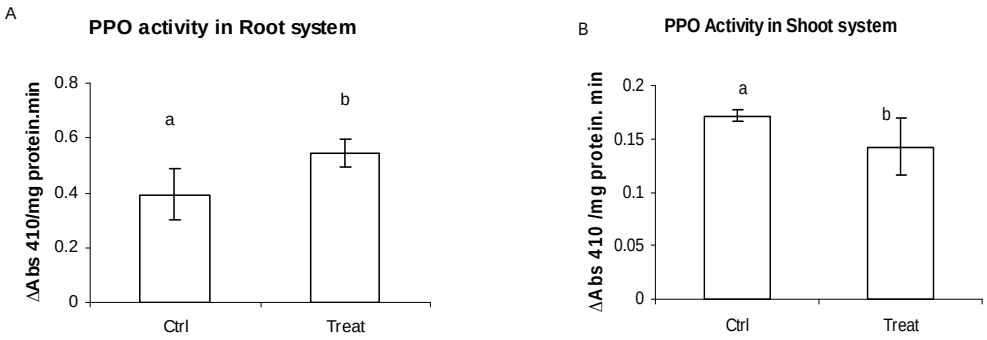


Fig. 1. Effect of Mf on the activity of PPO in root (A) and shoot (B) system of red cabbage. Data are means ± SD, n = 3. different characters refer to significant differences at P< 0.05 according to student' s T-test.

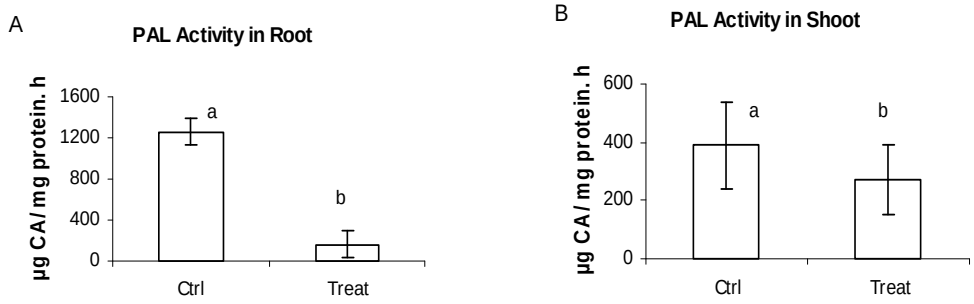


Fig. 2. Effect of MF on the activity of PAL in root (A) and shoot (B) system of red cabbage. Data are means ± SD, n = 3. different characters refer to significant differences at P< 0.05 according to student' s T-test.(CA: Cinnamic Acid)

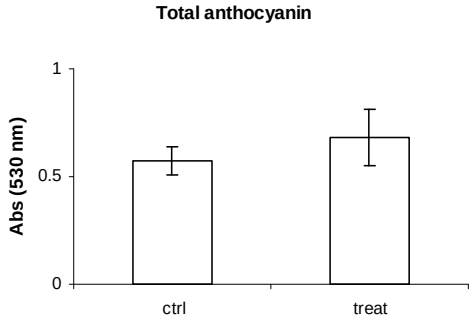


Fig. 3. Effect of Mf on total anthocyanin in aerial part of red cabbage. . Data are means ± SD, n = 3. different characters refer to significant differences at P< 0.05 according to student' s T-test.

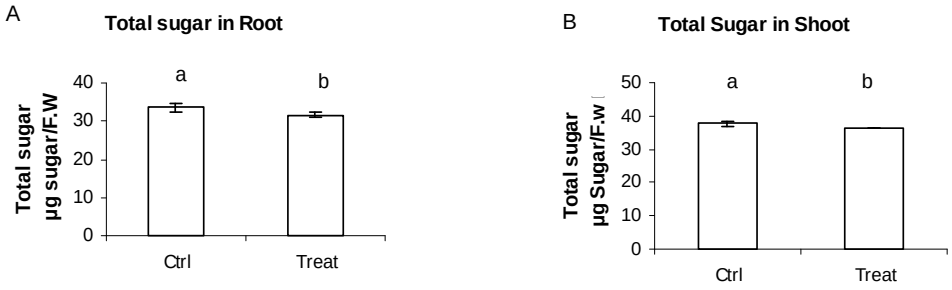


Fig. 4. Effect of MF on the lignin content of root (A) and shoot (B) system of red cabbage. Data are means ± SD, n = 3. different characters refer to significant differences at P< 0.05 according to student' s T-test.

Table. 1. Effect of MF on the activities of soluble, ionically and covalently bound cell fractions PO of root and shoot system of red cabbage

Peroxidase enzyme	Root		Shoot	
	Control	Treatment	Control	Treatment
Soluble PO Δ Abs 470 / mg protein.min	0.41± 0.2	0.4± 0.1	0.007± 0.0007	0.008± 0.001
Ionically bound PO Δ Abs 470 / mg protein.min	0.47± 0.05	0.41± 0.03	0.28± 0.03	0.54± 0.12
Covalently bound PO Δ Abs 470 / Cell Wall dry Weight.min	0.51± 0.01	0.44± 0.01	0.29± 0.009	0.55± 0.008

Data are means ± SD, n = 3.

Table. 2. Effect of MF on lignin content and cell wall phenolic compounds of root and shoot system of red cabbage.

Plant tissue	Lignin content (٪Lignin/ Cell Wall dry Weight)		Cell Wall Phenolic Compounds (µg phenol/ g Cell Wall dry Weight)	
	Control	Treat	Control	Treat
Root	4.1± 0.5	3.22± 0.7	3665.5± 282.7	7401.67± 2191.54
Shoot	5.04± 0.9	3.04± 0.46	2034.4± 594.8	4144.3± 968.43

Data are means ± SD, n = 3.

Summary

A magnetic field is an inescapable environmental factor for plants on the earth (Negishi et al. 1999). However, it´s impact on plant growth is not well understand(Negishi et al. 1999).In the current studies, contradictory results have been gained by scientists (Negishi et al. 1999). Static magnetic field, sometimes, has been received attention as a stress for beings (Aladjadjiyan 2002) and sometimes, it has been talked the co-operations of static MF with environmental factors, instance nourishing stresses, water deficit and heavy metals.

In the present paper the effect of SMF on the metabolism of certain phenolic compounds was investigated.

PPo is a bi-functional enzyme, that plays roles at both oxidation of phenols and conjugation of phenols to polyphenols. Increase of PPO activity in root system of treated plants can be related to accumulation of phenolic compounds. Also increase of PPO activity has been reported in tobacco cells affected by some nourishing stresses(Ghanati et al. 2002). Also the possibilities that the low PPO activity of the shoot system of treated plants can be due to the presence of an inhibitor, an in-activator or to factors degrading the enzyme (Kahn 1975).

Increased PO activity has been demonstrated to be a metabolic response under various stress conditions, including water stress, air pollution, and heavy metals (Pandolfini et al. 1992). Among the various forms of this enzyme , the wall-bound forms appear to be more efficient at catalyzing bound formation between extension and feruloylated polysaccharides and for the polymerization of phenolic monomers (Ghanati et al. 2002). Also Pandolfini (1992) reported the effects of nickel on peroxidases are always more marked in shoot than roots. Decrease of PO activity in the roots of treatment plants can be leading to stretch ability, wall-loosing and expansion in cell wall. Also, the percent of lignin content in treated roots can be help to this loosing. The lignin synthesis accomplishes from photosynthesis precursors .using of marked glucose showed relation between lignin synthesis and photosynthesis (Kollattukudy 1984). Decrease of lignin synthesis in the MF exposed plants, can be due to disorder in photosynthesis. According to Kazimov et al (1984) the magnetic fields results in decline in contents of photosynthetic pigments, chlorophyll a and b, in kidney bean leaves (Kazimov 1984). Also decrease of total sugar in treated plants with MF can be confirm this subject. it´s may be that MF was effected on lignin and sugar content from a common course.

PAL is a one of the main enzymes of metabolism of phenolic compounds that it catalyze changing of phenylalanine to cinnamic acid. The reaction catalyzed by phenylalanine ammonialyase. PAL is commonly regarded as akey step in the biosynthesis of phenols, and is affected by a number of factors (Ruiz et al 1998). This enzyme acts in the initial stages of lignin biosynthesis. rapid induction of the PAL activity (12 to 24 h) was observed during nourish stress and then decrease of PAL activity was reported in the next stages.(Ghanati et al. 2002,2004). In the present investigation, the activity of PAL in treated plants decreased after 10 days. Anthocyanins are another group of phenolic compounds belong to the flavonoids group. Anthocyanins in autumn leaves seem to prevent photo- oxidative irradiation.

The most important environmental cue in anthocyanin synthesis is light, which affects signal transduction and gene expression involved in anthocyanin biosynthesis. Other factors, such as sugar addition, phosphate limitation, and cold stress, can enhance anthocyanin accumulation induced by light. In the present research increase of anthocyanin and wall-bound phenlics may be resulted of phenols changing to anthocyanin and wall-bound phenolics and deviation from the lignin synthesis.

References

Aladjadjiyan A.; Study of the influence of magnetic field on some biological characteristics of Zea Mays . Journal of central European Agriculture; 2002; 3; 2: 89-94.

Belyavskaya N. A. ; Biological effects due to weak magnetic field on plants. Advances in space Research. 2003; 34: 1566- 1574.

Calzoni GL; Borghini F; Delgindice E. et al; Weak extremely high frequency microwaves affect pollen-tube emergence and growth Kiwifruit : Pollen grain irradiation and water- mediated effects; J Altern Complement Med; 2003; 9; 2: 217-228.

Daniel Otto; Meier Matthias Samuel; Schlatter Josef et al; Selected phenolic compounds in cultivated plants: Ecologic function; Health implications and Modulation by pesticides; 1999; 107: 109-114.

Dubois, M; Gilles, K; Hamilton, s; Rebes, P. and Smith F; Colorimetric method determination of sugars and related substances; Anal. Chem.; 1956; 28; 350-356.

Ghanati Faezeh; Morita Akio; Yokota Hiromi; Deposition of suberin in roots of Soybean induced by exess boron; Plant science; 2004. (Article in press).

Ghanati Faezeh; Morita Akio; Yokota Hiromi; Induction of suberin and increase of lignin content by excess Boron in Tobacco cells; Soil Sci. Plant Nutr. ; 2002; 48; 3; 357-364.

Hara Masakazu; Oki Karin; Hoshino Kyoko et al; Enhancement of anthocyanin biosynthesis by sugar in radish (Raphanus sativus) hypocotyl; 2003; 164; 2: 259-265.

Hirota Noriyuki; Nakagawa Jun and Kitazawa Koichi; Effects of a magnetic field on the germination of plants; Journal of Applied Physics; 1999; 85; 8: 5717-5719.

Iiyama Kenji and Wallis Adrian F. A. ; Determination of lignin in herbaceous plants by an improved Acetyl Bromide procedure; J Sci Food Agric; 1990; 51; 145-161.

Kahn Varda; Polyphenol oxidase activity and browning of tree Avocado varieties ; J. Sci. Fd Agric; 1975; 26; 1319-1324.

Kollattukudy P. E. ; Biochemistry and function o cutin and suberin. Can. J. Bot. ; 1984; 62; 2918-2933.

Mc Cann. J. ; Khiefts L; Rafferty C. ; Cancer risk assessment of Extremely Low Frequency Electric and Magnetic fields: a critical review of Methodology; Environmental Health Perspective; 1998; 6; 11.

Negeshi Y. ; Hashimoto A. ; Tsushima M. et al; Growth of pea epicotyl in low magnetic field implication eor space research; Adv. Space Res. ; 1999; 23; 12: 2029- 2032.

Pandolfini T; Gabbrielli R. and Comparini C. ; Nickel toxicity and peroxidase activity in seedlings of *Triticum aestivum* L. ; Plant cell and environment ; 1992; 15; 719-725.

Piera Piacentini Maria; Fraternale Daniel ; Piatti Elena et al; Senescence delay and change of antioxidant enzyme levels in Cucumis sativus L. etiolated seedlings by ELF magnetic fields; Plant science; 2001; 101; 45-53.

Ruiz Juan M. ; Bretones German; Baghour Mouurad et al; Relationship between Boron and phenolic metabolism in Tobacco leaves; 1998; 48; 2: 269- 272.

Ruiz R; Vodnic D; Jerman I; Influence of aluminum in biologic effects of ELF magnetic field stimulation; Electro- magnetobial; 2000; 19; 57- 68.

THE EFFECT OF ACUTE EXPOSURE TO 950 MHz WAVES OF GSM MOBILE PHONE SYSTEM ON CONSOLIDATION OF SPATIAL MEMORY IN RAT

MAJID JADIDI

PHYSIOLOGY RESEARCH CENTER, SEMNAN UNIVERSITY OF MEDICAL SCIENCES, SEMNAN, IRAN

Jadidim@Hotmail.com

S. MOHAMMAD P. FIROOZABADI

DEPARTMENT OF MEDICAL PHYSICS, TARBIAT MODARES UNIVERSITY, TEHRAN, IRAN

Pourmir@Modares.ac.ir

ALI RASHIDY-POUR

PHYSIOLOGY RESEARCH CENTER, SEMNAN UNIVERSITY OF MEDICAL SCIENCES, SEMNAN, IRAN

Rashidy-pour@Sem-ums.ac.ir

BAHRAM BOLOURI

DEPARTMENT OF MEDICAL PHYSICS, IRAN UNIVERSITY OF MEDICAL SCIENCES, TEHRAN, IRAN

BBolouri@Iums.ac.ir

YAGHOUB FATHOLLAHI

DEPARTMENT OF PHYSIOLOGY, TARBIAT MODARES UNIVERSITY, TEHRAN, IRAN

Fatolahi@modares.ac.ir

Abstract

With increasing in mobile communications, exposure to electromagnetic fields due to base station antenna has increased. This study was planned for evaluating the effects of short whole-body exposure to 950 MHz GSM electromagnetic field on consolidation phase of spatial memory.

33 naive male wistar rats (200 $^{\pm}$15 g) were trained (10 trials at 2 blocks, with 3 minutes interval between blocks for one day) to locate a submerged platform in a circular water maze. Immediately after training, animals randomly divided into three groups: control n= 11, sham-exposed n=11 and exposed n=11. The last group was exposed to 950 MHz electromagnetic waves (mean power density = 0.835 mW/cm^2) for 45 minutes in a circular plastic chamber. Performances of animals were tested 48 hours later by a 60 second probe test. Evaluation indexes were escape latency at target and opposite quadrants, swim speed and length.

Analysis of the probe data test indicated that, there were no significant difference between control, sham and 950 MHz exposed groups.

Results of this study provide no evidence indicating that consolidation phase of spatial memory can be affected by the 45 min whole-body exposure to 950 MHz electromagnetic waves.

Keywords: Electromagnetic field, Base station, Consolidation, Morris water maze

Introduction

Memory is defined as the capacity of brain to store and retrieve the information. It consists of three phases: encoding or acquisition phase, consolidation or stabilization phase that is a process by which new labile memories convert to more stable long-term memories, and retrieval phase in which memory is expressed.

In the last decade, many researches studied the effects of exposure to electromagnetic fields (EMF) on different nervous system functions such as memory in human and animals. Some of these studies have revealed deficits on memory due to EMF exposure [4; 7-20], whereas other studies did not [2, 3, 5, 6, 28, 33]. Nowadays, with increase in mobile communications, exposure to EMF due to mobile handset and base station antenna has increased. There are concerns about the effects of mobile phone electromagnetic waves on human body functions. These concerns emerge from results of epidemiological studies contributed to effects of mobile phone on human body. For example some of reported data indicated that mobile phone waves not only in regular power density but also in power density less than allowed limit (1 mW/cm^2) can produce headaches, warmth on ear, memory loss and fatigue. These reports suggest that there is a significant association between calling time/number of calls per day and prevalence of these signs [9, 10, 11, 27, 31]. Although these results are important but in most of these studies the mobile phone handset frequency has been used and the effects of base station antenna waves have been less noticeable.

The GSM mobile phone system that is used in most of the countries has a frequency of either 900 or 1800 MHz (pulsed at 217 Hz, Band width of 200 KHz). The spectrum of 900 MHz has two band areas: 890-915 MHz that is specific for handset and 935-960 MHz that is specific for base station antenna.

To date, we know no reports regarding the effects of acute exposure to 950 MHz waves, as a frequency in middle of base station band (935-960 MHz) on the memory processes. On the other hand, most of the experiments contribute to effects of exposure to mobile phone electromagnetic waves on acquisition phase of memory and few experiments are about the effects of these waves on consolidation phase. Thus, the aim of this study was to examine the effects of acute exposure to 950 MHz waves, emitted by base station antenna, on consolidation phase of spatial memory in a Morris water maze.

Materials and methods

Animals

Thirty three naive male Wistar rats (3 month old, 200 $^{\pm}$15 g) were used in three groups: control (n=11), sham-exposed (n=11) and EMF exposed (n=11). Rats were maintained on a 12-h light-dark cycle and with an ambient temperature of 21^{o}C.They were housed in a maximum of six rats per breeding cage and allowed access to food and water ad libitum. All experiments were performed between 9:00 a.m and 13:00 p.m during the light cycle.

Morris Water Maze training

The water maze was a blue circular pool (diameter: 140 cm, height: 50 cm) filled with water (22± 2°C) to a depth of 25 cm [29]. A circular glass platform (diameter: 11cm) was placed at the center of one quadrant (North-East quadrant) of the maze and submerged 3 cm below the surface of the water. The maze was located in a room containing several visual extra-maze cues. Each animal was released into the water from the wall of the maze at arbitrarily defined east, south, west, and north points. The sequence of points of release into the water

followed a random order. The animal was allowed to find the platform and land on it. If it could not find the platform within 1 minute, it was guided manually to the platform.

After finding the platform, it was allowed to stay there for 45 second before another trial. Performance in the maze was carried out and saved in a computer by an infrared receiver mounted on the roof. For spatial training, animals were given 10 trials (one training session) at 2 blocks, with 3 minutes interval between them for one day in Morris Water Maze. **Immediately after the last trial**, Rats were exposed to electromagnetic waves or sham exposed for a 45 minute.

Performance of each rat was tested 48 hours after the training session in a probe trial (60s), during which the platform was removed. Evaluation indexes were time spent in target quadrant, swim speed and total swim length during the probe test.

Electromagnetic field exposure

For whole body exposure to EMF, a 950 MHz GSM simulator (pulsed at 217 Hz and band width of 200 KHz, made by Khaje–Nasir Toosi University, Tehran, Iran) was used. It was connected to a 15 cm rod antenna fixed at the center of a circular plastic chamber (diameter = 30 cm). The animal could freely move inside the chamber. To prevent unknown exposure to reactive area of EMF, some of the near field restricted by a plastic mesh (radius = 5 cm). The power density inside the chamber was measured with RF meter (Narda 8716, USA) in different distances with 5 cm height from the base of antenna. With these records, the average value for power density was 0.835 mW/cm^2. The exposure room was adjacent to the experimental room.

Data analysis

The training data was analyzed with a one way analysis of variance (ANOVA) with trials as a repeated measure. Probe trial retention measures were analyzed with a two–way ANOVA. Tukey's *posthoc* test was performed to determine the source of detected significances. Values of $P<0.05$ were considered as significant

Results

The results of escape time during the 10 trials are shown in fig.1. Data analysis showed a significant trial effect (i.e., a significant decrease in escape time with training). There was no significant difference in time during the training session trials between three groups [F (2, 29) = 0.358, p=0.702].

Results of the probe trial are presented in fig.2, which shows the average time for the three groups of rats during the 1-minute probe trial period in the platform and opposite quadrants. There was no significant difference in time during the training session trials between three groups [F (2, 36) =1.03, p=0.364].

Fig.3, illustrates the swim path data during the probe test. One- way ANOVA indicated no significant differences among the groups [F (2, 27) =1.82, p=0.180]. Fig. 4, illustrates mean swim speed of rats during probe test. A one way ANOVA showed no significant differences between groups [F (2, 27) =1.72, p=0.198].

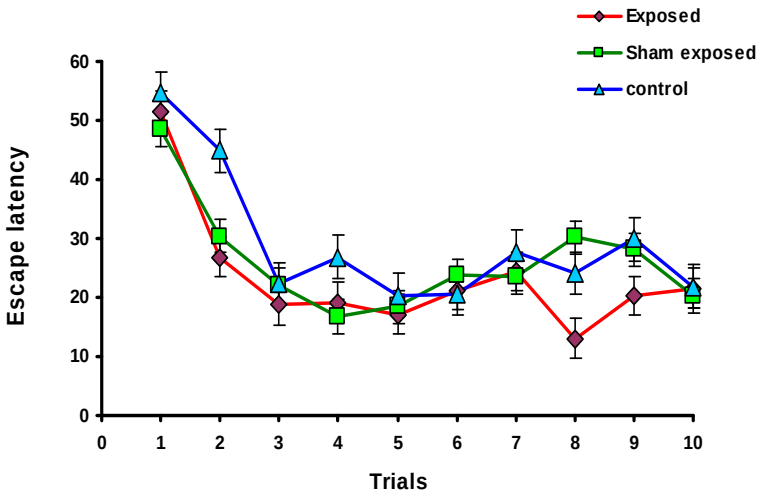


Fig. 1: Average escape time (Mean ± SEM); time to reach the platform after release into the water, during the trials.

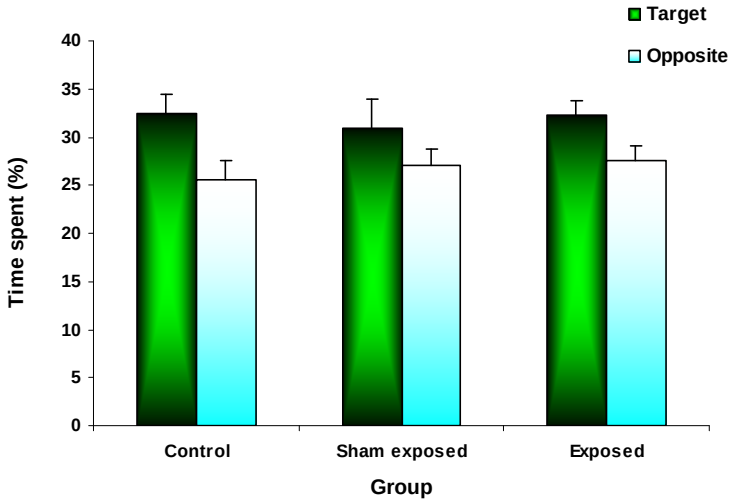


Fig 2: Average time spent (Mean + SEM) in three groups for target and opposite areas during probe trials.

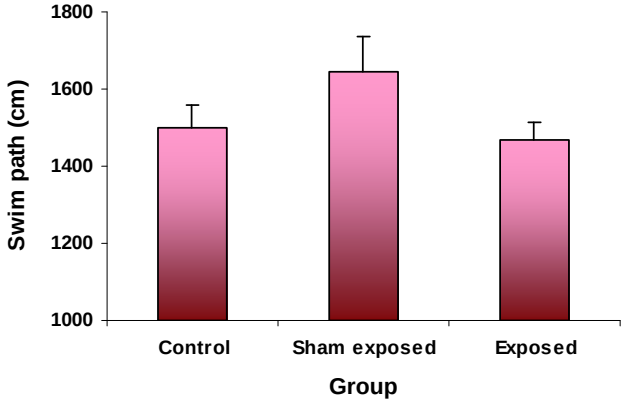


Fig. 3: Average swim path (Mean + SEM) in four groups during probe trials of consolidation experiment.

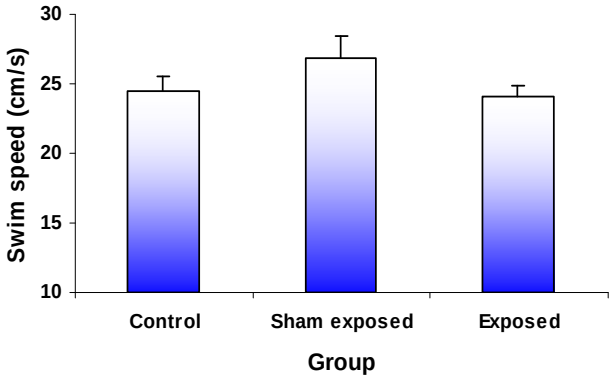


Fig. 4: Average swim speed (Mean + SEM) of the rats during probe trials in consolidation experiment.

Discussion

The mobile phones and their base station electromagnetic fields have low specific absorption rate that induce very low rise in brain temperature, thus, the possible biological effects of mobile phone systems on brain would be expected to be the non-thermal effects [12]. Data from this experiment showed that acute exposure (45 minute) of 950 MHz waves of GSM mobile phone system (pulsed at 217 Hz) does not affect the consolidation phase of rat spatial memory. This is in agreement with recent studies showing electromagnetic field dose not alter performance in an 8-arm radial-maze, either in mice [33] or in rats [16]. In addition, another study shows that 900MHz GSM electromagnetic field, in head-only exposure conditions, can not alter performances of rats in spatial memory and non-spatial memory tasks [5, 6].

On the other hand, Lai and Carino found that low level microwave irradiations can alter the cholinergic functions in the rat hippocampus and cortex [17]. This decrease in cholinergic activity in the brain can impair rat spatial memory [18]. Cassel et al. could not access the same results like the Lai et al findings, although their testing protocol was as similar as possible to that of the Lai et al. study [2]. Sienkiewicz et al. found similar results in radial-arm maze too [33]. But Wang and Lai showed that 45-minute exposure 2.45 GHz microwaves can alter spatial memory in Morris water maze [35]. Because it has showed that hyperthermia can produce amnesic effects, the memory impairment reported by Lai et al and Wang and Lai can be related to a hyperthermia due to the whole-body exposure [6].

McKay et al [23] indicated that exposure to magnetic field can impair memory consolidation of contextual conditioned fear rats. Consolidation is defined as a process by which new labile memories convert to more stable long-term memories. It is showed that consolidation requires RNA and protein synthesis [22, 25]. Sienkiewics et al [34] suggests that magnetic fields have no effects on the well-established long-term memories.

The epidemiological studies were performed on human cases showed different results like animal experiments. Hocking et al., Oftedal et al. and Sandstrom et al. reported that mobile phone waves can produce dizziness, headaches, discomfort, warmth on ear, memory loss, and fatigue not only in regular power density but also in power density less than allowed limit (1 mW/cm^2). They suggest that there is a direct relationship between these signs and calling time/number of calls per day [9, 10, 11, 27, 31]. In addition to studies performed on effects of waves emitted by phone handset, results of epidemiologic studies were done by Roosli et al and Navarro et al. on persons who lived in areas near the antenna, showed that 74% of people's complaints (sleep disorders, headaches, concentration difficulties and fatigue) are due to antenna. These signs appeared after exposure and decreased slowly [26, 30]. Santini et al suggest that the signs of persons, who live in areas near antenna, differ with increase of distance from antenna [32]. In addition to distance it seems that the antenna characteristics are important factors.

Bornkessel and Stocker-Meier studies on 24 antennas showed that although electrical fields' intensities of these antennas are in standard limit. These results are time dependent and can differ with different antenna traffic along day [1]. Although some of these studies suggest that exposure level is less than allowed level by ICNIRP in areas near the base station antenna, but the probability of long term exposure dangers of these waves for whom live in these areas are not rejected. In agreement with this point, Lai et al showed that intensity and duration of exposure have interactions in effectiveness of the field on memory so that high-intensity/short-duration exposure and lower-intensity/longer-duration exposure have similar effects on frontal cortex and hippocampus cholinergic activity and memory [17]. In addition, it is showed that chronic exposure to EMF can increase plasma corticosterone level [24]. This elevated level of corticosterone can induce time–dependent neuronal damage in hippocampus and impair cognitive function [21].

In the present research, the effect of acute exposure of 950 MHz waves emitted by base station antenna on the consolidation phase of spatial memory was investigated via the Morris water maze. This set of experiment provides no evidence indicating that spatial memory can be affected by the 45 minute whole-body exposure to 950 MHz electromagnetic field. Although this study was used as a model for understanding the effect of GSM electromagnetic field on consolidation phase of memory, further studies are needed to test other durations and intensities on this phase of memory.

Acknowledgements

This study was supported by Iran Telecommunication Research Center, Tarbiat Modares University and Semnan University of Medical Sciences.

References

1] Bornkessel C, Stocker-Meier E. 2003. Results of a measurement programme concerning mobile phone base station emissions in North Rhine-Westphalia. Mobile Phone Base Station and Health. Dublin, May 15th and 16th, 2003.

2] Cassel JC, Cosquer B, Galiani R, Kuster N. 2004. Whole body exposure to 2.45 GHz electromagnetic fields does not alter radial-maze performance in rats. Behav Brain Res 155(1):37-43.

3] Cosquer B, Galini R, Kuster N, Cassel JC. 2005. Whole-body exposure to 2.45 GHz electromagnetic fields does not alter anxiety responses in rats: a plus-maze study including test validation. Behav Brain Res 156 (1):65-74.

4] Croft RJ, Chandler JS, Burgess AP, Barry RJ, Williams JD, Clarke AR. 2002. Acute mobile phone operation affects neural function in human. Clin Neurophysiol 113:1623-1632.

5] Dubreuil D, Jay T, Edeline JM. 2002. Does head-only exposure to GSM-900 electromagnetic fields effect the performance of rats in spatial learning tasks? Behav Brain Res 129:203-210.

6] Dubreuil D, Jay T, Edeline JM. 2003. Head only exposure to GSM 900 MHz electromagnetic fields does not alter rats memory in spatial and non-spatial tasks. Behav Brain Res 145:51-61.

7] Haarala C, Bjornberg L, Ek M, Laine M, Revonsuo A, Koivisto M, Hamalainen H. 2003. Effect of 902 MHz electromagnetic field emitted by mobile phone on human cognitive function: A replication study. Bioelectromagnetics 24(4):283-288.

8] Hermann DM, Hossmann KA. 1997. Neurological effects of microwave exposure related to mobile communication. J Neurol Sci 152:1-14.

9] Hocking B. 1998. Preliminary report: Symptoms associated with mobile phone use. Occup Med 48(6):357-360.

10] Hocking B, Westerman R. 2001. Neurological abnormalities associated with CDMA exposure. Occup Med 51(6):410-413.1

11] Hocking B, Westerman R. 2003. Neurological effects of radiofrequency radiation. Occup Med 53:123-127.1

12] Ilhan A, Gurel A, Armutcu F, Kamisli S, Iraz M, Akyol O, Ozen S. 2004. Ginkgo biloba prevents mobile phone-induced oxidative stress in rat brain. Clinica Chimica Acta 340:153-162.

13] Jadidi M, Firoozabadi SMP, Sajadi AA, Taherian AA. 2005. Acute exposure to 50 Hz, 8 mT Magnetic field can impair rat spatial memory. 3rd European Medical & Biological Engineering Conference. Prague, November 20th -25th, 2005.

14] Koivisto M, Krause CM, Revonsuo A, Laine M, Hamalainnen H. 2000a. The effects of electromagnetic field emitted by GSM phones on working memory. Neuroreport 11:1641-1643.

15] Koivisto M, Revonsvo A, Krause C, Haarola C, Sillanmaki L, Laine M, Hamalainen H. 2000b. Effects of 902 MHz electromagnetic field emitted by cellular telephones on response times in humans. Neuroreport 11:413-415.

16] Lai H. 2004. Interaction of microwaves and a temporally incoherent magnetic field on spatial learning in the rat. Physiology & Behavior 82:785-789.

17] Lai H, Carino M. 1999. 60 Hz magnetic fields and central cholinergic activity: effects of exposure intensity and duration. Bioelectromagnetics 20:284-289.

18] Lai H, Horita A, Guy AW. 1994. Microwave irradiation affects radial-arm maze performance in the Rat. Bioelectromagnetics 15:95-104.

19] Lass J, Tuulik V, Ferenets R, Riisalo R, Hinrikus H. 2002. Effects of 7 Hz-modulated 450 MHz electromagnetic radiation on human performance in visual memory tasks. Int J Radiat Biol 78(10):937-944.

20] Mann K, Roschke J. 1996. Effects of pulsed high-frequency electromagnetic fields on human sleep. Neuropsychology 33: 41-47.

21] McEwen BS, Sapolsky RM. 1995. Stress and cognitive function. Current Opinion in Neurobiology 5:205–216.

22] McGaugh JL. 2000. Memory- A century of consolidation. Science 14:248-251.

23] McKay BE, Persinger MA. 2000. Application timing of complex magnetic fields delineates windows of posttraining- pretesting vulnerability for spatial and motivational behaviors in rats. Intern J Nuroscience 103:69-77.

24] Mickley GA, Cobb BL, Mason PA, Farrell S. 1994. Disruption of a pulsative working memory task and selective expression of brain c-fos following microwave-induced hyperthermia. Physiol Behav 55:1029-1038.

25] Nader K, Schafe GE, LE Doux JE. 2000,b. The labile nature of consolidation theory. Nat Rev Neurosci 1:216-219.

26] Navarro EA, Segura J, Gomez-Perretta C, Portoles M, Maestu C, Bardasano JL. 2003. About the effects of microwave exposure from cellular phone base stations: A first approach. Mobile Phone Base Station and Health. Dublin, May 15th and 16th, 2003.

27] Oftedal G, Wilen J, Sandstrom M, Mild KH. 2000. Symptoms experienced in connection with mobile phone use. Occup Med 50(4):237-245.
28] Preece AW, Davies-smith A, Wesnes K, Butler S, Lim E, Varey A. 1999. Effect of 915 MHz simulated mobile phone signal on cognitive function in man. Int J Biol. 75(4):447-456.
29] Rashidy-Pour A, Motamedi F, Motaghed-Laijani, Z. 1996. Effects of reversible inactivation of the medial septal area on reference and working memory versions of the Morris water maze. Brain Res 709:131-40.
30] Roosli M, Moser M, Meier M, Braun-Fahlander C. 2003. Health symptoms associated with electromagnetic radiation – A questionnaire survey. Mobile Phone Base Station and Health. Dublin, May 15th and 16th, 2003.
31] Sandstrom M, Wilen J, Oftedal G, Hansson Mild K. 2001. Mobile phone use and subject symptoms.Comparision of symptoms experienced by users of analogue and digital mobile phones. Occup Med 51(1):25-35.
32] Santini R, Santini P, Danze JM, Le Ruz P, Seigne M. 2002. Study of the health of people living in the vicinity of mobile phone base stations: I. Influences of distance and sex. Pathol Biol 50:369-73.
33] Sienkiewicz ZJ, Blackwell RP, Haylock RG, Saunders RD, Cobb BL. 2000. Low-level exposure to pulsed 900 MHz microwave radiation does not cause deficits in the performance of a spatial learning task in mice. Bioelectromagnetics 21:151-158.
34] Sienkiewicz ZJ, Haylock RG, Bartrum R, Saunders RD. 1998. 50 Hz magnetic field effects on the performance of a spatial learning task by mice. Bioelectromagnetics 19:486-493.
35] Wang B, Lai H. 2000. Acute exposure to pulsed 2450 MHz microwaves affects water-maze performance of rats. Bioelectromagnetics 21:52-56.

EXPOSURE OF MEDICAL STAFF TO STATIC MAGNETIC FIELDS FROM MAGNETIC RESONANCE IMAGING (MRI) SCANNERS

JOLANTA KARPOWICZ, MAILA HIETANEN[*)], KRZYSZTOF GRYZ

CENTRAL INSTITUTE FOR LABOUR PROTECTION – NATIONAL RESEARCH INSTITUTE, LABORATORY OF ELECTROMAGNETIC HAZARDS WARSZAWA, POLAND, e-mail: jokar@ciop.pl

[*)]FINNISH INSTITUTE OF OCCUPATIONAL HEALTH, HELSINKI, FINLAND, e-mail:maila.hietanen@ttl.fi

Abstract

The health care staff operating MRI devices are exposed to static magnetic field of significant spatial heterogenity (dB/dx) and high level of flux density – usually existing permanently during the work shift. They can be also exposed to pulses of magnetic field of high rate of rise/fall dB/dt, so-called gradient fields - existing only during examination of patients. The level of the workers' exposure depends both on the type of the magnet and ergonomical design of the particular MRI device.

The paper presents current state of the art on the occupational exposure to static magnetic field health effects, gaps in scientific data, MRI workers' exposure characteristic, research needs and suggestions for the exposure assessment protocol for further investigations.

Keywords: MRI, occupational exposure, electromagnetic fields, exposure assessment

1. Introduction – MRI EMF and exposure results

Electromagnetic fields associated with Magnetic Resonance Imaging

Nuclear magnetic resonance (NMR) is research method which can be used for medical imaging or spectral analysis of chemical structure of samples. The basic physical phenomenon in NMR is resonant absorption and re-emission of radiofrequency (RF) radiation by protons in a strong static magnetic field. In the magnetic resonance imaging (MRI) scanners, magnetic field useful for medical examination is result of summation of 2 components: static field produced constantly by strong magnets (permanent, resistive or superconductive) and pulses of time-varying so-called gradient field produced by gradient coils placed inside the housing of the MRI scanner [10]. The dynamic changes of spatial distribution of field produced in the result enables 3D changes of RF resonating absorption by patients tissues and in consequences the 3D imaging of the internal structure of the patient's body. Diagnostic coils placed at the MRI table or directly on the body of examined patient produce pulses of RF radiation used for such imaging.

Magnets of magnetic flux density of 0.2 - 3 T are currently used as a source of static magnetic field. Higher field's (up to 8 T) MR imaging is under intensive pre-clinical investigations. Workers operating MRI scanners are one of the highest exposed group to static magnetic fields because usually superconductive or permanent magnets generate the field constantly. Only resistive magnets can be switched off when the shift is over. Exposure of workers to RF and gradient fields is not common among MRI workers because during patients' examination medical staff is usually far from the magnet, controlling examination by a computer-console.

Biological and health consequences of electromagnetic fields exposure

Biological and health consequences of RF and gradient fields, associated with thermal effects and electro-sensitive tissues excitations, are relatively well investigated. In contrary, health effects of static magnetic fields are still under question, especially in case of chronic exposure of high level. Recent World Health Organization (WHO) monograph 232 [6] concluded that there is not sufficient scientific data for establishing health risk of static magnetic field exposure.

Physical effects of static magnetic fields (translation and orientation of charged molecules) cause electrodynamic

forces on moving electrolytes, and effects on electron spin states of chemical reaction intermediates [7]. Translation and orientation of molecular and cellular substances such as retinal rods, and some living cells have been experimentally observed in vitro in static fields of high level (above 1 tesla (T)), in various materials - dia- and paramagnetic such as hemoglobin, collagen, fibrin, and also on ferromagnetic particles such as magnetite. Water distribution can be also affected by high-gradient magnetic fields of high flux density (e.g., 8 T, 50 T/m; Ueno and Iwasaka 1994, following [7]), producing the force directly proportional to the square of the magnetic field strength and inversely proportional to the radius of the magnet e.g. force up to 30% the force of gravity in above-mentioned 8 T magnetic field, but only about 1% of gravity in whole-body 4 T magnet.

Static magnetic fields exert electrodynamic forces on moving ions in blood vessels, generating an electric potential across the blood vessels (Hall effect) and theoretically a reduction of blood flow velocity (Tenforde 1992, following [7]) - a 5 and 10% reduction in blood flow in the aorta was predicted to occur in static fields of 10 and 15 T, respectively, due to magneto-hydrodynamic interactions (Kinouchi et al. 1996, following [7]). Related observations included a 0.2–3% change in blood velocity between 1–10 T (Dorfman; Keltner, following [9]). Experimental examination of the scale of biomedical effects associated with electrodynamic and magnetodynamic forces in exposed human body are still under examination, frequently using electrocardiogram (ECG) technique. In addition, vertigo and other sensations, as difficulty with balance, nausea, headaches, numbness and tingling, phosphenes, and unusual taste sensations, were recorded during movement in high field. The other investigated endpoint were: cognitive function, assessed during exposure using standard neuropsychological tests, effects of exposure to fields of up to 8 T on heart rate, respiratory rate, systolic and diastolic blood pressure, finger pulse oxygenation levels, and core body temperature [7]. The exposed volunteers moved very slowly in comparison with normal workers activities in the vicinity of magnets (one or two feet over a few seconds, followed by a 15–30 s pause, taking overall about 3–4 min) into the magnet bore in order to avoid the transient, movement-induced sensations described above. Nevertheless, nine subjects reported sensations of dizziness, and two reported a metallic taste, assumed to be due to electrolysis of metallic chemicals in the subjects' teeth fillings (Schenck et al. 1992, following [7]).

IARC (2002) [12] notes that two somewhat dated studies (Neurath 1968; Ueno et al. 1984) report that exposure to 1 T fields with high spatial gradients (10–1,000 T/m) can adversely effect the development of frogs and toads, but notes that most studies indicate a lack of effect of static field exposure.

With static magnetic fields, reactions under laboratory conditions include a 17% increase in human cardiac cycle length at 2 T (Jehesen et al., following [9]). The authors suggested that the observed effect is probably harmless in healthy subjects, but that its safety in dysrhythmic persons was not certain. Such question is very important in the case of health examination for workers, who are going to start or continue MRI scanners operation.

2. Pattern of occupational exposure during MRI scanners operation

For health care staff (nurses, technicians, radiologists), the static magnetic field from MRI units is of special concern as during the shift the field is permanently on. Inside the MRI's room, the highest exposure occurs in the direct proximity to the magnet's housing. The workers are exposed to the static magnetic field while attending patients before and after examination and also while operating the MRI unit by the console situated on the housing of the magnet. Exposure to gradient and RF pulses is possible only during the examination and affects workers only in special cases, e.g. during so-called dynamic examination, interventional MRI procedure or because of emerging needs (even inside the bore of magnet). During patient's examination, the attendants usually stay in front of the monitor of computer controlling the examination, outside the MRI room (which is usually electromagnetically shielded to screen MRI device from all kinds of outside electromagnetic radiation).

During MRI examination, examined subject (selected part of patient's body) lies at the MRI's table located within the area of static magnetic field of very high spatial distribution's homogeneity in the bore of magnet's housing (in the case of so-called close MRI device) or in the open space between magnet's legs (in the case of so-called open MRI device). Medical staff activities are carried out in the vicinity of magnet housing, in the static field of significant spatial heterogeneity. The standing with the patient before/after examination, usually at the distance of 0.3 - 1.5 m from the housing of the magnet, last in the most cases 2 - 15 minutes [9]. The basic activities are as follows (fig. 1):

- attending at the MRI room during patient's access and lay down on the MRI's table (area A + B)
- positioning of diagnostic's RF coils on the MRI's table or patient's body (area A + B)
- plugging-in/off the RF coils' cables into the supplying socket (area A + B or D or E)

- MRI table positioning for fixing its initial geometrical position and put in/out it into/from the area of uniform field (inside magnet's bore or within open space of open device) (area A + C)
- attending at the room while patient is getting off from the MRI table (area A + B).

In the case of certain types of examination, a patient is dosed with some pharmaceutical components, e.g. contrast, frequently when patient is placed inside the magnet. In the most of cases dosing/injection is made by nurses, even if the use of infusion pumps is technically possible. These activities last 1 - 2 minutes and is frequently the reason of high exposure of the staff within area D at fig. 1.

Cleaners can be also exposed to high level of static magnetic fields inside MRI room or inside the bore of magnet because permanent and superconductive magnets are permanently on.

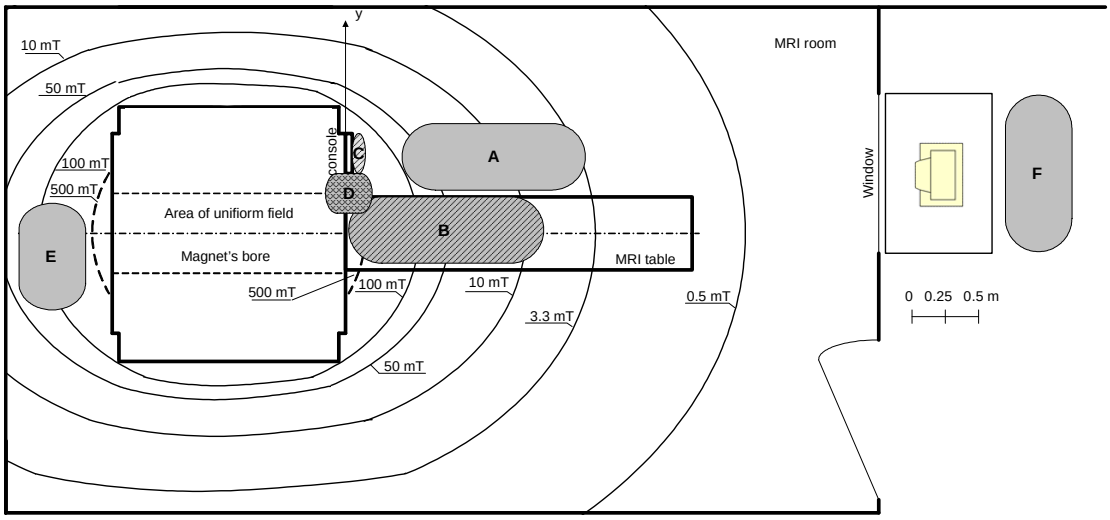


Fig. 1. Characteristic of the health care staff exposure while MRI examination attending: area A, E, F - whole body exposure; area B - hands exposure or head while worker is leaning towards the patient; C - hands exposure; D - hands or whole body exposure when worker have to approach very close to the area of uniform field (or is leaned against magnet housing) [9]

The exposure of medical staff to static magnetic fields while positioning the patient can be as high as the main field in the system, although locally and for limited periods of time. The trend towards the routine use of high field MRI systems (3–4 T) is increasing concern that exposure of workers and patients can exceed the existing recommended guidelines (tab. 1).

Table 1. Permissible occupational exposure to a static magnetic field.

Recommendations from	Whole body		Limbs		Cardiac stimulators and implanted electronically activated devices
	Whole working day	Ceiling value	Whole working day	Ceiling value	
ICNIRP guidelines, 1994 [7]	200 mT	2 T	not fixed	5 T	0.5 mT
EMF directive, 2004 [4]	200 mT	not fixed	not fixed	not fixed	mentioned but not fixed
IEEE standard, 2002 [8]	500 mT	500 mT	500 mT	500 mT	mentioned but not fixed
ACGIH, 2005 [1]	60 mT	2 T	600 mT	5 T	0.5 mT

Static field exposure levels must be quantified and controlled for medical staff safety. In the near future, ICNIRP is going to review its guidelines on limiting exposure to static magnetic fields [7]. Medical or paramedical staff may be exposed at low magnetic and electromagnetic fields around the device or outside the room for hours daily.

Concerning open or interventional MRI devices with magnetic field strength below 1.0 T, staff operating such devices are not exposed at levels higher than the currently recommended limits for occupational exposure. However, there are only limited data on the exposure of surgeons at open MRI devices.

Medical workers exposure to static fields from 20 various MRI devices of 0.2 - 2 T magnets, used for medical examination of various tissues (with head's examinations carried out the most frequently) presented by Karpowicz and Gryz [9] can be consider as the typical example of medical staff exposure pattern. The level of static magnetic field decreases rapidly with the distance from the magnet housing - app. 100-fold at a distance of about 2 m. In each of the cases, the area of controlled access for persons with cardiac pacemakers (B > 0.5 mT) exist, up to the distance no longer than approx. 5 m from magnet. Magnetic fields of B = 10 - 500 mT can be found in a distance up to approx. 1.5 m from the magnet. In the case of 0.5 - 2 T MRI units, the area of the high field, where occupational exposure limitations should be consider (B > 100 mT) can be found up to approx. 0.5 m from the border of the magnet's bore. The spatial distribution of the field levels are significantly non-isotropic around the bore magnets' housings - in front of and behind them much wider than sidelong. In the case of open MRI units, the spatial distribution of the field is isotropic around the magnet's housing.

Inside MRI rooms, the maximum exposure level in front of the magnet can reach 1 T. Exposure level in the area of workers' routine activities can reach 150 mT (for whole body exposure) and 600 mT (for hands exposure) (tab. 2). In the case of performing professional activities very close or inside the magnet's bore, workers can be exposed to higher fields. Exposure of hands to a static magnetic field up to 1,5 T was found. Exposure of workers outside the MRI room is lower, at a distance of 5 - 10 m, the magnetic field is normally less than 0.5 mT.

Table 2. Static magnetic field in the most possible places where health care staff attending patients before/after MRI examination [9].

Activities types	Health care staff exposure level, mT / MRI unit		
	0.2 T open	0.5 T bore	1.5 T bore
diagnostic RF coils positioning on the MRI table or patient's body - whole body exposure	3–50	5-100	50-150
diagnostic RF coils positioning on the MRI table or patient's body - hands exposure	5-100	20-250	100-600
plugging-in/off the RF coils cables into the supplying socket and console use - hands exposure	60-100	30-40	20-500 up to 1500*)
maximum field existing on the accessible for workers cover of magnet	200-270	80-300	250-600

*) - in case of location the supplying socket inside a magnet bore

3. Research needs concerning MRI exposure assessment

No serious adverse health effects from the whole-body exposure of healthy human subjects up to 8 T have been reported in the literature, but also no epidemiological studies have been performed yet to assess possible long term health effects in patients, workers, or volunteers. Only few informative studies have been performed using exposures above 2 T. This fact is very confusing against the growing up, the use of static magnetic fields in medicine, which lead to exposures of patients and workers to very high fields, even significantly exceeding the level of scientifically investigated exposure results (4 to 8 T). The main conclusions from WHO's health risk assessment of static magnetic fields [6], including the analysis of gaps in knowledge about possible health effects, indicated that, research carried out to date has not been systematic and has often been performed without appropriate methodology and exposure information. In consequences, no sufficient knowledge concerning safety conditions are available today for static magnetic fields exposure existing in the vicinity of MRI devices.

This lack of information resulted among others in the EU Directive 2004/40/EC provisions, which does not contain exposure limit value for static magnetic fields. To solve this serious problem for occupational safety and health engineering, further investigations concerning health risk assessments for static magnetic field exposure have been recently identified by international bodies [5, 6, 7, 14] as being of high priority for health risk assessment. The main areas identified for such research include:

- monitoring of occupational exposure, especially above 4 T, suitable to allow epidemiological studies

- epidemiological studies of possible long-term health effects in patients, volunteers, and staff with occupational exposure, particularly those with high levels of cumulative exposure

- epidemiological studies on pregnancy outcome, of high interest for patients as well as pregnant workers

- studies on biological effects of strong static magnetic fields, especially of chronic exposure on reproduction and development.

Further studies should be more systematic and coordinated. Appropriate dosimetry is important for all kind of research. There is a need to investigate the importance of physical parameters of exposure such as:

- field intensity

- exposure duration

- field gradient on biological outcome.

It means in practice the need of the use of investigations protocol, which allow the performance of the analysis of exposure level's distribution during the shift.

Epidemiological studies are of primary importance in health risk assessment [14]. The use of adequate estimates of exposure from all relevant sources and to establish real exposure pattern and it's variability among various countries is essential for quantitative analysis of research results and exposure's risk. High quality epidemiological studies, not executed yet, should focus on workers involved in high exposure areas and address endpoints such as cancer and pregnancy outcomes in occupational situations. Attention should be paid also to the important confounding variables, such as toxic fumes, vibration or other kinds of non-ionizing or ionizing radiation. Highly exposed occupational groups, as medical staff operating MRI scanners should be identified and followed over time with focus on common health outcomes with short latency periods (e.g. effects on CNS functions and cardiovascular effects). A health survey of surgeons, nurses and other workers using interventional MRI would provide useful information as to levels, durations and frequency of exposures of workers to static fields in these systems.

Experience with other frequencies has shown that obtaining reliable estimates of exposure to EMF for use in epidemiological studies can be very difficult, and surrogate measures of exposure, such as job title or distance from a particular source, may not always provide sufficiently accurate assessments. Investigations concerning low frequency exposure shown, that pocket-personal dosimeters would significantly improve exposure assessment for epidemiological studies and risk assessment. Adequate exposure assessment protocol for such method should be focused on:

- magnetic field strength
- magnetic field gradients
- exposure durations
- the rate of change of the magnetic due to motion.

Development of methods and tools for reliable assessment of human body exposure levels taking into account exposure metrics other than average field strength; criteria, improving exposure monitoring strategies both for static magnetic field and time-varying components, for complex and inhomogeneous exposure situations and for personal exposure assessment (personal dosimeters) is included in the high priority research needs [5] crucial for investigations on exposure risk for MRI technology. Numerical and experimental validation of the dosimeters is required and should consider technical properties of dosimeter coming from EMF sensor, its calibration, dynamic and frequency respond, spatial respond, sensitivity to human body, motion speed, sampling, etc. For the possibility of the use of monitoring results for various kind of analysis, it is very important to develop standardized exposure assessment protocol.

Studies in tissues, living cells and cell-free systems play a supporting role in health risk assessments [14]. Long-term and acute studies on experimental animals are needed using endpoints such as life-span, cancer, development, cardiovascular, immune system and CNS responses [5]. In vitro studies should investigate interaction mechanisms such as radical pair reactions and enzymatic activity, as well as effects on gene expression, mutagenicity and cell transformation.

Static magnetic fields may interact with biological systems in a number of ways, although the most likely means of causing health effects are via field-induced effects on charged molecules and alterations in the rate of biochemical reactions. Theoretical and computational studies are needed to investigate the magnitude and direction of induced currents and fields under various magnetic field exposure conditions.

Human laboratory studies on acute transient effects of exposure to static field effects studied in controlled exposure parameters can bring additional knowledge concerning thresholds of particular exposure effects and physical measures of exposure which should be monitored for exposure assessment in real situations. The priorities for such research [14] were identified including studies on field-induced vestibular dysfunction

including vertigo, head and eye coordination in a gradient and static magnetic field. Such investigations are focused on the MRI interventional procedures, when medical staff are in close proximity to patients within a magnet and are consequently exposed to relatively high fields. Further investigation of such mechanisms and intensity is considered of special interest because of the increasing likelihood that medical staff will be performing complicated tasks for extended periods of time within a magnetic field high exposure. Additional attention should be paid on cognitive and behavioral effects of static magnetic fields. Possible investigations could be executed as a battery of cognitive tasks that encompass standard tests of attention, reaction time and memory, as an initial work with exposed volunteers to find topics for further more focused work.

Proper design and interpretation of all types of above mentioned studies are not possible without expert dosimetric support. Computational dosimetry can provide the link between an external static magnetic field and the internal electric fields and induced currents caused by movement of living tissues in the field, taking into consideration specific tissues and organs. Precise investigations can be focused on the electric fields and currents associated with visual phosphenes and vertigo, fields and currents generated by head and eye movements in a static magnetic field, whole-body movement by staff around the interventional MRI system. Such investigations should be performed with the use of a very fine resolution head-and-shoulder phantom and are considered of particular relevance to interventional MRI procedures where reduced head movements of surgeons and other clinical staff may necessitate increased movement of the eyes.

The ability of non-error performing of such work can be of high importance for the patient’s safety, and should be also considered within occupational risk assessment.

4. Conclusion

There are many gaps in knowledge of biological effects and interaction mechanisms of MRI-related electromagnetic fields with tissues. High priority research needs cover the studies to fill important gaps in knowledge focused on health risk assessment that are needed to significantly reduce the uncertainty in the current scientific information. In the case of very specific occupational situation of medical staff operating MRI scanners, additional attention should take notice of the occupational risk assessment. Further investigations and exposure assessment should include the safety of patients from non-error work ability of medical staff and safety requirements preventing hazards from "flying metallic objects" (3 mT) and possible destroying of magnetic memories/cards (0.5 mT). Further investigations should provide knowledge for current scientific gaps, but also to allow verification of the protection level from exposure limitations published by various international and national bodies. Such needs indicate that exposure assessment should allow multi-level analysis of exposure pattern, harmonized with exposure limitations mentioned in Table 1. The most important topics for exposure assessment from MRI scanners should include static and gradient fields exposure, exposure results from workers movement in the area of spatially heterogeneous fields, medical staff, technicians, cleaners and other possible exposed workers groups, open and close magnets, low and high field magnets, diagnostic and interventional use, various types of medical procedures, availability of technical staff for the reduction exposure level and duration. In any case of further research, detailed exposure assessment protocol published with the biomedical research results will be of high importance for combined analysis of various studies and determination of the groups of highly exposed or at high risk groups of workers.

Acknowledgements

This paper was prepared as a part of the activities of European project EMF-NET (FP6 Co-ordination Action "EFFECTS OF THE EXPOSURE TO ELECTROMAGNETIC FIELDS: FROM SCIENCE TO PUBLIC HEALTH AND SAFER WORKPLACE", project No SSPE-CT-2004-502173)

References

1. ACGIH TLVs and BEIs. Based on the Documentations for Threshold Limit Values for Chemical Substances and Physical Agents & Biological Exposure Indices. American Conference Governmental and Industrial Hygienists, Cincinnati, OH, 2006.
2. Bassen H., Schaefer D. J., Zaremba L., Bushberg J., Ziskin M., Foster K. R., IEEE Committee on Man and Radiation (COMAR) Technical Information Statement “Exposure of Medical Personnel to Electromagnetic Fields from Open Magnetic Resonance Imaging Systems”, Health Physics, vol. 89, No. 6 (December), 684-689, 2005.

3. Cavin I. at all, Monitoring Occupational Exposure to MRI Static Magnetic Fields at 3T and & T, ICNIRP Workshop on EMF dosimetry, Berlin, March 2006 (poster)
4. Directive 2004/40/EC of the European Parliament and of the Council of 29 April 2004 on the minimum health and safety requirements regarding the exposure of workers to the risks arising from physical agents (electromagnetic fields) (18th individual Directive within the meaning of Article 16(1) of Directive 89/391/EEC), O.J. nr L-184 of 24 May 2004.
5. ENVIRONMENT AND HEALTH IMPLICATIONS OF ELECTROMAGNETIC FIELD EXPOSURE - Report on Research Needs, EMF-NET/WHO COMMITTEE on RESEARCH NEEDS - Elisabeth Cardis, Guglielmo D'Inzeo, Maria Feychting, Jukka Juutilainen, Jolanta Karpowicz, Norbert Leitgeb, Paolo Ravazzani (Chairman) , Mike Repacholi, Theo Samaras, Richard Saunders, Gyorgy Thuroczy, Emilie Van Deventer, Paolo Vecchia, and Bernard Veyret, sierpień, 2005 [http://www.jrc.cec.eu.int/emf-net/reports.cfm]
6. Environmental Health Criteria 232, Static Fields, World Health Organization, 2006
7. ICNIRP Statement on Medical Magnetic Resonance (MR) Procedures: Protection Of Patients. Health Physics 87(2): 197-216; 2004.
8. IEEE Standard for Safety Levels with Respect to Human Exposure to Electromagnetic Fields, 0-3 kHz, Std C.95.6, 2002.
9. Karpowicz J., Gryz K. - Health Risk Assessment of Occupational Exposure to a Magnetic Field From Magnetic Resonance Imaging Devices, International Journal of Occupational Safety and Ergonomics (JOSE), 2006, vol. 12, No. 2, 155-167.
10. Markisz J., Aquilia M., Technical Magnetic Resonance Imaging, Appleton&Lange, 1996.
11. Merkle E.M. et al – Safety, Compatibility, and Visualization Issues in Interventional MR Imaging, in: Practical MR Safety Considerations for Physicians, Physicists, and Technologists, ed. E. Kanal, Pittsburgh, USA, November 2001, pp 77-84.
12. Non-ionizing radiation, Part 1: Static and extremely low-frequency (ELF) electric and magnetic fields, IARC Monographs 80, IARC Press: Lyon, 2002.
13. Reilly P.J., Applied Bioelectricity. From Electrical Stimulation to Electropathology, Springer-Verlag New York, Inc., 1998.
14. WHO Research Agenda for Static Fields, World Health Organization, Geneva, 2006

CYTOTOXIC EFFECTS OF A SN MERCAPTONICOTINIC ACID COMPLEX ON WISTAR RAT LEIOMYOSARCOMA CELLS IN VITRO AND SIMULTANEOUS EXPOSURE AT LOW INTENSITY STATIC ELECTROMAGNETIC FIELDS: EVIDENCES OF A SYNERGY WITH STATIC ELECTROMAGNETIC FIELDS

IOANNIS VERGINADIS[1], IOANNIS ZELOVITIS[1], ANTONIOS AVDIKOS[1], TELEMACHOS DASKALOU[1], IOANNIS TOLIOPOULOS[1], IOANNIS SIMOS[1], MICHALIS BALLAS[1], SOTIRIS HADJIKAKOU[2], KONSTANTINOS HAVELAS[1], GEORGIOS HADZIAVAZIS[1], ANGELOS EVANGELOU[1], KONSTANTINOS CHARALABOPOULOS[1] AND SPYRIDON KARKABOUNAS[1]

[1]LABORATORY OF EXPERIMENTAL PHYSIOLOGY, DEPARTMENT OF MEDICINE, UNIVERSITY OF IOANNINA, GREECE,
[2]LABORATORY OF INORGANIC CHEMISTRY, DEPARTMENT OF CHEMISTRY, UNIVERSITY OF IOANNINA, GREECE

E-mail addresses: johnasterix20012001@yahoo.gr (Ioannis Verginadis), aevaggel@cc.uoi.gr (Angelos M. Evangelou), (Spyridon CH. Karkabounas).

Corresponding author: Dr Spyridon CH. Karkabounas, Lecturer of Physiology, Lab of Physiology, Dept of Medicine, University of Ioannina, Greece, Tel: 0030-26510-97576, Fax: 0030-26510-97850, E-mail : skarkabou@cc.uoi.gr.

Abstract

The aim of this study is to examine the possible synergistic action between the cytotoxic $Ph_3Sn(MNA)SnPh_3$ complex (SNMNA) and its electromagnetic resonance radiofrequencies on proliferation and viability of a cancer cell line. Leiomyosarcoma tumor cells (LMS cells) were isolated from cancer bearing Wistar rats and tested for their proliferation and viability after administration of the SNMNA complex in various concentrations. We used an appropriate system to take the resonance radiofrequencies spectrum of the SNMNA complex. Then the LMS cells were exposed to two groups of frequencies for 45 min every 24h to determinate their proliferation and viability. Lastly we studied the simultaneous administration of the SNMNA complex and exposure to two groups of its radiofrequencies. The data collected reveal that the SNMNA: 1) Is a very cytotoxic and antiproliferative agent against cancer cells and 2) In low concentrations exercises synergistic action with Electromagnetic Resonance Frequencies (ERFs) and promotes obvious cytotoxic and antiproliferative action. In conclusion, SNMNA complex presents a relatively strong anticarcinogenic and cytotoxic activity. The mechanism of SNMNA complex action on the LMS cells seems to be related with the inhibition of the glycolytic metabolism of the cancer cells. Possibly the SNMNA complex acts as an anti-metabolite competing nicotinic acid in energy production metabolic pathways in which it participates as a coenzyme. The cytotoxicity of the SNMNA complex can be modified with the use of electromagnetic fields which can result beneficial for its future therapeutic actions.

Introduction

LMS tumor is a type of cancer which presents great resistance to chemotherapy. Until, cis-platinum is the preferred therapeutic agent [1,2,3,4]. Due to its chemical characteristics and the ability to form bonds between DNA strands, the main intercellular target of cis-platinum is the cell's DNA [5] The Pt derivatives interpolate between DNA strands and provoke structural deformation to DNA molecules inhibiting the functional rotations around the histones resulting to DNA fragmentation. [5]. It is not really clear if cis-platinum as well as other forms of Pt complexes is metabolically activated by cell's microsomial system in order to react with DNA molecule [6]. Platinum is the preferred element used to construct metal complexes with antitumoral effects. Various Tin complexes are used in the same therapeutic approach as platinum, for cancer experimental therapy [7,8,9,10,11,12,13,14,15,16,17]. A restrict number of experimental studies indicated that Tin complexes may act with a different mechanism of cis-Pt [11,12,13,14,15,16,17]. The present project studies the cytotoxic and antiproliferative effects of SNMNA complex and the synergistic action between the SNMNA complex and its electromagnetic resonance radiofrequencies on cancer cells *in vitro*.

Material and Methods

Tumor cell line development: LMS cells were produced the following way: 3 male and 3 female Wistar rats were selected from a group of syngenic laboratory animals (7th generation). After anaesthetization with ketamine and midazolam, B[a]P was administered using the procedure described by Karkabounas et al [18,19,20,21,22]. 110 to 128 days late, all animals developed tumors. Biopsies were performed after anaesthetization with diethyl ether and a sample of malignant cells was attained using a bioptic needle. Tumors of 4 animals were histological identified as LMS tumors (65%). One of them developed fibromyosarcoma and another rhabdomyosarcoma. Aseptic samples of LMS tumors sizing about 0,5 cm^3 were placed into cold Ringer sterile solution. Then they were aseptically cut into smaller pieces (around 1mm^3) and placed in a sterilized glass beaker with 20 ml of Trypsin 0,25% solution. Incubation of the pieces was performed by a gently stir and every 15 minutes 20 ml of the supernatant were collected and placed into sterile plastic tubes (falcon) for further process. Before we commence the second round of trypsinisation 10ml of Dulbeco's Modified Eagles Medium (DMEM) were added to protect tumors from the trypsin action. Afterwards 10 ml of DMEM were rejected and 20 ml of trypsin 0,25% solution were added again and the same trypsinization process was repeated until the tumor pieces were dissolved in released tumor cells. In each tube with the collected tumor cells after trypsinization, we added 1 ml of Foetal Bovine Serum (FBS) in order to stop the action of trypsin. The tubes containing the initial trypsinised samples of the tumors centrifuged at 1200 rpm for 5 minutes in order to form a pellet all the remaining cells. Supernatant was rejected, 10ml of Phosphate Buffer Saline (PBS) were added and the cell suspension was gently mixed using pipette before the second centrifugation at 1200 rpm for 5 minutes. Supernatant was again rejected, 10 ml of DMEM with 10% FBS were added, mixed with the cells and a sample of 1 ml suspension was cultured in a Petri dish (9 ml DMEM, 1 ml FBS). Cells incubated at 37% ^oC, 95% O_2, 5% CO_2 and examined once a day by light microscopy. Cells were subcultured in order to obtain large numbers of tumor cells. The confluent tumor cells in each Petri dish washed with 10 ml of PBS to digress the dead cells, added 1 ml of trypsin 0,25% solution in order to be detached and 10 ml of DMEM to stop the trypsin action. The cell suspension from Petri dish transferred into sterilized plastic tubes and centrifuged at 3000 rpm for 5 minutes. The supernatant rejected and the pellet of cells resuspended in a cryopreservation solution of FBS and Dimethyl Sulfoxide (DMSO) at 9:1 ratio, placed in cryotubes (1ml of total volume) and stored in liquid nitrogen in order to be used again when needed. Examination the nature of these cells was performed using two techniques: 1) Classic diagnostic after Giemsa dyeing**,** 2) Biological testing. We used large numbers of viable tumor cells collected from a recent cell culture as described above. These cells were inoculated into Wistar rats, belonging to a homogenic line, to whom the initial tumor sample was taken (syngenic animals). Before the inoculation the rats anaesthetized with ketamine and midazolam (20mgr+6mgr per Kg BWt) followed by a 2 cm surgical incision performed aseptically on the left shoulder blade. The tissues removed and severed lightly until a small bleeding. $4x10^6$ LMS cells suspended in 1 ml of Hanke's solution and inoculated on the traumatized tissues by a gentle injection. The edges of the wound ascended και stitched so as the LMS cells to remain in the wound. Tumors were developed after a period of around 10-20 days. Small tumor pieces were cut for histopathological examination. All tumor samples were identified as Leiomyosarcomas. All the inoculated animals developed the characteristics of the neoplastic disease. Tumor's size at death was around 38-45% of the total animal weight.

SNMNA complex cytotoxicity and antiproliferative effects on LMS cells *in vitro*: For these experiments we used LMS cells taken from liquid nitrogen. The LMS cells were cultured in a Petri dish and incubated for 10 days in order to control the proliferation rate and viability. When the LMS cells become confluent, the DMEM rejected, washed with PBS and 1ml of trypsin 0,25% solution added. After five minutes incubation the LMS cells were detached and we added 10 ml of DMEM in Petri dish. We counted the LMS cells on a cymometer Newbauer and seeded in Petri dish containing 24 wells totally (25.000 LMS cells per well, total volume 1 ml). We seeded 3 Petri dishes for 24, 48 and 72 hours. After 24 hours incubation we renewed the DMEM in 12 wells of each Petri (control wells). At the remaining 12 wells of each Petri we rejected the DMEM and added the dissolved in DMEM SNMNA complex in various concentrations (test wells). The total volume was 1 ml per well. We examined the following concentrations of the SNMNA complex: $0,5x10^{-9}$ M, $0,75x10^{-9}$ M, $1x10^{-9}$ M, $5x10^{-9}$ M, $20x10^{-9}$ M, $50x10^{-9}$ M, $75x10^{-9}$ M, $100x10^{-9}$ M, $125x10^{-9}$ M, $150x10^{-9}$ M, 200 $x10^{-9}$ M, 250 $x10^{-9}$ M. After 24 hours incubation we rejected the DMEM, washed with 1 ml of PBS, added 0,25 ml of trypsin 0,25% solution and incubated again for 5 minutes. When the LMS cells were detached we added 0,25 ml of PBS and 0,5 ml of trypan blue 0,4% solution (total volume 1 ml). After 5 minutes we counted the LMS cells of each well on a cymometer Newbauer. The above procedure for 24 hours cell testing was repeated for 48 and 72 hours incubation.

Chemicals: DMEM, DMSO, PBS and Trypan Blue 0,4% were purchased from Sigma; Trypsin 0,25% and FBS were purchased from PAA (Cell culture company); Stereochemical formula of SNMNA complex is shown at photo 1.

Simultaneous administration of the tin complex and its electromagnetic resonance radio frequencies on LMS cells *in vitro*: This experiment included 5 different tests. Cell viability was the comparable parameter in every test. Cell viability was tested by using Trypan Blue 0,4% solution, counting only live cells. For all the 5 different tests, 25.000 LMS cells were cultured in each well of a Petri (24 wells totally), using 6 wells for each count at 24, 48 and 72 hours. Each test was performed as follows:
1st test line (control of the controls): The results of these tests were used to confirm the controls (double blinded) and were characterized as E1 test. Particularly, 24h after cell culture, DMEM was rejected, each well was washed with 1ml PBS and fresh DMEM was added to a final volume of 1ml. Cells were incubated for 24h at 37oC, 95% O_2, 5% CO_2. DMEM was again rejected in the first 6 wells which was washed using 1ml of PBS. 0,25 ml of trypsin solution 0,25%, was then added in each well and cells were incubated for 3 minutes in order to detach. After 3 minutes period 0,25ml of PBS and 0,5ml Trypan Blue (0,4%) solution were added. Following 5 minutes of incubation cell viability was measured using a microscope. This procedure was repeated at 48 and 72h.
2nd test line (control): The results of these experiments were used as controls (blind) and were characterized as E2 tests. LMS cell culture, 24h incubation, dead cell rejection, PBS wash, DMEM renewal was performed as descript above. The next step was to let the Petri outside the incubation chamber at RT (25 ^oC) and normal atmosphere (N_2 80% and O_2 20% approximately) under sterilized conditions for 45 minutes. LMS cell viability was measured after 24h incubation (Trypan Blue method described above). The same treatment was repeated at 48 and 72h in order to determinate the LMS cell viability.

3rd test line (substance activity): This line of experiments was characterized as E3 and was conducted the same way as E1 with the exception that before the first 24h incubation the SNMNA complex was dissolved in DMEM (1ml of total volume) and added in each well at various concentrations (1st group: 10^{-12} M, 10^{-15} M, 10^{-18} M and 2nd group: $5x10^{-9}$ M, $20x10^{-9}$ M, $50x10^{-9}$ M). LMS cell viability control was performed at the same time periods using the same methods as described above.

4th test line (electromagnetic field activity): This line of experiments was characterized as E4 and was performed in the same way as E2 with a simultaneous exposure of the Petri at a range EFRs of SNMNA complex for 45 minutes (1st group of exposure included 10 frequencies, 2nd 328 frequencies). LMS cell viability control was determinated at the same time periods using the same methods. The conditions of exposure were the same as E2.

5th test line (simultaneous activity of the SNMNA complex and the electromagnetic field): This line of experiments was characterized as E5 and included the simultaneous study of the SNMNA complex actions (2 groups of concentrations) and exposure to its ERFs (2 groups of frequencies) on the LMS cells. Experiments were performed by combining E3 and E4 test lines (addition of the SNMNA complex at known concentrations and exposure at known frequency groups of the LMS cells for 45min/24h). All cell lines experiments were repeated 5 times.

Equipment and used apparatus

Recording-storing-frequency broadcasting system: The used system is called Multi Channel Dynamic Exciter (MCDE) and it is composed of: a) the diagnostic system, b) the storing system and c) the field generator. The diagnostic system is based on Bohm-Aharonov effect, which was discovered by them in 1959 during a study involving experiments of recording beams of electrons (β rays) through a number of various solenoids [23,24]. A substance or a biological sample is put in a determinate part of the diagnostic apparatus in connection with a solenoid and the electromagnetic frequencies generator. The generator is activated and scan a broad spectrum of radiofrequencies from 0,1 Hz to 1 MHz. The frequencies in which observed resonance between electromagnetic radiofrequencies emitted by the sample (substance or biological material) and the generator's radiofrequencies are stored. In this manner is determinated a spectrum of resonating radiofrequencies that characterize the chemical substance or the biological material. This spectrum is called as the specific fingerprint of this chemical substance or biological material. This spectrum is registered at the memory of the storing system and transformed at different radiofrequencies by an appropriate algorithm. The transformed radiofrequencies can be used as input in the field generator and emitted back to the target to influence this chemical or biological material. The generator of electromagnetic fields used in the current study produce static electromagnetic fields with the following characteristics: the intensity of the electric field is 1,1-1,11±0,01 V/m and 0,0027-0,0029±0,00005 A/m for the magnetic field. The radiofrequencies broad ranged from 10Hz to 1MHz. The energy density of the MCDE system generated electromagnetic fields is approximately 100mW/cm^3. The MCDE system [photo 2] was examined for its safety application in animal and humans by the National (Greek) Center for Scientific Research «Demokritos» (Greek Department of the International Committee of Atomic Energy). The MCDE system was found safe for prolonging exposure humans, animals and other living systems. The MCDE system was placed inside a Faraday cage, in order not to be affected by external electromagnetic fields.

Results

Cytotoxicity of SNMNA complex: SNMNA complex is a very cytotoxic agent against LMS cells [figure 1-4]. The Inhibitory Concentration (IC_{50}) for this complex according to these figures is calculated between 5 and 20 nM for 24h, 48h and 72h. Minimal lethal concentration (MLC) of the complex at 24h ranges between 50-75nM, at 48h around 75nM and at 72h between 30-40nM. At all time points (24h, 48h, 72h) there was no significant different between the values of MLC. Thus, LMS cells seem sensitive to the SNMNA complex cytotoxic effects. The SNMNA complex presents a time depending cytotoxic action, and MLC reaches minimum value at 72h. At 48h MLC value is rather steady at 75nM which can be explained as a cell homeostasis adaptation for neutralize the SNMNA complex cytotoxic effects.

Synergistic activity of the complex and its ERFs:

Considering data from test lines E1, E2, E3, E4 and E5 we can conclude that: 1) LMS cell proliferation rate from 24h to 72h shows an increasing rate (control of controls E1). Thus, LMS cells present high viability during incubation without the presence of a substance or electromagnetic field [fig 1,2,3,4], [photo 3], 2) LMS cell proliferation rate (control E2) shows a slight decrease. Cells seem to be affective by stress when they are outside the incubating chamber (45minues/24h) although they continue to proliferate with increasing rates, 3) LMS cell proliferation rate at test line E3 is significantly lower compared with E1 and E2. Proliferation rate drop is smaller at low concentrations (10^{-12}, 10^{-15}, 10^{-18} M) [fig 5,7], [photo 4] and higher at high concentrations ($5x10^{-9}$, $20x10^{-9}$, $50x10^{-9}$ M) [fig 6,8],. These data imply the strong cytotoxic activity of the SNMNA complex, 4) LMS cell proliferation rate at test line E4 is lower compared with E1 and E2. Thus, even when the SNMNA complex is absent the exposure of the LMS cells to its resonance frequencies provokes the death of the cancer cells. The electromagnetic field exposure is more cytotoxic in comparison with the activity of the SNMNA complex at low concentrations (10^{-12}, 10^{-15}, 10^{-18} M) [fig 5,7]. At higher concentrations ($5x10^{-9}$, $20x10^{-9}$, $50x10^{-9}$ M) [fig 6,8] the fields shows smaller cytotoxic activity than the SNMNA complex, 5) LMS cell proliferation rate at test line E5 is significantly lower. The decrease of the proliferation rate is the highest among the test lines [fig 5,6,7,8] especially at 48h and 72h. In contrast a small increase is observed at 24h in relation with E2 test line and E1 (smaller than E2), [photo 5]. The decrease of the proliferation rate observed by simultaneous administration of the lowest SNMNA complex concentration (10^{-18} M) and the exposure to its electromagnetic radiofrequencies is the highest among the other low concentrations (10^{-12}, 10^{-15} M) with the presence of the electromagnetic field [Table 1,2]. There is a 54,79% (72h) [Table 1] decrease of the proliferation rate of E5 (C=10^{-18} and 10

radiofrequencies) and 51,35% (72h) [Table 1] decrease of the proliferation rate of E5 ($C=10^{-18}$ and 328 radiofrequencies), in comparison to E2. This result indicates a synergistic effect on LMS cells between the SNMNA complex and its electromagnetic radiofrequencies. The decrease of the LMS cell proliferation rate is related to the exposure time rather than the number of frequencies used in each group.

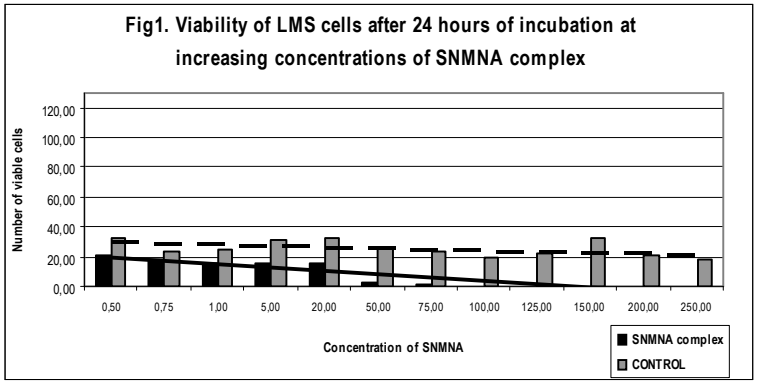


fig 1: We measure the viability of LMS cells after 24 hours of incubation at increasing concentrations ($0,5x10^{-9}$ M, $0,75x10^{-9}$ M, $1x10^{-9}$ M, $5x10^{-9}$ M, $20x10^{-9}$ M, $50x10^{-9}$ M, $75x10^{-9}$ M, $100x10^{-9}$ M, $125x10^{-9}$ M, $150x10^{-9}$ M, 200 $x10^{-9}$ M, 250 $x10^{-9}$ M) of SNMNA complex.

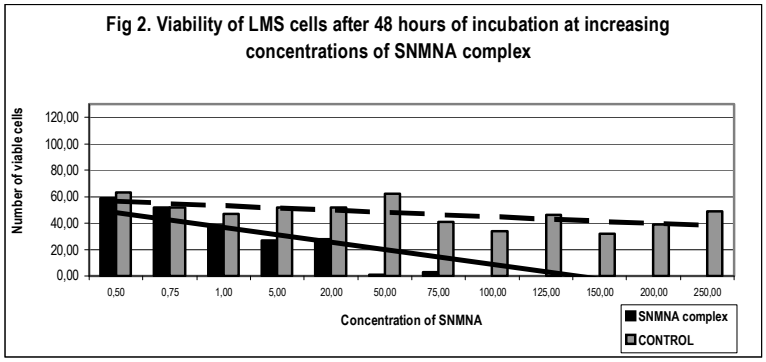


fig 2: We measure the viability of LMS cells after 48 hours of incubation at increasing concentrations ($0,5x10^{-9}$ M, $0,75x10^{-9}$ M, $1x10^{-9}$ M, $5x10^{-9}$ M, $20x10^{-9}$ M, $50x10^{-9}$ M, $75x10^{-9}$ M, $100x10^{-9}$ M, $125x10^{-9}$ M, $150x10^{-9}$ M, 200 $x10^{-9}$ M, 250 $x10^{-9}$ M) of SNMNA complex

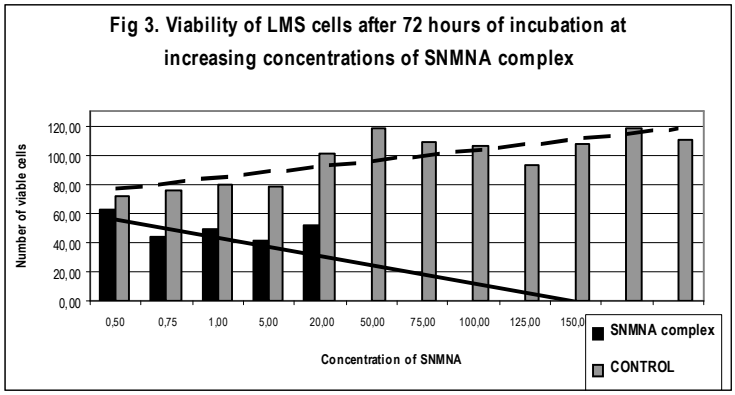


fig 3: We measure the viability of LMS cells after 72 hours of incubation at increasing concentrations ($0,5x10^{-9}$ M, $0,75x10^{-9}$ M, $1x10^{-9}$ M, $5x10^{-9}$ M, $20x10^{-9}$ M, $50x10^{-9}$ M, $75x10^{-9}$ M, $100x10^{-9}$ M, $125x10^{-9}$ M, $150x10^{-9}$ M, 200 $x10^{-9}$ M, 250 $x10^{-9}$ M) of SNMNA complex

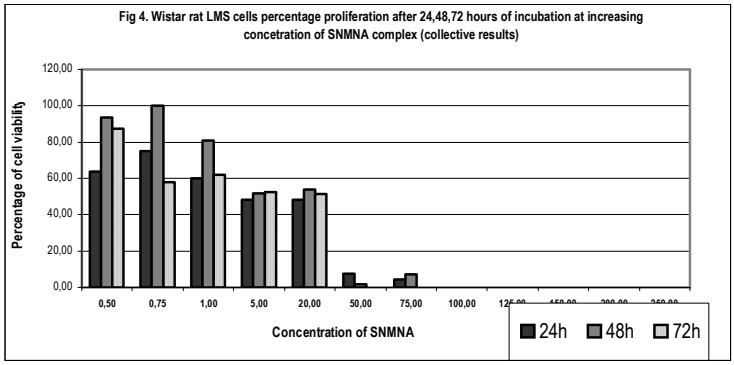


fig 4: Wistar rat LMS cells percentage proliferation after 24,48,72 hours of incubation at increasing concentrations (0,5x10^{-9} M, 0,75x10^{-9} M, 1x10^{-9} M, 5x10^{-9} M, 20x10^{-9} M, 50x10^{-9} M, 75x10^{-9} M, 100x10^{-9} M, 125x10^{-9} M, 150x10^{-9} M, 200 x10^{-9} M, 250 x10^{-9} M) of SNMNA complex (collective results)

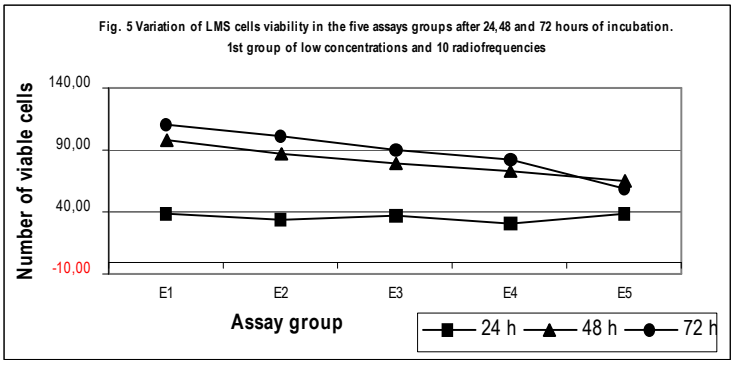


fig 5: In this one we measure the variation of LMS cells viability in the five assays groups (E1, E2, E3, E4, E5) after 24,48 and 72 hours of incubation. 1st group of low concentrations (10^{-12} M, 10^{-15} M, 10^{-18} M) and 10 radiofrequencies

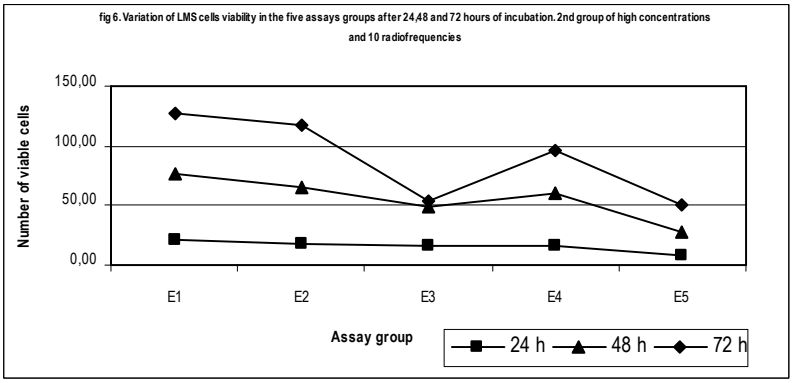


fig 6: We measure the variation of LMS cells viability in the five assays groups (E1, E2, E3, E4, E5) after 24,48 and 72 hours of incubation. 2nd group of high concentrations (5x10^{-9} M, 20x10^{-9} M, 50x10^{-9} M) and 10 radiofrequencies.

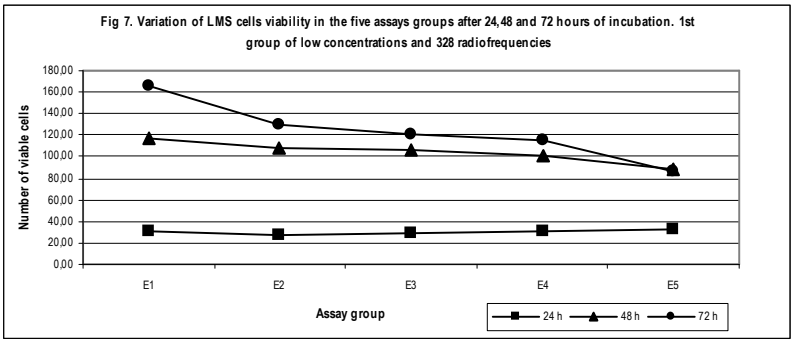


fig 7: We measure the variation of LMS cells viability in the five assays groups (E1, E2, E3, E4, E5) after 24,48 and 72 hours of incubation. 1st group of low concentrations (10^{-12} M, 10^{-15} M, 10^{-18} M) and 328 radiofrequencies

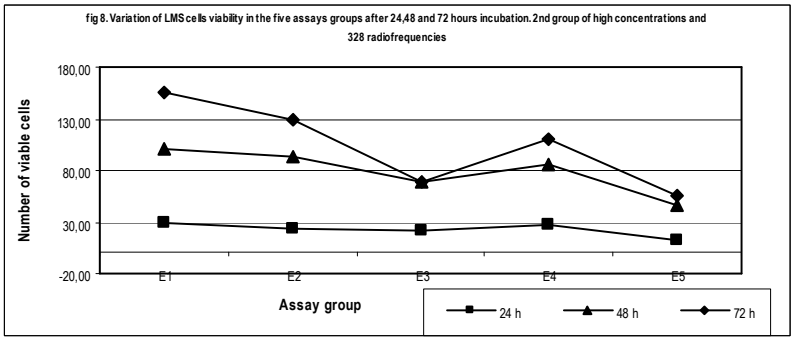


fig 8: We measure the variation of LMS cells viability in the five assays groups (E1, E2, E3, E4, E5) after 24,48 and 72 hours incubation. 2nd group of high concentrations ($5x10^{-9}$ M, $20x10^{-9}$ M, $50x10^{-9}$ M) and 328 radiofrequencies.

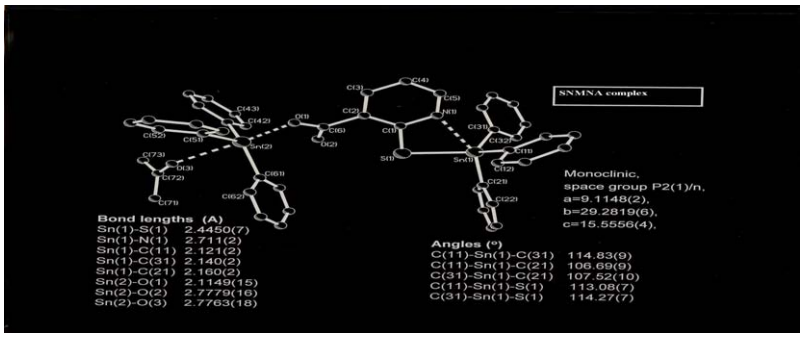


Photo 1: Formula and structural characteristics of the SNMNA complex.



Photo 2: The MCDE system in Faraday cage.

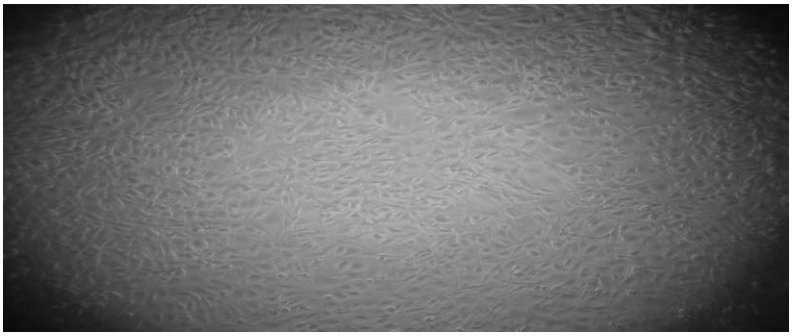


Photo 3: E1 assay (control of the controls). The LMS cells was confluent.



Photo 4: E3 assay (substance activity). Decrease of LMS cell population after 72 h incubation at 10^{-18} M of SNMNA complex.

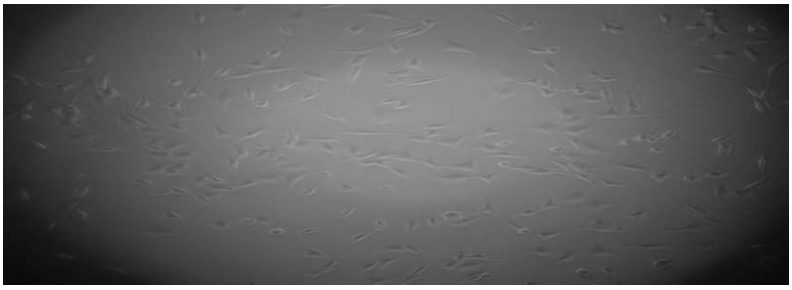


Photo 5: E5 assay (simultaneous activity of the SNMNA complex and the electromagnetic field). Synergistic decrease of LMS population after 72 h incubation at 10^{-18} M of SNMNA complex and 3x45 min total exposure at the electromagnetic field.

		(L+10)	
10^{-12} M	28,43	-15,96	-32,33
10^{-15} M	0,90	-31,19	-36,09
10^{-18} M	-5,68	-42,98	-54,79
		(L+328)	
10^{-12} M	18,32	2,99	-8,37
10^{-15} M	48,85	0,69	-50,13
10^{-18} M	1,15	-48,05	-51,35

Table 1: Shows the time dependent declination of LMS cell proliferation in low concentrations (10^{-12} M, 10^{-15} M, 10^{-18} M) of SNMNA complex. The decrease of the LMS cell proliferation is independent to the

number of radiofrequencies. The lowest concentration (10^{-18} M) shows the highest cell proliferation decrease. The table shows the percentage LMS cell proliferation (E5 in comparison with E2 assay).

		(H+10)	
5nM	-22,34	-35,44	-27,55
20nM	-41,08	-43,04	-44,60
50nM	-94,64	-100,00	-100,00
		(H+328)	
5nM	-25,98	-31,30	-27,02
20nM	-36,33	-39,23	-40,15
50nM	-91,63	-100,00	-100,00

Table 2: Shows the time dependent declination of LMS cell proliferation in high concentrations ($5x10^{-9}$ M, $20x10^{-9}$ M, $50x10^{-9}$ M) of SNMNA complex. The accumulative decrease (SNMNA complex+electromagnetic field) is minor in comparison with results in table 1. The prevalence of SNMNA complex concentration on the electromagnetic field effects is obvious. The table shows the percentage LMS cell proliferation (E5 in comparison with E2 assay).

Discussion

We have studied the effects of the SNMNA complex on a Wistar rat LMS cancer cell line. We also studied if it is possible to modify the cytotoxicity of the SNMNA complex using electromagnetic fields at radiofrequencies of the complex resonance spectrum. SNMNA complex is a strong cytotoxic agent on LMS cancer cells *in vitro* [11,12,13]. Mercaptonicotinic acid is an essential moiety of the complex and it is possible to act as anti-metabolite. Nicotinic acid participates in coenzymes (NAD^+, $NADP^+$), which take place as reduced equivalents carriers in glycolysis pathway and Krebs cycle in cancer cells [25]. Thus, nicotinic acid seems as a very important agent at energy production of tumors energetic metabolism [25]. Mercaptonicotinic acid of the SNMNA complex may compete nicotinic acid coenzymes in the above metabolic energy production pathways. The used LMS cells, such as other cancer cell types, seem to produce energy by glycolytic pathway [26,27,28,29,30,31,32]. This point has been shown by preliminary experiments in which the LMS cells are very sensitive to iodoacetic acid [31,32]. Iodoacetic acid is a strong inhibitor of the glyceraldehyde-3-phosphate dehydrogenase [29]. This enzyme plays a critical role for the whole glycolytic pathway and so the ATP glycolytic production stops by inhibiting this enzyme [33]. The SNMNA complex acts in very low concentrations lower than the iodoacetic acid. On the other hand the SNMNA complex is a strong inhibitor of the 5-lipoxygenase [13,14]. Generally the lipoxygenase, cyclooxygenase 1 and cyclooxygenase 2 inhibitors of synthetic or natural origins are still used as anti-cancer substances with target action [34,35]. It is possible that SNMNA complex acts as a non steroid antinflammation derivative (NSAID) inhibiting 5-lipoxygenase on LMS cells [13,14]. In a recently published work, we find that the SNMNA complex produces free radicals in aquatic solutions [13,14]. This is verified from the EPR spectrums of the SNMNA complex [13,14]. The energy of electromagnetic fields may activate the electrons of the SNMNA complex bonds causing electron excitation. Exposure of SNMNA complex aquatic solutions to UV radiation causes the immediate production of free radicals [13,14]. The chemical reactions can be accelerated when an external electromagnetic field influences a chemical system [36,37,38,39]. For example the Belluzov – Zhabotinsky (BZ) reaction of malic acid catalyzed by Fe^{+2} – Fe^{+3} ions (and not Ce) can be accelerated with the use of a low intensity external electromagnetic field (0,1 μT) [37]. Metal complexes such as SNMNA complex can be activated by external electromagnetic fields. The characteristic (fingerprint) resonance radiofrequencies spectrum of a substance can reduce the energy threshold activation of this substance and catalyse its chemical and biological effects.

Acknowledgements: We want to thank the Hellenic Hepirus Biotechnology R&D JS Company for the offer of many reagents.

References

1. K. Charalambopoulos , S. Karkabounas , E. Ioachim , V. Papalimneou , K. Sirigos , A. Evangelou , N. Agnantis and N. Hadjiliadis. Antitumour and toxic effects on Wistar rats of two new platinum complexes. European Journal of Clinical Investigation 2002;32(2):129-33

2. Pautier P, Rev A, Haie-Meder C, Kerbrat P, Dutel JL, Gesta P, Bryard F, Morice P, Duvillard P, Lhomme C. Adjuvant chemotherapy with cisplatin, ifosfamide, and doxorubicin followed by radiotherapy in localized uterine sarcomas: results of a case-control study with radiotherapy alone. Int J Gynecol Cancer. 2004;14(6):1112-7

3. Sagae S, Yamashita K, Ishioka S, Nishioka Y, Terasawa K, Mori M, Yamashiro K, Kanemoto T, Kudo R. Preoperative diagnosis and treatment results in 106 patients with uterine sarcoma in Hokkaido, Japan. Oncology. 2004;67(1):33-9

4. Resnik E, Chambers SK, Carcangiu ML, Kohorn EI, Schwartz PE, Chambers IT. Malignant uterine smooth muscle tumors: role of etoposide, cisplatin, and doxorubicin (EPA) chemotherapy. J Surg Oncol 1996;63(3):145-7

5. Ruiz J, Lorenzo J, Sanglas L, Cutillas N, Vicente C, Villa MD, Aviles FX, Lopez G, Moreno V, Perez J, Bautista D. Palladium(II) and Platinum(II) Organometallic Complexes with the Model Nucleobase Anions of Thymine, Uracil, and Cytosine: Antitumor Activity and Interactions with DNA of the Platinum Compounds. Inorg Chem. 2006;45(16):6347-60

6. LeBlanc GA, Sundseth SS, Weber GF, Waxman DJ. Platinum anticancer drugs modulate P-450 mRNA levels and differentially alter hepatic drug and steroid hormone metabolism in male and female rats. Cancer Res. 1992;52(3):540-7

7. Federica Barbieri, Fabio Sparatore, Monica Cagnoli, Cristina Bruzzo, Federica Novelli and Angela Alama. Antiproliferative activity and interactions with cell-cycle related proteins of the organotin compound triethyltin(IV)lupinylsulfide hydrochloride. Chem Biol Interact 2001;134(1): 27-39

8. Ruslan Sarimov, Eva Markova, Fredrick Johansson , Dag Jenssen, and Igor Belyaev. Exposure to ELF magnetic field tuned to Zn inhibits growth of cancer cells. Bioelectromagnetics 2005;26:631-638

9. Saxena A, Tandon JP. Antitumor activity of some diorganotin and tin(IV) complexes of Schiff bases. Cancer Lett 1983;19(1):73-6.

10. Martin Blank and Lily Soo. Electromagnetic acceleration of the Belousov–Zhabotinski reaction. Bioelectrochemistry 2003;61(1-2):93-97

11. Xanthopoulou M, Hadjikakou S, Hadjiliadis N, Schurmann M, Jurkschat K, Michaelidis A, Skoulika S, Bakas T, Binolis J, Karkabounas S and Charalabopoulos K. Synhesis, structural characterization and in vitro cytotoxicity of organotin[IV] derivatives of heterocyclic thioanides 2-mercapto-benzothiazole, 5-chloro-2-mercapto-benzothiazole, 3-methyl-2-mercapto-benzothiazole, and 2-mercaptonicotinic acid. Journal of Inorganic Biochemistry. 2003;96(2-3):425-34.

12. Xanthopoulou M, Hadjikakou S, Hadjiliadis N, Schurmann M, Jurkschat K, Binolis J, Karkabounas S, Charalabopoulos K. Synthesis of a novel triphenyltin[IV] derivative of 2-mercaptonicotinic acid with strong cytotoxicity in vitro. Bioinorganic Chemistry and Applications. 2003;1(3-4):227 – 231.

13. Xanthopoulou M, Hadjikakou S, Hadjiliadis N, Kubicki M, Karkabounas S, Charalabopoulos K, Kourkoumelis N, Bakas T. Synthesis and characterization of a new chloro – di – phenytin[IV] complex with 2-mercaptonicotinic acid : study of its influence upon a catalytic oxidation of linoleic acid to hydroperoxylinoleic acid by the enzyme lipoxygenase. Journal of Organometalic Chemistry, 2006;691:1780 – 1789.

14. Xanthopoulou M. Biomedical Applications of Thioamides. Synthesis and study of new organotin[IV] thioamides derivatives with biological actions. PhD Thesis, 2006, Department of Chemistry. University of Ioannina.

15. Li Q, da Silva MF, Pombeiro AJ. Diorganotin(IV) derivatives of substituted benzohydroxamic acids with high antitumor activity. Chemistry. 2004;10(6):1456-62

16. Han G, Yang P. Synthesis and characterization of water-insoluble and water-soluble dibutyltin(IV) porphinate complexes based on the tris(pyridinyl)porphyrin moiety, their anti-tumor activity in vitro and interaction with DNA.J Inorg Biochem. 2002;91(1):230-6

17. Syng-Ai C, Basu Baul TS, Chatterjee A. Inhibition of cell proliferation and antitumor activity of a novel organotin compound. J Environ Pathol Toxicol Oncol. 2001;20(4):333-42

18. Karkabounas S, Binolis J, Zelovitis J, Kotsis N, Charalabopoulos A, Avdilos A, Zuridakis A,, Liasko R, Giannakopoulos X, Charalabopoulos K. Inhibition and modification of benzo[a]pyrene induced chemical carcinogenesis of ascorbic acid alone or in combination wih a-tocopherol in Wistar rats .Experimental Oncology, 2002;24: 274-78

19. Karkabounas S, Kostoula O, Daskalou T, Veltsistas P, Karamouzis M, Zelovitis J, Metsios A, Lekkas P, Evangelou AM, Kotsis N, Skoufos I Anticarcinogenic and antiplatelet effects of carvacrol. Exp Oncol 2006;28(2):121-5

20. Karkabounas S., Assimakopoulos D., Malamas M.,. Skaltsounis A.L, Leonce S., Zelovitis J., Stefanou D. and Evangelou A.. Antiproliferative and anticarcinogenic effects of an aqueous preparation of Abies alba and Viscum album se abies , on a L-1210 malignant cell line and tumor-bearing Wistar rats. Anticancer Research 2000;20(6B)4391-5.

21. A. Charalabopoulos , S. Karkabounas , A. Charalampopoulos , V. Papalimneou , E. Ioachim , X. Giannakopoulos. Inhibition of benzo[a]pyrene induced carcinogenesis by vitamin C alone and by pairs of vitamin C –vitamin E and Selenium-Glutathion. Biol Trace Elem Res 2003;93(1-3):201-12

22. A Evangelou, S. Karkabounas, G. Kalpouzos, M. Malamas, R. Liasko, D. Stefanou, A. Vlahos, T. Kabanos. Comparison of the therapeutic effects of two Vanadium complexes administrated at low doses on benzo(a)-pyrene-induced malignant tumors in rats. Cancer Letters. 1997;119(2):221-5

23. Aharonov Y. and D. Bohm. Significance of electromagnetic potentials in quantum theory. Phys. Rev. 1959;115:485–491.

24. Peshkin M. and Tonomura A. The Aharonov-Bohm effect. Springer-Verlag: Berlin, 1989. ISBN 3-540-51567-4.

25. Muruganandham M, Alfieri AA, Matei C, Chen Y, Sukenick G, Schemainda I, Hasmann M, Saltz LB, Koutcher JA. Metabolic signatures associated with a NAD synthesis inhibitor-induced tumor apoptosis identified by 1H-decoupled-31P magnetic resonance spectroscopy. Clin Cancer Res. 2005;11(9):3503-13

26. Baggetto LG. Deviant energetic metabolism of glycolytic cancer cells. Biochimie 1992;74(11):959-74

27. Ristow M. Oxidative metabolism in cancer growth. Curr Opin Clin Nutr Metab Care 2006;9(4):339-45

28. Zu XL, Guppy M. Cancer metabolism: facts, fantasy, and fiction. Biochem Biophys Res Commun 2004;313(3):459-65

29. Tatton WG, Chalmers-Redman RM, Elstner M, Leesch W, Zagodzinski FB, Stupak DP, Sugrue MM, Tatton NA. Glyceraldehyde-3-phosphate dehydrogenase in neurodegeneration and apoptosis signaling. J Neural Transm Suppl 2000;(60):77-100

30. Mathupala SP, Rembel A, Pedersen PL. Aberrant glycolytic metabolism of cancer cells: a remarkable coordination of genetic, transcriptional, post-transcriptional, and mutational events that lead to a critical role for type II hexokinase. J Bioenerg Biomembr 1997;29(4):339-43

31. McKee RW, Parks ME, Dickey A. Influence of iodoacetate on glycolytic intermediates and on respiration in Ehrlich-Lettre ascites carcinoma cells. Arch Biochem Biophys 1968;124(1):450-5
32. Karkabounas S, Kartsiouni D, Stefanou A, Zelovitis J, Lekkas P, Theodosopoulou E, Yioti I, Batistatou A, and Evangelou A. Iodoacetic acid effects on Wistar rat leiomyosarcoma cells in vitro and on cancer bearing Wistar rats.2004, Nov 26 – 28. 5th Greek Congress on Tumor Markers and Target Therapy of Cancer. Book of Abstracts P-28, pg 82.

33. Foxall DL, Brindle KM, Campbell ID, Simpson RJ. The inhibition of erythrocyte glyceraldehyde-3-phosphate dehydrogenase. In situ PMR studies. Biochim Biophys Acta. 1984;804(2):209-15.

34. Matsuyama M, Yoshimura R, Mitsuhashi M, Tsuchida K, Takemoto Y, Kawahito Y, Sano H, Nakatani T. 5-Lipoxygenase inhibitors attenuate growth of human renal cell carcinoma and induce apoptosis through arachidonic acid pathway. Oncol Rep. 2005;14(1):73-9

35. Ye YN, Wu WK, Shin VY, Bruce IC, Wong BC, Cho CH. Dual inhibition of 5-LOX and COX-2 suppresses colon cancer formation promoted by cigarette smoke. Carcinogenesis 2005;26(4):827-34.

36. Kopf-Maier P, Janiak C, Schumann H.Antitumor properties of organometallic metallocene complexes of tin and germanium. J Cancer Res Clin Oncol 1988;114(5):502-6.

37. Kopf-Maier P. Complexes of metals other than platinum as antitumour agents. Eur J Clin Pharmacol 1994;47(1):1-16.

38. Blank M, Soo L. Electromagnetic acceleration of electron transfer reactions. J Cell Biochem. 2001;81(2):278-83

39. Blank M. Do electromagnetic fields interact with electrons in the Na,K-ATPase? Bioelectromagnetics 2005;26(8):677-83

EFFECTS OF LOW INTENSITY STATIC ELECTROMAGNETIC FIELDS ON LEIOMYOSARCOMA CELL LINES

SPYRIDON KARKABOUNAS[1], IOANNIS TOLIOPOULOS[1] , TELEMACHOS DASKALOU[1], KONSTANTINOS HAVELAS[1], OLGA KOSTOULA[1,2], PATRA VEZYRAKI[1], ANTONIOS AVDIKOS[1], JAYNE BINOLIS[1], GEORGE HADZIAVAZIS[1], APOSTOLOS METSIOS[1], IOANNIS VERGINADIS[1], ANGELOS EVANGELOU[1]

[1]Laboratory of Experimental Physiology, Faculty of Medicine, University of Ioannina, Greece
[2]Department of Applied Biology and Technology, University of Ioannina, Greece

Correspondence author: Spyridon Karkabounas, PhD, Lecturer of Experimental Physiology, Laboratory of Experimental Physiology, Faculty of Medicine, University of Ioannina, University Campus, 451 10 Greece. Tel: +30-26510-97751, +30-26510-97576, Fax: +30-26510-97850, E-mail: skarkabu@cc.uoi.gr

Abstract
In this study we investigated the effects of low intensity static electromagnetic field (EMF) causing no thermal effects, on leiomyosarcoma cells (LSC), isolated from tumors of Wistar rats. Electromagnetic resonance frequencies measurements and exposure of cells to static EMF's were performed by a device called Multi Channel Dynamic Exciter 100 V1 (MCDE). The tumors were developed in the rats via a 3,4-benzopyrene injection. The LSC were exposed to electromagnetic resonance frequencies (ERF's) between 10 kHz to 120 kHz, for 45 min. During a 24h period, after the exposure of the LSC to ERF's, there was no inhibition of cells proliferation. In contrast, at the end of a 48h incubation period, LSC proliferation dramatically decreased by more than 98%. At that time, the survived LSC were only 2% of the total cell population exposed to ERF's, and under the same culture conditions showed significant decrease of proliferation. These cells were exposed once again to ERF's for 45 min (totally 4 sessions of exposure, of 45 min duration each) and tested using a flow cytometer. It was found that 45% of these double exposed to ERF's, LSC (EMF cells) were apoptotic and only a small percentage 2%, underwent mitosis. In order to determinate their metastatic potential, these EMF cells were also counted and tested by an aggregometer for their ability to aggregate platelets and found to maintain this ability. They showed no difference in comparison to the LSC not exposed to ERF's (control cells). *In conclusion,* exposure of LSC to specific ERF's decreases dramatically their proliferation rate and induces a high rate of cell apoptosis. Also, the LSC that survived after exposed to ERF's, had a lower proliferation rate compared to the LSC controls but did not loose their potential for metastasis. The use of specific ERF's generated from the MCDE electronic device, is safe for humans and animals according to the international safety standards, and appropriate for the experimental treatment of cancer in vitro and in vivo.

Introduction
There are quite a few of data on the effects of electromagnetic field (EMF) on various kinds of malignant cells in experimental animals and in humans, some of them referring to the application of electromagnetic resonance principles [1,2]. The main concepts expressed so far referring to the effects of EMF on malignancies are: the intensity, frequency and duration of application of the electromagnetic waves. The EMF may act as co-carcinogen combined with the primary carcinogen, especially in experimental animals but can also exert anticarcinogenic effects, inhibiting the proliferation of malignant cells in vitro as well as decreasing the size of the experimental tumors in vivo [3-6]. Studies of the EMF pro-carcinogenic effects in experimental animals are not numerous and seem to have many uncertainties [3,4]. On the contrary, studies on the EMF anticancer effects are abundant and their methodology is well documented [7]. It has been also shown, that the cytostatic effects of the EMF on cancer cells are not related to their thermal effects but are temperature-

independent [8-10]. The purpose of the present study is to investigate the effects exerted by low intensity static electromagnetic field on a) the proliferation and the viability of the leiomyosarcoma cells line (LSC) and b) the cell cycle of LSC and c) the platelet's aggregation from a physiological agonist and LSC cells.

Materials and methods

Production of leiomyosarcoma cells (LSC) and smooth muscle cells (SMC): The malignant cells were isolated from selected leiomyosarcoma tumors of Wistar rats. Fifteen (7 male and 8 female) Wistar rats, of the fifth generation of a certain couple, 60 days old, were subcutaneously injected in their right scapula by 1 ml of 3,4-benzopyrene solution (B[a]P) in tricapryline in a dose of 10.08 mg/ml. The rat leiomyosarcomatic tumors B[a]P induced have the following characteristics: a) sensitivity to antioxidant substances and free radical scavengers indicating that their proliferation is related to the release of reactive oxygen species [11-13], b) their proliferation can be inhibited via the administration of cycloxygenase-2 (COX-2) and 5-lipoxygenase (5-LOX) inhibitors [14] and c) ability to induce leiomyosarcoma tumors when inoculated into Wistar rats. After 110 days (maximum 135 days) of B[a]P injection, all animals developed malignant tumors at the site of injection. All tumors were histologically identified as leiomyosarcomas. The tumors were surgically removed and cut under aseptic conditions into pieces of 0.5 cm^3 in volume. Each piece was placed immediately in cold Ringer's solution and sliced down again to smaller pieces (1 mm^3). All smaller pieces were inserted for 5 min into 5 ml of cold Dulbecco's modified Eagles medium (DMEM) solution which contained small quantities of trypsin and then these pieces were incubated in the same DMEM solution at 37º C for 4 h, with gentle mixing every 15 min. After incubation the DMEM solutions containing the tumor pieces were centrifuged at 900 rpm for 10 min and the supernatant was rejected. The remaining cells were resuspended in DMEM+10% fetal bovine serum (FBS) solution and seeded in plastic coated dishes of 52 mm in diameter. Tumor cells after been subcultured, were examined histologically and were characterized as leiomyosarcoma cells. In order to verify if these LSC were active and able to induce the same type of malignancy in rats, $4x10^6$ of them were suspended in Hanks salt solution and inoculated into every Wistar rat as follows: the animals were anaesthetized with midazolame and ketamine, and a surgical opening was made in their outer skin layer at the middle of their back. The tissue underneath was traumatized by lancing with a sharp blade in order to bring fresh blood to the surface. LSC were then aseptically infused into the operated area, and the incision was immediately sutured. The animals developed medium-sized malignant tumors approximately 12 cm^3 in volume, within the first 10 days after inoculation. Smooth muscle cells (SMC) were isolated from the aorta of Wistar rats and cultured again by the methods described above. The animal experimentation performed according to the European Community Directives and International Legacy for the animal protection. All the in vivo experiments were accomplished according to the European Union Directive for the Protection of Vertebrate Animals Used for Experimental and other Scientific Purposes (86/609/EEC, article 9 §§1,2).

Electromagnetic field equipment: Electromagnetic resonance frequencies measurement and exposure of cells to static EMF's were performed by a device called Multi Channel Dynamic Exciter 100 V1 (MCDE) invented by K. Havelas [17]. The MCDE has been certified by the Greek National Centre for Scientific Research "Democritos" and its Department of International Committee of Atomic Energy for its safe use in humans and animals. This device is consisted of two basic parts: A) an electromagnetic field generator of various intensities. The range intensities for the electrical field are 1.1 to 1.11 ± 0.01 V/m and for the magnetic field are 0.0027 to 0.0029 ± 0.00005 A/m. The radiofrequencies which generate from MCDE system range of 10 Hz to 1 MHz. The power density of the electromagnetic field is 100 mV/cm^3 approximately, B) an electron paramagnetic resonance spectrometer with specific characteristics. This spectrometer is a scanner-recorder of the ERF's emitted from biological systems (targets), such as localized tumors in experimental animal, or cultured cancer cells, exposed to EMF. It is well known that the normal function of any biological system produce electromagnetic waves of specific frequencies caused by cell electromagnetic properties (electric membrane potential, transport of ions charges etc). The specific ERF's emitted from an EMF excited biological system, is recorded as an electromagnetic resonance fingerprint of this system. This is due to the electromagnetic resonance taking part between ERF's produced by the generator and ERF's emitted from the biological system. The MCDE is supported by a sophisticated software easy to use (submitted for accreditation). First, it is necessary to record the electromagnetic resonance fingerprints emitted from the biological systems (targets). Then, by selecting the specific MCDE's programs of the software, the appropriate ERF's for the exposure of the target are calculated and then are emitted to the target.

Estimation of leiomyosarcoma cells and smooth muscle cells electromagnetic resonance frequencies: Electromagnetic resonance fringerprintings of LSC and SMC were recorded before and after their exposure to EMF (10 Hz-1 MHz). The ERF's of LSC electromagnetic resonance fingerprints are modulated using the software and after that, the cancer cells are exposed to these modulated

electromagnetic fingeprintings for 45 min. The cell proliferation and cell morphology were checked every 24 h. A total of 492 different frequencies emitted from LSC cells were recorded (fig 5).

Method of leiomyosarcoma cells and smooth muscle cells exposure to electromagnetic field

Leiomyosarcoma cells treatment: Twelve Petri dishes with 10 ml growth medium were seeded with $1x10^5$ LSC (zero time). The LSC cultures were incubated in 37º C at 95% O_2 + 5% CO_2 atmosphere for 48 h. Then the medium was replaced by 10 ml of new DMEM. At 72 h from zero time, six LSC cultures (EMF cells) were placed into a Faraday apparatus at room temperature (RT) and exposed to modulated electromagnetic fingerprints (from 10 kHz to 120 kHz and intensities from 1.1 to 1.11 +/- 0.01 V/m for the electric field and 0.0027 to 0.0029+/-0.00005 A/m for the magnetic field), for 45 min. A total of 492 frequencies were used for LSC exposure to EMF. The used frequencies were derived from a transformation of the 492 frequencies recorded as the LSC electromagnetic fingerprints (Fig 1) by an specific algorithm [$\sum f(r) + f(em) = c$, f(r) = registrated frequence, f(em)= emitted frequence, c = a constant] The other six LSC cultures (control cells) remained at RT for the same time as EMF cells but without being exposed to EMF. The control and EMF cells were incubated once again at the same conditions as before, for about seven hours. At 79h and 96h from zero time, the cells of each culture were counted, subcultured at about $1x10^5$ cells per plate and incubated at the same as above conditions. At 120h from zero time, the EMF cells were re-exposed to EMF as before and 24 h later, both EMF and control cells in each plate were counted and examined microscopically. Then, to examine their proliferation rate in relation to time, both groups (EMF and control cells) were subcultured and incubated at the same described conditions, in order to estimate the time till cell confluence. The cells were then preserved in liquid nitrogen.

Smooth Muscle Cells treatment: The SMC isolated from Wistar rat aorta were subcultured in the same conditions as described above for LSC and exposed to EMF in the same manner and frequencies as rat LSC.

Leiomyosarcoma cells manipulations: The preserved in liquid nitrogen EMF and control cells were defrost and cultured again till cell confluence. Twelve plates were then seeded with the same number of LSC and incubated for 24 h. The EMF cells were again exposed to EMF for 45 min after 24 h and 48 h. Six hours after the last session, cell samples from each plate were taken for testing their cell cycle phases by a flow cytometer Bexton Dickinson system.

Estimation of platelet aggregation ability of leiomyosarcoma cells

The potential for metastasis of the **LSC** was determined from their ability to aggregate platelets before and after their exposure to EMF using the aggregometer CA-500, Cronolog, USA and the Cronolog kit for platelets aggregation. The Cronolog kit was used to verify the normal platelet responses. A total of 120 tests were performed on blood samples taken from six healthy volunteers who abstained from the use of drugs and alcohol for ten days before the tests. The tests were performed in platelet rich plasma (PRP) isolated from the blood samples and prepared according to the manual of the apparatus. The platelet aggregation tests were performed after the suspension of either $5X10^5$ EMF cells or of the same number of control cells, in PRP.

Statistics

Student's t-test was used for the statistical evaluation of the results and $P<0.05$ was considered statistically significant.

Results

Cell proliferation rate: Our results were as follows: a) Twenty-four hours after the first and second session of exposure to the EMF, the proliferation rate of the LSC was slightly decreased, in comparison to the control cells proliferation ($P<0.05$). Also the microscopic examination showed that the highest percentage of LSC was under stress, showing round-shaped cells with abortive pseudopodia and formation of nuclear membrane blebs. b) The multiplication rate of the EMF exposed LSC after 48 h of incubation was dramatically decreased at a percentage higher than 98%, ($P< 0,0001$ compared to the control cells) and most of the exposed malignant cells were found either dead (mainly apoptotic) or extremely stressed: round shaped cells, formation of bleeds in the outer cell membrane, absence of pseudopodia (fig 1) c) The survived LSC after one session of EMF exposure, showed a great difficulty in proliferating according to the time needed till cell confluence (6 days of incubation) in with comparison to the time needed till control cells confluence (3 days), (fig 2). Also, the survived LSC developed a remarkable resistance to EMF, showing only 20% decrease of cell proliferation rate compared to the much higher decrease in proliferation rate of 98%, shown after their first EMF exposure.

Leiomyosarcoma cells distribution in the cell cycle phases: Flow cytometry revealed that after the fourth cell exposure to EMF, 33% of the **LSC** were found to be in G0/G1, 9% in S phase, 2% in mitosis and 45% were undergoing apoptosis, while the control cells were found to be: 36% in G0/G1, 38% in S phase, 19% in mitosis and 2% undergoing apoptosis (Table 1).

SMC viability after exposure to EMF: The SMC seem not to be affected by electromagnetic fields exposure at 24 and 48 h (fig 3). The exposed SMC have a proliferation rate 10% lower than the non exposed SMC (control). This difference is not statistically significant (P<0,4).

Estimation of sarcoma cells " potential for metastasis" by platelet aggregation: The aggregation ability of the control as well as of the exposed to EMF cells, was 78%, and almost equal to the ability to aggregate of the ADP (82%). According to the above, LSC exposure to EMF did not affect significantly the "potential for metastasis" of LSC (fig 4).

Estimation of cell electromagnetic resonance – frequencies: Electromagnetic resonance frequencies of the: a) unexposed to EMF LSC were ranging between 10.5 to 120.5 kHz, b) exposed to EMF LSC, between 10 to 120 kHz and c) SMC between 10 to 120 kHz. Spectrum analysis of the above estimations revealed that the electromagnetic resonance frequencies of LSC exposed to EMF showed significant differences as compared to those of the unexposed LSC (control cells) presenting an almost 70% similarity to the electromagnetic resonance frequencies recorded from the SMC (data not shown).

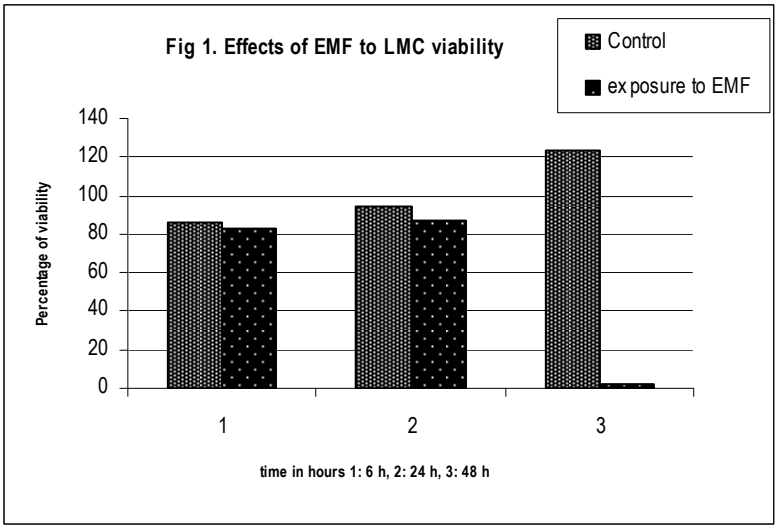


Fig 1. The viability of the EMF exposed LSC after 48 h of incubation was dramatically decreased at a percentage higher than 98%, (P< 0,0001 compared to the control cells)

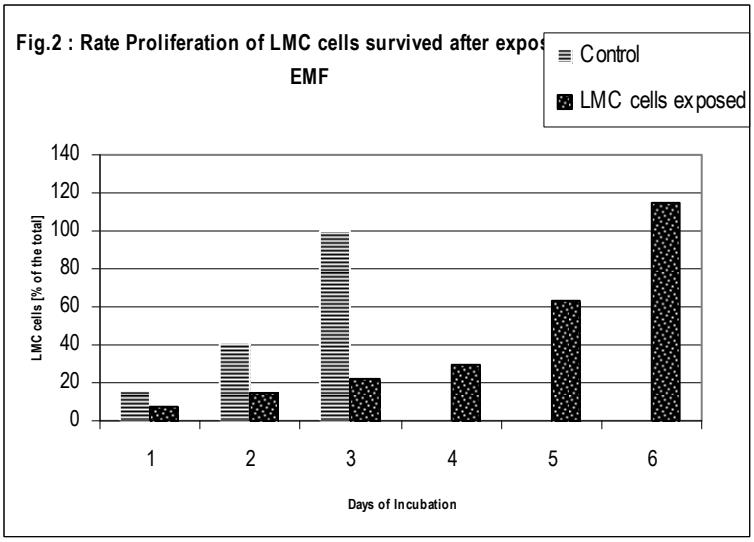


Fig 2. The survived LSC after one session of EMF exposure, showed a significant difficulty in proliferating according to the time needed till cell confluence (6 days of incubation) in with comparison to the time needed till control cells confluence (3 days)

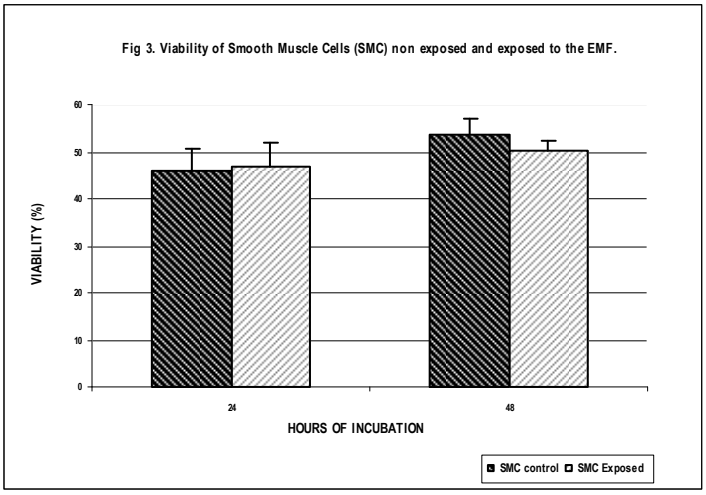


Fig.3 : Viability of Smooth Muscle Cells (SMC) not exposed and exposed to EMF. The non exposed SMC have a rate of growth 10% larger from the exposed ones [P< 0,4].

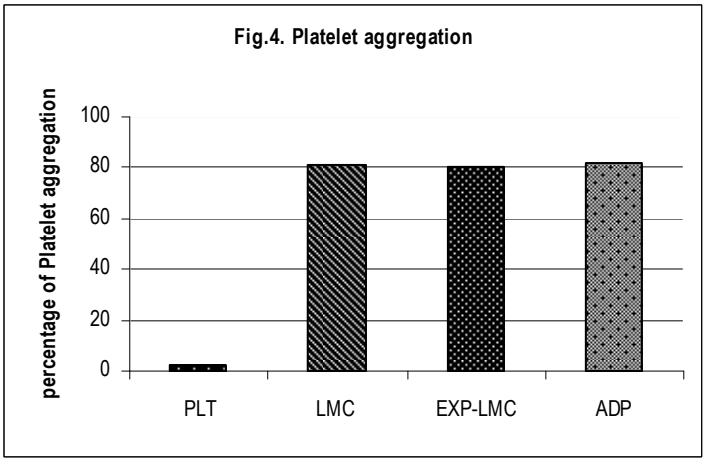


Fig 4. LSC exposure to EMF did not affect significantly the capacity of LSC to aggregate human platelets. PLT : resting platelets, LMC : platelet aggregation LMC induced, EXP-LMC: platelet aggregation induced by exposed LMC, ADP: control of platelet aggregation by ADP as agonist.

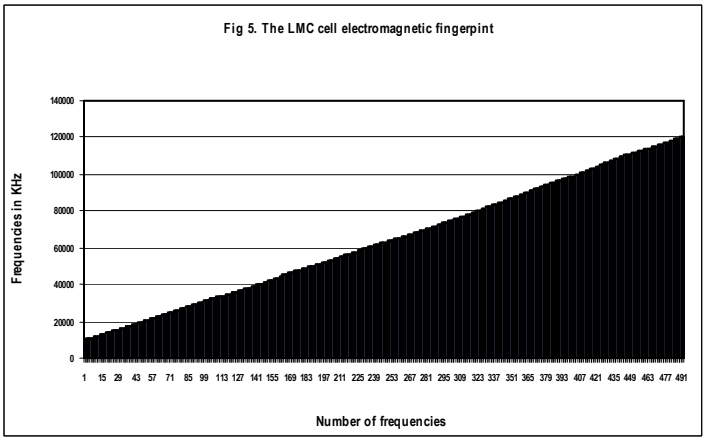


Fig 5. The fingerprint spectrum of 492 frequencies emitted from leiomyosarcoma cells of Wistar rat after an accurate registration by the resonating system of the MCDE apparatus

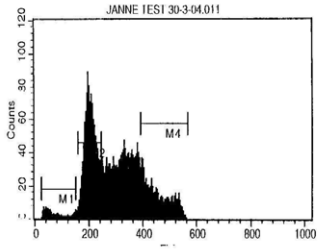
Table 1 : Flow cytometry for non exposed and exposed to EMF sarcoma cells .

The percentage of apoptotic nucleus in the group of control cells is very low (1,79 %) when the percentage of apoptotic nucleus in the group of exposed cells to EMF is much greater (45,34 %) .

Control (non exposed sarcoma cells)

Marker	Left	Right	Events	% Gated	Total
All	0	1023	9461	100.00	49,07
M1	26	149	169	1,79	0,88
M2	15	242	3366	35,58	17,46
M3	262	386	35,49	37,51	18,41
M4	391	565	1774	18,75	9,20

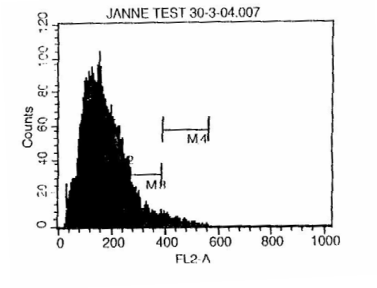
G0/G1 : 35,58%, S : 37,51% , G2/M : 18,75% , Apoptosis : 1,79%



Exposed sarcoma cells to EMF

Marker	Left	Right	Events	% Gated	Total
All	0	1023	13232	100,00	17,89
M1	26	149	5999	45,34	8,11
M2	159	242	4396	33,22	5,94
M3	262	386	1232	9,31	1,67
M4	391	565	217	1,64	0,29

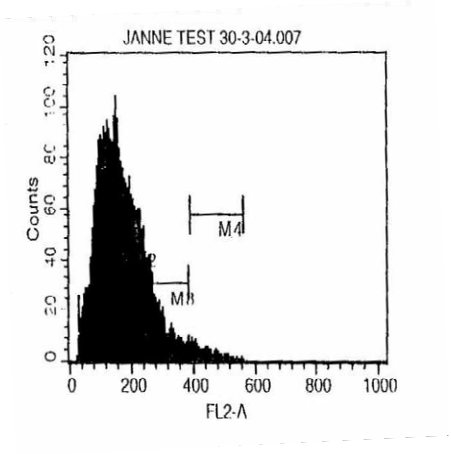
G0/G1 : 33,22%, S : 9,31%, G2/M : 1,61% , Apoptosis : 45,34%



Exposed sarcoma cells to EMF

Marker	Left	Right	Events	% Gated	Total
All	0	1023	13232	100,00	17,89
M1	26	149	5999	45,34	8,11
M2	159	242	4396	33,22	5,94
M3	262	386	1232	9,31	1,67
M4	391	565	217	1,64	0,29

G0/G1 : 33,22%, S : 9,31%, G2/M : 1,61% , Apoptosis : 45,34%



Discussion

Our findings indicate that high growth inhibition of LSC of more than 95% can be accomplished by the applying an EMF according to electromagnetic resonance principles. The results of this study reinforce the other authors findings on the proliferation inhibition and on the significant morphological alterations of human melanoma cell lines exposed to low power electromagnetic waves of 50-80 GHz [15] and also on the apoptotic effects of static EMF of 1.95 GHz on human epidermoid cancer cells [16]. In the present study antiproliferative and apoptotic effects have been achieved by exposing LSC to a static EMF of low energy waves and frequencies between 10 kHz to 120 kHz. This field is far lower in frequency and in power than the upper limit of permitted exposure (power: 200m Watt/cm^3), being thus, safe for use in animals and humans [17]. It is also evident from the literature, that the EMF effect is dependent on immediate interactions that affect the electronic spin of the atoms or molecules with uncoupled electrons in their external orbit, enhancing electron spin coupling; thus may help the neutralization of free radicals, especially those produced by the activation of arachidonic acid cascades [14,16,18-21]. It is also known that the EMF induce free radicals production that may act as activators of signal transduction pathways [10,19,20]. According to the above, it is possible that the effects of these EMF, could be similar to the effects of antioxidants and free radical scavengers on LSC lines. The high percentage of the exposed LSC found in apoptosis (45%) in comparison to that of the unexposed to EMF, control cells (2%), could be explained as the effect of the EMF's on cellular membranes activating signal transduction pathways leading to genes expression of cell apoptosis [5,7,16,22] or to inactivation of anti-apoptotic genes [15]. The low percentage of cells found in synthesis and in mitosis (9% and 2% respectively) compared to that of the control cells (38% and 19% respectively), indicates that radiofrequency of the EMF can act as cell cycle inhibitor, similarly to the effect of magnetic field on DNA synthesis [23,24,7]. There is also evidence that exposure to the EMF may reduce the immunoreactive p53 expression in tumor bearing mice [19], which has been found increased in BaP-induced leiomyosarcomas in Wistar rats [25]. The lower sensitivity of LSC after their fourth exposure to ERF's, compared to their higher sensitivity after the first exposure, indicates that LSC may have developed some type of resistance to EMF. Our finding, that the electromagnetic resonance fingerprints of LSC changed after their exposure to EMF and resembled to that of the SMC, may indicate that some differentiation in the LSC function has taken place. This differentiation is supported by our -yet unpublished- data indicating that the EMF treated LSC, after being inoculated to Wistar rats, retard the tumor development or even fail to develop tumor, in contrary to inoculated but unexposed to EMF LSC that develop tumors in a 100% of the experimental animals. There are also bibliographic references indicating that the EMF, specific or generalized is able to induce differentiation of cancer and non cancer cells [26,27]. Nevertheless, the LSC exposed to the EMF seem to retain their potential for metastasis as they can still aggregate platelets. It must be emphasized that for the first time a low intensity EMF has been used and it is essential that this EMF is carefully designed on the basis of the emitted electromagnetic frequencies from the target cells, in order to be effective. Also, the intensity of the electric field we used was 75 times lower and the intensity of the magnetic field was more than 1800 times lower than the average of the international safety standards according to the National Centre for Physical Sciences of Greece ("Demokritos", Athens Greece) [17]. Because of that, the use of this electronic device for the treatment of cancer cells seems to be safe. Unpublished data of ours, from the follow up of tumor-bearing animals and cancer patients treated with EMF by the above method, confirm the above. Our data, concerning the changes of LSC electromagnetic resonance fingerprints after repeated exposures to EMF, indicate that, in order to affect the cells functions, it is crucial to make regular readjustments of the electromagnetic resonance fingerprints, in order to differentiate the LSC phenotype to a phenotype with an electromagmetic resonance fingerprinting as close as possible to that of the normal cells (SMC). In this case, the LSC should loose their malignant phenotype, so that their inoculation to Wistar rats could not cause malignant disease. Experiments going on, in our lab, seem to confirm this hypothesis.

Acknowledgements: This research has been supported by funds of the Center for Energy Frequencies Studies in Physical and Mental Balance (Greece), through the Research Committee of the University of Ioannina. We thank Dr. Georgios Vartholomatos for his valuable assistance in flow cytometry and Nikos Papadopoulos for his contribution in the management and administration of this project.

References

1. Suss S. Bioresonace therapy in treatment of allergies. Every person has its own vibration pattern. *Fortschr Med* 1997; 115: 16-18.
2. Islamov BI, Balabanova RN, Funtikov VA, et al. Effect of bioresonance therapy on antioxidant system in lymphocytes in patients with rheumatoid arthritis. *Bull Exp Biol Med* 2002; 134: 248-250.

3. Foster KR, Repacholi MH. Biological effects of radiofrequency fields: does modulation matter? *Rad Res* 2004; 162: 219-225.
4. Heynick LN, Johnston SA, Mason PA. Radio frequency electromagnetic fields: cancer, mutagenesis and genotoxicity. *Bioelectromagnetics* 2003; Suppl 6: S 74-100.
5. Marinelli F, La Sala D, Cicciotti G, et al. Exposure to 900 MHz electromagnetic field induces an unbalance between pro-apoptotic and pro-survival signals in T-lymphoblastoid leukaemia CCRF-CEM cells. *J Cell Physiol* 2004; 198: 324-332.
6. Repacholi MH. Low-level exposure to radiofrequency electromagnetic fields: health effects and research needs. *Bioelectromagnetics* 1998; 19: 1-19.
7. Tofani S, Cintorino M, Barone D, et al. Increased mouse survival, tumor growth inhibition and decreased immunoreactive P53 after exposure to magnetic fields. *Bioelectromagnetics* 2002; 23: 230-238.
8. Han L, Lin H, Head M, et al. Application of magnetic fields induced heat shock protein 70 for presurgical cytoprotection. *J Cell Biochem* 1998; 78: 371-379.
9. Junkersdorf B, Bauer H, Gutzeit H.O. Electromagnetic fields enhance the stress response at elevated temperature in the nematode caenorabditis elegans. *Bioelectromagnetics* 2000; 21: 100-106.
10. Grundler W, Kaiser F, Keilmann F, Walleczek J. Mechanisms of electromagnetic interaction with cellular systems *Naturwissenschaften* 1992; 79: 551-559.
11. Kallistratos G, Evangelou A, Agnantis N, et al. Enhancement of the antineoplastic effect of anticarcinogens on benzo[a]pyrene treated Wistar rats, in relation of their number and biological activity. *Cancer Lett* 1994; 82: 153-165.
12. Evangelou A, Kalpouzos G, Karkabounas S, et al. Dose related preventive and therapeutic effects of antioxidants-anticarcinogens on experimentally induced malignant tumours in Wistar rats. *Cancer Lett* 1997; 115: 105-111.
13. Charalabopoulos K, Karkabounas S, Charalabopoulos AK, et al. Inhibition of benzo[a]pyrene-induced carcinogenesis by vitamin C alone and by vitamin C/ vitamin E and Selenium/glutathione. *Biol Trace Elem Res* 2003; 93: 201-212.
14. Xanthopoulou M, Hadjikakou S, Hadjiliadis N et al. Synthesis and characterization of a new chloro diphenyl (VI) complex with 2-mercapto nicotinic acid. A study of its influence upon the catalytic oxidation of linoleic acid to hydroperoxylinoleic acid by the enzyme lipoxygenase. *Organometal Chem 2006; 691: 1780-1789.*
15. Beneduci A, Chidichimo G, Rose R, et al. Frequency and irradiation time-dependant antiproliferative effects of low-power millimeter waves on RPMI 7932 human melanoma cell lines. *Anticancer Res* 2005; 25(2A): 1023-1028.
16. Caraglia M, Marra M, Mancinelli F, et al. Electromagnetic fields at mobile phone frequency induce apoptosis and inactivation of the multi-chaperone complex in human epidermoid cancer cells. *J Cellular Physiol* 2005; 204: 539-548.
17. Karabetsos E. Measurements report of electromagnetic radiation levels emitted from the device Multi Channel Dynamic Exciter 100 v.1 Report of ΕΕΑΕ: ΜΙΑ ΕΕΠ 2, 15-11-2000, Karabetsos E, ed, *Bulletin no 2, National Centre of Physics Research "Democritos"*publ, Athens, Greece, 2000.
18. Grudler W, Kaiser F, Keilmann F, Walleczek J. Mechanisms of electromagnetic interactions with cellular systems. *Naturwissenschaften* 1992; 79: 551-559.
19. Clejan S, Ide C, Walker C, et al. Electromagnetic fields induced changes in lipid second messengers. *J Lipid Mediat Cell Signal* 1996, 13: 301-324.
20. Lander M. An essential role of free radicals and derived species in signal transduction. *FASEB J* 1997; 11: 118-124.
21. Del Carratore R, Morichetti E, Della Croce C, Bronzelli G. Effect of magnetic fields on rodend monooxygenase enzymes. *Bioelectromagnetics* 1995; 16: 324-329.
22. Polyak K, Xia Y, Zweier JL, et al. A model for P53 induced apoptosis. *Nature* 1997; 389: 300-305.
23. Liboff AR, Wikkiams T Jr, Strong DM, Wistar R Jr. Time varying magnetic fields: effect on DNA synthesis. *Science* 1984; 223: 818-820.
24. Takahashi K, Kaneko I, Date M, Fukada E. Effects of pulsed electromagnetic fields on DNA synthesis in mammalian cells culture. *Experientia* 1986; 42:185-186.
25. Stefanou DG, Nonni AV, Kalpouzos G, et al. Immunophenotype ras oncogenes and p53 onco-suppressor genes on bezo(a)pyrene induced malignant soft tissue tumors in Wistar rats. *In Vivo* 1998; 12: 511-521.
26. Tao Q, Henderson A. EMF induces differentiation in HL-60 cells. *J Cell Biochem* 1999; 73: 212-217.
27. Rodenman HP, Peterson HP, Schwenke K, von Wangenheim KH. Terminal differentiation of human fibroblasts is induced by radiation. *Scanning Microscop* 1991; 5: 1135-1142.

CAN BE INCREASED EFFICIENCY OF ALA PHOTODYNAMIC THERAPY BY ELECTROPORATION?

F. CIOBANU, M.G. MOISESCU, I. STOIAN, M. RADU, E. KOVACS

CAROL DAVILA UNIVERSITY OF MEDICINE AND PHARMACY, PO BOX 35-43, BUCHAREST, 050461, ROMANIA, MRADU@NIPNE.RO

Abstract

One of the most used photosensitizer in photodynamic therapy of cancer is the aminolevulinic acid (ALA), a precursor in synthesis of protoporphyrin IX (PpIX). One of the disadvantages using this photosensitizer is the small rate of ALA uptake of the cells. Our work aim was to increase by electroporation the PpIX level in ALA treated cells. Electroinduced pores in membrane would facilitate an enhanced uptake rate of ALA forcing an increased level of PpIX and consequently a better efficiency of ALA photodynamic therapy. B16F10 melanocytes cultures were incubated with 1 mM ALA for 4 h and PpIX level was monitored by the fluorescent emission at 635 nm. The viability of cells was analysed by MTT test. The electroporation of cells in the presence of ALA was done with exponential decay electric pulses in the range of 500-4500 V/cm, 100 μs, 1-4 pulses. In the control experiment (without electroporation) a rate of PpIX production comparable with results in literature was obtained. Exposing the ALA treated cell cultures to light (633 nm) for various periods the apoptosis or necrosis of cells was triggered. This observation was confirmed by the results of cells viability tests. The electroporation of cells in the presence of ALA did not show significantly increase the cellular PpIX level. In conclusion our *in vitro* preliminary results did not supply evidences that the electroporation of cells can be a way to improve the ALA uptake of the cells and consequently to improve the efficiency of photodynamic therapy with ALA.

Introduction

Photodynamic therapy (PDT) concept is based on a combined effect of the light and chemicals. A photosensitive chemical species incorporated into cell and afterwards exposed to irradiation with light of appropriate wavelength produces very reactive chemical radicals which are able to trigger the apoptosis or necrosis of the cell. This type of therapy was proposed as an alternative to classical surgical techniques. The photosensitive molecules can be an exogenous (an appropriate techniques has to be used to uptake this molecules by the cell) or an endogenous one as protoporphyrin IX (PpIX). 5-aminolevulinic acid being a precursor of PpIX is one of the most used chemical in PDT. ALA is an endogenous precursor of PpIX. In normal conditions the rate of PpIX synthesis is regulated by means of a negative feedback loop limiting in this way the level of endogenous ALA. An enforced uptake of ALA allows overcoming this limiting mechanism resulting in an increased rate of PpIX production by the cells. PpIX absorption spectrum shows a high peak located 635 nm (Ma et al, 2001). Under the light irradiation the PpIX produces several photo-induced products having as final results an unbalanced oxidative status of the cell. As a consequence the cell triggers the apoptosis program. The technique was successfully used in *in vitro* and *in vivo* experiments.

The main disadvantage of this ALA-PDT method is the limiting step of ALA incorporation into the cell. ALA is a hydrophilic molecule and consequently has a very low diffusion coefficient through the membrane lipid bilayer. There are several reports concerning the mechanism of ALA uptake through the cell membrane. Mainly two paths are proposed: (i) the passive diffusion which would be important only during a short period of incubation, till 15 min (Bermudez Moretti et al, 2002) and (ii) an active mechanism mediated by a BETA family transporter (Rud et al, 2000; Bermudez Moretti et al, 2002).

An alternative proposed to improve the rate of ALA influx is the cell electroporation. The action of a short electric pulse of appropriate amplitude is able to produce a reversible permeabilisation of the membrane. During this state the exogenous molecules, for which normally the membrane is not permeable, can pass through the membrane barrier by diffusion. In cancer therapy the technique was successfully used to improve the efficiency of cytostatics (Orlowski, Belehradek et al.,1988). A derived method is the transdermal electroporation. The electric pulses are applied across the dermal layer increasing the diffusion of drugs through it. This method was proposed to improve the efficiency of ALA – PDT when ALA is topically applied (Johnson et al, 2002) and an increase of transdermal transport rate was reached.

In this report we present our preliminary results concerning the possibility to use the electroporation at the cell level in order to increase the uptake of ALA and consequently the production of PpIX.

Materials and Methods

B16F10 murine metastatic melanoma cells were used as biological experimental object. They were cultured in 3 cm Petri dishes, at 37°C, 5% CO_2, in Dulbecco's MEM (Gibco) supplemented with 10% foetal calf serum (Gibco), 100 units/ml of penicillin and 100 µg/ml of streptomycin (BioClone). The B16F10 cell line was kindly provided by Dr. L.M.Mir, Gustave-Roussy Institute (Villejuif), France.

1mM ALA (Sigma) was added in the fresh Dulbecco's MEM medium without foetal calf serum and without phenol red (Gibco) and the cells were incubated with at 37°C for 4 hours. A longer ALA incubation period did not increase the PpIX production (data not shown). After this incubation the ALA-treated cells were harvested by mild trypsination and the level of PpIX was measured by fluorescence. The PpIX excited at 510 nm has two emission peaks at 635 and 706 nm (Orenstein et al, 1997). The emission spectrum in the range of 600 – 750 nm was recorded in a SPEX spectrofluorometer. The intensity at 635 nm was considered as a measure of PpIX production.

In order to produce the photo-degradation of PpIX the cells attached to Petri dishes and incubated with ALA, were exposed to red He-Ne laser beam (power at the level of the dish surface was 16 mw) expanded by a simple lens system to cover the all dish surface. After different exposure durations (4-35 min) the cells were harvested by mild trypsination and the fluorescence spectrum recorded.

The level of toxic photo-induced products was evaluated using the MTT cell viability test after exposure to laser beam. The cells were seeded at appropriate concentration on a 96wells plate for 24h, than incubated for 4 h, at 37°C, with 0.5mg/ml thiazolyl blue tetrazolium bromide (TBTB, Sigma). The viable cells are transforming the TBTB into coloured formazan precipitate. The production of formazan was quantified using a spectrophotometer plate reader (Awarness).

The cell suspension electroporation was done using an Eppendorf electroporator. The suspension medium was the same as Eppendorf recommended. An exponential electric pulse (time constant of 100 µs) was applied between the electrodes of an electroporation cuvette (BioRad) where the cell suspension was introduced. The electric field intensity ranged from 0.5 to 6 kV/cm. In order to evaluate the efficiency of electroporation the uptake of a membrane impermeable molecule (ethidium bromide, EB) was followed. The dye was added to the cell suspension just before the electroporation. The labelled cells were counted under a fluorescence microscope (Zeiss Axiovert 200) equipped with an appropriate filter set and the percentage of the coloured cells was calculated. To evaluate the cells 'death' (at high electric field intensity a large number of cells die) the EB was added to the electroporated cell suspension after 10 min. It was considered that during this period the permeability membrane of surviving cells was recovered and only the irreversible permeabilized cells will uptake the dye.

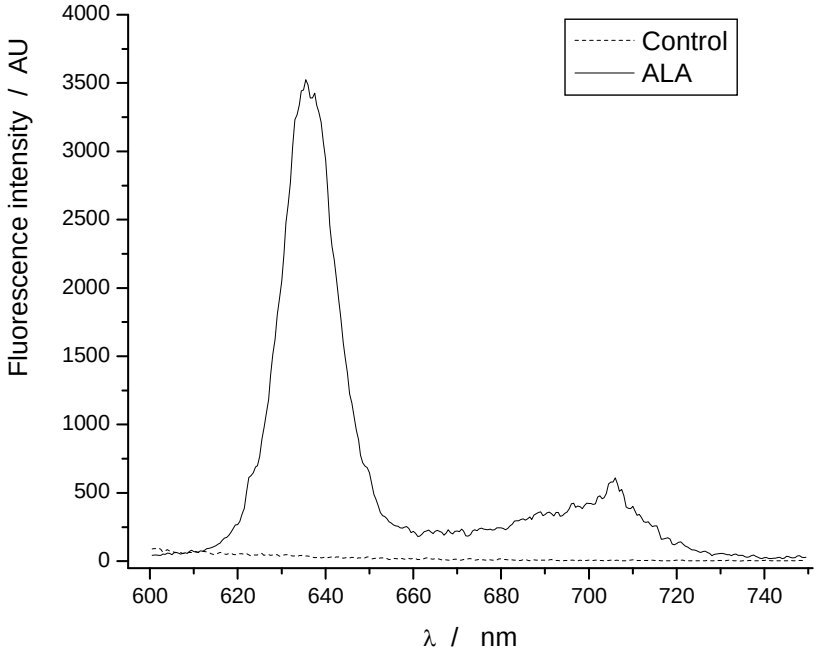


Figure 1. Fluorescence spectra of cells incubated with ALA, 1 mM, 4 hours (ALA) and without ALA (Control). λ_{ex} = 510 nm

Results and Discussions

The cells incubated with ALA, 1 mM, 4 hours, had a strongly increase of PpIX production (fig. 1). The spectrum is very similar with other reported results (Orenstein et al, 1997; Dysart and Patterson, 2006) and two peaks can be observed at 635 nm, the main one, and at 706 nm. In contrast, the control cells (without ALA) did not present observable levels of PpIX.

The effect of light irradiation on cells incubated with ALA was revealed by means of decrease of PpIX level in cells after irradiation (fig. 2). The PpIX level decreases with irradiation time confirming other results reported in the literature (Orenstein et al, 1997). Plotting the maximal intensity at 635 nm against irradiation time a linear decrease of PpIX level in irradiated cells can be observed (fig 3). Over 35 min of irradiation the fluorescence intensity at 635 decrease much slowly suggesting a saturation of the process (data not shown).

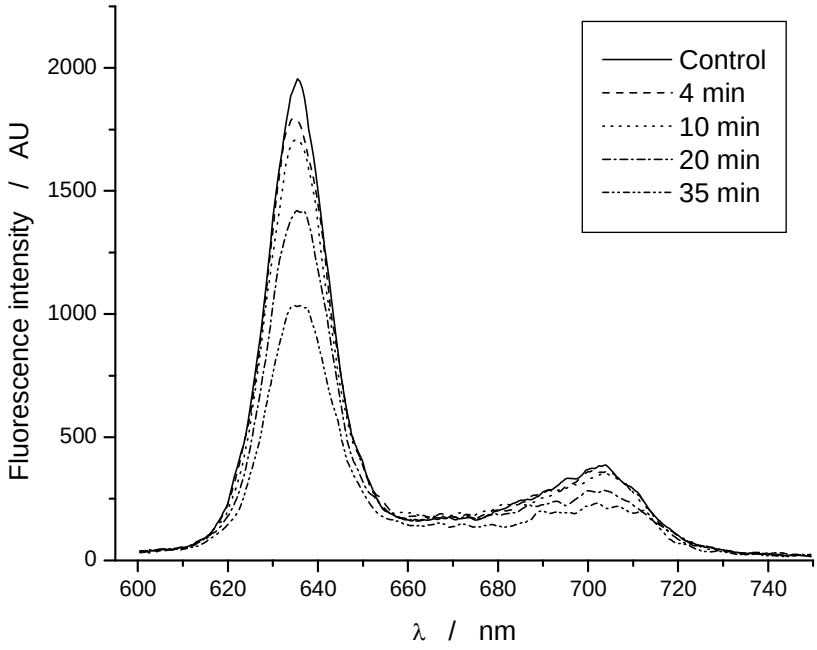


Figure 2. Fluorescence spectra of cells incubated with ALA, 1 mM, 4 hours (ALA) and irradiated with red laser light (633 nm) for different periods. λ_{ex} = 510 nm.

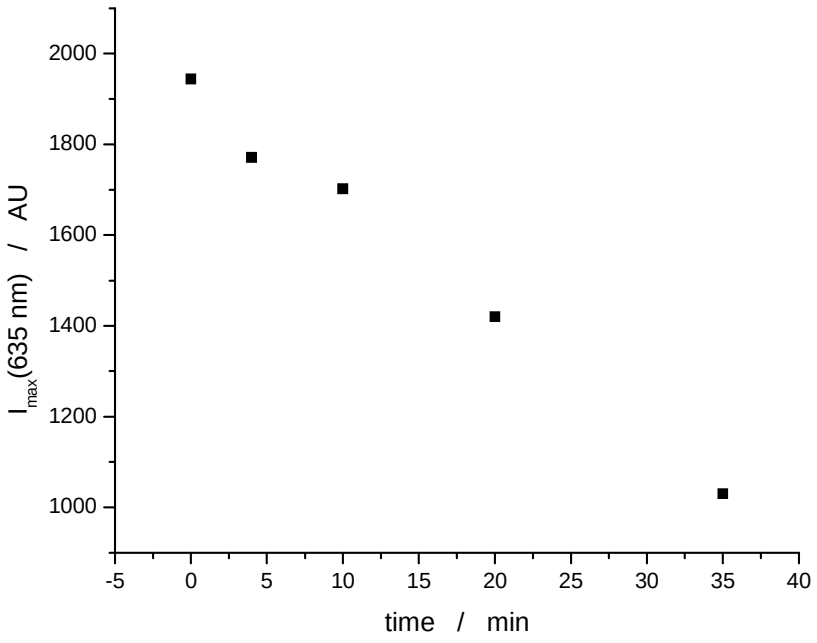


Figure 3. Fluorescence intensity at 635 nm (λ_{ex} = 510nm) of cells incubated with ALA, 1mM, 4 hours and irradiated with red laser light (633 nm) for different periods.

In order to check the effects of irradiation on the viability of the cells the MTT test was applied. Four variant of cell cultures were tested: a control consisting in cells without ALA, a second control without ALA but irradiated at 633 nm, a non-irradiated but ALA incubated culture cells and a culture cells incubated with ALA and irradiated with 633 nm laser light. The period of irradiation was 30 min. ALA incubation was performed as above. The results are in presented in Figure 4. The red light irradiation and ALA incubation did not affect the viability of cells with respect to the controls. Only the cells incubated with ALA and irradiated with red light show more than two times smaller viability. This experiment actually proves the fact that our experimental conditions are appropriate for an *in vitro* experiments revealing the presence of photo-induced products in ALA incubated cells and irradiated with red light.

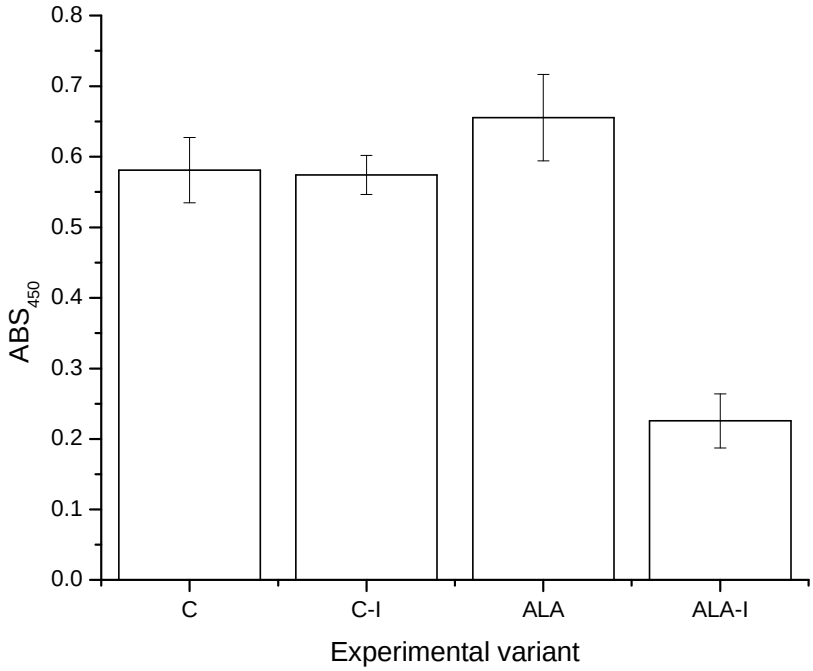


Figure 4. Viability of the cells evaluated by MTT test: C – control, C-I – control cells irradiated with red light, ALA – ALA incubated cells, ALA-I – ALA incubated cells and irradiated with red light.

In order to find out the optimal conditions for the electroporation a range from 0.5 to 6 kV/cm was used. One exponential pulse (time constant of 100 μs) was applied to the cell suspension with or without EB. The results are in Figure 5. At low level of electric field intensity a rapid increase of porated cells percentage is observed reaching a plateau for higher values of electric field. On the other hand, at low field intensity the viability of cells is very close to maximum (100%) and decreases when the electric field increases. For medium values of the field intensity (between 2 and 4 kV/cm) the cells have simultaneously a maximal level of poration and of viability. Considering the conditions of minimal stress for the cells we used in our experimental trials to increase the uptake of ALA in the cells by electroporation the following electric conditions: one exponential pulse of 2 kV/cm and 100 μs time constant.

After all these preparatory experiments which allow us to have proper conditions to reveal the photosensitizer effect and to have optimal electroporation parameters we performed experiments trying to find out an increase of PpIX production in cells electroporated in presence of ALA. The following conditions were used: ALA 1mM, one exponential pulse of 2 kV/cm and 100 μs time constant. 15 min after electroporation the cells were incubated in a fresh culture medium without ALA and after 1 h the cells PpIX level was recorded. For control cells the same experimental conditions were used without electroporation step but with a 4h incubation with ALA.

An unexpected result was obtained. In the electroporated cells no PpIX was revealed. The spectrum was very similar to the spectrum of control cells without ALA (data not shown).

In order to check if the electroporation step disturb or not the metabolism of cells a further control experiment was performed. Cells electroporated without ALA were incubated immediately after the electroporation in fresh medium with 1mM ALA for 4 hours. The level of PpIX was recorded by fluorescence spectrum and the PpIX value was similar to the control cells incubated with ALA for 4 h, without electroporation. This is an evidence for the fact that electroporated cells were able to develop the biochemical processes needed for PpIX synthesis.

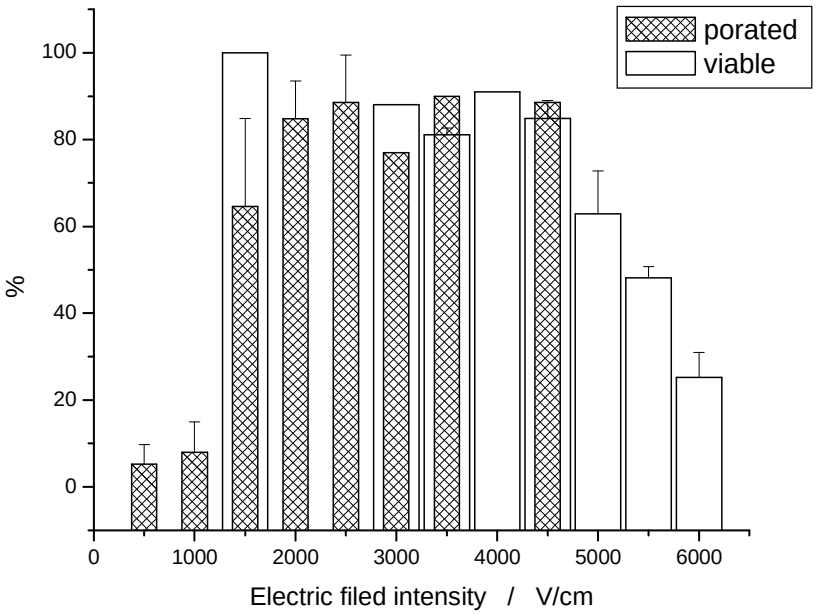


Figure 5. The electroporation yield and the viability of electroporated cells.

Summary

In this paper we report our preliminary results concerning the possibility to improve the efficiency of ALA – PDT method by electroporation. Our *in vitro* trials did not supply evidences that the electroporation of cells in suspension can be a way to increase the rate of ALA uptake of the cells. These results are apparently in contradiction with reports of other authors which successfully increase the transdermal transport rate of ALA and the level of PpIX production in *in vivo* experiments on mice (Johnson et al, 2002).

Refferences

Ma LW, Bagdonas S and Moan J, 2001 – The photosensitizing effect of the photoproduct of protoporphyrin IX – J Photochem Photobiol B, **60**: 108-113

Bermudez Moretti M, Correa Garcia S, Perotti C, and Casas A, 2002 – δ-aminolevulinic acid transport in murine mammary adenocarcinoma cells is mediated by BETA transporters – Br J Cancer, 87: 471-474

Rud E, Gederaas O, Hogset A, and Berg K, 2000 – 5-aminolevulinic acid, but not 5-aminolevulinic acid esters, is transported into adenocarcinoma cells by system BETA transporters – Photochem Photobiol, **73**:164-169

Johnson PG, Hui SW, Oseroff AR, 2002 - Electrically enhanced percutaneous delivery of delta-aminolevulinic acid using electric pulses and a DC potential - Photochem Photobiol., **75**: 534-40.

Dysart JS and Patterson MS, 2006 – Photobleaching kinetics, photoproduct formation, and dose estimation during ALA induced PpIX PDT of MLL cells uder well oxygenated and hypoxic conditions – Photochem Photobiol Sci, **5:** 73-81

Orenstein A, Kostenich G and Malik V, 1997 – The kinetics of protoporphyrin fluorescence during ALA-PDT in human malignant skin tumors – Cancer Lett, **120**: 229-234

Orlowski, S., J. Belehradek, Jr., et al.,1988 -- Transient electropermeabilization of cells in culture. Increase of the cytotoxicity of anticancer drugs -- Biochem Pharmacol, **37(24)**: 4727-33.

REGULATORY COMPLIANCE OF MOBILE PHONE BASE STATIONS IN AUSTRALIA

TANYA STOIANOFF BAgrEc MPS
EXECUTIVE DIRECTOR, MOBILE CARRIERS FORUM
L6, 46 MARKET STREET, SYDNEY 2000

Abstract

Mobile phone base stations in Australia are governed by a mix of regulatory and self-regulatory instruments ranging from how base stations are built, through to cumulative EME compliance on existing shared sites.

This paper explores various levels of regulatory compliance required of Australia's mobile phone carriers when it comes to siting, designing and operating mobile phone infrastructure.

The regulatory and self-regulatory mix aims to address both the science underlying human exposure safety and the public perception of health risks from mobile phone infrastructure - so there is a mix of both the ICNIRP standard for human exposure as well as the adoption of precautionary behaviours when carriers build base stations in Australia.

The ACIF Code for the Deployment of Mobile Phone Networks is the key instrument which has adopted precautionary behaviours requiring carriers to:

- Have written procedures for site selection;
- Improve notification and community consultation procedures;
- Design and operate base stations with the objective of minimizing electromagnetic emissions; and
- Provide electromagnetic radiation emission reports, or Environmental Reports for every site, as per the Federal Department of Health's requirements.

Australia's Mobile Carriers Forum (MCF) has played an important role in this regulatory/self-regulatory mix. It is an industry forum comprised of the four mobile phone carriers building networks in Australia, and was formed in 2000 to address a number of issues in the area of wireless infrastructure network operations and mobile base station deployment. Of particular relevance was responding to issues of community concern and improving inter-carrier cooperation.

The MCF has either contributed to the creation of the various regulatory and self-regulatory instruments discussed in this paper, or has developed operational programs and systems for the carriers to use in practice to ensure regulatory compliance. While it does not claim to be a complete analysis, this paper explores the main instruments and initiatives.

Introduction to the Australian Scene

Mobile phones have become an integral part of day to day life for individuals, businesses and the community at large. According to Credit Suisse First Boston 2005, the Australian mobile telecommunications industry today has approximately 19 million subscribers with various mobile technologies being used by about 95% of the Australian population. Although it may seem surprising, a penetration rate exceeding 100% has been achieved in a number of countries and research suggests that it will be achieved in Australia by the end of 2008.

The Allen Consulting Group states in its publication *Australian Mobile Telecommunications Industry – Economic Significance (2005*) that the mobile telecommunications industry is a high revenue, high cost industry that makes a substantial and growing contribution to the wider telecommunications industry and the Australian economy. Industry gross product for the financial year 2004/05 was $6.1 billion, up

from $5.3 billion in the previous year. Since 1997, capital expenditure by the industry on new networks has exceeded $10 billion. Revenue from the mobiles sector of the telecommunications industry was $9.9 billion in 2004/05 according to Credit Suisse First Boston 2005. Australia's mobile phone networks reach over 98 percent of the population and cover just over 20 percent of the Australian land mass.

Data such as industry gross product, mobiles revenue and capital expenditure figures are important in demonstrating the economic contribution of Australia's mobile phone industry, however those measures do not convey the many ways in which mobile telephony contributes to improvements in the quality of people's lives and increases in social equity.

For many people, mobile telecommunications is more than a tool to make voice calls; instead, the extensive coverage, array of services and information available mean that the mobile phone can "make life mobile". The accessibility and freedom for people on the move to maintain contact with other people is a significant benefit. From an emergency perspective, a third of all calls to emergency services in Australia are made from mobile phones. Furthermore, emerging technology such as 3G and video phones will help to increase social equity by expanding access to groups such as the hearing impaired. Mobile telephony is increasingly more affordable in Australia particularly through low-cost and capped plans, allowing more people to benefit from the connectivity of mobile telecommunications services.

The MCF found in its publication *Third Generation Mobile Networks in Australia, Broadband For Your Mobile Phone (2005)*, that 3G applications in the Australian business sector are also growing, ranging from video-calling to location based mobile data services and telecommuting for employees.

Regulatory Environment

In Australia, telecommunications facilities are primarily regulated under Commonwealth law. This is largely due to Section 51(V) of the Australian Constitution which reads:

"The Parliament shall, subject to this Constitution, have power to make laws for the peace, order and good government of the Commonwealth with respect to:…(V) postal, telephonic and other like services:…"

In 1991 the Commonwealth Parliament enacted the *Telecommunications Act 1991*. The *Telecommunications Act 1991* and subsequent Carrier licences obligated Carriers to provide mobile telecommunications services to a large percentage of the Australian population. To assist Carriers meet these obligations the *Telecommunications Act 1991* also provided broad ranging powers to Carriers to install all types of mobile telecommunications facilities by granting exemptions from State and Territory environmental planning laws. These exemptions allowed Carriers to build quite substantial structures such as, for example, 30-metre towers without regard to State and Territory planning law.

However in 1997 the telecommunications regulatory environment was reshaped with the introduction of the *Telecommunications Act 1997*. This Act significantly curtailed the carriers' powers to install telecommunications facilities by limiting those exemptions from State and Local planning laws. Carriers must now comply with State and Territory planning and environmental assessment laws in relation to the installation of certain types of telecommunications facilities.

The Australian Government recognised however, that there are some telecommunications facilities and activities that are "unlikely to cause significant community disruption or significant environmental disturbance". These are exempt from certain State and Territory laws. These new telecommunications facilities and activities are described in the *Telecommunications Act 1997 (as amended)*, (referred to as "the Act") and in a Ministerial determination made under the Act – the *Telecommunications (Low-impact Facilities) Determination 1997* (referred to as the "Low-impact Determination") as amended.

The Act and the Low-impact Determination define what low-impact installation activities may be undertaken in certain areas without reference to particular State and Territory laws. Low-impact facilities are those which are considered essential to maintaining telecommunications that cause minimal detrimental visual impacts. Common examples of low-impact facilities are smaller scale structures such as panel antennas on light poles, building facades and rooftop installations. The

Determination sets out performance criteria for certain types of facilities based on the proposed location (an area classification criteria) of the facility and the dimensions of the proposed facility (a dimension criteria).

Facilities that do not meet the performance criteria outlined in the Determination cannot be defined as low-impact facilities. Those activities which are not exempt require consent from the local council as they are subject to State planning laws which vary in each of the States of Australia. For the purposes of brevity, this paper will not outline each State's planning regime.

Mix of Regulation and Self-Regulation

The Australian Communications and Media Authority, the ACMA, (formerly known as the Australian Communications Authority) is the regulator of the Australian communications industry. Since 1997 it has regulated telecommunications consumer and technical matters, and manages radio-communications. Specifically, the ACMA is responsible for the issuing of carrier licenses, the regulation of service providers, the registration and enforcement of industry (including consumer, operations and technical) codes of practice and the setting of industry standards, to name a few of its responsibilities.

The issue of electro-magnetic radiation (EMR) is an important issue for consideration in the deployment of telecommunications infrastructure. Some members of the public perceive that exposure to this type of radiation from mobile telephony could be harmful to human health. For the purposes of this paper it is necessary to outline that in Australia, exposure to EMR is regulated by the ACMA. The applicable standard is the "Radiation Protection Standard – Maximum Exposure Levels to Radiofrequency Fields – 3kHz to 300 GHz. The standard prescribes "fundamental limits designed to ensure that known health effects do not arise from exposure to radio frequency fields".

The Australian Radiation Protection and Nuclear Safety Agency (ARPANSA) is an Australian Government agency under the Department of Health, charged with responsibility for protecting the health and safety of people, and the environment, from the harmful effects of ionizing and non-ionizing radiation. ARPANSA builds and maintains expertise in the measurement of radiation and assessment of health impacts, it advises Government and provides information to the public, on issues related to radiation protection and nuclear safety, and it leads in the development of standards, codes of practice, guidelines and other relevant material to support radiation protection and nuclear safety throughout Australia. For example, the ACMA changed its Radio-communications (Electromagnetic Radiation) Human Exposure Standard 2001 to incorporate the limits of the new radiation protection standard recommended by ARPANSA – harmonising Australia with the ICNIRP guidelines a few years ago.

The considered scientific opinion from ARPANSA about possible health effects from this type of infrastructure is that "the weight of national and international scientific opinion is that there is no substantiated evidence that RF emissions associated with living near a mobile phone base station of telecommunications tower poses a health risk". The Australian Government and its regulatory bodies commonly refer to the World Health Organisation's position on this issue. Comprehensive reviews of over 2200 research publications, including more than 410 studies specifically on mobile phones and base stations, by governments and health authorities continue, without exception, to find there is no substantiated scientific evidence of health effects.

The World Health Organisation (WHO) in May 2006 updated their fact sheet entitled "Electromagnetic Fields and Public Health – Base Stations and Wireless Technologies", saying:

> *"Considering the very low exposure levels and research results collected to date, there is no convincing scientific evidence that the weak RF signals from base stations and wireless networks cause adverse health effects"*

Only recently the WHO said that despite the feeling of some people that more research needs to be done, scientific knowledge in this area is now more extensive than for most chemicals.

The Australian Communications Industry Forum (ACIF) is an industry owned, resourced and operated company established by the telecommunications industry in 1997 to help implement and manage

communication self-regulation within Australia. ACIF develops Standards and Codes to support competition and protect consumers, and administer technical and operating arrangements.

ACIF developed an *Industry Code for the Deployment of Radio-communications Infrastructure* (referred to as "the Code") which was registered by the ACMA in 2002. The Code applies the precautionary approach to the siting, design and operation of mobile phone base station infrastructure in Australia. It requires carriers to:

- Have written procedures for site selection;
- Improve notification and community consultation procedures for low-impact sites;
- Design and operate base stations with the objective of minimizing electromagnetic emissions; and
- Provide electromagnetic radiation emission reports upon request, as per the Federal Department of Health's ARPANSA requirements.

The Code was developed in response to calls for greater council and community involvement and more information when mobile phone base stations are installed. It was developed and agreed to by carriers, local government, unions, community groups and the ACMA.

It is important to note that the Code was developed to increase the transparency and accountability of carriers and increase consultation with the community when low-impact mobile phone base stations are built. The Australian community now has rights of access to information about any proposed base station in their area.

Self-Regulatory Aspects to Code Implementation – Industry Activity

As the industry approached the introduction of the above mentioned Code, the MCF recognised that the industry needed to be well prepared for the significant changes the Code would make to Australia's traditional deployment processes. The Code introduced new notification and consultation requirements for low-impact sites that were not required previously by law. It requires carriers to provide certain EME information about all sites across the country and it requires carriers to demonstrate that they had investigated possible co-location opportunities in the first instance.

In order for the Code to succeed, the carriers needed an implementation program of proforma documentation and flowcharts which guided carrier staff to ensure industry compliance with the Code. The MCF created such documentation with the input and ownership of each carrier on the Code drafting committee. The implementation process was then transferred into an interactive web based system which each carrier utilises. The program has provided some industry consistency in what could have become a myriad of interpretations which may have resulted in poorer compliance and would have made it even more difficult for the regulator, the ACMA, to monitor. The ACMA records all legitimate complaints made to it about a carrier's compliance or lack of compliance with the Code and assesses whether in fact the Code has been breached. Fines of up to $250,000 per breach may be charged by the regulator.

Other countries have introduced similar industry policies to the Code, but none have been supported by industry-consistent implementation documentation and processes which provide a paper trail demonstrating industry compliance with such a regime.

As part of the implementation program it was important to engage with the key stakeholders in the Code. The MCF organised a series of National Workshops in partnership with each State Local Government Association (LGA), the ACA and ARPANSA, to improve council awareness of the new Code. The MCF also produced an Information Kit for councils, distributed via LGA channels.

One particular Council in Sydney even made a specific report to its full council on the MCF's Code Information Kit and Workshop and stated that "the Code appears to be a genuine attempt by the Carriers to gain some community and Council trust". This feedback was an important message confirming to the industry that its efforts had not gone unnoticed.

In addition to this work, the MCF embarked upon a project with State Local Government Associations in Australia, which resulted in the creation of *Guidelines for Local Government on the ACIF Code* in

2006. The Guidelines were created with extensive consultation with local councils and they provide a useful toolkit for local council staff to monitor carrier compliance with the Code, despite the fact that low-impact sites do not require local council consent.

Demonstrably, the MCF's promotional and operational activities have been world leading in that the adoption of the code was strengthened with the development of an implementation program for demonstrating industry compliance and process, as well as providing local government with enhanced awareness of required carrier processes. This has reinforced Australia's self-regulatory regime for telecommunications.

Coordinated Strategy for On-site Regulatory Compliance

The MCF has facilitated the creation of a regulatory compliance strategy for carriers to assist them in managing their cumulative EME exposure obligations at both carrier and non-carrier owned sites. This strategy involves inter-carrier data exchange as well as liaison with third party property owners and radio licensees.

The strategy, which is now known as the MCF EME Regulatory Compliance Strategy (MERCS) was first tested via a national trial of fifty rooftop sites each containing two or more carrier facilities. A process for inter-carrier information exchange, cumulative radio hazard assessment by accredited specialists and communicating compliance to the property owner through a standard form Radio-communications Site Management Book (RCSMB) was developed and tested. This strategy is now being used by the industry across the country.

The MCF Rooftop Trial, as it was known, was also transferred into an electronic repository or database of carrier sites by one of the MCF's members, Telstra. It is now being populated by all carriers. This database, known as the National Site Archive (NSA), facilitates an electronic information exchange amongst carriers. Each carrier site, as it is built, is uploaded onto the NSA and the public are provided access to each site's environmental EME report (ARPANSA report) and compliance certificate as part of the industry's objective of transparency and accountability.

During the Trial, a National Antenna Database (NAD) was developed as the centralised database of mobile carrier antenna data. The NAD is an essential system to ensure that consistent and standard antenna data is available to carriers for EME software applications. The NAD is also critical to further automation of the NSA e.g. producing automatic environmental reports from STAD tables.

The MCF Rooftop Trial created a system for ensuring cumulative assessment of EME at shared sites given the regulatory requirements placed on the carriers by the ACMA and ARPANSA which included occupational health and safety (OH&S) obligations for workers who would access such rooftop sites. It is not an overstatement to say that the MCF Rooftop Trial revolutionized how carriers ensured compliance with cumulative exposure standards and OH&S laws on non-carrier owned sites.

The resulting NSA is also linked to an electronic system for managing the afore mentioned ACIF Code. Australia's largest (majority Government owned) carrier, Telstra assisted the industry by taking the MCF's Code implementation documentation and transferring it into an electronic system for compliance, linked to the NSA. Carriers in Australia can now upload site data onto the NSA, record the required compliance documentation, upload the required site management book, and document the completion of their ACIF Code requirements through a linked MCF web based electronic system.

The efficiencies and benefits to the industry from these initiatives are significant. The MCF's ability to facilitate such a consistent industry owned and used system is laudable and is testimony to the growing maturity of the MCF's members - the Australian mobile telecommunications carriers.

Visual Impact of Mobile Phone Base Stations

As was outlined by Stoianoff (2004), when communities convey concerns over base station deployment, it usually arises in three areas, not in any particular order – firstly, EMR emissions and health, secondly, visual amenity concerns about infrastructure and thirdly, a perceived lack of community empowerment when base stations are being built.

In Australia, the third concern has somewhat been addressed via the previously described ACIF Code, however, this instrument, nor any other similar instrument, can ever fully satisfy every community member's desire to control development in their area.

The first concern in relation to emissions and health is a world-wide phenomenon and can only be managed with the assistance of ongoing replicated research and the communication of information and education to the community from independent expert bodies such as the World Health Organization and local authorities such as ARPANSA in Australia.

The second concern, visual amenity is a somewhat different issue in that it is influenced by a number of factors such as cost, technical RF requirements, topography and vegetation and land owner requirements. Given the varying range of issues, the most aesthetic design is not always an available option when building base stations, however, industry needed to make an effort wherever possible.

Early on in the MCF's formation, a set of Guidelines were created incorporating urban design principles with the requirements of the infrastructure regulatory regime in Australia. The *Guidelines for Better Visual Outcomes – Low-impact Mobile Facilities* book was published by the MCF in 2001. It was well received by planners, government and local councils. Some local councils even sought permission to extract sections of the Guidelines to insert into local government policies and planning schemes. A second edition of the Guidelines was produced in 2004 to include the ACIF Code in the chapter which outlines Australia's telecommunications regulatory regime.

More recently, with the imprimatur of the Australian Government, the MCF has convened a *Design and Innovation Taskforce* inviting key stakeholders to participate including the property sector, structural designers and engineers, local government, town planners and telecommunications industry representatives. This group of stakeholders was identified as those who are best placed to make either a technical contribution to the Taskforce or those who have a direct involvement in the siting and design component of mobile phone base station deployment.

The Taskforce's key objectives are to:

- help investigate the national and international scene for improving the visual amenity of infrastructure – what designs are in use globally,
- gain a better understanding of the real life impediments to the adoption of "aesthetic design options" in Australia; and
- identify practical methods or opportunities to improve the visual amenity of facilities in Australia - providing recommendations within the context of the Australian marketplace.

The MCF Taskforce intends to generate a technical paper drafted by a specialist planner which should focus on the above key objectives. The Technical paper will also focus on typical types of telecommunications sites including: building rooftops, base stations in parks and recreational space, and on telegraph/electricity poles and other utility structures.

Summary

This paper has outlined the main regulatory instruments which govern mobile phone base station deployment in Australia. It is clear to see that a balanced mix of regulatory and self-regulatory mechanisms are at play ranging from legislation and Codes of Practice through to industry initiatives geared towards ensuring compliance with regulatory expectations from Government and the community's perspective.

This paper has also outlined a summary of MCF initiatives from devising regulatory compliance programs to creating publications which assist in industry performance and stakeholder appreciation of the limitations in network deployment options. Each of the MCF's initiatives may assist other country's organisations in addressing similar issues of concern.

While the telecommunications industry is governed by a largely self regulatory regime, the industry must take a proactive and responsible approach to deployment in order to honour such a regime.

References

Australian Communications Media Authority, FSC 44 7/2001, *Mobile Base Stations and EMR* (www.aca.gov.au)

Australian Radiation Protection and Nuclear Safety Agency, (2002) *Prediction Methodologies for Radiated Electromagnetic Energy (EME) Exposure Levels from Mobile Phone Base Station Antennas - Technical Report,* Australia (www.arpansa.gov.au)

Credit Suisse First Boston (2005) *Australian Telecommunications 2005*, Equity Research.

Mobile Carriers Forum, (2002) *Your Right to Information about Mobile Phone Base Stations,* Sydney Australia (www.mcf.amta.org.au)

Mobile Carriers Forum, (2001) first and second edition (2004), *Guidelines for Better Visual Outcomes – Low-impact Mobile Facilities,* Sydney Australia (www.mcf.amta.org.au)

Mobile Carriers Forum, (2005) *Third Generation Mobile Networks in Australia, Broadband for Your Mobile Phone,* Sydney Australia (www.mcf.amta.org.au)

Stoianoff, T. (2004) *World Leading Activities of the Mobile Carriers Forum*, as presented at 3rd International Workshop Biological Effects of Electromagnetic Fields, Kos Greece

The Allen Consulting Group (2005) – research commissioned by AMTA, *Australian Mobile Telecommunications Industry – Economic Significance,* Canberra Australia

World Health Organisation (May 2006) Fact Sheet No. 304 *Electromagnetic Fields and Public Health, Base Stations and Wireless Technologies*, Geneva

NEUROPHYSIOLOGICAL AND BEHAVIORAL EFFECTS OF HUMAN ACUTE EXPOSURE TO A 60 HZ MAGNETIC FIELD UP TO 1800 µT: PRELIMINARY RESULTS

A. LEGROS[1], A. BEUTER[2], L. KEENLISIDE[1], D. GOULET[3], M. PLANTE[3], D. NGUYEN[3], F.S. PRATO[1], A.W. THOMAS[1]

[1] LAWSON HEALTH RESEARCH INSTITUTE AND UNIVERSITY OF WESTERN ONTARIO, ST JOSEPH HEALTH'S CARE, 268 GROSVENOR STREET, LONDON, ON, N6A 4V2, CANADA

[2] UNIVERSITE VICTOR SEGALEN BORDEAUX 2, INSTITUT DE COGNITIQUE, 146 RUE LEO SAIGNAT, 33076 BORDEAUX CEDEX, FRANCE

[3] HYDRO-QUEBEC, 800 BD DE MAISONNEUVE EST, 21^{E} ETAGE, MONTREAL, QC, H2L 4M8 CANADA

Abstract

For the past two decades, researchers have actively been studying the effects of time-varying magnetic fields (MF) on humans, principally examining the potential for the field to have acute effects on human physiology, neurophysiology and behaviour. The more consistent results reported in recent literature seem to show an increase in occipital alpha rhythm of resting electroencephalographic activity (EEG) with exposure (Cook et al., 2004; Ghione et al. 2005). Interestingly, other studies have demonstrated that human motor behavior can be modulated by exposure to an Extremely Low Frequency (ELF) MF, showing a reduction in anteroposterior standing balance oscillations (Thomas et al., 2001) and a decrease in physiological tremor intensity (Legros et al, 2006). However, to establish a connection between these observations would require a project that, in one procedure, investigates physiological, neurophysiological and behavioural parameters. Therefore, subject testing has begun, in a project approved by the University of Western Ontario (Health Sciences Research Ethics Board # 11956E), to investigate the effects of a 60 Hz, 1800 µT MF on heart rate (frequency and variability), peripheral blood perfusion, brain electrical activity (EEG), postural oscillations, voluntary motor functions, and physiological tremor. Preliminary results will be presented and should provide reliable information concerning human exposure to power-line frequency MF.

A. LEGROS, A. BEUTER, L. KEENLISIDE, D. GOULET, M. PLANTE, D. NGUYEN, F.S. PRATO, A.W. THOMAS

Introduction

Domestic electrical appliances, distribution and transport power-lines, and residential wiring are some of the numerous sources of magnetic field (MF) in our everyday environment. Over the past several years, studies have been conducted with the aim of characterizing the effects of Extremely Low Frequency (ELF, below 300Hz) MF on human health and performance. Despite the amount of work that has been done in this area, there remains no consensus as to the effects of ELF MF on humans.

From brain electrical activity to motor behaviour, a number of aspects of human physiology and behaviour have been examined in scientific literature in response to acute exposure to ELF MF. Among the potential effects, many studies detected neuropsychological changes induced by the exposure (Keetley *et al.* 2001; Preece *et al.* 1998). That these studies are still relatively rare, and often have conflicting findings prevents the confident characterization of the field's effects. Further, exposure protocol and neuropsychological evaluating tools differ between studies, and reported effects are tenuous or even absent. Nevertheless, the examination of these studies shows that any notable cognitive effects generally appear to affect high level cognitive processes such as attention mechanisms, learning and memory; and executive functions such as working memory, flexibility, categorization, deduction and problem solving (see Kazantzis *et al.* 1998; Podd *et al.* 2002; Preece *et al.* 1998; Stollery 1986). Moreover, authors have found that the changes influence the quality and the precision of high level cognitive mechanisms rather than the velocity of execution.

If such neuropsychological functions are effectively modulated by the exposure to ELF MF, effects should be detectable at a neurophysiological level. Several studies have shown effects of MF exposure on human electroencephalogram (EEG) or evoked potentials (Bell *et al.* 1992; Bell *et al.* 1994a; Bell *et al.* 1994b; Cook *et al.* 2005; Cook *et al.* 2004; Ghione *et al.* 2005; Heusser *et al.* 1997; Lyskov *et al.* 1993a; Lyskov *et al.* 1993b; Marino *et al.* 2004). Still, no consensus exists on the direction of these effects, though the most conspicuous results seem to suggest a higher resting EEG in the alpha rhythm after exposure (8-13 Hz, see for example Cook *et al.* 2004; Ghione *et al.* 2005).

Other studies analyzing the interaction between heart rate (HR) behavior and MF have shown that electrophysiological rhythms can also be modified at the peripheral level and that the exposure to 60 Hz MF could induce a slowing of the HR that may or may not be associated with changes in HR variability (Cook *et al.* 1992; Graham *et al.* 2000a; Maresh *et al.* 1988; Sastre *et al.* 1998; Sastre *et al.* 2000). Again, other works did not detect any exposure effect on HR (Graham *et al.* 2000b; Graham *et al.* 2000c; Kurokawa *et al.* 2003). For a better understanding of the mechanisms underlying observed changes in HR, electrophysiological data should be completed by the monitoring of hemodynamic parameters such as blood flow.

Another way to investigate the effects of MF on the human body in its entirety is to evaluate human motricity. A few studies have demonstrated an effect on human motor control resulting from exposure to time-varying MF. Thomas *et al.* 2001a, for example, explored human postural oscillations and reported significant decrease in anteroposterior balance using a pulsed MF at 200 µT. Legros *et al.* explored human physiological tremor (Legros and Beuter 2005; Legros and Beuter 2006; Legros *et al.* 2006). They did not report any significant effect of a 50 Hz, 1000 µT MF on physiological tremor occurring during a goal directed task. However, the analysis of tremor occurring during a postural task of the index finger suggested a relaxing effect induced by the exposure, decreasing tremor size. Interestingly, Cook et al. who, in 2004, showed an effect of a pulsed 200 µT MF on EEG alpha activity, also underlined the link between resting posterior alpha activity and the state of relaxed wakefulness (Niedermeyer 1999).

Reported results are subtle and often not replicated. These discrepancies defining the effect of an ELF MF on humans can be attributed to the heterogeneity in intensity, shape and frequency of the MF used, as well as the differences in exposure duration. Furthermore, results differ with continuous versus intermittent exposure, and depending on whether the testing of the subjects is performed during or after the exposure.

Objective

The main objective of this study is to evaluate subtle effects of a 60 Hz MF exposure up to 1800 µT on human physiology, neurophysiology and motor functions in a single procedure. This intensity has been chosen because the International Commission on Non-Ionizing Radiation Protection (ICNIRP) guidelines establishes that current density induced by MF occupational exposure "should be limited to fields that induce current densities less than 10mA/m2" (ICNIRP 1998), and this corresponds to computed MF value which can reach 1800 µT (Stuchly and Dawson 2002, http://www.emfs.info/sci_Numerical.asp). This global approach will then establish a better understanding of the effects of high intensity MF on these functions. Conclusions will be drawn from the examination of human blood perfusion, HR (frequency and variability), brain electrical activity (EEG), posturo-kinetic activity as postural sway, voluntary motor functions as rapidly alternating movements and involuntary movements through the measurement of postural tremor.

Based on results in the literature, we hypothesize that MF exposure will (1) not affect ECG or blood flow, (2) increase EEG power in alpha band activity, especially in the posterior regions of the brain, (3) decrease the quantity and the variability of anteroposterior displacements of postural sway, (4) increase the rapid voluntary movements' maximum frequency, and (5) decrease postural tremor amplitude. Effects should appear after several minutes of exposure. The results could be useful in the development of public policy regarding the safety of MF exposure.

Methods

This is a currently ongoing study. To date, 8 subjects have completed at least 1 of the 2 sessions of testing. All participants give their informed consent before participating (University of Western Ontario Health Sciences Research Ethics Board # 11956E). At term, 70 healthy adults between 18 and 55 years of age will have completed the full protocol consisting of 2 counterbalanced exposure sessions given on 2 separate days (with at least 2 days in between): 1 active exposure condition (real) and 1 control exposure condition (sham) as detailed in Figure 1a. None of the participants have ever experienced an epileptic seizure; have motor limitation; suffer from chronic illness (e.g., diabetes, severe psychiatric, cardiovascular or neurological diseases); or have a cardiac or cerebral pacemaker. They have no history of head, eye or thorax injury involving metal fragments; they do not wear metal braces on their teeth. Finally, women cannot be pregnant, nor have an intrauterine device. A double blind computer driven procedure controlling for variables is used such that neither the participant nor the experimenter know when the real or sham condition occurs. Each session lasts 1 hour and 45 minutes and is composed of four 15 minute blocks of testing with 15 minutes rest in between. 1 hour of MF exposure is given from minute 15 to minute 75 of the real exposure session. There is no MF exposure in the sham session.

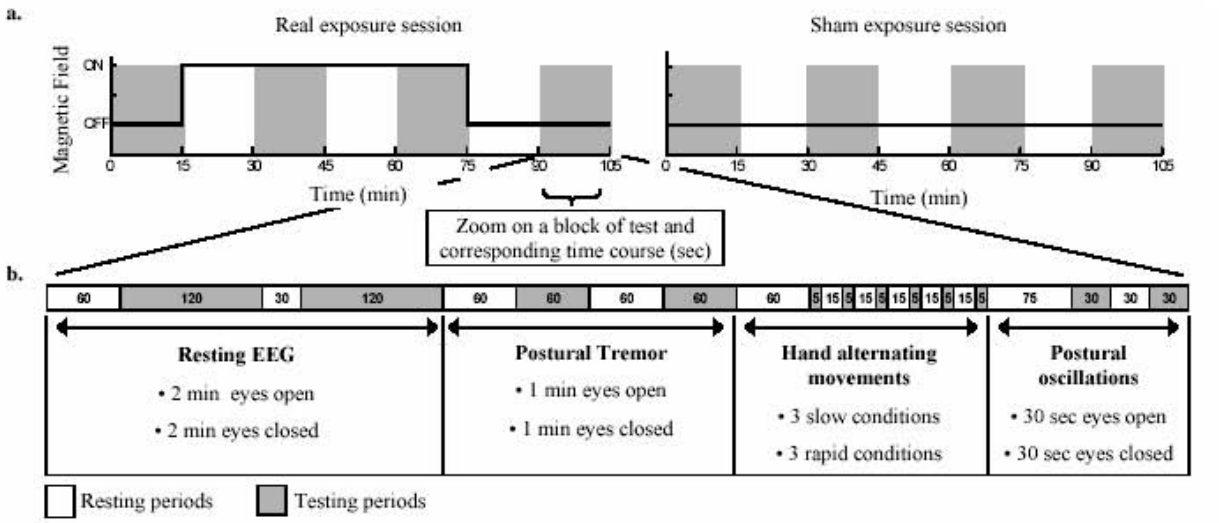


Figure 1: a. Time course of the 2 exposure sessions (real and sham). The horizontal black line represents the MF status (OFF when down, ON when up). Note that during the sham exposure session, the MF is never ON. Vertical grey bands represent the four 15-minute blocks of testing. **b.** Zoom on the time course of a block of testing (the same for each block). White cells represent resting periods and grey cells represent testing periods (duration is displayed in seconds inside the cells). The table below indicates the tests to which these periods correspond.

Each subject is equipped with the recording devices and his handedness is determined with the Oldfield questionnaire (Oldfield 1971). For the experiment, he is seated in an armchair in the exposure facility. The exposure system generating the MF has been designed for this experiment. It is composed of 2 octagonal coils, 1.6 meters in diameter, running parallel to each other 1.2 meters apart. Each coil contains 80 turns of AWG-10 wire mounted with a nonconductive cooling/heating tubing system. The system is configured to generate a homogenous 60 Hz field, up to 1800 µT, centred at the level of the head.

Prior to testing, the subject receives written directions, and is shown an audio-video demonstration of each task through a LCD screen and speakers, both positioned 1 meter in front of him. The room temperature is maintained at 23 °C. From the beginning of the testing session, both the subject and experimenter wear ear plugs to make it impossible to detect the subtle noise produced by the coils when the field is generated. The time course of the testing, as well as the MF generation and data acquisition, are entirely automated and computer driven (Labview 8.0 and Data acquisition card NI PCI-6289, National Instrument Inc., USA); except for recording of EEG, ECG and blood flow data. Automatic audio directions are given to the subject throughout the

duration of the experiment. He obtains visual information about the timing of the experiment through the screen in front of him.

Each of the 4 blocks of testing in each session follows the same time course (Figure 1b). The subject first relaxes for 1 min. Then his resting eyes-open-EEG is recorded for 2 min. After 30 sec of inactivity, his resting eyes-close-EEG is recorded for another 2 min. Baseline local blood perfusion (recorded at the tip of the non dominant index finger, PF 5010 Laser Doppler Perfusion Monitoring unit and probe 407-1, Perimed, Sweden) and ECG are recorded simultaneously. EEG and ECG are recorded at 512 Hz with a 32 channels ambulatory unit (Siesta unit, Compumedics Inc., USA). During the real exposure session, the MF is switched OFF during the second minute of both EEG recordings (eyes open and eyes closed) to keep 1 minute free of MF artefact in the data.

The subject is then asked to open his eyes, and after a resting period of 1 minute, his eyes-open postural tremor is recorded at the extremity of his dominant index finger for 1 minute. A Class II laser diode pointing toward the ground (Micro laser sensor LM10, series ARN11, Matsushita Electronic Work, Ltd., Osaka, Japan) and located 8 cm above the piece of white cardboard fixed on nail of the index finger enables 1000 Hz vertical displacement recording. A target horizontal line gives feedback about the index finger's vertical position, and is also displayed on the LCD screen. In this test, the subject must point the index finger (in extension at the level of the metacarpophalangeal joint) to keep the target line centred in the middle of the screen for 1 minute at the "zero position". After another 1 minute rest, he performs the same test with his eyes closed and therefore, with no visual feedback.

After another 1 min period, the subject is asked to extend his arms in front of him, parallel to the floor, and then to bend them to a 90 degree angle at the elbow, with hands open, palms facing each other. From this starting position, he has to execute alternating hand movements that involve rotating the hands at the wrist axis: (1) with the right hand at a natural rhythm; (2) with the left hand, natural rhythm; (3) with both hands, natural rhythm; (4) with the right hand at a higher frequency; (5) with the left hand, higher frequency; and (6) both hands, higher frequency. For the higher frequency condition, the subject is asked to rotate his hands "as fast and as far as possible". Recordings last 5 sec each, with a 15 sec rest between any two. Recordings are done with the liberty system (Polhemus inc., USA), with 2 transducers fixed like watches on the dorsal side of the wrists, allowing recording of movement kinematics with 6 degrees of freedom at 200 Hz in the used configuration (3D and 3 angles of rotation, accuracy of 0.03 RMS for X, Y, Z position and 0.15° RMS for orientation). The Liberty system is an electromagnetic tracking system and therefore, during MF exposure session, the field has to be turned OFF during each 5 sec recording periods so as not to affect data.

Finally, the subject has 75 sec to step onto a force plate (standardized socks, feet parallel, 1 cm apart) and to relax before his postural sway is recorded during 30 sec eyes open, and 30 sec eyes closed, with a 30 sec period in between. The 3-D force plate used in previous works (Thomas *et al.* 2001a; Thomas *et al.* 2001b, OR6-7-1000, AMTI, Watertown MA) is mounted on the floor in the centre of the MF exposure system, and measures the force and momentum applied by the subject's feet at a sampling rate of 1000 Hz. These measurements can be converted to centre of pressure (COP) values, i.e. the perpendicular projection of the centre of gravity through the force plate. Postural sway is then the change the COP over time.

As detailed in the Figure 1b, this block of testing is given 4 times over a session. During a real exposure session, this would mean that the testing begins: 15 minutes before the beginning of the exposure period, 15 minutes after the beginning of the MF exposure, 45 minutes after the beginning of the MF exposure, and 15 minutes after the end of the MF exposure. Skin temperature is monitored throughout the experiment. After each block, the subject has to answer the Field Status Questionnaire (FSQ, Cook *et al.* 1992) to assess his ability to detect the presence of the field.

Data processing and Analysis

As an ongoing study, data are still being collected and analysed. Therefore, given the advancement of the study and in a concern of clarity of the purpose, it has been chosen to focus here on a limited set of data, including EEG in the occipital region of the brain (O1, O2), postural tremor data, and postural sway data.

First, the ambulatory EEG data are recorded on a flash memory card, and then an averaged reference montage is used to import data in Matlab for processing (The MathWorks Inc., Natick, USA). Fast Fourier Transform (FFT) and inverse Fast Fourier Transform (iFFT) are used to extract time series in the theta (4-7 Hz), alpha (8-13 Hz), and beta (14-35 Hz) frequency bands. The average amplitude in each band is then computed for each electrode (O1, O2 here, see example in Figure 2).

Secondly, the laser system records vertical displacement with a resolution of 13 µm (i.e. 2σ, where σ is the standard deviation of a recording on a stationary target) which is effectively reduced to 5 µm after filtering out high frequencies (above 25 Hz, FFT, iFFT). Data are transferred to Matlab for A/D conversion to mm given a calibration constant (-3.97). Position and velocity data (obtained by differentiation of the raw displacement data) are used for indexes computation in time and frequency domains (Beuter and Edwards 1999; Edwards and

Beuter 2000) allowing the characterization and the examination of temporal, frequential and morphological components of the signals (see also Legros and Beuter 2005; Legros and Beuter 2006). Here, amplitude, drift, median frequency and frequency concentration are computed (see Appendix 1 for index definitions and Figure 3 for an example).

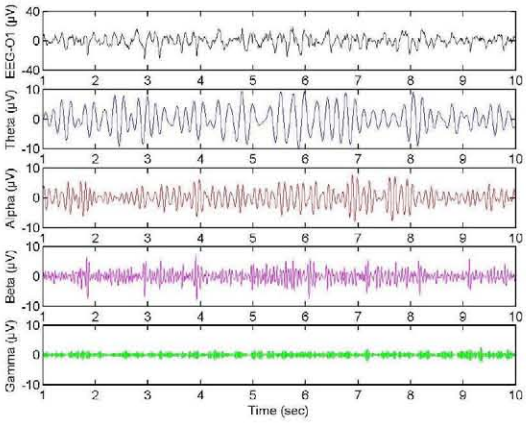


Figure 2: From the top to the bottom: 10 sec of O1 EEG trace and corresponding theta, alpha, beta and gamma components respectively extracted using FFT and iFFT. Averaged amplitude for this sample are: Theta = 3.909 µV, alpha = 2.485 µV, beta = 1.757 µV; gamma = 0.641 µV.

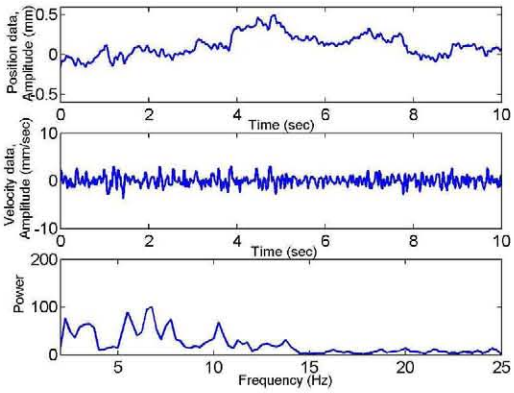


Figure 3: Position data (top), velocity data (middle) and corresponding power spectrum (bottom) for 10 sec of recording during MF exposure with eyes open (block 3). The computed values on this sample are: Amplitude = 0.032 mm; drift = 0.106 mm, median frequency = 7.04 Hz; and frequency concentration = 6.31 Hz.

Third, postural sway data are exported under Matlab and converted from volts to COP trajectories (in meters) using a calibration matrix. Through the inclusion of two dimensional trajectories (X vs. Y), the following validated characteristics have been computed (Despres *et al.* 2000; Thomas *et al.* 2001a): Mean sway, sway, velocity and sway area (see Appendix 1 for index definition and Figure 4 for an example).

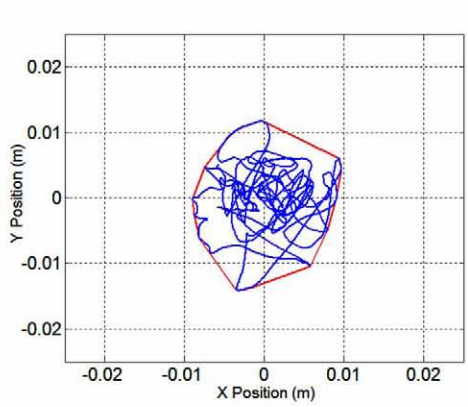


Figure 4: 30 sec of postural sway recording during MF exposure (block 3) with the eyes are closed. The smallest polygon including the entire trajectory is also displayed. The computed characteristics on this sample are: Mean sway = 0.53 cm; sway velocity = 1.62 cm/sec, sway area = 3.41 cm^2.

Preliminary results

For 3 of the 8 subjects who have completed at least 1 of the 2 sessions of testing, the first session was a real exposure condition. Therefore 3 subjects who have completed the sham session first have been chosen to afford a control group (i.e. the sham condition), which allowed providing a preliminary assessment of the exposure effects on their behaviour. According to the small sample size available at this step, a simplified statistical procedure has been chosen, focusing on the data acquired in the block 1 (before exposure) and the block 3 (during exposure, and after a 45 min period of continuous exposure, see Figure 1). A within-subject ANOVA including a between-subject factor (sham vs. real) have been conducted on each of the above

mentioned indexes: ANOVA 2 (eyes open vs. eyes closed) x 2 (block1 vs. block3) x 2 (sham vs. real). The level of significance has been set at $p < .05$ and no adjustment for multiple comparisons has been applied.

No Block main significant effect has been found either for EEG, postural tremor or postural sway recordings. However, with eyes closed, subjects had significantly higher EEG alpha activity in the occipital region (O1: $F = 24.85$, $p < .01$, $Eta^2 = .86$; O2: $F = 20.54$, $p < .05$, $Eta^2 = .83$), larger and faster postural oscillations (mean sway: $F = 17.38$, $p < .05$, $Eta^2 = .81$; sway velocity: $F = 51.47$, $p < .005$, $Eta^2 = .92$; sway area: $F = 35.14$, $p < .005$, $Eta^2 = .89$), and higher index finger drift ($F = 12.19$, $p < .05$, $Eta^2 = .75$) with eyes closed than with eyes open. No interaction effect was found.

Discussion-Conclusion

Preliminary results confirm that this experimental protocol is adapted to detect subtle changes in the neurophysiological characteristics investigated, despite the small number of subjects tested at this point. Indeed, as expected we observed significant differences between open and closed eyes conditions in EEG, tremor and postural sway. However due to the small number of subjects tested we did not detect a significant effect due to the presence of MF. This is why we performed a sample size analysis.

The sample size calculation for 2 independent samples with common variance was done on the sway velocity characteristic because this is the lowest p value for the interaction block x sham/real ($F = .509$, $p = .51$, $Eta^2 = .113$). In the present configuration, the decrease of .072 cm/sec observed for the real exposure group would be significant with two groups of 34 subjects (p fixed at .05, power = .80). We have planned to test a sample of $n = 70$ subjects which should be sufficient to detect the MF effects on the characteristics examined. We have to keep in mind that, at this stage of the study, 2 groups of subjects were evaluated. However in the final study all participants will have been tested under both MF conditions with a counterbalanced protocol. This should contribute to make the protocol more sensitive to subtle effects (reducing the impact of the between-subjects variability).

The results presented in this paper are only partial results on selected tests recorded. They will be completed by heart rate frequency and variability, blood flow perfusion, alternating movement performance. Finally data acquisition will be completed in 2007.

Acknowledgements

This research is funded in part by Hydro-Québec, Réseaux Transport Electricité (RTE), Electricitié de France (EDF), Ontario Research and Development Challenge Fund (ORDCF), Canadian Institutes of Health Research (CIHR) and Lawson Health Research Institute.

References

[1] Bell, GB, Marino, AA and Chesson, AL. 1992. "Alterations in brain electrical activity caused by magnetic fields: detecting the detection process." Electroencephalogr Clin Neurophysiol **83**(6): 389-97.

[2] Bell, GB, Marino, AA and Chesson, AL. 1994a. "Frequency-specific blocking in the human brain caused by electromagnetic fields." Neuroreport **5**(4): 510-2.

[3] Bell, GB, Marino, AA and Chesson, AL. 1994b. "Frequency-specific responses in the human brain caused by electromagnetic fields." J Neurol Sci **123**(1-2): 26-32.

[4] Beuter, A and Edwards, R. 1999. "Using frequency domain characteristics to discriminate physiologic and parkinsonian tremors." J Clin Neurophysiol **16**(5): 484-94.

[5] Cook, CM, Thomas, AW, Keenliside, L and Prato, FS. 2005. "Resting EEG effects during exposure to a pulsed ELF magnetic field." Bioelectromagnetics **26**(5): 367-76.

[6] Cook, CM, Thomas, AW and Prato, FS. 2004. "Resting EEG is affected by exposure to a pulsed ELF magnetic field." Bioelectromagnetics **25**(3): 196-203.

[7] Cook, MR, Graham, C, Cohen, HD and Gerkovich, MM. 1992. "A replication study of human exposure to 60-Hz fields: effects on neurobehavioral measures." Bioelectromagnetics **13**(4): 261-85.

[8] Despres, C, Lamoureux, D and Beuter, A. 2000. "Standardization of a neuromotor test battery: the CATSYS system." Neurotoxicology **21**(5): 725-35.

[9] Edwards, R and Beuter, A. 2000. "Using time domain characteristics to discriminate physiologic and parkinsonian tremors." J Clin Neurophysiol **17**(1): 87-100.

[10] Ghione, S, Seppia, CD, Mezzasalma, L and Bonfiglio, L. 2005. "Effects of 50 Hz electromagnetic fields on electroencephalographic alpha activity, dental pain threshold and cardiovascular parameters in humans." Neurosci Lett **382**(1-2): 112-7.

[11] Graham, C, Sastre, A, Cook, MR and Gerkovich, MM. 2000a. "Nocturnal magnetic field exposure: gender-specific effects on heart rate variability and sleep." Clin Neurophysiol **111**(11): 1936-41.

[12] Graham, C, Sastre, A, Cook, MR and Kavet, R. 2000b. "Heart rate variability and physiological arousal in men exposed to 60 Hz magnetic fields." Bioelectromagnetics **21**(6): 480-2.
[13] Graham, C, Sastre, A, Cook, MR, Kavet, R, Gerkovich, MM and Riffle, DW. 2000c. "Exposure to strong ELF magnetic fields does not alter cardiac autonomic control mechanisms." Bioelectromagnetics **21**(6): 413-21.
[14] Heusser, K, Tellschaft, D and Thoss, F. 1997. "Influence of an alternating 3 Hz magnetic field with an induction of 0.1 millitesla on chosen parameters of the human occipital EEG." Neurosci Lett **239**(2-3): 57-60.
[15] ICNIRP. 1998. "Guidelines for limiting exposure to time-varying electric, magnetic, and electromagnetic fields (up to 300 GHz). International Commission on Non-Ionizing Radiation Protection." Health Phys **74**(4): 494-522.
[16] Kazantzis, N, Podd, J and Whittington, C. 1998. "Acute effects of 50 Hz, 100 microT magnetic field exposure on visual duration discrimination at two different times of the day." Bioelectromagnetics **19**(5): 310-7.
[17] Keetley, V, Wood, A, Sadafi, H and Stough, C. 2001. "Neuropsychological sequelae of 50 Hz magnetic fields." Int J Radiat Biol **77**(6): 735-42.
[18] Kurokawa, Y, Nitta, H, Imai, H and Kabuto, M. 2003. "Can extremely low frequency alternating magnetic fields modulate heart rate or its variability in humans?" Auton Neurosci **105**(1): 53-61.
[19] Legros, A and Beuter, A. 2005. "Effect of a low intensity magnetic field on human motor behavior." Bioelectromagnetics **26**(8): 657-69.
[20] Legros, A and Beuter, A. 2006. "Individual subject sensitivity to extremely low frequency magnetic field." Neurotoxicology **27**(4): 534-46.
[21] Legros, A, Gaillot, P and Beuter, A. 2006. "Transient effect of low-intensity magnetic field on human motor control." Med Eng Phys **28**(8): 827-36.
[22] Lyskov, EB, Aleksanian, ZA, Iousmiaki, V, Medvedev, SV, Partanen, I, Safonova, TE, Khanninen, O and Iutilainen, I. 1993a. "[Neurophysiologic effects of short-term exposure to ultra-low-frequency magnetic field]." Fiziol Cheloveka **19**(6): 121-5.
[23] Lyskov, EB, Juutilainen, J, Jousmaki, V, Partanen, J, Medvedev, S and Hanninen, O. 1993b. "Effects of 45-Hz magnetic fields on the functional state of the human brain." Bioelectromagnetics **14**(2): 87-95.
[24] Maresh, CM, Cook, MR, Cohen, HD, Graham, C and Gunn, WS. 1988. "Exercise testing in the evaluation of human responses to powerline frequency fields." Aviat Space Environ Med **59**(12): 1139-45.
[25] Marino, AA, Nilsen, E, Chesson, AL, Jr. and Frilot, C. 2004. "Effect of low-frequency magnetic fields on brain electrical activity in human subjects." Clin Neurophysiol **115**(5): 1195-201.
[26] Niedermeyer, E (1999). The normal EEG of the waking adult. Electroencephalography.Basic principals, clinical applications, and related fields. ELdSF Niedermeyer. Baltimore, Williams and Willkins**:** 149–173.
[27] Oldfield, RC. 1971. "The assessment and analysis of handedness: the Edinburgh inventory." Neuropsychologia **9**(1): 97-113.
[28] Podd, J, Abbott, J, Kazantzis, N and Rowland, A. 2002. "Brief exposure to a 50 Hz, 100 microT magnetic field: effects on reaction time, accuracy, and recognition memory." Bioelectromagnetics **23**(3): 189-95.
[29] Preece, AW, Wesnes, KA and Iwi, GR. 1998. "The effect of a 50 Hz magnetic field on cognitive function in humans." Int J Radiat Biol **74**(4): 463-70.
[30] Sastre, A, Cook, MR and Graham, C. 1998. "Nocturnal exposure to intermittent 60 Hz magnetic fields alters human cardiac rhythm." Bioelectromagnetics **19**(2): 98-106.
[31] Sastre, A, Graham, C and Cook, MR. 2000. "Brain frequency magnetic fields alter cardiac autonomic control mechanisms." Clin Neurophysiol **111**(11): 1942-8.
[32] Stollery, BT. 1986. "Effects of 50 Hz electric currents on mood and verbal reasoning skills." Br J Ind Med **43**(5): 339-49.
[33] Stuchly, MA and Dawson, TW. 2002. "Human body exposure to power lines: relation of induced quantities to external magnetic fields." Health Phys **83**(3): 333-40.
[34] Thomas, AW, Drost, DJ and Prato, FS. 2001a. "Human subjects exposed to a specific pulsed (200 microT) magnetic field: effects on normal standing balance." Neurosci Lett **297**(2): 121-4.
[35] Thomas, AW, Drost, DJ and Prato, FS. 2001b. "Magnetic field exposure and behavioral monitoring system." Bioelectromagnetics **22**(6): 401-7.

Appendix 1

Postural tremor characteristics:

Amplitude: Root Mean Square (RMS) of position time series centered on their mean (highpass and lowpass filtered, between 2 and 25 Hz).

Drift: RMS of the low frequency component of the time series (below .01 Hz), quantifying slow movements of the finger.

Median frequency: Determines the value at which 50% of the power spectrum is below this frequency, and 50% is above. It is computed on the power spectrum between 2 and 25 Hz.

Frequency concentration: Quantifies the degree of organization of tremor by computing the width of the interval containing 68% of the power of the spectrum between 2 and 25 Hz.

Postural sway characteristics:

Mean Sway: Average distance between the geometric center of all recorded forces and each point visited by the Center of Pressure (COP) during a test.

Sway Velocity: Average velocity of the COP displacements.

Sway Area: Area of the smallest polygon including the entire trajectory of the COP.

ELECTROMAGNETIC FIELDS EFFECTS ON WITHDRAWAL SYNDROME SIGNS OF MORPHINE (WSSM)

A. SAFARI[1], H.JAFARI[2], H.JAHANI HASHEMI[3]

1. **Department of Occupational Health, Qazvin University of Medical Sciences.**
2. **Department of pharmacology, Qazvin University of Medical Sciences.**
3. **Department of Biostatics, Qazvin University of Medical Sciences.**

Abstract:

Background: Many studies have showed that electromagnetic field decreased WSSM.
Objectives: Effect of electromagnetic fields on WSSM investigated on rats.
Materials and methods: In this study 102 male rats with weight (225 ± 25) gr were classified in 17 groups (n = 6). They were addicted by morphine injection according to Pinelli Method. 16 groups of them exposed to electromagnetic fields with 25, 50, 75 and 100 Hz frequency and with magnetic field 0.5, 1.5, 2.5 and 3.5 G intensity. One group was chosen as control. WSSM jumping, climbing, rearing, diarrhea, weight loss, ptosis and yawning by naloxone injection in pretoon (5mg/kg) at all animals were investigated.
Findings: WSSM were obtained by counting the jumoing, wawing, alimbing, rearing and the ptosis, diarrhea were scrod from +1 to +4. Also weight losses were measured in all groups.
Results: This study showed that magnetic fields caused the significant decreased on waving, ptosis, weight loss and diarrhea at all of the exposure groups ($P<0.001$). Rearing and climbing decrease significantly in groups that exposed to electromagnetic fields and this fields with 25 Hz frequency and 0.5 G intensity have minimum and with 100 and 75 Hz frequency 3.5 G intensity have maximum effects on WSSM.
Keywords: Electromagnetic field, Withdrawal syndrome signs, Morphine, Rat.

Introduction:

About the role of electricity for curing addiction, some studies have been performed as bellow that about the laboratorial addicted animal has been used so that two metal electrodes have been touched around the two sides of its body, so that it would be done under special condition, and this action must be done daily for several times. This action is called Transcutanous Electrical Nerve Stimulation or TENS. And according to the Frequency and Voltage that is given two kinds of TENS can be done so that the low TENS and high TENS would have electrical changes in the epidictic system in this case this currency of addiction would be activated and then released. So if TENS be given to an addicted animal to morphine many of the signs in this field would be removed (1,2). In the recent years, the electromagnetic fields (EMF) in the medical sciences have many usages and they have indicated that the resulted energy from this field for curing the wound, reduction of all the kinds of pain can be effective, in a way that today the electromagnetic fields have found an important place as the alternative medicine and then they are mentioned like that.

Naturally the electromagnetic waves by high TENS would have some effects to the talent and focusing point and they would reduce the memory. Anyway in the animal tests it has been shown that the actions of electromagnetic fields in the addicted mice to morphine would cause the reduction of the signs of Syndrome especially for pain (3). The electromagnetic waves have some effects to the channels in the brain and also the environmental tissues would cause some changes in the physiological operation and the operation of these hormones, neurotransmitters, and some other medicine effects that strongly are related to the tissue of mind (4).

According to the last information of National Center for Complementary Alternative Medicine(NCCAM) National Institute of Health(NIH) the subsistent, electrical, magnetic, methods and electromagnetic fields and the electrical stimulations the nervous stimulation methods have been replaced(5). Some of the researchers about the role of electromagnetic in the addiction to morphine have provided some reports that would reduce the signs of dependency role,. They believe that the serotonin and triptophan surfaces and Hydroxide indol astic acid during the electromagnetism would be increased and following it some changes in some of the channels that are calcium in the brain (3). Some reports have been available that during electromagnetic therapy beta endorphins were increased. And this action will prevent the occurrence of syndrome in the body (3). It is possible that the increase of endorphin system and the increase of chemical materials in the brain be released (3). The last research of Magnet Therapy has caused the reduction of pain in the Post-Polio patients and this kind of therapy has little third effects (6). One of the usages of electromagnets is during the time of intensified pain. In the northern America the expenditures more than 10 to 15 thousands dollars for the reduction of pain for each person is used. 17 % of the population over 15 suffer from the pain that they get from the daily activities and in the United States of America about 93 millions dollars daily and more than 5 milliards dollars per year would be wasted for this purpose(7). Some evaluations would be done in the static and some channels that are similar to each other. Many researches about Pulsed Electromagnetic Filed have been done for reduction of pain and the provided results indicate the following effects:

1. Increase of pain field
2. Activation of anti-contagious system
3. Stimulation of producing aphetic points
4. Betterment of blood currency and the resulted effects of it including the increase of oxygen transferring and etc.
5. Improvement of blood thickness
6. Betterment of metabolism in the brain
7. Improvement of the movement of blood in body and brain

Pain is the important parameter that caused to become addicted patients. Some of researches showed that nerve systems affected by PEME curing (8).

Materials and methods

In this study 102 rat with 200-250g weight were divided in 17 group (n=6). That each group contains 6 muse. And these groups were Group one considers as the control group and the groups 2-17 as study groups that were expose to magnetic field as below detail.

Group2 (B= 0.5G, F = 100Hz), Group 3(B= 1.5G, F = 100Hz), group 4(B= 2.5G. F = 100Hz)
Group 5(B= 3.5G, F = 100Hz), Group 6 (B= 0.5G, F=75Hz), Group 7(B=1.5G.F= 75Hz)
Group 8(B=2.5G, F=75Hz), Group9 (B= 3.5G, F = 75Hz), Group 10 (B= 0.5G, F = 50Hz)
Group11 (B= 1.5G, F=50Hz), Group12 (B=2.5G, F = 50Hz), Group13 (B=3.5G, F = 50Hz)
Group14 (B= 0.5G, F = 25Hz), Group15 (B=1.5G, F=25Hz), Group16 (B=2.5G, F= 25Hz), Group 17 (B= 3.5G. F = 25Hz)

The animals were addicted according to Poinelli Method, and then animals of 16 groups as mention above condition were exposed to magnetic field for 30 minutes.

The syndrome signs of morphine stop were studied after Naloxone injection in pretoon. Jumping, Rearing, Climbing, yawning, diarrhea and ptosis, as syndrome signs were studied in this research after 2 hour naloxone injection. In this research we used the analyze variance, Dunnet and crouscal valis for data analyzing.

Findings

Seven signs for the stopping point of morphine in all the groups were considered. The most important sign was jumping, the number of Jumping in the groups 17, 16, 15, 12, 11 and 10 not only was not reduced but also ratio to other groups were more. In the groups 2, 6, 8, 13 and 14 the number of jumping was reduced but this reduction was not so much. In the groups 3, 4, 5, 7 and 9 the reduction of jumping was observed and it was so much in a way that in the groups 5 and 9 $P< 0.001$ was observed. In the groups 4^{th} and 7^{th} $P< 0.01$ and in the 3^{rd} group $P<0.05$ was seen. Except the group 14 and 15 which the reduction was so much. In the 9^{th} group more than other groups the reduction could be seen and it was as $p<0.001$. In all the groups the magnetic field except the group 4^{th} has an important

reduction which was P< 0.001. In the groups 9 and 12 the reduction was more than other groups. In the group 10, 14 and 15 there was not so much reduction but in the other 13 groups the reduction was so much. In way that other 14 groups had the weight reduction by p< 0.001. The little weight for reduction in the second and fourth groups is shown in the diagram 2. Generally it can be stated that the lesser response was in the groups 5^{th} and 9^{th} which had the best operation and the response would be provided.

Discussion

Present study showed that magnetic field with various intensity and frequency have affected on syndrome signs of morphine stop in rat magnetic field decrease jumping in exposure groups(3.4, 5 , 7 , 9) and also decries rearing in exposure groups (2-13 , 16 , 17) significantly (P<0.05).This study showed the magnetic field with various condition cause to reduce syndrome sings of morphine stop in rat such as climbing, yawning, Ptosis, diarrhea and weight significantly (P < 0.05).The magnetic field affected on the number of jumping depend on intensity, frequency and time exposure.

Morphine is an alkaline material and ionizes in body. The ionized form of morphine can't pass the Blood Brian Barrier (B.B.B), the magnetic field caused to ionizing the acidic and alkaline drug (9) for this reason the magnetic field can reduce the syndrome signs of morphine stop. The result of this study showed that the magnetic field with high frequency and high intensity reduce the syndrome signs of morphine in rat. This reduction can explain by this reason.

1- Increase the polarity of Naloxone
2- Alteration of receptors instruction
3- Reduction of morphine in brain cells

This study showed that rearing and climbing reduced significant in exposed groups (P<0.05).We think that these reduction is because of increase the induction and releasing the androgen peptides opiate and alteration of nerve mediator induction and releasing such as dopamine, glutamate, serotonin, Spartant.This nerve mediator affected to jumping, another study showed that Spartant system can increase the jumping in rat(10).Also other researcher showed that the electromagnetic field caused to induction and releasing the acetylcholine in animals cells(11).In this study we showed that magnetic field didn't have any effect on weight loss and this finding accompany with our result of previous study(1).The magnetic field with high frequency and high intensity decrease diarrhea but acetylcholine and piocarpin increase diarrhea(12). By considering the results of this study, we obtained that magnetic field reduce the cholinergic system and acetylcholine in brain cells and also other reports indicated dopamine has affected on climbing and yawning (13,14,15). According to results of others study we can guess the electromagnetic field increase serotonin and dinorphine and decrease dopamine and acetylcholine.

Reference

1. Jafari H., Vaez M. M., Gharebaghi R., Consideration the level of sufficiency of electrical stimulations as (IENS) and reasonable stress of (ICWS) against with the dependency to morphine in the desert mice and the comparison of these two methods. Daneshaver (Shahed collage) Vol.29, 2000, pp: 2-10.
2. Jafari H., Vaez M. M., Gharebaghi R., Study for the effect of TENS and ICWS in the reduction of syndrome signs of morphine in Rat, scientific magazine of medical sciences university of QazvinVol. 18, 2001, pp: 12- 16.
3. http:// www. Therrionresearch.com/learing-center-articles.html.(Drug addiction and brain. By Paul Tyler).
4. Albert E. Desantis M Microwaves alter nervous system structure? In: Tyler p. biological effect of non ionizing radiation. Proceeding of conferences. Ann New York Acad. Sci, 1975, 247: 87-108.
5. The first congress of paramedical therapy and traditional therapy from Islamic Azad university unit Qom 2001 and the introduction of replacement therapy.
6. Www. Therrionresearch.com/learing-center-articles.html. (Magnet Therapy Reduces pain in Post-polio Patients. By Carlos Vallbona).
7. Pawlo W. MD, MSC. Pain Management with Pulsed electromagnetic field. 2002, Black well Science, PP: 175-182.
8. Http//www. Rush star. Com/ health care/ magnetic therapy. Rush star magnetic therapeutic kit rush star health care.
9. Edward H. Microwave: Industrial, scientific and medical application (part IV- Biological affects and Medical application), pp: 445-450.
10. Nadia M. Pharmacology & Behavior Vol. 20. pp: 631-633.

11. Kalantari, Z., Jafari H., Riyahi, A., Using of electromagnet as the replacing therapy for using the medicine for addicted people. The collection of province conference for addiction by Islamic Azad University Unit Astara. pp. 227-229.
12. Clark, Barter, Janson, Goths Medical pharmacology.1992, Vol. (1):112-116.
13. Muore Na. Axton M. Production of climbing behavior in mice requires both D, Fe D2 receptors activation. Psychopharmacology. 94: 263-66.
14. Ramanda k. Tanaka M. Involvement of sepatel and stratal dopamine D2 receptors in yawning rats. J. Psychopharmacology. 1986, 90: 9-13.
15. Zarrindas Mr. Bromocriptine induced climbing behavior: possible D1 & D2 receptors J. psychopharmacology. 1990, 100: 275-280.

LEGISLATIVE NEEDS FOR COMPUTATIONAL EMF EXPOSURE ASSESSMENT THE EUROPEAN DIRECTIVE 2004/40/CE

PAOLO ROSSI, ROSARIA FALSAPERLA

National Institute of Occupational Safety and Prevention (ISPESL) – Rome – Italy
paolo.rossi@ispesl.it, rosaria.falsaperla@ispesl.it

Abstract

The European directive 2004/40/CE on the minimum health and safety requirements regarding the exposure of workers to the risks arising from electromagnetic fields, based on ICNIRP guidelines for occupational exposure, is presented and commented. The resulting needs for computational assessment of workers' exposure in terms of dosimetric quantities is considered and discussed.

I. The European Directive 2004/40/CE

The directive 2004/40/CE [1], on the minimum health and safety requirements regarding the exposure of workers to the risks arising from electromagnetic fields, has been issued in the European Official Journal on May 25, 2004, as the 18th individual directive within the meaning of framework directive on health and safety at work (391/89/EEC). The EMF directive follows the publication of directives on other physical agents, namely 2002/44/CE on vibration and 2003/10/CE on noise. The aim of the directive is the protection from established adverse effects caused by induced currents and by energy absorption, as well as by contact currents. Suggested long-term effects are not addressed, due to the lack of conclusive scientific evidence. The directive lays down minimum requirements giving EU member states the option of maintaining or adopting more favourable provisions for the protection of workers. Like in the previous directives on physical agents, the framework is based on the definition of "exposure limit values" and "action values". The exposure limit values can never be exceeded, whereas the action values are levels at which the employer must undertake technical or organizational measures to reduce exposure. The numerical definition of such values is based, respectively, on basic restrictions (dosimetric quantities) and reference levels (unperturbed fields) established for the workers in the relevant guidelines of the International Commission on Non-Ionizing Radiation Protection (ICNIRP) [2]. The directive claims the employer to give particular attention to any indirect effects, such as interference with medical devices like cardiac pacemakers, and adapt risk assessment and mitigation measures for workers at particular risk. Member states have to transpose the directive into national law within April 2008.

Directive 2004/40 CE claims the employer to a specific risk assessment, and to verify the respect of limits of exposure that are expressed in terms of dosimetric quantities, induction of current and Specific Absorption Rate (SAR). Such evaluation is achievable only by means of simulation computational methods, and in fact the directive often refers to calculations. Moreover, the directive shall be taken into account in the definition of product standards for special families of equipment emitting EMFs, to be used at the workplace. Compliance verification of the basic limits by calculations calls for the use of proper numerical methods able to solve Maxwell's equations, in combination with high resolution models of worker's body, and satisfactory representation of sources and workplace environment.

II. Computational exposure assessment for workers – Critical points

As information technology, numerical methods are increasing and developing very rapidly. Application to more and more complex problems is expectable, like multiple sources and complex environments, but the reliability of results critically depends on the representation of the real problem; any obtainable result refers in fact to the representation scenario and not to the actual problem, otherwise than *in situ* field measurements.

Many of the available numerical methods, that are listed in [3], are implemented on commercial SW packages mostly developed by research teams, provided with digital human body models and CAD tools able to realistically represent sources and environment. A lot of scientific work and applications have been developed, mostly addressed to relatively simply exposure evaluations, like in the case of mobile phones (head) or base

stations and broadcasting (whole body), and specific standards for calculations have been issued by CENELEC and IEC, but extensive application to more complex occupational exposures has not been carried out yet, due to lower public and authority concern.

All simulation packages and components are affected by limitations, advantages and disadvantages, so that the proper choice in a given situation may not be easy. The duration of calculation is one aspect to be considered in relation with the efficiency of the representation. Concerning human body models, the knowledge of dielectric properties of human tissues is still affected by gaps especially at low and intermediate frequencies range, and the available models only refer to very simple postures (erect), even if in occupational exposures the posture of the workers may be very complex. Methods have been introduced for scaling and obtain different body postures but results need to be carefully validated in a wide number of conditions.

III. Needs for computational exposure assessment - Discussion

The provisions from Directive 2004/40/CE pose the need to answer to some basic questions, and identify a logical pathway in order to manage the dosimetry problem. A basic question is to address when numerical dosimetry must be invoked in EMF occupational risk assessment. The first case is a condition where reference/action levels are exceeded, but basic/exposure limits are probably not. Such condition may occur for instance in the case of RF fields strictly confined close to the source, similarly to head exposure from a mobile phone. A second case, to be carefully considered, deals with compliance with local basic restrictions. Guidelines of ICINIRP [2] clearly states that: "*the reference levels are intended to be spatially averaged values over the entire body of the exposed individual, but with the important proviso that the basic restrictions on localized exposure are not exceeded"*. In other words, reference/action levels are able to guarantee compliance with body averaged SAR but don't assure compliance with restrictions on local SAR, which is however crucial when the source is very close to the worker and directly coupled to the body. In the frequency range 10 MHz - 110 MHz, where the electromagnetic energy is mostly absorbed inside legs and limbs, ICNIRP Guidelines [2] and Directive 2004/40/CE provide a reference/action level for feet current that is helpful in order to verify compliance with local SAR limits in the limbs. On the opposite hand, in the "hot spot" frequency range (400 MHz - 3 GHz) localized peaks of energy absorption may concern internal organs, and in such condition the assessment of local SAR by means of numerical dosimetry should be recommended even when the exposure levels (as spatially averaged values over the body) approach the reference/action levels.

Another critical point to be addressed is the accuracy, or approximation, of the representation of the exposure problem. This point needs consideration on sources characteristics, human model, but the surrounding work-place must be taken into account too, especially in the case of presence of metal objects or structures. The choice of proper resolution of the human model is crucial again; too low resolution could lead to unreliable results, but too high one could overload computational time and HW resources.

As a matter of fact occupational exposure assessments based on numerical methods are very complicated and require high level education, to-date available only in research centres or institutes. The possibility of practical use of numerical modeling by the employers for real cases in working environment seems to be very limited, in contrast to the relatively effective use of such technique for large scale manufacturing in standardized condition, bearing in mind however that occupational exposure patterns are much more complicated than general public ones (e.g. SAR in the head with mobile phones), and standardization bodies should carefully consider it.

Simplified models could be useful for performing rough assessment on occupational EMF sources and workers' exposure levels. Worst-case models could be used as intermediate step between field measurements and refined dosimetry. To such aim, extensive comparisons of standard case-studies should be carried out, analyzing the performance of simplified models compared to more sophisticated ones.

References

[1] Directive 2004/40/EC of the European Parliament and of the Council of 29 April 2004 on the minimum health and safety requirements regarding the exposure of workers to the risks arising from physical agents (electromagnetic fields) (18th individual Directive within the meaning of Article 16(1) of Directive 89/391/EEC), O.J. L-184 of 24 May 2004.

[2] INTERNATIONAL COMMISSION ON NON-IONIZING RADIATION PROTECTION (ICNIRP). Guidelines for Limiting Exposure to Time-Varying Electric, Magnetic, and Electromagnetic Fields (Up to 300 GHz). Health Physics 1998; 74: 494-522..

[3] EN 50392: 2004-01: Generic standard to demonstrate the compliance of electronic and electrical apparatus with the basis restrictions related to human exposure to electromagnetic fields (0 Hz – 300 GHz), CENELEC Standard.

EXISTING ELF, IF AND HF ELECTRICAL APPLIANCES AND TECHNOLOGIES PRODUCING HIGH EMF EXPOSURE

MONICA SANDSTRÖM, JONNA WILÉN, KJELL HANSSON MILD

NATIONAL INSTITUTE FOR WORKING LIFE, UMEÅ, SWEDEN

The new EU directive, 2004/40/EU, issued on occupational exposure to electromagnetic fields (EMF), calls for occupational risk assessment and implementation in the EU states national occupational safety and health regulations before April 2008. Commonly, workers are exposed to EMF with a mixture of different frequencies. In most cases the exposure levels are low and not in conflict with the new directive. However, some work situations or occupations need special attention due to risk of high exposure. Following the protocol in the directive, workers exposure to EMFs should be estimated, measured or calculated depending on type of workplace and possible risk of over exposure. One of the assigned issues in the EMF-NET MT2 group is to identify work situations that might be in conflict with the new EU directive. In this review, a number of work situations where there is a risk of high EMF levels will be presented and a few examples are listed below.

At electrolytic processes static magnetic field levels at the operator's location can be about 8-15 mT with an AC rectification's component about 30 %. The fundamental frequency is usually 50-300 Hz.

Magnetic resonance imaging systems use magnets typically from 0.05 T to about 3 T. In addition to static magnetic fields, RF fields (10-100 MHz) and rapidly changing gradient magnetic fields occur in pulse sequences within MRI equipment. The time derivatives of gradient fields (dB/dt) affecting patients vary typically from 1-3 T/s, and exposure of staff to EMF can be significant inside treatment rooms surrounding MRI equipment. The maximum exposure level is about 1 T in front of the magnet, and nurses/technicians staying with patients can be exposed to magnetic flux densities up to 0.2 T, approaching the protection guideline. In the case of performing professional activities very close or inside the magnet's tube, workers can be exposed to higher fields (up to 1-2 T), e.g. during adjutancy or plugging in RF cables of treatment coils, or device cleaning.

Transcranial magnetic stimulation or repetitive transcranial magnetic stimulation (TMS/rTMS) is currently being used in treatments of the central nervous system diseases, for instance, depressive states. During the treatment the therapeutic staff is exposed to a pulsed 100 kHz magnetic field that might exceed the reference values in the EU directive. The time derivative, in some of the measured tests, was in the order of kT/s!

Operators of induction furnaces and heaters are highly exposed to magnetic fields. At a distance of 1 meter from a 1-10 kHz heating equipment, flux densities typically range from 0.03 to 0.5 mT, and may reach 5 mT at 10 cm. Measurements of devices operating at 50 Hz, have shown that at a distance of 20 cm the flux density of the field might exceed 5 mT. At a distance of several meters 0.1 mT have been measured. The reference values in the EU directive (30.7 µT for 1-10 kHz and 500 µT for 50 Hz) are exceeded during work procedures close to furnaces.

Welders are one of the occupations that are highly exposed to EMF and thereby in conflict with the new EU directive. Arc welding uses high electric currents up to several hundreds of Amperes. The current, provided by the welding power source, flow through the torch-cable and torch to the welding arc, and into the workpiece and back to the power source via the ground cable. This provides a source for magnetic field to which the worker is exposed during the welding process as the cable can touch the welder or even be wrapped around the shoulder of the welder. Magnetic flux densities are about 1 mT at the surface of the welding cable and power supply, exposing the welders to strong ELF fields. (ref)

Glue dryers in the wood industry and plastic welders are using RF energi by applying a strong RF current between metal electrodes. The output powers range from 1 to 200 kW at the ISMfrequencies of 13.56, 27.12 or 40.68 MHz. Most plastic sealers are operated manually and require the presence of the operator close to the RF electrodes. In some applications, pieces of plastic materials to be heated must be held by hand, so that the operator's hands will be highly exposed to RF fields. Electric field strengths range in areas of operators typically from 1 to 300 V/m, and magnetic fields from 0.1 to 20 A/m, respectively.

Broadcast stations are using high RF energy intentionally radiated into the air. Typical maximum radio and TV transmitting powers fed to the antennas are about 500 kW for LF, MF and HF antennas and 10-50 kW for VHF and UHF antennas. Since the antennas are mounted near the top of a mast at the height of over 200 m, the exposure levels at the ground level are very low, but the occupational exposure can, however, be high during maintenance and installing work inside a mast, and special precautionary actions has to be taken.

A mobile phone base station emit RF fields in the range 450-2200 MHz. With a maximal output power of let say 50 W the EU directive might be exceed within a couple of dm in front of the antenna. In other positions or at a longer distance from the antenna there is no conflict with the directive.

References

Figueroa Karlström E., R. Lundström, O. Stensson, K. Hansson Mild. *Therapeutic staff exposure to magnetic field pulses during TMS/rTMS treatments*. Bioelectromagnetics, 2006, 27: 156-158.

International Journal of Occupational Safety and Ergonomics (JOSE) 2006, 12;2. *Special issue electromagnetic fields in the workplace*. http://www.ciop.pl/jose

Sandström M., K. Hansson Mild, O. Stensson. *Elektromagnetic fields associated with Arc welding - examples of measurements for compliance.* Workshop in welding, Mol, Belgium, 6 April 2006. http://www.vito.be/english/environment/pdf/welding_workshop.pdf

Wilén J., R. Hörnsten, M. Sandström, P. Bjerle, U. Wiklund, O. Stensson, E. Lyskov, and K. Hansson Mild, *Electromagnetic field exposure and health among RF plastic sealer operators.* Bioelectromagnetics, 2004. **25**(1): p. 5-15.

This project was partially funded by the Coordination Action EMF-NET "Effects of the Exposure to Electromagnetic Fields: from Science to Public Health and Safer Workplace" (European Commission FP6 Coordination Action, Thematic Priority 8, Policy support and anticipating scientific and technological needs, Contract N° SSPE-CT-2004-502173, 2004-2008)

THE FUNDAMENTALS OF OCCUPATIONAL EXPOSURE ASSESSMENT IN REAL LOW AND INTERMEDIATE FREQUENCY EMF ENVIRONMENT

JOLANTA KARPOWICZ, KRZYSZTOF GRYZ

CENTRAL INSTITUTE FOR LABOUR PROTECTION – NATIONAL RESEARCH INSTITUTE, LABORATORY OF ELECTROMAGNETIC HAZARDS WARSZAWA, POLAND, e-mail: jokar@ciop.pl

Abstract

The presentation is based on analysis of the fundamental problems defined for the use of numerical calculations for workers exposure assessment in real occupational situations. The examples of data from workplaces in the vicinity of LF or IF sources will be presented, focusing: space distribution of EMF, complex characteristics of the frequency content, workers activities/moving in the workplace, field impedance, etc., as well as discussion concerning situations when the use of calculations is required.

Keywords: EMF exposure, exposure assessment, numerical calculations, low frequency, intermediate frequency

1. Introduction

Electromagnetic field's (EMF's) exposure assessment adequate to the real exposure level is the crucial step towards appropriate risk assessment for occupational safety and health (OSH) engineering, epidemiological studies of EMF-exposed groups, environmental monitoring. The highest requirements concerning detailed EMF exposure assessment come from the legislations concerning mandatory control of occupational or environmental EMF exposure, e.g. European Directive on workers EMF exposure limitation.

The provisions of the Directive 2004/40/EC permit the employer to use exposure level (external measures of exposure like electric and magnetic field strength, *E* and *H*) or dosimetric quantities (internal measures of exposure results like induced current, *J*, and Specific Absorption Rate, *SAR*) for the mandatory risk assessment. In the case of EMF of low and intermediate frequencies (LF and IF) the basic internal measure used for exposure assessment is induced current density in head and torso. IEEE standards offer also the use of *E* field induced in exposed tissues. Both parameters can be used till low MHz frequencies. The use of internal measures require numerical calculations and detailed analysis and interpretation of data obtained from modeling.

EMF from LF and IF range, affecting workers are usually so-called near fields. The impedance of such fields (the ratio of electric fields strength to magnetic field strength) is defined by the technical properties of the EMF-source-worker-body system. Electric voltages and currents in the electric device, producing EMF play important role, but in many cases also the direct coupling between workers body and EMF source modify the exposure conditions. The sources of high level of EMF exposure to time-varying LF or IF fields are basically: high voltages power distribution systems, welding devices, industrial induction heating devices, electro surgery devices. In consequences the most important external measure of exposure is magnetic field strength (or magnetic flux density) assessed following the frequency-dependent exposure limitation in the case of very huge number of welding and induction heating devices. Significant exposure to electric component can be found in practice in the vicinity of high voltage electricity distribution systems. The most complicated situation can be found, when both components (*E* and *H*) should be consider, especially when the field impedance can varying significantly during the application, as in the case of electro surgery use.

For the practical EMF exposure assessment at workplace, first of all it should be discussed when it is acceptable to make the EMF exposure assessment by spot measurements with a broad-band RMS meter (i.e. the most convenient and less expensive method). For the other situations, it should be decided the use of more complicated (and more expensive) exposure assessment method: more detailed measurements or dosimetrical calculations.

2. Method

Professional activities of authors is focused on the detailed analysis of occupational EMF exposure characteristics in various enterprises and application of EMF measurements and/or numerical calculations

technique for workers exposure assessment. The presentation is based on analysis of the fundamental problems defined for the use of numerical calculations for workers exposure assessment in real occupational situations.

3. Results

Electromagnetic field (EMF) in the workplace has often very specific characteristics in comparison with the fields from general environment. In working conditions not only the locations of the EMF source and worker's body, but also the geometry of the source, frequency and level of produced EMF in its vicinity, can change significantly, exposure level can be high, even exceeding international safety guidelines.

The analysis of detailed data obtained from various work place and experience with the numerical calculations modeling realistic exposure scenarios for the assessment of the exposure following the internal measures' limitations have shown a number of practical problems, identified for the worker's exposure assessment.

In the most of cases of high level exposure of workers to LF or IF EMF, their professional activities need hand operation of the EMF sources. For the exposure assessment of such cases the modeling of realistic posture of worker's body and possible simplifications of it to reduce the complication and costs of exposure assessment process is of high priority. Important question is on the exposure assessment of hands, especially while hand-operating of EMF sources of high level. The use of calculations for exposure assessment in LF and IF band is more difficult, that RF (with huge experience obtained from mobile phones research) because of:

- the lack of models, transferable from one software to other one, representing realistic EMF occupational sources, already verified by reference data from workplaces and taken as standardized models

- the lack of well verified data on electrical properties of various elements of workplace, as shoes, floor cover, furniture's, etc.

- relatively small number of the scientific data concerning human body models, electrical properties of tissues, numerical calculations procedures, etc. for the assessment of IF fields.

For the wider use of numerical calculations for the assessment of workers EMF exposure, it is of high priority to obtained well verified scientific data concerning

- the possibility to use simplified numerical models of working places and EMF exposure conditions

- the uncertainty of exposure assessment for checking the compliance with the Directive

- the role of frequency components within the exposure assessment procedures

- the assessment of pulsed fields, especially in the case of hand-operated devices, when the repetition time of pulses is not fixed.

The practical use of numerical calculations for the EMF exposure assessment is also problematic because it was not defined when various software packages can be use, and non of currently available software is specialized for workers exposure. Additionally, a few commercial human body models are applicable for selected specialized software only. Separate problem is the calculations of induced and contacts currents, which can be also measured.

4. Conclusion

The use of internal measures of exposure results for risk evaluation is possible only by simulation computational methods, with the use of adequate representation of the workplace environment and worker’s body models. Such calculations for particular exposure situations require highly skilled professionals and specialized software. The modeling of real exposure scenario, validation of calculations result and interpretation of obtained data is usually very time-consuming and currently achievable by research centers only. These are reasons why, the possibility of practical use of numerical modeling by the particular employers, especially from SMEs is very limited in contrast to the relatively effective use of such technique for large series manufacturing (e.g. common use electrical devices, like mobile phones handsets). In this respect, the question arises if more simple models are powerful enough for performing roughly assessment of the occupational EMF sources and workers exposure level, while every day's occupational safety and health practice.

Acknowledgment
This review has been prepared from results obtained from the investigations supported by the State Committee for Scientific Research and Ministry of Economy, Labour and Social Policy of Poland (individual grants focused on occupational EMF exposure investigations).

ISSUES IN ACTUAL RF ENVIRONMENT OCCUPATIONAL EXPOSURE ASSESSMENT

DINA SIMUNIC

UNIVERSITY OF ZAGREB, FACULTY OF ELECTRICAL ENGINEERING AND COMPUTING, UNSKA 3, HR-10000 ZAGREB, CROATIA

Introduction

Exposure assessment of electromagnetic fields is a topic that gets more importance every day, especially related to Directive 2004/40/EC and EC Recommendation 1999/519. The complexity of interaction between electromagnetic fields and human body makes any kind of analysis (theoretical-analytical, numerical, experimental) difficult. In an actual multi-source radiofrequency environment situation is even worse, due to a consequent complex distribution of electromagnetic fields.

Method

Issues related to actual RF environment, specifically related to multi-frequency, multi-source environment require sound analysis. The number of issues is even bigger in the indoor environment, where a building structure influences the electromagnetic field distribution. In such environment a number of reflections exist, which forms a complex environment of standing waves. Thus, it is necessary to perform a detailed analysis of the field distribution.

The field distribution is the first step in performing exposimetry analysis, as well as dosimetry analysis.

Results

The results of exposimetry and dosimetry analysis indicate the issues addressed by the process, especially related to uncertainty of the analysis. The concerned sources are wireless communications devices, i.e., mobile telephony, Bluetooth and wireless LAN devices, which are located in the indoor and outdoor space. The devices in the outdoor space are treated by analytical methods, whereas in the indoor space, it is impossible to perform even exposimetry analysis without a numerical tool.

Conclusion

The complete dosimetric and exposimetric analysis of the human body in electromagnetic fields can be performed only by a numerical analysis. The needs and necessary requirements of the analysis for a full application for existing legislative acts, especially for Directive, are related to the complex electromagnetic environment which makes albeit difficult dosimetric analysis more complex.

NUMERICAL CODE VALIDATION WITH EMPIRICAL DATA

Dr. PETER GAJŠEK

INSTITUTE OF NON-IONIZING RADIATION, LJUBLJANA, SLOVENIA

Abstract

The development of mathematical dosimetry modeling techniques and powerful computer hardware has resulted in dosimetry modeling as a principle tool in determining EMF exposure. The results of any anatomical model are questionable if the model has not been validated with empirical data obtained from *in vivo* or *in vitro* experiments. Validation of the theoretical with empirical results and the subsequent refining of a model are essential in order to earn the credibility when using these models to establish or revise exposure standards. The increasing acceptance and use of FDTD modeling within the EMF community make it imperative that predictions be compared, and validated against experimental data. With the development of the Finite-Difference Time-Domain (FDTD) code, it is possible to predict whole body and localized SAR values under a wide range of exposure conditions in phantoms and laboratory animals, as well as humans.

In the past, FDTD predictions have been validated mainly for very simplistic geometric models. For far-field sources, simulation results have been compared with analytical results for square [Umashakar and Taflove, 1982], cylinders [Furse et al., 1990], spheres [Gandhi et al., 1992; Gandhi et al., 1999], and plates [Taflove et al., 1985]. Calculations of currents induced in a standing human have compared well with empirical data [Furse et al., 1997]. For near-field sources, simulation results have been compared with analytical, measured or method of moment results for dipole antennas in front of layered half-spaces, layered boxes and homogeneous spheres [Furse and Gandhi, 1998]. In addition, the FDTD method has been validated for near-field testing of realistic cellular telephones next to the human head [Dimbylow and Mann, 1994; Gandhi and Chen, 1995]. Agreement between FDTD code and experimental results (e.g. E-field measurements on simplistic canonical geometries such as box or sphere filled with tissue equivalent material) was excellent and generally within ±20 % (±1 dB) [Gandhi et al., 1999]. However, little direct comparison of empirical data obtained by actual type of organism with SAR values predicted by FDTD modeling exists in the published literature [Walters et al., 2000; Mason et al., 2000].

In this paper, we report on the use of the convergent technologies to validate the use of computational codes to predict SAR values in both, simplistic models (spheres) and actual biological organisms. Since experimental validation requires the implantation of thermal or e-field probes, it is not feasible to perform such studies in human subjects, therefore laboratory animals and phantoms were used. The brain of the rat offers an ideal organ for comparison, due to the reliability of stereotaxic probe placement, as well as the ability to easily confirm probe placements in tissue sections following experimentation [Walters et al., 1998].

Our predicted SAR values obtained by computer models based on FDTD code of spheres and Sprague-Dawley rat were compared to temperature measurements made with implanted probes and infrared thermography model [Gajsek et al., 2001].

The SAR values were determined thermally. Irradiation was performed at a high exposure level (above 700 mW/cm^2) and short exposure duration (30 seconds) to produce a measurable linear temperature rise. This was done to allow accurate quantification of the rate of temperature rise in the absence of any significant thermoregulatory effects. Good correlation between the predicted and empirical phantom and animal data would provide increased confidence in the results predicted by the man model [Mason et al., 2000].

REFERENCES:

Dimbylow PJ, and Mann SM (1994): SAR Calculations in an Anatomically Based Realistic Model of the Head for Mobile Communication Transceivers at 900 MHz and 1.8 GHz," Physics in Medicine and Biology, vol. 39, 1537-1553.

Furse CM, and Gandhi OP (1998): Calculation of Electric Fields and Currents Induced in a Milli mete r-Resolution Human Model at 60 Hz Using the FDTD Method, Bidelectromagnetics, Vol. 19, 293-299.

Furse CM, Mathur SP, and Gandhi OP (1990): Improvements in the FiniteDifference Time-Domain Method for Calculating the Radar Cross Section of a Perfectly Conducting Target, IEEE Transactions on Microwave Theory and Techniques, Vol. 38, no. 7, 919-927.

Furse CM, Yu SQ, Gandhi OP (1997): Improvements in the FDTD method for near field bioelectromagnetic simulations, Microwave and Optical Technology letters, Vol.16, 341-345.

Gajšek P, Ziriax JM, Hurt WD, Walters TJ, and Mason PA (2001): Predicted SAR in Sprague-Dawley rat as a function of permittivity values, Bioelectromagnetics 24, 1-17.

Gandhi OP, and Chen JY (1992): Numerical Dosimetry at Power-Line Frequencies using Anatomically Based Models, Bioelectromagnetics Supplement, 1, 43-60.

Gandhi OP, and Chen JY (1995): Electromagnetic Absorption in the Human Head from Experimental 6 GHz Hand-Held Transceivers, IEEE Transactions on Electromagnetic Compatibility, vol. EMC-37, 547-558.

Gandhi OP, Lazzi G, Tinniswood A, and Yu Q, (1999): Comparison of numerical and experimental Methods for determination of SAR and Radiation patterns of Handheld Wireless Telephones, Bioelectromagnetics, No. 20, 93-101.

Mason PA, Hurt WD, Walters TJ, D'Andrea JA, Gajšek P, Ryan KL, Nelson PA, and Ziriax JA (2000): Effects of frequency, permittivity, and voxel size on predicted specific absorption rate values in biological tissue during electromagnetic field exposure, IEEE Microw. Theory & Techn, Vol.48, No 11, 2050-2057.

Taflove A., Umashankar KR, and Jurgens TG (1985): Validation of FD-TD Modeling of the Radar Cross Section of Three-Dimensional Structures Spanning up to Nine Wavelengths, IEEE Transactions on Antennas and Propagation, pp. 662-666, June 1985.

Umashankar KR, and Taflove A (1982): A Novel Method to Analyze Electromagnetic Scattering of Complex Objects, IEEE Transactions on Electromagnetic Compatibility, vol. EMC-24, pp. 397-405.

Walters TJ, Blick DW, Johnson LR, Adair ER, and Foster KR (2000): Heating and pain sensation produced in human skin by millimeter waves. Health Phys., Vol. 78, No.3, 259-267.

Walters TJ, Ryan KL, Belcher JC, Doyle JM, Tehrany MR, and Mason PA (1998): Regional brain heating during microwave exposure (2.06 GHz), warm-water immersion, environmental heating and exercise, Bioelectromagnetics 19, 341-353.

SIMULATION OF ELECTROMAGNETIC FIELDS INCLUDING BIOLOGICAL MODELS WITH CST STUDIO SUITE

MONIKA BALK

CST – COMPUTER SIMULATION TECHNOLOGY

In our modern society technology and simultaneously electronics play an important role. It is almost impossible to avoid electromagnetic field exposure. When evaluation the human body field exposure the always occurring problem is: How to measure it. Most of the time it can't be measure in vivo. Thus, the interaction of electromagnetic fields and biological tissues is a topic of intense research. Therefore, 3D numerical EM simulations have been established as tool to analyse the effect of the electromagnetic fields caused by the environment on human beings. This effect is usually described by the Specific Absorption Rate (SAR).

The software package CST STUDIO SUITE™ is a specialised tool for evaluating 3D electromagnetic fields, which is based on the Finite Integration Technique (FIT). The software package offers the possibility to import data obtained by medical imaging. With this voxel import the characteristics of the biological tissues are translated in material information used by the simulation software to evaluate the electric and magnetic fields. Based on electric and magnetic field, the specific absorption rate can be calculated using a mass averaging approach compliant to the IEEE C95.3 standard. Alternatively, own procedures are offered that show improved consistency for structure rotations.

In this talk first of all the Finite Integration Technique fundamentals are described. Furthermore the simulation work flow within the software package is shown. Finally several examples concerning SAR calculations are shown

Dr. Monika Balk, Application Engineer

CST – Computer Simulation Technology

Bad Nauheimer Str. 19, 64289 Darmstadt, Germany

Tel: +49-6151-7303-0, Fax +49-6151-7303-100

Email: monika.balk@cst.com

BIOLOGICAL EFFECTS OF EXTREMELY LOW FREQUENCY ELECTRIC AND MAGNETIC FIELDS

AHMAD YOONESSI, ARASH MIRHASHEMI

KHAJE NASIR TOOSI UNIVERSITY OF TECHNOLOGY, TEHRAN,IRAN
AMIRKABIR UNIVERSITY OF TECHNOLOGY,TEHRAN,IRAN

Abstract- There has been numerous evidence that exposure to extremely low frequency magnetic and electric fields can produce biological effects. Many of these effects are not clearly understood so far. Most of these researches emphasize on power frequency (50 or 60Hz) and the biological effects at these frequencies. The following paper attempts to describe the current researches toward emphasizing the effects in the Extremely Low Frequency (ELF) range. Lab experiments regarding biological effects of ELF fields have been shown in various organs and the results have been discussed. There is presently no clear and convincing evidence from animal or cellular studies that demonstrates harmful effects of EMF. There are, however, some studies that are suggestive of potential health impacts. From the perspective of laboratory studies, this presentation will discuss biological responses to extremely low frequency electric and magnetic field exposures.

Introduction

With the ongoing advancement in electrical and electronic devices the odds of exposure to electrical and magnetic fields have raised dramatically. More and more people are exposed to electrical and magnetic fields daily. Therefore the need to understanding the effect that these fields have on the human body is significantly important. One of the areas that are often neglected is in the Extremely low Frequency Range (up to 300Hz). At the frequencies this low, the wavelength in air is very long (6000km at 50 Hz and 5000Km at 60Hz) The only area within this range that is on the main focus is the power frequency (50Hz or 60Hz) Since it is the widely found frequency in the environment. This paper tries to summarize the effect on the ELF range without focusing on any special frequency.

Biological effects may sometimes lead to adverse health effects. Biological effect is when exposure to an electromagnetic field produces a noticeable or detectable change in a biological system. An adverse health effect occurs when the biological effect is outside the normal range for the body to compensate and thus leads to some detrimental health conditions. [1], [9], [13]

The primary mechanism of interaction between elf fields and biological system is in the induction of electrical charge and current.

ELF electric fields exist whenever a voltage is present regardless of the current flowing. Almost none of the electric field penetrates into the human body. On the other hand ELF magnetic fields exist whenever a current is flowing. They can easily penetrate into the human body. [1], [9]

Circulatory System

Heart

There have been some studies suggesting that exposure to ELF electric and magnetic fields decreases heart rate [3]. While this studies report this incident, they often characterize it as temporary and within the normal physiological variation. The boundary for this effect is reported as low as 0.1μA/cm2.[3] There have been reports of effect on the blood pressure, Heart rate and electrocardiograph waveform but these studies are limited by uncertainties regarding exposure duration and subsequent control group.[3], [4], [5].

Endocrine system

Melatonin

Some studies suggest that exposure to ELF fields may suppress secretion of melatonin, a hormone related to human day-night rhythm [1], [6]. It has been suggested that melatonin is effective in the prevention of breast cancer and therefore suppressing it will result in an increased incident of breast cancer. Although there is some evidence in laboratory animals, human volunteer studies have not confirmed this report. [1], [7], [8]

Musculoskeletal System
Bone growth and fracture repair
Electrical and magnetic stimulation have been known to have effect on bone fracture repair since 1970. The mechanism which enables these fields to increase new bone formation is still not known. Effect of pulsed EMF on fracture healing have been proven in numerous clinical studies on human and animal subjects.[10],[11] However the mechanism that this interaction takes place is not clearly known so far. Some studies suggest that EMF can increase the secretion of growth hormone IGF-I and IGF-II and therefore increase the healing rate. [12], [14], [15]

Nervous System
Behavior
Many studies have been done to demonstrate the effect of elf magnetic and electric field on human and animal behavior Since nervous system plays a major role in function of all the body and since many of the nervous signals communicate in a form of electrical signal it can be predicted that the elf could alter the behavior.
There has been numerous studies showing the effect of E field on animals such as rats, mice, pigs and birds.[16] Most animals try to avoid exposure to E fields over 50-75kV/m. The exposure to B field shows little evidence on animal behavior in general. [13], [14]
In humans a phenomena known as phosphene is reported in the B fields as low as 20 mT. [13], [19]

Reproductive System
It is known that the developing system is more prone to various environmental hazards. Therefore it is assumed that a developing system is more sensitive in response to electrical and magnetic fields. Studies have been done mostly on animals such as chicken, rats and rabbits. Few studies have been done on human growing organisms such as hair follicles. [13], [16], [17]

Immune System
Cancer and Mutation
The EMF effects on promoting cancer have been studied more than anything else. However few life long studies have been reported. There have been some studies on the effect of 50 or 60 Hz B field on the male and female rats which showed that although the B field can increase the carcinogenic activity it is not effect is not significant.
Evidence of effect of ELF B and E fields on the DNA breaking and tumor initiation has been minimal. Since these frequencies do not possess enough energy to break bonds between molecules and damage DNA. [14], [15]

Summary
The health effects of extremely low frequency EMF still remains a controversial subject as the mechanism of interaction is not yet known. The biggest issue in various experiments regarding these fields is the lack of reproducibility of different outcomes. This will be the case until the clear mechanism of interaction between living systems and electric and magnetic fields

References:

[1] Electromagnetic fields and public health: extremely low frequency, WHO Fact sheet N205, Nov.1998
[2] Exposure to extremely low frequency electromagnetic fields and radiofrequency radiation: cardiovascular effects in humans, James R. Jauchem, Vol.70, No.1, Pages 9-21, 1997
[3] Effects of 50 Hz magnetic field exposure on human heart rate variability with passive tilting, Mardi L Sait, Andrew W wood, Richard L G Kirsner,Physiological Measurement, Vol 27, Pages 73-83, 2006
[4] Influence of exposure to electromagnetic field on the cardiovascular system.. Jeong J.H. Kim J.S. et all, Auton Autacoid Pharmacol, Vol 25, No1, Pages 17-23, Jan 2005

[5] Influence of 50 Hz electric and magnetic fields on the human heart, J. Korpinen, J. Partanen,A Uusitalo, Bioelectromagnetism , Vol 14 ,Issue 4, Pages 329 – 340, 1994
[6] Effects of extremely low frequency magnetic fields on pain thresholds in mice: roles of melatonin and opioids, J.H. Jeong, K.B. Choi et all,Journal of autonomic pharmacology, Vol 20, Issue 4, pages 259, 2000
[7] Static and extremely low frequency electromagnetic field exposure: reported effects on the circadian production of melatonin.. Reiter RJ, Journal Cell Biochemistry, Vol. 51, No.4 Pages 394-403, Apr 1993
[8] Human melatonin during continuous magnetic field exposure, Charles Graham, Mary R. Cook,Donald W. Riffle, Bioelectromagnetism, vol 18, issue 2, pages 166-171, 1998
[9] Biological Effects of low-level low frequency electric and magnetic fields, Charles Polk, IEEE transaction on education, Vol 34, NO 3, August 1991
[10] Effects of Pulsed Electromagnetic Fields on Bone Healing in a Rabbit Tibial Osteotomy Model.,Fredricks, Douglas C., Nepola, James V., Journal of orthopaedic trauma ,Vol. 14, No.2,Pages 93-100, February 2000
[11] Pulsing electromagnetic field treatment in ununited fractures and failed arthrodeses , Bassett C.A.L., S.N. Mitchell and S.R. Gaston, JAMA, Vol. 247, Pages 623-628, 1982
[12] Inhibition of gap junction intercellular communication by extremely low frequency electromagnetic fields in osteoblast like models is dependent on cell differentiation, Dean T. Yamaguchi, Jason Huang, Defang Ma, Paul K.C. Wang, Journal of cellular physiology, Vol. 190, Issue 2, Pages 180-188, 2002
[13] Biological effects of Magnetic Fields: Laboratory Studies, Larry E. Anderson, Proceeding of the 20th Annual International Conference of The IEEE Engineering in Medicine and Biology Society, Vol.20, No 6, 1998
[14] A Three generation animal study of the biological effects of very strong low frequency electromagnetic fields, W.Z. Fam, E.L, Mikhail, Engineering in Medicine and Biology Society, 1994. Engineering Advances: New Opportunities for Biomedical Engineers. Proceedings of the 16th Annual International Conference of the IEEE Volume 2, Page(s):756 – 757, 1994
[15] Where are the thresholds for biological effects of non-endogenous low frequency low intensity electric and magnetic fields?, Charles Polk, Engineering in Medicine and Biology Society, 1992. Vol.14. Proceedings of the Annual International Conference of the IEEE Volume 7, Issue , 29 Oct-1 Page(s):2879 – 2880, Nov 1992
[16] Biological effects of low frequency electric and magnetic fields: an overview, Charles Polk, Bioengineering Conference, 1992., Proceedings of the 1992 Eighteenth IEEE Annual Northeast Volume , Issue , 12-13 Page(s):55 – 57, Mar 1992
[17] Biological effects of electric and magnetic fields: what do we know?, Indira Nair, IEEE International Magnetics Conference, Stockholm, Sweden, April 13-16, 1993.
[18] Interaction of static and extremely low frequency electric and magnetic fields with living systems: health effects and research needs,Michael H. Repacholi, B. Greenebaum,Bioelectromagnetism, Vol 20, Issue 3, Pages 133-160, 1999
[19] Weak electric field interactions in the central nervous system, RD Saunders, JGR Jefferys, Health Physics, 83(3):366-375, 2002